University of Lille

Doctoral School Biology- Health of Lille

Deciphering Flax dew retting by a multimodal approach

Suvajit Mukherjee

Defend on December 16th, 2024

For the grade of Doctor in Plant Glycobiology at Lille University (France)

(Amphitheater-IEMN, 59650 Villeneuve-d'Ascq, Lille)

Members of jury

Dr. Anne Harduin-Lepers (DR, CNRS, University of Lille, France)..... President of the jury

Dr. Gabriel Paes (DR, INRAE/URCA Reims, France)..... Thesis reporter

Prof. Craig Faulds (PR, University of Aix Marseille, France)..... Thesis reporter

Prof. Catherine Rayon (PR, University of Picardie Jules Verne, Amiens, France) ..... Thesis examiner

Dr. Brigitte Chabbert (Mission in charge, INRAE/ FARE, Reims, France) ..... Thesis examiner

Dr. Anne-Sophie Blervacq (PR, Udl, University of Lille, France) .....Thesis director

Prof. Simon Hawkins (PR retired, University of Lille, France).....Ex-Thesis director

Dr. Stephen Arscott (CNRS/IEMN, France)..... Thesis co-director

Dr. Sébastien Grec (MCF, Udl, University of Lille, France)..... Thesis supervisor

Université de Lille

École Doctorale Biologie-Santé de Lille

Analyse multimodale du processus de rouissage sur champs du lin : étude fonctionnelle et spectrales en vue d'améliorer la qualité des fibres

Suvajit Mukherjee

Soutenance de thèse le 16 décembre 2024

Pour l'obtention du grade de Docteur en Glycobiologie Végétale à l'Université de Lille (France)

(Amphithéâtre IEMN, 59650 Villeneuve-d'Ascq, Lille)

Membres du jury

Dr. Anne Harduin-Lepers (DR, Université de Lille, France) ..... Président du jury

Dr. Gabriel Paes (DR, INRAE/URCA Reims, France) ..... Rapporteur de thèse

Prof. Craig Faulds (PR, Université d'Aix Marseille, France) ..... Rapporteur de thèse

Prof. Catherine Rayon (PR, Université de Picardie Jules Verne, Amiens, France) Examinateur de thèse

Dr. Brigitte Chabbert (Chargée Mission INRAE/ FARE, Reims, France)..... Examinateur de thèse

Dr. Anne-Sophie Blervacq (PR, Udl, Université de Lille, France) ..... Directeur de thèse

Prof. Simon Hawkins (PR retraité, Université de Lille, France) .....Ancien directeur de thèse

Dr. Stephen Arscott (DR, CNRS/IEMN, France) ..... Co-directeur de thèse

Dr. Sébastien Grec (MCF, Udl, Université de Lille, France) ..... Encadrant de thèse

Résumé

Les fibres issues des plantes sont traditionnellement utilisées dans les textiles et représentent une alternative durable aux fibres synthétiques, notamment dans les matériaux composites. Les fibres de lin sont produites dans la tige, entre le parenchyme cortical et le phloème secondaire.

L'extraction de ces fibres à partir de la tige commence par le processus de rouissage, au cours duquel les tiges de lin sont laissées sur le champ. Cette étape permet aux microorganismes de dégrader les polymères qui lient les fibres à la tige, principalement les pectines de la lamelle~~s~~ moyenne~~s~~. Après le rouissage, des étapes mécaniques telles que le teillage, le peignage et la filature permettent de séparer et nettoyer les fibres.

Le rouissage sur champs, pratiqué en Europe a l'inconvénient d'introduire de la variabilité dans les lots de fibres. Le rouissage est un processus biologique naturel complexe influencé par divers facteurs ce qui rend sa maîtrise difficile. Il est donc essentiel pour garantir une qualité constante des fibres de pouvoir contrôler ce process.

Pour l'instant aucune méthode fiable permettant de mesurer l'avancée du rouissage directement sur champs n'a encore été établie. Nous pensons que l'utilisation de capteurs de l'intelligence artificielle pourraient être utilisés (Agriculture 4.0). Cependant, le déploiement de telles stratégies nécessite une connaissance plus approfondie des changements biologiques, biochimiques et physiques qui se produisent pendant le rouissage. Cette étape permettra d'identifier des marqueurs de rouissage fiables permettant de suivre l'avancée du rouissage. C'est l'objectif du projet Flaxtronic (I-Site PEARL 2021-24) dans lequel ces travaux de thèse s'inscrivent.

Les principaux objectifs sont (i) d'accroître notre connaissance biologique du processus du rouissage en combinant des approches d'enzymologie, de chimie et de métaprotéomique, (ii) d'explorer la possibilité d'utiliser la spectroscopie vibrationnelle (FT-IR/Raman) pour suivre les modifications biochimiques qui s'opèrent pendant le rouissage, et (iii) Evaluer l'utilisation des changements de couleurs de la tige au niveau du spectre comme marqueur physique et non destructif du rouissage.

Dans ce travail, nous avons utilisé pour la première fois une approche basée sur la métaprotéomique pour étudier le rouissage sur champs du lin. La combinaison de la métaprotéomique et des approches enzymologiques et chimiques classiques, a permis, pour la première fois, d'identifier les enzymes microbiennes et végétales (CAZymes) impliquées dans la dégradation de la paroi cellulaire, ainsi que leur dynamique tout au long du rouissage. La comparaison de deux champs adjacents a montré que, malgré une majorité de microorganismes et d'enzymes soient communs, une certaine variabilité

inter-champs (enzymes/microorganismes spécifiques) pourrait expliquer la différence de qualité dans les fibres obtenues pour chacun.

Le suivi spectroscopique de pailles prélevées tout au long du rouissage et sur plusieurs champs a permis d'établir que la spectroscopie vibrationnelle FT-IR peut être utilisée pour suivre efficacement le rouissage. Des marqueurs clés ont pu être identifiés, comme par exemple le pic de 1733,8 cm^{-1} pour la pectine estérifiée et le pic de 1317 cm^{-1} pour l'hémicellulose. La significativité de ces liaisons chimiques permet d'indiquer le moment optimal de récolter les tiges rouies.

Les changements de couleur des tiges qui s'opère pendant le rouissage ont été mesurés et quantifiés. L'analyse statistique des données a révélé que les changements associés aux longueurs d'onde spécifiques (480-490 nm et 600-610 nm) permettent de prédire de manière fiable la fin du rouissage.

L'ensemble de ces résultats pourra faire l'objet d'intégrations statistiques poussées pour produire un modèle prédictif multimodale. Cela constituera une « boite à outils » sur laquelle un capteur permettant de suivre le rouissage sur champs pourra être construit.

Mots-clés : Rouissage, Fibre végétale, Métaprotéomique, Spectroscopie vibrationnelle, Spectroscolorimetrie, Enzymes.

Abstract

Plant bast fibers, traditionally used in textiles, are gaining attention as sustainable alternatives to synthetic fibers, especially in composite materials. Flax (*Linum usitatissimum L.*) is a key crop in France's textile and materials industries due to its strong, flexible bast fibers found in the outer stem. The extraction of these fibers begins with the retting process, during which the flax stems are left in the field, allowing microbes to break down the pectic substances binding the fibers to the stem. After retting, mechanical steps like scutching, combing, and spinning are employed to fully separate and refine the fibers.

Dew retting, the most common method used in Europe, is environmentally friendly but can introduce variability in the quality between fiber batches. Insufficient retting makes further extraction difficult and so fiber damages, while excessive retting weakens them by degrading fiber cell wall integrity. Retting is a complex natural process influenced by various factors that make it difficult to obtain fiber batches of standard quality. Standardizing the retting is essential to ensure consistent quality for sustainable textile production.

Although several studies have attempted to develop tools for assessing the degree of retting, a reliable, non-destructive method has yet to be established. We believe that employing sensors and artificial intelligence could help overcome this challenge. However, this requires a deeper understanding of the biological, biochemical, and physical changes occurring during retting to identify reliable and consistent retting markers to monitor the retting from the fields. This is the objective of the FlaxTronic project (I-Site PEARL 2021-24) in which this thesis work is done.

Key objectives of this thesis included (i) understanding biological and biochemical processes that occur during the retting, (ii) exploring vibrational spectroscopy (FT-IR/Raman) for monitoring chemical changes, and (iii) assessing stem color changes as non-invasive physical retting markers.

While previous research has advanced our understanding of the bacterial and fungal communities involved in retting, the specific enzymes and their producing organisms remain unidentified. In this work, we employed a metaproteomic-based approach for the first time in the context of flax dew retting, significantly enhancing the understanding of retting dynamics by identifying microbial and plant enzymes (carbohydrate-active enzymes) involved in cell wall degradation. Comparing two adjacent field studies revealed that despite a majority of enzymes and microbes being commonly found, inter-field variability in retting enzymes and microbes might explain the obtained “in fine” contrasting fiber quality.

FT-IR vibrational spectroscopy effectively monitors the retting process by identifying key markers, including the 1733.8 cm^{-1} peak for esterified pectin and the 1317 cm^{-1} peak for hemicellulose, whose changes indicate the optimal retting endpoint in both “a priori” and “without a priori” approaches.

Our spectrophotometric analysis of stem color changes demonstrated promise for a predictive model to monitor retting progress by linking color intensity shifts at specific wavelengths (480-490 nm and 600-610 nm) to advanced stages.

Integration of these multi-scale data obtained to build predictive models will be the next step to provide a comprehensive “toolbox” that can be used to develop a device solution for monitoring retting and optimizing fiber quality. This would contribute to the introduction of sustainable textiles under Agriculture 4.0.

Keywords: Retting, Plant Fiber, Metaproteomics, Vibrational spectroscopy, spectrocolorimetry, Enzymes.

Acknowledgment

I would like to express my deepest gratitude to the members of the jury, Dr. Gabriel Paes, Prof. Craig Faulds, Prof. Catherine Rayon, Dr. Brigitte Chabbert, and Dr. Anne Harduin, for agreeing to evaluate my work and participate in the discussion during the defense.

My sincere thanks go to my 1st and 2nd-year CSI juries, Dr. Marie-Noëlle Rosso and Dr. Bernard Kurek, whose advice significantly influenced the shape of this thesis.

I gratefully acknowledge the support of the PEARL FlaxTronic project, financed by the European Union's Horizon 2020 research and innovation program under the Marie Skłodowska-Curie grant agreement N°847568, as well as the I-SITE ULNE Foundation (ANR). Special thanks to Mr. Alexis Boulet (from I-SITE, Pearl) for his ongoing management and to Mr. Phillipe Ducamp from Euraxes Lille, who ensured all our bureaucratic needs were addressed.

I extend my thanks to our collaborators, particularly Van Robays Ferrers, with special appreciation to Mr. Pierre D'Arras (Chairman), Mr. Nicolas Ryckeboer (Manager), and Mr. Hubert Vancappel (flax grower) for their support during multiple years of flax sampling, sharing industrial evaluation details, and introducing us to the industrial flax processing chain. A special mention goes to those who accompanied me to the fields during sampling, including my supervisors Dr. Sébastien Grec, Dr. Stephen Arscott, my teacher Dr. Anne Creach, my colleague Dr. Oriane Morel, Dr. Ali Reda and always-supportive Dr. Dmitry Galinousky. I would also like to thank Dr. Damien Saulat from the GEMTEX ENSIT lab for assisting with fiber quality analysis.

Thanks to Dr. Jean Michel Salou and Dr. Anne-Sophie Lacoste (from the PLBS platform) for their contributions to proteomics work. Special thanks to our hemp collaborators, Dr. Eliane Bou Orm and Ecole des Mines, for trusting us with the enzymatic portion of their research.

My sincerest cordial gratitude goes to my thesis supervisors, Dr. Sébastien Grec, Prof. Simon Hawkins, Dr. Anne-Sophie Blervacq, and Dr. Stephen Arscott for guiding me through each step of this journey, offering valuable advice, and granting me the autonomy needed to carry out this work. I am grateful to Dr. Anne Creach who first introduced me to working with flax enzymes, and to Dr. Estelle Goulas, who taught me the discipline required for working with proteins. I would like to thank Dr. Fredric Krzewinski for his guidance on HPLC and monosaccharide analysis. Again, I want to thank my supervisor Dr. Anne-Sophie Blervacq along with technicians Dr. Isabelle De Waele and Dr. Myriam Moreau for introducing me to Raman and FT-IR vibrational spectroscopy. A special mention to Dr. Chrystelle Le Danvic for guiding the work with volatile organic compounds.

I owe a huge thanks to my supervisor Dr. Sébastien Grec for pushing me to improve my statistical analysis skills, and who was always there beside me in every situation since the beginning. And to Dr. Dmitry Galinousky for his help, support, care, and encouragement. I also deeply appreciate Prof. Simon Hawkins, who always provided the right answers during difficult times. Thanks to Dr. Brigitte Huss and Prof. Godfrey Neutelings, who checked and encouraged me regularly; also, for all the treats during both national and international conferences.

My thanks extend to the master's students, Mrs. Sarah Rathary and Mrs. Alicia Mengue, for their hard work and contributions to the project. I would also like to thank all the wonderful people at UGSF—colleagues, friends, and staff—for the moments we shared, both big and small, that I will cherish forever. Special thanks to Dr. Alessandra Gaetano, Dr. Ryma Benlakehal for their help, support, and company.

A special note of appreciation to my friends from the PEARL program, training sessions and Euraxess gatherings, where I met some truly exceptional individuals like Dr. My Nghe Tran and his wife Mrs. Le Nhu Ngoc Nguyen, Dr. Athulya Nadol, Mr. Nguyen Duc Manh, and Dr. Smritijit Sen and his wife Dr. Rapti deb, whose friendship and emotional support have been invaluable throughout this journey.

I owe a debt of gratitude to my Master's supervisor and mentor, Prof. Rajib Bandopadhyay, whose inspiration set me on this path, and to Dr. Subhojit Dutta, whose guidance and encouragement have been critical to my growth.

Finally, I would like to thank my family—my parents, my sister and guruji—for being my guiding light and for making me who I am today. You are the most important person in my life. A special thank you to my great friend Mr. Saikat Sain back home, who has always supported me without question.

I end with a huge thanks and congratulations to myself, with whom I carried all this adventure.

Suvajit Mukherjee

October, 2024

Lille, France

Contribution to thesis work and scientific valorization

Publications

Publication 1:

Mukherjee S.[a], Goulas E.[a], Creach A.[a], Galinousky D.[a], Blervacq A-S.[a], Krzewinski F[a], D'Arras P.[d], Ratahiry S.[a], Menuge A.[b], Soulat D.[b], Saliou J-M.[c], Lacoste A-S.[c], Hawkins S.[a] and Grec S[a*], 2024. Metaproteomics identifies key cell wall degrading enzymes and proteins potentially related to inter-field variability in fiber quality during flax dew retting. https://doi.org/10.1016/j.indcrop.2024.119907.

Publication 2:

Mukherjee Suvajit[1], Goulas Estelle[1], De Waele Isabelle[2], Hawkins Simon[1], Grec Sébastien[1], Blervacq Anne-Sophie*[1], 2024. Flax dew retting tracking: biomarkers for retting processing and estimation of retting dynamics in fields. https://doi.org/10.1016/j.indcrop.2025.120798.

Publication 3:

Mukherjee Suvajit[1,2], Grec Sébastien[1*], Blervacq Anne- Sophie[1], Arscott Steve[2], 2024. Quantifying flax stem surface color change for the development of a smart tool to monitor the degree of retting [in preparation].

Publication 4:

Bou Orm, E., Mukherjee, S., Rifa, E., Créach, A., Grec, S., Bayle, S., Benezet, J.C., Bergeret, A., & Luc Malhautier, 2024. High-throughput sequencing reveals microbial community dynamics during hemp field retting [in review].

Oral presentations

Mukherjee S.[a]*, Goulas E.[a], Galinousky D.[a], Creach A.[a], Blervacq A-S.[a], Krzewinski F[a], D'Arras P.[d], Ratahiry S.[a], Menuge A.[b], Soulat D.[b], Saliou J-M.[c], Lacoste A-S.[c], Hawkins S.[a] and Grec S[a], "Metaproteomics identifies key cell wall degrading enzymes during flax dew retting", (14[e] Journées du Réseau Français des Parois, Saint-Malo, France, august 2024).

Deciphering flax dew retting by a multimodal approach; Lille, 22/09/2023, Séminaire hebdomadaire de l'UGSF, Lille, France.

Suvajit Mukerjhee[1,2], Anne Creach[1], Anne Sophie Blervacq[1], Estelle Goulas[1], Ali Reda[2,1], Steve Arscott[2], Simon Hawkins[1] and Sébastien Grec[1], "Deciphering bast fiber retting by a multimodal approach", 01/11/2023, ICAR-CRIJAF, Barrackpore, India.

Poster presentations

Mukherjee S.[1,2], Creach A.[1], Blervacq A-S.[1], Goulas E.[1], Reda A.[2,1], Saliou J-M.[3], Lacoste A-S.[3], Arscott S.[2], Hawkins S.[1] and Grec S.[1], "Flax dew retting, a unique and specific plant cell wall degradation process" (Plant Cell Wall Meeting: XVI, Malaga, Spain, juin, 2023).

Blervacq A.-S.[1], Mukherjee S.[1*], Moreau M.[2], Duputié A.[3], Duponchel L.[2], Hawkins S.[1], "Proprioception in plant? Comparison of flax bast fibers and G-layers induced by long-term gravitropic stress." (Plant Cell Wall Meeting: XVI, Malaga, Spain, juin, 2023).

Table of content

Résume i
Abstract iii
Acknowledgment v
Contribution to thesis work and scientific Valorization vii
List of Figures xi
List of Tables xiv
Abbreviations xv

Chapter I: Bibliographic Synthesis 1
I.1. Flax Fibers: A Potential green replacement of petrobased fibers? 3
I.2. All About Flax 17
I.3. All about Hemp (a collaborative study). 41
I.4. The Retting. 46
I.5. Microbiology of retting. 55
I.6. (Enzyme) Biochemistry of Retting 60
I.7. Evaluation of (physicochemical changes of) flax straw during dew retting. 67
I.8. Factors affecting field retting. 70
I.9. Determination of degree of flax dew retting. 71
I.10. Possibility of artificial intelligence-based decision-making tool-box (Emerging Agriculture 4.0) 73
I.11. Objective of the thesis work 75
I.12. References. 81

Chapter II: Material and Methods 96
II.1. Context of the chapter 98
II.2. Sampling of materials 98
II.3. Soil analysis of retting 2021 102
II.4. Fiber quality assessment of retting 2021 102
II.5. Anatomy of stems and histochemical staining 104
II.6. Spectrophotometric/ fluorometric enzyme assay 105
II.7. Monosaccharide analysis with HPLC-HPAEC-PAD 107
II.8. Preparation, and measurements for 2D-LC-MS/MS-based metaproteomics 110
II.9. Proteomic data analysis 111
II.10. FTIR-vibrational-spectroscopy 113

II.11. Color spectroscopy 118
II.12. References 122

Chapter III: Biological insight of flax and hemp dew retting, identification of key enzymes and microorganisms 124
III.1. Context and structure of the chapter 126
III.2. Metaproteomics of flax dew retting (2021) in adjacent fields 128
III.3. Enzyme dynamics study in hemp retting 159
III.4. Conclusion of the chapter 162
III.5. Reference: 164

Chapter IV: Evaluation of flax dew retting progression and field dynamics 169
IV.1. Context and structure of the chapter 170
IV.2. Flax dew retting tracking: biomarkers of retting and fields dynamics 172
IV.3. Conclusions of the chapter 203
IV.4. Reference 204
ANNEXE A: Table FT-IR assignment band 208
ANNEXE B: Table FT-IR assignment band 210

Chapter V: Studying color change of flax stem surface during dew retting 211
V.1. Context and structure of the chapter 212
V.2. Quantifying flax stem surface color change for the development of a smart tool to monitor the degree of retting 214
V.3. Reference: 236

Chapter VI: Overall Discussion, Conclusion, and Perspective of the Thesis 239
VI.1. Discussion 240
VI.2. General Conclusion of the Thesis 249
VI.3. Perspective of the Thesis 250
VI.4. References 252

List of Figures

I.1. Classification of fiber based on nature of origin 5
I.2. Classification of plant base cellulosic fibers 6
I.3. Infographics of selected events through evolution of human history of fiber and textile 8
I.4. Examples of the uses of flax in ancient Egypt 8
I.5. Global textile market according to '*PFMR – Textile Exchange, 2022'* report 10
I.6. Life cycle analysis comparison between different fibers. 13
I.7. Stress-strain curve showing elastic, plastic and strain-hardened zone followed by fracture point. 15
I.8. Taxonomic classification of flax 17
I.9. Members of the *Liniodeae* tribe 18
I.10. Morphology of Flax (*Linum usitatissimum*) 19
I.11. Flax Anatomy 20
I.12. Flax Anatomy: focus on the outer and inner tissues 21
I.13. Flax stem's outer and inner issues in detail 21
I.14. Flax bast fiber 23
I.15. The upper scheme illustrates the fiber elongation, with fibers represented in green 24
I.16. Bast fiber composition, cell wall structural, and chemical organization 27
I.17. Categorization of bast fibers and G-layer in stressed wood 28
I.18. Flax fiber bundle before and during retting 29
I.19. Structure of pectin 30
I.20. Structure of Hemicellulose 32
I.21. Cellulose in plant bast fiber 35
I.22. Flax cultivation and processing - Where does retting stand from seed to woven linen 37
I.23. Production share of flax (raw or retted) on average between 1994-2022; by region 38
I.24. Various use of flax fibers 40
I.25. Hemp plant 42
I.26. Structure of flax and hemp stem 43
I.27. Use of Hemp plant in various usages 45
I.28. Different types of retting and degumming 49
I.29. Dew retting of flax 50
I.30. Timeline of Microbiology of Flax retting 56
I.31. Timeline of Microbiology of Hemp retting 59
I.32. Classification of glycosyl hydrolases 64
I.33. Retting disorganizes flax stem tissues and facilities easy fiber detachment by applying mechanical force 68

I.34. Factors affecting field retting 71
I.35. Use of sensors in agriculture 75
I.36. Three major segments for multimodal analysis of flax dew retting 78

II.1. Sampling location and techniques 99
II.2. Sampling location in different years 101
II.3. Method of classifying retted and scutched flax fiber according to USTRL standards. .. 102
II.4. In-lab fiber quality assessment using the single fiber tensile test 103
II.5. Technovit embedding and microtomy 105
II.6. Schematic representation of the sampling 115
II.7. Flax straw surface color change reading with spectrophotometer Konica cm23d 119
II.8. Schematic representation of experimental steps 120

III.1. Anatomy of flax stem during retting 130
III.2. Abiotic parameters affecting flax growth and retting 132
III.3. Fiber yield and industrial quality assessments 133
III.4. Enzyme activity dynamics in outer tissues of flax stems during dew retting in field A 135
III.5. Enzyme activity dynamics in outer tissues of flax stems during dew retting in field B 136
III.6. Changes in cell wall monosaccharide composition in outer tissues of flax during dew retting in field A 138
III.7. Changes in cell wall monosaccharide composition in outer tissues of flax during dew retting in field B 139
III.8. Venn diagrams of proteins identified during retting in Fields A and B 140
III.9. Distribution of proteins by GO category according to GO aspects for field A and field B. 142
III.10. Venn diagrams of proteins identified during retting in Fields A and B 143
III.11. Distribution of CAZymes identified in the metaproteome of field A and field B presented by class and families 146
III.12. Dynamic changes in CAZyme abundances during flax retting in fields A and B 149
III.13. Taxonomic origins of CAZymes associated with plant cell wall degradation identified in the metaproteomes of fields A and B 150
III.14. Enzyme activity dynamics in outer tissues of hemp stems during dew retting in watered (A) and non-watered (N-A) conditions 161

IV.1. Average spectra of the different dew retting time according to the field A 178
IV.2. Comparative analysis of Zone A in field A 179
IV.3. Comparative analysis of Zone B in field A 180
IV.4. Comparative analysis of Zone C in field A 180
IV.5. Comparative analysis of Zone D in field A 181

IV.6. Comparative analysis of Zone E in field A 181
IV.7. Definition of the workflow followed for the multivariate analysis of FT-IR datasets 184
IV.8. [Start vs End] points retting process (R0 vs R7) in field A 186
IV.9. Early retting process (R0 vs R2) in field A 187
IV.10. Late retting process (R6 vs R7) in Field A 189
IV.11. Venn Diagrams highlighting significant peaks in Field A 190
IV.12. Timeline of retting with common and specific peaks characterizing steps 191
IV.13. Average spectra of the different dew retting time according to the field B 192
IV.14. Comparative analysis of the five zones, in field B 193
ANNEXE B Stem water-content evolution during retting. 210

V.1. Climate data (temperature and rainfall) during flax dew retting in three sampling years 218
V.2. Photographs of flax stem bundles in various stages of retting 219
V.3. Box plot of L*a*b* values of color retting samples (where L* = lightness, a* = green-redness, b* = blue-yellowness). 220
V.4. Spectral analysis of retting 2014 222
V.5. Spectral analysis of retting 2021 filed A 224
V.6. Spectral analysis of retting 2021 filed B 225
V.7. Spectral analysis of retting 2022 filed A 226
V.8. Spectral analysis of retting 2022 filed B 227
V.9. Spectral analysis of pooled color data with selected four variables from comp-1, from all five retting color data sets 230
V.10. ROC curve with AUC score of different retting color data sets 231
V.11. Spectral analysis of color data from retting 2022 Field A with over-retted samples 232

VI.1. Biology of Retting and the Search for Retting Markers 241
VI.2. A concept of a toolbox combining proposed methods 248

List of Tables

I.1. Comparison of fiber mechanical properties of Flax with synthetic and others natural fibers 16
I.2. Characteristics and approximate composition of the different cell wall layers of flax fibers 25
I.3. Comparing the physicochemical properties of Hemp and Flax fibers 44
I.4. Comparative retting methods according to the fiber plants 51
I.5. Most abundant microbes during flax dew retting 57
I.6. Most abundant microbes during hemp dew retting 58
I.7. PICRUSt prediction of dew retting CAZymes from falx metagenomics 62
I.8. CAZymes from living flax plant and from dead wood decomposition 66

II.1. Details of sampling (for color analysis) from five flax dew retting experimental sets 118

III.1. Single fiber tensile test on Filed A and Filed B fibers, following French standard NFT 25-501-2 (for SFTT) and NFG 07-004 (for diameter and fineness) 134
III.2. Protein numbers obtained during the different filtering and processing steps of metaproteomic data 140
III.3. Taxonomic origin of identified nonredundant proteins and respective cell wall-related CAZymes 144
III.4. List of CAZy families, corresponding enzyme activities, target polymers, biological origin, kingdom, UniProt ID and presence/absence in fields A and B from all identified nonredundant proteins 147

IV.1. One-way ANOVA of i_{max} value from spectra during the three main steps of the retting process for the field A 182
IV.2. One-way ANOVA of i_{max} value from spectra during the three main steps of the retting process for the field B 194
IV.3. Comparison of the two methods '*a priori*' and 'without *a priori*' 202
ANNEXE A. Table FT-IR assignment band 208

V.1. Details of sampling from five flax dew retting experimental sets 216
V.2. Loadings of principle component 1 with positive and negative contributions, from respective retting color data sets 228
V.3. Pooling of five retting color data sets (from three years with different durations) into Early, Middle, and Advanced stages based on clustered image analysis 228

Abbreviations

<taxon> L. Carl Linnaeus

<taxon> Spp. Several Species

µm Micrometer

AIR Alcohol insoluble residues

BC Before Christ

BCE Before Common Era

CFRP Carbon fiber reinforced polymers

CIELab Commission Internationale de l'Éclairage L*a*b*

DAPI 4,6-diamidino-2-phenylindole

GPa Gigapascal

ISCC International Sustainability and Carbon Certified

Kwh kilowatt-hour

LCA Life Cycle Assessement

MPa Megapascal

Objective *NA* Numerical aperture

PA Polyamide

PE Polyethylene

PET Polyethylene terephthalate

PLA Polylactic acid

PP Polypropylene

ppm Parts per million

SCE Specular Component Excluded

SCI Specular ComponentIncluded

SFTT Single Fiber Tensile Test

UN United Nations

UNICEF United Nations International Children’s Emergency Fund

USTRL Union Syndicale des Rouisseurs-Teilleurs de Lin

WMO World Meteorological Organization

CHAPTER I

Bibliographic Synthesis

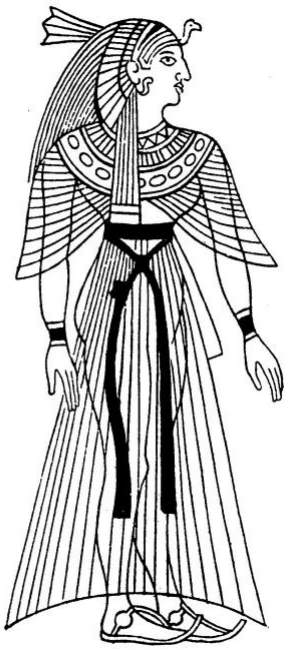

@Manali bhanushali (https://textilevaluechain.in/)

(www.historicalpicturearchive.com)

Chapter I: Bibliographic Synthesis

Contents

Chapter I: Bibliographic Synthesis 1
I.1. Flax Fibers: A Potential green replacement of petrobased fibers? 3
I.1.1. The Need for Fibers: Textile & Other 3
I.1.2. Classification of Fibers 4
I.1.3. (Quick)_History of Fibers 7
I.1.4. Global Textile Market & Today's Fibers 9
I.1.5. Textile pollution 10
I.1.5.1. Textile-Carbon-footprint 11
I.1.5.2. Textile-Energy-footprint 11
I.1.5.3. Textile-Water-footprint 11
I.1.6. (Rough) LCA-comparison: Are bast fibers a sustainable replacement? 12
I.1.7. Physical and Mechanical Properties of Flax Fiber are ideal for composite material reinforcement 14
I.2. All About Flax 17
I.2.1. Taxonomy and Systematics 17
I.2.2. Morphology of Flax (Stem/Flower/Fruit) 18
I.2.3. Antomy of Flax 20
I.2.3.1. Flax stems outer vs inner tissue 20
I.2.3.2. The bast fibers 22
I.2.4. Flax plant polymers in outer stem tissues 26
I.2.4.1. Pectins 28
I.2.4.2. Hemicelluloses. 31
I.2.4.3. The glycoproteins arabinogalactan proteins (AGPs) in Flax. 33
I.2.4.4. Cellulose 34
I.2.5. Flax Cultivation and Processing: From Flax to Linen. 36
I.2.6. Flax: Use and Demand (global production). 37
I.3. All about Hemp (a collaborative study). 41
I.3.1. General Introduction. 41
I.3.2. Hemp Stem anatomy (in comparison to flax). 42
I.3.3. Hemp Cultivation. 44
I.3.4. Global production and use of Hemp: Productions and Consumption. 44
I.4. The Retting. 46
I.4.1. All about retting. 46

I.4.2. Changes in fibers due to retting. 52
I.4.3. Methods used to study retting. 53
I.5. Microbiology of retting. 55
I.5.1. Flax retting. 55
I.5.2. Hemp retting. 58
I.5.3. Other retting studies (metagenomics based). 60
I.6. (Enzyme) Biochemistry of Retting 60
I.6.1. Dynamics of plant cell wall degrading enzyme in dew retting. 60
I.6.2. Details on plant cell wall degrading enzymes (CAZymes). 63
I.6.2.1. Cell-wall pectin degrading enzyme. 64
I.6.2.2. Cell-wall hemicellulose degrading enzyme. 65
I.6.2.3. Cell-wall cellulose degrading enzyme. 65
I.6.2.4. Lignin degrading enzymes. 67
I.7. Evaluation of (physicochemical changes of) flax straw during dew retting. 67
I.8. Factors affecting field retting. 70
I.9. Determination of degree of flax dew retting. 71
I.10. Possibility of artificial intelligence-based decision-making tool-box (Emerging Agriculture 4.0) 73
I.11. Objective of the thesis work. 75
I.12. References. 81

I.1. Flax Fibers: A Potential green replacement of petrobased fibers?

I.1.1. The Need for Fibers: Textile & Other

Textiles play an essential role in all stages of human life Therefore, a thorough understanding of textile fibers is important to avoid common mistakes (in judging durability, comfort, allergic reactions, textile-care, environment impact, appropriate use case etc.) when purchasing, selling, and using textile materials. The term "textile" comes from the Latin "textilis" and the French "texere", both meaning weaving (Murthy, 2016) and the French term for clothes i.e. ‘linge’ comes from linen (Flax). Textiles include the lengths of thread required to produce yarn and materials that can be processed into fabric (Cook, 1984; Murthy, 2016). As a noun, textile refers to woven or woven materials, including fabrics, fibers, and yarns made by weaving, felting, or stitching. Textile as an adjective refers to the materials, machines, and processes involved in production, such as textile factories, laboratories, engineers, research, printing, design, and technology (Murthy, 2016). Fibers are basic units of fabrics and textiles (Kadolph, n.d.). Natural or artificial fibers form the basic components of fabrics. It is defined as the fine hair-like components of plant or animal tissue that can be woven into thread. Physical analysis of the fibers emphasizes that the length-to-diameter ratio is at least 100 times (Cook, 1984; Murthy, 2016). According to technologists, textile fibers are fibers suitable for spinning into yarn or fabric using weaving techniques such as weaving, knitting, or felting (Murthy, 2016). Fibers exist in two basic forms: staple fibers, which are limited lengths that require twisting to produce yarn, and filaments, which are continuous lengths suitable for direct use in textiles (Kadolph, n.d.; Murthy, 2016). Natural fibers, for example, silk, have amazing length-to-width ratios. Silk fibers are often millions of times longer than their diameter (Murthy, 2016). Man-made fibers also have a high length-to-diameter ratio and are generally similar in diameter to natural fibers (Cook, 1984; Murthy, 2016).

Fibers have a wide range of industrial applications outside textiles. They are used to make ropes, twines, nonwoven fabrics, and biocompatible surgical equipment, gauze, bandages, cotton swabs, implants, etc. Carbon and glass fibers are used in the automotive industry to make lightweight, high-strength components, which improve fuel efficiency. Aerospace uses metal-coated fibers and carbon composites because of their excellent strength-to-weight ratio. Sporting items benefit from fibers' toughness and impact resistance (Elfaleh et al., 2023).

The desirable properties of a good fiber include strength, cohesion, flexibility (less rigidity), fineness, elasticity, uniformity, porosity, gloss or luster, and durability (Cook, 1984; Kadolph, n.d.; Murthy, 2016). Strength, measured as tensile strength, reflects the load-bearing capacity of the fiber, while cohesion refers to the ability of fibers to adhere to each other during spinning, influenced by surface properties such as flakes or wrinkles. Flexibility ensures that fibers wrap around each other during rotation, while rigidity makes the fabric difficult to use. Fineness, expressed in various units, refers to fiber diameter or weight per unit length. Elasticity, the ability of a fiber to return to its original

state after deformation, is crucial for fabric performance. Uniformity in thickness and length improves fabric quality, with man-made fibers often exhibiting greater uniformity than natural fibers. Porosity promotes moisture absorption, important for wet processing, as natural fibers are generally more porous than synthetic ones. Preferences vary, but luster adds value to the fiber. Durability, encompassing a fiber's resistance to abrasion, chemicals, and physical damage, is influenced by strength, flexibility and cohesion (Murthy, 2016).

Natural fibers like flax, hemp, and jute offer significant advantages over synthetic fibers such as carbon and glass in composite materials, particularly in terms of environmental sustainability and weight reduction. While synthetic fibers offer higher tensile strength and modulus, natural fibers are biodegradable, renewable, and have a less carbon footprint. They result in lighter composites, which improve fuel efficiency and weight reduction while also providing great vibration and noise reduction. These qualities make natural fibers a viable option for a variety of industrial applications.

I.1.2. Classification of Fibers

Classification of textile fibers is important for selecting the right fiber for a particular application (Kadolph, n.d.; Murthy, 2016). The classification method can vary depending on the desired specificity. Some of the examples are - classification based on personality and origin; classification based on botanical, zoological, and chemical names; classification according to their ability to absorb moisture; classification according to thermoplasticity; classification by usefulness, etc. (Murthy, 2016).

Based on the nature of origin, broadly fibers can be divided into natural and synthetic or man-made fiber (**Fig. I.1**).

Natural fibers can be further classified into animal, plant, and inorganic fibers.

- Animal fibers are mainly composed of protein and include silk, wool, mohair (goat), llama and alpaca wool, vicuna wool, camel hair, horsehair, rabbit fur, beaver fur, pig bristle, badger fur, sable fur, etc.
- Plant fibers consist primarily of cellulose and can be classified as short fibers (such as cotton and kapok) or long fibers, including flax, hemp, manila-hemp (abaca), jute, ixtle, ramie, sisal, Spanish moss, etc. (**Fig. I.2**)
- The main natural inorganic fiber is asbestos, a hazardous material that can cause asbestosis, mesothelioma, lung cancer, and other health issues if inhaled. Fibers can also be obtained from other inorganic materials, such as metals (especially gold and silver) that can be spun into yarn.

Natural fibers (obtained from plants, animals, minerals, etc.) are sometimes called miscellaneous fibers (Murthy, 2016).

Non-natural or artificial fibers are developed by humans and often mimic natural fibers using natural resources and/or chemicals. Artificial fibers can be divided into regenerated fibers, synthetic fibers, and various inorganic fibers (Murthy, 2016).

- Regenerated fibers made from natural polymers are regenerated using natural resources as a base and chemically moulded into filaments such as rayon, copper-ammonium fiber, acetate fiber, alginate, and protein fibers.
- Synthetic fibers are made using only chemicals such as nylon and polyester. Synthetic fibers can also be divided into heterochain fibers (e.g. polyester, polyamide) and carbon chain fibers (e.g. polyacrylonitrile, polyvinyl alcohol).
- Various inorganic fibers are made from materials such as metal and glass and have traditionally been used for purposes other than textile fibers. However, modern developments have made it possible to convert it into textiles for regular use.

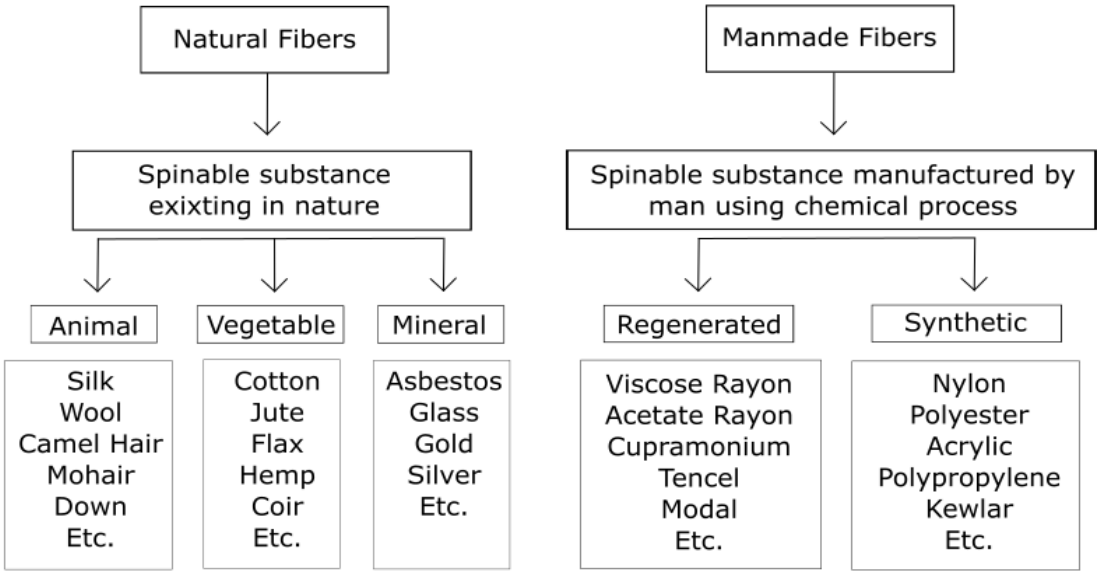

Fig. I.1. Classification of fiber based on nature of origin. Source: adapted from (Murthy, 2016).

Natural plant fibers found in stems and leaves are made up of cellulose, hemicelluloses, lignins, aromatics, waxes, lipids, ash, and water-soluble chemicals, which define their structural composition. The chemical composition and structural characteristics of these fibers define their qualities, functions, and processing efficiencies, which have an impact on their wide range of applications (Murthy, 2016; Müssig, 2010).

Fibers are notably characterized by their extreme length and length-to-diameter ratio exceeding 1000 (Cook, 1984; van Dam and Gorshkova, 2003; Gorshkova et al., 2022). Based on origin, plant fibers are classified into different fibers; such as (a) Bast fiber (sclerenchyma in secondary phloem); also known as phloem fiber, extracted from the inner bark or bast surrounding the stem of certain dicotyledonous

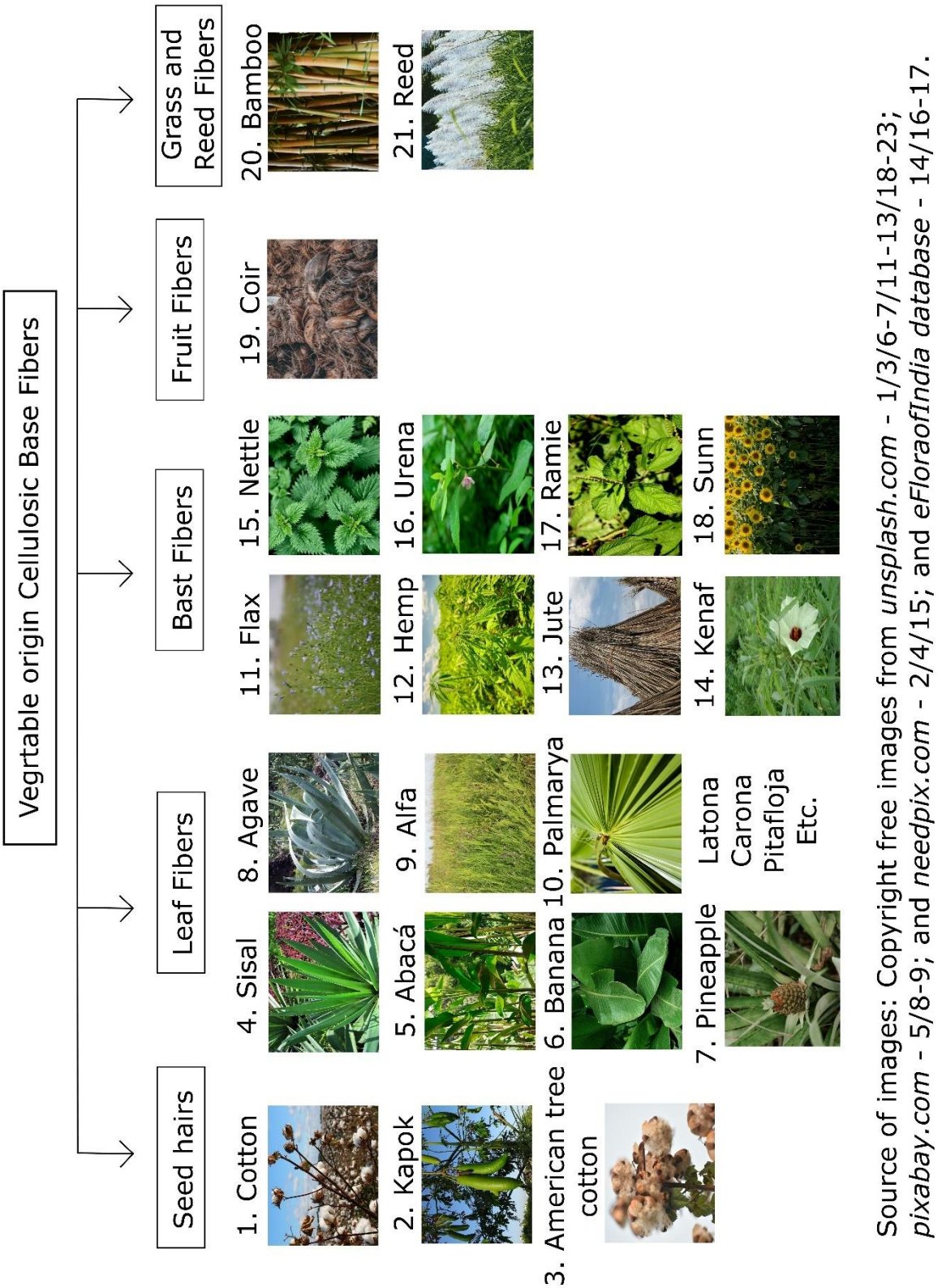

Fig. I.2. Classification of plant base cellulosic fibers.

pant. Common examples are – Flax (*Linum usitatissimim*), Hemp (*Cannabis sativa*), Jute (*Corchorus spp*.), Ramie (*Boehmeria nivea*), Kenaf (*Hibiscus cannabinus*), etc. (b) Leaf fiber (sclerenchyma and specialized epidermal cells); also known as hard fibers, obtained from leaves of monocotyledonous plant such as Sisal (*Agava sisalana*), Abaca (*Musa textilis*), Pineapple (*Ananas comosus*) etc. These fibers are stiffer and coarser than bast fiber, used mainly for making ropes, mats; brushes, etc. (c) Seed or fruit fibers (specialized epidermal cells or trichome, sclerenchyma cells); collected from seeds or fruit of plants, are typically softer and more flexible, making them ideal for textile. Common examples are cotton (*Gossypium spp*.), kapok (*Ceiba pentandra*), coir (*Cocos nucifera*), etc. (d) Grass and reed fibers (specialized sclerenchyma cells); are obtained from bamboo (Bambusoideae), reed (*Phragmites spp*.), Esparto (*Stipa tenacissima*) etc., are generally coarse and used for making mats, baskets, paper etc.

There are also wood fibers (xylem sclerenchyma cells), originating from vascular cambial initials (secondary meristem), unlike other textile fibers like cotton (carpel epidermis extension) or flax (procambium/ primary meristem); which also differs in fiber polymer compositions (wood fiber has cellulose, lignin and hemicellulose). These wood cells, mainly from Spruce (*Picea spp*.) or Pine (*Pinus spp*.) are primarily used for paper, cardboard production and to produce regenerated cellulose fibers for textiles (Kadolph, n.d.; Kozłowski et al., 2020; Murthy, 2016; Paridah et al., 2011).

In this monograph, our main focus will be cellulosic plant fiber, more exclusively bast fibers of Flax.

I.1.3. (Quick)_History of Fibers

The utilization of fibers and textiles in human history predates history itself and followed many developments until now (**Fig. I.3**) (Allaby et al., 2005; Bergfjord et al., 2010; Fisher, 1981; McDonald, 2011; van Zeist and Bakker-Heeres, 1975). The oldest artifacts, including basketwork, mats, and cordage, have been found in the caves at Lascaux (France), dating back to 13,000 BCE (Fisher, 1981; McDonald, 2011); and a net bag excavated in Utah cave (US), about 9000BCE indicates the achievement of human skills in plant fiber processing (Fisher, 1981). The discovery of dyed flax fibers in a cave in the Republic of Georgia 34,000 years ago suggests textile-like materials were made even in prehistoric times (Balter, 2009; Bergfjord et al., 2010; McDonald, 2011). The Swiss Lake dwellers cultivated flax and wove it to linen to make clothing, household items, and even fishing nets, dating back to 8000 BCE (Fisher, 1981; McDonald, 2011). In ancient Egypt, during the Middle Kingdom period (around 2033–1963 BCE), flax was cultivated primarily in the fertile Nile valley. Egyptians used flax extensively for high-quality textiles, creating clothing, workwear, sails, fishing nets, and especially mummy wraps and funeral linens for burials (**Fig. I.4**). The flax textiles' fine quality and comfort were highly prized, demonstrating Egyptians' advanced textile manufacturing skills (Melelli et al., 2022).

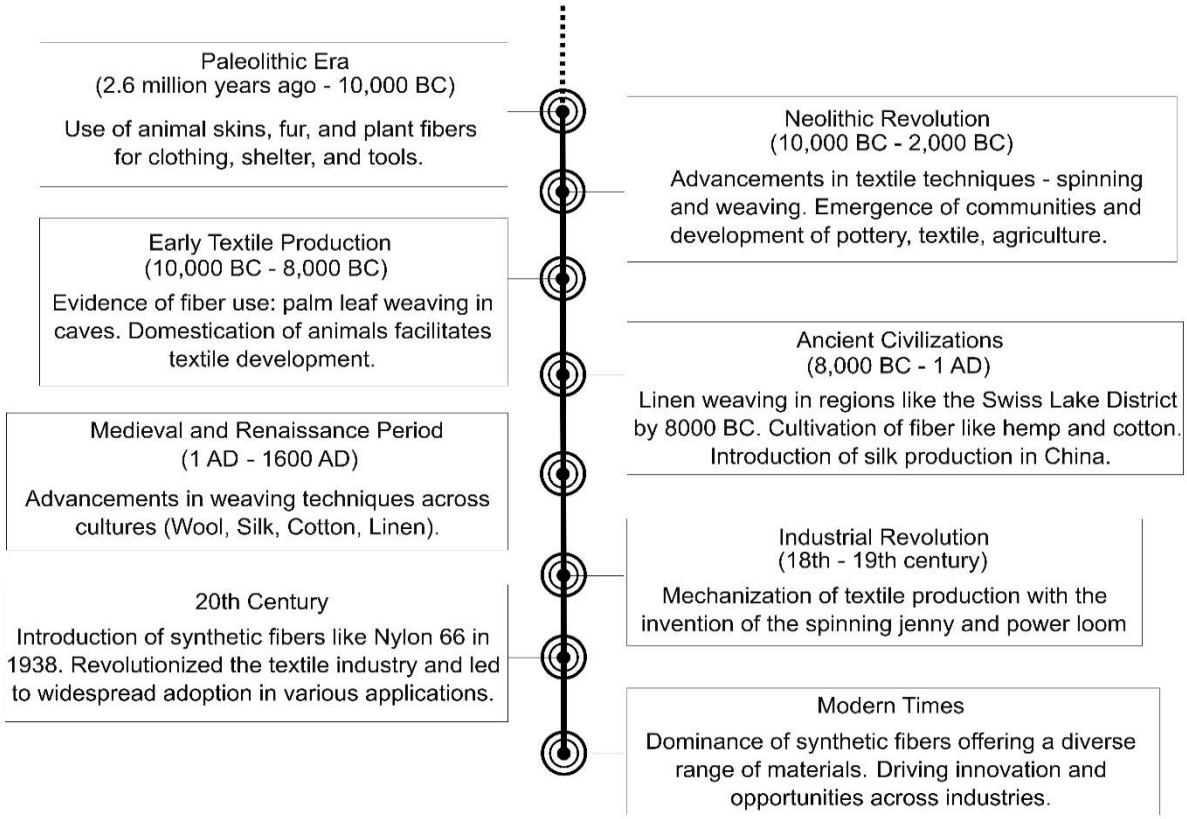

Fig. I3. Infographics of selected events through evolution of human history of fiber and textile.

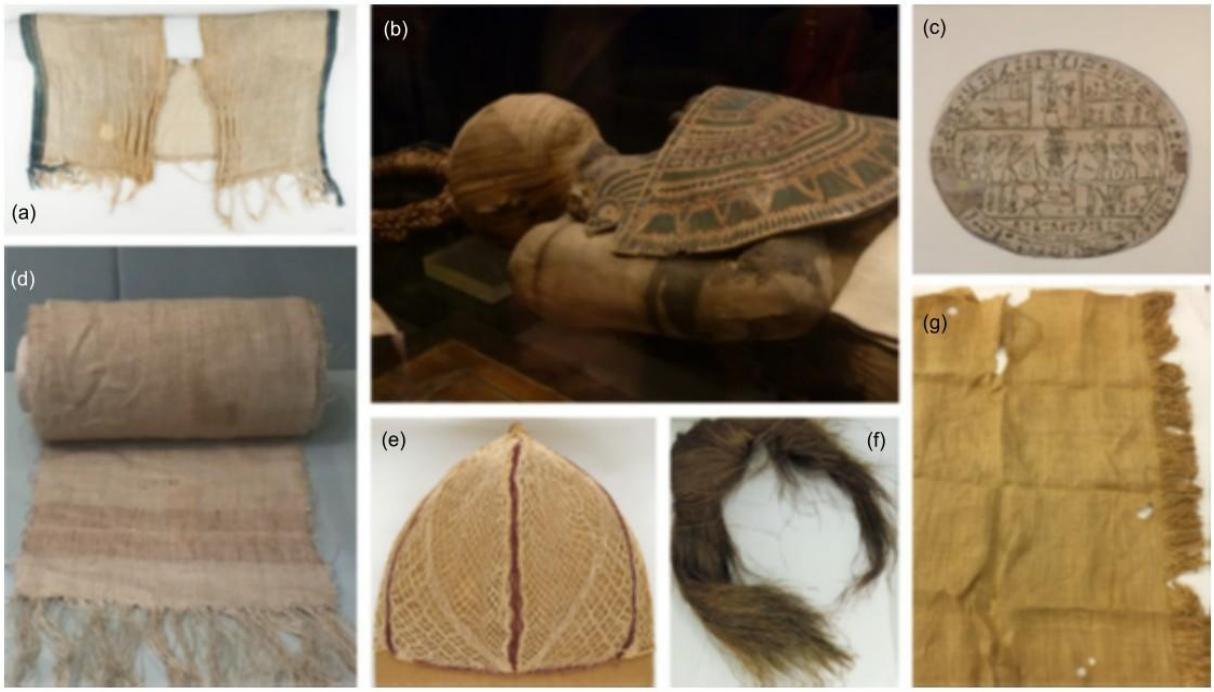

Fig. I.4. Examples of the uses of flax in ancient Egypt.

a) Child's vest with dyed blue edges, 800–720 or 700–540 BCE, b) Mummy of man with agglomerated and stuccoed flax fabric, 332–30 BCE, c) Flax hypocephalus, 305–30 BCE, d) Fragment of flax shroud, 1550–1295 BCE. e) Hairnet cap, fifth or sixth-century ad., f) Unspun flax hank, 1420–1230 BCE, g) Mortuary linen, 2140–1976 BCE. Objects, c & d are from the British Museum (London, UK). Objects a, b, e, f, and g are from Le Louvre Museum (Paris, France). Image taken from (Melelli et al., 2022).

Animal skins have also been used since the earliest humans for apparel and other uses (Fisher, 1981). The history of spinning yarn is lost in prehistory, but evidence exists that spinning was known to the ancient Middle East, at least as far back as 5000 BC. For example, pictographs were found in the tomb of the 4th-millennium pharaoh (Fisher, 1981; McDonald, 2011). The following millennia saw the popularity of fibers like flax, hemp and cotton, the development of weaving throughout many different cultures, and, in the modern age, the development of synthetic fibers (McDonald, 2011). The discovery of Rayon in 1884 (synthetic cellulosic fiber); the "artificial silk", drew the attention of scientific communities and led to the invention of Nylon 66 in 1938, enabling the material to be mass-produced and turned synthetic fibers into a fabric-building block (El Nemr, 2012; Fisher, 1981; McDonald, 2011; Morgan, 1981). Eventually, the lack of parachute clothes during World War II was the final push that replaced the natural fiber market more or less! "By 1990, 45% by weight of world fiber production consisted of artificial materials" (Jenkins and Jenkins, 2003; Melsted and Pallua, 2018). Now, synthetic fibers dominate the landscape, with the material coming in all forms from polyesters to polyolefins, enabling innovation and new solutions to a wide variety of problems (but at what cost?).

I.1.4. Global Textile Market & Today's Fibers

Being considered a basic need, 'Clothes' i.e. the textile industry is responsible for fulfilling the needs of 8 billion, and that makes the global textile market huge! According to '*PFMR - Textile Exchange*, 2022', global fiber production was 113.6 million tons in 2021 (almost tripled since 1975) which is expected to be 149 million tons in 2030. Global per capita fiber production was 13kg per person, which became 14.3kg in 2021, which is 2.4 times higher than in 1975 (5.9kg/person) (Munasinghe et al., 2021; Peters et al., 2019). Industries have a large variety of fibers to choose from, based on their origin, usage, quality, and price (profit). Finally, "the choice of consumers" decides market dominance! Currently, 64% of the global market (72.2 mt) is owned by synthetic fibers followed by 28% plant-based, 1.62% animal-based, and 6.4% manmade natural cellulosic fibers. Polyester is leading in the synthetic segment with 54% (60.5 mt) share alone, followed by plant-based cotton fiber with 22% (24.7 mt) share (*Textile Exchange Reports*, https://textileexchange.org/) (**Fig. I.5**).

The synthetic fibers include polyester, polyamide, polypropylene, acrylics, elastane, etc. The plant-based fibers include cotton, jute, coir, flax, hemp, sisal, abaca, kapok, ramie, agave, and other bast fibers. Although, the market share of other than cotton plant fibers are only 5.9% (6.7mt) altogether, flax shares only 1% (1.1mt) of the global fiber production. Animal-based fibers, with a total of 1.8mt yearly global production, include mainly sheep wool, down, and silk; and also, mohair, cashmere, alpaca, and others (angora rabbit, camel, guanaco, llama, vicuna, and yak hair etc.). Manmade cellulosic fibers include mainly viscose; also, acetate, lyocell, modal, cupro, etc. (Cook, 1984) (Materials and Market report, https://textileexchange.org/) (**Fig. I.5**).

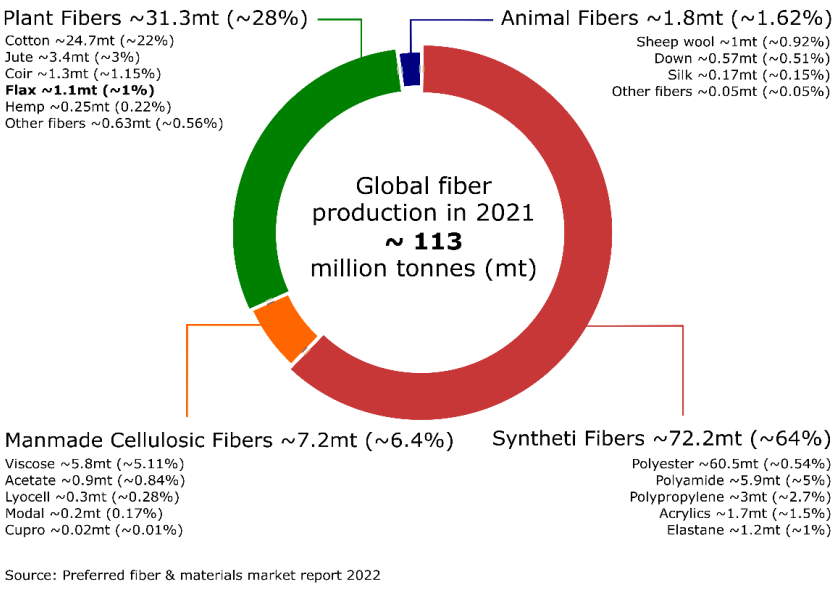

Fig. I.5. Global textile market according to '*PFMR – Textile Exchange, 2022*' report.

Source:(*https://textileexchange.org/2022-preferred-fiber-materials-market-report-recycled-polyester-submission-form/?gad_source=1&gclid=CjwKCAjw8fu1BhBsEiwAwDrsjKViLj16iw4vKpA_ivT8or7HYAbVfIKKO90mPYCT8AXTqyVSi0M27BoC7sYQAvD_BwE*).

How the drastic changes in fiber usage in the global textile market within 70-80 years with (still uprising) synthetic dominance affects the environment and possible alternatives; will be quickly explored in **Chapter I** of the manuscript (literature review) to enrich the context by emphasizing the importance of developing green textile technologies for a possible sustainable future.

I.1.5. Textile pollution

"The availability of power sources determines the amount of work activity that can exist, and control of these power flows determines the power in man's affairs and his relative influence on nature" – Odum, 1971. Energy, described as the universal currency, has driven social advancement since the Industrial Revolution (Smil, 2018). The discovery of fossil fuels provided us with enough energy to support the 'Industrial Revolution'- in the 18th century, creating this advanced modern-day civilization in a very short time (Melsted and Pallua, 2018; Smil, 2018; Yahya, 2018). Today, our activities, including fossil fuel burning and deforestation, emit 11 billion metric tons of carbon annually, elevating atmospheric CO2 concentrations above 400 ppm (Friedlingstein et al., 2022). This contributes to rising global temperatures, predicted to increase by ~5°F by the century's end (UNEP Emissions Gap report 2022, *https://www.pbl.nl/en/publications/unep-emissions-gap-report-2022*). Climate change exacerbates droughts (UN Water), affecting 1.4 billion people with half the world potentially facing water scarcity by 2025 (WMO 2021; UNICEF). Fossil fuel reserves are depleting, with estimates suggesting oil, gas, and coal could last approximately 50, 52, and 114 years respectively (Ritchie et al., 2024). Reducing dependency on fossil fuels is crucial across energy and related industries like textiles.

I.1.5.1. Textile-Carbon-footprint

The global yearly production of petroleum-based synthetic fibers is more or less 72 million tons. Approx. 70 million oil barrels are used to produce this polyester (*European Environment Agency Report*, https://www.eea.europa.eu/publications/textiles-in-europes-circular-economy). The industrial report says, 1kg of plastic-based synthetic fiber production requires 1.1kg of oil (*New Textile Economy Reports*, https://archive.ellenmacarthurfoundation.org/assets/downloads/A-New-Textiles-Economy.pdf; *Quantis Report*, https://quantis.com/wp-content/uploads/2018/03/measuringfashion_globalimpactstudy_full-report_quantis_cwf_2018a.pdf).

EU report estimates textile production generates around 15 to 35 tons of CO2 equivalent per ton for textile produced (*European Environment Agency Report*). An estimated 10% of global greenhouse emissions come from clothing & footwear production which is more than the combined emission of all international flight & maritime shipping (Niinimäki et al., 2020), (*Européen Parlement Reports*, https://www.europarl.europa.eu/topics/fr/article/20201208STO93327/production-et-dechets-textiles-les-impacts-sur-l-environnement infographies#:~:text=Selon%20l'Agence%20europ%C3%A9enne%20pour,de%20121%20millions%20de%20tonnes). It's not only just the oil-based origin of synthetic fibers but also the global transport of materials and processing at various stages of textile production that contributes to this carbon footprint (Leal Filho et al., 2022; Niinimäki et al., 2020), which is also true for natural fibers.

I.1.5.2. Textile-Energy-footprint

Mechanized production of fiber; as well as transport needs energy, which adds up to the overall fiber's energy footprint in a Life cycle analysis. A study in 2008 showed that to produce ~60 billion kg of fabric (globally), 1 trillion kWh of electricity (which equals to ~132 million tons of coal), and approx. 9 trillion liters of water were consumed (in one year) (Kousar et al., 2022; Rana et al., 2015). On average in the composite textile industry, 41% of the electricity is used for spinning, 5% for weaving preparation, 13% for weaving, 19% for humidification, 10% for wet processing, 4% for lighting, and 8% for all other equipment respectively for a certain amount of fiber (Rana et al., 2015).

I.1.5.3. Textile-Water-footprint

The growing population and resource-intensive economic development are increasing the demand for freshwater, a finite resource, leading to water scarcity when demand exceeds supply. Climate change exacerbates this by affecting natural water storage. UN-Water (2021) reports that 2.3 billion people live in water-stressed countries and nearly 4 billion experience severe water scarcity for at least one month annually. Per capita water use varies significantly by population, industrial activity, and climate. Industries in developed countries consume more water than agriculture in developing countries annually (*UN World Water Development Report 2021*). The global textile industry used approximately 79 billion cubic meters of water in 2015, with a single cotton T-shirt requiring 2700 liters of fresh water (*Européen Parlement Reports*). The industry also pollutes water through dyed wastewater and pesticide use, with

cotton accounting for about 25% of the world's insecticides (Clay, 2013). Additionally, textile washing releases 0.5 million tons of microfibers annually, representing 35% of global microplastic pollution (Barrett et al., 2020), *Européen Parlement Reports*, *Eunomia reports*, https://www.eunomia.co.uk/reports-tools/plastics-in-the-marine-environment/). Recent studies say "We are eating a credit card's worth of plastic every week" (https://nautil.us/you-eat-a-credits-card-worth-of-plastic-every-week-238481/); they even found traces of microplastic inside human placentas, which is even more disturbing (Ragusa et al., 2021).

I.1.6. (Rough) LCA-comparison: Are bast fibers a sustainable replacement?

The carbon, energy and water footprint significantly vary between fiber types. From cradle to grave of a fiber material & product, the environmental footprints are assayed in a method called Life Cycle Assessment (LCA). This is an important tool for comparing the environmental impact of products or processes. It helps identify hot spots and informs decision-making. Comparative LCA requires features such as comprehensiveness, methods, constraints, and data consistency. They are important for debates such as nature and man-made textiles by providing objective insights into environmental performance (Dissanayake et al., n.d.; Eady et al., 2012; Gomez-Campos et al., 2021; La Rosa and Grammatikos, 2019a; Laursen et al., 2007; Sandin et al., 2019). Although in recent years, the life cycle assessment has been well undertaken by industries, the lack of standard interpretation, transparency, scarcity of open-source data availability, old-out dated data, *etc*., led to gaps in understanding and gave us only rough estimates (van der Velden et al., 2014).

Comparing carbon, energy, and water footprint from available life cycle assessment (LCA) studies of various textile fibers (until textile production stage) from published journals (Astudillo et al., 2014; Bevilacqua et al., 2014, 2011; Brock et al., 2013; Chapagain et al., 2006; Chen et al., 2021; Eady et al., 2012; Gomez-Campos et al., 2021; Gonzalez et al., 2023; Kalliala and Nousiainen, 1999a, 1999b; La Rosa and Grammatikos, 2019a, 2019b; Le Duigou et al., 2011; Munasinghe et al., 2021; Muthu et al., 2012; Peters et al., 2019; Sandin et al., 2013; Sandin and Peters, 2018; Shen et al., 2012, 2010; Shen and Patel, 2010; van der Velden et al., 2014; Wiedemann et al., 2015; Yacout et al., 2016; Zampori et al., 2013), reports (Barber and Pellow, n.d.; Das et al., 2022; Dissanayake et al., n.d.; Laursen et al., 2007; Sandin et al., 2019), Textile Exchange Reports (https://textileexchange.org/), and databases (e.g. Ecoinvent 3.4, Idemat 2018, etc.) reveals the possibility of reducing textile pollution with other than synthetic and conventional-cotton based fibers (**Fig. I.6**). The comparison shows that in general synthetic fibers have a higher CO2 release and energy consumption per kg of fiber production than other fibers; whereas conventional cotton has higher water usage than others. Plant-based bast fibers like Flax (dew-retted), Organic-cotton (Better cotton, Reel, myBMP, BASFe3, Fairtrade, ISCC, CmiA, etc.), and somewhat manmade fibers like Lyocell, and Modal have the least environmental effects (till textile

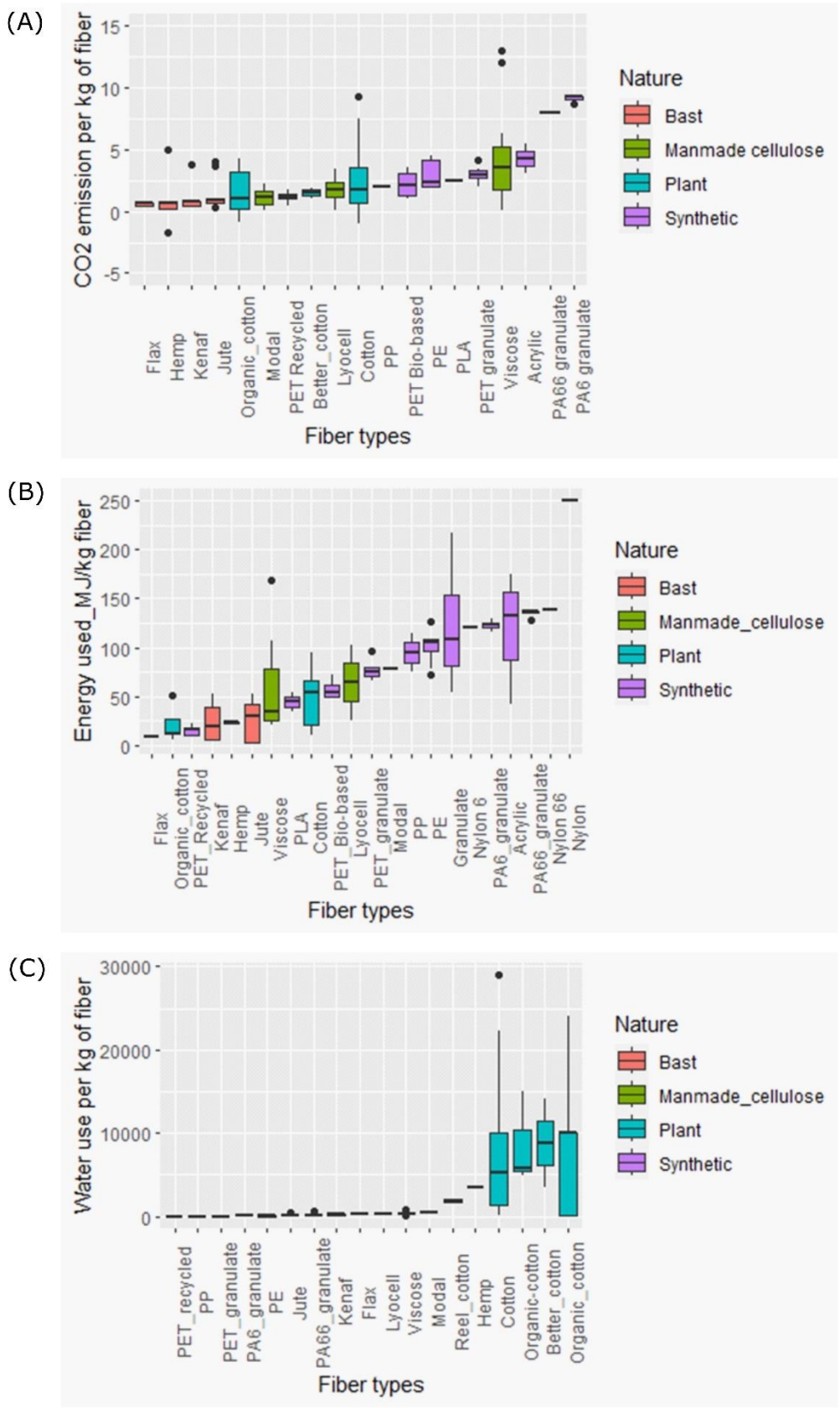

Fig. I.6. Life cycle analysis comparison between different fibers.

A, B, and C show a comparison of carbon footprint, energy footprint, and water footprint respectively. Data taken from literature, reports, and databases mentioned in section (§) I.1.6.

production stage) (**Fig. I.6**). Then again, multiplying the footprints (per Kg-fiber production) by their global annual production might give us a clearer insight into their actual environmental effects. However, the issue is more complex, as one could argue that utilizing arable land for non-food applications, given the context of global hunger, could decrease food production and drive-up prices.

This study excludes the widely used carbon and glass fibers (primarily in the composite industry), as well as wool and silk fibers, due to their significantly high carbon and energy footprints (*Novapress - Renewable Carbon News*, https://renewable-carbon.eu/news/natural-fibres-show-outstandingly-low-co2-footprint-compared-to-glass-and-mineral-fibres/). Carbon fiber and CFRPs are critical lightweight materials for the aerospace, automotive, and renewable energy industries, with increasing demand, particularly from wind energy, whereas glass fibers are valuable for their cost-effectiveness and low density, which aid in weight reduction and efficiency (Zhang et al., 2023). However, natural fiber composites have become viable alternatives to glass-reinforced composites since the 1990s, particularly in the automotive industry, due to their reduced cost and density (Joshi et al., 2004). Flax fibers have a density of around 1.5 g/cm³ and cost \$0.22 to \$1.10/kg, while glass fibers have a density of around 2.6 g/cm³ and cost \$1.30 to \$2.00/kg (Foulk et al., 2000; Joshi et al., 2004). Natural fiber-reinforced thermoplastics, such as polypropylene composites, are also gaining appeal due to their recyclable nature. These composites provide additional environmental benefits, such as less reliance on nonrenewable resources, lower emissions, and biodegradability (Foulk et al., 2000; Joshi et al., 2004; More, 2022). As a result, comparing natural fiber composites to conventional composites necessitates a thorough life cycle analysis (Joshi et al., 2004).

I.1.7. Physical and Mechanical Properties of Flax Fiber are ideal for composite material reinforcement

Flax fibers, extracted from the flax plant's bast, have attracted a lot of interest because of their remarkable mechanical qualities (Baley et al., 2018; Chand and Fahim, 2020; Djafari Petroudy, 2017; Goudenhooft, 2018; Müssig, 2010; Yan et al., 2014). These fibers are well-known for their exceptional wearability, high strength, and biocompatibility, making them ideal for various uses, including reinforcement in composite materials (Foulk et al., n.d.; Yan et al., 2014; Zhu et al., 2013). Individual flax fibers subjected to tensile testing revealed a tensile strength of between 343 and 2000 MPa and elastic modulus ranging from 27.6 to 103 GPa (**Table I.1**). The values can vary in different experiments primarily due to the method and sample used (Baley et al., 2018; Goudenhooft, 2018). Tensile strength is the maximum stress a material can endure before breaking (measured in Pascals or MPa). The elastic modulus, or Young's modulus, indicates a material's stiffness, defined as the stress-to-strain ratio in the elastic region (expressed in Pascals or GPa) and strain at break measures the elongation a material undergoes at fracture, shown as a dimensionless ratio or percentage of the original length (**Fig. I.7**).

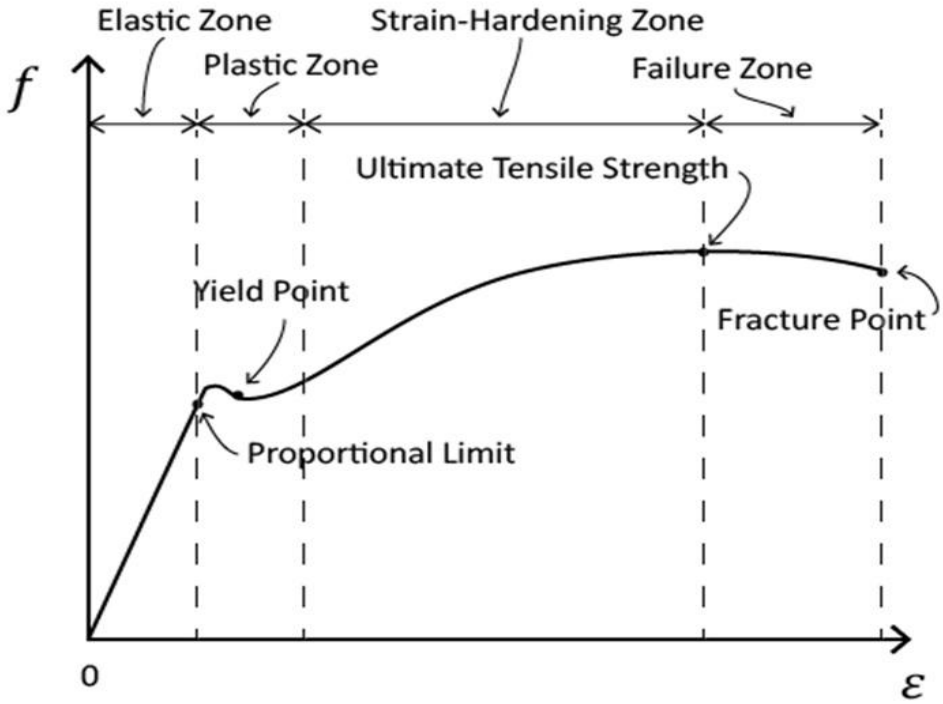

Fig. I.7. Stress-strain curve showing elastic, plastic and strain-hardened zone followed by fracture point. (Pandey et al., 2023)

Strain (ε) in X-axis and stress (f) in Y-axis. Tensile strength = ε/f.

A comparison study between flax and glass fiber (using the same method) by Goudenhooft 2018 revealed, that flax fiber exhibits greater elastic modulus variability (47.2 ± 18.1 to 58.7 ± 21.3) than glass fiber, but the variability in strength and strain at break is similar for both materials (**Table I.1**) (Goudenhooft, 2018). While flax fibers generally show more scattered properties (as a natural) than glass fibers, this does not necessarily translate to deviations in composite properties. Despite flax fibers generally having slightly lower strength than glass fibers, their tangent modulus is typically higher, demonstrating their good mechanical performance and suitability for composite manufacturing (Goudenhooft, 2018).

When compared to other natural fibers (like hemp, ramie, etc.) (**Table I.1**), flax fibers are positioned favorably due to their high tensile strength, softness, and fewer structural flaws, making them particularly suitable for high-quality textiles and clothing (Chand and Fahim, 2020; Foulk et al., n.d.; Goudenhooft, 2018; Kozłowski et al., 2020; Müssig, 2010). The distinct blend of characteristics found in flax fibers—especially their high cellulose content—significantly improves their mechanical performance, making them a top option for long-term and multipurpose uses in the expanding market for green products (Baley et al., 2018; Gorshkova et al., 2022; Müssig, 2010; Yan et al., 2014).

Fiber type	Tensile Strength (MPa)	Elastic Modulus (GPa)	Strain at break (%)	Reference
Flax	1339 ± 486	58 ± 15	3.27	(Zhu et al., 2013)
	343-1035	27-80	2.7 – 3.2	(Kozłowski et al., 2020)
	712 ± 238	29 ± 6.3	2.53 ± 0.51	(Goudenhooft, 2018)
	875 ± 318	35.4 ± 9.9	3.27 ± 0.84	(Baley, 2002; Goudenhooft, 2018)
	343-2000	27.6 – 103	1.2 – 3.3	(Dittenber and GangaRao, 2012; Yan et al., 2014)
Hemp	580-1110	3-90	1.4 – 3.1	(Kozłowski et al., 2020; Djafari Petroudy, 2017)
	920	70	1.7	(Zhu et al., 2013)
	270-900	23.5 – 90	1 – 3.5	(Dittenber and GangaRao, 2012; Yan et al., 2014)
Cotton	287-597	5-13	7-8	(Djafari Petroudy, 2017)
	287-800	5.5 – 12.6	3 – 10	(Yan et al., 2014)
Jute	187 - 773	3 - 55	1.4 – 3.1	(Kozłowski et al., 2020)
	860	60	2	(Zhu et al., 2013)
	320-800	30	1 – 1.8	(Dittenber and GangaRao, 2012; Yan et al., 2014)
Kenaf	240-600	14-38	-	(Zhu et al., 2013)
	295-930	53	2.7-6.9	(Djafari Petroudy, 2017)
	223 – 930	15.5 – 53	1.5 – 2.7	
Ramie	400-938	44-128	3.6 – 3.8	
	400-1000	24.5 – 128	1.2 – 4	(Dittenber and GangaRao, 2012; Yan et al., 2014)
E-glass	3400	71	3.4	(Zhu et al., 2013)
	2000-3500	73	2.5	(Kozłowski et al., 2020; Djafari Petroudy, 2017)
	2000-3500	70-76	1.8-4.8	(Dittenber and GangaRao, 2012; Yan et al., 2014)
	972±221	26.2±3.5	3.49±0.68	(Goudenhooft, 2018)
Carbon	4000	230-500	1.4-1.8	(Mirdehghan, 2021)

Table I.1. Comparison of fiber mechanical properties of Flax with synthetic and other natural fibers.

I.2. All About Flax

I.2.1. Taxonomy and Systematics

Cultivated Flax or more specifically *Linum usitattisimum* (L.) is an herbaceous, annual, self-pollinating, dicot flowering plant belonging to the family *Linaceae*, well known in textile, material, cooking-oil (from flax seed) and other industries (paint, varnishes, animal feed, etc.). Such a name, *Linum*, most useful, reflects its long history of usefulness and its contribution (The name *Linum* originated from the Celtic word "*lin*" or "thread" and the word "*usutattisimum*" is the Latin word for "most useful") (Kolodziejczyk et al., 1995; MUIR and WESTCOTT, 2003). Grown primarily in temperate climates (also in subtropical areas under short-day conditions), flax takes 90 to 150 days from seeding to harvest. The biogeographic distribution of *Linum* covers all the lands except Antarctica with approx. 180 species (300 species according to Hickey 1998), is the largest among the 8 genera of Linaceae (McDill et al., 2009; Muir and Westcott, 2003; Wang et al., 2012). The position of the flax family in the plant kingdom is described in **Fig. I.8**.

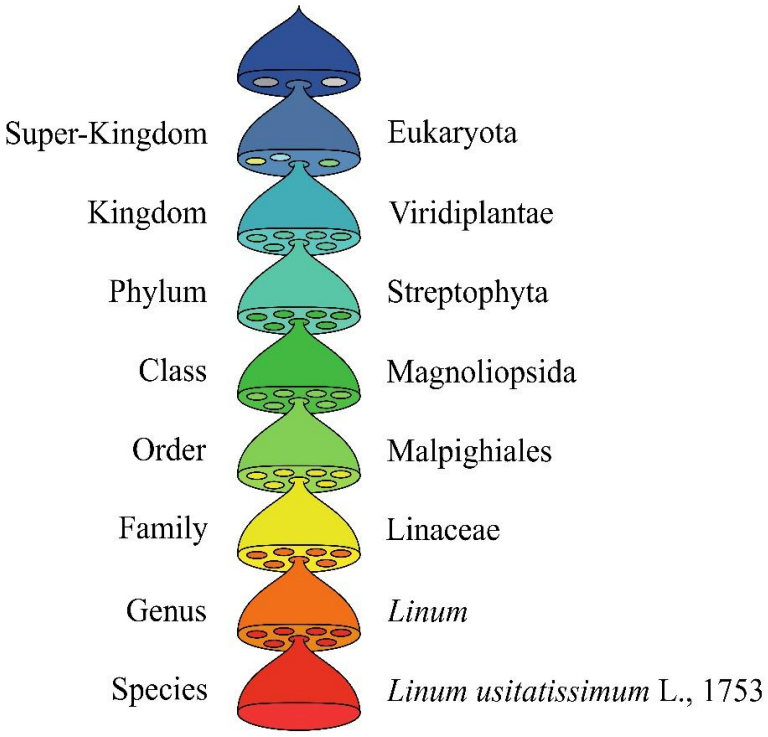

Fig. I.8. Taxonomic classification of flax. Source: NCBI (*https://www.ncbi.nlm.nih.gov/datasets/taxonomy/4006/.*)

Within the flax family, the genus *Linum* belongs to the tribe *Linioideae* H. Winkl. Within this tribe, there are four other genera (**Fig I.9**): (1) Reinwardtia Dumort., found in India and Southeast Asia; (2) Tirpitzia Hallier, native to South China; (3) Hesperolinon (A. Gray) Small, located in Western USA; and (4) Radiola (Dillen.) Roth., present in Europe and also found as an introduced species in the USA. (Muir and Westcott, 2003).

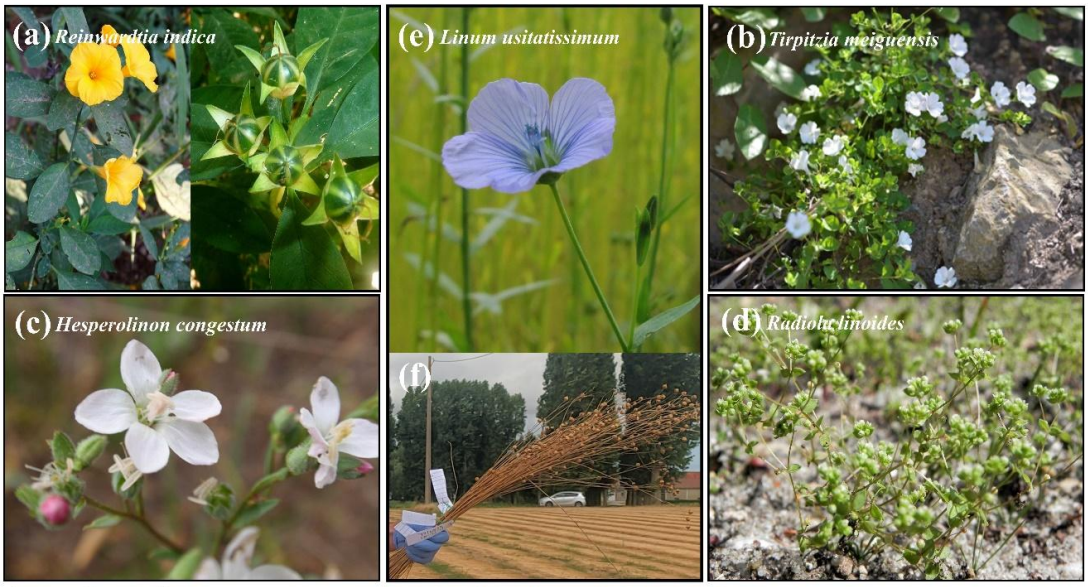

Source of image: (a) By JMK CC BY-SA 3.0 https://en.wikipedia.org/wiki/Reinwardtia;(b) DOI: 10.11646/PHYTOTAXA.626.1.6 (c) By tom hilton - originally uploaded to Flickr as Marin Dwarf Flax, CC BY 2.0, https://commons.wikimedia.org/w/index.php?curid=7687119; (d) By Hajotthu, CC BY-SA 3.0, https://commons.wikimedia.org/w/index.php?curid=10991620; (e) Djemiel (c) ugsf (150), (f) Mukherjee (c) ugsf.

Fig. I.9. Members of the *Liniodeae* tribe.

(A) is *Reinwardtia sp*., (B) is *Tirpitzia sp*., (C) is *Hesperolinon sp*., (D) is *Radiola sp*. and (E) and (F) is *Linum usitatissimum*.

The genus *Linum* has been a significant focus for botanists over the past three centuries due to its extensive diversity, which poses ongoing challenges for systematic classification. Within the genus *Linum*, the chromosome number varies between 2n = 16 and 2n = 60, with most species having either 2n = 18 or 2n = 30 (in the case of Linum usitatissimum L.). Various proposals to divide the genus into sections have been suggested, yet the classification and status of many species within the genus still require further clarification (Muir and Westcott, 2003; Rogers, 1982).

I.2.2. Morphology of Flax (Stem/Flower/Fruit)

Domestication and careful selection of favored genotypes by man, introduce a range of variations in several agrobotanic (phenotypic) characteristics in cultivated flax (Muir and Westcott, 2003; Goudenhooft, 2018; Galinousky et al., 2020). The morphology of flax is described in **Fig. I.10**. The plant features a tap root with an erect leading shoot, which can develop multiple secondary basal shoots if injured (Muir and Westcott, 2003). Flax growth, including height and branching pattern, varies based on genotype and soil fertility. Plant height ranges from 20 to 150 cm. Flax cultivars for linseed oil differ from fiber Flax cultivars in the aspects of plant height, branching, and the number of seed production per plant along with their location of cultivation based on climatic adaptations (Gill, 1987; McKeon et al., 2016). Fiber flax tends to grow taller (80-120cm) and branches in the upper part of the stem, while large-seeded flax is shorter (60-80cm) with branching from the middle (Muir and Westcott, 2003; Salmon-minotte and Franck, 2005).

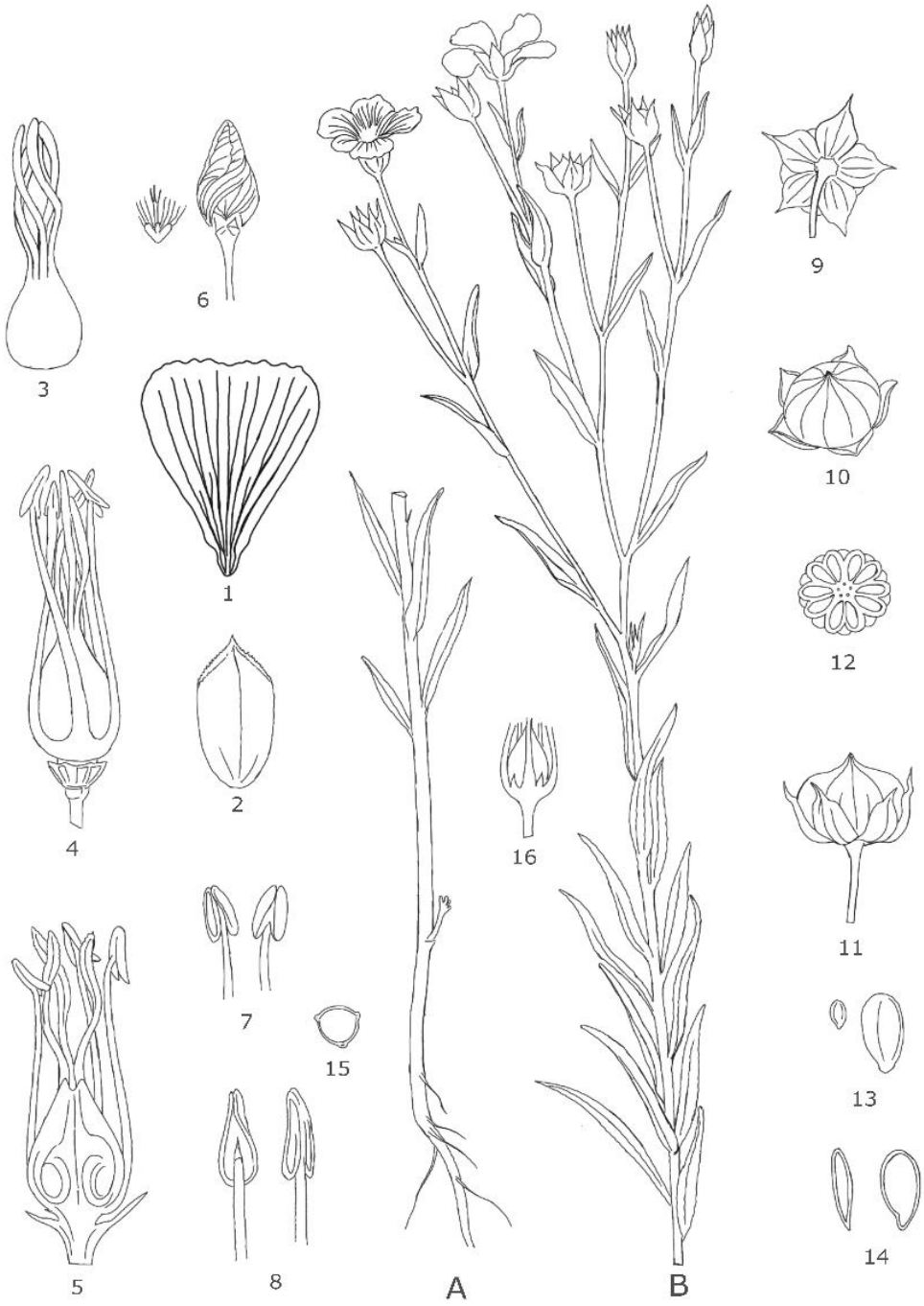

Fig. I.10. Morphology of flax (Linum usitatissimum) drawn from Köhler's Medizinal-Pflanzen, 1887.

Figure (B) shows a flax plant with flowers, fruits, buds, and leaves; (A) shows the lower part of (B) with roots; 1. Single petal of flax flower, 2. Sepal of flax flower, 3. Pistil of flax flower, 4. Pistil and Stamen of flax flower, 5. A transverse section of figure 4 shows a superior syncarpous ovary, 6. Flax flower corolla before blooming, 7. Stamen filament of flax flower showing basifixed anther with two lobes, 8. A transverse section of anther shows two pollen sacs per lobe, 9. Figure shows a persistent green calyx with five sepals, 10. Capsule fruit of flax (top view), 11. Flax fruit side view, 12. Transverse section of flax fruit exposing 10 ovule chambers with seed, 13. Flax seed (3-5mm), 14. Transverse section of flax seed, 15. Colporate pollen of flax.

The leaves are alternately arranged, linear to linear-lanceolate (80-100/stem), senescing during ripening (Muir and Westcott, 2003; Salmon-minotte and Franck, 2005). Flax flowers are arranged in a panicle-like structure with the shoot terminating in flowers. The flower parts, including sepals, petals, and stamens, display a range of colors, with blue and white being predominant. The corolla can be tubular, funnel-shaped, or bowl-shaped. Self-pollination is common and occurs at flower openings (Muir and Westcott, 2003; Rogers, 1982; Salmon-minotte and Franck, 2005).

The fruit is a capsule, typically with ten lodicules and a maximum seed capacity of ten (Muir and Westcott, 2003; Salmon-minotte and Franck, 2005). Fiber flax varieties tend to have slightly opening capsules, while oilseed types do not open, reducing seed shattering. Seeds are ovoid or oblong, with considerable variation in size and color, weighing between 4 and 13 grams per 1,000 seeds (Muir and Westcott, 2003).

Flax stems are of special interest because they have fibers. The flax stem is round and slender with a hollow pith in the center and phloem fiber beneath the cortex. The quality of the fiber depends on "technical stem length", i.e. how long the stem is before it starts branching out. Technical stem height of various varieties of fiber flax varies between 60-90cm, with a diameter of 1.5-3mm. The stem diameter reduces with height (Charlet et al., 2010; Goudenhooft, 2018).

I.2.3. Antomy of Flax

I.2.3.1. Flax stems outer vs inner tissue

Many articles provide detailed information about the anatomy of flax stems and the chemical composition of cell types (Akin, 2013; Akin et al., 1996; Müssig, 2010; Van Sumere, 1992).

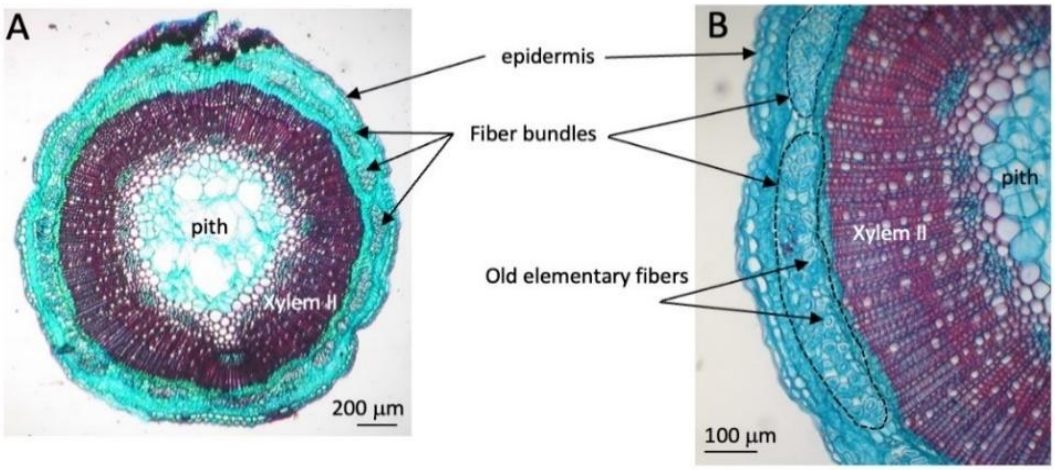

Fig. I.11. Flax Anatomy.

A: hand section of a whole stem. Inner wood is stained in red, outer tissues are stained in blue as cell walls are mainly cellulosic. At three months old, clear fiber bundles are defined. B: zoom on outer tissues. SAB (Safranin- Alcian Blue).

Like any other dicot plant, structurally it has an outer cuticle and epidermis layer, followed by the parenchymatous cortex, phloem (containing fiber cells), and inner core cells (Akin, 2013; Esau, 1942; Gorshkova et al., 2003) (**Fig. I.11**). Flax stems can be easily peeled in order to only examine outer versus inner tissues (**Fig. I.12**).

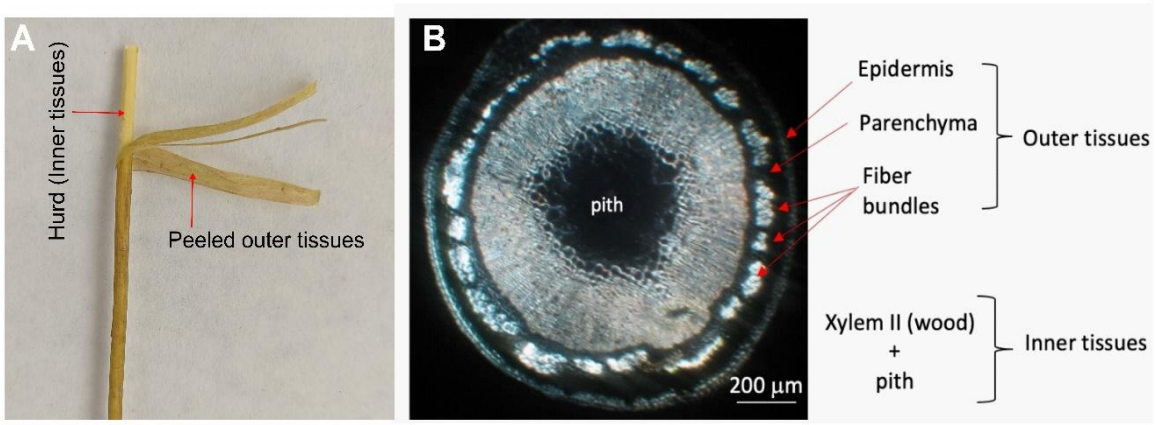

Fig. I.12: Flax Anatomy: focus on the outer and inner tissues.

A: Flax stem with peeled outer tissue part and the inner tissue. B: relative position of outer versus inner tissues in a flax stem (hand section, darkfield optical microscopy with Normaski's filter).

The outer tissues contain the epidermis (including the cuticle), chlorophyllous parenchyma (either cortical or inner), and the fiber bundle (containing elementary fibers) (**Fig. I.13**). Inner tissue contains xylem-I and xylem-II followed by a hollow pith (**Fig. I.13C**) (Akin, 2013; Esau, 1942; Goudenhooft, 2018). It provides structural reinforcement and facilitates water transport (xylem vessels) (Esau, 1942; Goudenhooft, 2018; Nuez et al., 2021). The core tissue makes more or less 65%–75% of stem material (Akin, 2013; Day et al., 2009; Akin et al., 1996) (**Fig. I.13**). The pith progressively degrades to form a hollow pith (**Fig. I.12B**).

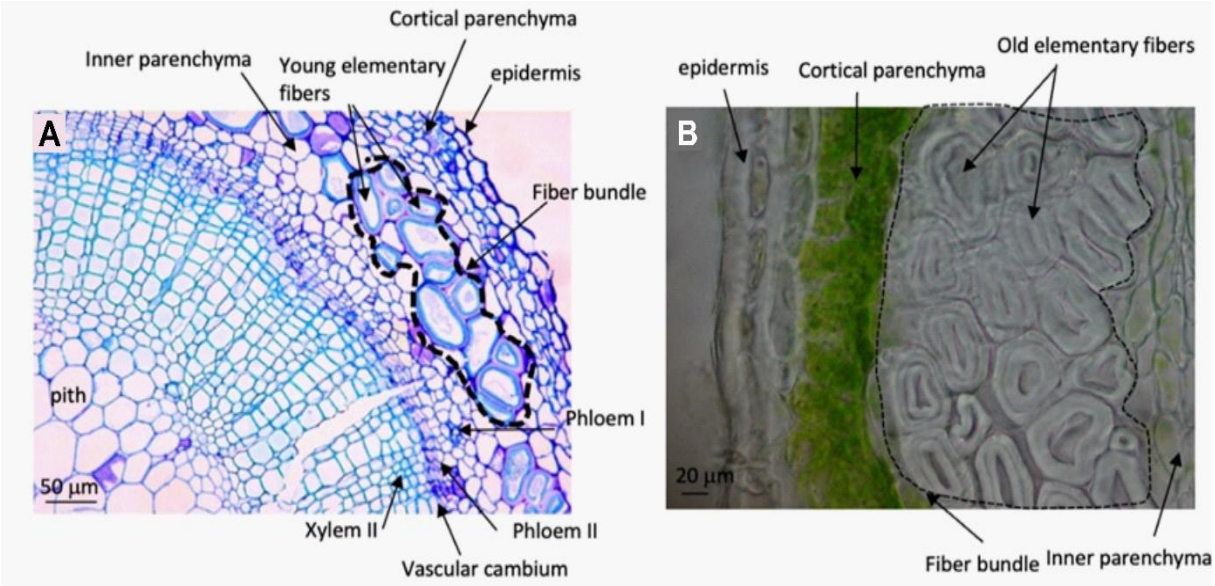

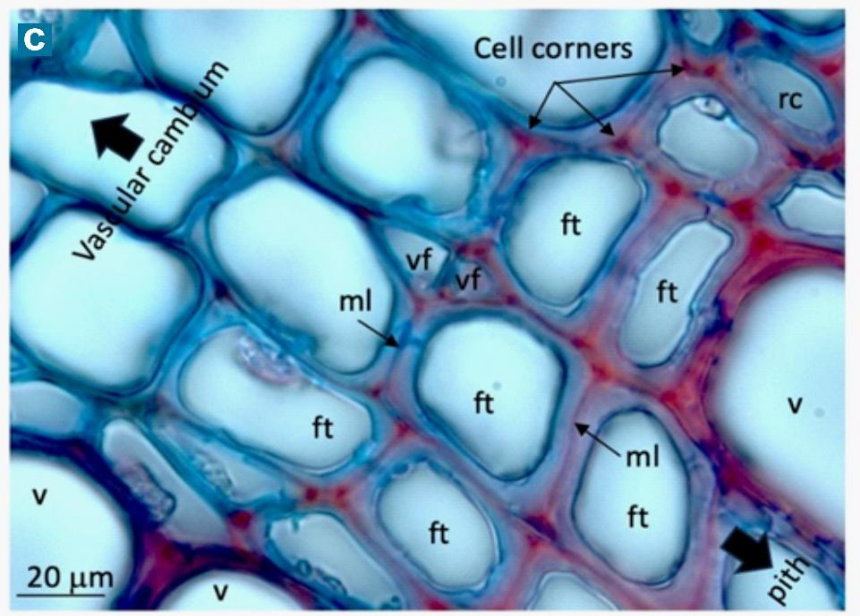

Fig. I.13. Flax stem's outer and inner issues in detail.

A: semi-thin section (5µm) stained with TBO. The different categories of outer tissues are localized. B: hand section, no stain showing chlorophyllous cortical parenchyma and large fiber bundles with old (filled) elementary fibers. C: Inner tissues: Cell types present in differentiation secondary xylem (wood): progressive lignification occurs from cell corners and from the middle lamella (ml). Different cell types involved in mineral sap transport are present: fiber-tracheid (ft), huge vessel (v), and ray cell (rc, for horizontal transport). Strengthening is supported by lignification, and vascular fiber (vf) originating from vascular cambium initials. A: TBO (Toluidine Blue O); C: SAB (Safranin- Alcian Blue) staining (cellulose in blue, lignin in red). Credits: A-S Blervacq and M. Delay.

I.2.3.2. The bast fibers

In between the inner core tissue and cuticle-epidermal, we have pectin-rich cortical parenchyma and extra-phloemien, cellulose-rich (65-80% of dry weight), bast fiber cells with specialized primary and secondary cell walls (**Fig. I.14**) (Akin, 2013; Esau, 1942; Gorshkova et al., 2003; Goudenhooft, 2018). In general, a mature Flax stem contains 20-50 fiber bundles (which is 25% of stem dry weight or 9-15% of stem tissue area) and 10-50 spindle-shaped ultimate fibers, 2 to 3 cm long and 15 to 20µm in diameter (Akin, 2013; Goudenhooft, 2018; Salmon-minotte and Franck, 2005). (The following paragraphs will be dedicated to bast fiber description).

These attributes, especially the extensive elongation and thick cell walls, make flax fibers an ideal model for studying plant cell growth. Flax fibers begin their development through primary growth originating from the apical meristem (Ageeva et al., 2005; Anderson, 1927). This process includes two main stages: **elongation** and **cell wall thickening**. During the elongation phase, flax fibers can grow to lengths of up to 65 mm, averaging around 25 mm (Roach and Deyholos, 2007). This substantial growth

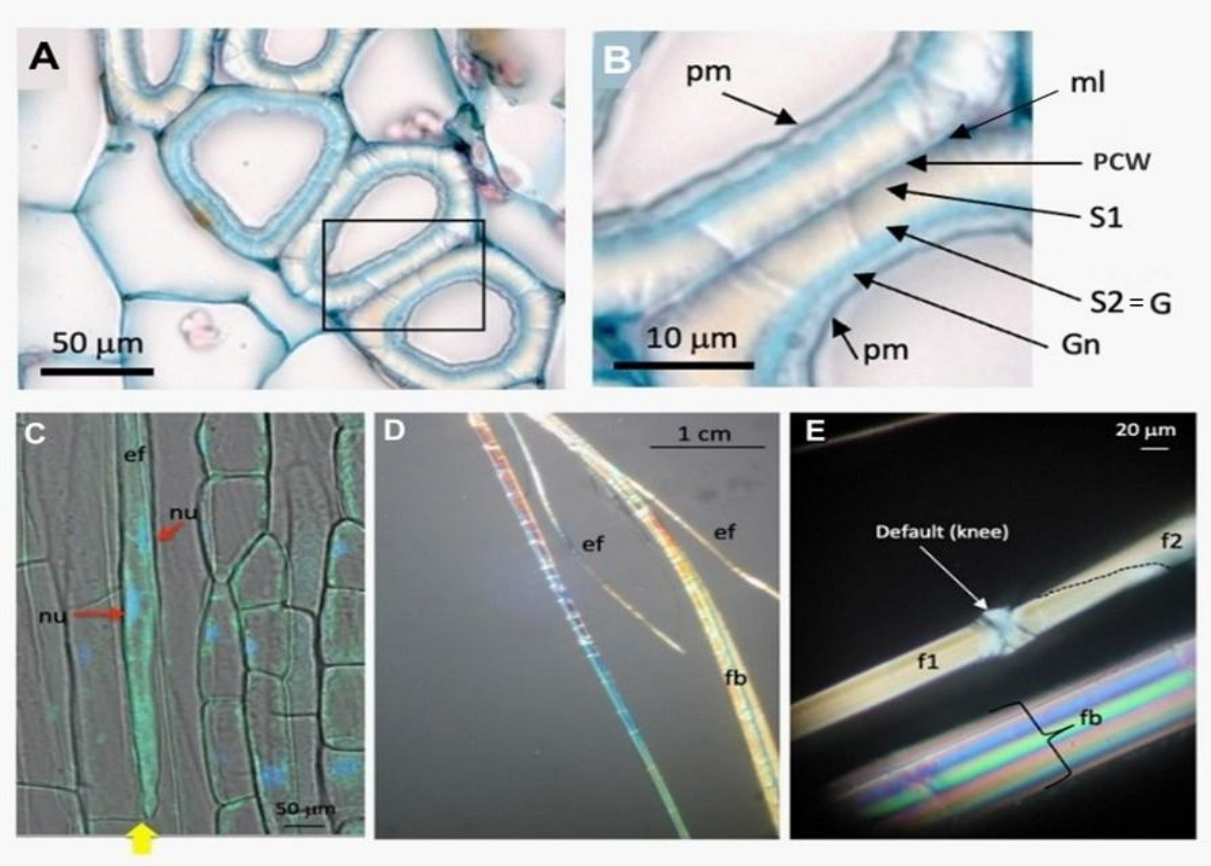

Fig. I.14: Flax bast fiber.

A-B: Paraffin sections (10 µm) stained with SAB (Safranin-Alcian Blue). Primary thin cellulosic cell wall (PCW) is stained in blue. As the bast fibers exhibit secondary cell wall, mainly cellulosic, some white zones and blue ones are observed. pm: plasma membrane; ml: middle lamella; S1, (S2) = G and Gn = the different cell wall layers. C: Longitudinal section of one elementary fiber (ef) showing it polynucleated status (nuclei- nu are stained in blue). D, E: fiber bundles (fb) and old elementary fibers (ef, f1, f2) decorticated from up-rooted flax stem. Such a single cell is really long. E: some future industrial default as knee (that causes dislocation) could be detected close to the junction of two elementary fibers (f1-f2). C: merge brightfield optical microscopy and DAPI nucleus staining. D-E: polarized optical microscopy. Credits: AS Blervacq.

occurs in two steps: **coordinated growth** and **intrusive growth** (McDougall et al., 1993). In the coordinated growth phase, flax fibers initially elongate in sync with neighbouring cells, which lasts only a few hours and results in multinucleate cells (Fig. I.14C) (Roach and Deyholos, 2007). At this stage, fibers reach about 100µm in length with a diameter of approximately 5µm (Ageeva et al., 2005; Snegireva et al., 2010). During the second growth phase i.e. intrusive growth, fibers elongate faster than neighbouring cells and force their way between other cells. This phase is characterized by the formation of "**knees**" at the ends of the fibers (Fig. I.14E), which eventually smooth out into a spindle-like shape with tapered ends (Ageeva et al., 2005; McDougall et al., 1993). These knees, which are perpendicular dislocations, may result from tissue development or mechanical strain. Fiber nodes, or knees, are critical in the initial reactions to dyes, enzymes, and cellulases and are often the primary points of failure in

stress tests. The presence of these knees makes individual fibers more susceptible to crushing (Akin, 2013; Baley, 2002; Goudenhooft, 2018). Intrusive growth can last several days, with fibers elongating at a rate of 1-2 cm per day, ultimately reaching an average length of 25 mm and a diameter of 20 µm (Ageeva et al., 2005; Goudenhooft, 2018).

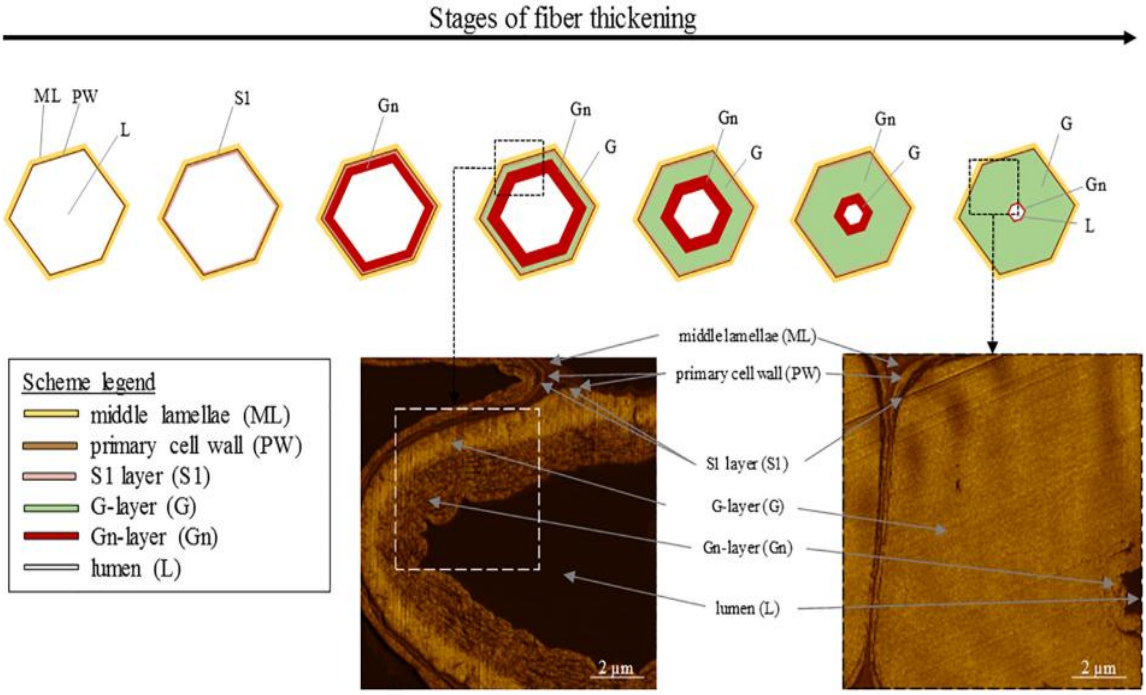

Fig. I.15. The upper scheme illustrates the fiber elongation, with fibers represented in green.

(A) First phase of the coordinated growth; (B) more advanced step of the coordinated growth; (C) beginning of the intrusive growth with fibers having "knees" on both ends; (D) more advanced phase of the intrusive growth, with fibers becoming a much longer structure than the neighbouring cells and showing tapered ends. The lower scheme illustrates the cell wall thickening in relation to the remodelling of the Gn-layer. Cellulose microfibrils are originally separated by long galactan chains present in nascent RG I. The long galactan chains are then trimmed off which leads to the G-layer with compact cellulose microfibrils. Source (Gorshkova et al., 2022; Goudenhooft et al., 2019).

The end of fiber elongation and the beginning of cell wall thickening is called the "snap point" (Gorshkova et al., 2003). This point moves along the stem as the plant grows and is identified by a noticeable change in stem stiffness. Above the snap point, the stem is softer, leading to a vertical position in the top part of the plant due to its weight and wind. Cell wall thickening, occurring primarily below the snap point, is a lengthy process that can take up to 60 days (Ageeva et al., 2005; Gorshkova et al., 2003). This stage (around five weeks old flax) involves the deposition of multiple cell wall layers (especially Gn layer), significantly increasing the cell wall's thickness (**Fig. I.15**) (Goudenhooft, 2018). Flax fiber cell walls can exceed 10µm in thickness, compared to the few micrometers typical of most cell walls (Ven and Godbout, 2013).

From the outside inward toward the cell lumen, the flax bast fiber cell wall is composed of multiple layers, which are ordered structurally as follows: the middle lamella, the primary cell wall (PCW), the secondary cell wall (SCW), and an inner gelatinous layer (G-layer), which forms subsequent to the SCW (**Fig. I.14a, I.15**) (**Table I.2**) (Blervacq et al., 2023; Cosgrove and Jarvis, 2012; Gorshkova et al., 2022, 1996). On the other hand, G-layers are typically absent from the xylem cell walls of flax and other species. But since 1860, it has been known that in the "reaction wood" of dicots, a gelatinous cell wall layer—dubbed the G-layer (because of its gel-like appearance)—forms in response to gravitational stimuli (Blervacq et al., 2023). Remarkably, inclined flax plants have also been reported to exhibit G-layers in their xylem cells (Blervacq et al., 2023; Gorshkova et al., 2022, 2018; Goudenhooft, 2018). However, the fact that the term G-layer is used to define the innermost cell wall layer of extraaxillary bast fibers, which is also being used to define the tertiary cell wall layer or xylem G-layer is quite confusing and currently debated. A recent study shows that G-layers in flax bast fibers and xylem cells, whether in flax or other species, are not identical, differing both ontogenetically and chemically. However, their overall structure and polymer distribution are similar (Blervacq et al., 2023).

Cell wall layer	Average thickness	Microfibril orientation	Approximate composition
PW	0.2µm	disperse orientation, preferentially 0°	~25–40% Cellulose ~30% Hemicelluloses (mainly xyloglucan and lesser amounts of arabinoxylan) ~30% Pectins (mainly homogalacturonan; possibly rhamnogalacturonan (RG) I; RG II and arabinogalactan)
S1	0.5µm	60–80◦	~30–50% Cellulose ~30% Hemicelluloses (xylan, xyloglucan) ~5% Pectins (homogalacturonan and RG I) ~10–20% Lignin
G	Up to 15µm or 90% of the total cell wall area at maturity	8–10◦	~75–90% Cellulose ~15–20% Hemicelluloses (glucomanan) ~5–10% Pectins (RG I)
Gn	0.5–1µm through thickening	Loosely packed as a heterogeneous structure	Cellulose, Hemicelluloses (glucomanan), Pectins [nascent RG I (i.e., long galactan chains)]

Table I.2. Characteristics and approximate composition of the different cell wall layers of flax fibers. Source (Goudenhooft et al., 2019).

I.2.4. Flax plant polymers in outer stem tissues

The outermost section of flax stem, the cuticle layer, making up 13-24% of the flax stem's dry weight, primarily consists of lipids such as waxes (4.4%) and cutin (6%), with smaller amounts of aromatics (0.46%). This layer protects against water loss and microbial invasion and is easily stained with oil red due to its wax content. Spectroscopic techniques (FTIR, Raman, UV) confirm the presence of these compounds in the cuticle, not in the underlying tissues. The cuticle often comes off with the epidermal cells during processing, leading to contamination that reduces fiber quality by leaving waxy residues and large, undesirable fragments on the fibers. The cortical parenchyma cells surrounding the bast cell are rich in pectin and devote of any aromatics (Akin, 2013).

The structural integrity and mechanical qualities of flax (*Linum usitatissimum*) stems are mostly influenced by their cell wall polymers, which include cellulose, hemicelluloses, lignins, and pectins. Celluloses (made up of β-1,4-linked D-glucose units), create microfibrils that give tensile strength and rigidity when implanted in a hemicellulose and pectin matrix. Hemicelluloses, which include xylans and xyloglucans, bond to the microfibrils, providing flexibility and compression resistance. Lignins are aromatic polymers found in secondary cell walls that provide compressive strength, rigidity, and microbial resistance; yet, they are in a reduced amount in flax bast fibers as compared to woody plants improving fiber flexibility and tensile strength. Pectins, which contain galacturonic acid, create a gel-like matrix in primary cell walls and intermediate lamellae (phloem fiber and cortical parenchyma cells), aiding cell adhesion, wall porosity, and growth control, contributing to stem flexibility and extensibility. Furthermore, structural proteins such as extensions and phenolic substances like ferulic and coumaric acids strengthen and stiffen the cell wall. The chemical ratio in bast fiber changes with maturity (Gorshkova et al., 1996, 2003, 2004). The flax bast fibers' primary and secondary cell walls are made up of **cellulose** (65-80%) (**Fig. I.16A**) embedded in the concentric lamella of 2% pectin and 15% hemicellulose (Akin, 2013). **Pectin** is the main cementing material between the fiber and non-fiber tissues followed by **hemicellulose** (**Fig. I.15B-C**). The lignin in trace amounts (1.5–4% of dry cell wall residues) gave the "hypolignified" status to the bast fibers (**Fig. I.15E**) (Day et al., 2005).

The hypothesis of a new "tertiary cell wall" category was recently debated (Gorshkova et al., 2022, 2018, 1996; Mokshina et al., 2018). For Gorshova's team, the flax bast fiber exhibits a G-layer that creates a new category of cell wall, the tertiary one. In this context, the xylem G-layer that appears in tension wood also belongs to this third recent category. New current data on flax bast fibers obtained through spectroscopy led us to demonstrate that if similarities seemed present in both Raman spectral profiles, the PCA and PLS-DA established that they are significantly different (**Fig. I.17**) (Blervacq et al., 2023).

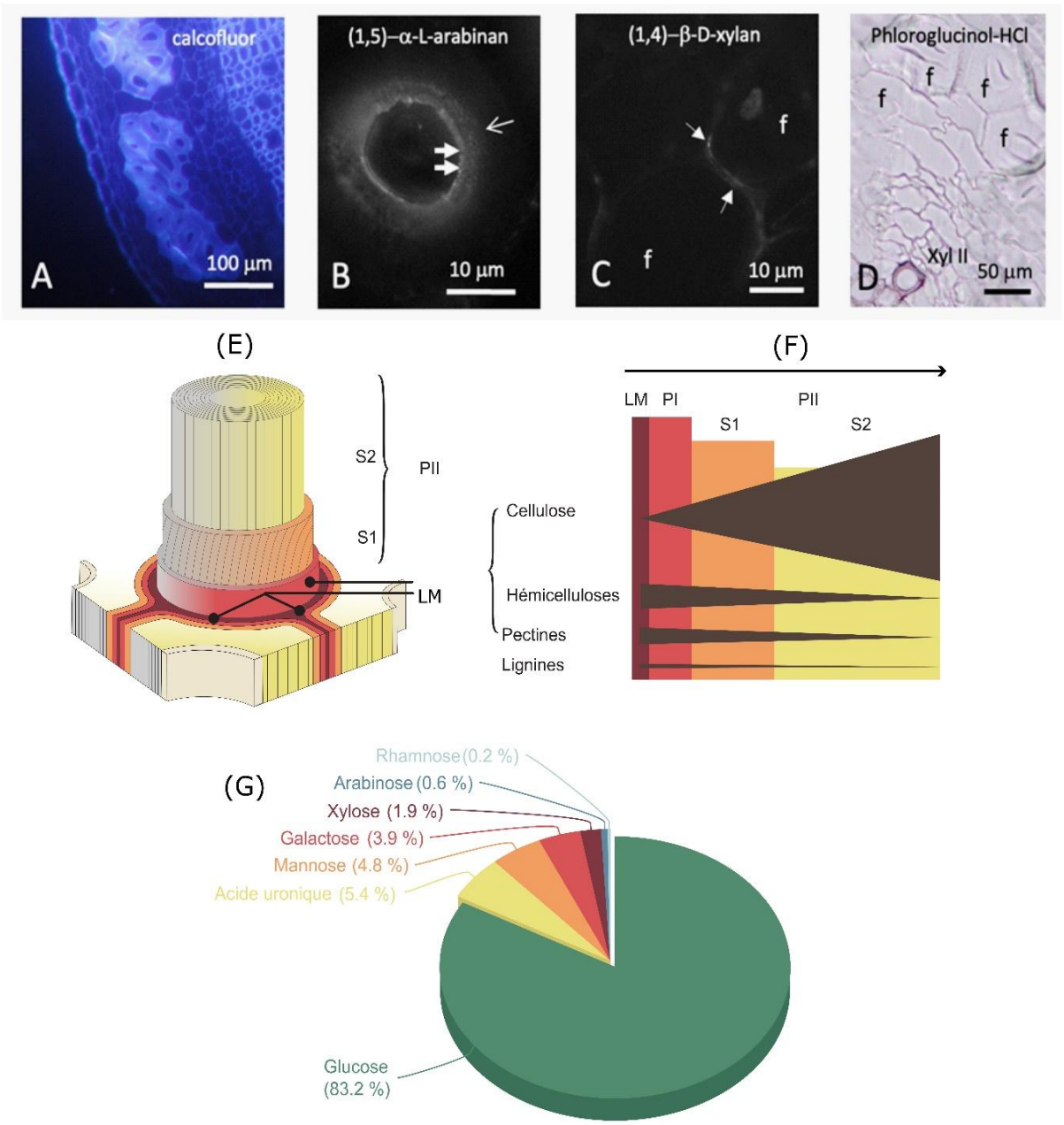

Fig. I.16. Bast fiber composition, cell wall structural and chemical organization.

A: calcofluor white stains cellulose (epifluorescence microscopy, λem nm, λexc nm); B-C: Immunolocation of (1,5)- α-L-arabinan and (1,4)- β-D-xylan, respectively with LM6 and LM10 (epifluorescence microscopy, λem = 515-521 nm, λexc = 495-499 nm); D: identification of lignin with the Wiesner reaction (phloroglucinol-HCl). Only vessel (xyl II) with lignified secondary cell walls is stained in dark red. (E) shows structural feature of a fiber (M = midle lamella, PI = primary cell wall, PII = secondary cell wall); (F) distribution of polymers in different segmets of fiber cell wall; (G) composition of monoscaccharide in mature peripholem fiber. Source A-D (Blervacq et al., 2023), E-G (Djemiel, 2017).

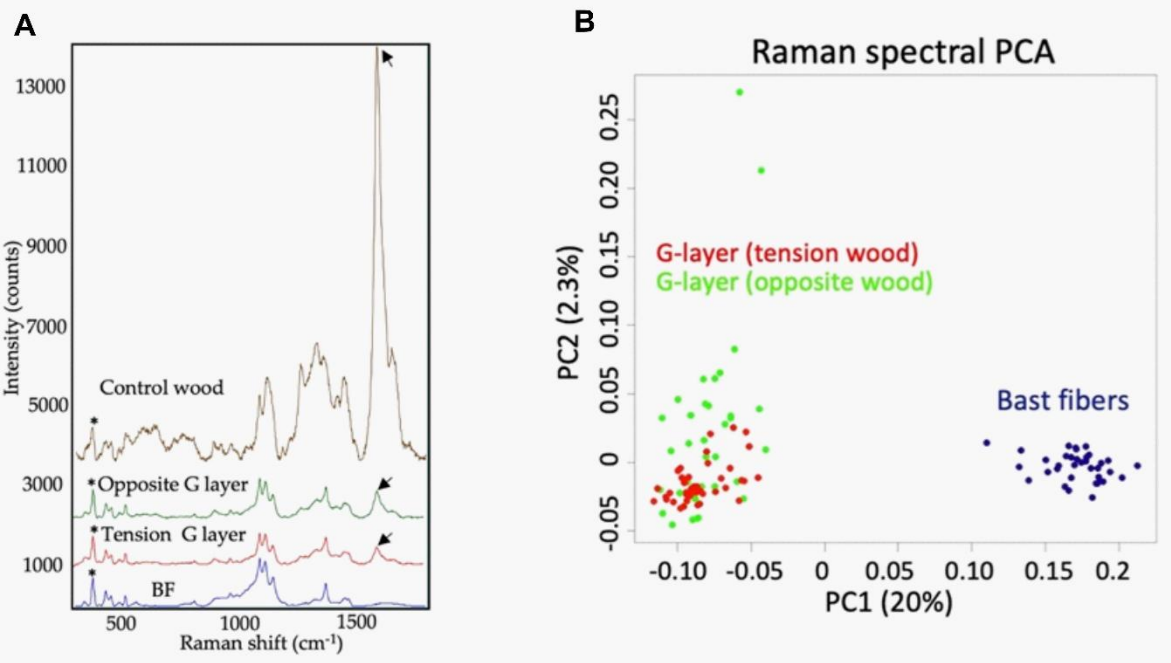

Fig. I.17. Categorization of bast fibers and G-layer in stressed wood.

Even if Raman spectral profiles between flax bast fibers (blue) and flax vessel G-layer (in woods) (red, green) are similar (A), PCA exhibited significant differences between bast fibers (blue dots) and vessel G-layers (red and green dots) (B). Source: (Blervacq et al., 2023).

The G-layer in flax fibers is characterized by its lack of lignin and xylan, high cellulose content (up to 90%), significant porosity, and flexible properties. t is transient and less visible as fibers mature but can persist under stress conditions like drought (Gorshkova et al., 2022, 2018, 1996; Mokshina et al., 2018). Over time, the Gn-layer gradually transforms into a compact, homogenous G-layer, contributing to its thickening (Gorshkova et al., 2022, 2018; Goudenhooft, 2018; Mokshina et al., 2018). This transformation involves the modification of the Gn-layer's structure, particularly through the trimming of long galactan chains in rhamnogalacturonan-I (RGI), leading to stronger interactions between cellulose microfibrils and the formation of a dense, mature G-layer (Gorshkova et al., 2022, 2004; Goudenhooft, 2018).

I.2.4.1. Pectins

In flax stem cells, pectins are present mainly in the **middle lamella** region of cortical parenchyma and bast cells (**Fig. I.18**), which is degraded by microbial enzymes during retting. Looking at the chemical compositions; **pectins** are galacturonic acid-rich (70%), highly branched plant polysaccharides (or structural heteropolysaccharides) (Joseleau and Pérez, n.d.; Mohnen, 2008; Srivastava et al., 2017) (**Fig. I.19**). Depending on factors, such as source (stem/ leaf/ fruit), condition (growth stage), degree of

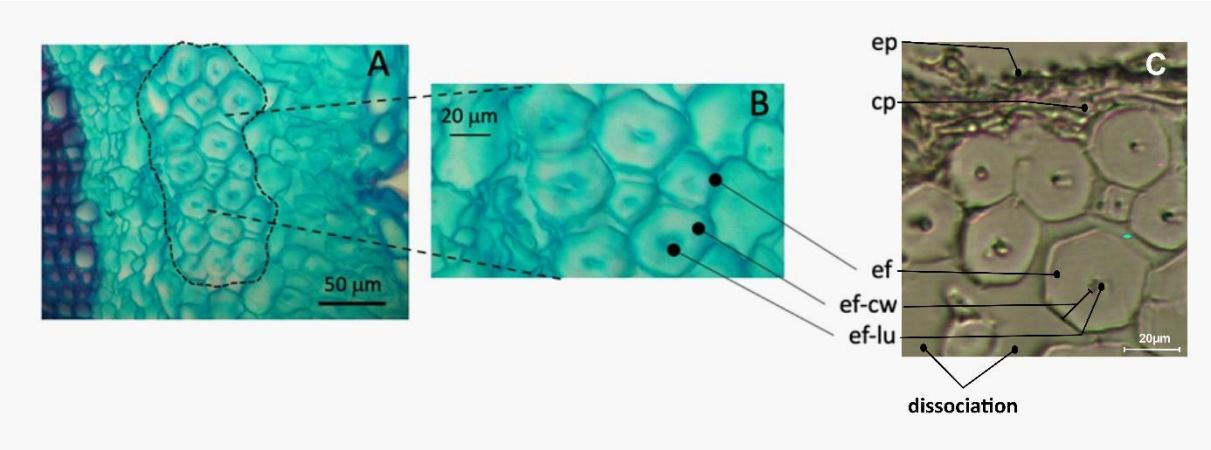

Fig. I.18. Flax fiber bundle before and during retting.

A-B: before retting, fiber-bundle (dotted line) is still compact and all elementary fibers are stuck together due to the middle lamella being rich in pectins. C: during retting, a disorganization is observed and more and more elementary fibers dissociate from each other. Ep: epidermis; cp: cortical parenchyma; ef: elementary fiber; cw: cell wall, lu: lumen. Source: A-B: AS Blervacq.

esterification, etc; its structure can vary. Pectins are broadly categorized into three main groups; (a) **homogalacturonan** (HG), which is a linear chain of alpha-1,4 linked galacturonic acids (65% of pectin) (partially methylated at C6 carboxyl group or maybe O-acetylated at O-2/O-3 or may contain other potential crosslinking esters of uncertain structure) (Mohnen, 2008); (b) more structurally complex substituted HGs **rhamnogalacturonan II** (RGII)(10% of pectins), with a commonly conserved structure consisting of 8 (or more) α-D-GalA backbone decorated with 12 different types of sugars in side branching with 20 different linkages; (c) and structurally more variable **rhamnogalacturonan I** (RGI) (20-35% of pectins) (Mohnen, 2008). The carboxyl group of galacturonic acids often forms **calcium bridges** (in the presence of calcium ions**)** together in a reticulated manner which resembles an eggbox structure (Shin et al., 2021, *Encyclopedia of Applied Plant Sciences*, 2016), and holds pectin in a gelatinous form.

In flax (*Linum usitatissimum*), pectins play a crucial role in the composition of cell walls, exhibiting significant variation based on tissue type and developmental stage (Davis et al., 1990; Gorshkova et al., 1996; Goubet et al., 1995). In the cortex, cell walls are particularly rich in methylated pectins, making up about 10% of the cell wall's dry weight, alongside homogalacturonans, which account for approximately 5%. In contrast, the walls of phloem cells, which differentiate into fibers, mainly consist of cellulose and galactans, with pectins constituting less than 10% and being depleted in arabinose but enriched in galactose, rhamnose, and glucose (Davis et al., 1990).

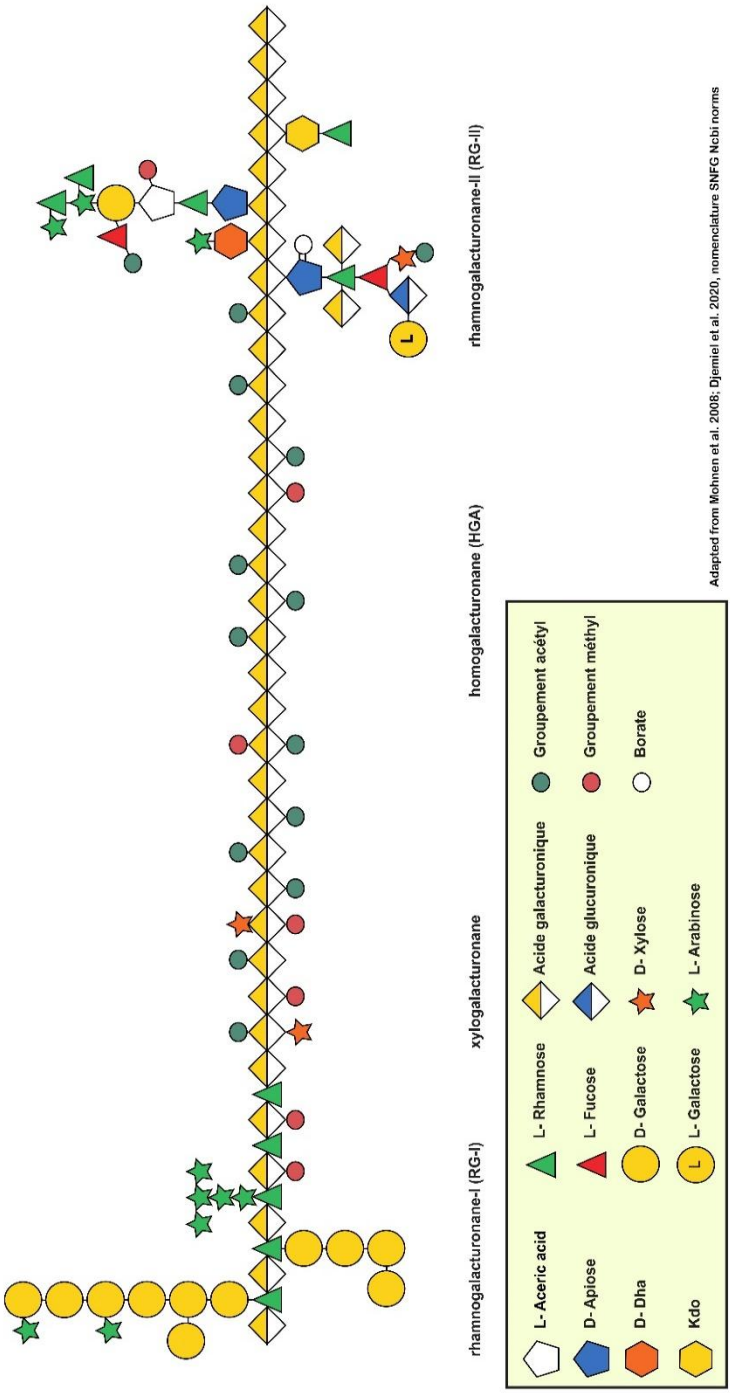

Fig. I.19. Structure of pectin.

The figure shows structural components (monosaccharides) of principal pectin polymers present in the plant cell wall.

EDTA-extracted pectins from flax (supposedly RG-I side branches from primary cell wall) reveal a diverse array of polysaccharides (mainly beta-1,4 galactans), including substantial amounts of galactose, galacturonic acid, rhamnose, glucose, and traces of arabinose. In addition, the extraction also revealed β-1,3/1,6 linked galactans associated with proteins, as well as β-1,3 glucan, β-1,4 glucan, and polymers resembling glucomannan (Goubet et al., 1995).

The primary structure of these pectins includes high-molecular-weight galactans composed predominantly of β-(1→4)-linked galactopyranose (Galp) chains with non-reducing terminal β-Galp units, as identified by 1D ^{1}H- and ^{13}C-NMR analysis (Davis et al., 1990). Additionally, low-molecular-weight fractions are enriched in rhamnose and galacturonic acid, forming a rhamnogalacturonan type I structure with β-Galp units attached to the hydroxyl group at position 4 (HO-4) of the rhamnose residues. This structure likely constitutes the backbone of the high-molecular-weight polysaccharides (Davis et al., 1990), and introduces variation in plant pectins (Gorshkova et al., 1996).

Gorshkova et al., explain flax pectic substances include two main neutral-sugar polymers: 5-arabinan and 4-galactan, with infrequent branching. The high-molecular-mass 4-galactan is notably associated with phloem fiber development. Unlike type-I arabinogalactans (AGs), which have terminal arabinose (t-Ara) units at the O-3 position of 4-galactans, flax 4-galactans exhibit branching at both O-2 and O-3 positions, terminating with galactosyl rather than arabinosyl units (Gorshkova et al., 1996). Overall, the structural diversity and specific localization of pectins and interaction with other polymers within flax cell walls underscore their critical role in cell wall architecture and function.

I.2.4.2. Hemicelluloses

Hemicelluloses are key non-cellulosic components of plant cell walls, generally making up about one-third of their dry mass. They are also found in smaller amounts in the middle lamella. They act as a cementing matrix for cellulosic microfibrils, as well as lignins in the cell wall (Pauly et al., 2013). Hemicelluloses are complex carbohydrate heteropolymers (with mainly β-1,4 linked backbone) that encompass a group of different plant polysaccharides; mainly divided into four groups (**Fig. I.20**) (Pauly et al., 2013); (a) **mannans** (abundant in algal cell wall and gymnosperms secondary cell wall); made up of mainly mannose and glucose backbone and galactose side chains (for galactoglucomanans) (b) **xyloglucans**, most abundant hemicellulose (primary cell wall) composed of β-1,4 linked glucan backbone with xylosyl substituents at O-6 position; (c) **xylans**, are major secondary cell wall hemicelluloses (i.e. load bearing tissue), comprising β-1,4 linked xylose backbone, with diverse substitution pattern (by rhamnose/glucuronic acid/ O-acetyl, etc) depending on species and tissue type;

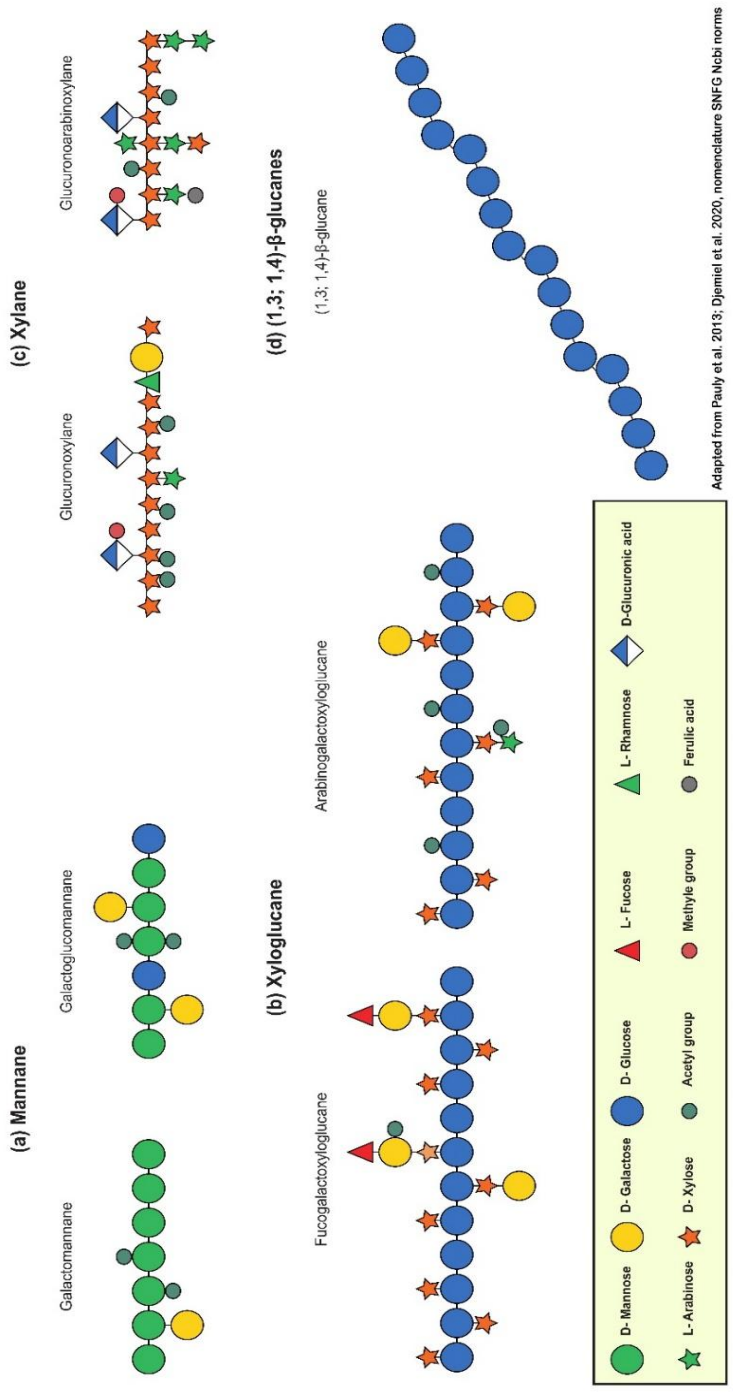

Fig. I.20. Structure of Hemicellulose.

The figure shows structural components (monosaccharides) of principal hemicellulose polymers present in plant cell wall.

and finally (d) **mixed linked glucans**, a glucose-based, unsubstituted, non-branched homopolymer (mainly found in grass, algae, bryophytes, etc) (Joseleau and Pérez, n.d.; Pauly et al., 2013; Srivastava et al., 2017).

In xylem tracheary elements, 4-O-methylglucuronoxylan is the predominant noncellulosic polysaccharide, accounting for over 60% of the composition, with cellulose comprising about 30% at maturity (Gorshkova et al., 1996). The 4-xylans in flax contain 4-O-methylglucuronic acid side groups spaced about 12 to 13 residues apart, attached solely to the O-2 of xylosyl units. Additionally, (galacto)glucomannans exhibit a small amount of branching with terminal Galactose (t-Gal) units at the mannosyl O-6 position. The fiber-rich peels are enriched in 5-arabinan, 4-O-methyl-glucuronoxylan, glucomannan, and cellulose (Carpita and Gibeaut, 1993; Gorshkova et al., 1996). These findings align with enzymological studies which revealed diagnostic β-D-xylobiosyl, isoprimeverose, and β-D-manno-oligosaccharides from alkali- and boric-acid-soluble polysaccharides from retted flax fibers (Gorshkova et al., 1996; McDougall et al., 1993).

I.2.4.3. The glycoproteins arabinogalactan proteins (AGPs) in Flax

Flax fibers have been shown to contain arabinogalactan proteins (AGPs), which are closely linked to the secondary walls (Girault et al., 2000; Gorshkova et al., 1996). The structural importance of these AGPs within the cell walls is indicated by their significant reactivity with anti-AGP monoclonal antibodies (JIM13, JIM14, MAC 207) and β-glucosyl Yariv reagent (Girault et al., 2000). These AGPs exhibit a strong attraction for homogalacturonan sequences and include galactose as their primary sugar component (Kido et al., 1996; Girault et al., 2000). The main encrusting polysaccharides in flax fibers are long chains of 1,4-β-galactans (Gorshkova et al., 1996; Girault et al., 1997), which are probably attached to a backbone of rhamnogalacturonan I. Potentially, this structure facilitates the cross-linking of AGP-like polymers found in flax fibers (hydroxyproline deficient 2YP1 and 2YP2) (Gorshkova et al., 1996; Girault and Morvan, 1999).

Given that they require severe treatments (like alkali treatment) for their release, suggesting strong cross-linking within the cell walls, the proteins in flax fibers likely play structural roles (Cassab, 1998; Girault et al., 2000). Alanine, glycine, serine, glutamic acid/glutamine, and aspartic acid/asparagine are all abundant in these proteins. According to Keller et al. (Keller et al., 1989), the glycine-rich proteins (GRPs) present in flax fibers are comparable to those found in other plants, and they help to improve the mechanical characteristics of the cell walls by preventing shattering (Girault et al., 2000). Similar to tomato-derived leucine-rich proteins (LRPs), some proteins in flax, may feature a leucine-rich-protein (LRP)-type domain, potentially influencing protophloem-derived flax fiber differentiation (Tornero et al., 1996; Girault et al., 2000).

AGPs and the associated proteins, such as GRPs and LRPs, in flax fibers are crucial for cell differentiation and the mechanical properties of the secondary walls (Cassab, 1998; Keller, 1993). Immunocytological approaches can further elucidate their developmental expression and interactions with other polymers like 1,4-β-galactans, which are significant components of the cellulose matrix (Girault et al., 1997; Gorshkova et al., 1997).

I.2.4.4. Cellulose

Cellulose, a linear chain of β-glucose (linked with β-1,4 glycosidic bond) (**Fig. I.21b**); is the main structural component of plant cell wall (**Fig. I.21a**) (Srivastava et al., 2017). Cellulose molecules make microfibrils (10-210 nm) through hydrogen bonding; which further aggregates into large structures, contributing to the overall strength and integrity of plant cell walls (Srivastava et al., 2017; van Dam and Gorshkova, 2003). The degree of organization of these cellulose molecules is referred to as crystallinity, where they are closely packed forming a rigid stable structure; on the other hand, loosely packed cellulose regain are called amorphous regions, susceptible to chemical/biological degradation (Srivastava et al., 2017; van Dam and Gorshkova, 2003).

Flax cellulose exhibits a highly crystalline structure composed of cellulose fibrils embedded in an amorphous matrix of hemicellulose (and hypolignified). These fibrils are arranged unidirectionally with a tilt angle of approximately 10 degrees relative to the fiber axis (Baley, 2002; Bos, 2004). At a finer scale, cellulose fibrils consist of microfibrils, each about 10-20 nm in diameter, which are further composed of micelles—elementary fibrils formed from 50 to 100 cellulose molecules spaced approximately 1 nm apart (Baley, 2002). The microfibrils are surrounded by water in their natural state, contributing to the cell wall's swollen appearance (Baley, 2002). Defects such as nodes or dislocations, observable under microscopy, can significantly influence the mechanical properties of flax fibers during tensile stress (Davies and Bruce, 1998; Baley, 2002). The density of flax fibers, considering their porous nature, averages around 1.53 g/cm³ (Baley, 2002; Ganster and Fink, 2003). This hierarchical cellulose organization in flax fibers plays a critical role in determining their mechanical strength and overall performance in various applications (Baley, 2002). At that stage, and considering flax fiber, it is now possible to draw a fiber definition at different scales as described in **Fig. I.21c**, starting from technical fibers (unit considered by industrials), elementary fibers (unit considered by cytologists) and microfibrils (unit considered by structural chemists).

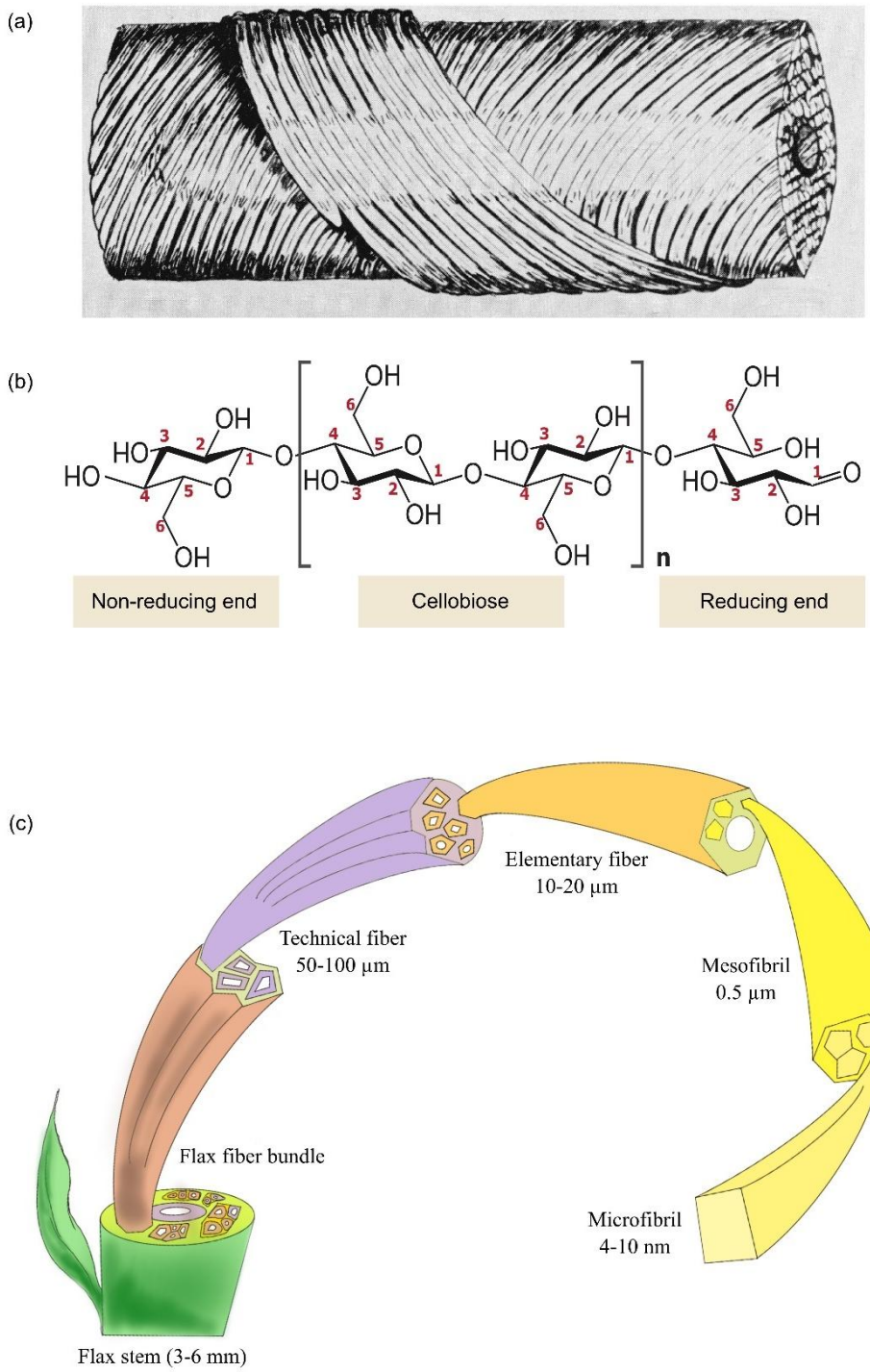

Fig. 21. Cellulose in plant bast fiber.

(a) the arrangement of crystalline cellulose in flax fiber, (b) the chemical structure of cellulose units, (c) The construction of a flax fiber. Source: (Bos, 2004; Djemiel, 2017; Hock, 1942).

I.2.5. Flax Cultivation and Processing: From Flax to Linen

Preparing linen from flax is a long process, starting from cultivation, harvest, retting, mechanical scutching, hackling, and finally weaving into linen **(**Fig. I.22**)** (Kozłowski et al., 2020; Müssig, 2010; Sharma, 1992; Summerscales et al., 2010). Flax cultivation thrives in cool and humid climates (with stable cloud cover), ideal temperatures of 18-20°C, and annual rainfall of 600-650 mm. The best soil includes fertile, medium-heavy sandy clay soil with an average pH of about 6.5-6.9 (Kozłowski et al., 2020; MARCHENKOV and ROZHMINA, 2003; Muir and Westcott, 2003; Sharma, 1992). Oilseed and fiber flax varieties perform best in well-drained silty-loam and clay-loam soils but perform poorly in poor or sandy soils (MARCHENKOV and ROZHMINA, 2003). Oilseed flax prefers high temperatures and post-flowering cold will increase oil content, especially linolenic acid, while fibrous flax should be cool throughout its growth, best found in temperate coastal waters at around 45° latitude (Kozłowski et al., 2020; MARCHENKOV and ROZHMINA, 2003). Crop rotation is important; especially flax after grains such as oats and pre-winter wheat with little soil to retain moisture and control weeds. Fertilization should comply with the ratio N: P2O5: K2O = 1: 2: 3 and add micronutrients such as boron and zinc (Kozłowski et al., 2020; Muir and Westcott, 2003). Effective post-care includes the use of technology that prevents soil crusting and herbicides when plants reach 6-12 cm tall (Kozłowski et al., 2020). Control of pests and diseases depends on the use of resistant varieties and the use of crop rotation. This combination of soil management, fertilization, and pesticides ensures good and productive flax production. Flax is usually planted in spring; for spring-varieties and early October for winter varieties. In areas like Hauts-de-France, the best planting time is mid-March to mid-April. Harvesting involves using special machinery to uproot by pooling (for fiber-flax) and spreading the crops to ensure good drainage (during field retting) before they are shaded and baled using fiber ropes (Kozłowski et al., 2020; MARCHENKOV and ROZHMINA, 2003).

Dew-retted & rolled straw is then sent to a mill for fiber extraction & processing (MARCHENKOV and ROZHMINA, 2003; Müssig, 2010; Sharma, 1992). Processing flax requires a number of important procedures in order to convert the raw plant material into useful fibers (Dhirhi et al., 2015). First, **breaking** is necessary to break the straw into short segments and loosen it from the fibers by beating the flax bundles with a breaking machine. This step ensures that the woody parts are separated, making the fibers more accessible. Next, **scutching** involves swinging a wooden scutching knife down the hanging fibers to scrape off more pieces of the stalk. This step further cleans the fibers, though some fiber loss is inevitable. Then, **heckling** pulls the fibers through progressively finer combs to remove the remaining straw and split, and polish the fibers. This refinement is essential for achieving the desired quality and smoothness. Finally, **weaving** involves interlacing linen yarn into sheets on a loom, creating fabric. High-quality linen is still primarily handmade due to the delicate nature of flax fibers, even with mechanization. The labor-intensive nature of linen manufacture sets it apart from other industrially produced fabrics such as rayon and cotton (Dhirhi et al., 2015).

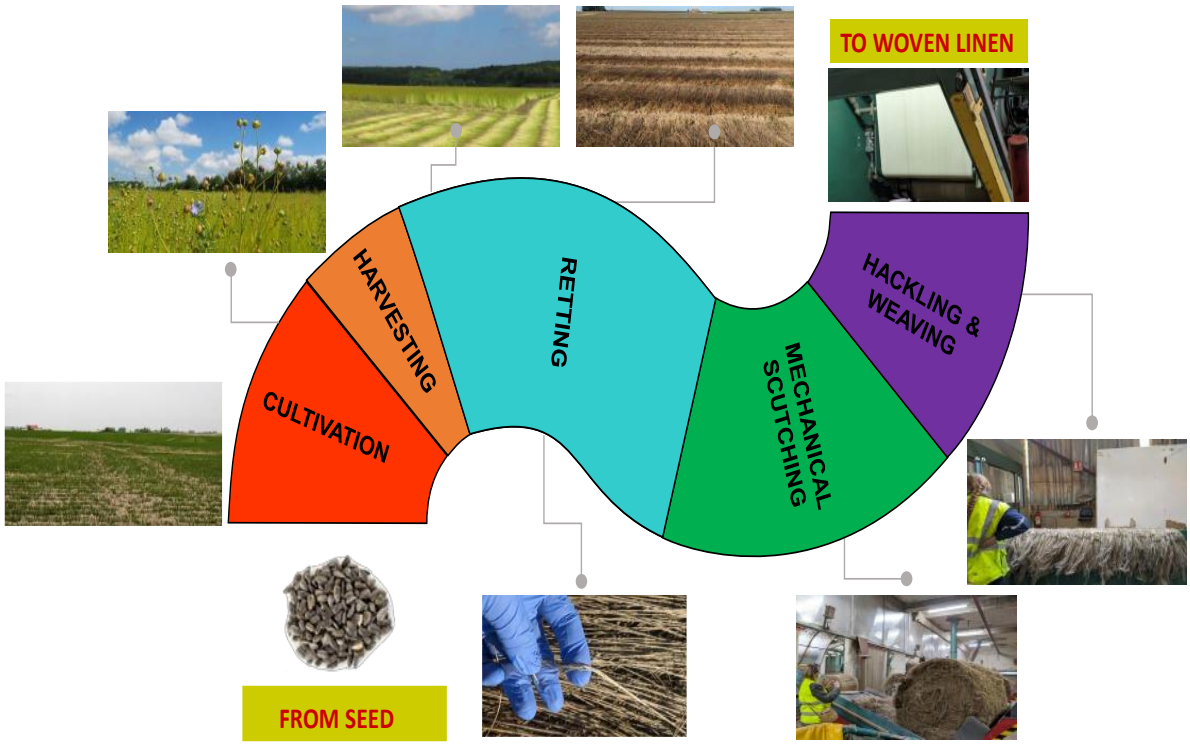

Fig. I.22: Flax cultivation and processing - Where does retting stand from seed to woven linen.

Water retting, which produces a lot of sludge, is now uncommon. Dew retting, despite occasional crop loss, is widely practiced in Europe (Kozłowski et al., 2020; Lee et al., 2020; Paridah et al., 2011). This efficient method enables flax to be processed more efficiently, while also reducing environmental impact.

I.2.6. Flax: Use and Demand (global production)

Flax production has increased modestly in recent years, from 0.77 million tons in 1962 to 0.897 million tons in 2021 and 0.875 million tons in 2022, according to UN FAOSTAT. However, in 2022 this figure will barely reach 1% of global textile production (Data from *FAOSTAT*, https://www.fao.org/faostat/en/#data/QCL; *Textile Exchange Reports*, https://textileexchange.org/). Most flax in the global market comes from Europe. This accounts for nearly 76.7%, followed by Asia (21.7%) (**Fig. I.23**). In Europe, France leads flax production, with production in 2022 estimated at 0.652 million tons, or 78% of Europe's flax production. This is followed by Belgium (9%), Belarus (6%), and other countries (Data from *FAOSTAT*, https://www.fao.org/faostat/en/#data/QCL).

The historical use of flax dates back to ancient civilizations such as Greece and Egypt, primarily as a staple food and natural laxative (Jhala and Hall, 2010). In recent times, flax fiber has had applications in the food industry (edible oil, margarine, functional food for promoting health, etc), textile

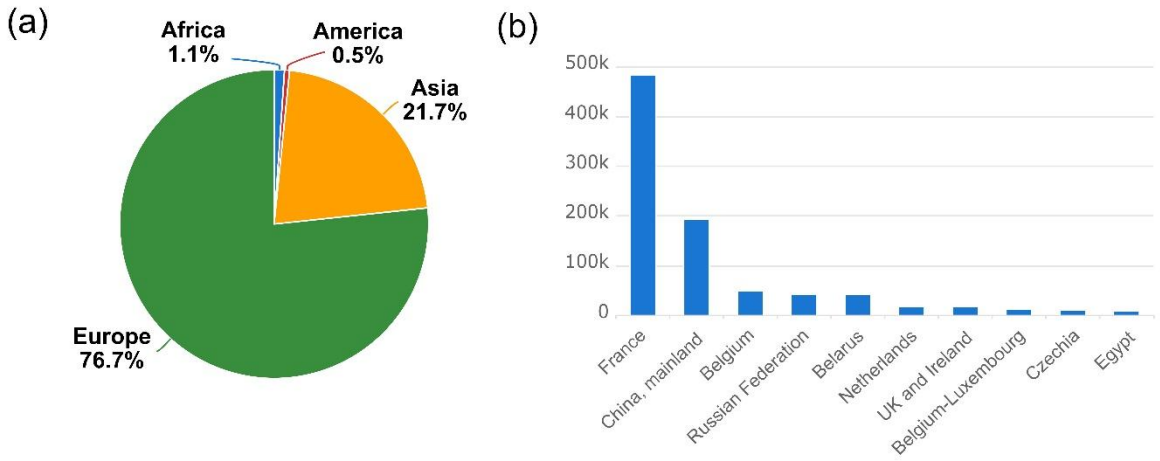

Fig. I.23. Production share of flax (raw or retted) on average between 1994-2022; by region.

(a) Continent and (b) top 10 producers. Source FAOSTAT, *https://www.fao.org/faostat/en/#data/QCL*, August 22, 2024.

and bio-composite industries (wearables, automotive parts, building materials, packaging materials, consumer goods, etc.), paper production, and other industrial products (curing agents; linoleum, oilcloth, painting, printer's ink, varnish, etc.) (CALHOUN, 2011; Célino et al., 2014; Chand and Fahim, 2021, 2020; Djemiel, 2017; Jhala and Hall, 2010; More, 2022; MUIR and WESTCOTT, 2003; Müssig, 2010; Yan et al., 2014; Zhu et al., 2013). Flax has significant economic value in France and Europe for its dual-purpose (multiple use) nature, providing both oil and fiber. In 2015, 861 thousand tons of flax were harvested, of which 137 thousand tons were mainly used in industries such as textile and paper industries (*FranceAgriMer Report*, *https://www.franceagrimer.fr/Actualite/Filieres/Tabac/2016*). The dominance of synthetic fiber and its effect on the environment has already been discussed. Despite competition from synthetic materials such as nylon and polyester, the comfort, drape, and unique look that linen provides has maintained a significant market share, especially in the luxury fabric market. The recent climate changes and challenges influence countries to achieve net zero carbon emissions, which can't be realized without reducing industrial carbon footprints (European Green Deal) and shifting more towards green textiles. With ongoing technological research and advancements in line with EU policies, the textile industries are being encouraged to adapt to other fibers (like flax and hemp) smoothly; giving the already existing **green** textile market a clear commercial advantage.

Flax-in-food-industry: Flax consumption has been linked to a variety of health benefits, most notably helping to balance the omega-6 to omega-3 ratio, which is important for cardiovascular health and reducing the risk of chronic diseases such as diabetes, arthritis, and some cancers (Jhala and Hall, 2010; MUIR and WESTCOTT, 2003). Flax seeds are rich in essential fatty acids, especially alpha-linolenic acid (ALA) and linoleic acid (LA), with ALA accounting for approximately 57% of total fatty acids (Jhala and Hall, 2010). This unique composition highlights its potential as a functional food (acting

on disease prevention and boosting health) (De Silva and Alcorn, 2019; Jhala and Hall, 2010; MUIR and WESTCOTT, 2003). Flax lignans have been shown to help inhibit the initiation and progression of tumours, potentially reducing the risk of breast and prostate cancer (De Silva and Alcorn, 2019; Jhala and Hall, 2010).

Flaxseed oil (also known as linseed oil) has limited dietary application because of its high linolenic acid content (susceptible to oxidation polymerization), but this makes it suitable for other industrial usages, such as the production of varnishes, paints, linoleum, etc. (Jhala and Hall, 2010; MUIR and WESTCOTT, 2003). Efforts are currently underway to overcome the stability issues of flaxseed oil for direct human consumption, with research aimed at improving its usability and mimicking the fatty acid profile of other oils (Jhala and Hall, 2010).

Flax-in-textile-industry (Fig. I.24): Flax, renowned for its sustainability, drape, and distinctiveness, is a vital crop in the textile industry primarily used to produce linen (Foulk et al., n.d.; Franck, 1992; Müssig, 2010; Potluri and Chaitanya Krishna, 2020). Linen, derived from flax fibers, is famous for its durability, breathability, and natural luster, making it ideal for high-quality fabrics and garments (Akin, 2013; Zhu et al., 2013). The production of linen involves several steps, including retting, dying, and spinning which transform flax fibers into yarn (Gomez-Campos et al., 2021). This yarn is then woven into various textile products such as clothing, home textile, and industrial fabrics. Linen's natural properties include moisture-wicking, hypoallergenic, and anti-bacterial characteristics, contributing to its popularity in bedding and clothing (Jhala and Hall, 2010; Salmon-minotte and Franck, 2005). Certification like the Global Organic Textile Standards (GOTS) and MASTERS OF LINEN® ensure that linen products meet stringent environmental and quality standards, reinforcing their appeal in the sustainable fashion market.

Flax-in bio-composite industry (Fig. I.24): Emerging bio-composite industries are using natural fibers as reinforcements within a synthetic matrix, often from petroleum or biodegradable materials such as polylactic acids (PLA) or poly-hydroxy-alkanoates (PHA) as plant fibers have promising mechanical properties and lower densities compared to glass fibers, benefiting applications such as transportation and construction (Chand and Fahim, 2020). In the field of bio-composites, flax fibers have shown great promise as a lightweight, strong, and sustainable substitute for conventional synthetic fibers like carbon or glass (More, 2022; Yan et al., 2014; Zhu et al., 2013). Because of its renewable qualities and capacity to lessen environmental effects, flax is a desirable alternative for various industries, including consumer products, building, and automotive. Despite these benefits, flax-reinforced composites nevertheless confront obstacles to their economic viability, mainly related to moisture resistance and durability (Chand and Fahim, 2020; Joshi et al., 2004; Yan et al., 2014).

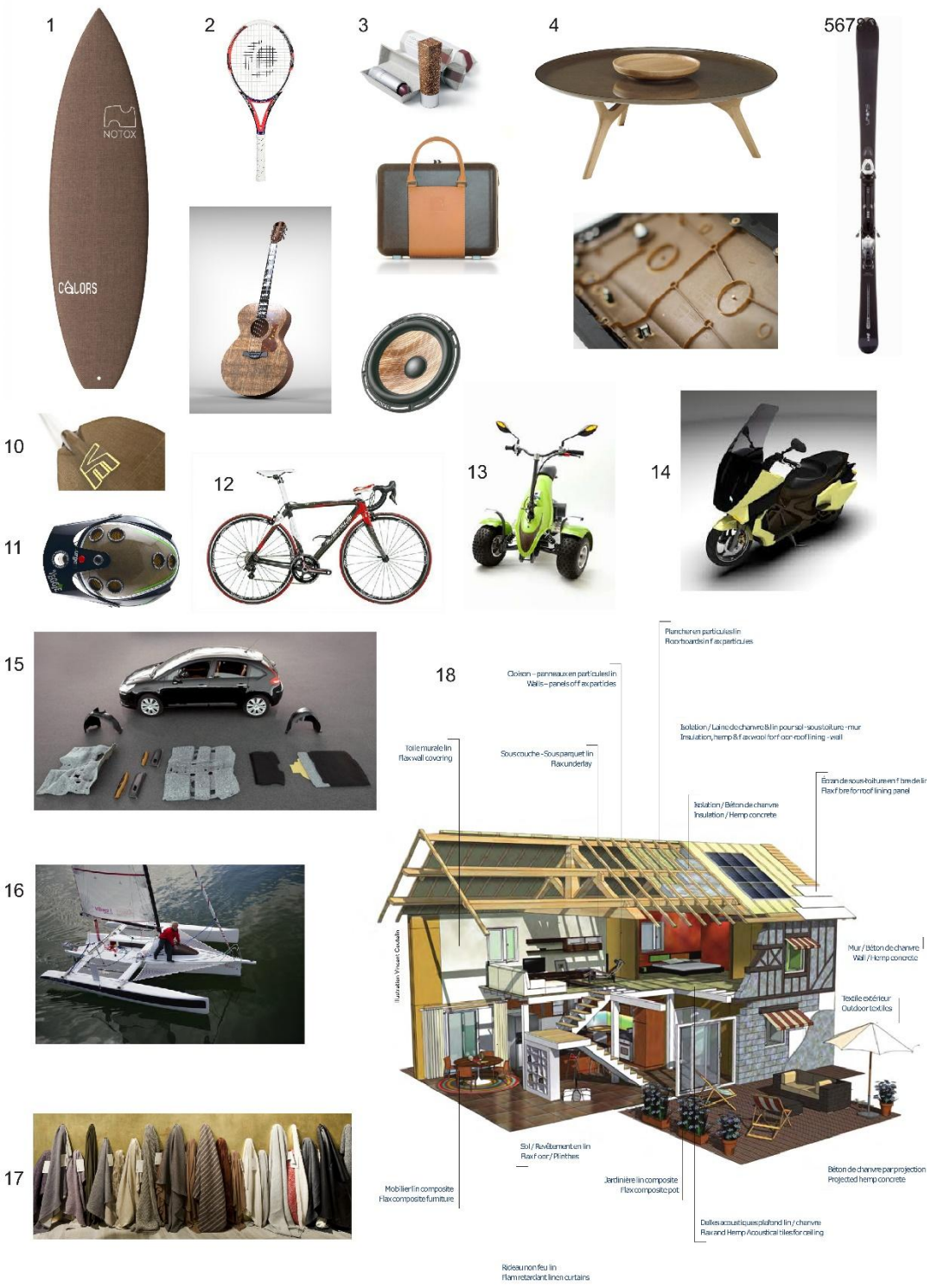

Fig. I.24: Various use of flax fibers.

Source : (Djemiel, 2017). Source des images : 1/ Planche de surf © Notox, 2/ Raquette de tennis © Artengo, 3/ Packaging cosmétique© Aveda, 4/ Table basse par Noé Duchaufour-Lawrance © Saintluc Editions, 5 /Ski © Wed'ze, 6/ Guitare acoustique Blackbird El-Capitan, 7/ Valise 24h © Delsey, 8/ Pièce de porte automobile © Faurecia, 9/ Mem-brane acoustique © Focal, 10/ Pagaie de Kayak © Ve Paddles, 11/ Casque de VTT © Urge bike, 12/ Vélo de compétition © Museeuw, 13/ Véhicule électrique tri-porté © Scube, 14/ Carrosserie de scooter Ek'O © Citi Technologies, 15/ Composants habitacle automobile © PSA, 16/ Trimaran "Gwalaz" © Kairos, 17/ Mur de linge © CELC, 18/ Construction et aménagement © CELC.

Because of their hydroxyl groups, flax fibers naturally absorb moisture, which weakens their interfacial attachment to the polymer matrix and lowers their mechanical characteristics (Yan et al., 2014). To address these issues, scientists have concentrated on making flax fibers more hydrophobic with chemical treatments and coupling agents like maleic anhydride-polypropylene copolymers and silanes, which enhance fiber-matrix adhesion and decrease moisture absorption (Torres et al., 2017; Yan et al., 2014; Zhu et al., 2013). Indeed, combining flax with synthetic fibers like carbon or glass creates hybrid composites that improve mechanical strength and moisture resistance while balancing performance and cost (Chand and Fahim, 2021, 2020; Yan et al., 2014). In the bio-composite sector, flax's future rests in resolving these durability concerns and advancing the creation of novel, eco-friendly materials that satisfy the demanding specifications of contemporary engineering and sustainability objectives (Yan et al., 2014).

I.3. All about Hemp (a collaborative study)

I.3.1. General Introduction

Like flax, hemp is a bast fiber plant that has been used in textiles since ancient times (Fisher, 1981). Scientists are also exploring hemp as a potential green alternative to synthetic fibers. Hemp is more resilient than other plants, requiring minimal water and sequestering atmospheric carbon, resulting in a low carbon and water footprint (as shown in **§ I.1.6**, **Fig. I.6,** page 13). Additionally, hemp fibers possess sufficient strength (270-1110 MPa) and elastic modulus (23.5 – 90 GPa), making them suitable for use in the textile and composite industries (as shown in **§ I.1.7**, **Table I.1,** page 15).

Cannabis, from the *Cannabaceae* family, includes the genera Cannabis (hemp) and Humulus (hop). Cannabis comprises two species, *Cannabis sativa* L. and *Cannabis indica*. LAM (Small and Marcus, n.d.; McPartland, 2018).

C. sativa, known for tall, sparsely branched plants with large leaves and grey-brown seeds, is primarily cultivated for fiber and seeds and includes both wild (ssp. *spontanea*) and cultivated (ssp. *culta*) subspecies. *Cannabis indica*, characterized by short, densely branched plants with small, dark seeds and high tetrahydrocannabinol (THC) content, is notable for its psychoactive properties (**Fig. I.25**) (Small and Marcus, n.d.; McPartland, 2018).

Hemp, an annual herbaceous plant, is typically dioecious, flowering with the shortening days post-summer solstice, although some commercial varieties are monoecious (Small and Marcus, n.d.; Raman et al., 2017).

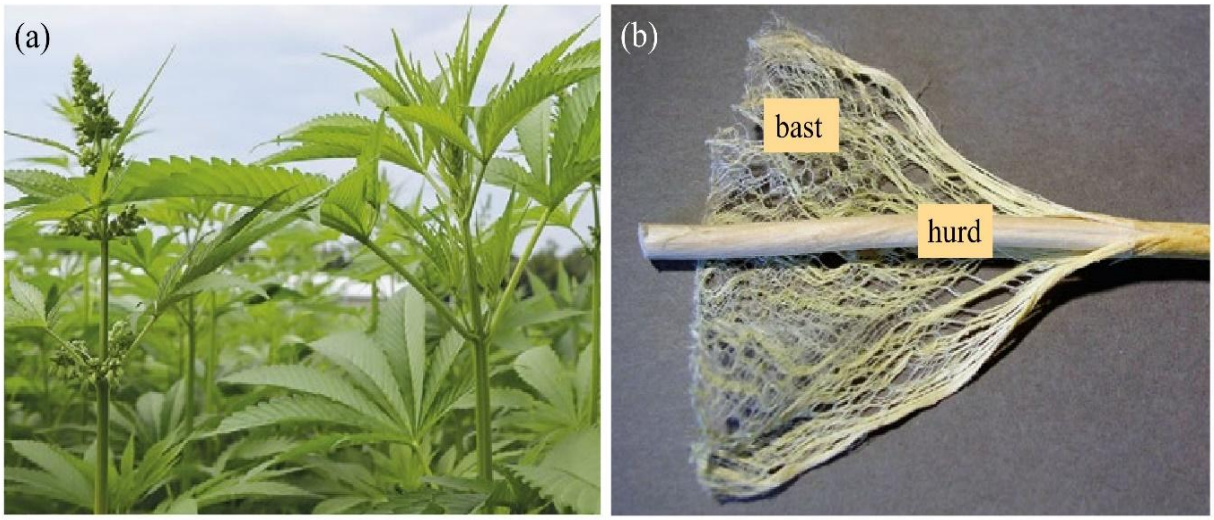

Fig. I.25: Hemp plant.

(a) growing hemp plant; (b) wood and bast of the mature hemp plant.
Source https://www.ncat.edu/caes/cooperative-extension/files/all-about-hemp.pdf.

I.3.2. Hemp Stem anatomy (in comparison to flax)

Like flax, ramie, jute, and kenaf, hemp's bast fibers surround the center of the xylem (wood) and are glued together to form bundles under the epidermis parallel to the longitudinal axis of the stem (**Fig. I.26**) (Raman et al., 2017; Zimniewska et al., 2022). A comparison of flax and hemp fiber characteristics and composition is proposed in **Fig. I.26** and **Table I.3** Each fiber or primary fiber corresponds to a cell surrounded by a cellulose-rich wall. Fiber cells are glued together in bundles using anchoring materials, especially pectin (Crônier et al., 2005; Vignon and Garcia-Jaldon, 1996). Hemp fibers are composed of primary fibers (sclerenchyma cells derived from the ground meristem) and secondary fibers (generated from the vascular cambium) (Crônier et al., 2005). This contrasts with flax fiber, which contains only primary fiber (**Fig. I.26**). Primary fibers can be distinguished from secondary fibers by their length, cell wall thickness, and degree of rigidification, and are of industrial interest for high-quality applications such as textiles and reinforced composites (Crônier et al., 2005; Raman et al., 2017; Zimniewska et al., 2022).

Compared to wood fibers (5–55 mm), hemp primary fibers are substantially longer, reaching up to 100 mm at maturity, and 15-25 µm in diameter. The secondary fibers are shorter (~2 mm), thinner, and less in proportion (Crônier et al., 2005). The primary fibers have a thick crystalline cellulose secondary wall, with microfibrils arranged almost parallel to the main axis of the cell (Bonatti et al., 2004; Crônier et al., 2005). Along with non-cellulosic polysaccharides including hemicellulose (10–16%), pectin (8%), fibers contain low amounts of lignin (4%) and trace of proteins (less than 5%), the major bast fiber cell wall is primarily composed of cellulose (55%) (Bonatti et al., 2004). Polymer

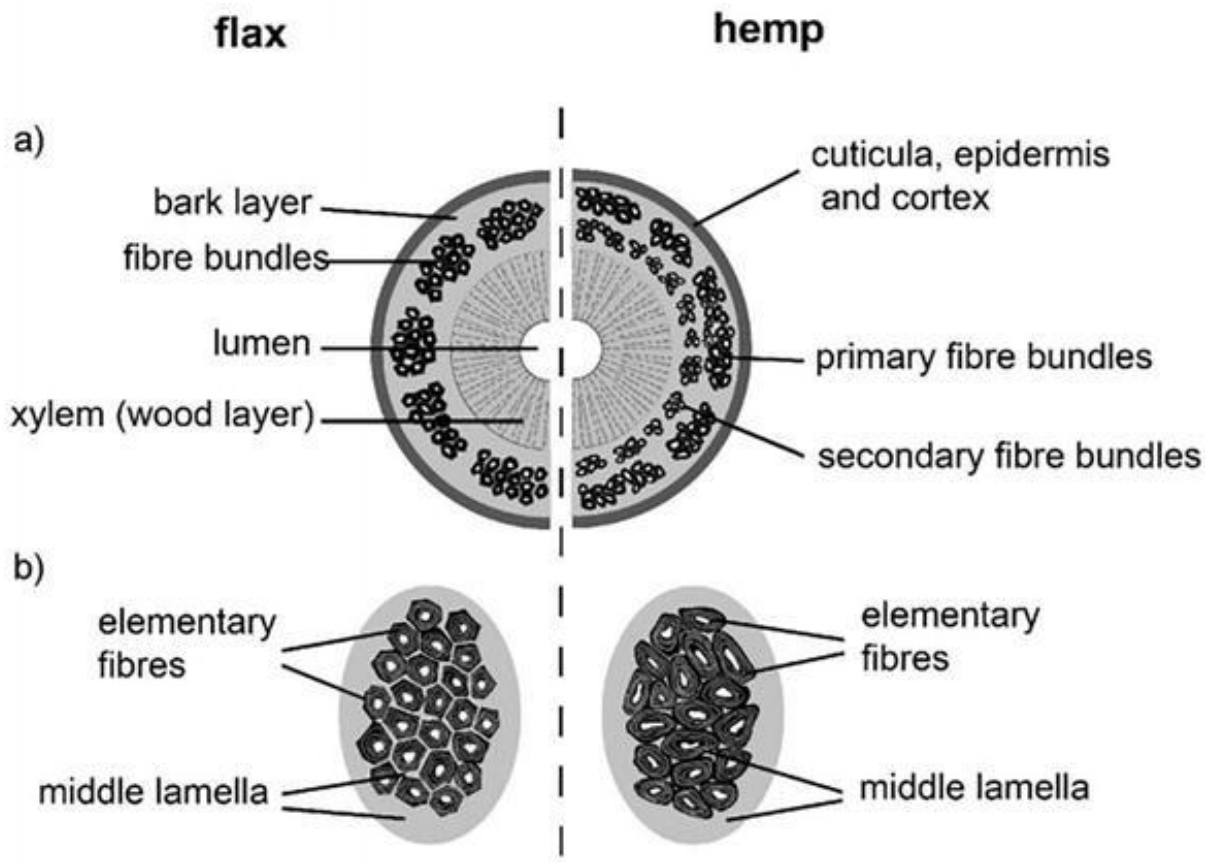

Fig. I.26. Structure of flax and hemp stem.

a) comparison of transverse section of flax and hemp stem, b) comparison of elementary fibers. Source: (Zimniewska et al., 2022); Under license CCBY 3.0.

distribution within cell wall layers impacts fiber properties. Glucomannan makes up the majority of the secondary wall of hemp fibers with very little beta-1-4-galactan in contrast to flax (Bonatti et al., 2004; Crônier et al., 2005; Morvan et al., 2003; Vignon and Garcia-Jaldon, 1996). Additionally, hemp fiber's secondary cell wall contains arabinogalactan protein and has almost no lignin content (Blake et al., 2008; Crônier et al., 2005). The middle lamellae and primary wall layers are held together by a pectin- and xylan-rich matrix with some lignin (Blake et al., 2008; Crônier et al., 2005). The lignin distribution in hemp primary fibers is more uniform compared to flax (Fernandez-Tendero, 2013; Djemiel, 2017; Mazian, 2018). The secondary hemp fiber presents a similar chemical composition to primary fiber but with slightly higher lignin and xylan content (Fernandez-Tendero, 2013). The chemical composition and spatial distribution of cell wall polymers in hemp fibers vary with the harvest date (maturity), showing increased levels of lignins and glucomannan when harvested after flowering. Fiber quality is influenced by growing conditions, such as soil quality and climate (Amaducci et al., 2015; van der Werf and Turunen, 2008).

Fiber attributes	Hemp	Flax
Length (mm)	5-55	10-60
Diameter (µm)	13-40	8-30
Crystallinity of cellulose (%)	55	70
Cellulose content (%)	55	70-80
Non-cellulosic polysaccharides (%)	15-25	10-15
Lignin (%)	3-4	2-3

Table I.3. Comparing the physicochemical properties of Hemp and Flax fibers.
Source : (Bonatti et al., 2004; Crônier et al., 2005; Djemiel, 2017).

I.3.3. Hemp Cultivation

Hemp is grown worldwide in various climatic conditions, and cultivation is possible in more than 30 countries in the Northern Hemisphere Despite its wide adaptability, hemp grows best in mild, humid climates with annual rainfall ranging from 625 to 750 mm. Prefers well-drained, silty clay soil with plenty of organic matter, rich in minerals, and a pH of 6 to 7.5 (Amaducci et al., 2015). Hemp growth and development are affected by photoperiod and temperature, so even for the same variety, flowering and harvest times vary depending on latitude (van der Werf and Turunen, 2008). Thus, the production is deliberately boosted by choosing late-flowering hemp types in high latitudes, which produce larger plants and more biomass (van der Werf and Turunen, 2008). In Western Europe (the second largest hemp fiber-producing region after China), hemp is typically sown in April and harvested from mid-August (mid-flowering stage) to mid-September (seed maturity stage), depending on the farmer's harvest plan (either with just a stem or with both stem and seeds, respectively) (Müssig, 2010). Harvest timing and stage significantly impact the deterioration process, as differences in leaf biomass, stem dry matter, and fiber histochemistry alter deterioration dynamics (Djemiel, 2017; M. Liu et al., 2015).

I.3.4. Global production and use of Hemp: Productions and Consumption

The global hemp production in 2021 was 254,692 tons (around 0.2% of the global fiber market) and has been increasing since 1990 (Textile Exchange *PFMM* Report 2022). According to FAO (*FAOSTAT*), US (*USDA*) and Turkish (*TURKSTAT*) database reports in 2021, France is the highest global hemp producer by volume, with ~47% of global hemp production (141,110 tons), followed by China with 24% (72,878 tonnes) and others (US, Poland, North Korea, Netherlands, Austria, Italy, Chile, Romania, Lithuania, Russia, Spain, etc.).

The use of hemp in bio-based materials has become widespread, primarily due to its long-stemmed fiber properties (Crônier et al., 2005). These fibers can be used as reinforcements in a variety of industries, including construction (e.g., concrete, appliances) (**Fig. I.27**) (Barbhuiya and Bhusan Das,

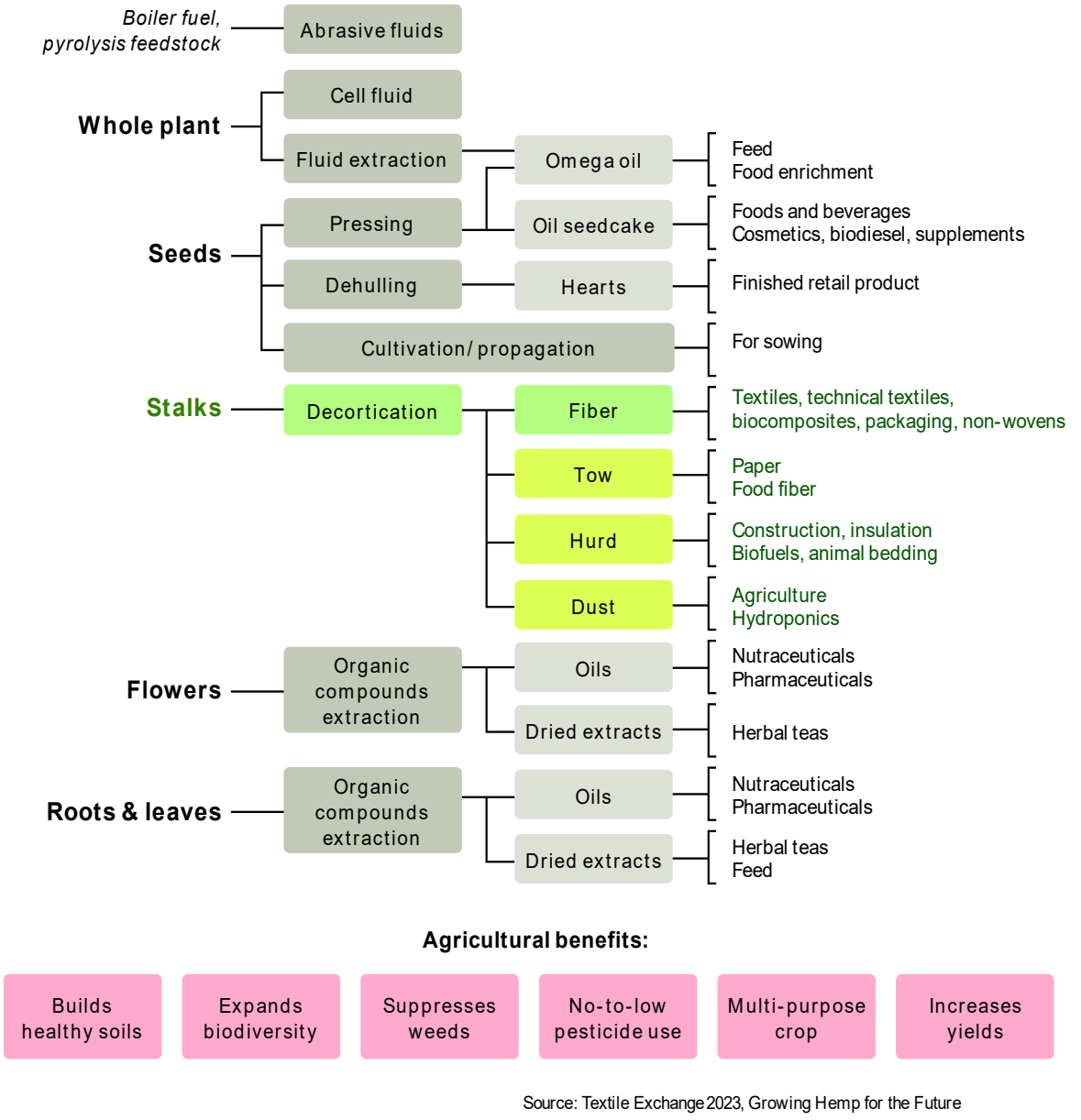

Fig. I.27: Use of Hemp plant in various usages.

Source: Growing Hemp for the Future, Textile Exchange 2023 report, (https://textileexchange.org/knowledge-center/reports/growing-hemp-for-the-future-a-global-fibeguide/?gad_source=1&gclid=Cj0KCQjwrKu2BhDkARIsAD7GBosjHTeLQZ_eYHABIh2k8BmhSbeQLJzBzsBgMbn4OEsIPhHHdl3i0xUaAmPHEALw_wcB).

2022), transportation, sports, and recreation (Amaducci et al., 2015; Fike, 2016). When compared to synthetic (or conventional cotton) fibers, hemp fibers have a reduced carbon and water footprint, according to LCA research (**Fig.I.6, § I.1.6**, page 13)**.** Hemp has many benefits in place of conventional fibers, such as low density, appropriate strength, biodegradability, renewable resources, and decreased cost and environmental effects (Chand and Fahim, 2020; Müssig, 2010). Hemp fiber has been used since ancient times to make fabric, rope, and paper (Iwańska et al., 2022; McDonald, 2011).

Although end uses have varied over the centuries, the key step before fiber extraction (i.e. retting) is very similar (Fernandez-Tendero, 2013; Mazian, 2018).

The retting process significantly impacts the future value of hemp fibers, affecting their extraction efficiency and properties (chemical composition, mechanical properties, length-to-diameter ratio, and fineness) (M. Liu et al., 2015), and its precise control is essential despite its long historical use (Amaducci et al., 2015), to provide high-quality and standardized raw materials to the composites and construction industries (Fernandez-Tendero, 2013; Mazian, 2018; Chabbert et al., 2023; Bou Orm et al., 2024). Inconsistencies in hemp fiber quality, introduced by the necessary retting processes, can affect the quality-based fiber cost evaluation and final product price.

I.4. The Retting

Retting is an essential process that links flax cultivation to linen production (as discussed in **§ I.2.5**, **Fig. I.22,** page 37). However, despite its necessity, retting also introduces variability in fiber quality, posing a significant challenge to the widespread industrial use of flax.

I.4.1. All about retting

Retting facilitates the separation of fibers from other stem tissues (epidermis, parenchyma, and woody parts) and can be considered as a controlled rotting process (Chabbert et al., 2020; Meijer et al., 1995; Sharma, 1992). The main objective is to degrade pectins and other compounds binding the bast fibers and fiber bundles to other tissues, thereby separating fibers and non-fiber materials (Akin, 2013; Chabbert et al., 2020; Paridah et al., 2011). It can be achieved by various methods, like natural water retting, dew retting, or man-made processes, like osmotic degumming, chemical retting, enzyme degumming, and more (Kozłowski et al., 2020; Lee et al., 2020; Paridah et al., 2011).

Pectin hydrolyzing enzymes, known as pectinases, play an important role in retting along with other cell wall-degrading enzymes such as hemicellulases and cellulases (Henriksson et al., 1999; Meijer et al., 1995), described in **§ I.6.1**. Although retting mainly affects the pectin-rich middle lamella, depending on the duration of retting, it can also affect the fiber's primary and secondary cell walls (Brown et al., 1986; Chabbert et al., 2020; Djemiel et al., 2020). The effect of retting on fiber is described in **§ I.4.2**. Considering the impact of retting on fiber quality and end use, numerous publications have described various methods to mimic, optimize, or replace the natural process of retting (Angulu and Gusovius, 2024; Paridah et al., 2011; Sharma, 1992). However, to our knowledge, none of them has led to cost-effective implementation for industrial applications. Various types of retting techniques for bast and allied fibers are described below.

The ancient traditional method of retting involves soaking harvested straw (flax/hemp/jute etc.) in water (river or pond), where anaerobic bacteria (such as *Clostridium sp*.) ferment the straw (Kozłowski et al., 2020; Lee et al., 2020; Paridah et al., 2011). This is known as **water retting** which produces the highest quality uniformly retted fibers since historical times (**Fig. I.28a-b**). This process requires 7-14 days on average (Lee et al., 2020; Paridah et al., 2011). However, retting (fermentation) by-products and released phenolics from straw result in severe water pollution; releasing a foul smell, a lot of slugs, and causing darkening of water, respectively (Kozłowski et al., 2020; Lee et al., 2020; Paridah et al., 2011). Released large amounts of organic matter, increases biochemical (BOD) and chemical oxygen demand (COD) leading to depletion of dissolved oxygen and harming aquatic life. Nutrition released during retting contributes to eutrophication. Toxic phenolics affect aquatic organisms and potentially enter the food chain. Increased water turbidity reduces light penetration and affects aquatic photosynthesis. Finally, the anaerobic condition promotes the growth of harmful bacteria and pathogens posing risk to both aquatic life and human health (Kozłowski et al., 2020; Lee et al., 2020; Paridah et al., 2011). Without treatment, this wastewater is harmful to release into the environment (Lee et al., 2020; Majumder et al., 2013; Zawani et al., 2015). Numerous research endeavors have focused on enhancing water retting and wastewater treatment methodologies (Kozłowski et al., 2020; Lee et al., 2020). To name a few; retting in saline water (Zhang et al., 2008); use of urea-soaking to reduce water-retting time and improve quality (Kozłowski et al., 2020); radio-frequency treatment to improve water-retted fiber with high crystallinity index (Ruan et al., 2015); ribbon-retting of jute (practiced in Bangladesh) (Jahan et al., 2016); wastewater treatment (organic & inorganic pollutants) by Fenton oxidation (Abou-Elela et al., 2016).

Koncevic et al. (2019) developed a new water system called **osmotic degumming**, which involves water (continuous or changing flow) flowing into the stem causing the fibers to swell, which in turn causes the pectin to swell and weaken (**Fig. I.28h**). A strong hydrostatic pressure helps tighten the epidermis in longitudinal and circumferential directions, causing soluble substances (such as dyes, bacteria, pectins, and mineral salts) in the stem to dissolve (Konczewicz et al., 2013; Lee et al., 2020; Paridah et al., 2011). High-quality fibers are obtained by this process, continuing at 40°C for 96 hours. This method is considered to be especially suitable for fiber reinforcement applications (Lee et al., 2020).

In **dew retting**, (**Fig. I.29**) uprooted plants (flax/hemp etc.) are left on fields for several weeks under heavy dew falls during night-time and warm summer days accompanied by frequent rainfall. These changing meteorological conditions promote phyllospheric micro-organisms' growth (fungi and bacteria) on the flax stem swaths. These microorganisms start feeding upon the stem by releasing a spectrum of polysaccharide-degrading enzymes, primarily pectinolytic and hemicellulolytic (Meijer et al., 1995). These help in breaking down the tissue binders that hold the bundles of natural fibers together, (Djemiel et al., 2017) letting loose the single fibers from fiber bundles and other plant tissues (Akin,

2013). Dew retting is very much weather-dependent and ceases working in dry weather, which can cause under-retting (Meijer et al., 1995). This process takes 2-3 weeks [88] or more based on optimal weather. Higher enzyme activity on the other hand can destroy cell wall polymers, affecting the fiber quality; is known as over-retting (Akin et al., 2001; Djemiel et al., 2020; Lee et al., 2020). Dew retting, despite occasional crop loss and having lesser and often intermittent fiber quality (than water retting), is widely practiced in Europe, due to its ease of use, cheaper cost, and environment friendliness (Kozłowski et al., 2020; Lee et al., 2020; Paridah et al., 2011).

In search of a low-cost alternative, scientists explored a simpler method called **Stand retting** (**Fig. I.28d-e**), where hemp or flax stems were left standing on the field either after maturity or with glyphosate treatment at the desired maturity state (Assirelli et al., 2020; Sampaio et al., 2005; Sharma, 1986a). Compared to flax desiccated two or six weeks after mid-flowering, flax desiccated at mid-flowering, followed by stand retting and high-speed decortication, generated finer, stronger fibers with lower acid-insoluble lignin and lighter color (Sampaio et al., 2005; Sharma, 1986a). The resulting fibers were good for bleeding with wool but the early desiccated fiber worked well when blended with cotton and spun on cotton systems. Lower lignin content at mid-flowering allowed more complete fiber retting, yielding finer fibers (Sampaio et al., 2005). This cotton-compatible fiber was cost-competitive with cotton, suggesting further desiccation timing optimization could increase yields. Assirelli et al. (2020) conducted a stand retting experiment on hemp, focusing on optimizing fiber extraction efficiency in the field. They utilized existing machinery with minimal adaptations, emphasizing a prolonged 4-month standing maceration period. This approach achieved a high fiber-to-shive separation rate above 46%, demonstrating the potential to lower production costs and improve industrial efficiency (Assirelli et al., 2020).

Chemical retting is the most effective method for eliminating non-cellulosic elements (pectin) in 60-75min and keeping fiber quality on par with water retting, but excessive retting leads to cellulose degradation (Basu et al., 2015; Lee et al., 2020). However, the use of chemicals usually leads to higher expenses and harms the environment by contaminating wastewater if released untreated (Lee et al., 2020). The quality of retted fiber is influenced by factors such as retting time, chemical concentration, and temperature. The chemical reaction mixture can be reused (at lower efficiency) with additional chemicals to achieve the same level of fiber quality. Utilizing sodium carbonate, sodium hydroxide, and sodium sulphide, in the reaction mixture significantly reduces the reaction time (Basu et al., 2015). Electrocoagulation treatment (90min) effectively decreases wastewater contamination (Jose et al., 2019). Chemical-retted fiber is appropriate for nonwoven applications in the automotive industry with shorter retting periods (Lee et al., 2020).

Enzyme retting (**Fig. I.28f-g**) is becoming a promising option in regions with dry climates where dew retting may be ineffective. This environment-friendly process not only improves yield/time

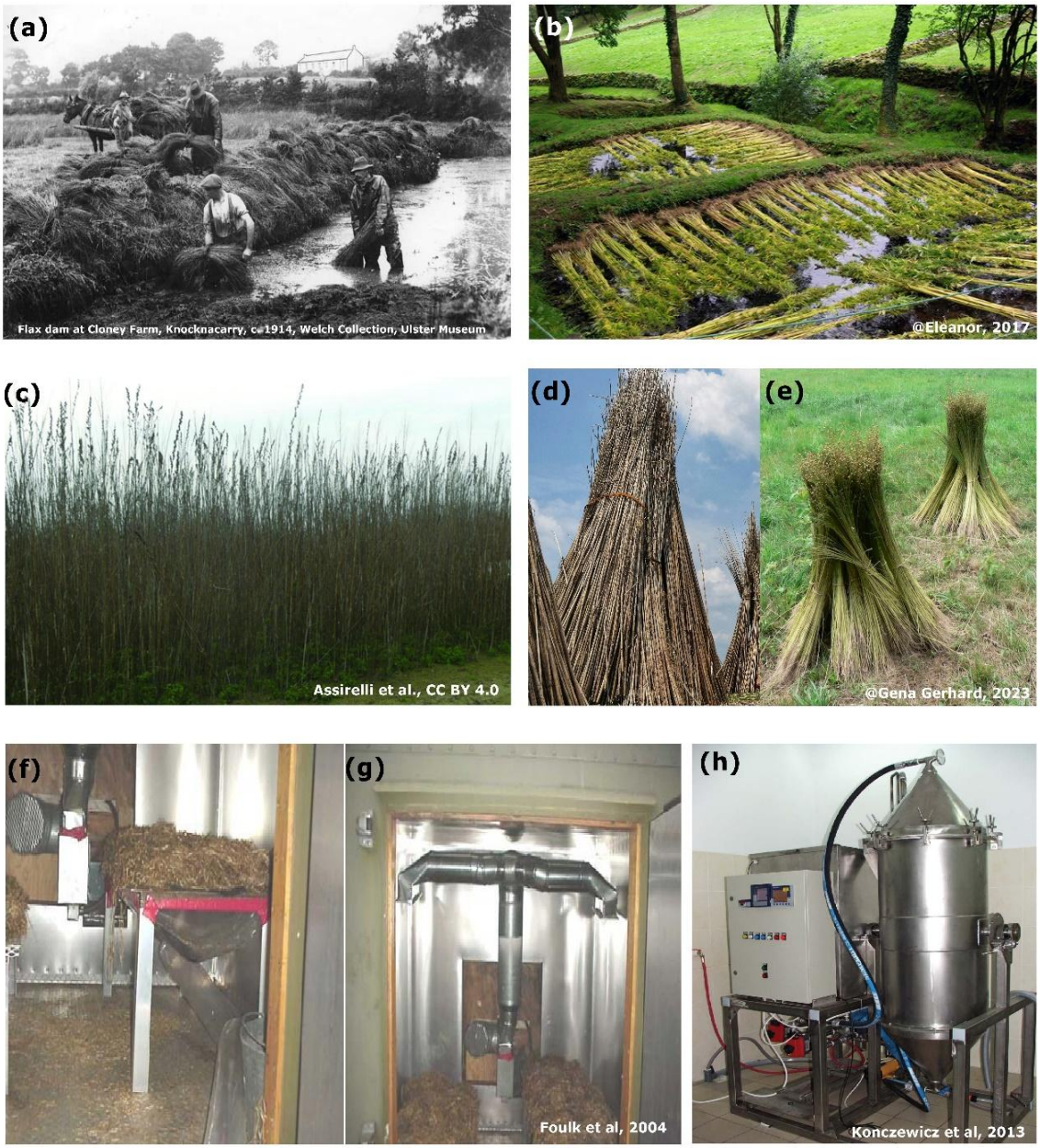

Fig. I.28. Different types of retting and degumming.

(a-b) water retting: upon harvest, flax stems are submerged into water in a flowing river (a); or placed into stagnant water beds (b); where anaerobic bacteria proliferate and favor flax stem degradation (but pollutes water). (c-e) stand retting: upon maturity hemp stems are treated with glyphosate and left standing for weeks (c), jute stem swaths (d), and flax stem swaths (e) are left standing upon harvest for retting. (f-g) enzyme retting: flax stems are treated with an enzyme mixture in a controlled environment (chamber). (h) osmotic degumming: flax stems are introduced to stem treatment in a tank facilitating fiber detachment. Image source: (a) https://antrimhistory.net/the-lint-pulling-dance-by-cahal-dailat-with-additional-comments-by-pat-mc-cambridge/, (b) https://www.sloweurope.com/community/media/poul-fetan-flax-retting-pools.3116/, (c) (Assirelli et al., 2020), (d) https://unsplash.com/s/photos/jute-retting, (e) https://localcolordyes.com/2012/08/14/michelles-excellent-flax-adventure/, (f-g) (Foulk et al., 2004), (h) (Konczewicz et al., 2013).

Fig. I.29. Dew retting of flax.

(a) flax stems are being uprooted and left on the field in rows for dew retting. (b) after five weeks of retting, flax swaths are turned for uniform retting (using vehicles), and (c) flax swaths after 8 weeks of retting, are almost retted and ready for harvest.

Retting types	Description	Advantages	Disadvantages	Duration	Type of bast fibers
Dew retting (Used extensively)	Mature plant stems are pulled and left on the field to rot	Pectin material could easily be removed by microbes.	Reduced strength (over retting), inconsistent quality, limited by climate, and prone to soil contamination.	2-3 weeks	Flax, Hemp
Water retting (Used)	Plant stems are immersed in water (rivers, ponds, or tanks) and frequently monitored (microbial retting).	Produces fiber of greater uniformity and higher quality.	Anaerobic bacterial fermentation of plants leads to extensive stench and pollution, high costs, environmental issues, low-grade fiber, and requires rigorous water treatment.	7-14 days	Flax, Hemp, Kenaf, Jute
Enzymatic retting (specific-Use)	Enzymes like pectinase and xylanase are used to break down the gum and pectin in the bast. This process is conducted under controlled conditions, tailored to the specific type of enzyme used.	Easier refining for pulping degrades selectively for different applications. Enzymatic reactions partially degrade components, separating cellulosic fiber from non-fiber tissues, making the process faster and cleaner.	Lower fiber strength.	12-24 hours	Flax
Chemical retting (specific-Use)	Boiling and applying chemicals, typically sodium hydroxide, sodium benzoate, and hydrogen peroxide.	It quickly produces clean, consistent, long, smooth bast fibers.	Fiber retted in more than 1% NaOH shows decreased tensile strength, unfavorable color, and increased processing costs.	75 minutes – 1 hour	Kenaf, Jute, Flax
Mechanical retting (specific-Use)	Fibers are separated by hammering or using a hammermill or decorticator.	Produces large quantities of short fiber quickly.	High cost and lower fiber quality.		Kenaf
Stand retting (experi-mental)	plants are macerated while standing in the field, facilitated by microbial activity and environmental effects.	Stand retting after mid-flowering desiccation produces finer, stronger fibers with lower lignin and paler color, ideal for mechanical processing and blending with cotton or wool at competitive costs.	Stand retting requires careful timing and conditions to achieve optimal fiber quality, which may vary with environmental factors and crop management practices.	40-120 days	Hemp, Flax, Jute
Osmotic degumming (experi-mental)	Treating fiber straw with water (30°C) and a neutral pH solution & washing with cold water under pressure.	Lightened color, no odor, enhanced uniformity, and reduced non-cellulosic substances and VOC emissions.	High variability in fiber diameter, lower linear mass of fibers ratio, and chance of thermal decomposition.	72 (flax) – 144 (hemp) hours	Hemp, Flax

Table I.4. Comparative retting methods according to the fiber plants.

Source: (Assirelli et al., 2020; Konczewicz et al., 2013, 2018; Lee et al., 2020; Paridah et al., 2011; Sampaio et al., 2005; Sharma, 1986a).

but also enhances the fiber quality, especially when utilizing pectinase-rich commercial enzymes, such as Flaxzyme (Akin, 2013; Kozłowski et al., 2020; Lee et al., 2020; Sharma, 1992). Factors, such as type of substrate, type, and dosage of enzyme, pH, temperature, reaction duration, etc., at the right combination, are crucial for efficient enzyme retting, enhancing fiber characteristics suited for particular uses (Akin, 2013; Sharma, 1992). Enzymes such as cellulases, xylanases, laccases, and pectinases are used in enzymatic hydrolysis to break down cellulose, hemicellulose, lignin, and pectin in the plant cell wall. Chelating agents such as EDTA improve the effectiveness of retting by attaching to calcium ions, making it easier to break down the plant cell wall. Although commercial enzymes are convenient, they can be costly, which is why scientists are investigating different formulations and conditions to achieve efficient retting. In order to reduce the amount of formulation required in a tank and to enable the mixture to be reused for a predetermined amount of time, the enzyme-retting method was optimized (Akin et al., 2001; Van Sumere, 1992). In general, enzyme retting demonstrates potential in creating top-notch fibers with enhanced characteristics, providing a practical choice for fiber production in different situations (Akin, 2013; Lee et al., 2020; Paridah et al., 2011; Sharma, 1992).

Finally, each of these retting methods offers unique advantages and poses specific challenges, (for comparison, see **Table I.4**) resulting in different flax fiber qualities suitable for a variety of textile applications. The choice of method depends on the desired fiber quality, cost, ease of doing, environmental norms and laws as in Europe, and the specific requirements of the textile industry. In the north of France, dew retting is widely practiced due to its eco-friendliness and lower cost. Further discussion on our work will be based on **dew retting of flax and understanding the basis of its biology**.

I.4.2. Changes in fibers due to retting

Decortication effect: The ability of the stalk to be decorticated is determined by retting, which impacts its integrity. Bast fibers are separated from epidermal and woody tissues by conventional industrial methods that involve mechanical and thermal pressures (Djemiel, 2017; Mazian, 2018). Retting results in cleaner fibers with less physical damage and woody residues by lowering the energy required for tissue separation during scutching (Diquélou et al., 2015; Hobson et al., 2001). Retting extent and decortication techniques can also alter the length-to-diameter ratio of fiber bundles (Hobson et al., 2001).

Surface properties: The surface that remains visible following decortication is determined by the breakage of fiber-to-tissue contacts, which are mostly caused by retting microbes and weather changes (sunny/rainy). The degree of retting-induced degradation and leaching can disclose various surface compositions, including lignins, hemicelluloses, and cellulose. Furthermore, the global accessible surface concerning the volume and form of the fiber bundle can change, as can the physical

characteristics of the fiber at the micro and mesoscales as a result of decortication processes (Bourmaud et al., 2010; Truss et al., 2016).

Mechanical properties: The arrangement of plant cell wall polymers within each technical fiber, how elementary fibers are bundled together, and the combined mechanical and biological stresses that occur during retting and decortication, all affect the mechanical properties of technical bast fibers (Andersons et al., 2011; Martin et al., 2013). Biochemical similarities with flax imply that microbial and enzymatic degradation of hemp during retting can influence the mechanical characteristics of extracted fibers, even if detailed research on the effect of retting on hemp fibers is scarce (Djemiel, 2017). The modification of mechanical characteristics is also influenced by intrinsic flaws and those created during decortication (Akin et al., 2001; Andersons et al., 2011; Baley et al., 2020; Djemiel, 2017; Jeannin et al., 2024).

Retting is not perfect but necessary: In every application, fibers must come into contact with other fibers or components, hence surface quality is crucial (Bourmaud et al., 2010; Chand and Fahim, 2021; Fike, 2016). When retting falls short of requirements, qualities can be managed by surface treatments (Bergeret, 2021; Sharma, 1992). The cohesiveness of the polymers in the fiber cell walls and the interactions within the fiber bundles determine the mechanical properties (Bergeret, 2021; Chand and Fahim, 2020). While over-retting facilitates decortication but might harm fibers due to cellulose degradation, incomplete retting protects structures but may result in damage during decortication (Chabbert et al., 2020; Djemiel et al., 2020; Sharma, 1992). In order to attain the optimal compromise for morphology, surface characteristics, and mechanical performance, fiber quality management thus necessitates rigorous identification of the retting process steps and events, especially in developing applications (Djemiel, 2017; Meijer et al., 1995; Sharma and Faughey, 1999).

I.4.3. Methods used to study retting

With a multimodal approach to study retting, researchers have consistently explored several key questions: who is involved in the retting process (Chabbert et al., 2020; Djemiel et al., 2017; Rosemberg, 1965; Sharma, 1986b; Brown et al., 1986; Henrissat and Davies, 1997), how is retting performed (drawing insights from wood degradation), and what are the dynamics of enzymes and physio-biochemical changes occurring in the stem (Akin et al., 2000; Bleuze et al., 2018; Bou Orm et al., 2024; Chabbert et al., 2020; Mazian et al., 2020). They further investigate the mechanical and organoleptic analyses of retted fibers and stems (Baley, 2002; Goudenhooft, 2018; Mazian et al., 2019).

Studying physical changes of straw during retting (mainly surface color) includes **Colorimetry** and **FTIR spectroscopy** to support the analysis of CIELAB components that link these color changes as well as surface chemical changes to microbial colonization and plant pigment degradation (Akin et

al., 2000; Bleuze et al., 2018; Mazian et al., 2019; Bou Orm et al., 2024). It also includes **organoleptic** and **chromatographic** studies of volatile organic compound release during retting (Mazian et al., 2019).

Effect of retting on mechanical properties has been studied on **single fiber** (SFTT) [using various standards such as NF T25-501–2 (Chabbert et al., 2020; Goudenhooft, 2018; Jeannin et al., 2024), NFT 25-704, ASTM D 3379-75 (Baley, 2002)], and in composites (**IFBT** or Beam test) (Chabbert et al., 2020).

Biochemical studies of retting include mainly **spectrophotometric/ fluorometric enzyme assay** (on **selected enzymes** from literature), **sugar analysis** by **colorimetry** or **chromatography**, and often **X-ray diffraction** analysis to study changes in cellulose crystallinity, which are done to answer what happens during retting (Bleuze et al., 2018; Chabbert et al., 2020; Mazian et al., 2018). **Thermogravimetric** analysis is also done to monitor changes in biomass (Bou Orm et al., 2024).

Answering who is there involves **microbial studies**. The methods used to identify microbiota have historically limited research into the microbial communities involved in retting of flax, hemp and allied fibers. Conventional methods concentrate on cultivating bacteria, investigating their morphologies and metabolisms, and studying the cellular kinds and nutrition levels of fungi (Djemiel, 2017). Culture-based methods of flax/hemp water and dew retting have identified only a handful of retting microbes (13 fungal and 16 bacterial genera for flax; 23 fungal and 3 bacterial genera for hemp). Because only a small percentage of microorganisms can be grown in lab conditions, these techniques frequently fall short of capturing the full diversity of microorganisms, a phenomenon known as "The Great Plate Count Anomaly". In the 1970s, Woese and Fox, presented a new taxonomy of living things based on DNA sequences, specifically employing molecular markers such as 18S rDNA or Internal Transcribed Spacer (ITS) for fungi and 16S rDNA for bacteria (Woese and Fox, 1977). These markers contain variable areas for microbe identification and conserved regions for multiplying a variety of bacteria. These genes could be sequenced concurrently with the advancement of Sanger sequencing, giving classification a molecular foundation. Microbiota research has undergone a radical change with the introduction of Next-Generation Sequencing (NGS) technologies (Handelsman, 2004).

Comprehensive metagenomics investigation of microbial communities is made possible by these high-throughput techniques, which include platforms such as Roche 454, Illumina MiSeq, Ion Torrent, and Single-Molecule Real-Time Sequencing. By multiplexing up to 384 samples, NGS methods optimize bioinformatic processing rates, reagent use, and time. Visi et al. (2013) conducted the first study to use NGS (Ion Torrent PGM) for retting community analysis in Kenaf retting (Visi et al., 2013). Phyllosphere communities, litter decomposers, root-associated communities, and soil communities have all been the subject of several meta-omics investigations (Chirania et al., 2022; Tláskal et al., 2021; Voříšková and Baldrian, 2013; Wallenstein et al., 2010). With its development in the early 21st century, this method seeks to evaluate the roles of microbes in many ecosystems and provides a thorough grasp

of the microbial dynamics in hemp retting (discussed in section 1.3.2.) (Law et al., 2020; Ribeiro et al., 2015; Tamburini et al., 2004).

I.5. Microbiology of retting

I.5.1. Flax retting

The process of controlled natural degradation or retting traditionally relies on microorganisms to break down the plant polysaccharides while they're feeding on it. The enzyme pool coming from microbes affects the efficiency of degradation. As microbes are the lead performers, numerous studies have focused on identifying them and assessing their efficiency in fiber release during traditionally practiced water and dew retting. The scientific exploits till 2020 have been very well documented in a review by Djemiel et al (Djemiel et al., 2020).

Short history in microbial research of **water-retting** (**Fig. I.30**): The first significant research on retting of flax with water was carried out by Philippe àdouard Léon Van Tieghem in 1879 that revealed *Bacillus amyloides* was responsible for the breakdown of pectin (Van Tieghem, 1879). Subsequent studies in 1950 unveiled the role of *Clostridium* species, especially *Clostridium felsineum*, in water retting (Lanigan, 1950). Later, the study of Rosemberg in 1965 isolated a variety of bacteria involved in water retting, including *Clostridium* and *Pseudomonas* species, where *Pseudomonas aeruginosa* was recognized for its rapid fiber de-cohesion ability (Rosemberg, 1965). In 1990, researchers from Northern Ireland, isolated anaerobic bacteria from water retting, from mainly Firmicutes phylum. Isolated *Bacillus licheniformis* and *Bacillus subtilis*, were found to be dominant in the early stages of retting, while *Clostridium acetobutylicum* and *Clostridium felsinium* were present at a later stage (Donaghy et al., 1990). From 2003, the use of molecular markers such as 16S rRNA gene amplification precisely assigned, identified anaerobic strains in water retting, to the genus *Clostridium* and aerobic strains to the genus *Bacillus* or *Paenibacillus* (Tamburini et al., 2003). Recent high-throughput sequencing techniques have expanded this knowledge by identifying five bacterial phyla and eight classes involved in water retting of flax, including some not previously associated with the process, such as Cyanobacteria and Bacteroidetes (Zhao et al., 2016).

Short-history in microbial research of **dew-retting** (**Fig. I.30**): Inaugural studies on microbiology of flax dew-retting in 1984 by Brown et al, recognize the role of fungus, mainly from phyla Ascomycota (*Epicoccum sp*., *Cladosporium sp*., *Fusarium sp*., *Botrytis sp*., *Alternaria sp*., *Phoma sp*., and yeast) and Mucoromycota (*Rhizopus sp*., and *Mucor sp*.) (Brown, 1984). Later, Sharma 1986, successfully isolated 6 bacterial species belonging to Actinobacteria (*Micrococcus sp*.), Firmicutes (*Bacillus sp*.), and Proteobacteria (*Pseudomonas sp*., *Erinia carotovora*) phyla; and 5 fungal species from *Ascomycota* phylum (*Cladosporium sp*., *Fusarium sp*., *Epicoccum sp*., *Botrytis sp*. and Yeast) in

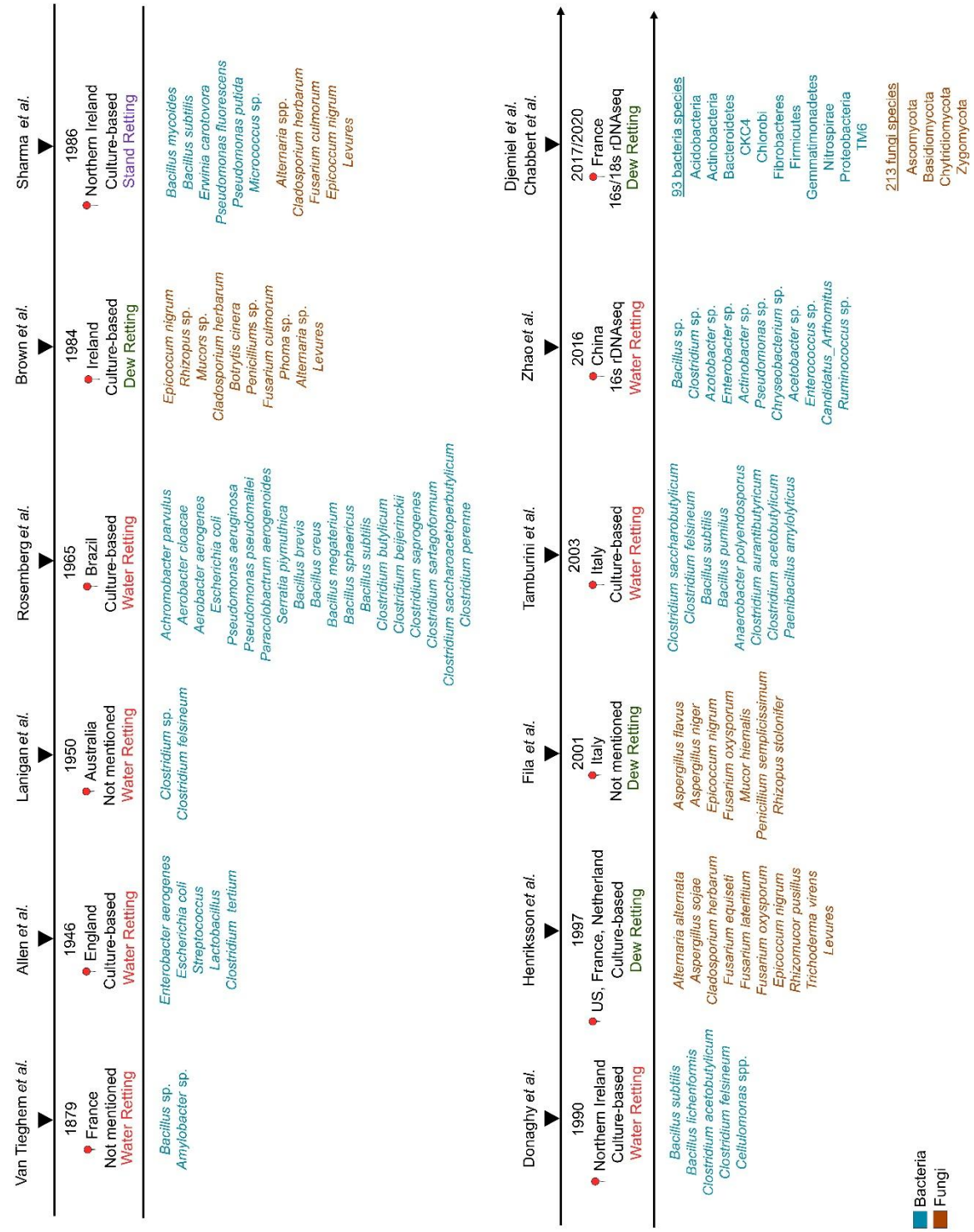

Fig. I.30. Timeline of Microbiology of Flax retting.

The different micro-organisms (bacteria, fungi) established as involved during retting have been indicated by (Van Tieghem, 1879; Allen, 1946; Lanigan, 1950; Rosemberg, 1965; Brown, 1984; Sharma, 1986b; Donaghy et al., 1990; Henriksson et al., 1997; Fila et al., 2001; Tamburini et al., 2003; Zhao et al., 2016; Djemiel et al., 2020; Chabbert et al., 2020).

culture-based approach from dew retting of flax (Sharma, 1986b). Henricksson et al. 1997; isolated strains of fungal species from *Ascomycota* (*Fusarium sp*., *Cladosporium sp*., *Epicoccum sp*., *Alternaria sp*., *Trichoderma sp*. and yeast) and *Mucoromycota* (*Rhizomucor pusillus*) phylum with a same culture-dependent approach from flax dew retting taking place in US, France, and Holland (Henriksson et al., 1999). Another culture-dependent study on flax dew retting in Italy (Budrio) in 2001, identified already reported fungal species from Ascomycota (*Aspergillus sp*., *Epicoccum sp*., *Fusarium sp*. and yeast) and *Mucoromycota* (*Rhizopus sp*., *Mucor sp*.) phylum.

Recently, Djemiel et al. (2017) and Chabbert et al. (2020) identified 93 bacterial species and 213 fungal species (**Table I.5**) from flax dew retting using a high-throughput sequencing DNA metabarcoding approach (16s rRNA/ITS). Identified dominant bacterial species belong to Proteobacteria (*Pseudomonas sp., Sphingomonas sp*.), Bacteroidetes (*Flavobactereium sp*., *Pedobacter sp*.), *Actinobacteria*, and Firmicutes (bacteria) phylum whereas dominant fungal species are coming from Ascomycota (*Cladosporium sp*., *Epicoccum sp*., *Alternaria sp*., *Botrytis sp*.), *Basidiomycota* (*Itersonilia sp*., *Kondoa sp*.) and *Zygomycota* phylum. Some fungi, such as *Fusarium lateritium*, *Epicoccum niger*, etc. are recognized as primary saprophytic species in retting, marked as over-retting actors while *Rhizomucor pusillus* has been recognized to degrade cuticle layers, marked as a pioneer (Akin et al., 1996; Brown, 1984; Henriksson et al., 1999).

Domain	**Djemiel *et al.*, 2017** **16s_18s_rDNAseq (Top 10)**	**Chabbert *et al.*, 2020** **16s_rDNAseq (Top 10)**
Bacteria	*Pedobacter* sp. * *Pantoea vagnas* * *Pseudomonas rhizosphaerae* * *Rhizobium* sp. * *Massilia* sp. * *Sphingomonas* sp. * *Epilithonimonas* sp. *Flavobacterium* sp.	*Pedobacter* sp. * *Pantoea vagnas* * *Pseudomonas graminis* * *Rhizobium* sp. * *Massilia* sp. * *Sphingomonas olei* * *Stenotrophomonas* sp. *Chryseobacterium* sp.
Fungus	*Cladosporium herbarum* * *Alternaria* sp. * *Epicoccum nigrum* * *Konda* sp. *Botrytis cinerea* *Aureobasidium* sp. * *Itersoniia perplexans* *Neoascochyta* sp.	*Cladosporium herbarum* * *Alternaria infectoria* * *Epicoccum nigrum* * *Phoma* sp. *Sporobolomyces* sp. *Aureobasidium pullulans* * *Periconia byssoides* *Gibellulopsis* sp. *Apiotrichum gracile*

Table I.5. Most abundant microbes during flax dew retting.

Culture-independent (16s/18s rDNAseq) studies from (Chabbert et al., 2020; Djemiel et al., 2017). The overall common species are denoted with '*'.

I.5.2. Hemp retting

The 16s/18s-rRNA-based method expanded the microbial inventory of hemp retting, identifying 25 fungal phyla and 9 bacterial phyla, compared to the 4 bacterial and 3 fungal phyla found in culture-based studies (**Fig. I.31**) (Law et al., 2020; Ribeiro et al., 2015; Tamburini et al., 2004). In three separate culture-independent studies conducted with nearly 5-year intervals and in different regions, bacterial species such as *Pantoea* sp., *Pseudomonas* sp., *Sphingomonas* sp., *Methylobacterium* sp., and *Rhizobium* sp. were consistently prevalent and dominant during hemp dew retting. Among fungal species, *Cladosporium* sp., *Phoma* sp., and the genus *Plectosphaerellaceae* were commonly identified, with *Cladosporium* sp. and *Phoma* sp. being particularly dominant. (**Table I.6**) (Law et al., 2020; Ribeiro et al., 2015). Comparing the microbial communities involved in flax retting, the top 10 bacteria include the same dominant species such as *Pseudomonas* sp., *Sphingomonas* sp., *Rhizobium* sp., and *Massilia* sp., and the top 10 fungi such as *Cladosporium* sp., *Phoma* sp., and *Aureobasidium* sp. are also significant contributors to the process (Chabbert et al., 2020; Djemiel et al., 2017).

Domain	**Riberio *et al.*, 2015 16s_18s_rDNAseq (Most abundant)**	**AD Law *et al.*, 2020 16s_rDNAseq (Top 10)**	**Bou Orm *et al.*, 2024 16s_18s_rDNAseq (Top10)**
Bacteria	*Escherichia coli* *Pantoea agglomerans* * *Pseudomonas fulva* * *Rhizobium huautlense* * *Massilia timonae* *Sphingomonas* sp. * *Methylobacterium* sp. * *Roseomonas aerophile* *Stenotrophomonas* sp.	*Aureimonas* sp. *Pantoea* sp. * *Pseudomonas* sp. * *Neorhizobium* sp. * *Massilia* sp. *Sphingomonas* sp. * *Methylobacterium* sp. * *Roseomonas* sp. *Stenotrophomonas* sp. *Polaromonas* sp.	*Pantoea* sp. *Pantoea agglomerans* * *Pseudomonas* sp. * *Allo-Neo-Para-Rhizobium* * *Sphingomonas* sp. * *Methylobacterium* sp. *
Fungus	*Cladosporium* sp. *Phoma* sp. *Plectosphaerella cucumerina* *Cryptococcus* sp.		*Cladosporium* sp. *Phoma* sp. Plectosphaerellaceae genus *Lectera* sp. *Didymosphaeria* sp. *Aureobasidium* sp. *Vishniacozyma* sp. Filobasidiaceae genus *Tilletiopsis* sp. Fungi genus

Table I.6. Most abundant microbes during hemp dew retting.

Culture-independent (16s/18s rDNAseq) studies from (Law et al., 2020; Ribeiro et al., 2015). The overall common species are denoted with '*'.

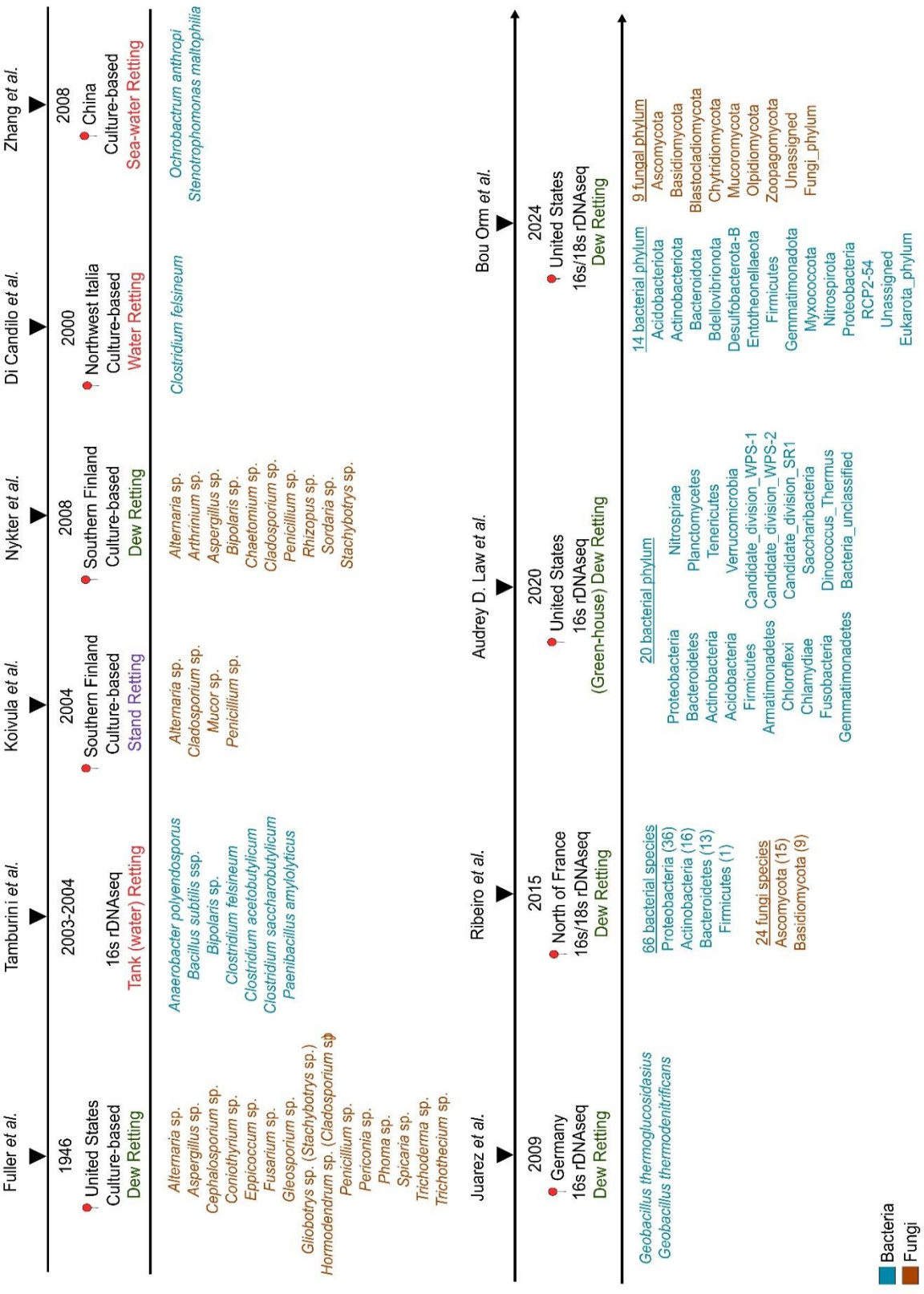

Fig. I.31. Timeline of Microbiology of Hemp retting.

The different micro-organisms (bacteria, fungi) established as involved during retting have been indicated by (Fuller et al., 1946; Di Candilo et al., 2000; Tamburini et al., 2004; Koivula et al., 2004; Nykter et al., 2008; Zhang et al., 2008; Valladares Juárez et al., 2009; Ribeiro et al., 2015; Law et al., 2020; Bou Orm et al., 2023).

I.5.3. Other retting studies (metagenomics based)

In other studies, Visi et al; 2013, identified Firmicutes, Proteobacteria, and *Bacteoidetes* as major phyla in **kenaf water retting** with 16s rRNA-based high throughput sequencing method (Visi et al., 2013) while in **2020**, Duan et al. (16s; 18s rRNA) found the presence of Ascomycota and Basidiomycota along with Proteobacteria and *Bacteoidetes* on the same (Duan et al., 2020). In 2022, (Xu et al., 2022) reported the dominance of *Bacteoidetes*, Proteobacteria and Firmicutes in kenaf water retting looking at the dynamic activities of *Actinobacteria* and *Clostridium*. On **jute water retting**, (Aktar et al., 2024) reported 915 genera (belonging to 53 phylotypes) where proteobacteria are dominating (60%). The most abundant genera are *Aeromonas* (7%), *Bacteroides* (3%), *Clostridium* (6%), *Desulfovibrio* (4%), *Acinetobacter* (4%), *Enterobacter* (1%), *Prevotella* (2%), *Acidovorax* (3%), *Bacillus* (1%), *Burkholderia* (1%), *Dechloromonas* (2%), *Caulobacter* (1%) and *Pseudomonas* (7%) (Aktar et al., 2024).

To summarize; the microbiology of retting significantly varies based on the type of retting process i.e. either aerobic dew retting or predominantly anaerobic water retting. In dew retting both fungal and bacterial strains are identified but fungal species, mainly from the *Ascomycota* phylum (and more or less *Mucoromycota* phylum) dominate. Proteobacteria is predominant among bacterial participants. On the other hand, water retting mainly involves anaerobic microorganisms, dominated by bacteria (Firmicutes) and a few fungi (from *Ascomycota* and *Basidomycota*) (Djemiel et al., 2017; Duan et al., 2020). All the culture-dependent and culture-independent studies applying powerful high-throughput DNA sequencing methods significantly enrich our understanding of the microbial communities involved in retting and their community dynamics. The role of these microbes in retting is to secrete various enzymes while feeding on the stem polysaccharides. The cumulative action of these enzymes (specifically cell wall degrading carbohydrate-active enzymes) degrades the tissue binding pectin's/xyloglucans, letting loose the fiber cells for easy mechanical extraction.

I.6. (Enzyme) Biochemistry of Retting

I.6.1. Dynamics of plant cell wall degrading enzyme in dew retting

The complexity of the plant cell wall, being a lignocellulosic material, led to the assumption that a mixture of enzymes, including cellulases, hemicellulases, and especially pectinases, is necessary for the retting of flax, similar to the natural microbial process associated with plant degradation into forest litter (Jenkins and Jenkins, 2003; D. Liu et al., 2015; Peters et al., 2019; Tláskal et al., 2021; Voříšková and Baldrian, 2013). However, the special feature of retting compared to the degradation of plant matter in the litter is its "controlled" nature, which should prevent the degradation of the cellulose wall of the fibers maintaining their optimal mechanical properties. It appears that while the decomposition process

may be similar to the degradation of plant matter in terms of the microorganisms and enzymes involved, the dynamics must be different. The work of Sharma and colleagues on retting enzyme was patented by Novo Nordisk and gave us Flaxzyme (Van Sumere, 1992) with successful retting qualities. But couldn't replace dew retting due to complex reasons including cost and industrial support (Akin, 2013; Sharma, 1992). Further studies at Clemson University, South Carolina, revealed that purified EPG from *Rhizopus oryzae* with oxalic acid alone was sufficient to separate flax fibers and other enzymes were not required (Akin, 2013; Akin et al., 2001).

The enzyme dynamics study, indeed showcases a fascinating interplay between all these enzymes from start to end of retting. Among a few studies (enzyme dynamics), Chabbert. et al. (2020), in their multimodal study of flax field retting, show the dynamics of 7 groups of enzymes (namely peroxidase, phenol oxidase, polygalacturonase, glucosidase, galactosidase, cellobiohydrolase, and xylosidase) interacting throughout the retting process and the resulting physicochemical changes in flax straw (Chabbert et al., 2020). The study found that polygalacturonase, phenol-oxidase, and peroxidase exhibit peak activity shortly after uprooting flax, followed by a gradual decline; while enzymes targeting hemicellulose (β-D-galactosidase, β-D-xylosidase) and cellulose (glucosidase, cellobiohydrolase) showed increasing activity during initial two weeks of retting before declining. This pattern is more or less consistent with the previous study of hemp dew retting under controlled conditions by Bleuze et al., 2018, where the activity of pectinase and hemicellulase increased during first two weeks and then continued without any significant changes.

PICRUSt predictions of bacterial enzyme dynamics from metagenomics, as demonstrated by Djemiel et al., 2017 (**Table I.7**), revealed that the hydrolytic enzyme potential for degrading various polymers is greater during the initial stages of flax dew retting (R0-R2/R3) compared to later stages (R2/R3-R6) (Djemiel et al., 2017). These predictive models provide insights into the enzymatic activities resulting from enzyme cocktails, such as glucanase activity, which is contributed by multiple Glucanases observed in global enzyme assays. PICRUSt, or Phylogenetic Investigation of Communities by Reconstruction of Unobserved States, is a bioinformatics tool designed to predict the functional potential of bacterial communities by inferring the abundance of enzyme activities and metabolic pathways using known sequences in databases like KEGG Orthologs, COGs, and CAZy (Langille et al., 2013). However, PICRUSt is limited to bacterial communities (until recently) and cannot predict the enzyme potential for fungal OTUs, showing the necessity of alternative direct methods like **metaproteomics** to study enzymes (especially cell wall degrading carbohydrate-active enzymes) in detail with precision, as shown by (Chirania et al., 2022; Tláskal et al., 2021).

Groups	Enzymes	PICRUSt CAZymes in Flax (Djemiel et al. 2017)
Xylanase	endo-β-1,4-xylanase exo-β-1,4-xylosidase	GH8, GH10, GH11, GH30, GH43, GH3, GH39, GH52, GH54
Arabinanase	eno-α-1,5-arabinanase	GH43, GH93
Arabinofuranosidase	α-L-arabinofuranosidase	GH3, GH43, GH51, GH54, GH62
Glucuronidase	β-glucuronidase α-1,2- glucuronidase	GH2, GH79, GH67, GH115
Xyloglucanase	endo-β-1,4-glucanase	GH5, GH12, GH16, GH74
Mannanase	endo-1,4-β-mannanosidase	GH5, GH26
Mannanase	endo- β-1,4- mannanosidase	GH1, GH2, GH5
Galactanase	endo-galactanase	GH53
Glucosidase	β-glucosidase	GH1, GH3
	ferulic acid esterase	CE1
	Acetyl xylan esterase	CE1, 2, 3, 4, 5, 6, 7
Endo-glucanases		GH5, GH6, GH7, GH8, GH9, GH12, GH23, GH48, GH44, GH45, GH51, GH61, GH74
Exo-glucanases _ cellobiohydrolase		GH7, GH48, GH5, GH6, GH9
LPMOs		AA9, AA10, AA11, AA13
Peroxidases	LIPs, MnPs, VPs, DyPs	AA2
Laccases		AA1_1

Table I.7. PICRUSt prediction of dew retting CAZymes from falx metagenomics.

Source: (Djemiel et al., 2017).

I.6.2. Details on plant cell wall degrading enzymes (CAZymes)

The predominant plant cell wall polymers such as pectin, hemicellulose and cellulose, together with aromatic polymers (lignin) and protein form a complex rigid structure, often called lignocellulose (Kubicek and Druzhinina, 2007). The proportions of these components vary between different plant species, leading to the need for different enzymes and methods to break down the plant cell walls. It requires a consortium of organisms (mainly fungi), starting with the colonization of living plants and ending with soil humus formation, or in our case the proceeding of the retting. Microorganisms use two main types of extracellular enzymatic systems – (a) hydrolytic systems (mainly pectinases, hemicellulases and cellulases) and (b) oxidative ligninolytic systems (mainly peroxidases and laccases) (Kubicek and Druzhinina, 2007). All these enzymes can be classified into two groups according to their targets and activities. Enzymes that act on carbohydrates are classified as CAZy (Carbohydrate-Active enzymes) (Cantarel et al., 2009), whereas enzymes that act on lignins in fungi are described as FOLy (Fungal Oxidative Lignin Enzymes) (Levasseur et al., 2008).

In the early 1990s, Bernard Henrissat and Pedro Coutinho developed the CAZy database, which classifies enzymes involved in glycobiology into CAZymes (Henrissat and Davies, 1997; Cantarel et al., 2009; Drula et al., 2022). CAZymes are categorized into five main classes – glycosyl hydrolases (GHs), glycosyl transferases (GTs), polysaccharide lyases (PLs), carbohydrate esterases (CEs), and auxiliary activities (AAs), with almost 7% containing a carbohydrate-binding motif (CBM) (Cantarel et al., 2009; Drula et al., 2022). GHs, PLs, CEs and AAs are particularly significant in case of plant cell wall degradation. CAZy enzymes are classified based on their amino acid sequences, which are compared and grouped into families using algorithmic methods like sequence alignment and Hidden Markov Models (Henrissat, 1991). For example, glycosyl hydrolases are classified into families and clans based on sequence similarity, catalytic mechanism, and structural features (**Fig. I.32**). (https://www.cazypedia.org/index.php/Sequence-based_classification).

GHs or Glycosyl hydrolases are enzymes, with currently 189 families (in 20 clans), mainly catalyze hydrolytic cleaving of glycosidic bonds and produce carbohydrate hemiacetal; but with exceptions (such as transglycosylases, phosphorylases, α-glucan lyases, and NAD-dependent glycoside hydrolases) that structurally and sequentially resembles GHs but without any hydrolytic activity (Davies et al., 2005; Henrissat and Davies, 1997).

PLs or polysaccharide lyses (currently with 43 families), break down polysaccharides with uronic acids using a β-elimination process resulting in unsaturated hexanuronic acid residue (and a new reducing end at the cleavage site) (Garron and Cygler, 2010; Henrissat and Davies, 1997).

CEs or carbohydrate esterases (currently with 20 families) remove acyl group from substituted saccharides. They can act on sugars acting as either ‘acid’ or ‘alcohol’ in the ester link. The most

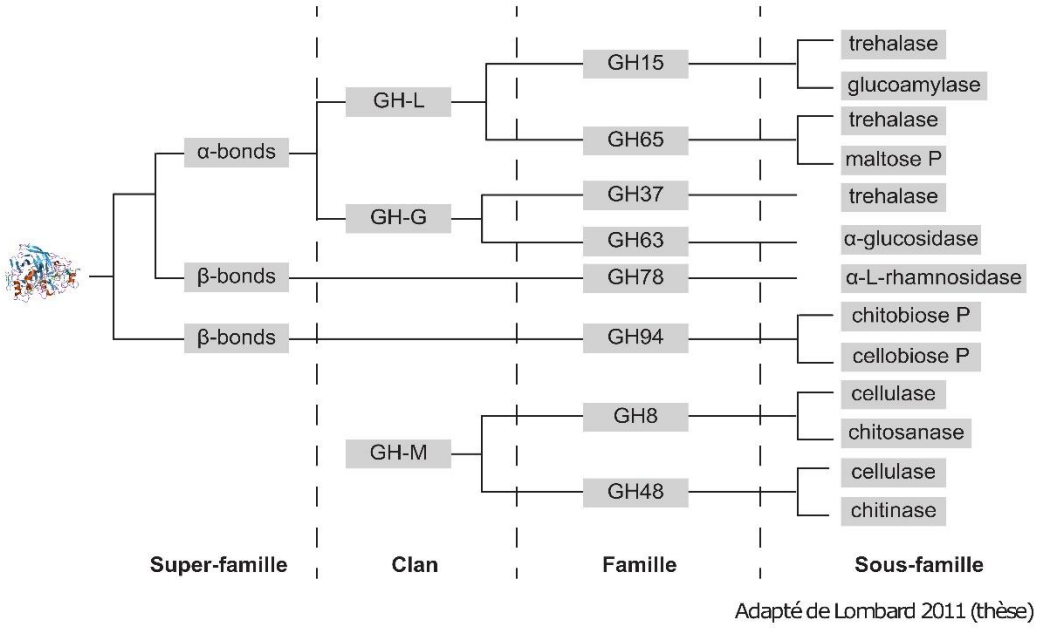

Fig. I.32. Classification of glycosyl hydrolases.

Source (Djemiel, 2017).

common mechanism involves a serine-histidine-aspartic acid catalytic triad (similar to classical lipase or serine protease) but some families also perform zinc-based catalysis (Davies et al., 2005; Henrissat and Davies, 1997).

The recently added auxiliary activity (AA) classes are catalytic proteins that help GHs, PLs, and CEs access carbohydrates. This class is currently comprised of 9 families of lignolytic enzymes and 7 families of lytic polysaccharide monooxygenases (LPMOs), reflecting their structural similarity (Davies et al., 2005; Levasseur et al., 2013). Identified CAZymes found in flax plants and during forest wood decomposition are proposed in Table 8.

I.6.2.1. Cell-wall pectin degrading enzyme

The pectinases are produced by various kinds of micro-organisms and are used extensively in multiple industries such as – the wine industry, agro-food processing industries, paper industry, extraction of plant fibers, etc. (Garg et al., 2016). Based on the mode of action, pectinase is broadly classified into three types – pectin esterase (CEs), pectin hydrolase (GHs), and pectin lyase (PLs). Pectin esterase (or specifically PMEs) removes ester-linked (methoxy) group from pectin (forming pectic acid) and makes it more accessible for other pectinases. Pectin hydrolase (polygalacturonase/PG and polymethylgalacturonase /PMG) breaks down alpha-1,4-D-galacturonic bonds in pectin. Based on the type of cleavage, they can be endo-acting (Endo-PGs) or exo-acting (Exo-PGs). Lastly, the pectin lyase (polygalacturonate lyase and polymethylgalacturonate lyase) catalyzes the cleavage of alpha-1,4-

glycosidic linkage (by trans-elimination reaction) between pectic acid and pectin and forms unsaturated galacturonan and methyl galacturonates, respectively; also classified based on cleavage type as endo and exo-acting pectin lyase. Moreover, endo and exo-acting rhamnogalacturonan hydrolase (RGA) and lyase (RGL) also help in pectin degradation, observed in pectinolytic system of *Aspergillus niger* (Garg et al., 2016; Kubicek and Druzhinina, 2007). The pectinases present in mature flax plants and released from microbes during dead wood decomposition is shown in **Table I.8**.

I.6.2.2. Cell-wall hemicellulose degrading enzyme

Hemicelluloses, accounting for 20-30% of plant cell wall biomass, are degraded by a diverse set of enzymes due to their heterogeneous nature. The key types of hemicelluloses include **xylans**, **xyloglucans**, and **(galacto-)glucomannans**, each requiring specific enzymatic actions for breakdown (Kubicek and Druzhinina, 2007). Hemicellulases have a simple structure with a catalytic domain (CD) and often a carbohydrate-binding domain (CBM). Catalytic domains are either glycosyl hydrolases (GHs) (eg. Mannanases, arabinofuranosidases, glucuronidases, etc) or carbohydrate esterases (CEs) (eg. Acetyl-xylan-esterase, feruloyl esterases, etc) (Juturu and Wu, 2013). **Xylans**, composed of β-1,4-linked β-D-xylose, are broken down primarily by endo and exo-acting β-1,4-xylanases and β-xylosidases. Xylanases cleave xylans into oligomers, which are then further broken down into xylose monomers by xylosidases. In the meantime, α-L-arabinofuranosidases remove arabinose from arabinoxylan side chain. In case of **xyloglucan**, it has β-D-glucopyranose backbone with xylopyranose substitution which is broken down by xyloglucan-specific hydrolases (exo and endo-acting xyloglucanase) and endoglucanases (eg. endo β-1,4-glucanase); while β-galactosidases hydrolyze the galactose containing sidechains. The β-1,4-mannosidic linkage in the **galacto-glucomannan** backbone is broken down by (endo and exo-acting) mannanases, while β-mannosidases remove β-D-mannose residues from the oligosaccharides. The efficiency of these enzymes is influenced by the number and position of side chains. Enzyme β-galactosidases also work here in removing galactose-containing side chains in galacto-glucomanan (Kubicek and Druzhinina, 2007). All these enzymatic systems operate synergistically (both inside chains and main backbone) to achieve complete hydrolysis of hemicellulose (Juturu and Wu, 2013; Kubicek and Druzhinina, 2007). The hemicellulases present in mature flax plants and released from microbes during dead wood decomposition are shown in **Table I.8**.

I.6.2.3. Cell-wall cellulose degrading enzyme

Cellulose (the most abundant biopolymer on earth) constitutes approximately 50% of plant biomass, comprised of β-1,4-glycosidic linked repeated D-glucose subunits, forming highly insoluble microfibrils via hydrogen bonds. Enzyme degradation of cellulose needs three key enzymes – cellobiohydrolases, endoglucanases, and β-glucosidases -

Groups	Enzymes	CAZymes in mature Flax (Chabi et al., 2017)	CAZymes in wood decomposition (Tlàskal et al., 2021)
Glycosyl hydrolases (GH)			
Hemicellulase	endo-β-1,4-xylanase	GH10_3,	GH10, GH11, GH141, GH30, GH43, GH5,
	exo-β-1,4-xylosidase	GH3, CBM22, GH31	GH120, GH30_2, GH39, GH43, GH5, GH52
	β-mannanase	GH5_7	GH113, GH134, GH26, GH5
	xyloglucan hydrolase	GH16	
	α-L-arabinofuranosidase	GH51, GH3,	
Cellulase/ Hemicellulase	β-glucosidase	GH1, GH3, GH17, GH31	GH1, GH116, GH3, GH30_6
	α -glucosidase		GH30
	β-galactosidase	GH35	GH110, GH27, GH36, GH97
	glucuronidase		GH115, GH67
Cellulase	endo/exo-β-1,4-glucanase	-	GH2, GH124, GH44, GH45, GH5, GH8, GH9
	cellobiohydrolase		GH48, GH6, GH7
AGP	β-glucuronidase	GH79_2	-
	α-1,2- glucuronidase		
Callose	glucanase	GH9, CBM43	GH128, GH152, GH157, GH17, GH158, GH87, GH81, GH64, GH71
Glycoprotein	mannosidase	GH38	GH5
Pectinase	polygalacturonase	GH28	GH28
	rhamnogalacturonase		GH78, GH106
Chitin	Chitinase, glucosaminidaase	-	GH18, GH19
starch	α-glucosidase		GH122, GH13, GH133, GH31
	glucoamylase	-	GH15, GH77
	α- amylase, β - amylase		GH119, GH13, GH57, GH14
Carbohydrate esterase (CE)			
Pectinase	pectin methyl esterase	CE8	CE8
	pectin acetyl esterase	CE13	
Glucoroxylan	acetyl xylan esterase		CE1, CE3, CE4, CE5, CE6, CE12, CE15
Polysaccharide lyase (PL)			
Pectinase	rhamnogalacturonan endolyase	PL4	PL4, PL11, PL9
	pectate lyase	-	PL1, PL10, PL2, PL3
Auxiliary activity (AA)			
Lignin/ phenolics	oxidoreductase	AA1	
	Peroxidase	AA2	
Chitin		-	AA10, AA11

Table I.8. CAZymes from living flax plant and from dead wood decomposition.
Source: (Chabi et al., 2017; Tláskal et al., 2021).

(Kubicek and Druzhinina, 2007) (all from GHs). Cellobiohydrolase (CBH) cleaves cellulose ends, while endoglucanase (EGL) targets amorphous regions (internal β-1,4-glycosidic bond in glucose chain), creating sites for CBH action. Beta-glucosidase converts oligosaccharides (cellobiose) to glucose. Often cellulases contain carbohydrate-binding modules (CBM) helping it to attach to the substrate (Kubicek and Druzhinina, 2007; Obeng et al., 2017).

The coper-dependent lytic polysaccharide monooxygenases (LPMOs) enzymes are also known to hydrolyze (or enhance the hydrolysis of) complex polysaccharides such as cellulose, hemicellulose, and chitin; by oxidatively cleaving the β-1,4- glycosidic bonds and creating more chain ends (oxidized C1 or C4) that makes these polysaccharides more accessible to hydrolytic enzymes. This oxidative cleaving mechanism involves the insertion of an oxygen atom into the glycosidic bond, facilitated by a copper ion at the enzyme's active site (Agger et al., 2014). The cellulases present in mature flax plants and released from microbes during dead wood decomposition are shown in **Table I.8**.

I.6.2.4. Lignin degrading enzymes

Lignin, a major component of cell walls, poses a significant obstacle to efficient saccharification of cellulose and hemicellulose. Fungi, particularly white-rot basidiomycetes, employ peroxidases and laccases (AAs) to degrade lignin. Peroxidases like lignin peroxidases (LiPs) and manganese peroxidases (MnPs) generate free radicles to break down lignin. Laccases, on the other hand, directly oxidize phenol and aromatic amines. Enzymes such as cellobiose dehydrogenase (CDH) play auxiliary roles, aiding in radical reduction and production of hydroxyl radicals for cellulose and hemicellulose modification (Kubicek and Druzhinina, 2007). The lignin/ phenolics degrading enzymes present in mature flax plants and released from microbes during dead wood decomposition are shown in **Table I.8**.

Microbes employ a combination of oxidative and hydrolytic mechanisms to degrade lignocellulosic material, making them important players in wood decomposition and maintaining the atmospheric carbon-nitrogen cycle (Kubicek and Druzhinina, 2007; Tláskal et al., 2021).

I.7. Evaluation of (physicochemical changes of) flax straw during dew retting

Dew retting reveals a fascinating interplay between microbes/plants and the environment. As the flax stem decomposes, serving as a food source for a constantly evolving community of microorganisms, their physical and chemical properties are dramatically transformed (Meijer et al., 1995; Sharma, 1986b), (**Fig. I.33A**). This is evident in the changing color of the stem surface, the break-down of its

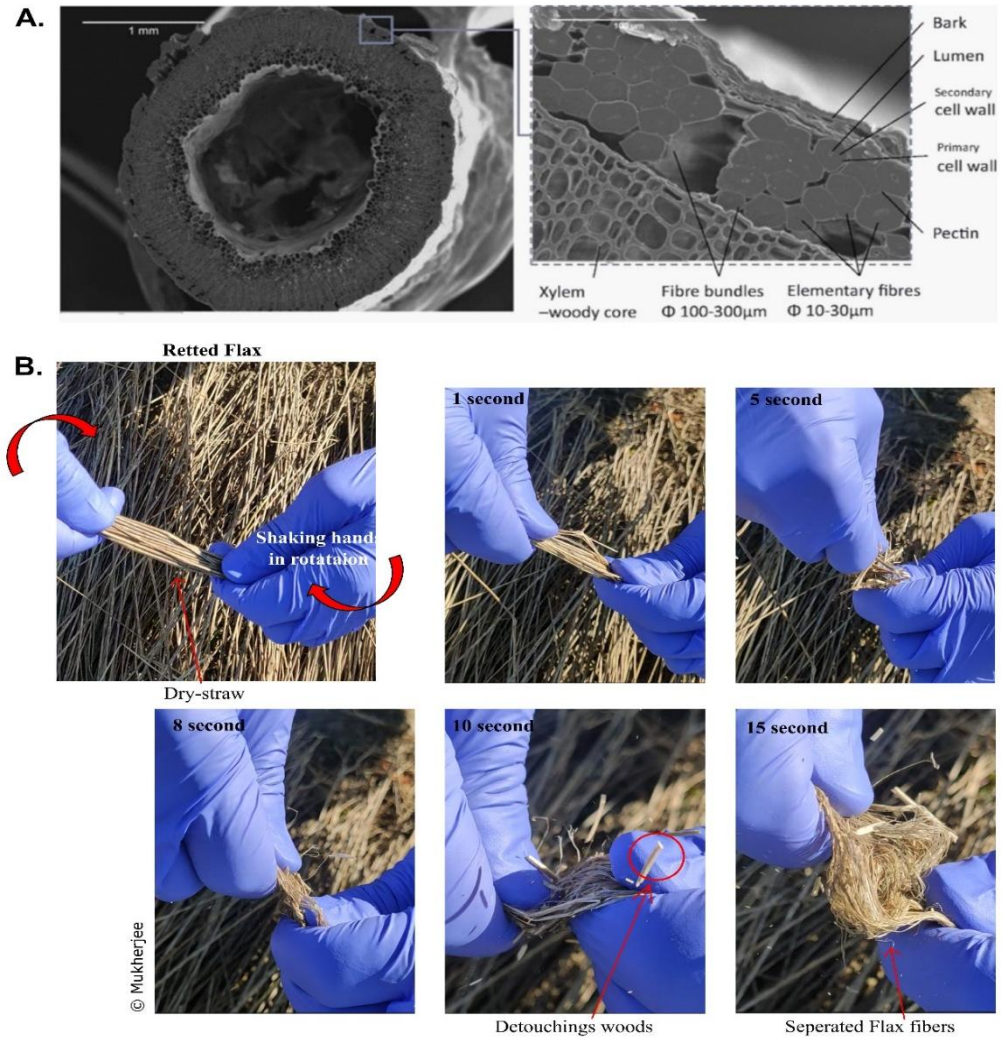

Fig. I.33. Retting disorganizes flax stem tissues and facilitates easy fiber detachment by applying mechanical force.

A: The (SEM) image shows effect of retting on flax stem. Source (Zhang et al., 2008). B: The image shows how after retting fibers are easily extracted from straw.

internal structure, reduced moisture content, and fiber characteristics like strength and diameter (Akin et al., 2000; Chabbert et al., 2020). All these changes lead to making fiber extraction easy. Indeed, **Fig. I.33B**, shows how the retting efficiency can be hand monitored. This parameter combined with color changes will help the farmer to decide if the retting should be continued or stopped. Otherwise, this approach that is simple to perform is empirical and might lead to variability from one farmer to another, resulting in a certain variability between the fiber batches.

During retting significant visual and colorimetric changes occur in plant stem. Colorimetry, a rapid and non-destructive technique, offers an objective method for determining colors and is thus valuably used for characterizing and classifying plant fibers (Akin et al., 2000; Bleuze et al., 2018;

Chabbert et al., 2020). The colorimetric study on hemp dew retting by Bleuze et al (2018) categorized the retting process into three stages; initial (pre-retting), intermediate (Day 7-28), and final (Day 42), highlighting the dynamic changes in stem color. Initially, bright green stems become yellow after one week with black spots appearing in two weeks; and pale grey (with more back spots) in four weeks, finally turning black grey with wide-spread black spots in six weeks (Bleuze et al., 2018; Mazian et al., 2018). These changes are quantified with the CIELab color space system; which quantifies color using coordinates in 3-D space: L*(lightness), a*(red-green), and b*(yellow-blue) (Bleuze et al., 2018). The study reported a significant decrease in L* a* and b* values; explaining a transition from light to dark colors and a shift from green to achromatic grey. A similar feature has been reported on flax stem surface color change in dew retting by Chabbert et al (2020), where decreasing a* and b* values are accompanied by increasing L*, indicating (deep-colored) yellow-green stems are becoming (pale-colored) grey. These changes are explained by associating with degrading plant pigments (photodegradation, biodegradation) and microbial colonization on plant stems during retting (Akin et al., 2000; Bleuze et al., 2018; Chabbert et al., 2020; Martin et al., 2013).

The microbial degradation process of retting significantly impacts the chemical composition of plant stems. Scanning electron microscopy and chemical analysis showed that in dew retting of flax, the pectin-rich portion of the flax stem decomposes primarily, with a significant decrease in galacturonic acid and arabinose within first two weeks (Chabbert et al., 2020). This decomposition occurs not only in the middle layer and primary cell walls of the outer tissue but also in the cambium and differentiated xylem cells of the inner tissue. Microbial colonization and enzyme activity initiate the dissociation of fiber bundles in the outer tissue while in the inner tissue, the cambium layer and outermost differentiated xylem layer disappear. Cellulose and hemicellulose of the secondary cell wall remain virtually unchanged, as evidenced by stable levels of glucose and mannose (Chabbert et al., 2020). Overall, a similar pattern has been found in hemp dew retting (Bleuze et al., 2018; Mazian et al., 2018). Environmental factors such as severe water loss may also contribute to these changes (Chabbert et al., 2020).

Technical flax fibers with longer retting duration (4 to 8 weeks) showed a progressive increase in thermal stability, according to thermogravimetric analysis (TGA) by Chabbert et al, 2020 (Chabbert et al., 2020). This is demonstrated by a change towards higher values in later retting stages in peak degradation temperature of the main component, cellulose (Barneto et al., 2010; Chabbert et al., 2020). This pattern is consistent with the reported decline in the content of non-cellulosic polysaccharides (hemicellulose and pectin), which suggests the removal of these components during retting, might positively impact the cellulose crystallinity (Barneto et al., 2010; Chabbert et al., 2020; Mazian et al., 2018).

The study of flax fiber mechanical strength during retting shows, that tensile strength and Young's modulus are higher at the latter stages of retting (week 6 to 8) as compared to the early stage (week 4) (Chabbert et al., 2020). The stem diameters/retting week are said to be responsible for this, as week 4 has a bigger diameter compared to later stages (Chabbert et al., 2020). A similar trend has been seen in hemp dew retting, where the tensile strength and tensile modulus of un-retted fiber (day 0) increase by two-fold at week 5 of retting, followed by a very slight decrease in week 9 (Mazian et al., 2018). Although prolonged retting is reported to have minimal impact on fiber tensile properties (Charlet et al., 2010; Mazian et al., 2018), over-retting can significantly degrade them (Chabbert et al., 2020; Placet et al., 2017). Tensile properties can vary more or less, depending on the method and of course cultivars.

I.8. Factors affecting field retting

Retting is a complex natural process affected by many variables, both biotic and abiotic (**Fig. I.34**), and obtaining uniform good quality fiber is a hard and empirical challenge (Chabbert et al., 2020; Sharma and Faughey, 1999). These factors affecting retting include; climatic conditions during retting, microbial population and load in and around the niche (soil and stem), stem's maturity at harvest, weed contamination, soil pH, and water holding capacity, etc. In field retting, uprooted flax stems are left on the ground for several weeks. Under damp weather conditions (European summer), the flax stems become colonized by various fungi and yeast species, producing a spectrum of polysaccharide-degrading enzymes, primarily pectinolytic (Meijer et al., 1995). These enzymes play a pivotal role in macerating and disrupting the middle lamella of the cortical cells surrounding fiber bundles (Akin, 2013; Brown and Sharma, 1984; Meijer et al., 1995). Notably, Field retting's efficacy is weather-dependent, ceasing in dry weather and causing under-retted straw. Continuous wet conditions lead to cellulase production, inducing non-enzymic degradation and fiber decay (Bratt et al., 1988; Brown and Sharma, 1984), resulting in unfavorable variations in fiber characteristics. The effects of microbial enzymes are naturally substrate-dependent; the substrate, the flax straw, depends on the flax cultivar, maturity at harvest, showing density, etc.

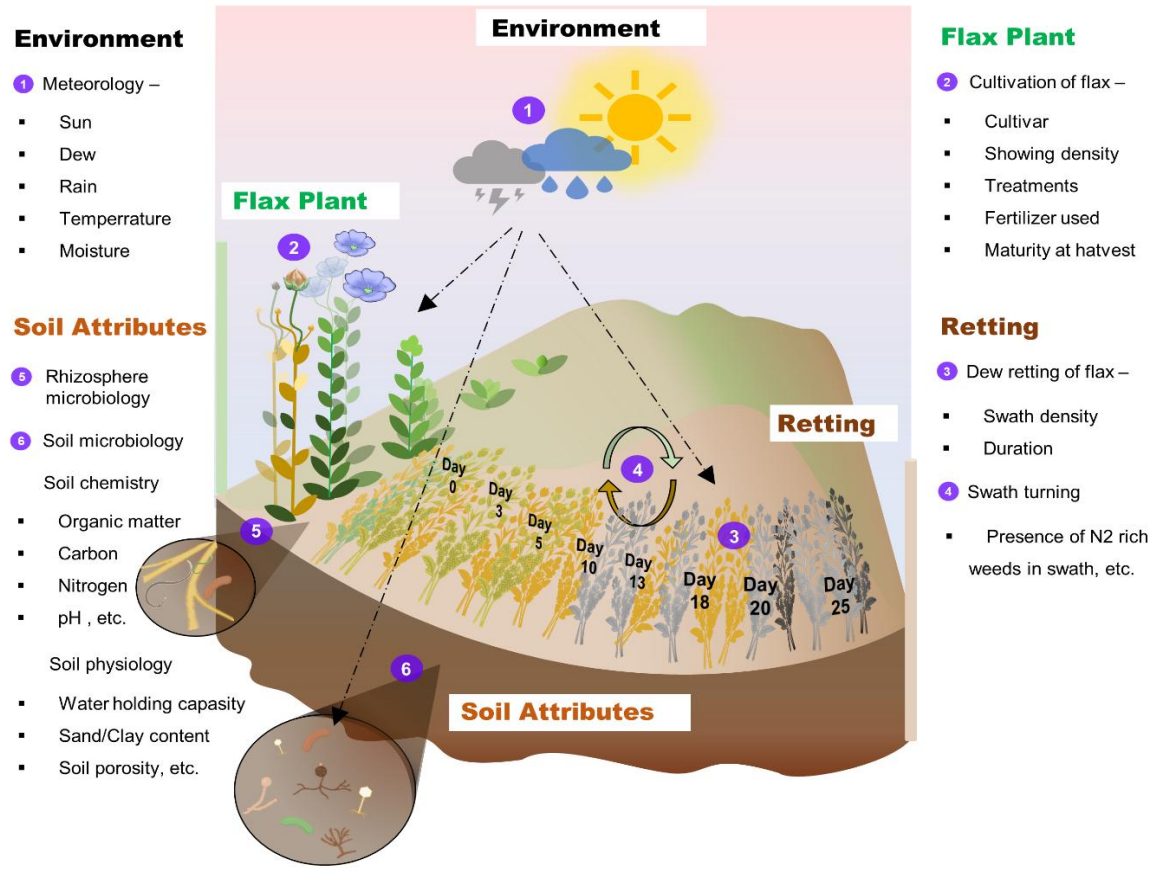

Fig. I.34. Factors affecting field retting.

Farmers commonly acknowledge that the maturity of flax plants directly impacts, the retting process, with younger plants, typically at the flowering or green capsule stage, rets more rapidly compared to more mature flax with yellow or brown capsules (Djemiel et al., 2017). This difference is thought to be due to the variability in the proportion of cellulosic and non-cellulosic components (deposition or modification of pectin /lignin content during growth) (Akin et al., 2001; Brown and Sharma, 1984; Djemiel et al., 2017; Meijer et al., 1995; Sharma, 1992). Metagenomic studies by Djemiel et al, 2017 support this hypothesis after finding no significant difference in microbial communities and colony dynamics between early and standard harvested flax retting (Djemiel et al., 2017).

I.9. Determination of degree of flax dew retting

The few studies aimed at controlling field retting until 2024 suggested that a more sensitive method is needed to determine flax's initial rettability and monitor the degree of retting during field retting (Meijer et al., 1995). Seaby and Mercer (1984) (Seaby and Mercer, 1984) described a device to measure retting

in individual stems, producing consistent results. But, it needs many trials, and the results might be influenced by harvest time and different varieties (Meijer et al., 1995; Seaby and Mercer, 1984). Other approaches, including assessing loss of dry weight (Donaghy et al., 1992; Meijer et al., 1995) and caustic weight loss (dry weight loss after treatment with caustic soda, Brown et al., 1986 (Brown et al., 1986)), prove insufficiently sensitive for accurately gauging the degree of retting. While Kessler et al. (1994) explored near-infrared spectroscopy for this purpose, its potential remains unclear, requiring direct measurements for calibration (Meijer et al., 1995). In 2004, Sharma and Reinard examined the use of visible and near-infrared spectroscopy to assess fiber fineness during the mechanical processing of dew-retted fibers. While they obtained significant results, they highlighted the method's expense and the need for expertise in operating the instrument (Sharma and Reinard, 2004). Later in 2008, JA. de Haseth et al. successfully adapted a near-infrared (NIR)-chemometric method for assessing flax shive to a low-cost, durable instrument suitable for at-line use in processing plants (de Haseth et al., 2008). However, monitoring the retting of flax straw still poses challenges. The cation exchange capacity and ash content measurements suggested by Morvan et al. (1985) and Kessler et al. (1994) are only applicable to scutched fibers and do not extend to intact stems (Meijer et al., 1995).

Rosemberg and de Franca (1967) made strides in monitoring water retting by measuring the galacturonic acid content of the retting liquid, reflecting pectin hydrolysis. However, the organic acid's metabolism complicates the reliance on galacturonic acid content as a sole indicator of retting (Meijer et al., 1995). Evaluating pectin content and its reduction during controlled water retting in flax stems is effective for monitoring retting and assessing stem rettability. Meijer (1995), shows the initial pectin content, starting at 25-30 g/kg of the stem, decreases to 7-10 g/kg upon completion of retting, whether in the field or through water retting. Water retting after partial or total field retting yields a similar final pectin content, suggesting the persistence of the same pectin fraction. However, the scientists conclude measuring pectin content is time-consuming and less practical for a large-scale, periodic recording of retting degrees in flax crops (Meijer et al., 1995).

Estimating the degree of retting appears challenging when relying solely on a single factor. Scientific studies revealed that the quality of the flax fibers depends on many factors (as described in **§ I.8**). A comparative approach involving the examination of both **subjective** and **objective methods** to assess flax straw cultivars & fiber quality after dew retting was undertaken by Sharma and Faughey in 1999 (Sharma and Faughey, 1999). They conclude that the microbial breakdown of stems during retting can be detected from the reducing lipid, ash, and nitrogen contents but precision requires studying many replicates.

Now the question arises; complementing chemical changes in straw during retting with other biological changes can increase the chance of a good degree of retting estimation?

Still, the succession of enzyme mixtures during filed retting is not known. Many scientists thus delved into the intricacies of multiscale analysis to define retting and the rettability of bast fibers. Chabbert. et al. (2020) reported changes in (selected groups of) enzyme dynamics, biochemical compositions, straw color, and fiber mechanical properties during field retting. The trick might be to correlate all these changes together. In this study, we recreate the multimodal analysis of the biology of flax field retting; but with a comparative approach between adjacent fields. This is to define any possible pattern in retting. Statistical correlation (and a huge data set) may give us the model (resembling multimodal remote sensing) to specify the retting and rettability of the flax stem (Karmakar et al., 2024).

I.10. Possibility of artificial intelligence-based decision-making tool-box (Emerging Agriculture 4.0)

Agriculture, the backbone of civilization, faces a critical challenge, with a projected global population of 11 billion by 2050; ensuring food security requires a significant boost in production. Here's where smart agriculture, also known as Agriculture 4.0, steps in as a game-changer (Klerkx et al., 2019; Mukherjee et al., 2021). The advanced approach can be a breakthrough for non-food agriculture such as fiber production.

Simply increasing production isn't enough, sustainable practices are key, as highlighted by the UN's Food and Agriculture Organization (FAO). Smart agriculture tackles this by utilizing cutting-edge technologies like AI, robotics, and the Internet of Things (IoT) to optimize resource use and agricultural practices, aiming for sustainability, increased production, and reduced quality variability (Fortino et al., 2018; Yang et al., 2021). For instance, sensors monitor soil health and weather patterns, while robots (vehicles/drones) precisely apply fertilizers (Yahya, 2018). Through real-time data collection, farmers can make informed decisions, resulting in increased productivity (more food with fewer resources), reduced environmental impact (less water usage, optimized fertilizer/fungicides/pesticides application, and so improved soil health), and enhanced efficiency (automated tasks and optimized workflows) (Griesche and Baeumner, 2020; Klerkx et al., 2019; Rose et al., 2021; Yahya, 2018).

Smart agriculture is not a sudden invention. It's the culmination of past industrial revolutions that paved the way for advanced machinery and technology (Rose et al., 2021; Yahya, 2018). The synergy of these revolutions has led to the era of smart agriculture. Similar to how steam engines initiated ‘Industry 1.0’ and ‘Agriculture 1.0’ relied on muscle power, electricity-powered ‘Industry 2.0’ and

'Agriculture 2.0' saw production increases with steam and electricity. 'Industry 3.0' introduced robots and automation, reflected in 'Agriculture 3.0' with complex machinery automating tasks (Smil, 2018).

Currently, in 'Agriculture 4.0', the era of Digital Farming, technologies like AI, Big Data, and IoT, combined with advanced biological and chemical sciences, enable the creation of **biosensors** and **data-driven farms (Fig. I.35)**. This includes activities such as analyzing soil moisture and air humidity, predicting harvest times with drones (by color sensing), enhancing yields (cumulative monitoring of soil & plant health), reducing environmental impact (by eliminating weeds without insecticides, using standardized quantity of fertilizer, water), and improving product quality.

Biosensors, as defined by the International Union of Pure and Applied Chemistry (IUPAC), utilize biochemical reactions mediated by various elements like **enzymes**, **antibodies**, and whole cells **to detect chemical compounds** through electrical, thermal, or optical signals. Biorecognition elements in biosensors primarily include antibodies, aptamers, nucleic acids, enzymes, and occasionally other proteins or bacteriophages. Antibodies are crucial for their high binding constants in detecting contaminants and pathogens, while aptamers offer a cost-effective and reproducible alternative. Nucleic acids find use in DNA hybridization assays, particularly for detecting microorganisms. Enzymes serve dual roles as labels and biorecognition elements, while bacteriophages provide specificity in detecting bacterial cells (Griesche and Baeumner, 2020).

Between 2015 and 2019, research on biosensors for sustainable agriculture lagged behind those focused-on food safety, with an emphasis on detecting pathogens and marker molecules relevant to plant health and fertilizer management (Griesche and Baeumner, 2020; Wang et al., 2022). Electrochemical biosensors were prevalent due to their simplicity and cost-effectiveness, with some optical lateral flow assays also used. Notable advancements included biosensors for viruses, fungi, and to a lesser extent, bacteria or oomycetes, with methyl salicylate and nitrate being significant markers. For instance, a methyl salicylate **bio-enzyme biosensor enabled plant infection detection via volatile organic compound analysis**, while a nitrate biosensor by Nicolas Plumeré's group facilitated electrochemical quantification in plant juice (Griesche and Baeumner, 2020). Soil analysis biosensors targeted heavy metals and pesticides using various biorecognition elements, including DNAzymes, aptamers, and whole-cell biosensors, with engineered bacteria offering colorimetric outputs for contaminants. Prospects foresee expanded biosensor applications in agriculture, bolstering sustainable practices by optimizing resource utilization and reducing toxin and pesticide overuse (Griesche and Baeumner, 2020; Wang et al., 2022; Yahya, 2018). Optimizing a biosensor that can detect optimal dew retting is indeed possible with accurate retting markers. In our work, along with studying the retting at different scales (biology, chemistry, biochemistry, biophysical /physical level), we will try to find biological markers to

distinguish good standards for retting that can improve fiber quality homogeneity. These markers can be, the sudden changes in certain enzyme ratios (polygalacturonase: cellulase), a ratio of peri phloem trace-monosaccharides (fucose: xylose: galacturonic acid: galactose), a decrease in major pectin peak (near 1732,9cm-1) from retting stem surface detected by FTIR or the series of straw color change detected by remote sensing.

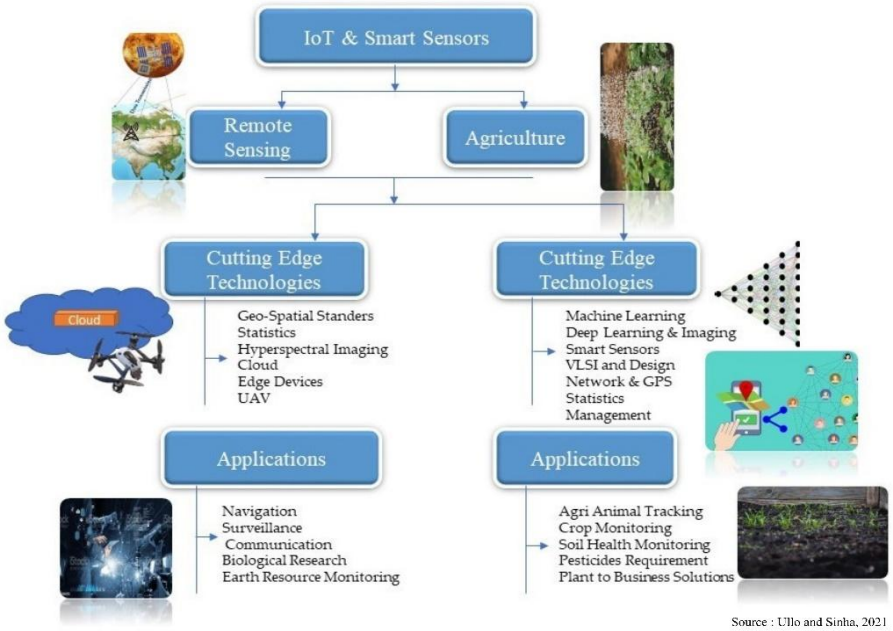

Fig. I.35. Use of sensors in agriculture. Source: (Ullo and Sinha, 2021).

I.11. Objective of the thesis work

As it has been assessed in the introduction chapter, plant bast fibers, traditionally exploited in the textile industry, can represent an ecologically virtuous alternative to the synthetic fibers currently massively used in the textile industry. In addition, natural fibers are now being used to replace synthetic fibers in composite materials as they are more respectful of the environment and will contribute to the planned end of petro-based resources. Among fiber crops, flax (*Linum usitatissimum* L.) is an economically important species in France with a production of 861 kt in 2015, including 137 kt, mainly used for the materials industry (FranceAgrimer, February 2016 edition, https://www.franceagrimer.fr/Actualite/Filieres/Tabac/2016). The need for plant fiber will increase in the very near future, and improving production techniques to obtain fiber of homogenous quality in large amounts will be the challenge of these next years.

Industrially, the fibers must be dissociated from the plant stem by a succession of processes that start with the retting step (Paridah et al., 2011). As mentioned in the introduction, retting introduces

variability in fiber quality both within and between flax batches, varying from year to year and across different fields. In Europe, this step is primarily conducted via dew or field retting, where the entire uprooted flax plant is left on the ground for several weeks. During this period, microorganisms begin to colonize the stem's surface and interior, leading to the partial degradation of specific plant tissues and cell wall components (Djemiel et al., 2017; Chabbert et al., 2020). The process starts with the breakdown of outer tissues like the epidermis, cortical parenchyma, and fiber bundles. To release the elementary fibers, the cohesion between cells in these tissues, as well as between fibers within the bundles, must be enzymatically degraded. Microorganisms play a key role in this step, breaking down pectins and hemicelluloses, the cell wall polymers responsible for binding fibers. This degradation facilitates mechanical fiber extraction and improves the quality and performance of the fibers (Martin et al., 2013).

It appears from the literature that despite an increasing knowledge of the biological, chemical, and physical mechanisms that occur during retting, there is no real-time standardization of flax dew retting and farmers still decide when to stop retting depending on their experience. Constant fiber quality management of dew-retted flax is still very much empirical. Farmers, inmany cases, depend upon the straw color change or manual in-hand evaluation of ease of fiber separation (Fried test) and decide to stop retting (Martin et al., 2013). As retting is a complex natural process affected by many variables (Chabbert et al., 2020; Djemiel et al., 2020; Meijer et al., 1995; Sharma, 1992), obtaining uniform good quality fiber is still challenging. Therefore, retting, although it is necessary for obtaining the fibers, introduces a significant variability in the quality of the latter. This variability is a brake on the introduction of plant fibers in mass industries.

We believe that the use of sensors and artificial intelligence to help the farmer in deciding to harvest flax stems after retting will help to remove this lock. However, this requires a deeper understanding of the biological, biochemical, and physical changes during retting to identify reliable and consistent retting markers, making it a complex but crucial endeavor. This is the objectives of the “FlaxTronic” (I-Site PEARL 2021:2024) project that has been proposed by the consortium including the Unité de Glycobiologie Structurale et Fonctionnelle (UGSF, UMR 8576) and the Institut d’Electronique de Microélectronique et de Nanotechnologie (IEMN, UMR 8520), the GEMTEX laboratory (expertise in textile and composites; led by Prof. Damien Soulat, they provided in-lab fiber mechanical characteristics) and the company “Van Robaeys Fréres ®”. The Van Robaeys Fréres ® contributes its expertise in monitoring flax dew retting and provides the fields in Bavinchove (2021) and Killem (2022) for research purposes. This project aims to develop a comprehensive database of biological, biochemical, and physical parameters involved in the retting process, which will be further used to create an intelligent toolbox that would enable farmers to monitor and objectively characterize the maturation

of the flax fiber during dew retting. The objectives and the work that has been performed during the thesis are derived from this project. To reach its objective, the 'FlaxTronic' program was planned to be achieved through the following steps (**Fig. I.36**), representing the objectives of the thesis:

1. Acquiring a deeper understanding of the biology of dew retting and assessment of the biological origin of the variability introduced by the retting process.
2. Question the relevance of using vibrational spectral approaches (with RAMAN/FT-IR) to provide a tool (at the level of chemical bonds) for monitoring retting in the field.
3. Evaluate the feasibility of using physical markers such as the color spectral changes of the stem to monitor retting in the field.
4. Discuss how to obtain a toolbox by combining literature, biological, spectral, and physical results.

Objective 1 : Acquiring a deeper understanding of the biology of dew retting and assessment of the biological origin of the variability introduced by the retting process.

As we saw previously from the bibliography in the introduction part, the retting process involves the controlled microbial decomposition of the plant cell wall polymers that bind the fibers together and to surrounding tissues inside the stem, to allow an easier separation. Although enzyme assays have been employed to define the enzymatic dynamics in cell wall-degrading enzymes during the retting process in both flax (Chabbert et al., 2020; Sharma, 1992) and hemp (Bleuze et al., 2018; Liu et al., 2017), they still represent global activities and do not allow for the identification of individual proteins and the microorganisms that secrete them. The metabarcoding was successfully used to inventory the microorganisms involved in retting (Chabbert et al., 2020; Djemiel et al., 2017) but only gave truncated predictions about the protein involved in the process. However, these two approaches, as informative as they are, may not fully describe the link between microbial communities and their enzymes involved in the retting process. To overcome these limitations, we propose to use metaproteomics for the first time to study flax dew retting. Recent studies on the degradation of forest litter and lignocellulosic biomass (Chirania et al., 2022; Hori et al., 2018) have shown that a metaproteomic approach represents an interesting strategy that can be used to precisely identify individual enzymes as well as the microorganisms producing them. Applying this approach to flax retting, combined with global

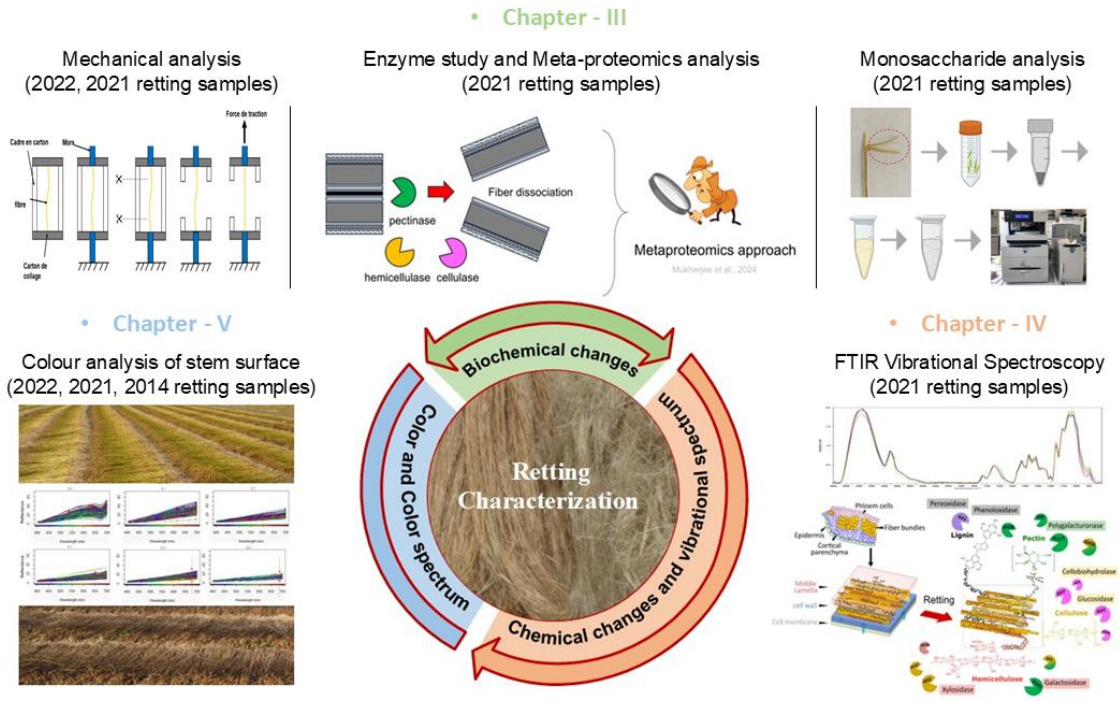

Fig. I.36: Three major segments for multimodal analysis of flax dew retting.

enzymatic activities and wet chemistry of cell wall polymers will allow the identification of the enzymes produced by the retting microbial communities, potentially leading to a more comprehensive understanding of the retting process. In addition, we sampled three adjacent fields showing contrasting "in fine" fiber qualities. We propose to apply the combined analysis on the two most contrasted of them to determine whether differences in the dynamics of enzymes and microorganisms can explain these differences. The details of these studies are described in **Chapter III** (submitted article entitled "Metaproteomics identifies key cell wall degrading enzymes and proteins potentially related to inter-field variability in fiber quality during flax dew retting").

The microbiology of hemp dew retting is explored with the same approach already used for flax (Chabbert et al., 2020). Identified for its expertise in flax retting, our laboratory was required to take part in a project to study hemp retting. The project aims to make the links between global enzymatic changes and microbiological dynamics during the hemp dew retting in the south of France, questioning the effect of watering retting swaths during the process. In that study global enzymatic activities were combined with a metagenomics approach, added with PICRUSt-based CAZymes prediction to describe the biology of hemp retting. We establish the global enzymatic activities dynamic presented in **Chapter III**. The Transferability of the metaproteomic approach to study hemp retting will be discussed. The

results of this collaboration are featured in a submitted article entitled “High-throughput sequencing reveals microbial community dynamics during hemp field retting” (Bou Orm et al., 2024).

Objective 2 : Question the relevance of using spectral approaches such as RAMAN/FTIR to provide a fine tool for monitoring retting in the field.

For many decades, vibrational spectroscopies such as RAMAN or FT-IR (Fourier Transform Infra-Red) have been often used in industry, to establish diagnostics, the quality of alimentary products, the origins of raw nutritional components, genius/species of plants, etc. FT-IR appears to also be a valuable tool to monitor cotonisation of flax fibers (Zimniewska et al., 2022), the comparison of osmotic- water- or dew retting of flax and hemp (Różańska et al., 2023), the comparison of retting processes (mechanical, enzymatic, chemical and dew retting) in many natural plant fibers (including flax and hemp) in the context of fiber-reinforced composites (Lee et al., 2020).

Looking for an efficient monitoring method that can be applied in the field and can lead to the identification of a significant “peak/marker” that indicates its completion, we propose to follow the chemical transformation of flax outer tissues during specific stages of dew retting using FT-IR. To question the inter-field variability aspect already evoked and so to improve the reproducibility of the method, the monitoring of the retting process in two adjacent fields was undergone. These fields present different scutched fiber qualities. Two approaches were investigated: ‘*a priori*’ in which only one single chosen peak/marker (from literature) was tested, and a ‘without *a priori*’ approach, whole spectra, were considered. To achieve this second approach, multivariate analysis (PCA, (s)PLS-DA), has been defined in order to identify significant peaks/markers characteristic of each retting stage. These peaks/markers will help to determine the well-starting retting process and help to estimate the optimal endpoint retting time. Both approaches aim to standardize and enhance control over the variability introduced by the retting process. Once established, those peaks/markers could be applied on a standard theoretical spectrum in portable FT-IR handle-device, in order to evaluate the level of retting, directly in distinct fields (Cebi et al., 2023). The details of FT-IR spectroscopic studies of retting are discussed in **Chapter IV**.

Objective 3: Evaluate the feasibility of using physical markers such as spectral changes in stem color to monitor retting in the field.

The visual changes in stem surface color during dew retting have been described a few times in the literature (Bleuze et al., 2018; Bou Orm et al., 2024) and are still used as a criterion to define the state of retting by experts (Fried test). Until now, the color changes had been evaluated with the CLEb method (RGB) and no comparison between different years or different retting processes has been carried out to confirm the reproducibility, and therefore, the relevance of using this approach to monitor retting. We

propose to enrich the database by measuring color changes as a spectrum extending over all wavelengths of the visible spectrum (400 nm to 700 nm). The laboratory has a collection of dried stems from different retting campaigns (2014, 2021, 2022), corresponding to samples taken at different time points of the kinetics. We believe that acquiring the spectra of each sample, coupled with a multivariate statistical analysis of all the spectra, will enable us to identify wavelengths or patterns of interest for the main stages in the retting process. Color analysis might represent a convenient non-destructive method to monitor retting stages and to question its progress. Moreover, this method can be easily applied and automated using for example cameras fixed on drones driven by artificial intelligence which can not only acquire the data but also interpret the spectral images and send warnings when retting is at its optimum. The details of the visual color change of flax straw surface during retting are discussed in **Chapter V**.

Objective 4 : Based on the results obtained and the literature, discuss how to obtain a toolbox combining biological, spectral, and physical approaches.

The ultimate objective of 'FlaxTronic' project was the construction of an intelligent "toolbox" combining several relevant markers that can reliably and stably describe the progress of the retting process and identify the best time to harvest the stems. Unfortunately, objectives 1 to 3 took longer time than expected, and each of the methods used has required a more or less long optimization and development time. Finally, we do not have the time within the framework of this thesis to set up the statistical analyses that would be required to identify relevant markers among all the parameters that were evaluated. Nonetheless, in the last chapter entitled "Discussion and Perspective", all results will be discussed together and statistical solutions that can be used to complete the construction of the toolbox will be proposed. Moreover, we will also discuss how all these results taken together can be useful to design tools to rationalize retting (in **Chapter VI**, via discussions, conclusions, and perspectives).

I.12. Reference

Abou-Elela, S.I., Ali, M.E.M., Ibrahim, H.S., 2016. Combined treatment of retting flax wastewater using Fenton oxidation and granular activated carbon. Arabian Journal of Chemistry 9, 511–517. https://doi.org/10.1016/j.arabjc.2014.01.010

Ageeva, M.V., Petrovská, B., Kieft, H., Sal'nikov, V.V., Snegireva, A.V., van Dam, J.E.G., van Veenendaal, W.L.H., Emons, A.M.C., Gorshkova, T.A., van Lammeren, A.A.M., 2005. Intrusive growth of flax phloem fibers is of intercalary type. Planta 222, 565–574. https://doi.org/10.1007/s00425-005-1536-2

Agger, J.W., Isaksen, T., Várnai, A., Vidal-Melgosa, S., Willats, W.G.T., Ludwig, R., Horn, S.J., Eijsink, V.G.H., Westereng, B., 2014. Discovery of LPMO activity on hemicelluloses shows the importance of oxidative processes in plant cell wall degradation. Proceedings of the National Academy of Sciences 111, 6287–6292. https://doi.org/10.1073/pnas.1323629111

Akin, D.E., 2013. Linen Most Useful: Perspectives on Structure, Chemistry, and Enzymes for Retting Flax. ISRN Biotechnology 2013, 1–23. https://doi.org/10.5402/2013/186534

Akin, D.E., Epps, H.H., Archibald, D.D., Sharma, H.S.S., 2000. Color Measurement of Flax Retted by Various Means. Textile Research Journal 70, 852–858. https://doi.org/10.1177/004051750007001002

Akin, D.E., Foulk, J.A., Dodd, R.B., McAlister, D.D., 2001. Enzyme-retting of flax and characterization of processed fibers. Journal of Biotechnology, Biotechnology in the Textile Industry - Perspectives for the New Millennium 89, 193–203. https://doi.org/10.1016/S0168-1656(01)00298-X

Akin, D.E., Gamble, G.R., Morrison III, W.H., Rigsby, L.L., Dodd, R.B., 1996. Chemical and Structural Analysis of Fibre and Core Tissues from Flax. Journal of the Science of Food and Agriculture 72, 155–165. https://doi.org/10.1002/(SICI)1097-0010(199610)72:2<155::AID-JSFA636>3.0.CO;2-X

Aktar, N., Mannan, E., Kabir, S.Md.T., Hasan, R., Hossain, M.S., Ahmed, R., Ahmed, B., Islam, Md.S., 2024. Comparative metagenomics and microbial dynamics of jute retting environment. Int Microbiol 27, 113–126. https://doi.org/10.1007/s10123-023-00377-7

Allaby, R.G., Peterson, G.W., Merriwether, D.A., Fu, Y.-B., 2005. Evidence of the domestication history of flax (Linum usitatissimum L.) from genetic diversity of the sad2 locus. Theor Appl Genet 112, 58–65. https://doi.org/10.1007/s00122-005-0103-3

Allen, L.A., 1946. Recent developments in the microbiology of retting. Part I.—the microbial flora in different systems of retting. Journal of the Society of Chemical Industry 65, 365–370. https://doi.org/10.1002/jctb.5000651110

Amaducci, S., Scordia, D., Liu, F.H., Zhang, Q., Guo, H., Testa, G., Cosentino, S.L., 2015. Key cultivation techniques for hemp in Europe and China. Industrial Crops and Products, FIBRE CROPS: from production to end use 68, 2–16. https://doi.org/10.1016/j.indcrop.2014.06.041

Anderson, D.B., 1927. A Microchemical Study of the Structure and Development of Flax Fibers. American Journal of Botany 14, 187–211. https://doi.org/10.2307/2435728

Andersons, J., Poriķe, E., Spārniņš, E., 2011. Modeling strength scatter of elementary flax fibers: The effect of mechanical damage and geometrical characteristics. Composites Part A: Applied Science and Manufacturing 42, 543–549. https://doi.org/10.1016/j.compositesa.2011.01.013

Angulu, M., Gusovius, H.-J., 2024. Retting of Bast Fiber Crops Like Hemp and Flax—A Review for Classification of Procedures. Fibers 12, 28. https://doi.org/10.3390/fib12030028

Assirelli, A., Dal Re, L., Esposito, S., Cocchi, A., Santangelo, E., 2020. The Mechanical Harvesting of Hemp Using In-Field Stand-Retting: A Simpler Approach Converted to the Production of Fibers for Industrial Use. Sustainability 12, 8795. https://doi.org/10.3390/su12218795

Astudillo, M.F., Thalwitz, G., Vollrath, F., 2014. Life cycle assessment of Indian silk. Journal of Cleaner Production 81, 158–167. https://doi.org/10.1016/j.jclepro.2014.06.007

Baley, C., 2002. Analysis of the flax fibres tensile behaviour and analysis of the tensile stiffness increase. Composites Part A: Applied Science and Manufacturing 33, 939–948. https://doi.org/10.1016/S1359-835X(02)00040-4

Baley, C., Gomina, M., Breard, J., Bourmaud, A., Davies, P., 2020. Variability of mechanical properties of flax fibres for composite reinforcement. A review. Industrial Crops and Products 145, 111984. https://doi.org/10.1016/j.indcrop.2019.111984

Baley, C., Goudenhooft, C., Gibaud, M., Bourmaud, A., 2018. Flax stems: from a specific architecture to an instructive model for bioinspired composite structures. Bioinspir. Biomim. 13, 026007. https://doi.org/10.1088/1748-3190/aaa6b7

Balter, M., 2009. Clothes Make the (Hu) Man. Science 325, 1329–1329. https://doi.org/10.1126/science.325_1329a

Barber, A., Pellow, G., n.d. LCA: NEW ZEALAND MERINO WOOL TOTAL ENERGY USE.

Barbhuiya, S., Bhusan Das, B., 2022. A comprehensive review on the use of hemp in concrete. Construction and Building Materials 341, 127857. https://doi.org/10.1016/j.conbuildmat.2022.127857

Barneto, A.G., Carmona, J.A., Alfonso, J.E.M., Serrano, R.S., 2010. Simulation of the thermogravimetry analysis of three non-wood pulps. Bioresource Technology 101, 3220–3229. https://doi.org/10.1016/j.biortech.2009.12.034

Barrett, J., Chase, Z., Zhang, J., Holl, M.M.B., Willis, K., Williams, A., Hardesty, B.D., Wilcox, C., 2020. Microplastic Pollution in Deep-Sea Sediments From the Great Australian Bight. Frontiers in Marine Science 7.

Basu, G., Mishra, L., Jose, S., Samanta, A.K., 2015. Accelerated retting cum softening of coconut fibre. Industrial Crops and Products 77, 66–73. https://doi.org/10.1016/j.indcrop.2015.08.012

Bergeret, A., 2021. 3 - Surface treatments in fiber-reinforced composites, in: Joseph, K., Oksman, K., George, G., Wilson, R., Appukuttan, S. (Eds.), Fiber Reinforced Composites, Woodhead Publishing Series in Composites Science and Engineering. Woodhead Publishing, pp. 47–81. https://doi.org/10.1016/B978-0-12-821090-1.00020-X

Bergfjord, C., Karg, S., Rast-Eicher, A., Nosch, M.-L., Mannering, U., Allaby, R.G., Murphy, B.M., Holst, B., 2010. Comment on "30,000-Year-Old Wild Flax Fibers." Science 328, 1634–1634. https://doi.org/10.1126/science.1186345

Bevilacqua, M., Ciarapica, F.E., Giacchetta, G., Marchetti, B., 2011. A carbon footprint analysis in the textile supply chain. International Journal of Sustainable Engineering 4, 24–36. https://doi.org/10.1080/19397038.2010.502582

Bevilacqua, M., Ciarapica, F.E., Mazzuto, G., Paciarotti, C., 2014. Environmental analysis of a cotton yarn supply chain. Journal of Cleaner Production 82, 154–165. https://doi.org/10.1016/j.jclepro.2014.06.082

Blake, A.W., Marcus, S.E., Copeland, J.E., Blackburn, R.S., Knox, J.P., 2008. In situ analysis of cell wall polymers associated with phloem fibre cells in stems of hemp, Cannabis sativa L. Planta 228, 1–13. https://doi.org/10.1007/s00425-008-0713-5

Blervacq, A.-S., Moreau, M., Duputié, A., Hawkins, S., 2023. Comparative Analysis of G-Layers in Bast Fiber and Xylem Cell Walls in Flax Using Raman Spectroscopy. Biomolecules 13, 435. https://doi.org/10.3390/biom13030435

Bleuze, L., Lashermes, G., Alavoine, G., Recous, S., Chabbert, B., 2018. Tracking the dynamics of hemp dew retting under controlled environmental conditions. Industrial Crops and Products 123, 55–63. https://doi.org/10.1016/j.indcrop.2018.06.054

Bonatti, P.M., Ferrari, C., Focher, B., Grippo, C., Torri, G., Cosentino, C., 2004. Histochemical and supramolecular studies in determining quality of hemp fibres for textile applications. Euphytica 140, 55–64. https://doi.org/10.1007/s10681-004-4755-x

Bos, H.L., 2004. The potential of flax fibres as reinforcement for composite materials (Phd Thesis 1 (Research TU/e / Graduation TU/e)). Technische Universiteit Eindhoven, Eindhoven. https://doi.org/10.6100/IR575360

Bou Orm, E., Sauvagère, S., Rocher, J., Benezet, J.-C., Bayle, S., Siatka, C., Bergeret, A., Malhautier, L., 2023. Estimating the bias related to DNA recovery from hemp stems for retting microbial community investigation. Appl Microbiol Biotechnol 107, 4665–4681. https://doi.org/10.1007/s00253-023-12582-5

Bou Orm, E., Sutton-Charani, N., Bayle, S., Benezet, J.-C., Bergeret, A., Malhautier, L., 2024. Influence of field retting on physicochemical and biological properties of “Futura 75” hemp stems. Industrial Crops and Products 214, 118487. https://doi.org/10.1016/j.indcrop.2024.118487

Bourmaud, A., Morvan, C., Baley, C., 2010. Importance of fiber preparation to optimize the surface and mechanical properties of unitary flax fiber. Industrial Crops and Products 32, 662–667. https://doi.org/10.1016/j.indcrop.2010.08.002

Bratt, R.P., Mercer, P.C., Brown, A.E., 1988. Degradation of flax stems by Botrytis cinerea. Transactions of the British Mycological Society 90, 537–544. https://doi.org/10.1016/S0007-1536(88)80004-4

Brock, P.M., Graham, P., Madden, P., Alcock, D.J., 2013. Greenhouse gas emissions profile for 1 kg of wool produced in the Yass Region, New South Wales: A Life Cycle Assessment approach. Anim. Prod. Sci. 53, 495–508. https://doi.org/10.1071/AN12208

Brown, A.E., 1984. *Epicoccum nigrum*, a primary saprophyte involved in the retting of flax. Transactions of the British Mycological Society 83, 29–35. https://doi.org/10.1016/S0007-1536(84)80242-9

Brown, A.E., Sharma, H. s. s., 1984. Production of polysaccharide-degrading enzymes by saprophytic fungi from glyphosate-treated flax and their involvement in retting. Annals of Applied Biology 105, 65–74. https://doi.org/10.1111/j.1744-7348.1984.tb02803.x

Brown, A.E., Sharma, H.S.S., Black, D.L.R., 1986. Relationship between pectin content of stems of flax cultivars, fungal cell wall-degrading enzymes and pre-harvest retting. Annals of Applied Biology 109, 345–351. https://doi.org/10.1111/j.1744-7348.1986.tb05326.x

CALHOUN, J., 2011. The Word Made Flax: Cheap Bibles, Textual Corruption, and the Poetics of Paper. PMLA 126, 327–344.

Cantarel, B.L., Coutinho, P.M., Rancurel, C., Bernard, T., Lombard, V., Henrissat, B., 2009. The Carbohydrate-Active EnZymes database (CAZy): an expert resource for Glycogenomics. Nucleic Acids Research 37, D233–D238. https://doi.org/10.1093/nar/gkn663

Carpita, N.C., Gibeaut, D.M., 1993. Structural models of primary cell walls in flowering plants: consistency of molecular structure with the physical properties of the walls during growth. The Plant Journal 3, 1–30. https://doi.org/10.1111/j.1365-313X.1993.tb00007.x

Cassab, G.I., 1998. PLANT CELL WALL PROTEINS. Annual Review of Plant Biology 49, 281–309. https://doi.org/10.1146/annurev.arplant.49.1.281

Cebi, N., Bekiroglu, H., Erarslan, A., Rodriguez-Saona, L., 2023. Rapid Sensing: Hand-Held and Portable FTIR Applications for On-Site Food Quality Control from Farm to Fork. Molecules 28, 3727. https://doi.org/10.3390/molecules28093727

Célino, A., Freour, S., Jacquemin, F., Casari, P., 2014. The hygroscopic behavior of plant fibers: a review. Front. Chem. 1. https://doi.org/10.3389/fchem.2013.00043

Chabbert, B., Padovani, J., Djemiel, C., Ossemond, J., Lemaître, A., Yoshinaga, A., Hawkins, S., Grec, S., Beaugrand, J., Kurek, B., 2020. Multimodal assessment of flax dew retting and its functional impact on fibers and natural fiber composites. Industrial Crops and Products 148, 112255. https://doi.org/10.1016/j.indcrop.2020.112255

Chabbert, B., Philippe, F., Thiébeau, P., Alavoine, G., Gaudard, F., Pernes, M., Day, A., Kurek, B., Recous, S., 2023. How the interplay between harvest time and climatic conditions drives the dynamics of hemp (Cannabis sativa L.) field retting. Industrial Crops and Products 204, 117294. https://doi.org/10.1016/j.indcrop.2023.117294

Chabi, M., Goulas, E., Leclercq, C.C., Waele, I. de, Rihouey, C., Cenci, U., Day, A., Blervacq, A.-S., Neutelings, G., Duponchel, L., Lerouge, P., Hausman, J.-F., Renaut, J., Hawkins, S., 2017. A Cell Wall Proteome and Targeted Cell Wall Analyses Provide Novel Information on Hemicellulose Metabolism in Flax *. Molecular & Cellular Proteomics 16, 1634–1651. https://doi.org/10.1074/mcp.M116.063727

Chand, N., Fahim, M., 2021. 1 - Natural fibers and their composites, in: Chand, N., Fahim, M. (Eds.), Tribology of Natural Fiber Polymer Composites (Second Edition), Woodhead Publishing Series in Composites Science and Engineering. Woodhead Publishing, pp. 1–59. https://doi.org/10.1016/B978-0-12-818983-2.00001-3

Chand, N., Fahim, M., 2020. Tribology of Natural Fiber Polymer Composites. Woodhead Publishing.
Chapagain, A.K., Hoekstra, A.Y., Savenije, H.H.G., Gautam, R., 2006. The water footprint of cotton consumption: An assessment of the impact of worldwide consumption of cotton products on the water resources in the cotton producing countries. Ecological Economics 60, 186–203. https://doi.org/10.1016/j.ecolecon.2005.11.027
Charlet, K., Jernot, J.P., Eve, S., Gomina, M., Bréard, J., 2010. Multi-scale morphological characterisation of flax: From the stem to the fibrils. Carbohydrate Polymers 82, 54–61. https://doi.org/10.1016/j.carbpol.2010.04.022
Chen, F., Ji, X., Chu, J., Xu, P., Wang, L., 2021. A review: life cycle assessment of cotton textiles. Industria Textila 72, 19–29. https://doi.org/10.35530/IT.072.01.1797
Chirania, P., Holwerda, E.K., Giannone, R.J., Liang, X., Poudel, S., Ellis, J.C., Bomble, Y.J., Hettich, R.L., Lynd, L.R., 2022. Metaproteomics reveals enzymatic strategies deployed by anaerobic microbiomes to maintain lignocellulose deconstruction at high solids. Nat Commun 13, 3870. https://doi.org/10.1038/s41467-022-31433-x
Clay, J., 2013. World Agriculture and the Environment: A Commodity-By-Commodity Guide To Impacts And Practices. Island Press.
Cook, J.G., 1984. Handbook of Textile Fibres: Man-Made Fibres. Elsevier.
Cosgrove, D., Jarvis, M., 2012. Comparative structure and biomechanics of plant primary and secondary cell walls. Front. Plant Sci. 3. https://doi.org/10.3389/fpls.2012.00204
Crônier, D., Monties, B., Chabbert, B., 2005. Structure and Chemical Composition of Bast Fibers Isolated from Developing Hemp Stem. J. Agric. Food Chem. 53, 8279–8289. https://doi.org/10.1021/jf051253k
Das, S.C., La Rosa, A.D., Grammatikos, S.A., 2022. Chapter 19 - Life cycle assessment of plant fibers and their composites, in: Mavinkere Rangappa, S., Parameswaranpillai, J., Siengchin, S., Ozbakkaloglu, T., Wang, H. (Eds.), Plant Fibers, Their Composites, and Applications, The Textile Institute Book Series. Woodhead Publishing, pp. 457–484. https://doi.org/10.1016/B978-0-12-824528-6.00015-1
Davies, G.C., Bruce, D.M., 1998. Effect of Environmental Relative Humidity and Damage on the Tensile Properties of Flax and Nettle Fibers. Textile Research Journal 68, 623–629. https://doi.org/10.1177/004051759806800901
Davies, G.J., Gloster, T.M., Henrissat, B., 2005. Recent structural insights into the expanding world of carbohydrate-active enzymes. Current Opinion in Structural Biology, Catalysis and regulation/Proteins 15, 637–645. https://doi.org/10.1016/j.sbi.2005.10.008
Davis, E.A., Derouet, C., Herve Du Penhoat, C., Morvan, C., 1990. Isolation and an N.M.R. study of pectins from flax (*linum usitatissimum* L.). Carbohydrate Research 197, 205–215. https://doi.org/10.1016/0008-6215(90)84143-I
Day, A., Neutelings, G., Nolin, F., Grec, S., Habrant, A., Crônier, D., ... & Hawkins, S. (2009). Caffeoyl coenzyme A O-methyltransferase down-regulation is associated with modifications in lignin and cell-wall architecture in flax secondary xylem. *Plant Physiology and Biochemistry*, *47*(1), 9-19.
Day, A., Ruel, K., Neutelings, G., Crônier, D., David, H., Hawkins, S., Chabbert, B., 2005. Lignification in the flax stem: evidence for an unusual lignin in bast fibers. Planta 222, 234–245. https://doi.org/10.1007/s00425-005-1537-1
de Haseth, J.A., Akin, D.E., Ii, F.E.B., 2008. Sensors and Chemometrics for Flax Fiber Quality and for Processing.
De Silva, S.F., Alcorn, J., 2019. Flaxseed Lignans as Important Dietary Polyphenols for Cancer Prevention and Treatment: Chemistry, Pharmacokinetics, and Molecular Targets. Pharmaceuticals 12, 68. https://doi.org/10.3390/ph12020068
Dhirhi, N., Shukla, R., Patel, N.B., Sahu, H., Mehta, N., 2015. Extraction method of flax fibre and its uses 15, 711–716.
Di Candilo, M., Ranalli, P., Bozzi, C., Focher, B., Mastromei, G., 2000. Preliminary results of tests facing with the controlled retting of hemp. Industrial Crops and Products 11, 197–203. https://doi.org/10.1016/S0926-6690(99)00047-3

Diquélou, Y., Gourlay, E., Arnaud, L., Kurek, B., 2015. Impact of hemp shiv on cement setting and hardening: Influence of the extracted components from the aggregates and study of the interfaces with the inorganic matrix. Cement and Concrete Composites 55, 112–121. https://doi.org/10.1016/j.cemconcomp.2014.09.004

Dissanayake, N., Summerscales, J., Grove, S., Singh, M., n.d. QUANTITATIVE LIFE CYCLE ANALYSIS FOR FLAX FIBRES.

Dittenber, D.B., GangaRao, H.V.S., 2012. Critical review of recent publications on use of natural composites in infrastructure. Composites Part A: Applied Science and Manufacturing 43, 1419–1429. https://doi.org/10.1016/j.compositesa.2011.11.019

Djafari Petroudy, S.R., 2017. 3 - Physical and mechanical properties of natural fibers, in: Fan, M., Fu, F. (Eds.), Advanced High Strength Natural Fibre Composites in Construction. Woodhead Publishing, pp. 59–83. https://doi.org/10.1016/B978-0-08-100411-1.00003-0

Djemiel, C., 2017. Étude de la diversité du domaine Bacteria et du règne Fungi au cours du rouissage du lin sur champ par une approche de metabarcoding (These de doctorat). Lille 1.

Djemiel, C., Goulas, E., Badalato, N., Chabbert, B., Hawkins, S., Grec, S., 2020. Targeted Metagenomics of Retting in Flax: The Beginning of the Quest to Harness the Secret Powers of the Microbiota. Frontiers in Genetics 11.

Djemiel, C., Grec, S., Hawkins, S., 2017. Characterization of Bacterial and Fungal Community Dynamics by High-Throughput Sequencing (HTS) Metabarcoding during Flax Dew-Retting. Frontiers in Microbiology 8. https://doi.org/doi.org/10.3389/fmicb.2017.02052

Donaghy, J. a., Levett, P. n., Haylock, R. w., 1990. Changes in microbial populations during anaerobic flax retting. Journal of Applied Bacteriology 69, 634–641. https://doi.org/10.1111/j.1365-2672.1990.tb01556.x

Donaghy, J.A., Boomer, J.H., Haylock, R.W., 1992. An assessment of the quality and yield of flax fiber produced by the use of pure bacterial cultures in flax rets. Enzyme and Microbial Technology 14, 131–134. https://doi.org/10.1016/0141-0229(92)90170-S

Drula, E., Garron, M.-L., Dogan, S., Lombard, V., Henrissat, B., Terrapon, N., 2022. The carbohydrate-active enzyme database: functions and literature. Nucleic Acids Res 50, D571–D577. https://doi.org/10.1093/nar/gkab1045

Duan, S.W., Cheng, L.F., Feng, X.Y., Yang, Q., Liu, Z.Y., Zheng, K., Peng, Y.D., 2020. Insights on bio-degumming of kenaf bast based on metagenomic and proteomics. BMC Genomics 21, 121. https://doi.org/10.1186/s12864-020-6531-2

Eady, S., Carre, A., Grant, T., 2012. Life cycle assessment modelling of complex agricultural systems with multiple food and fibre co-products. Journal of Cleaner Production, Working towards a more sustainable agri-food industry: Main findings from the Food LCA 2010 conference in Bari, Italy 28, 143–149. https://doi.org/10.1016/j.jclepro.2011.10.005

El Nemr, A., 2012. From natural to synthetic fibers, in: Textiles: Types, Uses and Production Methods. pp. 1–152.

Elfaleh, I., Abbassi, F., Habibi, M., Ahmad, F., Guedri, M., Nasri, M., Garnier, C., 2023. A comprehensive review of natural fibers and their composites: An eco-friendly alternative to conventional materials. Results in Engineering 19, 101271. https://doi.org/10.1016/j.rineng.2023.101271

Encyclopedia of Applied Plant Sciences, 2016. . Academic Press.

Esau, K., 1942. Vascular Differentiation in the Vegetative Shoot of Linum. I. The Procambium. American Journal of Botany 29, 738–747. https://doi.org/10.2307/2437727

Fernandez-Tendero E (2013) Origines biologiques et environnementales de la variabilité de la qualité des fibres de chanvre **(***Cannabis sativa* L.) à destination d'agromatériaux. Université Lille 1 Sciences et Technologie.

Fike, J., 2016. Industrial Hemp: Renewed Opportunities for an Ancient Crop. Critical Reviews in Plant Sciences 35, 406–424. https://doi.org/10.1080/07352689.2016.1257842

Fila, G., Manici, L.M., Caputo, F., 2001. In vitro evaluation of dew-retting of flax by fungi from southern Europe. Annals of Applied Biology 138, 343–351. https://doi.org/10.1111/j.1744-7348.2001.tb00119.x

Fisher, C.H., 1981. History of Natural Fibers. Journal of Macromolecular Science: Part A - Chemistry 15, 1345–1375. https://doi.org/10.1080/00222338108056788

Flax: new uses and demands. [WWW Document], n.d. URL https://www.cabdirect.org/cabdirect/abstract/20033159726 (accessed 8.21.22).

Fortino, G., Russo, W., Savaglio, C., Shen, W., Zhou, M., 2018. Agent-Oriented Cooperative Smart Objects: From IoT System Design to Implementation. IEEE Transactions on Systems, Man, and Cybernetics: Systems 48, 1939–1956. https://doi.org/10.1109/TSMC.2017.2780618

Foulk, J., Akin, D., Dodd, R., Mcalister, D., 2004. USDA Flax Fiber Pilot Plant. 60th Flax Institute Proceedings 1–12.

Foulk, J.A., Akin, D.E., Dodd, R.B., 2000. New Low Cost Flax Fibers for Composites (SAE Technical Paper No. 2000- 01–1133). SAE International, Warrendale, PA. https://doi.org/10.4271/2000-01-1133

Foulk, J.A., Akin, D.E., Dodd, R.B., Iii, D.D.M., n.d. Flax Fiber: Potential for a New Crop in the Southeast 10.

Franck, R.R., 1992. The history and present position of linen. The biology and processing of flax 1–9.

Friedlingstein, P., O'Sullivan, M., Jones, M.W., Andrew, R.M., Gregor, L., Hauck, J., Le Quéré, C., Luijkx, I.T., Olsen, A., Peters, G.P., Peters, W., Pongratz, J., Schwingshackl, C., Sitch, S., Canadell, J.G., Ciais, P., Jackson, R.B., Alin, S.R., Alkama, R., Arneth, A., Arora, V.K., Bates, N.R., Becker, M., Bellouin, N., Bittig, H.C., Bopp, L., Chevallier, F., Chini, L.P., Cronin, M., Evans, W., Falk, S., Feely, R.A., Gasser, T., Gehlen, M., Gkritzalis, T., Gloege, L., Grassi, G., Gruber, N., Gürses, Ö., Harris, I., Hefner, M., Houghton, R.A., Hurtt, G.C., Iida, Y., Ilyina, T., Jain, A.K., Jersild, A., Kadono, K., Kato, E., Kennedy, D., Klein Goldewijk, K., Knauer, J., Korsbakken, J.I., Landschützer, P., Lefèvre, N., Lindsay, K., Liu, J., Liu, Z., Marland, G., Mayot, N., McGrath, M.J., Metzl, N., Monacci, N.M., Munro, D.R., Nakaoka, S.-I., Niwa, Y., O'Brien, K., Ono, T., Palmer, P.I., Pan, N., Pierrot, D., Pocock, K., Poulter, B., Resplandy, L., Robertson, E., Rödenbeck, C., Rodriguez, C., Rosan, T.M., Schwinger, J., Séférian, R., Shutler, J.D., Skjelvan, I., Steinhoff, T., Sun, Q., Sutton, A.J., Sweeney, C., Takao, S., Tanhua, T., Tans, P.P., Tian, X., Tian, H., Tilbrook, B., Tsujino, H., Tubiello, F., van der Werf, G.R., Walker, A.P., Wanninkhof, R., Whitehead, C., Willstrand Wranne, A., Wright, R., Yuan, W., Yue, C., Yue, X., Zaehle, S., Zeng, J., Zheng, B., 2022. Global Carbon Budget 2022. Earth System Science Data 14, 4811–4900. https://doi.org/10.5194/essd-14-4811-2022

Fuller, W., Norman, A.G., Wilsie, C.P., 1946. The retting of hemp I. Field retting of hemp in Iowa.

Galinousky, D., Mokshina, N., Padvitski, T., Ageeva, M., Bogdan, V., Kilchevsky, A., Gorshkova, T., 2020. The Toolbox for Fiber Flax Breeding: A Pipeline From Gene Expression to Fiber Quality. Front. Genet. 11. https://doi.org/10.3389/fgene.2020.589881

Ganster, J., Fink, H.-P., 2003. Physical Constants of Cellulose, in: The Wiley Database of Polymer Properties. John Wiley & Sons, Ltd. https://doi.org/10.1002/0471532053.bra036

Garg, G., Singh, A., Kaur, A., Singh, R., Kaur, J., Mahajan, R., 2016. Microbial pectinases: an ecofriendly tool of nature for industries. 3 Biotech 6, 47. https://doi.org/10.1007/s13205-016-0371-4

Garron, M.-L., Cygler, M., 2010. Structural and mechanistic classification of uronic acid-containing polysaccharide lyases. Glycobiology 20, 1547–1573. https://doi.org/10.1093/glycob/cwq122

Gill, K.S., 1987. Linseed. Linseed.

Girault, R., Bert, F., Rihouey, C., Jauneau, A., Morvan, C., Jarvis, M., 1997. Galactans and cellulose in flax fibres: putative contributions to the tensile strength. International Journal of Biological Macromolecules 21, 179–188. https://doi.org/10.1016/S0141-8130(97)00059-7

Girault, R., His, I., Andeme-Onzighi, C., Driouich, A., Morvan, C., 2000. Identification and partial characterization of proteins and proteoglycans encrusting the secondary cell walls of flax fibres. Planta 211, 256–264. https://doi.org/10.1007/s004250000281

Girault, R., Morvan, C., 1999. CARACTERISATION BIOCHIMIQUE DES POLYMERES INCRUSTANT LES PAROIS SECONDAIRES DES FIBRES DE LIN.

Gomez-Campos, A., Vialle, C., Rouilly, A., Sablayrolles, C., Hamelin, L., 2021. Flax fiber for technical textile: A life cycle inventory. Journal of Cleaner Production 281, 125177. https://doi.org/10.1016/j.jclepro.2020.125177

Gonzalez, V., Lou, X., Chi, T., 2023. Evaluating Environmental Impact of Natural and Synthetic Fibers: A Life Cycle Assessment Approach. Sustainability 15, 7670. https://doi.org/10.3390/su15097670

Gorshkova, T., Chernova, T., Mokshina, N., Ageeva, M., Mikshina, P., 2018. Plant 'muscles': fibers with a tertiary cell wall. New Phytologist 218, 66–72. https://doi.org/10.1111/nph.14997

Gorshkova, T., Petrova, A., Mikshina, P., 2022. Review: Tertiary cell wall of plant fibers as a source of inspiration in material design. Carbohydrate Polymers 295, 119849. https://doi.org/10.1016/j.carbpol.2022.119849

Gorshkova, T.A., Chemikosova, S.B., Sal'nikov, V.V., Pavlencheva, N.V., Gur'janov, O.P., Stolle-Smits, T., van Dam, J.E.G., 2004. Occurrence of cell-specific galactan is coinciding with bast fiber developmental transition in flax. Industrial Crops and Products 19, 217–224. https://doi.org/10.1016/j.indcrop.2003.10.002

Gorshkova, T.A., Sal'nikov, V.V., Chemikosova, S.B., Ageeva, M.V., Pavlencheva, N.V., van Dam, J.E.G., 2003. The snap point: a transition point in *Linum usitatissimum* bast fiber development. Industrial Crops and Products 18, 213–221. https://doi.org/10.1016/S0926-6690(03)00043-8

Gorshkova, T.A., Wyatt, S.E., Salnikov, V.V., Gibeaut, D.M., Ibragimov, M.R., Lozovaya, V.V., Carpita, N.C., 1996. Cell-Wall Polysaccharides of Developing Flax Plants. Plant Physiology 110, 721–729. https://doi.org/10.1104/pp.110.3.721

Goubet, F., Bourlard, T., Girault, R., Alexandre, C., Vandevelde, M.-C., Morvan, C., 1995. Structural features of galactans from flax fibres. Carbohydrate Polymers 27, 221–227. https://doi.org/10.1016/0144-8617(95)00063-D

Goudenhooft, C., 2018. Multi-scale characterization of flax stems and fibers : structure and mechanical performances (These de doctorat). Lorient.

Goudenhooft, C., Bourmaud, A., Baley, C., 2019. Flax (Linum usitatissimum L.) Fibers for Composite Reinforcement: Exploring the Link Between Plant Growth, Cell Walls Development, and Fiber Properties. Frontiers in Plant Science 10.

Griesche, C., Baeumner, A.J., 2020. Biosensors to support sustainable agriculture and food safety. TrAC Trends in Analytical Chemistry 128, 115906. https://doi.org/10.1016/j.trac.2020.115906

Handelsman, J., 2004. Metagenomics: Application of Genomics to Uncultured Microorganisms. Microbiology and Molecular Biology Reviews 68, 669–685. https://doi.org/10.1128/mmbr.68.4.669-685.2004

Henriksson, G., Akin, D.E., Rigsby, L.L., Patel, N., Eriksson, K.-E.L., 1997. Influence of Chelating Agents and Mechanical Pretreatment on Enzymatic Retting of Flax. Textile Research Journal 67, 829–836. https://doi.org/10.1177/004051759706701107

Henriksson, G., Akin, D.E., Slomczynski, D., Eriksson, K.-E.L., 1999. Production of highly efficient enzymes for flax retting by *Rhizomucor pusillus*. Journal of Biotechnology 68, 115–123. https://doi.org/10.1016/S0168-1656(98)00192-8

Henrissat, B., 1991. A classification of glycosyl hydrolases based on amino acid sequence similarities. Biochemical Journal 280, 309–316. https://doi.org/10.1042/bj2800309

Henrissat, B., Davies, G., 1997. Structural and sequence-based classification of glycoside hydrolases. Current Opinion in Structural Biology 7, 637–644. https://doi.org/10.1016/S0959-440X(97)80072-3

Hobson, R.N., Hepworth, D.G., Bruce, D.M., 2001. PH—Postharvest Technology: Quality of Fibre Separated from Unretted Hemp Stems by Decortication. Journal of Agricultural Engineering Research 78, 153–158. https://doi.org/10.1006/jaer.2000.0631

Hock, C.W., 1942. Microscopic structure of flax and related bast fibers. J. RES. NATL. BUR. STAN. 29, 41. https://doi.org/10.6028/jres.029.024

Hori, C., Gaskell, J., Cullen, D., Sabat, G., Stewart, P.E., Lail, K., Peng, Y., Barry, K., Grigoriev, I.V., Kohler, A., Fauchery, L., Martin, F., Zeiner, C.A., Bhatnagar, J.M., 2018. Multi-omic Analyses of Extensively Decayed Pinus contorta Reveal Expression of a Diverse Array of Lignocellulose-

Degrading Enzymes. Applied and Environmental Microbiology 84, e01133-18. https://doi.org/10.1128/AEM.01133-18
Iwańska, O., Latoch, P., Suchora, M., Pidek, I.A., Huber, M., Bubak, I., Kopik, N., Kovalenko, M., Gąsiorowski, M., Armache, J.-P., Starosta, A.L., 2022. Lake microbiome and trophy fluctuations of the ancient hemp rettery. Sci Rep 12, 8846. https://doi.org/10.1038/s41598-022-12761-w
Jahan, M.S., Mostafizur Rahman, J.N.M., Islam, M., Quaiyyum, M.A., 2016. Chemical characteristics of ribbon retted jute and its effect on pulping and papermaking properties. Industrial Crops and Products 84, 116–120. https://doi.org/10.1016/j.indcrop.2016.01.054
Jeannin, T., Arnold, G., Bourmaud, A., Corn, S., De Luycker, E., Dumont, P.J.J., Ferreira, M., François, C., Grégoire, M., Harzallah, O., Heurtel, J., Joannès, S., Kervoelen, A., Labanieh, A.R., Le Moigne, N., Martoïa, F., Orgéas, L., Ouagne, P., Soulat, D., Vivet, A., Placet, V., 2024. A round-robin study on the tensile characterization of single fibres: A multifactorial analysis and recommendations for more reliable results. Composites Part A: Applied Science and Manufacturing 185, 108323. https://doi.org/10.1016/j.compositesa.2024.108323
Jenkins, D. T., Jenkins, David Trevor, 2003. The Cambridge History of Western Textiles. Cambridge University Press.
Jhala, A.J., Hall, L.M., 2010. Flax (Linum usitatissimum L.): Current Uses and Future Applications 10.
Jose, S., Mishra, L., Debnath, S., Pal, S., Munda, P.K., Basu, G., 2019. Improvement of water quality of remnant from chemical retting of coconut fibre through electrocoagulation and activated carbon treatment. Journal of Cleaner Production 210, 630–637. https://doi.org/10.1016/j.jclepro.2018.11.011
Joseleau, J.-P., Pérez, S., n.d. Complex Polysaccharide Nano-Composites.
Joshi, S.V., Drzal, L.T., Mohanty, A.K., Arora, S., 2004. Are natural fiber composites environmentally superior to glass fiber reinforced composites? Composites Part A: Applied Science and Manufacturing, AIChE 2002 35, 371–376. https://doi.org/10.1016/j.compositesa.2003.09.016
Juturu, V., Wu, J.C., 2013. Insight into microbial hemicellulases other than xylanases: a review. Journal of Chemical Technology & Biotechnology 88, 353–363. https://doi.org/10.1002/jctb.3969
Kadolph, S.J., n.d. Textiles. (No Title).
Kalliala, E.M., Nousiainen, P., 1999a. Life Cycle Assessment: ENVIRONMENTAL PROFILE OF COTTON AND POLYESTER-COTTON FABRICS. AUTEX Research Journal 1, 8–20. https://doi.org/10.1515/aut-1999-010102
Kalliala, E.M., Nousiainen, P., 1999b. Life Cycle Assessment: ENVIRONMENTAL PROFILE OF COTTON AND POLYESTER-COTTON FABRICS. AUTEX Research Journal 1, 8–20. https://doi.org/10.1515/aut-1999-010102
Karmakar, P., Teng, S.W., Murshed, M., Pang, S., Li, Y., Lin, H., 2024. Crop monitoring by multimodal remote sensing: A review. Remote Sensing Applications: Society and Environment 33, 101093. https://doi.org/10.1016/j.rsase.2023.101093
Keller, B., Templeton, M.D., Lamb, C.J., 1989. Specific localization of a plant cell wall glycine-rich protein in protoxylem cells of the vascular system. Proceedings of the National Academy of Sciences 86, 1529–1533. https://doi.org/10.1073/pnas.86.5.1529
Kessler, R. W., Quint, B., Kessler, W., Ullmeyer, D., Ungerer, P., 1994. Quality estimation of flax by modern instrumental methods. Industrial Crops and Products.
Kido, S., Yasufuku, H., Azuma, J., 1996. Isolation and Characterization of Arabinogalactan Proteins Released by Cellulase Digestion of Cabbage Leaves. J. Agric. Food Chem. 44, 3432–3436. https://doi.org/10.1021/jf960192a
Klerkx, L., Jakku, E., Labarthe, P., 2019. A review of social science on digital agriculture, smart farming and agriculture 4.0: New contributions and a future research agenda. NJAS - Wageningen Journal of Life Sciences 90–91, 100315. https://doi.org/10.1016/j.njas.2019.100315
Koivula, M., Kymäläinen, H.-R., Vanne, L., Levo, S., Pehkonen, A., Sjöberg, A.-M., 2004. Microbial quality of linseed and fibre hemp plants during growing and harvest seasons.
Kolodziejczyk, P., Fedec, P., Kozlowska, J., Kozlowski, R., 1995. Linseed in health food and nutrition. Zemedelska Technika - UZPI (Czech Republic).

Konczewicz, W., Kryszak, N., Nowaczkiewicz, E., Kozlowski, R., Wojtysiak, J., Podsiedlik, W., 2013. Osmosis Phenomena Based Degumming of Bast Fibrous Plants as a Promising Method in Primary Processing. Molecular Crystals and Liquid Crystals 571, 116–131. https://doi.org/10.1080/15421406.2012.703912

Konczewicz, W., Zimniewska, M., Valera, M.A., 2018. The selection of a retting method for the extraction of bast fibers as response to challenges in composite reinforcement. Textile Research Journal 88, 2104–2119. https://doi.org/10.1177/0040517517716902

Kousar, S., Shafqat, U., Kausar, N., Pamucar, D., Karaca, Y., Salman, M.A., 2022. Sustainable Energy Consumption Model for Textile Industry Using Fully Intuitionistic Fuzzy Optimization Approach. Computational Intelligence and Neuroscience 2022, e5724825. https://doi.org/10.1155/2022/5724825

Kozłowski, R., Mackiewicz-Talarczyk, M., Textile Institute (Manchester, England) (Eds.), 2020. Handbook of natural fibres, Second edition. ed, The Textile Institute book series. Woodhead Publishing, Duxford, United Kingdom ; Cambridge, MA, United States.

Kubicek, C.P., Druzhinina, I.S. (Eds.), 2007. Environmental and Microbial Relationships, The Mycota. Springer, Berlin, Heidelberg. https://doi.org/10.1007/978-3-540-71840-6

La Rosa, A.D., Grammatikos, S.A., 2019a. Comparative Life Cycle Assessment of Cotton and Other Natural Fibers for Textile Applications. Fibers 7, 101. https://doi.org/10.3390/fib7120101

La Rosa, A.D., Grammatikos, S.A., 2019b. Comparative Life Cycle Assessment of Cotton and Other Natural Fibers for Textile Applications. Fibers 7, 101. https://doi.org/10.3390/fib7120101

Langille, M.G.I., Zaneveld, J., Caporaso, J.G., McDonald, D., Knights, D., Reyes, J.A., Clemente, J.C., Burkepile, D.E., Vega Thurber, R.L., Knight, R., Beiko, R.G., Huttenhower, C., 2013. Predictive functional profiling of microbial communities using 16S rRNA marker gene sequences. Nat Biotechnol 31, 814–821. https://doi.org/10.1038/nbt.2676

Lanigan, G.W., 1950. Relationship of Fibre Quality to Bacterial Flora in Flax Retting. Nature 165, 516–517. https://doi.org/10.1038/165516a0

Laursen, S., Hansen, J., Knudsen, H., Wenzel, H., Larsen, H., Kristensen, F., 2007. EDIPTEX - Environmental assessment of textiles.

Law, A.D., McNees, C.R., Moe, L.A., 2020. The Microbiology of Hemp Retting in a Controlled Environment: Steering the Hemp Microbiome towards More Consistent Fiber Production. Agronomy 10, 492. https://doi.org/10.3390/agronomy10040492

Le Duigou, A., Davies, P., Baley, C., 2011. Environmental Impact Analysis of the Production of Flax Fibres to be Used as Composite Material Reinforcement. Journal of Biobased Materials and Bioenergy 5, 153–165. https://doi.org/10.1166/jbmb.2011.1116

Leal Filho, W., Perry, P., Heim, H., Dinis, M.A.P., Moda, H., Ebhuoma, E., Paço, A., 2022. An overview of the contribution of the textiles sector to climate change. Frontiers in Environmental Science 10.

Lee, C.H., Khalina, A., Lee, S.H., Liu, M., 2020. A Comprehensive Review on Bast Fibre Retting Process for Optimal Performance in Fibre-Reinforced Polymer Composites. Advances in Materials Science and Engineering 2020, e6074063. https://doi.org/10.1155/2020/6074063

Levasseur, A., Drula, E., Lombard, V., Coutinho, P.M., Henrissat, B., 2013. Expansion of the enzymatic repertoire of the CAZy database to integrate auxiliary redox enzymes. Biotechnology for Biofuels 6, 41. https://doi.org/10.1186/1754-6834-6-41

Levasseur, A., Piumi, F., Coutinho, P.M., Rancurel, C., Asther, Michèle, Delattre, M., Henrissat, B., Pontarotti, P., Asther, Marcel, Record, E., 2008. FOLy: An integrated database for the classification and functional annotation of fungal oxidoreductases potentially involved in the degradation of lignin and related aromatic compounds. Fungal Genetics and Biology 45, 638–645. https://doi.org/10.1016/j.fgb.2008.01.004

Liu, D., Li, M., Xi, B., Zhao, Y., Wei, Z., Song, C., Zhu, C., 2015. Metaproteomics reveals major microbial players and their biodegradation functions in a large-scale aerobic composting plant. Microbial Biotechnology 8, 950–960. https://doi.org/10.1111/1751-7915.12290

Liu, M., Ale, M.T., Kołaczkowski, B., Fernando, D., Daniel, G., Meyer, A.S., Thygesen, A., 2017. Comparison of traditional field retting and Phlebia radiata Cel 26 retting of hemp fibres for fibre-reinforced composites. AMB Expr 7, 58. https://doi.org/10.1186/s13568-017-0355-8

Liu, M., Fernando, D., Meyer, A.S., Madsen, B., Daniel, G., Thygesen, A., 2015. Characterization and biological depectinization of hemp fibers originating from different stem sections. Industrial Crops and Products 76, 880–891. https://doi.org/10.1016/j.indcrop.2015.07.046

Mirdehghan, S.A., 2021. 1 - Fibrous polymeric composites, in: Latifi, M. (Ed.), Engineered Polymeric Fibrous Materials, The Textile Institute Book Series. Woodhead Publishing, pp. 1–58. https://doi.org/10.1016/B978-0-12-824381-7.00012-3

Majumder, A., Bairagya, M.D., Basu, B., Gupta, P.C., Sarkar, S., 2013. Retting of jute grown in arsenic contaminated area and consequent arsenic pollution in surface water bodies. Science of The Total Environment 442, 247–254. https://doi.org/10.1016/j.scitotenv.2012.09.071

MARCHENKOV, A., ROZHMINA, T., 2003. Cultivation of flax, in: Flax. CRC Press.

Martin, N., Mouret, N., Davies, P., Baley, C., 2013. Influence of the degree of retting of flax fibers on the tensile properties of single fibers and short fiber/polypropylene composites. Industrial Crops and Products 49, 755–767. https://doi.org/10.1016/j.indcrop.2013.06.012

Mazian, B., 2018. Approche intégrée du procédé de rouissage des fibres de chanvre : Vers une amélioration de la qualité des intrants pour la fabrication des matériaux biocomposites (phdthesis). IMT - MINES ALES - IMT - Mines Alès Ecole Mines - Télécom.

Mazian, B., Bergeret, A., Benezet, J.-C., Malhautier, L., 2020. Impact of field retting and accelerated retting performed in a lab-scale pilot unit on the properties of hemp fibres/polypropylene biocomposites. Industrial Crops and Products 143, 111912. https://doi.org/10.1016/j.indcrop.2019.111912

Mazian, B., Bergeret, A., Benezet, J.-C., Malhautier, L., 2018. Influence of field retting duration on the biochemical, microstructural, thermal and mechanical properties of hemp fibres harvested at the beginning of flowering. Industrial Crops and Products 116, 170–181. https://doi.org/10.1016/j.indcrop.2018.02.062

Mazian, B., Cariou, S., Chaignaud, M., Fanlo, J.-L., Fauconnier, M.-L., Bergeret, A., Malhautier, L., 2019. Evolution of temporal dynamic of volatile organic compounds (VOCs) and odors of hemp stem during field retting. Planta 250, 1983–1996. https://doi.org/10.1007/s00425-019-03280-6

McDill, J., Repplinger, M., Simpson, B.B., Kadereit, J.W., 2009. The Phylogeny of Linum and Linaceae Subfamily Linoideae, with Implications for Their Systematics, Biogeography, and Evolution of Heterostyly. Systematic Botany 34, 386–405. https://doi.org/10.1600/036364409788606244

McDonald, F., 2011. Textiles: A History. Remember When.

McDougall, G.J., Morrison, I.M., Stewart, D., Weyers, J.D.B., Hillman, J.R., 1993. Plant fibres: Botany, chemistry and processing for industrial use. Journal of the Science of Food and Agriculture 62, 1–20. https://doi.org/10.1002/jsfa.2740620102

McKeon, T., Hayes, D.G., Hildebrand, D., Weselake, R., 2016. Industrial Oil Crops. Elsevier.

McPartland, J.M., 2018. Cannabis Systematics at the Levels of Family, Genus, and Species. Cannabis and Cannabinoid Research 3, 203–212. https://doi.org/10.1089/can.2018.0039

Meijer, W.J.M., Vertregt, N., Rutgers, B., van de Waart, M., 1995. The pectin content as a measure of the retting and rettability of flax. Industrial Crops and Products 4, 273–284. https://doi.org/10.1016/0926-6690(95)00041-0

Melelli, A., Jamme, F., Beaugrand, J., Bourmaud, A., 2022. Evolution of the ultrastructure and polysaccharide composition of flax fibres over time: When history meets science. Carbohydrate Polymers 291, 119584. https://doi.org/10.1016/j.carbpol.2022.119584

Melsted, O., Pallua, I., 2018. The Historical Transition from Coal to Hydrocarbons: Previous Explanations and the Need for an Integrative Perspective. Canadian Journal of History 53, 395–422. https://doi.org/10.3138/cjh.ach.53.3.03

Mohnen, D., 2008. Pectin structure and biosynthesis. Current Opinion in Plant Biology, Physiology and Metabolism - Edited by Markus Pauly and Kenneth Keegstra 11, 266–277. https://doi.org/10.1016/j.pbi.2008.03.006

Mokshina, N., Gorshkov, O., Ibragimova, N., Pozhvanov, G., Gorshkova, T., 2018. Screenplay of flax phloem fiber behavior during gravitropic reaction. Plant Signaling & Behavior 13, e1486144. https://doi.org/10.1080/15592324.2018.1486144

More, A.P., 2022. Flax fiber–based polymer composites: a review. Adv Compos Hybrid Mater 5, 1–20. https://doi.org/10.1007/s42114-021-00246-9

Morgan, P.W., 1981. Brief History of Fibers from Synthetic Polymers. Journal of Macromolecular Science: Part A - Chemistry 15, 1113–1131. https://doi.org/10.1080/00222338108066456

Morvan, C., Andème-Onzighi, C., Girault, R., Himmelsbach, D.S., Driouich, A., Akin, D.E., 2003. Building flax fibres: more than one brick in the walls. Plant Physiology and Biochemistry 41, 935–944. https://doi.org/10.1016/j.plaphy.2003.07.001

MUIR, A.D., WESTCOTT, N.D., 2003. Flaxseed constituents and human health, in: Flax. CRC Press.

Muir, A.D., Westcott, N.D., 2003. Flax: The genus Linum. CRC Press.

Mukherjee, S., Baral, M.M., Chittipaka, V., Srivastava, S.C., Pal, S.K., 2021. Discussing the Impact of Industry 4.0 in Agriculture Supply Chain, in: Agrawal, R., Jain, J.K., Yadav, V.S., Manupati, V.K., Varela, L. (Eds.), Recent Advances in Smart Manufacturing and Materials. Springer, Singapore, pp. 301–307. https://doi.org/10.1007/978-981-16-3033-0_28

Munasinghe, P., Druckman, A., Dissanayake, D.G.K., 2021. A systematic review of the life cycle inventory of clothing. Journal of Cleaner Production 320, 128852. https://doi.org/10.1016/j.jclepro.2021.128852

Murthy, H.V.S., 2016. Introduction to Textile Fibres. CRC Press.

Müssig, J., 2010. Industrial Applications of Natural Fibres: Structure, Properties and Technical Applications. John Wiley & Sons.

Muthu, S.S., Li, Y., Hu, J.Y., Mok, P.Y., 2012. Quantification of environmental impact and ecological sustainability for textile fibres. Ecological Indicators 13, 66–74. https://doi.org/10.1016/j.ecolind.2011.05.008

Niinimäki, K., Peters, G., Dahlbo, H., Perry, P., Rissanen, T., Gwilt, A., 2020. The environmental price of fast fashion. Nat Rev Earth Environ 1, 189–200. https://doi.org/10.1038/s43017-020-0039-9

Nuez, L., Magueresse, A., Lu, P., Day, A., Boursat, T., D'Arras, P., Perré, P., Bourmaud, A., Baley, C., 2021. Flax xylem as composite material reinforcement: Microstructure and mechanical properties. Composites Part A: Applied Science and Manufacturing 149, 106550. https://doi.org/10.1016/j.compositesa.2021.106550

Nykter, M., Kymäläinen, H.-R., Thomsen, A.B., Lilholt, H., Koponen, H., Sjöberg, A.-M., Thygesen, A., 2008. Effects of thermal and enzymatic treatments and harvesting time on the microbial quality and chemical composition of fibre hemp (*Cannabis sativa* L.). Biomass and Bioenergy 32, 392–399. https://doi.org/10.1016/j.biombioe.2007.10.015

Obeng, E.M., Adam, S.N.N., Budiman, C., Ongkudon, C.M., Maas, R., Jose, J., 2017. Lignocellulases: a review of emerging and developing enzymes, systems, and practices. Bioresour. Bioprocess. 4, 16. https://doi.org/10.1186/s40643-017-0146-8

Pandey, B.R., Knoblauch, H., Zenz, G., 2023. Slope Stability Evaluation Due to Reservoir Draw-Down Using LEM and Stress-Based FEM along with Mohr–Coulomb Criteria. Water 15, 4022. https://doi.org/10.3390/w15224022

Paridah, M.T., Basher, A.B., SaifulAzry, S., Ahmed, Z., 2011. RETTING PROCESS OF SOME BAST PLANT FIBRES AND ITS EFFECT ON FIBRE QUALITY: A REVIEW. BioResources 6, 5260–5281.

Pauly, M., Gille, S., Liu, L., Mansoori, N., de Souza, A., Schultink, A., Xiong, G., 2013. Hemicellulose biosynthesis. Planta 238, 627–642. https://doi.org/10.1007/s00425-013-1921-1

Peters, G.M., Sandin, G., Spak, B., 2019. Environmental Prospects for Mixed Textile Recycling in Sweden. ACS Sustainable Chem. Eng. 7, 11682–11690. https://doi.org/10.1021/acssuschemeng.9b01742

Placet, V., Day, A., Beaugrand, J., 2017. The influence of unintended field retting on the physicochemical and mechanical properties of industrial hemp bast fibres. J Mater Sci 52, 5759–5777. https://doi.org/10.1007/s10853-017-0811-5

Potluri, R., Chaitanya Krishna, N., 2020. Potential and Applications of Green Composites in Industrial Space. Materials Today: Proceedings, 2nd International Conference on Materials Manufacturing and Modelling, ICMMM – 2019, VIT University, Vellore, 29th - 31st March 2019 22, 2041–2048. https://doi.org/10.1016/j.matpr.2020.03.218

Ragusa, A., Svelato, A., Santacroce, C., Catalano, P., Notarstefano, V., Carnevali, O., Papa, F., Rongioletti, M.C.A., Baiocco, F., Draghi, S., D'Amore, E., Rinaldo, D., Matta, M., Giorgini, E., 2021. Plasticenta: First evidence of microplastics in human placenta. Environment International 146, 106274. https://doi.org/10.1016/j.envint.2020.106274

Raman, V., Lata, H., Chandra, S., Khan, I.A., ElSohly, M.A., 2017. Morpho-Anatomy of Marijuana (Cannabis sativa L.), in: Chandra, S., Lata, H., ElSohly, M.A. (Eds.), Cannabis Sativa L. - Botany and Biotechnology. Springer International Publishing, Cham, pp. 123–136. https://doi.org/10.1007/978-3-319-54564-6_5

Rana, S., Pichandi, S., Moorthy, S., Bhattacharyya, A., Parveen, S., Fangueiro, R., 2015. Carbon Footprint of Textile and Clothing Products. pp. 141–166. https://doi.org/10.1201/b18428-10

Ribeiro, A., Pochart, P., Day, A., Mennuni, S., Bono, P., Baret, J.-L., Spadoni, J.-L., Mangin, I., 2015. Microbial diversity observed during hemp retting. Appl Microbiol Biotechnol 99, 4471–4484. https://doi.org/10.1007/s00253-014-6356-5

Ritchie, H., Rosado, P., Roser, M., 2024. Fossil fuels. Our World in Data.

Roach, M.J., Deyholos, M.K., 2007. Microarray analysis of flax (Linum usitatissimum L.) stems identifies transcripts enriched in fibre-bearing phloem tissues. Mol Genet Genomics 278, 149–165. https://doi.org/10.1007/s00438-007-0241-1

Rogers, C.M., 1982. The systematics ofLinum sect.Linopsis (Linaceae). Pl Syst Evol 140, 225–234. https://doi.org/10.1007/BF02407299

Rose, D.C., Wheeler, R., Winter, M., Lobley, M., Chivers, C.-A., 2021. Agriculture 4.0: Making it work for people, production, and the planet. Land Use Policy 100, 104933. https://doi.org/10.1016/j.landusepol.2020.104933

Rosemberg, J.A., 1965. Bacteria Responsible for the Retting of Brazilian Flax. Applied Microbiology 13, 991–992. https://doi.org/10.1128/am.13.6.991-992.1965

Różańska, W., Romanowska, B., Rojewski, S., 2023. The Quantity and Quality of Flax and Hemp Fibers Obtained Using the Osmotic, Water-, and Dew-Retting Processes. Materials 16, 7436. https://doi.org/10.3390/ma16237436

Ruan, P., Du, J., Gariepy, Y., Raghavan, V., 2015. Characterization of radio frequency assisted water retting and flax fibers obtained. Industrial Crops and Products 69, 228–237. https://doi.org/10.1016/j.indcrop.2015.02.009

Salmon-minotte, J., Franck, R.R., 2005. 3 - Flax, in: Franck, R.E. (Ed.), Bast and Other Plant Fibres, Woodhead Publishing Series in Textiles. Woodhead Publishing, pp. 94–175. https://doi.org/10.1533/9781845690618.94

Sampaio, S., Bishop, D., Shen, J., 2005. Physical and chemical properties of flax fibres from stand-retted crops desiccated at different stages of maturity. Industrial Crops and Products 21, 275–284. https://doi.org/10.1016/j.indcrop.2004.04.001

Sandin, G., Peters, G.M., 2018. Environmental impact of textile reuse and recycling – A review. Journal of Cleaner Production 184, 353–365. https://doi.org/10.1016/j.jclepro.2018.02.266

Sandin, G., Peters, G.M., Svanström, M., 2013. Moving down the cause-effect chain of water and land use impacts: An LCA case study of textile fibres. Resources, Conservation and Recycling 73, 104–113. https://doi.org/10.1016/j.resconrec.2013.01.020

Sandin, G., Roos, S., Johansson, M., 2019. Environmental impact of textile fibers – what we know and what we don't know : Fiber Bible part 2.

Seaby, D.A., Mercer, P.C., 1984. Development of a hand tool to test the degree of retting of flax straw. Annals of Applied Biology 104, 567–573. https://doi.org/10.1111/j.1744-7348.1984.tb03040.x

Sharma, H.S.S., 1986a. An alternative method of flax retting during dry weather. Annals of Applied Biology 109, 605–611. https://doi.org/10.1111/j.1744-7348.1986.tb03217.x

Sharma, H.S.S., 1986b. The role of bacteria in retting of desiccated flax during damp weather. Appl Microbiol Biotechnol 24, 463–467. https://doi.org/10.1007/BF00250324

Sharma, H.S.S., Faughey, G.J., 1999. Comparison of subjective and objective methods to assess flax straw cultivars and fibre quality after dew-retting. Annals of Applied Biology 135, 495–501. https://doi.org/10.1111/j.1744-7348.1999.tb00879.x

Sharma, H.S.S., Reinard, N., 2004. Evaluation of Visible and Near-Infrared Spectroscopy as a Tool for Assessing Fiber Fineness during Mechanical Preparation of Dew-Retted Flax. Appl Spectrosc 58, 1431–1438. https://doi.org/10.1366/0003702042641272

Sharma, S., 1992. SHARMA, H.S.S. and VAN SUMERE, C.F. (1992). The Biology and Processing of Flax. M. Publications, Belfast, 576 pp.

Shen, L., Patel, M., 2010. Life Cycle Assessment of man-made cellulose fibres. Lenzinger Berichte 88: 1–59.

Shen, L., Worrell, E., Patel, M.K., 2012. Comparing life cycle energy and GHG emissions of bio-based PET, recycled PET, PLA, and man-made cellulosics. Biofuels, Bioproducts and Biorefining 6, 625–639. https://doi.org/10.1002/bbb.1368

Shen, L., Worrell, E., Patel, M.K., 2010. Environmental impact assessment of man-made cellulose fibres. Resources, Conservation and Recycling 55, 260–274. https://doi.org/10.1016/j.resconrec.2010.10.001

Small, E., Marcus, D., n.d. Hemp: A New Crop with New Uses for North America.

Smil, V., 2018. Energy and Civilization: A History. MIT Press.

Snegireva, A.V., Ageeva, M.V., Amenitskii, S.I., Chernova, T.E., Ebskamp, M., Gorshkova, T.A., 2010. Intrusive growth of sclerenchyma fibers. Russ J Plant Physiol 57, 342–355. https://doi.org/10.1134/S1021443710030052

Srivastava, V., McKee, L.S., Bulone, V., 2017. Plant Cell Walls, in: Encyclopedia of Life Sciences. John Wiley & Sons, Ltd, pp. 1–17. https://doi.org/10.1002/9780470015902.a0001682.pub3

Summerscales, J., Dissanayake, N.P.J., Virk, A.S., Hall, W., 2010. A review of bast fibres and their composites. Part 1 – Fibres as reinforcements. Composites Part A: Applied Science and Manufacturing 41, 1329–1335. https://doi.org/10.1016/j.compositesa.2010.06.001

Tamburini, E., León, A.G., Perito, B., Di Candilo, M., Mastromei, G., 2004. Exploitation of bacterial pectinolytic strains for improvement of hemp water retting. Euphytica 140, 47–54. https://doi.org/10.1007/s10681-004-4754-y

Tamburini, E., León, A.G., Perito, B., Mastromei, G., 2003. Characterization of bacterial pectinolytic strains involved in the water retting process. Environmental Microbiology 5, 730–736. https://doi.org/10.1046/j.1462-2920.2003.00462.x

Tláskal, V., Brabcová, V., Větrovský, T., Jomura, M., López-Mondéjar, R., Oliveira Monteiro, L.M., Saraiva, J.P., Human, Z.R., Cajthaml, T., Nunes da Rocha, U., Baldrian, P., 2021. Complementary Roles of Wood-Inhabiting Fungi and Bacteria Facilitate Deadwood Decomposition. mSystems 6, 10.1128/msystems.01078-20. https://doi.org/10.1128/msystems.01078-20

Tornero, P., Mayda, E., Gómez, M.D., Cañas, L., Conejero, V., Vera, P., 1996. Characterization of LRP, a leucine-rich repeat (LRR) protein from tomato plants that is processed during pathogenesis. The Plant Journal 10, 315–330. https://doi.org/10.1046/j.1365-313X.1996.10020315.x

Torres, J.P., Vandi, L.-J., Veidt, M., Heitzmann, M.T., 2017. The mechanical properties of natural fibre composite laminates: A statistical study. Composites Part A: Applied Science and Manufacturing 98, 99–104. https://doi.org/10.1016/j.compositesa.2017.03.010

Truss, R.W., Wood, B., Rasch, R., 2016. Quantitative surface analysis of hemp fibers using XPS, conventional and low voltage in-lens SEM. Journal of Applied Polymer Science 133. https://doi.org/10.1002/app.43023

Ullo, S.L., Sinha, G.R., 2021. Advances in IoT and Smart Sensors for Remote Sensing and Agriculture Applications. Remote Sensing 13, 2585. https://doi.org/10.3390/rs13132585

Valladares Juárez, A.G., Dreyer, J., Göpel, P.K., Koschke, N., Frank, D., Märkl, H., Müller, R., 2009. Characterisation of a new thermoalkaliphilic bacterium for the production of high-quality hemp fibres, Geobacillus thermoglucosidasius strain PB94A. Appl Microbiol Biotechnol 83, 521–527. https://doi.org/10.1007/s00253-009-1969-9

van Dam, J.E.G., Gorshkova, T.A., 2003. CELL WALLS AND FIBERS | Fiber Formation, in: Thomas, B. (Ed.), Encyclopedia of Applied Plant Sciences. Elsevier, Oxford, pp. 87–96. https://doi.org/10.1016/B0-12-227050-9/00046-6

van der Velden, N.M., Patel, M.K., Vogtländer, J.G., 2014. LCA benchmarking study on textiles made of cotton, polyester, nylon, acryl, or elastane. Int J Life Cycle Assess 19, 331–356. https://doi.org/10.1007/s11367-013-0626-9

van der Werf, H.M.G., Turunen, L., 2008. The environmental impacts of the production of hemp and flax textile yarn. Industrial Crops and Products 27, 1–10. https://doi.org/10.1016/j.indcrop.2007.05.003

Van Sumere, C., 1992. Retting of flax with special reference to enzyme-retting, in: The Biology and Processing of Flax. M Publications, pp. 153–193.

Van Tieghem, M.Ph., 1879. Sur La Fermentation De La Cellulose. Bulletin de la Société Botanique de France 26, 25–30. https://doi.org/10.1080/00378941.1879.10825719

van Zeist, W., Bakker-Heeres, J.A.H., 1975. Evidence for linseed cultivation before 6000 bc. Journal of Archaeological Science 2, 215–219. https://doi.org/10.1016/0305-4403(75)90059-X

Ven, T.G.M.V.D., Godbout, L., 2013. Cellulose: Fundamental Aspects. BoD – Books on Demand.

Vignon, M.R., Garcia-Jaldon, C., 1996. Structural features of the pectic polysaccharides isolated from retted hemp bast fibres. Carbohydrate Research 296, 249–260. https://doi.org/10.1016/S0008-6215(96)00226-1

Visi, D.K., D'Souza, N., Ayre, B.G., Webber III, C.L., Allen, M.S., 2013. Investigation of the bacterial retting community of kenaf (Hibiscus cannabinus) under different conditions using next-generation semiconductor sequencing. Journal of Industrial Microbiology and Biotechnology 40, 465–475. https://doi.org/10.1007/s10295-013-1242-1

Voříšková, J., Baldrian, P., 2013. Fungal community on decomposing leaf litter undergoes rapid successional changes. The ISME Journal 7, 477–486. https://doi.org/10.1038/ismej.2012.116

Wallenstein, M.D., Hess, A.M., Lewis, M.R., Steltzer, H., Ayres, E., 2010. Decomposition of aspen leaf litter results in unique metabolomes when decomposed under different tree species. Soil Biology and Biochemistry 42, 484–490. https://doi.org/10.1016/j.soilbio.2009.12.001

Wang, X., Luo, Y., Huang, K., Cheng, N., 2022. Biosensor for agriculture and food safety: Recent advances and future perspectives. Advanced Agrochem 1, 3–6. https://doi.org/10.1016/j.aac.2022.08.002

Wang, Z., Hobson, N., Galindo, L., Zhu, S., Shi, D., McDill, J., Yang, L., Hawkins, S., Neutelings, G., Datla, R., Lambert, G., Galbraith, D.W., Grassa, C.J., Geraldes, A., Cronk, Q.C., Cullis, C., Dash, P.K., Kumar, P.A., Cloutier, S., Sharpe, A.G., Wong, G.K.-S., Wang, J., Deyholos, M.K., 2012. The genome of flax (Linum usitatissimum) assembled de novo from short shotgun sequence reads. The Plant Journal 72, 461–473. https://doi.org/10.1111/j.1365-313X.2012.05093.x

Wiedemann, S.G., Ledgard, S.F., Henry, B.K., Yan, M.-J., Mao, N., Russell, S.J., 2015. Application of life cycle assessment to sheep production systems: investigating co-production of wool and meat using case studies from major global producers. Int J Life Cycle Assess 20, 463–476. https://doi.org/10.1007/s11367-015-0849-z

Woese, C.R., Fox, G.E., 1977. Phylogenetic structure of the prokaryotic domain: The primary kingdoms. Proceedings of the National Academy of Sciences 74, 5088–5090. https://doi.org/10.1073/pnas.74.11.5088

Xu, H., Zhang, L., Feng, X., Yang, Q., Zheng, K., Duan, S., Cheng, L., 2022. Metagenomic and proteomic analysis of bacterial retting community and proteome profile in the degumming process of kenaf bast. BMC Plant Biology 22, 516. https://doi.org/10.1186/s12870-022-03890-5

Yacout, D.M.M., Abd El-Kawi, M.A., Hassouna, M.S., 2016. Cradle to gate environmental impact assessment of acrylic fiber manufacturing. Int J Life Cycle Assess 21, 326–336. https://doi.org/10.1007/s11367-015-1023-3

Yahya, N., 2018. Agricultural 4.0: Its Implementation Toward Future Sustainability, in: Yahya, N. (Ed.), Green Urea : For Future Sustainability, Green Energy and Technology. Springer, Singapore, pp. 125–145. https://doi.org/10.1007/978-981-10-7578-0_5

Yan, L., Chouw, N., Jayaraman, K., 2014. Flax fibre and its composites – A review. Composites Part B: Engineering 56, 296–317. https://doi.org/10.1016/j.compositesb.2013.08.014

Yang, X., Shu, L., Chen, J., Ferrag, M.A., Wu, J., Nurellari, E., Huang, K., 2021. A Survey on Smart Agriculture: Development Modes, Technologies, and Security and Privacy Challenges. IEEE/CAA JAS 8, 273–302. https://doi.org/10.1109/JAS.2020.1003536

Zampori, L., Dotelli, G., Vernelli, V., 2013. Life Cycle Assessment of Hemp Cultivation and Use of Hemp-Based Thermal Insulator Materials in Buildings. Environ. Sci. Technol. 47, 7413–7420. https://doi.org/10.1021/es401326a

Zawani, Z., Luqman Chuah, A., Abdan, K., 2015. Characterization of Kenaf Fibre-Retting Wastewater.

Zhang, J., Lin, G., Vaidya, U., Wang, H., 2023. Past, present and future prospective of global carbon fibre composite developments and applications. Composites Part B: Engineering 250, 110463. https://doi.org/10.1016/j.compositesb.2022.110463

Zhang, L.L., Zhu, R.Y., Chen, J.Y., Chen, J.M., Feng, X.X., 2008. Seawater-retting treatment of hemp and characterization of bacterial strains involved in the retting process. Process Biochemistry 43, 1195–1201. https://doi.org/10.1016/j.procbio.2008.06.019

Zhao, D., Liu, P., Pan, C., Du, R., Ping, W., Ge, J., 2016. Bacterial succession and metabolite changes during flax (Linum usitatissimum L.) retting with Bacillus cereus HDYM-02. Sci Rep 6, 31812. https://doi.org/10.1038/srep31812

Zhu, J., Zhu, H., Njuguna, J., Abhyankar, H., 2013. Recent Development of Flax Fibres and Their Reinforced Composites Based on Different Polymeric Matrices. Materials 6, 5171–5198. https://doi.org/10.3390/ma6115171

Zimniewska, M., Romanowska, B., Zimniewska, M., Romanowska, B., 2022. Bast Fiber Textiles Addressed Improvement of Human Life, in: Natural Fiber. IntechOpen. https://doi.org/10.5772/intechopen.105161

CHAPTER II

Materials and Methods

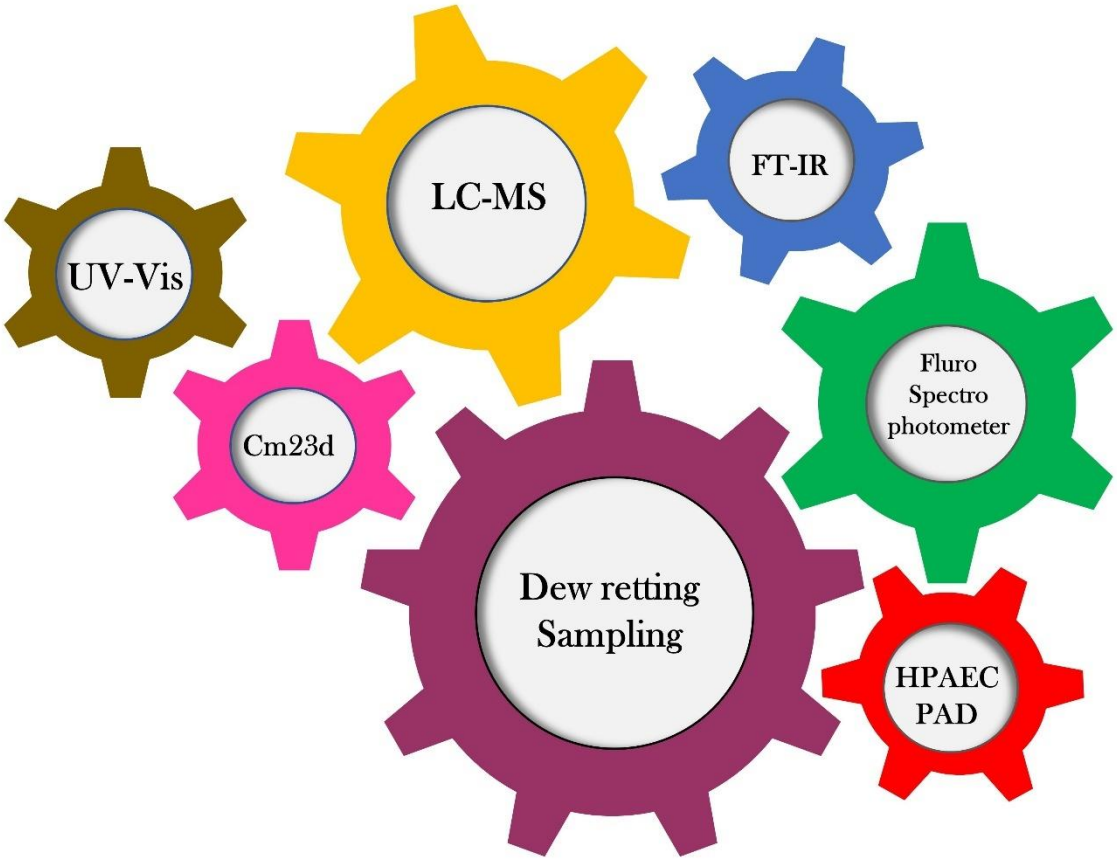

Chapter II: Material and Methods

Contents

Chapter II: Material and Methods 96
II.1. Context of the chapter 98
II.2. Sampling of materials 98
II.2.1. Sampling of flax dew retting 2021 and meteorological information 98
II.2.2. Sampling of flax dew retting 2022 and meteorological information 100
II.2.3. Description of collected flax retting sample 2014 100
II.2.4. Description of collected hemp retting sample 2021 101
II.3. Soil analysis of retting 2021 102
II.4. Fiber quality assessment of retting 2021 102
II.4.1. Industrial fiber assessment of retting 2021 102
II.4.2. In-lab fiber quality assessment 103
II.5. Anatomy of stems and histochemical staining 104
II.5.1. Sample preparation 104
II.5.1.1. Sample embedded in Technovit 7100 resin 104
II.5.2. Microtomy 104
II.5.3. Histochemical staining 104
II.6. Spectrophotometric/ fluorometric enzyme assay 105
II.6.1. Peroxidase/ Phenol-oxidase 106
II.6.2. Polygalacturonase 106
II.6.3. Glucosidase/ Cellobiohydrolase/ Xylosidase and Galactosidase 106
II.6.4. Statistical analysis of enzyme assay results 106
II.7. Monosaccharide analysis with HPLC-HPAEC-PAD 107
II.7.1 Sample preparation 107
II.7.1.1. Preparation 107
II.7.1.2. Starch degradation 107
II.7.3. AIR production 108
II.7.2. Hydrolysis 108
II.7.3. HPAEC-PAD run and calculations 109
II.7.4. Statistical analysis of monosaccharide assay results 109

II.8. Preparation, and measurements for 2D-LC-MS/MS-based metaproteomics..... 110
II.8.1. Choice of samples for metaproteomics..... 110
II.8.2. Extraction, quantification and preparation of protein samples..... 110
II.8.3. Nano LC-MS/MS and Mass Spectrometry..... 111
II.9. Proteomic data analysis..... 111
II.9.1. Spectra analysis and identification of proteins..... 111
II.9.2. Statistical analysis of resulting metaproteomic dataset..... 112
II.9.3. Functional and taxonomic analysis of proteomes..... 112
II.10. FTIR-vibrational-spectroscopy..... 113
II.10.1. Preparation of sample for FT-IR spectroscopy..... 113
II.10.2. FT-IR spectroscopy..... 114
II.10.3. Spectra treatments for average spectra illustrations..... 116
II.10.4. Statistical analysis for FT-IR data..... 116
II.10.4.1. Multiple pairwise comparisons by one way-ANOVA analysis (‘*a priori’* approach) 117
II.10.4.2. Global statistical analyses (‘without *a priori’* approach)..... 117
II.10.4.2.1. Unsupervised exploratory analysis by PCA..... 117
II.10.4.2.2. Supervised exploratory analysis by PLS-DA and sPLS-DA..... 117
II.11. Color spectroscopy..... 118
II.11.1. Collection of Spectral Reading..... 118
II.11.2. Statistical analysis of color data..... 119
II.11.2.1. Multiple pairwise comparisons of CL*a*b* data by one way-ANOVA analysis ... 119
II.11.2.2. Unsupervised exploratory analysis of visual spectral data by PCA..... 121
II.11.2.3. Supervised exploratory analysis of visual spectral data by PLS-DA and sPLS-DA 121
II.12. Reference..... 122

II.1. Context of the chapter

This chapter outlines the materials and methods used in the study, covering comprehensive details on sample collection and abiotic assessments, including soil analysis and weather data acquisition. It also encompasses industrial and laboratory-based fiber characterization, anatomical procedures of sample preparation (and staining), optimized protocols for enzyme assays, metaproteomic analysis, monosaccharide profiling, FTIR spectroscopy, color measurements, and statistical analyses applied throughout the research.

II.2. Sampling of materials

Sampling for flax dew retting was carried out twice during my thesis, in 2021 and 2022. Most of the biological experiments were performed on the 2021 flax retting samples. For color analysis, however, flax dew retting samples from three years (2022, 2021, and 2014) were used. The 2014 samples were collected and carefully stored by previous PhD student Christophe Djemiel under the supervision of Dr. Sebastien Grec. Additionally, hemp dew retting samples were collected by PhD student Eliane Bou Orm (Ecole des Mines d'Ales) and sent to us for enzymatic analysis.

II.2.1. Sampling of flax dew retting 2021 and meteorological information

Flax plants (*Linum usitatissimum* L., cultivar Evasion, Terre de Lin) were sown by flax farmers contracted to the Van Robaeys Frères company on the 30th March 2021, in a typical silty-clay soil field (50°47'05.5"N 2°27'07.4"E) near Bavinchove, Hauts-de-France, France (**Fig. II.1a**). Dew retting started at uprooting (23rd July, stage R0), swathes were turned on day 12 and then retting continued until the stem harvesting (15^{h} August, stage R7) (**Fig. II.1b**). Swath lines were marked at 5 plots (150×100cm) for 5 biological replicates (T1-T5-per time point) (**Fig. II.1c**) samples (30 cm-long sections from the middle regions of flax swathes) within each replicate were collected during retting on the following days (R0/day 1, R1/day 4, R2/day 6, R3/day 11, R4/day 13, R5/day 18, R6/day 20 and R7/day 25) and kept at -80 C° for further analysis. Samples are collected from three adjacent fields named filed A, filed B, and filed C (**Fig. II.1a**). Climatic data during field retting was obtained from the closest 'Infoclimat' weather station (https://www.infoclimat.fr/observations-meteo/temps-reel/mazinghem/000RL.html) (shown in Chapter III, IV & V).

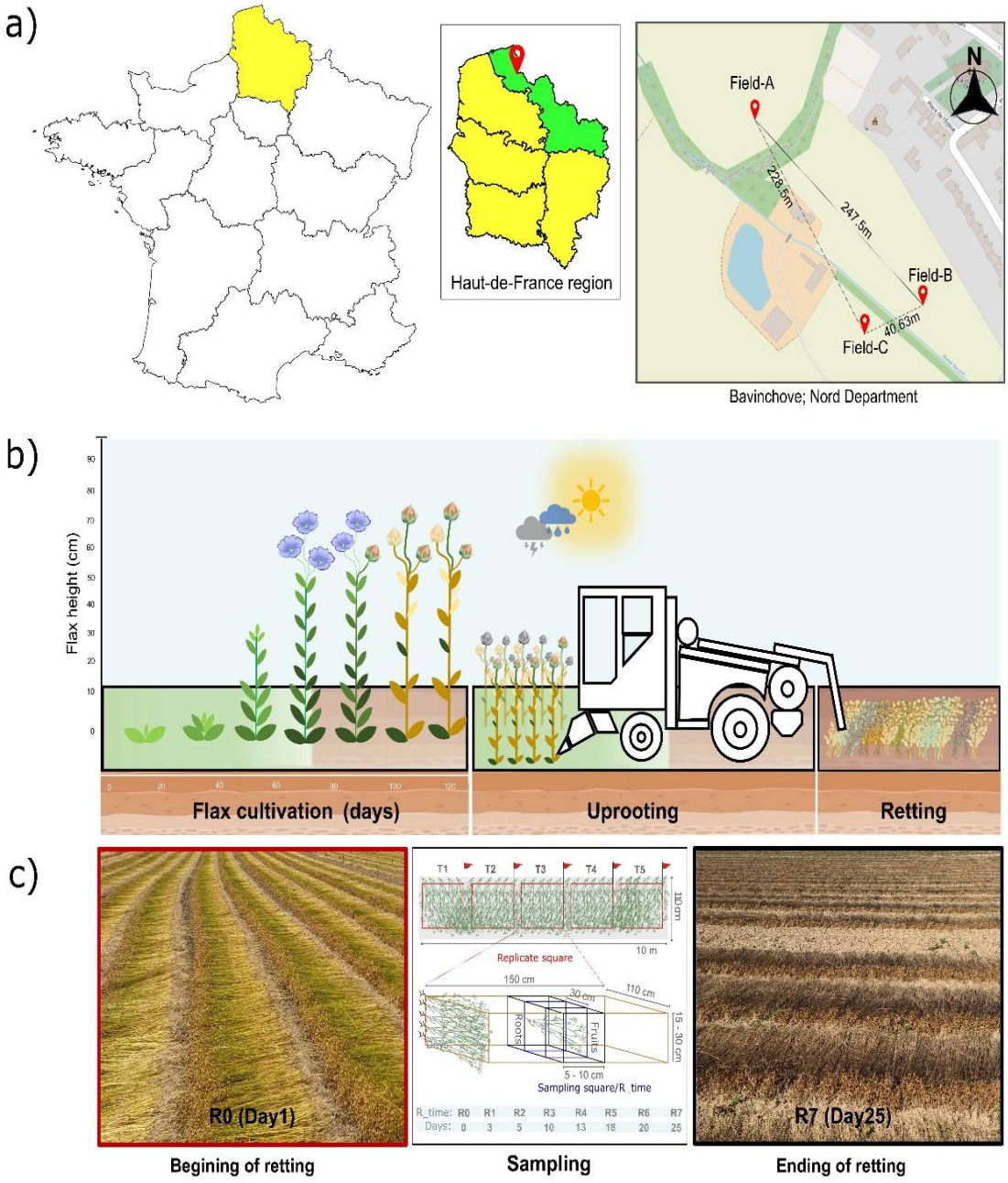

Figure II.1. Sampling location and techniques.

a) Map of France, showing the field location at department Nord, Hauts-de-France region (in the middle) and the three sampling fields (right side of reader). b) flax cultivation and harvesting of mature flax with the starting of field retting process. c) beginning of retting (left), end of retting (right), and the sampling technique infographics (in the middle) showing sample collection from five replicates (T1-T5) from day 1 (R0) till day 25 (R7).

II.2.2. Sampling of flax dew retting 2022 and meteorological information

In 2022, the second sampling of flax dew retting was conducted from the 6th of July until the 29th of August, focusing on the same cultivar (Evasion, Terre de Lin). This study took place in two fields located in Killem (coordinates: 50°57'04"N, 2°34'55"E) in the Hauts-de-France region (FR-59), in collaboration with Van Robaeys company and Mr. Nicolas RYCKEBOER. The retting process lasted for 55 days, and a total of 15 retting samples were collected at different time points. The samples were designated as follows: R0 (day 1), R1 (day 6), R2 (day 9), R3 (day 13), R4 (day 16), R5 (day 20), R6 (day 23), R7 (day 27), R8 (day 30), R9 (day 34), R10 (day 37), R11 (day 41), R12 (day 44), R13 (day 48), R14 (day 51), and R15 (day 55), with samples taken from each of the two fields. The collection methods strictly followed protocols established in previous years to maintain consistency in the experiment.

To investigate the effects of over-retting, sample collection in one of the fields (Field A) was extended beyond the initial 55-day period. Additional samples were taken on day 59 (R16) and day 69 (R17), while a subset of samples was left exposed to natural conditions until day 90 (R20). By day 90, the flax stems had entirely lost their mechanical properties, indicating the final stage of retting degradation.

Throughout the retting process, weather data was recorded using information from the nearest 'Infoclimat' weather station, located 9 km away in Bergues (https://www.infoclimat.fr/observations-meteo/temps-reel/bergues/000R5.html). This data was crucial in understanding the environmental conditions that influenced the retting dynamics in Killem (shown in Chapter V).

II.2.3. Description of collected flax retting sample 2014

The 2014 flax dew-retting sampling information was obtained from the thesis of Christophe Djemiel. Samples (*Linum usitatissimum* L., Cultivar Lorea) were collected from the fields of Martainneville (F-27210 Region Hauts-de-France) in northern France (50°00'03"N, 1°42'27"E) (**Fig. II.2**), starting on July 7th and continuing until September 5th, 2014, covering a period of 44 days. A swath of 50-60 stems was collected from five sampling spots (150×100 cm) in a W pattern, serving as biological replicates for each retting time point, which were named day 1, day 6, day 12, day 19, day 26, day 33, and day 44. The samples were dried at room temperature and stored in the dark. Spectral measurements were taken directly from these dried, stored samples. Details can be found in the thesis of Christophe Djemiel (Djemiel, 2017). (Climatic information, also taken from the thesis (Djemiel, 2017) shown in chapter V).

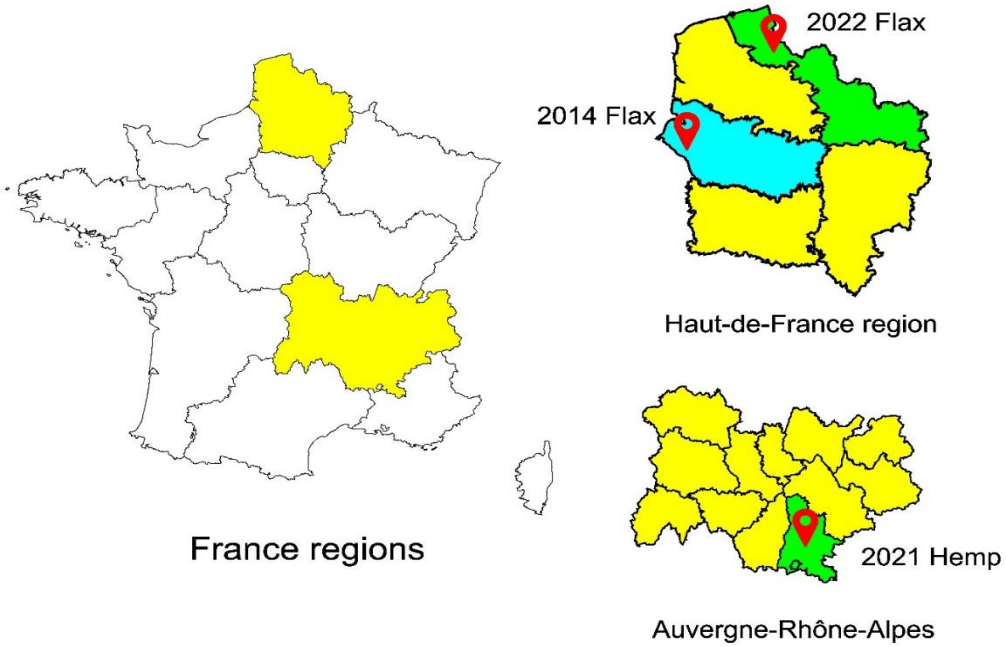

Figure II.2. Sampling location in different years.

In 2022, flax dew-retting samples were collected from the fields located at Department Nord, Hauts-de-France region. In 2014, dew-retting samples were collected from the fields of Somme department, Hauts-de-France region (by C. Djemiel). And in 2021, Hemp dew-retting samples were collected from fields of the Drôme department, Auvergne-Rhône-Alpes region.

II.2.4. Description of collected hemp retting sample 2021

The information on 2021 hemp dew retting sampling has been taken from the thesis of Eliane Bou Omr (Bou Orm et al., 2024). Hemp plants (*Cannabis sativa* L., Cultivar Futura 75) were sown at a rate of 40 kg/ha on April 15, 2021, in the south of France at the Drôme Chanvre association (Mirabel et Blacons, France, 44° 42′ 35″N, 5° 05′29″E) (**Fig. II.2**). The plants were harvested at the end of flowering on September 2, 2021, using a sectional mower adapted for hemp. After harvest, the hemp plants were transported to another field in the south of France, Mas de La Valus (Le Bouquet, France, 44°09′52″N, 4°16′56″E), for logistical convenience due to its proximity to the laboratory. The retting process took place in this field from September 3, 2021, to October 17, 2021. Stem samples were collected weekly from five swaths (250 stems/swath) arranged in a non-systematic W pattern. Hemp stems were regularly turned (once a week) to ensure uniform retting. For sampling, 20 stems were collected weekly, including un-retted stems (R0) and retted stems after 1 (R1), 2 (R2), 3 (R3), 4 (R4), and 6 (R6) weeks and immediately stored at -80°C for future analysis.

II.3. Soil analysis of retting 2021

Soil samples were also collected from the three fields for all replicate plots from retting 2021 and sent to *analyze soil composition to* the "Laboratoire d'Analyses des Sols d'Arras, ***INRAE*** (https://las.hautsdefrance.hub.inrae.fr/prestations).

II.4. Fiber quality assessment of retting 2021

II.4.1. Industrial fiber assessment of retting 2021

At the end of retting, flax samples (4 to 5 kg) from all three experimental fields were collected and fibers extracted (scutching) by the company Van Robaeys Frères (Killem, Hauts-de-France) for industrial classification according to USTRL (Union Syndicale des Rouisseurs-Teilleurs de Lin, https://www.usrtl-ifl.fr/, 2024) standards (**Fig. II.3**).

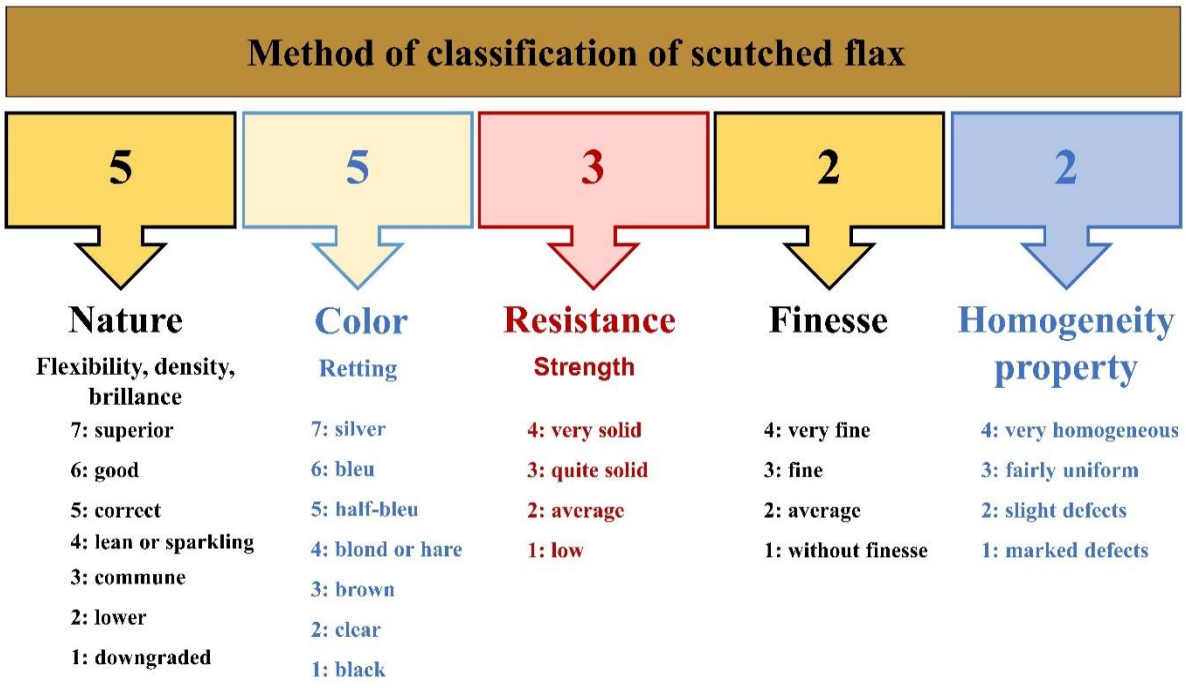

Figure II.3. Method of classifying retted and scutched flax fiber according to USTRL standards.

The Union Syndicale des Rouisseurs-Teilleurs de Lin de France (U.S.R.T.L.) is an association representing French flax retting and scutching companies, focusing on improving the quality, productivity, and profitability of flax fiber production. It plays a key role in setting industry standards, sharing technical insights, and providing support for investments. The U.S.R.T.L. helps monitor fiber

quality by evaluating parameters like fiber fineness, tensile strength, nature, homogeneity, color, etc., and giving them scores (from example: 55322) (**Fig. II.3**), ensuring consistency and competitiveness in the French and international flax markets.

II.4.2. In-lab fiber quality assessment

Scutched fibers from fields A and B were evaluated in the lab. Individual elementary fibers were manually individualized from factory-processed (scutched, hackled) flax fiber samples for the single fiber tensile tests. For fiber diameter measurement, 20mm long single fibers were glued to paper frames (to keep them straight) and diameters were measured every millimeter (20 times/fiber) with a Keyence VHX-6000 (500x) digital microscope & ImageJ software. Twelve to 14 single fibers were measured per sample group (field-A & field-B) (**Fig. II.4**). Fiber fineness was calculated from measured diameters according to the French Standard NFG 07-004 since literature considers that the cross-section of flax single fibers to be circular (Gogoli, 2022; Richely et al., 2022). Breaking stress, deformation (ε) at break & and two tensile moduli of single fibers were measured for samples using the single fiber tensile test (SFTT) according to the method of the French standard NFT 25-501-2 (Bourmaud et al., 2018; Charlet, 2008; Réquilé et al., 2021). The initial tensile modulus (E1) and a final apparent tensile modulus (E2) were determined using two different strain ranges (between 0.05% and 0.5 % for E1 and between εmax -0.2% and εmax for E2). Machine compliance was considered and the tensile force was measured with a 10N force sensor equipped on the MTS criterion bench, and the displacement rate was set at 1mm/min.

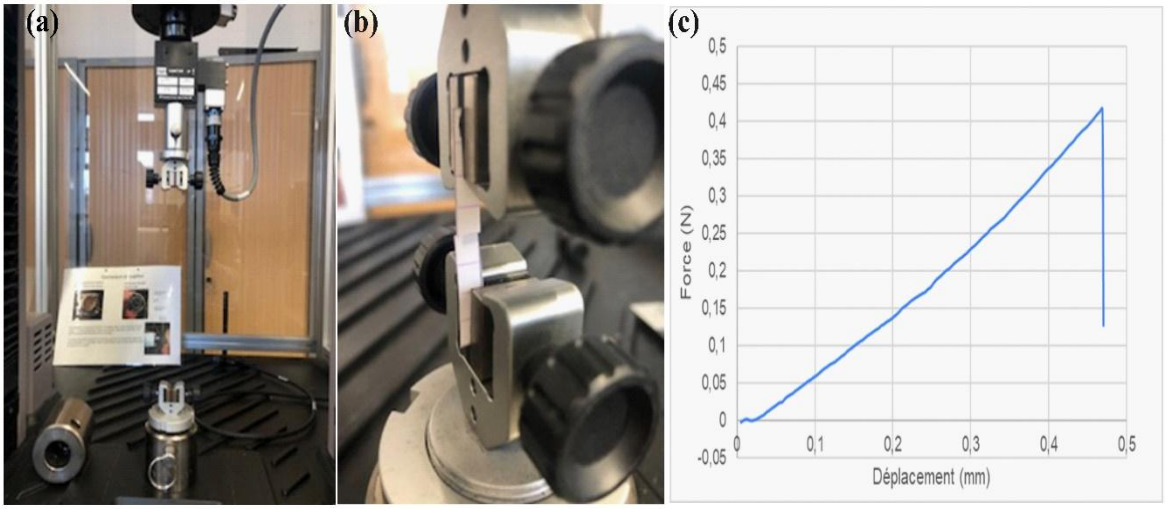

Figure II.4. In-lab fiber quality assessment using the single fiber tensile test.

(a) Installation of the 10N sensor on the MTS Criterion tensile tester; (b) Sample placed between the grips with a cut paper frame, ready for testing; (c) Force-displacement curve for a single fiber.

II.5. Anatomy of stems and histochemical staining

II.5.1. Sample preparation

To monitor structural changes in the stem during the early and late stages of retting, an anatomical study was conducted using simple transverse sections. At the beginning of retting, when the plant stem remains intact, preparing cross-sections is relatively straightforward. However, with the progress of retting, when the stem's integrity has significantly deteriorated, embedding the samples in a supporting medium such as Technovit resin or Paraffin/Paraplast is necessary. This ensures the production of intact sections, allowing detailed observation of the retting-induced changes in stem structure; which are also being used for our preliminary Raman vibrational spectroscopic analysis.

II.5.1.1. Sample embedded in Technovit 7100 resin

To prepare stem samples for embedding in Technovit 7100 resin, they must first be fully dehydrated. Stem segments, approximately 1-2 cm in length, undergo sequential treatment with graded ethanol solutions (70%, 95%, and 100%) for 20 minutes each, repeated twice for thorough dehydration. The dehydrated samples are then rinsed in Technovit solution-1 (A), to which one bag of catalyzer C powder is added (stored at 4°C). Subsequently, solution B, the hardener, is mixed with the A+C solution. The stem samples are then quickly transferred into this mixture within a gelatin capsule. Polymerization and hardening occur at room temperature (25°C) over a period of 2 hours. Once hardened, the gelatin capsules are removed, and the samples are labeled and prepared for microtomy (**Fig. II.5a**).

II.5.2. Microtomy

Microtome sections were prepared from embedded samples using different knives based on the embedding medium. For paraffin-embedded samples, steel knives were employed to cut sections with a thickness of 10–30 µm, while for resin-embedded samples, glass knives were used to obtain sections typically 3–5 µm thick. The sections were placed on labeled glass slides (added with water), on a hotplate maintained at 42°C, and subsequently covered with coverslips (**Fig. II.5b**). Staining procedures were performed prior to the application of the coverslips.

II.5.3. Histochemical staining

Staining was primarily performed using Toluidine Blue O (0.1% w/v in water) for general tissue staining. This metachromatic dye produces a range of colors depending on the chemical composition of the sample, from pink (pectin, galacturonic acid) to purple (acidic mucilage), to various shades of blue

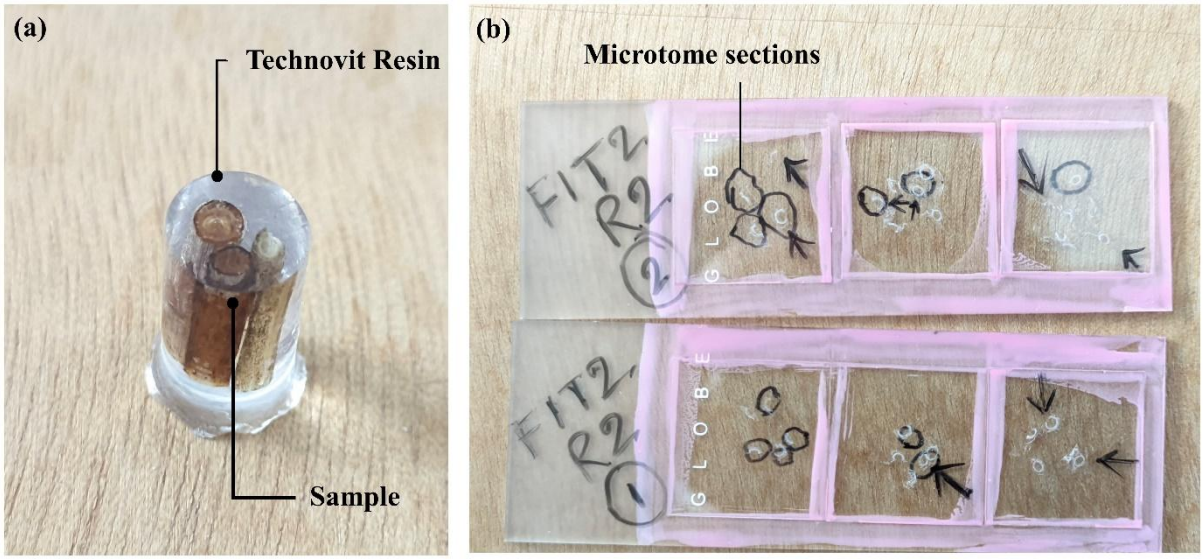

Figure II.5. Technovit embedding and microtomy.

(a) retted flax stem sample (1-2cm) embedded into Technovit-7100 resin; (b) microtome sections, with sealed cover slip on a labeled slide, prepared for staining purposes.

(cellulosic cell walls), and a luminescent light green-blue for polyphenols and lignin. Occasionally, orange staining indicated the presence of tannins or latex, while a brownish-orange hue identified cutin or suberin.

In addition, a double-staining protocol was employed using Safranin O (0.25% w/v in 100% ethanol) and Alcian Blue (0.1% w/v in water). The stains were either mixed and applied together or applied sequentially—Alcian Blue for 30 seconds followed by Safranin O for 3 seconds. After staining, the sections were rinsed with water until no excess stain remained. In plant tissues, Safranin O selectively stained lignified cell walls red, while Alcian Blue stained cellulosic cell walls blue.

II.6. Spectrophotometric/ fluorometric enzyme assay

Procedures were mainly adapted from (Chabbert et al., 2020). After removing the woody xylem part, frozen stems (2g of fresh weight) were blended in 100 mL of 50 mM phosphate buffer, pH 7 for 1 min and filtered with a GF/A filter (pore size 1.6 µm). This maximizes enzyme dynamics detection by focusing on the area of our interest. The soluble fraction of the extract from each of the five biological replicates per retting point was analyzed with five technical repetitions. All the enzyme activities were

determined at 25°C and expressed by nmol/gMS/h; except polygalacturonase (expressed in µmol/gMS/h). For flax samples (from retting 2021), 8 retting points, namely R0-R7 were analyzed whereas in hemp, stem samples from four retting stages (R0, R1, R4, and R6) have been analyzed.

II.6.1. Peroxidase/ Phenol-oxidase

The peroxidase and phenol oxidase enzyme activity were measured by using 5 mM L-DOPA (L-3,4-dihydroxyphenylalanine) as described previously (Sauvadet et al., 2016). Peroxidase enzyme hydrolyzes hydrogen peroxide into water and molecular oxygen and that reactive oxygen further oxidizes L-DOPA to D-IQC (3-hyroindole-5,6-quinone-2-carboxylate). The absorbance is taken at 460 nm to measure the enzyme activity.

II.6.2. Polygalacturonase

Polygalacturonase activity was quantified by the DNS method and a galacturonic acid calibration curve, as reported by (Bleuze et al., 2018). Enzyme endo-polygalacturonase (EPG) breaks the α-1,4-glycosidic bonds in polygalacturonic acid and releases galacturonic acid monomer units with a free-reducing sugar end group. They react with DNS and change the color. The enzyme (800 µL) substrate (200 µL) mixture was added with DNS (500 µL) after 1 h of incubation and treated with a boiling water bath for 15 min to finish the reaction. The color change of the reaction mixture is proportional to the free galacturonic monomers i.e. EPG activity. The absorbance change is measured at 540 nm to read the enzyme activity.

II.6.3. Glucosidase/ Cellobiohydrolase/ Xylosidase and Galactosidase

Cellobiohydrolase, β-D-glucosidase, β-D-xylosidase, and β-D-galactosidase activities were measured by measuring the release of 4MUB (4-methylumbelliferone) as described by (Sauvadet et al., 2016), and (Chabbert et al., 2020). 4MUB acts as a fluorophore. Esters of 4MUB do not fluoresce unless cleaved to release the fluorophore. The enzymatic hydrolysis of 4MUB-containing substrate i.e. MU-β-D-glucopyranoside releases fluorescence which is proportional to the enzyme activity. The reaction mixture (in 96 deep well plates) was incubated for 3 h in the dark and measured at 460 nm using a microplate spectrophotometer CLARIOstar.

II.6.4. Statistical analysis of enzyme assay results

Data normality was assessed with the Shapiro-Wilk test and checked for equal variances among groups using Levene's test. Outliers identified by interquartile range (IQR) were removed, and any missing values (if present), were replaced with the mean of the group. A one-way analysis of variance (ANOVA)

along with Tukey's HSD (Honestly Significant Difference) test was performed to assess the effect of retting time on enzyme dynamics. To compare the retting dynamics between two fields, a pairwise T-test is performed with FDR (False Discovery Rate) correction of p-value by multiple comparisons.

II.7. Monosaccharide analysis with HPLC-HPAEC-PAD

Procedures were mainly adapted from Yest et al and Menna et al. It is divided into three steps - sample preparation (starch degradation, AIR production), hydrolysis (matrix hydrolysis and seaman hydrolysis), single-run HPAEC-PAD quantification (high-performance anion exchange chromatography with pulsed amperometric detection), etc.

II.7.1 Sample preparation

II.7.1.1. Preparation

In the sample preparation step, plant materials (external tissue without woody core) are washed repeatedly with 70% ethanol until chlorophyll is depleted. The ethanol is removed and samples are dried in a hot-air oven for 2 days at 45°C. It is then grinded with Retsch Mixer Mill MM 400 in a 50 mL grinding jar and Ø25 mm metal balls, for 25 Hz for 2 min.

II.7.1.2. Starch degradation

In the next 'Starch degradation' step (Modified from Hostettler *et al*., 2011); ~250mg homogenized plant materials (up to ~0.5ml mark in a 2 ml microcentrifuge tube) are added with 1ml 80% ethanol and heated up to 95°C for 10 min. Each sample tube is vortexed for 10-15sec and centrifuged at room temperature at 3000g for 5 min. The supernatants are discarded. This step continued 4 more times, first by adding 1ml 50% ethanol, then 1ml 20% ethanol, then 1ml water, and finally 1ml 80% ethanol. Each time samples are vortexed to re-suspend the pellet and shaken it in a thermomixer (room temperature) for 10 minutes during each wash. The washed pellets are then dried using a speed-vacuum centrifuge (45°C, 2h) until completely dry and re-suspended in 400µL water. It is then boiled at 95°C for 10-15min and cooled at room temperature. 20µL of digestion mixture [9: 1 = amyloglucosidase (sigma 10102857001): α-amylase (sigma 10102814001)] is added to 380µL (0.22M) sodium acetate and combined with 400µL cooled sample and kept at 37°C overnight. Checking for remaining starch in the sample is done by staining a small portion with Lugol's solution. 20µL of the enzyme-sample mixture is added with 80µL 100% ethanol and boiled for 5min at 90°C and centrifuged for 5min at 5000g (supernatant is discarded). It is then added with 25µL Lugol solution (full concentration of purchased

solution) and observed for color change after 5min. No color change was observed (Colour change to a deep blue/black color indicates the presence of starch). Samples are centrifuged at 5000g for 5 minutes and proceed for final cleaning with the remaining insoluble fraction.

II.7.1.3. AIR production

In this step of 'Cleaning & final cell wall derived AIR production', the 250mg de-starched insoluble fraction (up to 0.5ml mark in a 2ml microcentrifuge tube) is added with 1.5ml of methanol: chloroform (1:1, v/v) mixture and vortexed to mix thoroughly. It is then centrifuged at 10000g for 5-10min at room temperature (supernatant discarded) and added with 1.5ml acetone (room temperature). The mixture is vortexed thoroughly and kept for 30 minutes in a tube rotator set at 15rpm. After it is centrifuged at 10000g for 5-10min at room temperature (supernatant discarded) the pellets are dried using a speed-vacuum centrifuge (45°C, 2h) until completely dry. The final product is the cell wall-derived alcohol insoluble residue (AIR).

II.7.2. Hydrolysis

1-3mg AIR per technical replicates are taken (minimum, two technical replicates per sample per hydrolysis) into 2ml screw-cap tubes (using any kind of plastic weighing paper towels) and hydrolysis is done with different acid concentrations.

In saeman hydrolysis, the tubes containing AIR are added with 50µl of 72% sulfuric acid (w/w) and immediately vortex vigorously (delayed or insufficient mixing can cause poor rehydration of the samples and incomplete hydrolysis). Samples are then incubated at room temperature for 1 hour and vortexed every 10 minutes. Next, 1400µl of miliQ water is added in each tube to adjust the sulfuric acid concentration to 4% (W/V) and mix well.

In matrix hydrolysis; 1400µl of water is added first and then 72% (w/w) sulfuric acid to have a 4% (w/v) concentration. Samples are vortexed well and left in a tube rotor for 1h at room temperature.

External recovery strands are prepared by mixing 9 sugars (of interest, Fuc, Rha, Ara, Gal, Glc, Xyl, Man, GalA, and GluA) each at a concentration of 100 µg ml-1. To account for sugar-specific losses during hydrolysis, a recovery standard is subjected to the same conditions as the matrix hydrolysis samples, where 500µl of the standard mixture is added with 900 µl of water and 50 µl of 72% (w/w) sulfuric acid (into a 2 ml microcentrifuge tubes). Samples and one set of standards are then autoclaved at 121 °C for 60 min. Cooled samples at room temperature are then centrifuged for 1 min at 20000g to pellet any insoluble material.

II.7.3. HPAEC-PAD run and calculations

Samples are analyzed on a 96-well microplate using several runs of high-performance anion exchange chromatography with pulsed amperometric detection (Dionex Ultimate 3000).
Neutral sugars from matrix hydrolyzed samples were separated with a 3mm CarboPac™ PA20 column (3×150mm) with a 3mm guard (3×50mm) (flow rate of 0.4ml/min at room temperature). Two isocratic elution was used:

- 2.4mM" (targeting fucose, galactose, glucose, xylose & mannose)
- 15mM" (targeting rhamnose & arabinose)

Standards and samples were diluted 1:1 (V/V) before injecting 25µl of the sample.

Uronic acid was analyzed with a 3mm CarboPac™ PA20 column (3×150mm) with a 3mm guard (3×50mm) (flow rate of 0.4ml/min at room temperature), a higher pH is required (Yeats et al., 2016), which was achieved by using a gradient of 1M sodium acetate (NaOAc) and water in the first program, and with a combination of 100mM sodium hydroxide (NaOH) and 1M NaOAc in the second program. For improved resolution, a program was developed, starting with an initial treatment of 100mM of NaOH and 50mM NaOAc for 2 minutes, which was then increased to 100mM of NaOH and 200mM NaOAc at 15 minutes. Standards and samples were diluted in a 1:1 ratio (v/v) before injecting 25 µL.

For Seaman hydrolysis, glucose was quantified using a 2mm CarboPac™ PA1 column (2×250mm), accompanied by a 2mm guard column (2×50mm) (flow rate of 0.25ml/min at room temperature) with an isocratic gradient of 24mM NaOH. The hydrolyzed samples were diluted 20:1, and a glucose external standard solution of 0.02 mg/mL was used.

The sugar concentration in the sample was calculated based on standard sugar concentration and peak area. For each retting time point (R0-R7) and 5 biological replicates (T), 2 technical repetitions were done in both fields (A & B).

II.7.4. Statistical analysis of monosaccharide assay results

Data normality was assessed with the Shapiro-Wilk test and checked for equal variances among groups using Levene's test. Outliers identified by interquartile range (IQR) were removed, and any missing values (if present), were replaced with the mean of the group. A one-way analysis of variance (ANOVA) along with Tukey's HSD (Honestly Significant Difference) test was performed to assess the effect of the degree of retting on the stem's chemical composition. To compare the retting dynamics between two

fields, a pairwise T-test is performed with FDR (False Discovery Rate) correction of p-value by multiple comparisons.

II.8. Preparation, and measurements for 2D-LC-MS/MS-based metaproteomics

II.8.1. Choice of samples for metaproteomics

Four protein samples [day 1 (R0); day 6 (R2), day 13 (R4), and day 25 (R7), (fields A and B)] corresponding to key points during the retting process were chosen for metaproteomics: Points R0 and R7 correspond to the start (R0), and end (R7) of the retting process. The point R2 was chosen because this sample showed statistically significant modifications in the activities of five out of the seven enzymes evaluated (increased xylosidase, galactosidase, and glucosidase activities; decreased peroxidase and phenoloxidase activities) compared to R0. The point R4 was chosen as it was the first point after swath turning that is generally considered by flax farmers to be an essential step during retting. this point would also be a good point for analysis by metaproteomics.

II.8.2. Extraction, quantification and preparation of protein samples

100 mL of soluble fractions (prepared as described above, M&M 2.2) from three biological replicates (T1, T2 and T3) for the retting points R0, R2, R4, and R7 (i.e. 12 samples) were processed as described in (Goulas et al., 2001), with the exceptions that, prior to acidic precipitation, i) soluble fractions were concentrated into a final volume of roughly 2mL with vivaspin-20 centrifugal concentrator (10kDa MWCO, Merck) and ii) protein quantification was performed according to Bradford using BSA as a standard (Bradford, 1976). Pellets were resuspended in 65 mM Tris-HCL buffer (pH 6.8) containing 20 % (v/v) glycerol, 2.3 % (w/v) sodium dodecyl sulfate (SDS), 100 mM dithiothreitol (DTT) and 0.04 % (w/v) bromophenol blue, boiled for 5 min to denature the proteins, and then cooled until required for electrophoresis. SDS-PAGE was denatured as described by Laemmli (1970) (Laemmli, 1970), using a 5.5% stacking gel and a 12% separation gel in a Mini-PROTEAN Tetra Cell system (BIO-RAD). Equal amounts of 20 micrograms of protein were loaded per lane, according to the protein quantification results. After a 2mm migration into the separation gel, migration was stopped and the gel was stained by using Quick Coomassie Stain (Generon, Slough, UK) according to manufacturer's instructions. Protein bands were excised, transferred into clean microtubes and stored at 4°C until further LC-MS/MS analysis.

II.8.3. Nano LC-MS/MS and Mass Spectrometry

Trypsin digestion was performed on each sample. Then peptides were extracted with 0.1% formic acid in acetonitrile, evaporated to reduce volume at 8µl, and injected on an UltiMate 3000 RSLCnano System (Thermo Fisher Scientific). Peptides were automatically fractionated onto a commercial C18 reversed-phase column (75 µm × 500 mm, 2-µm particle, PepMap100 RSLC column, Thermo Fisher Scientific, temperature 55 °C). Trapping was performed for 4 min at 5 µL/min, with solvent A (98% H2O, 2% acetonitrile, and 0.1% formic acid). The peptides were eluted using two solvents A (0,1% formic acid in water) and B (0.1% formic acid in acetonitrile) at a flow rate of 300 nL/min. Gradient separation was 3 min at 3% B, 170 min from 3 to 20% B, 20 min from 20% B to 80% B, and maintained for 15 min at 80% B. The column was equilibrated for 17 min with 3% buffer B prior to the next sample analysis. The eluted peptides from the C18 column were analyzed by Q-Exactive instruments (Thermo Fisher Scientific). The electrospray voltage was 1.9 kV, and the capillary temperature was 275 °C. Full MS scans were acquired in the Orbitrap mass analyzer over the *m*/*z* 400–1200 range with a 70,000 (*m*/*z* 200) resolution. The target value was 3.00E+06. Fifteen most intense peaks with charge state between 2 and 5 were fragmented in the higher-energy collision-activated dissociation cell with a normalized collision energy of 27%, and the tandem mass spectrum was acquired in the Orbitrap mass analyzer with a 17,500 (*m*/*z* 200) resolution. The target value was 1.00E+05. The ion selection threshold was 5.0E+04 counts, and the maximum allowed ion accumulation times were 250 ms for full MS scans and 100 ms for tandem mass spectrum. Dynamic exclusion was set to 30 seconds.

II.9. Proteomic data analysis

II.9.1. Spectra analysis and identification of proteins

Raw data collected during nanoLC–MS/MS analyses were processed and converted into a *.mgf peak list format with Proteome Discoverer 1.4 (Thermo Fisher Scientific). MS/MS data were analyzed using the search engine Mascot (version 2.4.0, Matrix Science, London, UK) installed on a local server. Searches were performed with a tolerance on mass measurement of 10 ppm for precursor and 0.02 Da for fragment ions, against a composite target-decoy database (372988*2 total entries) built with a Linum Uniprot database (taxonomy 4505, June 2022, 1404 entries), a Bacteria Swissprot database (taxonomy 2, June 2022, 335515 entries) and a Fungi Swissprot database (taxonomy 4751, June 2022, 35951 entries) fused with the sequences of recombinant trypsin and a list of classical contaminants (118

entries). Cysteine carbamidomethylation, methionine oxidation, protein N-terminal acetylation, and cysteine propionamidation were searched as variable modifications. Up to one missed trypsin cleavage was allowed. The identification results were imported into Proline software (http://proline.profiproteomics.fr) for validation. Peptide spectrum matches taller than 7 residues and ion scores >15 were retained. The false discovery rate was then optimized to be below 1% at the protein level using the Mascot Modified Mudpit score. Protein abundance was measured by Extracted Ion Current-based quantification with Proline 2.0. The data have been deposited to the ProteomeXchange Consortium via the PRIDE (Perez-Riverol et al., 2022) partner repository with the dataset identifier PXD055634 and 10.6019/PXD055634.

II.9.2. Statistical analysis of resulting metaproteomic dataset

Protein abundances were log2 transformed and distributions were checked for normality. Since the R0 sample group showed particular distributions compared to other groups of samples, this group was removed from the global dataset. Nevertheless, presence information for each protein was collected according to the following rule: a protein is considered present in R0 if, in at least two of the replicates, it shows an abundance value higher than the first quartile of the abundances of the whole dataset. Then distributions across samples of the remaining dataset (groups R2, R4 and R7) were normalized by the method of Quantiles using LIMMA procedure under R (https://www.bioconductor.org/packages/devel/bioc/vignettes/limma/inst/doc/usersguide.pdf). Proteins were then filtered for contaminants and assigned to field A and/or B according to the rule: a protein is considered present in a field if its abundance is higher than the first quartile of the dataset in at least two replicates of one of the retting points. Missing values at that stage represented less than 10% of the total values and so imputed to simulate the mass spectrometer's limit of detection according to the Perseus method (Tyanova et al., 2016; Yu et al., 2020) with a mean minus 1.8 times the standard deviation and a width of 0.4 times the standard deviation as parameters. For each field, significant differences in protein abundances between time points were assessed by pairwise Welsh's *t*-test followed by a Benjamini-Hochberg FDR correction (p-value ≤ 0.05, cut off: $0.66 \geq$ mean ratio ≥ 1.5).

II.9.3. Functional and taxonomic analysis of proteomes

For functional analysis, the metaproteome database was first annotated with Gene Ontology (GO) terms, using their UniProt ID and an in-house Python script written to use the UniProt QuickGO API (https://www.ebi.ac.uk/QuickGO/api/index.htm). Information about protein, gene name, organism name and ID were retrieved from the UniProt database using the R package UniProt.ws. For identification of

CAZymes in the metaproteome, a docker version of the dbCAN3 pipeline was run and proteins were categorized as "CAZymes" when it was annotated by the three dbCAN3 tools HMMER, DIAMOND, and E-CAMI. HMMER annotations took priority over DIAMOND and E-CAMI tools. Enzymatic functions and target polymers (plant cell wall polymers) were assigned manually integrating CAZy information about families (http://www.cazy.org/), as well as the functional assignment of CAZy families reported in the literature (Chirania et al., 2022; Djemiel et al., 2017; Tláskal et al., 2021). The taxonomic information concerning the organisms was reconstructed from the NCBI taxonomy (https://www.ncbi.nlm.nih.gov/guide/taxonomy/) using the "Taxizedb" package in an in-house script under R software. To examine statistical significance of categories of proteins (GO, CAZymes, by taxon) in retting time points, pairwise Welch's t-tests were performed between the considered R point and R2 (used as reference) followed by a Benjamini-Hochberg FDR correction. The log2 values of mean ratios are calculated and represented on heatmaps. All data representations were drawn using R software and specific packages: "ggplot2", heatmaps were constructed and drawn with "pheatmap" packages, Venn diagrams using the "ggVennDiagram" package, pie donuts with "webr" package, chord diagrams with "Circlize" package.

II.10. FTIR-vibrational-spectroscopy

For the FT-R analysis, flax dew retting samples from 2021 were used. After seeds were planted on March 30, 2021, and the plants were pulled out on July 23, 2021, a total of 116 days of culture and 25 days of retting transpired. For the purpose of dew retting, whole plants were placed directly on the field, and the flax layers were rotated throughout. R0 begins as soon as the plants are pulled up and placed on the ground, and R7 is the final stage in which samples are taken from the ground for mechanical scutching. Together, R0 and R7 represent a total of 25 days in the process. Four retting points—designated as R0, R2, R6, and R7, respectively—were chosen; these correspond to days 0–6, and 20–25.

II.10.1. Preparation of sample for FT-IR spectroscopy

Ten stems (30-40 cm in length), cut from the middle section of each stem (between the fruit and root), were collected from both Field A and Field B. Samples were taken from three distinct locations within each field (biological replicates: T1, T2, T3) at four key stages of the dew retting process (R0, R2, R6, R7).

Fragments were peeled in order to enrich samples with fiber bundles as well as epidermis and cortical parenchyma cell types. The inner tissue corresponding to the wood (lignified tissue) was discarded. According to the proportion of fiber bundles, such samples are enriched in bast fibers compared to the proportion of the other tissues that only present a thin primary cell wall. These outer tissues were gradually destroyed during natural dew retting. Peeled tissue samples were dried (at 45°C for 48h) to be grounded into powder.

A total of 24 samples (outer tissues), combining [F, T, R: 2 fields x 3 places in the field x 4 retting times = 24 samples] are to be analyzed. Each sample (= a mix of 10 stem fragments) was reduced in coarse powder with a Retsch Mixer Moll MM 400 in a 50 mL grinding jar and Ø25 mm metal balls, for 25 Hz, 2 min.

Two to three mg/sample were used for FT-IR spectra acquisition. KBr pellet (potassium bromide) method was firstly tested but did not give enough resolute spectra. Coarse powder was therefore placed between the two faces of a diamond compression cell (SpectraTec) and pressed. With this method, a fine powder is obtained. Such a powder appeared more homogenous than with the KBr method. Each face of this diamond cell was used to acquire spectra. A minimum of 10 spectra (technical repetitions) was acquired for each of the thirty samples. Global schematic diagram gathers the chart flow that was followed in this study (**Fig. II.6**). This work was carried out on the vibrational spectroscopy facility of the Advanced Characterization Platform of the Chevreul Institute ((FR2638).

II.10.2. FT-IR spectroscopy

A Bruker FT-IR microscope Hyperion 3000 was used to acquire micro-FT-IR spectra in transmission mode. This equipment was coupled to a Bruker Vertex 70 spectrometer in the laboratory of Infrared and Raman Spectrochemistry. The microscope was equipped with a liquid nitrogen-cooled MCT detector. 256 scans were recorded at 4 cm^{-1} spectral resolution in the spectral range from 650 cm^{-1} to 4000 cm^{-1} using a 36x Cassegrainian objective (NA=0.5). The area of interest was selected by adjusting knife edge aperture so that only the area of interest is exposed for analysis. Absorption bands maxima in the middle infra-red region at 3400-800 cm^{-1} were used to identify the main plant polymers and other residues (including those from microorganisms, as well as cellulose, hemicellulose and degrading products due to dew retting).

The spectra were recorded from 3400-800 cm^{-1} spectral ranges corresponding to the plant cell wall window (800-1900 cm^{-1}), total CH_2-CH_3 chemical bonds (2800-3000 cm^{-1}), and water (3000-3400 cm^{-1}).

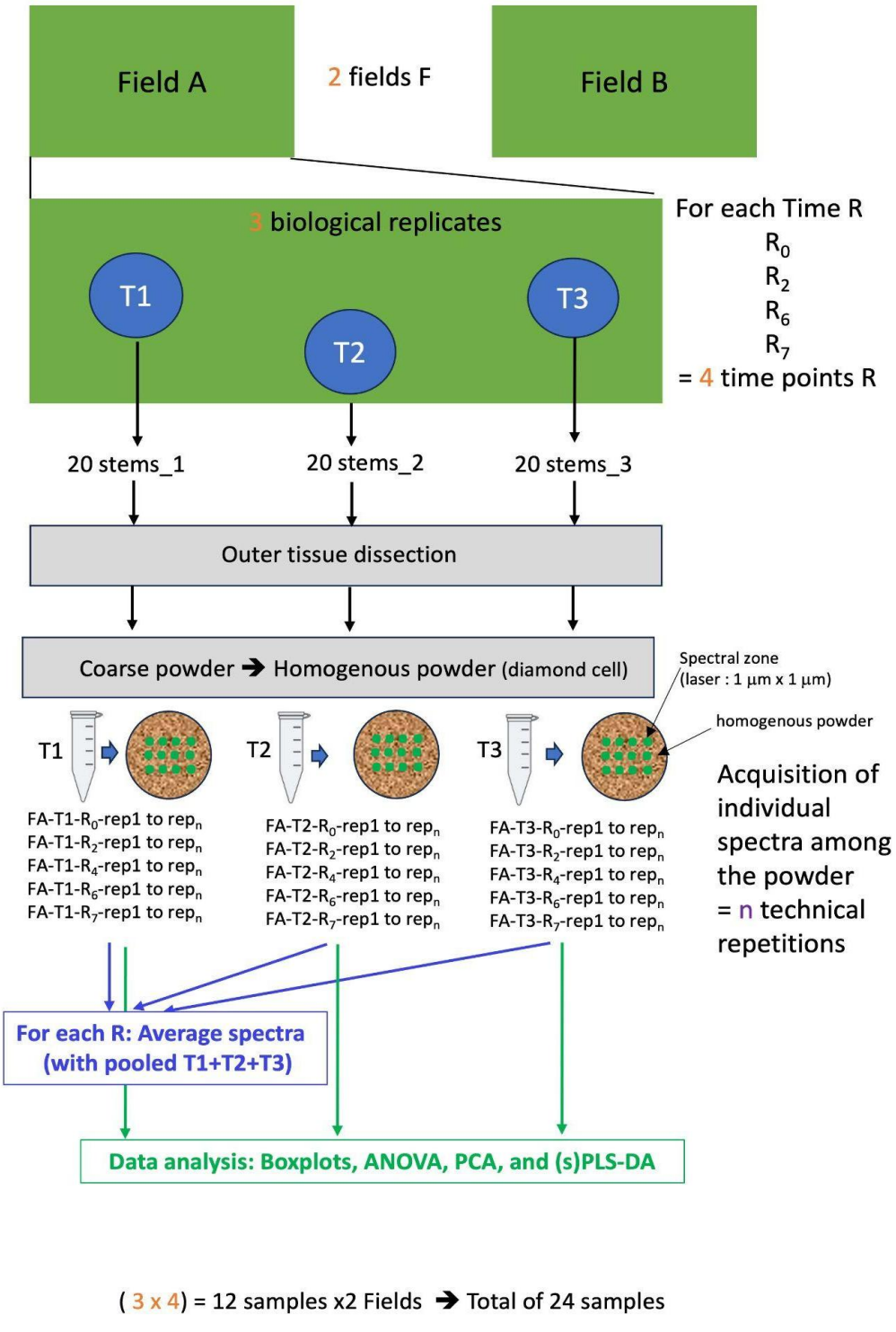

Figure II.6. Schematic representation of the sampling.

Field A and B are separated by 247.5 m. They show contrasted scutched fiber-industrial parameters.

II.10.3. Spectra treatments for average spectra illustrations

Baselines were corrected using OPUS-NT Software for each individual raw spectrum. Baseline correction was done according to the OPUS software. For illustration, the Min-Max method provided by OPUS-NT Software was used for normalization.

The average spectra were therefore calculated by cumulating individual spectra from each of the 10 samples (*i.e.* 2 fields x 5 retting times = 10 samples), and from a minimum of 15 individual spectra that correspond to technical repetition rep_1 to rep_{15} (*i.e.* 5 individual spectra x 3 biological repetitions T1+T2+T3 = total of 15 spectra minimum).

Some illustrations were done according to one specific field (Field A and Field B), with cumulated spectra from each biological repetition (T1+T2+T3) and for each retting kinetic time. In this case, the evolution of peak (= chemical bond assigned to plant cell wall) during the dew retting, in each field. However, no information is available about the potential differences that could occur in each biological repetition as T1+T2+T3 were pooled.

Other illustrations were done according to the retting kinetic time, to observe the behavior of each field (always with cumulated spectra T1+T2+T3). This approach led us to observe potential delays that could occur between fields, according to the retting speed of polymer degradation by enzymes.

II.10.4. Statistical analysis for FT-IR data

II.10.4.1. Multiple pairwise comparisons by one way-ANOVA analysis ('a priori' approach)

This study aims to address two key questions. The first is to identify significant peaks that characterize the spectral profiles during the retting process. The second is to analyze the dynamics between fields A and B to determine the optimal end-point of retting.

All spectra provided after spectra treatments described above (IV.2.2.4. part) were baseline corrected then normalized using the `TotInt` method (https://www.r-project.org/, 1st July 2024 accession). `TotInt` method normalized by total intensity. In this case, the y-data of a Spectra object is normalized by dividing each y-value by the sum of the y-values in a given spectrum. Thus each spectrum sums to 1. This method assumes that the total concentration of all substances giving peaks does not vary across samples.

The normality of spectral data was further assessed using the Shapiro-Wilk test, and equal variances among groups were verified with Levene's test. Outliers identified through the interquartile range (IQR) were removed, and any missing values were replaced with the group mean. To evaluate the

effect of the retting degree (R) on the modification of spectral profiles of outer-tissue powder, a one-way analysis of variance (ANOVA) was conducted, followed by Tukey's HSD (Honestly Significant Difference) test. To compare the retting dynamics between the two fields, a pairwise t-test was performed with a false discovery rate (FDR) correction of p-values for multiple comparisons. All analyses were performed with RStudio software and packages (https://www.r-project.org/, 1st July 2024 accession).

II.10.4.2. Global statistical analyses ('without a priori' approach)

II.10.4.2.1. Unsupervised exploratory analysis by PCA

As described above, all raw spectra were baseline corrected then normalized with TotInt method before any further analysis. Among the normalization methods, we choose the area-normalization one (Dinant et al., 2019; Blervacq et al., 2022, 2023). We performed Principal Component Analysis (PCA) processing for comparisons between biological repetition (T1-T2-T3) in a same field (Field A and Field B), and according the dew retting kinetic (R) were performed using the free R software using `ChemoSpec` and `MixOmics` libraries (https://www.r-project.org/, 1st July 2024 accession). The number of considered PC components was obtained with the scree plot. The PCA scree plots were firstly produced for each spectral zone (from zone A to zone E), for each retting point R, and firstly only for the field A. A number of PC components was identified in order to cover 75% of the explained variability. Usually, PC1 and PC2 components were enough. PLS-DA biplots were further generated according to these significant PC components.

II.10.4.2.2. Supervised exploratory analysis by PLS-DA and sPLS-DA

Statistical studies were performed by Sparse Partial Least-Squares Discriminant Analysis (sPLS-DA) by using R Studio software (2022.02.03 build 492) and the R-package mixOmics (v. 6.1.2) in order to select variables within spectroscopic peaks datasets, with the most explanatory of retting discrepancy (Le Cao et al., 2016). The `mixOmics` package is suitable for such an approach as it provides a wide range of linear multivariate methods for data exploration, integration and dimension reduction of large biological data sets and is also regularly updated, when undergoing most dimension reduction methods, latent components are produced. These latent components are defined by their corresponding loading vectors, which are vectors with the weight of each original variable's contribution to the corresponding latent component. Greater absolute values in loading vectors therefore means that a given variable has a greater "importance" *versus* another one. By undergoing classification in sPLS-DA, each variable's bar in plot loadings resulting from the analysis is colored according to whether the median is higher (or lower) in a given group of interest (R0, R2, R6 or R7).

II.11. Color spectroscopy

In this work, flax dew retting samples from multiple years (and different fields) have been used. It includes one retting field from 'flax dew retting 2014', two retting fields (named field A and B) from 'flax dew retting 2021', and two retting fields from 'flax dew retting 2022' (as explained in details in section II.2). In 2014, 6-time points were selected from a 44-day long retting (day1, day6, day12, day26, day33 and day44) for analysis. In 2021, retting was quick, completed in 25 days. Sampling from 6-time points (day1, day4, day6, day13, day20 and day25) were used to obtain the stem surface color changes during retting for spectral color analysis. In 2022, retting took 55 days; sampling from 6-time points (around - day1, day13, day24, day34, day44 and day55) are chosen for color analysis. Samples in 2022 filed A were over-retted till day 90 (since day 55) and two additional sampling points, on day 69 and day 90, were collected and classified as over-retted samples. These over-retted samples were subsequently compared in the analysis.

Flax dew retting sampling	Retting 2014	Retting 2021 Field A	Retting 2021 Field B	Retting 2022 Field A	Retting 2022 Field B
Duration (days)	44	25	25	55	52
Sampling point numbers (R)	R0 to R6	R0 to R7	R0 to R7	R0 to R18	R0 to R15
R point used in color study	R0, R1, R2, R4, R5, R6	R0, R1, R2, R4, R6, R7	R0, R1, R2, R4, R6, R7	R0, R3, R6, R9, R13, R15 (R17, R18)	R0, R4, R7, R10, R13, R15
In days	1, 6, 12, 26, 33, 44	1, 4, 6, 13, 18, 20, 25	1, 4, 6, 13, 18, 20, 25	1, 13, 23, 34, 44, 55 (69, 90)	1, 13, 24, 34, 45, 52
Readings SCI	630	288	288	150+ 50	150
Readings SCE	630	288	288	150 + 50	150

Table II.1. Details of sampling (for color analysis) from five flax dew retting experimental sets.

Number of sampling points (R) used in spectral color analysis and resulting total readings are mentioned. The over retting sampling points and respective readings are colored in red. SCI = specular component included and SCE = specular component excluded.

II.11.1. Collection of Spectral Reading

Color changes of the flax stem undergoing retting have been measured by a portable spectrophotometer CM-23d (KONICA MINOLTA). Measurements were taken at 5 places along the flax bundle either in real-time retted samples (2022) or dried stored samples (2021, 2014). The bundle was spread out in the

laboratory as it would be in the field (**Fig. II.7**). The parts of the stems were classed as "Top", "Middle", and "Bottom" (**Fig. II.8**). The spectrophotometer gives color measurements of stem surface in SCE (specular component excluded) & SCI (specular component included) including readings within the visual spectrum (400-700 nm), with one reading at every 10 nm gap, read with SpectraMagicNX (www.konicaminolta.fr) software.

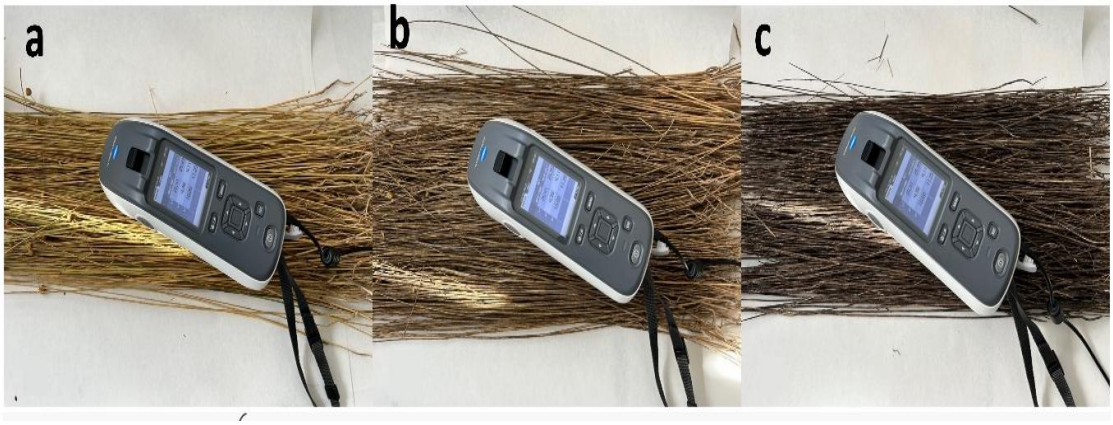

Figure II.7. Flax straw surface color change reading with spectrophotometer Konica cm23d.

(a) measurements of stem straw surface color after 1 week of retting in 2022, (b) straw surface color after 3 weeks of retting, (c) over-retted straw surface color measurements. About 60-70 straws are taken together resembling a swath in the field while taking the surface color readings.

For year 2022 samples, 5 technical measurements of 5 biological replicates from 19 retting time points in field A resulted in 950 total readings (16 usual retting time points with 800 readings + 3 over retting time points with additional 150 readings), and 800 in field B with 16 retting time points (SCI+SCE). For the year 2021, spectral readings on 6 retting time points with 3-5 biological replicates (& more than 16 technical measurements for each) resulted in 640 readings per field. For retting 2014, 7 retting points with 5 biological replicates are measured with 21 technical measurements each, resulting in 1470 total readings (SCI + SCE). The Cl*a*b* values generated by the spectrophotometer are taken for each five individual experimental sets.

Photographs of straw color change are taken with NIKON D5000 (24mega-pixel, aperture f/4.8), in auto settings (ISO 400, exposure time 1/90 second) with indoor light conditions and from 90° angle to present the changes visually, for each experiment set.

II.11.2. Statistical analysis of color data

II.11.2.1. Multiple pairwise comparisons of CL*a*b* data by one way-ANOVA analysis

CL*a*b* data obtained from the spectrophotometer (only SCI), are assessed with the Shapiro-Wilk test for normality and checked for equal variances among groups using Levene's test. Outliers identified by interquartile range (IQR) were removed, and any missing values (if present), were replaced with the mean. A one-way analysis of variance (ANOVA) along with Tukey's HSD (Honestly Significant Difference) test was performed in R software (https://www.r-project.org/, July, 2024) (Hanson, 2022; Rohart et al., 2017).

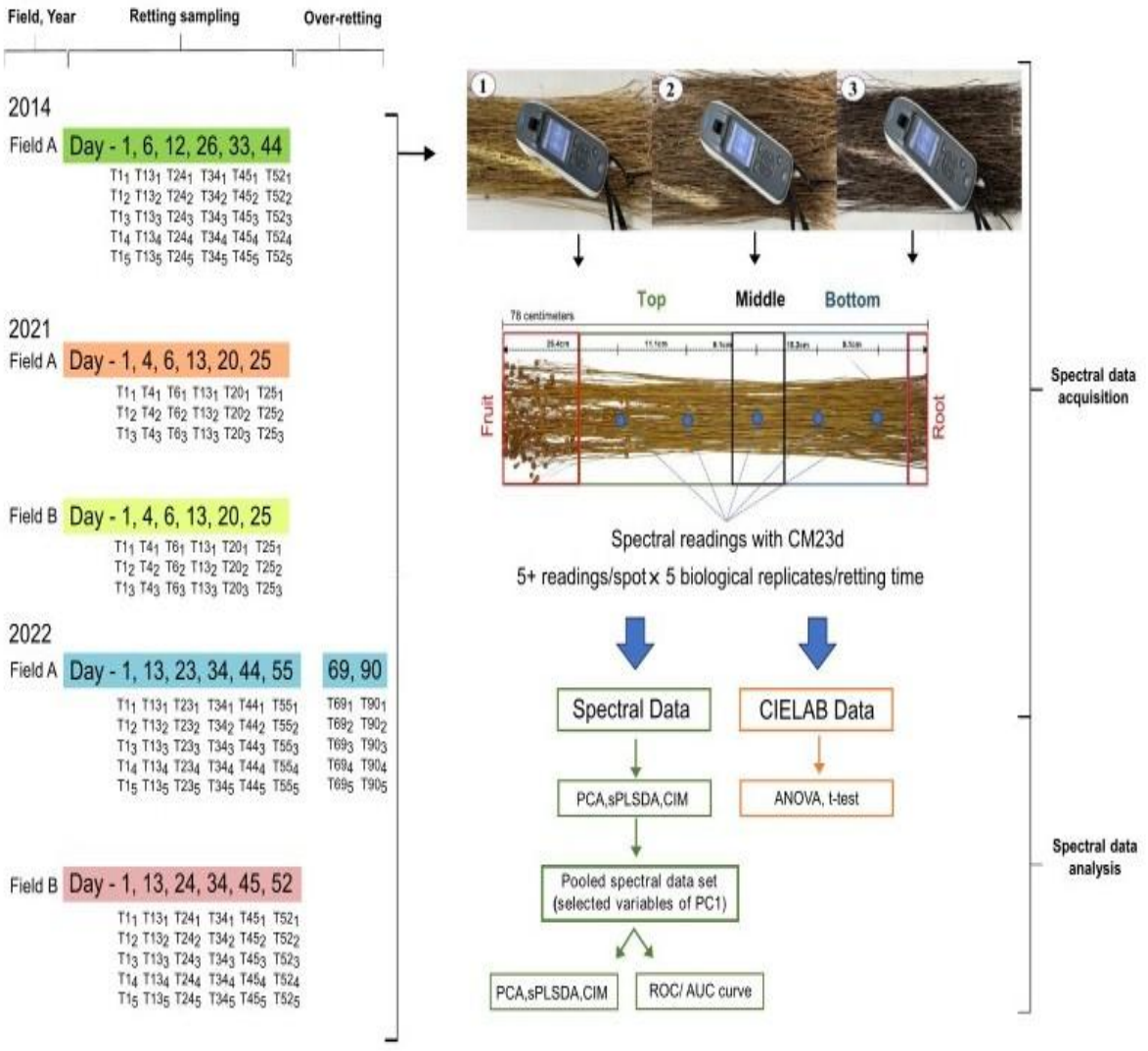

Figure II.8. Schematic representation of experimental steps.

II.11.2.2. Unsupervised exploratory analysis of visual spectral data by PCA

For spectral data (only SCI), a mean was done by technical measurements (keeping biological replicates separately) and position (Top, Middle, Bottom) per retting time points. The data was normalized using the `TotInt` method (area normalization) with the R software and Chemospec package and further analyzed with Mix-omics-R-package (https://www.r-project.org/, 1st July 2024 accession) (Hanson, 2022; Rohart et al., 2017) with unsupervised exploratory analysis or Principle component analysis (PCA). PCA processing is a dimensionality reduction technique that represents a multivariate dataset as a smaller set of variables. The number of principal components (PCs) was determined with a scree plot, selecting enough PCs to explain 75% of the variability, with PC1 and PC2 typically accounting for over 90%. PLS-DA biplots were then generated based on these key components.

II.11.2.3. Supervised exploratory analysis of visual spectral data by PLS-DA and sPLS-DA

Supervised Partial Least Squares Discriminant Analysis (PLS-DA) was applied to the simplified data (using PC1 and PC2) to identify differences between groups (retting-time points) and visualize feature contributions through Clustered Image Map (CIM) plotting. The analysis was conducted using R Studio (v. 2022.02.03) and the mixOmics package (v. 6.1.2), which is well-suited for multivariate data exploration, integration, and dimension reduction. Latent components were generated, with loading vectors highlighting each variable's contribution, where higher values indicate greater importance.

PLS-DA loadings, representing the key variables distinguishing groups, were identified separately for five datasets. From the top six common loadings of PC1, four were pooled across six selected retting time points (classified as early, middle, and advanced stages based on CIM plot patterns).

This pooled data was then analyzed with PLS-DA to train a confusion matrix and predict classification performance, determining the Area Under the Receiver Operating Characteristics Curve (AUC-ROC) for each year's data sets separately.

II.12. Reference

Blervacq, A.-S., Moreau, M., Duputié, A., De Waele, I., Duponchel, L., Hawkins, S., 2022. Raman spectroscopy mapping of changes in the organization and relative quantities of cell wall polymers in bast fiber cell walls of flax plants exposed to gravitropic stress. Frontiers in Plant Science 13.

Blervacq, A.-S., Moreau, M., Duputié, A., Hawkins, S., 2023. Comparative Analysis of G-Layers in Bast Fiber and Xylem Cell Walls in Flax Using Raman Spectroscopy. Biomolecules 13, 435. https://doi.org/10.3390/biom13030435

Bleuze, L., Lashermes, G., Alavoine, G., Recous, S., Chabbert, B., 2018. Tracking the dynamics of hemp dew retting under controlled environmental conditions. Industrial Crops and Products 123, 55–63. https://doi.org/10.1016/j.indcrop.2018.06.054

Bou Orm, E., Sutton-Charani, N., Bayle, S., Benezet, J.-C., Bergeret, A., Malhautier, L., 2024. Influence of field retting on physicochemical and biological properties of "Futura 75" hemp stems. Industrial Crops and Products 214, 118487. https://doi.org/10.1016/j.indcrop.2024.118487

Bourmaud, A., Beaugrand, J., Shah, D.U., Placet, V., Baley, C., 2018. Towards the design of high-performance plant fibre composites. Progress in Materials Science 97, 347–408. https://doi.org/10.1016/j.pmatsci.2018.05.005

Chabbert, B., Padovani, J., Djemiel, C., Ossemond, J., Lemaître, A., Yoshinaga, A., Hawkins, S., Grec, S., Beaugrand, J., Kurek, B., 2020. Multimodal assessment of flax dew retting and its functional impact on fibers and natural fiber composites. Industrial Crops and Products 148, 112255. https://doi.org/10.1016/j.indcrop.2020.112255

Charlet, K., 2008. Contribution à l'étude de composites unidirectionnels renforcés par des fibres de lin : relation entre la microstructure de la fibre et ses propriétés mécaniques (phdthesis). Université de Caen / Basse-Normandie.

Dinant, S., Wolff, N., De Marco, F., Vilaine, F., Gissot, L., Aubry, E., Sandt, C., Bellini, C., Le Hir, R., 2019. Synchrotron FTIR and Raman spectroscopy provide unique spectral fingerprints for Arabidopsis floral stem vascular tissues. Journal of experimental botany 70, 871–884. https://doi.org/10.1093/jxb/ery396

Djemiel, C., 2017. Étude de la diversité du domaine Bacteria et du règne Fungi au cours du rouissage du lin sur champ par une approche de metabarcoding (These de doctorat). Lille 1.

Gogoli, K., 2022. Contribution à l'étude des faisceaux de fibres de lin : analyse des relations morphologie-comportement mécanique-ultrastructure (phdthesis). Normandie Université.

Hanson, B.A., 2022. ChemoSpec: Exploratory Chemometrics for Spectroscopy. R package version 6.1.3; https://bryanhanson.github.io/ChemoSpec/.

Le Cao, K.A., Rohart, F., Gonzalez, I., 2016. with key contributors Benoit Gautier, S. D., Bartolo, F., contributions from Pierre Monget et al.

Perez-Riverol, Y., Bai, J., Bandla, C., García-Seisdedos, D., Hewapathirana, S., Kamatchinathan, S., Kundu, D.J., Prakash, A., Frericks-Zipper, A., Eisenacher, M., Walzer, M., Wang, S., Brazma, A., Vizcaíno, J.A., 2022. The PRIDE database resources in 2022: a hub for mass spectrometry-based proteomics evidences. Nucleic Acids Research 50, D543–D552. https://doi.org/10.1093/nar/gkab1038

Réquilé, S., Mazian, B., Grégoire, M., Musio, S., Gautreau, M., Nuez, L., Day, A., Thiébeau, P., Philippe, F., Chabbert, B., Chamussy, A., Shah, D.U., Beaugrand, J., Placet, V., Benezet, J.-C., le Duigou, A., Bar, M., Malhautier, L., De Luycker, E., Amaducci, S., Baley, C., Bergeret, A., Bourmaud, A., Ouagne, P., 2021. Exploring the dew retting feasibility of hemp in very contrasting European environments: Influence on the tensile mechanical properties of fibres and composites. Industrial Crops and Products 164, 113337. https://doi.org/10.1016/j.indcrop.2021.113337

Richely, E., Bourmaud, A., Placet, V., Guessasma, S., Beaugrand, J., 2022. A critical review of the ultrastructure, mechanics and modelling of flax fibres and their defects. Progress in Materials Science 124, 100851. https://doi.org/10.1016/j.pmatsci.2021.100851

Rohart, F., Gautier, B., Singh, A., Lê Cao, K.A., 2017. mixOmics: An R package for 'omics feature selection and multiple data integration. PLoS Computational Biology 13, 1–19. https://doi.org/10.1371/journal.pcbi.1005752

Sauvadet, M., Chauvat, M., Cluzeau, D., Maron, P.-A., Villenave, C., Bertrand, I., 2016. The dynamics of soil micro-food web structure and functions vary according to litter quality. Soil Biology and Biochemistry 95, 262–274. https://doi.org/10.1016/j.soilbio.2016.01.003

Yeats, T., Vellosillo, T., Sorek, N., Ibáñez, A., Bauer, S., 2016. Rapid Determination of Cellulose, Neutral Sugars, and Uronic Acids from Plant Cell Walls by One-step Two-step Hydrolysis and HPAEC-PAD. BIO-PROTOCOL 6. https://doi.org/10.21769/BioProtoc.1978

CHAPTER III

Biological insight of flax and hemp dew retting, identification of key enzymes and microorganisms

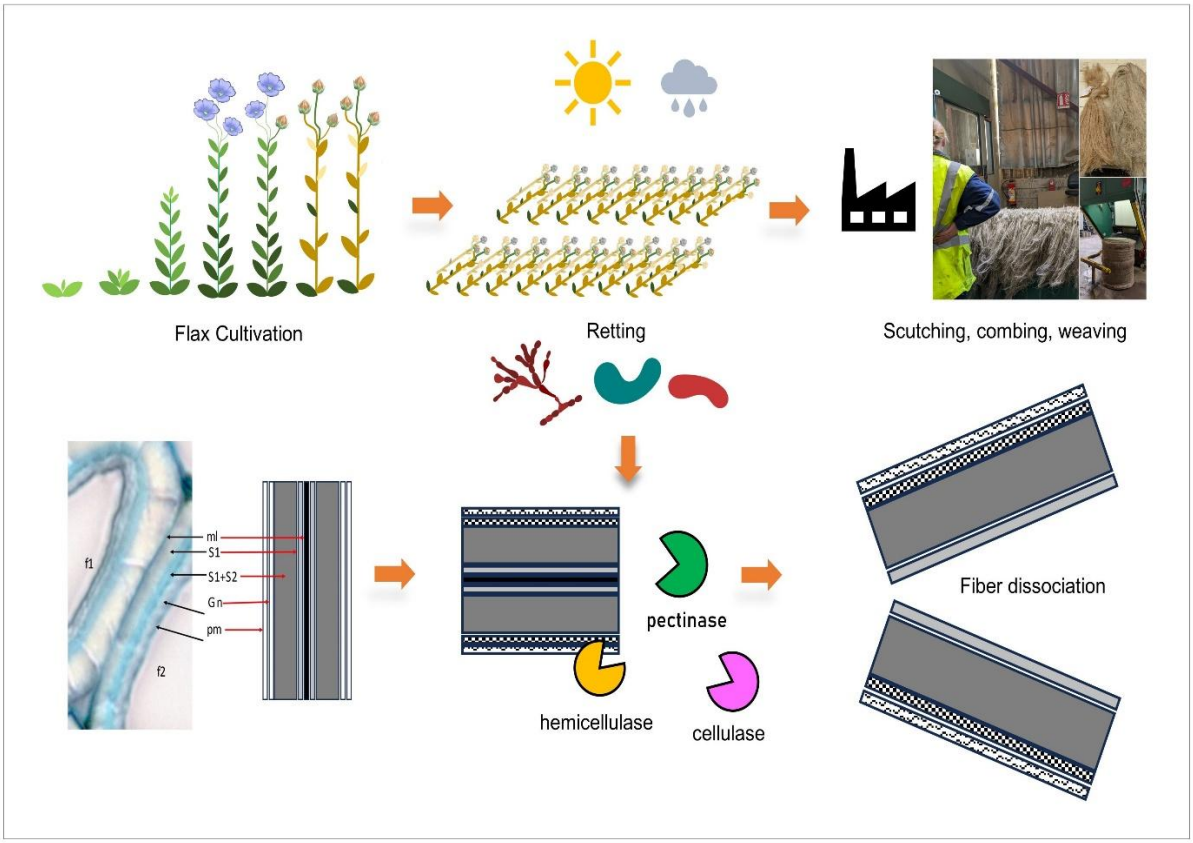

Chapter III: Biological insight of flax and hemp dew retting, identification of key enzymes and microorganisms

Contents

Chapter III: Biological insight of flax and hemp dew retting, identification of key enzymes and microorganisms 124
III.1. Context and structure of the chapter 126
III.2. Metaproteomics of flax dew retting (2021) in adjacent fields 128
III.2.1. Introduction 129
III.2.2. Material and methods 131
III.2.2.1. Sample collection, environmental data, and fiber characterization 131
III.2.2.2. Enzymatic activities measurements 131
III.2.2.3. Analysis of plant cell wall monosaccharides 131
III.2.2.4. Preparation, and measurements for 2D-LC-MS/MS-based metaproteomics 131
III.2.2.5. Proteomic data analysis 131
III.2.2.6. Other statistical analysis 131
III.2.3. Results 132
III.2.3.1. Climatic conditions and soil property 132
III.2.3.2. Inter-field variability exists in both fiber yield and industrial qualities 133
III.2.3.3. Fiber mechanical property assessment 134
III.2.3.4. Small differences are observed in cell wall degrading enzyme activities between both fields 134
III.2.3.5. Cell wall polymer composition evolution in stem outer tissues is similar in both fields 137
III.2.3.6. Metaproteomics of key retting points identifies 6032 unique proteins 137
III.2.3.7. Basic metabolism proteins are dominant in the metaproteome 141
III.2.3.8. The metaproteome is mainly composed of bacterial proteins 141
III.2.3.9. The abundance of about one-third of total proteins varies significantly during retting 144
III.2.3.10. The metaproteome contains key cell wall degrading enzymes belonging to Carbohydrate Active Enzymes (CAZy) families 145
III.2.3.11. CAZymes involved in the degradation of plant wall polymers come mainly from Fungi 149
III.2.4. Discussion 151

III.2.4.1. Biochemical analyses identify small differences in retting between fields A and B 151
III.2.4.2. Metaproteomics identifies specific proteins present during retting 153
III.2.4.3. Metaproteomics identifies plant enzymes potentially impacting cell wall structure 154
III.2.4.4. Metaproteomics identifies new retting micro-organisms 156
III.2.4.5. Metaproteomics potentially identifies the reasons for inter-field variability 156
III.2.5. Conclusion and perspectives 157
III.2.6. Supplementary material information 158
III.3. Enzyme dynamics study in hemp retting 159
III.3.1. Introduction 159
III.3.2. Materials and methods 159
III.3.3. Results 159
III.3.2.1. Enzyme dynamics of hemp dew retting are similar (watered and non-watered conditions) with flax dew retting. 159
III.3.4. Discussion 160
III.3.5. Conclusion 162
III.4. Conclusion of the chapter 162
III.5. Reference 164

III.1. Context and structure of the chapter

The increasing environmental pressures from climate change, water scarcity, and global warming have driven the textile industry to seek sustainable alternatives to synthetic and cotton fibers, which are associated with significant carbon, water, and energy footprints. Natural bast fibers, such as flax and hemp, have emerged as promising solutions due to their lower environmental impact. However, extracting these fibers from plant stems in a uniform, high-quality manner remains a challenge. Dew retting, an eco-friendly process widely practiced in Europe, is essential for fiber extraction but is heavily dependent on natural factors such as climate, soil chemistry, and microbial activity. This reliance on nature introduces variability in fiber quality, creating uncertainty in production lines, especially for fine textiles.

While considerable research has been done on the retting process—including studies on the chemical changes in dew-retted straw and technical fibers, microbial population dynamics using culture-based (Brown, 1984; Henriksson et al., 1999) and culture-independent approaches such as metabarcoding. Despite attempts to describe the involvement of enzymes and microorganisms in the dynamics of the overall enzymatic activities (Djemiel et al, 2017, Chabbert et al, 2020) the link between microorganisms, enzymes, and global enzyme activities still remains unclear. Some studies on the degradation of plant matter in forests have demonstrated the effectiveness of metaproteomics in identifying individual enzymes and the microorganisms that produce them during the process (Charania et al, 2020).

In this study, we aim to establish the dynamics of key retting enzymes using a metaproteomic approach and provide the missing link between enzymes, microorganisms that produce them, enzymatic activities and the chemical changes that occur during the process. We will also investigate whether differences in retting microbial communities and/or enzyme dynamics may be related to inter-field variability in fiber quality. Ultimately, the findings could lead to the development of precise biological tools to monitor and control the retting process, thereby reducing variability in flax fiber production and supporting its wider use in high-quality textiles.

The details of this study are provided in the first part of this chapter, This chapter was also structured as an article that was submitted for publication entitled "**Metaproteomics identifies key cell wall degrading enzymes and proteins potentially related to inter-field variability in fiber quality during flax dew retting**" in the *Industrial Crops and Products* journal, co-authored by Goulas E.[a], Creach A.[a] Krzewinski F[a], Galinousky D.[a], Blervacq A-S.[a], D'Arras P.[d], Ratahiry S.[a], Menuge A.[b], Soulat D.[b], Saliou J-M.[c], Lacoste A-S.[c], Hawkins S.[a] and Grec S[a] ([a]*Univ. Lille, CNRS, UMR 8576* -

UGSF - Unité de Glycobiologie Structurale et Fonctionnelle, F-59000 Lille, France ; [b]Univ. Lille, ENSAIT, GEMTEX – Laboratoire de Génie et Matériaux Textiles, 59056, Roubaix, France ; [c]Université de Lille, CNRS, Inserm, Centre Hospitalier Universitaire de Lille, Institut Pasteur de Lille, US 41 - UAR 2014 - Plateformes Lilloises de Biologie et Santé, Lille F-59000, France ; [d]Van Robaeys Fréres, 83 rue St-Michel CS 30014 59122 Killem, France, https://doi.org/10.1016/j.indcrop.2024.119907) and exposed by oral communication at national conference Réseau Français des Parois, St Malo 2024) and international poster communication at the (Plant Cell Wall Meeting, Malaga Spain, 2023).

In parallel with this work, our laboratory has been involved in a study concerning the retting of another fiber plant: hemp. This study, conducted by the PCH & LSR laboratory, and performed by Dr. Eliane Bou-Orme, questioned the establishment of hemp cultivation in the south of France, and in particular the feasibility of retting in this rather hot and dry region. The idea was to compare the biological (fungal and bacterial communities and enzymatic activities), physical and chemical aspects of a natural retting process with a second retting process supplemented by regular watering. Our laboratory carried out the enzymatic activity part of this project. This is described in a paragraph at the end of this chapter, and was the subject of a publication entitled "**High-throughput sequencing reveals microbial community dynamics during hemp field retting**" submitted to Environmental Microbiology Reports and co-authored by Eliane Bou Orm[1,2*], Suvajit Mukherjee[3], Etienne Rifa[4], Anne Créach[3], Sébastien Grec[3], Sandrine Bayle[2], Jean-Charles Benezet[1], Anne Bergeret[1], Luc Malhautier[2] ([1]Polymers, Composites and Hybrids (PCH), IMT Mines Alès, 6 avenue de Clavières, 30100, Alès, France ; [2]Laboratoire des Sciences des Risques (LSR), IMT Mines Alès, 6 avenue de Clavières, 30100, Alès, France; [3]Univ Lille, CNRS, UMR 8576 - UGSF - Unité de Glycobiologie Structurale et Fonctionnelle, 59000, Lille, France; [4]Toulouse Biotechnology Institute (TBI), Plateforme Genome et Transcriptome (GeT-Biopuces), Université de Toulouse, CNRS, INRAE, INSA, Toulouse, France).

III.2. Metaproteomics of flax dew retting (2021) in adjacent fields

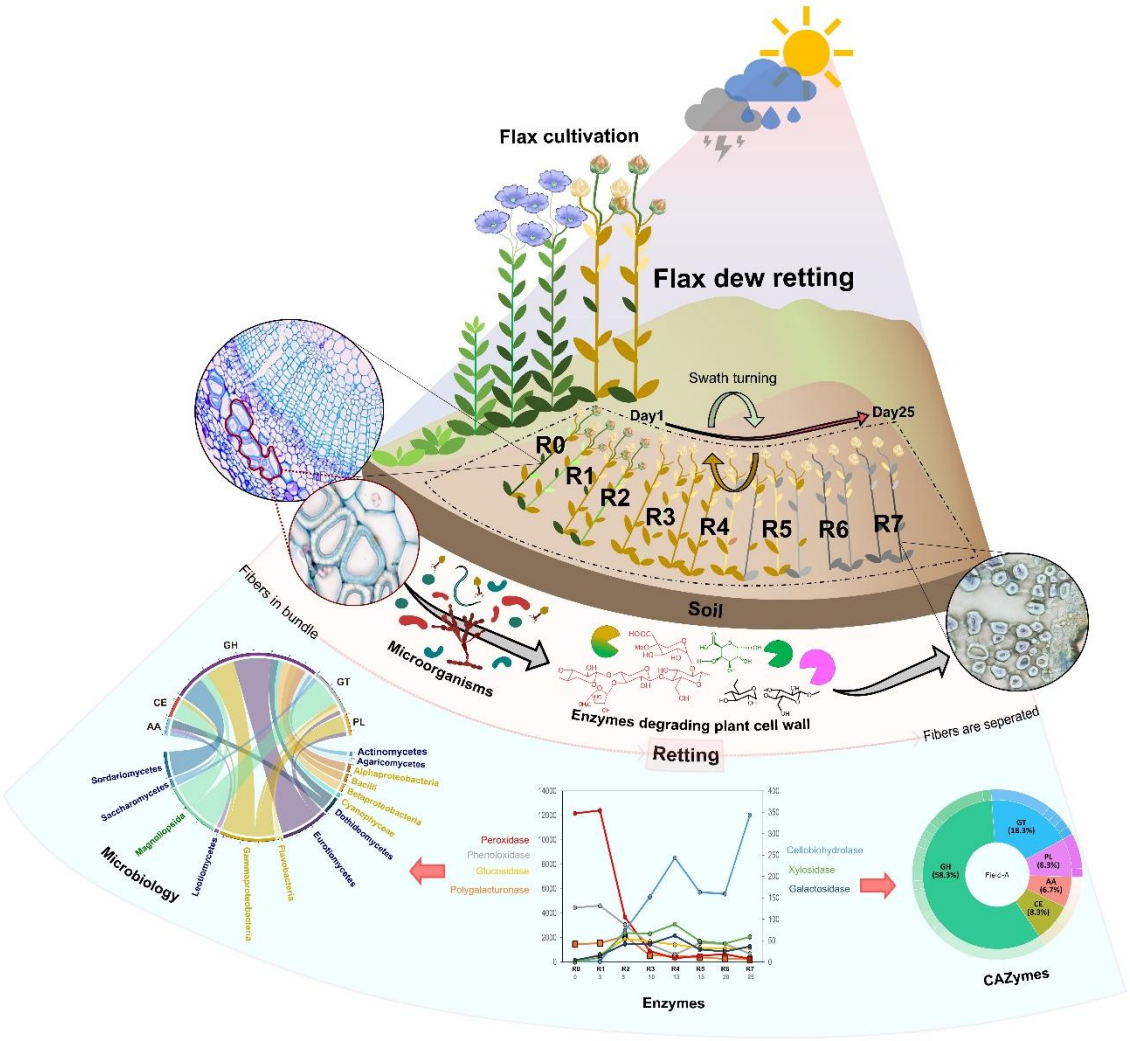

- What are the key cell wall-degrading enzymes involved in flax dew retting?
- Which microbial species or groups produce these enzymes during the retting process?
- How do these enzymes and microbes influence the retting process in nearby flax fields?

For this chapter, these persons collaborate (in alphabetical order):

Blervacq Anne-Sophie[1], Creach Anne[1], Goulas Estelle[1], Grec Sébastien[1], Galinousky Dimitry[1], Hawkins Simon[1], Krzewinski Frederic[1], Lacoste Anne-Sophie[2], Menuge Alycia[3], Pierre D'Arras[4], Ratahiry Sarah[1], Soulat Damien[3], Saliou Jean-Michel[2] ([1]Univ. Lille, CNRS, UMR 8576 - UGSF - Unité de Glycobiologie Structurale et Fonctionnelle, F-59000 Lille, France ;[2]Université de Lille, CNRS, Inserm, Centre Hospitalier Universitaire de Lille, Institut Pasteur de Lille, US 41 - UAR 2014 - Plateformes Lilloises de Biologie et Santé, Lille F-59000, France ; [3]Univ. Lille, ENSAIT, GEMTEX – Laboratoire de Génie et Matériaux Textiles, 59056, Roubaix, France ; [4]Van Robaeys Fréres, 83 rue St-Michel CS 30014 59122 Killem, France)

III.2.1. Introduction

Flax (*Linum usitatissimum* L) is an herbaceous, annual, self-pollinating dicot plant belonging to the family *Linaceae*. It is cultivated for both oil, and for its cellulose-rich bast fibers that are classically used in textiles (linen) and, more recently, composite materials (Mohanty et al., 2000; Chand and Fahim, 2020). Currently, quality variability between different fiber batches is an important factor holding back the widespread use of natural fibers in a range of different industrial applications (Müssig, 2010; Summerscales et al., 2010).

The qualities of both flax textiles and natural fiber composites (NFCs) are influenced by two main factors: firstly, the intrinsic mechanical and chemical attributes of individual fibers and/or fiber bundles, and secondly, the processing techniques used during fiber extraction and industrial manufacturing (Bourmaud et al., 2018). Variability in the quality of different fiber batches can be attributed to several different factors, some directly related to the plant (varieties, cultivation practices, soil type, meteorological conditions during growth etc.) (Chabi et al., 2023), while others concern post-harvest treatments (e.g., retting, scutching, combing, etc.) (Morgillo et al., 2023). In this article, we will look at field retting, which is considered to be one of the sources of variability (Martin et al., 2013; Baley et al., 2020).

Retting is a biological process used for the first stage of fiber extraction from the flax stem. In this organ, the individual fibers (elementary fibers) are elongated cells (reaching ~30mm in length, 15-20µm in diameter) organized into bundles of 30 to 40 cells embedded in the cortical parenchyma and located between the phloem and epidermis (Akin et al., 1996; Day et al., 2005; Salmon-minotte and Franck, 2005; Gorshkova et al., 2018). During retting, enzymes produced by microorganisms progressively degrade the cell wall polymers of fiber cells and surrounding tissues (**Fig. III.1**) thereby reducing inter-cell cohesion and facilitating fiber extraction (Sharma, 1992; Meijer et al., 1995). This operation cannot be achieved directly by a mechanical process as this would damage the fiber cell wall resulting in poor-quality fibers (Chabbert et al., 2020).

Historically, retting was often performed by placing flax stems in water tanks (water retting), however for both economic and ecological reasons, another type of retting - dew retting - is now the preferred process in Europe. The difference between these two processes is that in water retting, the flax stems are fermented anaerobically in a water tank, whereas in dew retting the stems lie on the field for several weeks, organized in swaths after being up-rooted (Paridah et al., 2011). Although similar to the natural microbial process associated with biomass degradation into forest litter (Voříšková and Baldrian, 2013; Tláskal et al., 2021), retting distinguishes itself by its "controlled" nature. Specifically, this means that cell wall degradation should be sufficient to facilitate fiber separation but must be stopped before

excessive degradation of the cellulose cell wall of fibers leads to a loss of mechanical properties (Akin et al., 1998; Goodman et al., 2002). In the light of such an observation, it is clear that retting is a major factor affecting fiber quality and homogeneity.

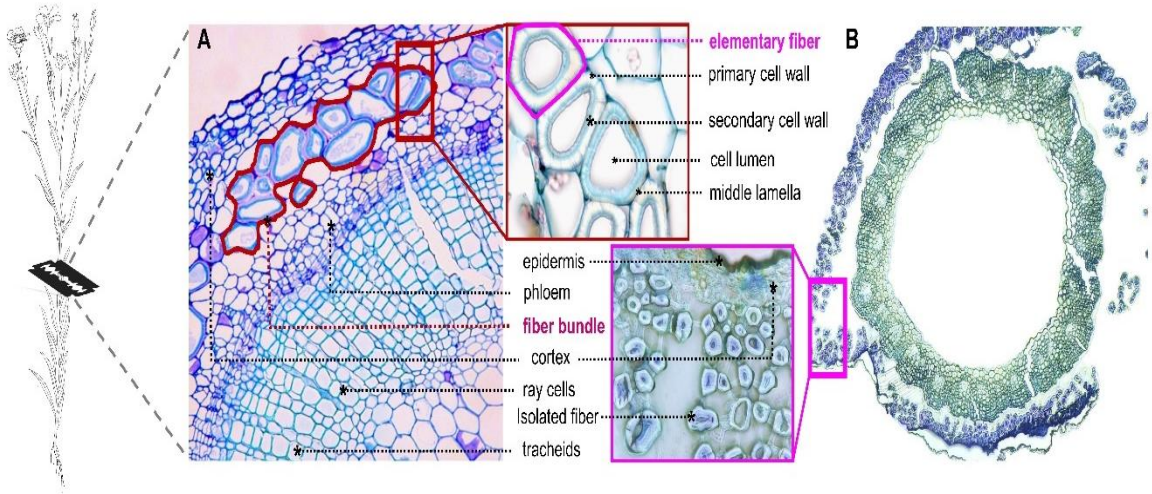

Fig. III.1. Anatomy of flax stem during retting.

A. Cross stem section of harvested Flax plants shows elementary fiber cells are grouped in bundles (red line) and with other tissues just before the retting started. B. After retting, fiber bundles are separated from other surrounding tissues and elementary fibers are individualized (pink line). Cross sections of flax stem, in Technovit 7100, 5µm semi-thin cross-section, TBO staining (Toluidine Blue O, 0.1% w/mL)

To decipher the biology that controls this complex process, researchers have used different approaches to both identify the different microorganisms involved, and to characterize the cell wall degrading enzyme activities involved in retting. Historically, conventional (culture-based) strategies allowed researchers to establish partial inventories of the bacterial and fungal consortia involved in dew retting (Brown and Sharma, 1984; Sharma, 1986; Henriksson et al., 1997; Fila et al., 2001). More recently, the composition and dynamics of the flax-retting microbial community have been studied with high throughput sequencing methods (targeted metagenomics on 16s rDNA and ITS markers) (Djemiel et al., 2017; Chabbert et al., 2020). However, while such studies have undoubtedly contributed to a better understanding about what microorganisms are present, they do not allow a precise identification of which cell-wall degrading enzymes are actually produced by these microorganisms during retting (Herbst et al., 2016; Djemiel et al., 2020). Although biochemical measurements (enzyme assays) have previously been used to evaluate the activities and dynamics of cell wall degrading enzymes during retting in flax (Sharma, 1992; Chabbert et al., 2020) and hemp (Liu et al., 2017; Bleuze et al., 2018), such approaches do not provide information about the individual enzymes contributing to such activity. Indeed, when biochemical approaches are used to measure enzyme activity during retting, what is actually being determined is a “global activity” resulting from the activities of a number of different

individual enzymes, all showing the same type of activity, but differing in structure and originating from different microorganisms. Nevertheless, recent studies on the degradation of forest litter and lignocellulosic biomass (Hori et al., 2018; Chirania et al., 2022) have shown that a metaproteomic approach represents an interesting strategy that can be used to precisely identify individual enzymes as well as the microorganisms producing them.

In this paper, we have attempted to reach two objectives. The first is to identify and establish the dynamics of the key retting enzymes using a metaproteomic approach, the second is to investigate whether differences in retting microbial communities and/or enzyme dynamics might be related to inter-field variability in fiber quality. It is well established that the Northern French climate is favourable for growing and retting flax, nevertheless, field-to-field variability in fiber quality still occurs even when the same variety is grown by the same farmer in the same geographical region. In an attempt to see whether such variability might be related to differences in retting, we sampled three adjacent retting fields and selected the two with the most contrasting fiber properties for further analysis.

III.2.2. Material and methods

III.2.2.1. Sample collection, environmental data, and fiber characterization

Refer to Section **(§) II.2**, **II.3**, **II.4** of Chapter 2

III.2.2.2. Enzymatic activities measurements

Refer to Section **(§) II.6** of Chapter 2

III.2.2.3. Analysis of plant cell wall monosaccharides

Refer to Section **(§) II.7** of Chapter 2

III.2.2.4. Preparation, and measurements for 2D-LC-MS/MS-based metaproteomics

Refer to Section **(§) II.8** of Chapter 2

III.2.2.5. Proteomic data analysis

Refer to Section **(§) II.9** of Chapter 2

III.2.2.6. Other statistical analysis

Refer to Section **(§) II.6.4**, **II.7.4** of Chapter 2

III.2.3. Results

III.2.3.1. Climatic conditions and soil property

Rainfall and temperature weren't evenly distributed during the retting period (23 July-16 August 2021). The highest precipitation was seen in the first week (24 July-27 July 2021) with a maximum value of 41.8 mm on the 26th of July (**Fig. III.2a**). Average temperature was around 20°C which increased at times with lack of rainfall. At this "dew point temperature", we saw a lot of dew in the morning (Beysens et al., 2017). Maximum temperature was around 25.5°C (23july, 12aug, 15aug) and minimum was around 9.5°C (4aug, 11aug). This weather condition promotes microbial metabolism and thus their growth (Robador et al., 2016; Stanaszek-Tomal, 2020).

The composition of soil samples from the three fields is shown in **Fig. III.2b**. The main difference is observed in the limestone content, other attributes are quite similar. The soils are silty-clay or loam type with low sand in it. This type of soil can hold a lot of water (high soil humidity) (Réquilé et al., 2021).

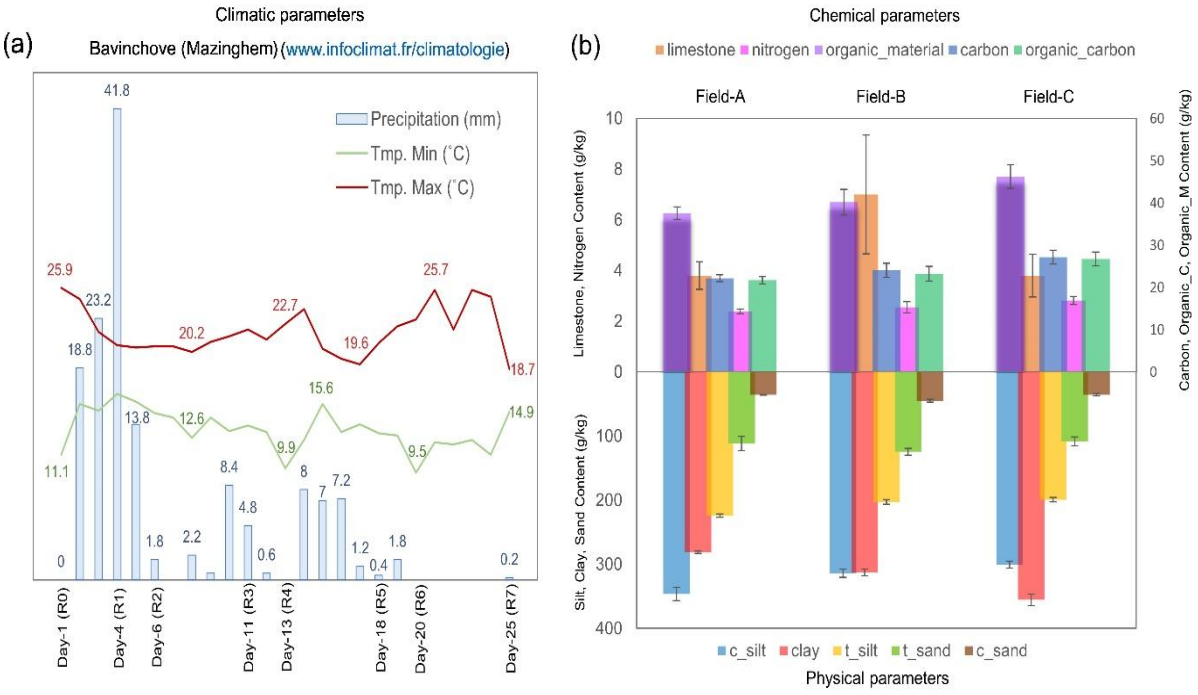

Fig. III.2. Abiotic parameters affecting flax growth and retting.

It includes the weather conditions during growth and retting (III.2a) and the physical and chemical parameters of soil in three experimental fields (III.2b).

III.2.3.2. Inter-field variability exists in both fiber yield and industrial qualities

Measurements showed that differences in the stem and fiber contents existed between the three fields indicating the existence of inter-field variability in terms of fiber extraction yield (Supplementary Data 1). Field A showed the highest fiber extraction yield compared to fields B and C which showed similar values (**Fig. III.3a**). Industrial evaluation of fiber qualities using the USTRL (Union Syndicale des Rouisseurs-Teilleurs de Lin, https://www.usrtl-ifl.fr/) standard (**Fig. II.3** in **§ II.4**, Supplementary Data 1) indicated that fibers from field A show the highest values (6,6,4,3,3) in all evaluated categories (nature, color, resistance, fineness, and homogeneity). The lowest values were obtained for field B (6,4,3,2,2), except for the 'nature' category where fibers from all 3 fields show the same value, and the 'homogeneity' and 'strength' categories where fibers from fields B and C have the same value (lower than field A) (**Fig.III.3**) (see Supplementary Data 1).

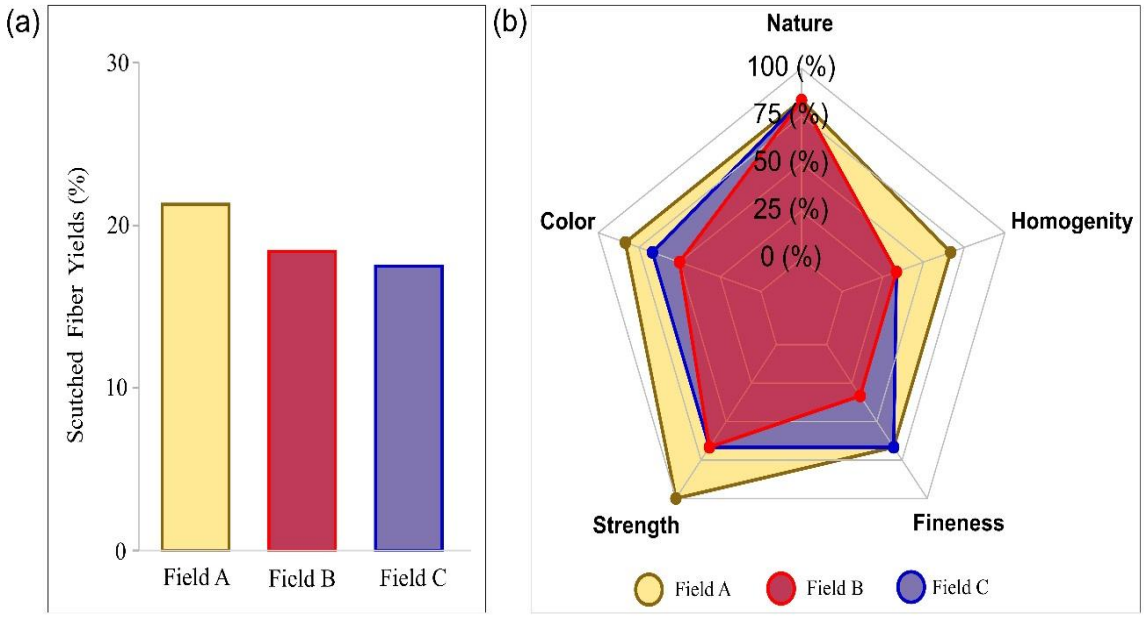

Fig. III.3. Fiber yield and industrial quality assessments.

(a) Comparison of scutched fiber yield (in %) between three experimental fields (A, in yellow, B, in red, and C, in blue). b) Comparison of industrially assessed retted fiber quality obtained from the three experimental fields (A, in yellow, B, in red, and C, in blue). Individual notation for each parameter, i.e. nature, homogeneity, fineness, strength and color, is represented as a % of the possible maximum quotation of the USTRL notation grid (**Fig. II.3** in **§ II.4.1**, page 102).

III.2.3.3. Fiber mechanical property assessment

The observed variability between fibers from fields A and B at the industrial scale was partially confirmed by morphometric and mechanical analyses (**Table III.1**). Significant differences at (93% confidence level) in diameter, fineness, and breaking stress were observed between field A and field B fibers. In contrast, no significant differences were seen for the other tested parameters (deformation at break, E1: tensile modulus, and E2: tensile modulus-2). The small sample size (12 single 20mm fibers) and the high percentage of defects in Field A (63.75% per mm of fiber) compared to Field B (22.91% per mm) led us to accept a P-value of 0.07 (Supplementary data 1). However, power analysis indicated that a sample size of 40 fibers per field would be needed for a more statistically significant result.

Fiber mechanical characteristics	Field-A	Field-B	P-Value (t-test)
Diameter (µm)	21.2± 3.39	18.6±2.49	P = 0.071
Fineness (Tex)	0.54 ± 0.175	0.414 ± 0.106	P = 0.071
Deformation at break (%)	2.2 ± 0.826	1.88 ± 0.698	P = 0.3
Breaking stress (Mpa)	881 ± 378	615± 212	P = 0.072
E1: Tensile modulus (Gpa)	42.5 ± 13	42.4 ± 17.3	P = 0.98
E2: Tensile modulus (Gpa)	48.2 ± 11.8	55± 20.8	P = 0.38

Table III.1. Single fiber tensile test on Filed A and Filed B fibers, following French standard NFT 25-501-2 (for SFTT) and NFG 07-004 (for diameter and fineness). T-test is performed on results in R software showing respective P-values.

Overall, field C fibers show intermediate values. In the light of these results, it was decided to continue subsequent analyses of the retting process by comparing fields A and B which showed the most inter-field variability in terms of fiber yield and quality.

III.2.3.4. Small differences are observed in cell wall degrading enzyme activities between both fields

The activities of seven cell wall degrading enzymes were determined at several time points (R0 – R7) throughout retting in fields A (**Fig. III.4**) and B (**Fig. III.5**). For all enzymes, except for glucosidases, no obvious difference in terms of dynamics between the two fields is observed. For field A, Endo-polygalacturonase activity shows a high level at the beginning of retting before decreasing about 10-fold at day 11 (R3) (**Fig. III.4a**). A similar pattern is observed for phenol-oxidase and peroxidase activities (**Fig. III.4c**), although the decrease in peroxidase activity is more marked. The activities of xylosidase and galactosidase are initially low but increase at R2 until R4 before decreasing at R5 (**Fig. III.4b**). Similarly, both glucosidase and cellobiohydrolase activities initially show low levels of

activities before increasing to a peak at R2 (glucosidase) and R4 (cellobiohydrolase) (**Fig. III.4d**). Comparing the two studied fields, the peak of glucosidase activity in field A seems to be reached as early as R2, whereas it is only attained at R3 in field B (**Fig. III.5**). For certain enzymes (xylosidase, galactosidase, cellobiohydrolase and glucosidase), activity levels are significantly higher in field B compared to field A.

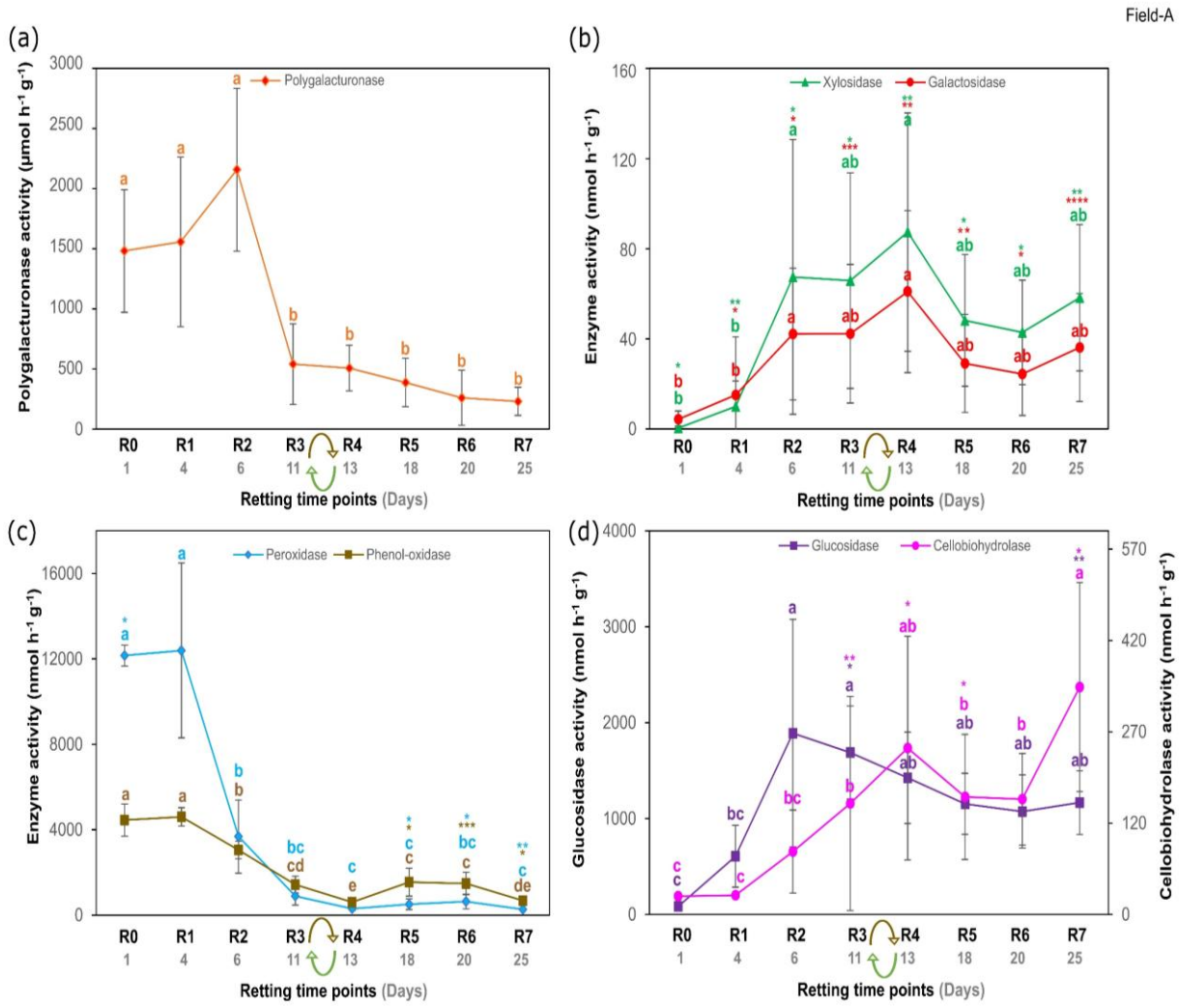

Fig. III.4. Enzyme activity dynamics in outer tissues of flax stems during dew retting in field A.
a) Polygalacturonase activity; b) Xylosidase and Galactosidase activities; c) Peroxidase and Phenol-oxidase activities; d) Cellobiohydrolase and Glucosidase activities. All enzyme activities are expressed in nmol.$h^{-1}g^{-1}$ dry matter except polygalacturonase (µmol.$h^{-1}g^{-1}$ dry matter); n = 5, with n being the mean of 3 technical replicates, Anova (Tukey's HSD) test between retting points are shown with different letter marking p-Value < 0.05; point to point comparison between two fields (A and B), tested with Pairwise T-Test (p.adjust: Fdr), p-Value < 0.05 are indicated with * (data and tests results are shown in supp-data 1). Brown/green arrows indicate swath turning.

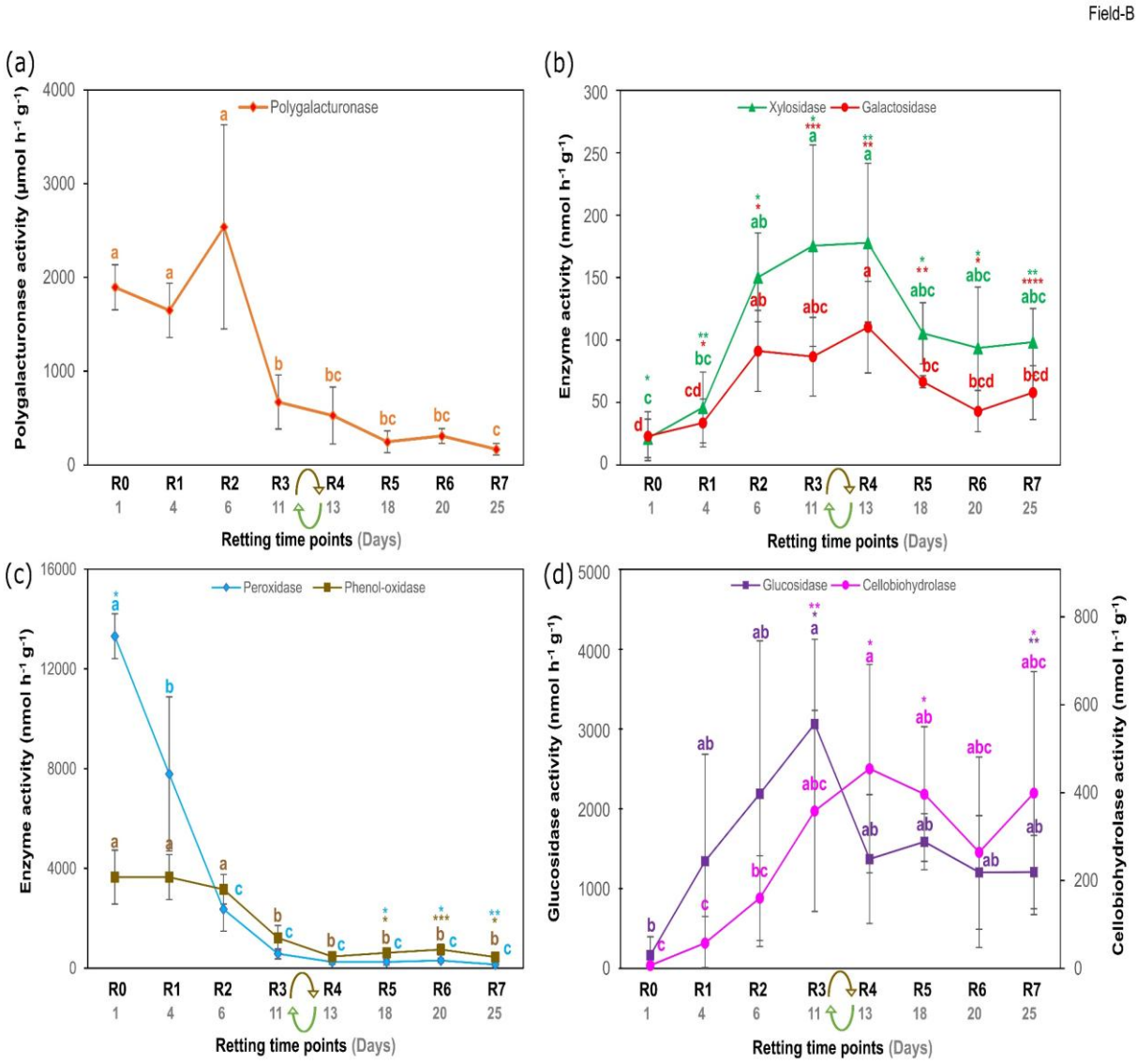

Fig. III.5. Enzyme activity dynamics in outer tissues of flax stems during dew retting in field B.

a) Polygalacturonase activity; b) Xylosidase and Galactosidase activities; c) Peroxidase and Phenol-oxidase activities; d) Cellobiohydrolase and Glucosidase activities. All enzyme activities are expressed in nmol.$h^{-1}g^{-1}$ dry matter except polygalacturonase (µmol.$h^{-1}g^{-1}$ dry matter); n = 5, with n being the mean of 3 technical replicates, Anova (Tukey's HSD) test between retting points are shown with different letter marking p-Value < 0.05; point to point comparison between two fields (A and B), tested with Pairwise T-Test (p.adjust: Fdr), p-Value < 0.05 are indicated with * (data and tests results are shown in supp-data 1). Brown/green arrows indicate swath turning.

The results show the overall global enzyme dynamics are very similar between the two fields and can be grouped into two events;

- In The first week (Early stage); peroxidase and phenol-oxidase activity decreases. Polygalacturonase activity reaches a maximum point (**Fig. III.4.a, c**, **Fig. III.5.a, c**).
- After the first week (Late stage); the beta-galactosidase, cellobiohydrolase, xylosidsae, and galactosidase gradually increase in both fields (from R2) before decreasing (near R6) (**Fig. III.4.b, d**, **Fig. III.5. b, d**). Interestingly, cellobiohydrolase shows again an increase in activity at the endpoint of retting.

III.2.3.5. Cell wall polymer composition evolution in stem outer tissues is similar in both fields

In order to monitor the degradation of cell wall polymers during retting, monosaccharide analyses were performed on hydrolyzed cell wall preparations (AIR) prepared from flax outer-stem samples. The yield from AIR was 70-58% (R0, R1 – R2, … R7). This 30% discrepancy in monosaccharide analysis can be attributed to: 1) non-carbohydrate components in AIR, 2) incomplete hydrolysis, or 3) analytical limitations. Our results (**Fig. III.6 & III.7**) indicated that sample monosaccharide profiles are very similar in both fields. Statistical analyses (ANOVA test, p.value<0.05) identified five monosaccharides (fucose, galactose, xylose, galacturonic acid, and arabinose) that showed statistically significant changes between retting points during the process of dew retting for both fields. The quantities of galactose, xylose, and galacturonic acid decreased gradually and smoothly by roughly 50% during retting. In contrast, the amount of arabinose decreased more abruptly (by approx. 70%) between R0 and R2. Finally, fucose decreased by 55% between R4 and R7 (Supplementary Data 1). Notably, 90-92% of the detected monosaccharides were glucose, of which 85-87% was crystalline, presumably the crystalline cellulose of fibers.

III.2.3.6. Metaproteomics of key retting points identifies 6032 unique proteins

Protein identification and quantification was performed on selected samples [day 1 (R0); day 6 (R2), day 13 (R4), and day 25 (R7), (fields A and B)] corresponding to key points during the retting process that were revealed by enzyme activities and cell wall composition kinetic. Analyses of all samples identified 7373 non-redundant proteins of which 102 were filtered as contaminants (mainly animal proteins; Supplementary Data 2). After normalization, proteins were further filtered to determine the effective metaproteome for field A (5702 proteins) and field B (5610 proteins). Overall, combined metaproteomes from field A and B led to the identification of 6032 unique proteins (**Table III.2**). The list of proteins, normalized values and information on whether proteins are present/absent at R0 is

provided in Supplementary Data 2. 5280 proteins (88%) are shared between the two fields, 422 proteins (7%) are specific to field A and 330 proteins (5%) to field B (**Fig. III.8**).

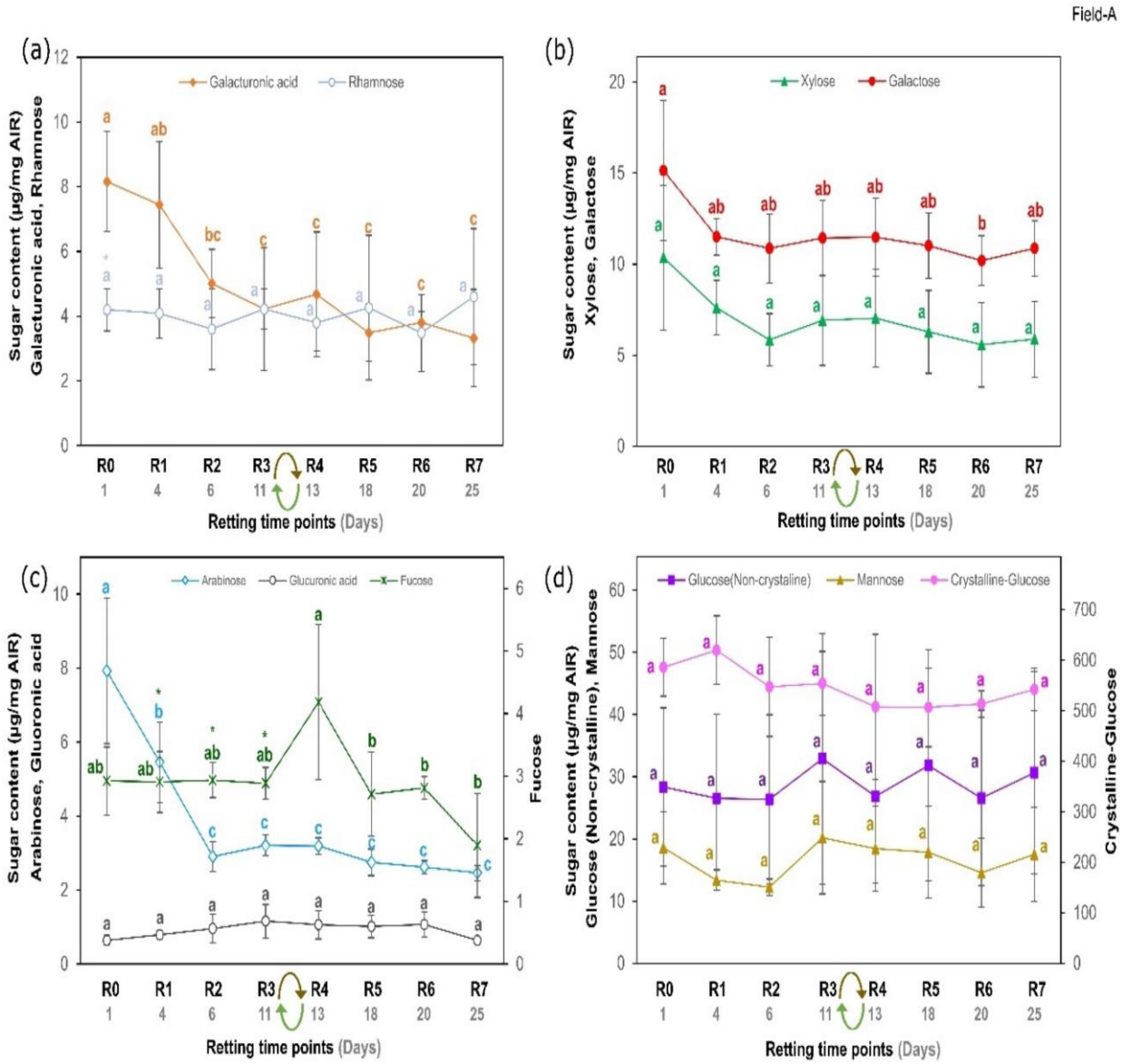

Fig.III.6. Changes in cell wall monosaccharide composition in outer tissues of flax during dew retting in field A.

a) Galacturonic acid and Rhamnose; b) Xylose and Galactose; c) Arabinose, Glucuronic acid and Fucose; d) Mannose, Glucose (coming from crystalline cellulose) Glucose (coming from non-crystalline polysaccharides) are expressed in µg/mg of Alcohol Insoluble Residue (AIR) obtained from flax stem outer tissue. n = 5, with n being the mean of 3 technical replicates, statistical significance with Anova (Tukey's HSD) test between retting points are shown with letter marking p-Value < 0.05; point to point comparison between two fields were tested with Pairwise T-Test (p.adjust: Fdr), p-Value < 0.05 are indicated with * (corresponding data and tests results are given in supp data 1). Brown/green arrows indicate swath turning.

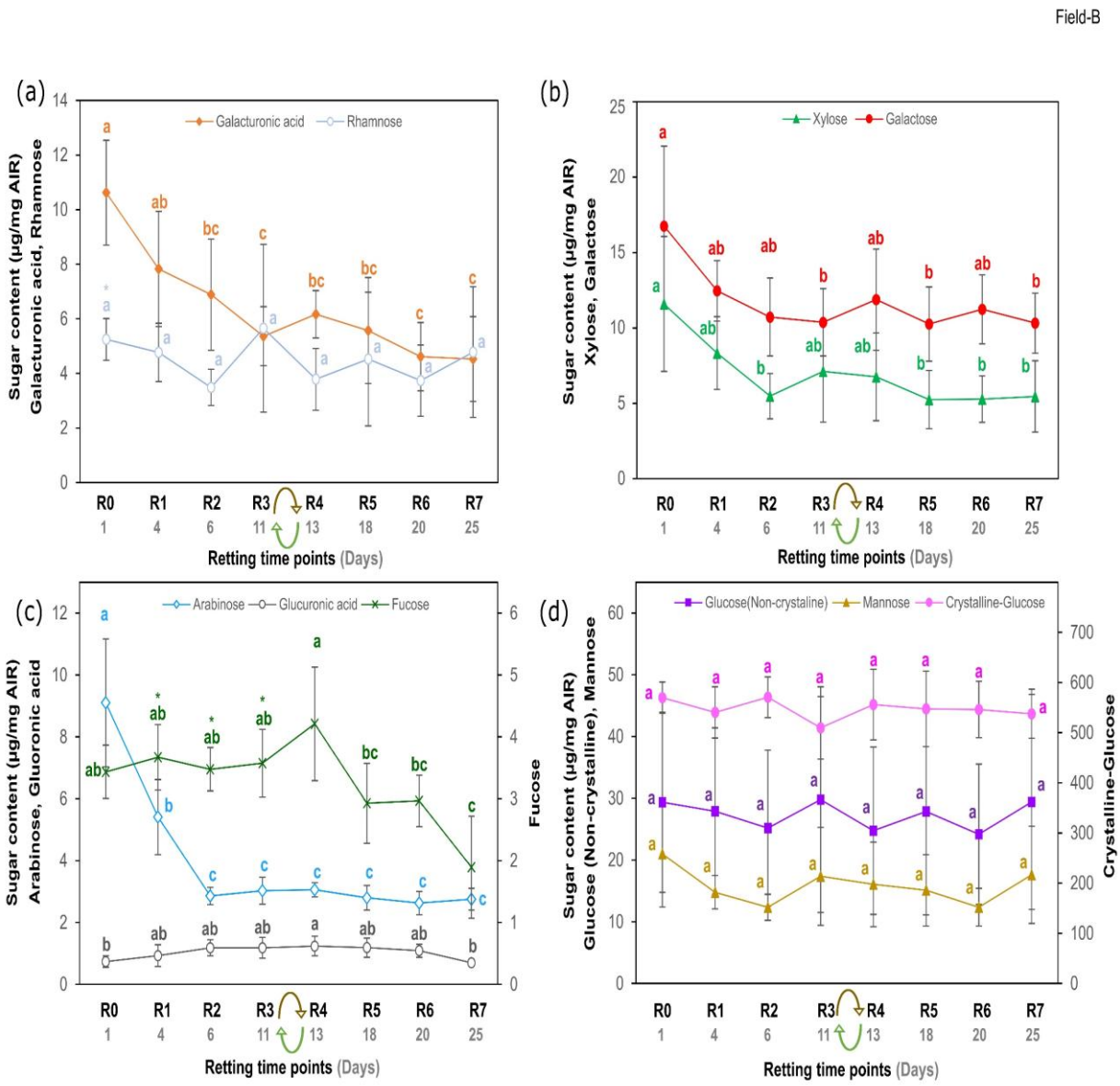

Fig.III.7. Changes in cell wall monosaccharide composition in outer tissues of flax during dew retting in field B.

a) Galacturonic acid and Rhamnose; b) Xylose and Galactose; c) Arabinose, Glucuronic acid and Fucose; d) Mannose, Glucose (coming from crystalline cellulose) Glucose (coming from non-crystalline polysaccharides), are expressed in µg/mg of Alcohol Insoluble Residue (AIR) obtained from flax stem outer tissue. n = 5, with n being the mean of 3 technical replicates, statistical significance with Anova (Tukey's HSD) test between retting points are shown with letter marking p-Value < 0.05; point to point comparison between two fields were tested with Pairwise T-Test (p.adjust: Fdr), test p-Value < 0.05 are indicated with * (corresponding data and tests results are given in supp data 1). Brown/green arrows indicate swath turning.

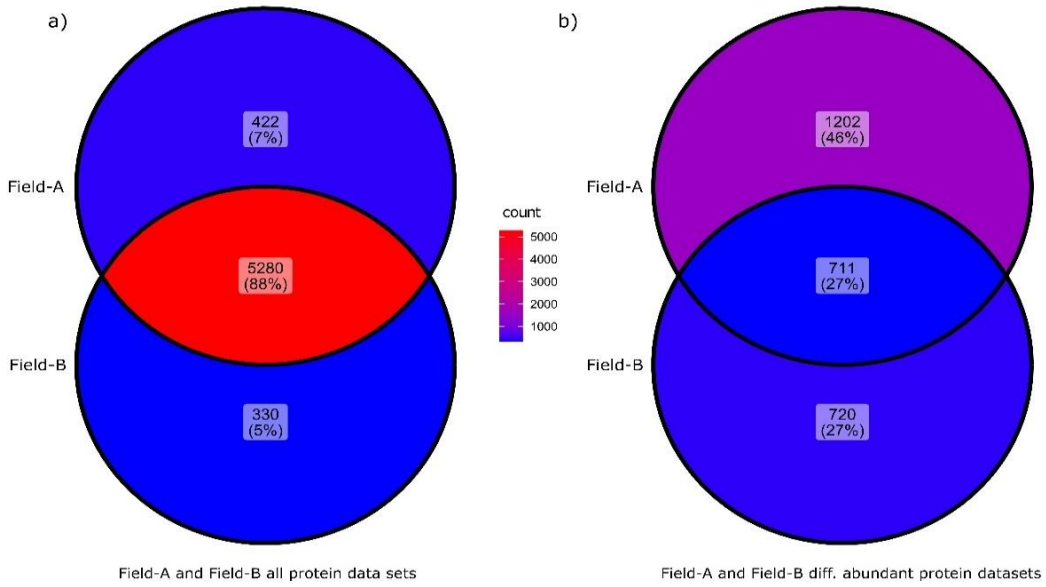

Fig. III.8. Venn diagrams of proteins identified during retting in Fields A and B

a) Venn diagram showing the number of specific and common identified proteins from fields A and B; b) Venn diagram showing the number of differentially abundant proteins identified in fields A and B. Color scale corresponds to the number of proteins.

Conditions	Field-A	Field-B	Common	Non-redundant
Initial total identified proteins			7373	
Initial contaminations			102	
Proteins left after sorting based on the condition explained in material and methods	1671	1763	2093	-
Sorted-proteins	5702	5610	5280	6032
Differentially abundant between R4_R2	1052	497	-	-
Differentially abundant between R7_R2	1637	1326	-	-
Differentially abundant between R7_R4	0	0	-	-
All differentially abundant proteins	1912	1431	711	-
Identified proteins with CAZy motif	60	58	44	75
Cell wall related CAZymes	31	30	24	37

Table III.2. Protein numbers obtained during the different filtering and processing steps of metaproteomic data.

III.2.3.7. Basic metabolism proteins are dominant in the metaproteome

Functional gene ontology (GO) assignation (https://geneontology.org/) was undertaken to provide an initial overview of the functional composition of the retting metaproteome. Full GO annotations by protein, counts of proteins by GO terms and filtering with GO slims metagenomic are presented in Supplementary Data 3. A comparison of the GO profiles for fields A and B shows that they are very similar (**Fig. III.9**). Among the molecular functions identified, approximately 33% are related to nucleic acid metabolism and 6% are ribosomal components. Functions related to degradation activities, such as peptidase, lyase, and hydrolase represent only 1%, 3.2% and 2.7%, respectively. In terms of processes, protein and nucleic acid metabolism dominate. Processes related to carbohydrate metabolism, which probably include enzymes involved in the degradation of plant polymers, account for about 7% of the GO annotations. Interestingly, the photosynthesis process is still represented within both metaproteomes indicating the presence of plant proteins (mainly from flax) but also cyanobacteria proteins. About half of all proteins are associated with the cytoplasm, while 3.7% and 1.4% of proteins are associated with the extracellular and periplasmic compartments, respectively.

III.2.3.8. The metaproteome is mainly composed of bacterial proteins

A taxonomic analysis of the metaproteome based on the NCBI organism database (https://www.ncbi.nlm.nih.gov/taxonomy) (**Fig. III.10**, Supplementary Data 4) showed that the majority of proteins come from the bacteria kingdom (85% for field A, 86% for field B). Most of these proteins correspond to bacteria belonging to the *Pseudomonadota phylum* (71.6% for both fields), which includes *Alpha, Beta and Gammaproteobacteria*, classes already identified in other studies on flax retting. Other phyla identified include *Bacillota* (around 7% in both fields), *Actinomycetota* (5 - 6%) and *Cyanobacteria* (around 3.2%). Thirteen percent (field A) and 12 % (field B) of identified proteins are of fungal origin. Fungal proteins come mainly from the *Ascomycetes* phylum (around 91%), and to a lesser extent from the *Basidiomycetes* phylum (around 7%). Two percent of proteins come from plants (*Streptophyta*), mainly flax (**Table III.3, Fig. III.10**).

Fig. III.9. Distribution of proteins by GO category according to GO aspects for field A and field B.

Identified proteins were annotated for GO aspects, sorted and counted by GO categories (Biological process in blue, Cellular components in red and Molecular function in green), and filtered according to GOslims metagenomic (https://www.ebi.ac.uk/QuickGO/). Percentages are presented in imbricated pie donuts chart. Color: Blue is related to basic cell metabolism (Process), Pink-Orange is related to cell structure components (Components), and Green is related to physiological functions (Functions).

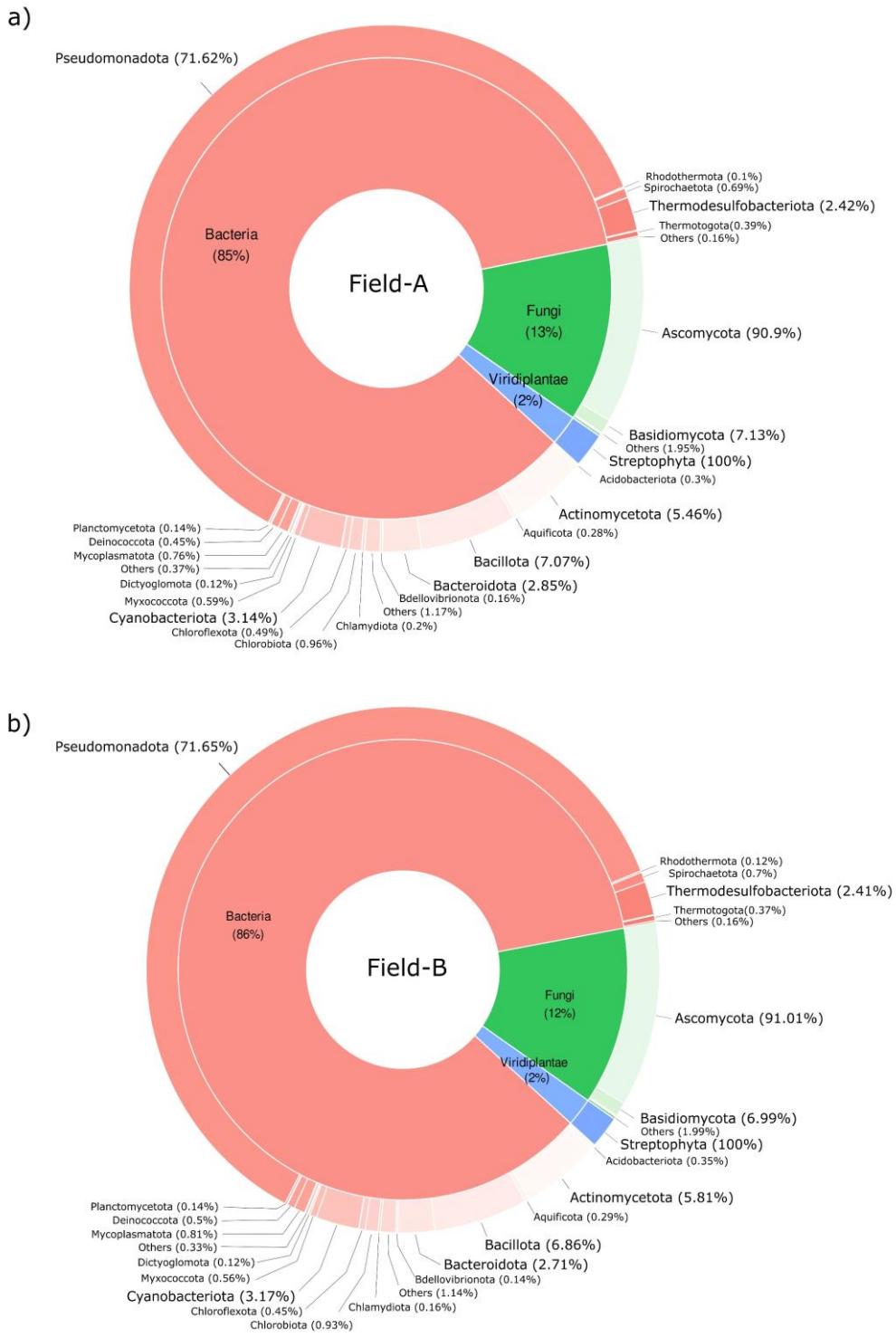

Fig. III.10. Taxonomic origin of proteins identified in the field A and B metaproteomes.

Proteins identified in field A (a) and in field B (b) metaproteomes were annotated with a reconstructed taxonomy (https://www.ncbi.nlm.nih.gov/taxonomy). Taxons were counted for proteins, then represented in an imbricated pie donuts chart showing kingdom and phyla. Pink-Orange is related to *Bacteria* domain, Green for Fungi domain, and pale Blue for *Viridiplantae* sub-domain (green plants).

Taxonomic origin of identified proteins	Field-A	Field-B
Identified protein coming from bacteria (genus level)	381	380
Identified protein coming from fungus (genus level)	97	96
Identified protein coming from plant (genus level)	1	1
Identified cell wall related CAZymes coming from bacteria (genus level)	4	3
Identified cell wall related CAZymes coming from fungus (genus level)	10	9
Identified cell wall related CAZymes coming from plant (genus level)	1	1

Table III.3. Taxonomic origin of identified nonredundant proteins and respective cell wall-related CAZymes.

III.2.3.9. The abundance of about one-third of total proteins varies significantly during retting

Pairwise differential analysis was performed on three different combinations of protein groups (R2 vs R4, R2 vs R7 and R4 vs R7). R0 proteins were not included in the pairwise analysis due to their particular distribution as previously explained. 1913 and 1431 proteins showing significant differences (FDR p-values $\leq 0{,}05$, $0.66 \geq$ mean ratio ≥ 1.5) in abundance between the compared retting points were identified for fields A and B, respectively (Supplementary Data 2). Among these differentially abundant proteins, 711 (27%) were identified in both fields A and B (**Fig. III.7b**). For each field, a list of the top 30 most over-expressed and most repressed proteins between the R2 and R7 retting points were generated (Supplementary Data 2). In the most over-expressed protein category for field A, the number one protein corresponds to an exoglucanase (cellobiohydrolase, Cel1) from an ascomycete parasite of *Poaceae* (*Cochliobolus carbonum*). A second exoglucanase (cellobiohydrolase, Cel2) from a basidiomycete (*Agaricus bisporus*), and a Beta-mannosidase (bmann9) from an ascomycete known for its cellulolytic activity (*Myceliophthora thermophila*) are also present in the over-expressed category. None of these proteins were present at the start of the retting process (R0). The repressed protein category for field A is dominated by flax proteins, including proteins related to pectin metabolism (pectinesterases pme5, pme3), and peroxidases (PER3, PER4) that are already present at R0. Regarding field B, it is surprising to observe that the top 2 proteins in the over-expressed category correspond to flax proteins encoding lignin/monolignol metabolism enzymes (CAD7 and CAD8). Nevertheless, two cellobiohydrolases, Cel1 and Cel2 from *Cochliobolus carbonum* and *Agaricus bisporus* are also present. In field B the repressed proteins are dominated by the same flax proteins (except for pme3) found in field A.

III.2.3.10. The metaproteome contains key cell wall degrading enzymes belonging to Carbohydrate Active Enzymes (CAZy) families

All identified protein sequences were subjected to CAZy (Carbohydrate-Active enzymes) motif searches. A total of 60 and 58 proteins presenting a CAZy motif were identified in fields A and B, respectively. Forty-four proteins (59%) are common to both fields. The identified CAZymes are distributed in 31 families from all 5 different CAZy classes: GTs = glycosyl transferases, GHs = glycosyl hydrolases, CEs = carbohydrate esterases, PLs = polysaccharide lyases and AAs = auxiliary activities (**Fig. III.11**, Supplementary Data 5). The percentage distribution of proteins in the different CAZy classes is quite similar between the two fields with GH representing the largest class (58 %) in both fields. Within the GH class, family GH13 proteins generally associated with starch degradation represent the largest category (37 % field A, 44 % field B). The second most represented CAZy family is GH7 (around 17% for both fields), whose activity is often associated with cellobiohydrolase-type exoglucanase activity. Other GH families associated with the degradation of plant wall polymers can also be identified for each field. It is interesting to note that the GH10, GH37, and GH31 families are only present in field B samples while the GH94, GH54, GH55, GH17 and GH18 families are only present for field A. Polysaccharide lyases account for 8.3 % of CAZymes (field A) and 12 % (field B), while carbohydrate esterases represent 8.5% CAZy proteins for both fields. These classes include enzyme families that degrade pectins. The GT (Glycosyl transferase) class accounts for a similar percentage value in both fields (18.3% field A; 15.5% field B) with the GT1 family representing over 60% of identified GTs.

In order to further characterize the enzymes potentially involved in the degradation of plant cell walls, a manual annotation was carried out by integrating the UniProt annotation of each protein, the description of the CAZy families (http://www.cazy.org/) and the functional assignment of CAZy families according to the literature (Djemiel et al., 2017; Tláskal et al., 2021; Chirania et al., 2022). This approach allowed the selection of 31 proteins (field A) and 30 proteins (field B), each associated with an enzymatic activity and target polymer(s) (**Fig. III.12,** Supplementary Data 5, **Table III.4**). Taken together, 36 non-redundant proteins belonging to 19 families putatively involved in the degradation of different plant cell wall polymers were identified including lignin (AA1), pectins (CE13_8, PL1_3, GH35, GH28), hemicelluloses (GH2, GH26, GH35, GH55, GH3, GH5, GH17) and cellulose (GH7, GH3, GH35, GH94). Analysis of how the relative abundance of these enzymes evolved during retting revealed a number of different profiles according to the CAZy family/enzyme activity and target polymer (**Fig. III.12**, Supplementary Data 5). The results firstly show that enzymes belonging to some

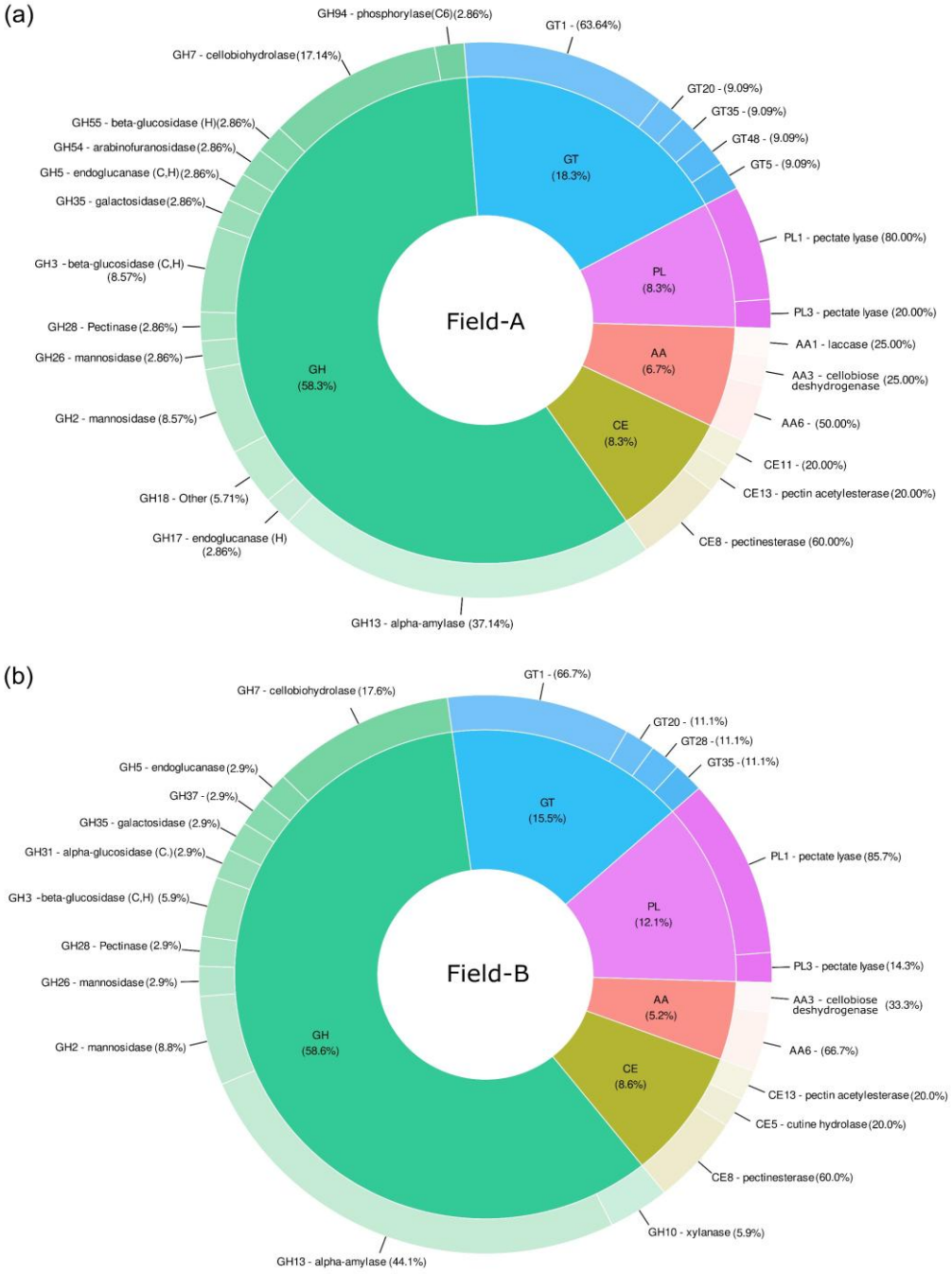

Fig. III.11. Distribution of CAZymes identified in the metaproteome of field A and field B presented by class and families.

Proteins within the flax metaproteome were sorted by the dbCAN3 pipeline (https://bcb.unl.edu/dbCAN2/) and are listed in Supp._Data 5. Percentages are presented in imbricated pie donuts chart. Green is related to GH: glycosylhydrolase, pale Blue to GT: glycosyltransferase, Purple to PL: pectate lyase, Pink-Orange to AA: auxiliary activities, and Khaki to CE: carbohydrate esterases.

Family	Names	Enzyme	Target-Polymer	Organism (Species-level)	Kingdoms	UniProt-ID	Field-A	Field-B
GH	GH5	Endoglucanase	Cellulose	*Paenibacillus lautus*	Bacteria	P23550	✓	✓
	GH7	Cellobiohydrolase	Cellulose	*Aspergillus clavatus*	Fungi	A1CE97	✓	✓
	GH7	Cellobiohydrolase	Cellulose	*Aspergillus aculeatus*	Fungi	O59843	✓	✓
	GH7	Cellobiohydrolase	Cellulose	*Fusarium oxysporum*	Fungi	P46238	✓	✓
	GH7	Cellobiohydrolase	Cellulose	*Cochliobolus carbonum*	Fungi	Q00328	✓	✓
	GH7	Cellobiohydrolase	Cellulose	*Neurospora crassa*	Fungi	Q7SA23	✓	✓
	GH7	Cellobiohydrolase	Cellulose	*Agaricus bisporus*	Fungi	Q92400	✓	✓
	GH94	Phosphorylase(C6)	Cellulose	*Neurospora crassa*	Fungi	Q7S0S2	✓	×
	GH3	Beta glucosidase	Cellulose & Hemicellulose	*Neosartorya fischeri*	Fungi	A1D451	✓	×
	GH3	Beta glucosidase	Cellulose & Hemicellulose	*Neosartorya fischeri*	Fungi	A1DFA8	✓	✓
	GH3	Beta glucosidase	Cellulose & Hemicellulose	*Escherichia coli*	Bacteria	P33363	✓	✓
	GH17	Endoglucanase	Hemicellulose	*Linum usitatissimum*	Plante	H9E8V8	✓	×
	GH10	Xylanase	Hemicellulose	*Fusarium oxysporum*	Fungi	B3A0S5	×	✓
	GH10	Xylanase	Hemicellulose	*Aureobasidium pullulans*	Fungi	Q2PGV8	×	✓
	GH2	Mannosidase	Hemicellulose	*Aspergillus clavatus*	Fungi	A1CGA8	✓	✓
	GH2	Mannosidase	Hemicellulose	*Aspergillus niger*	Fungi	A2QYN2	✓	✓
	GH2	Mannosidase	Hemicellulose	*Thermothelomyces thermophilus*	Fungi	I2C092	✓	✓
	GH26	Mannosidase	Hemicellulose	*Thermothelomyces thermophilus*	Fungi	G2Q4H7	✓	✓
	GH55	Beta-glucosidase	Hemicellulose	*Cochliobolus carbonum*	Fungi	P49426	✓	×
	GH35	Galactosidase	Hemicellulose & Pectin	*Linum usitatissimum*	Plante	F6LC68	✓	✓
	GH54	Arabinofuranosidase	Hemicellulose &Pectin & AGP	*Aspergillus clavatus*	Fungi	A1CGD1	✓	×
	GH28	Polygalacturonase	Pectin	*Neosartorya fischeri*	Fungi	A1DLC1	×	✓
	GH28	Polygalacturonase	Pectin	*Aspergillus flavus*	Fungi	B8N7Z8	✓	×
AA	AA3	Cellobiose dehydrogenase	Cellulose	*Pichia angusta*	Fungi	P04841	✓	✓
	AA1	Laccase	Lignin	*Botryotinia fuckeliana*	Fungi	Q96UM2	✓	×
CE	CE13	Pectin acetylesterase	Pectin	*Linum usitatissimum*	Plante	A0A172MLD6	✓	✓
	CE8	Pectinesterase	Pectin	*Linum usitatissimum*	Plante	Q94FS5	✓	✓
	CE8	Pectinesterase	Pectin	*Linum usitatissimum*	Plante	Q94FS6	✓	✓
	CE8	Pectinesterase	Pectin	*Linum usitatissimum*	Plante	Q9FVF9	✓	✓
	CE5	Cutine-Hydrolase	Cutine	*Colletotrichum gloesporioides*	Fungi	P11373	×	✓
PL	PL1	Pectate lyase	Pectin	*Pseudomonas amygdali*	Bacteria	P72242	✓	✓
	PL1	Pectate lyase	Pectin	*Pseudomonas marginalis*	Bacteria	Q51915	✓	✓
	PL1	Pectate lyase	Pectin	*Pseudomonas fluorescens*	Bacteria	Q59671	✓	✓
	PL1	Pectate lyase	Pectin	*Pseudomonas viridiflava*	Bacteria	Q60140	✓	✓
	PL1	Pectate lyase	Pectin	*Pectobacterium carotovorum*	Bacteria	P0C1C0	×	✓
	PL1	Pectate lyase	Pectin	*Pectobacterium carotovorum*	Bacteria	P0C1C1	×	✓
	PL3	Pectate lyase	Pectin	*Neosartorya fischeri*	Fungi	A1DBJ7	✓	✓

Table. III.4. List of CAZy families, corresponding enzyme activities, target polymers, biological origin, kingdom, UniProt ID and presence/absence in fields A and B from all identified nonredundant proteins.

of the CAZy families (GH5, GH17, CE8, CE13) were present since flax were up-rooted (R0) while others appeared later during retting.

The total abundance of cellulose-degrading enzymes increases significantly from R2 to the end of the retting process for both fields. In this group, the most important CAZy family is GH7 (exo-glucanase/ cellobiohydrolase), corresponding to six identified proteins, followed by GH3 (beta-glucosidase) with 3 enzymes targeting both cellulose and the xyloglucan hemicellulose backbone. In contrast to the GH7 group, the abundance of the GH3 group does not vary between R2 and R7. The only GH5 (endoglucanase) enzyme identified was already present at R0 in both fields, but only increased in abundance after point R2 in field A, but not field B. It is also noteworthy that the abundance of certain proteins involved in cellobiose degradation (AA3 - fields A and B; GH94 - field A only) increases sharply at the end of retting, most likely reflecting an increase in the abundance of cellulose-derived oligosaccharides.

With regards to hemicellulose metabolism, the mannosidase/mannanase group is the most represented, with 1 mannanase enzyme (GH26) and 3 beta-mannosidase enzymes (GH2). The abundance of proteins in the latter group increased significantly during retting in both fields. Two other enzymes classified in the GH17 (endoglucanase) and GH55 (beta-glucosidase) families are only found in field A. The abundance of both of these proteins decreased between R2 and R7. In contrast, 2 xylanase enzymes belonging to the GH10 family were only found in field B. The abundance of these proteins remained constant throughout retting. Finally, one enzyme belonging to the GH35 family (galactosidase) potentially targeting either hemicellulose or pectin was identified in both fields. The abundance of this protein decreased during retting in field A but remained stable in field B.

The same pectin-targeting CAZy families are represented in both field A and B samples and include CE13 (pectin acetylesterases), CE8 (pectin-esterases), PL1 and PL3 (pectate lysases), as well as GH28 (pectinases).

Metaproteomics also revealed other enzymes that potentially target components of the plant cell wall. Examples include arabinogalactan-proteins (AGPs), which are targeted by arabinofuranosidase (GH54), and lignin which could be targeted by laccases (AA1). These two enzymes are only found in the A-field samples. In contrast, a cutin hydrolase enzyme (CE5) was present in field B, but not field A samples. This enzyme might play a role in promoting flax stem penetration for certain fungi and bacteria at the beginning of the retting by degrading cutin in epidermal cell walls.

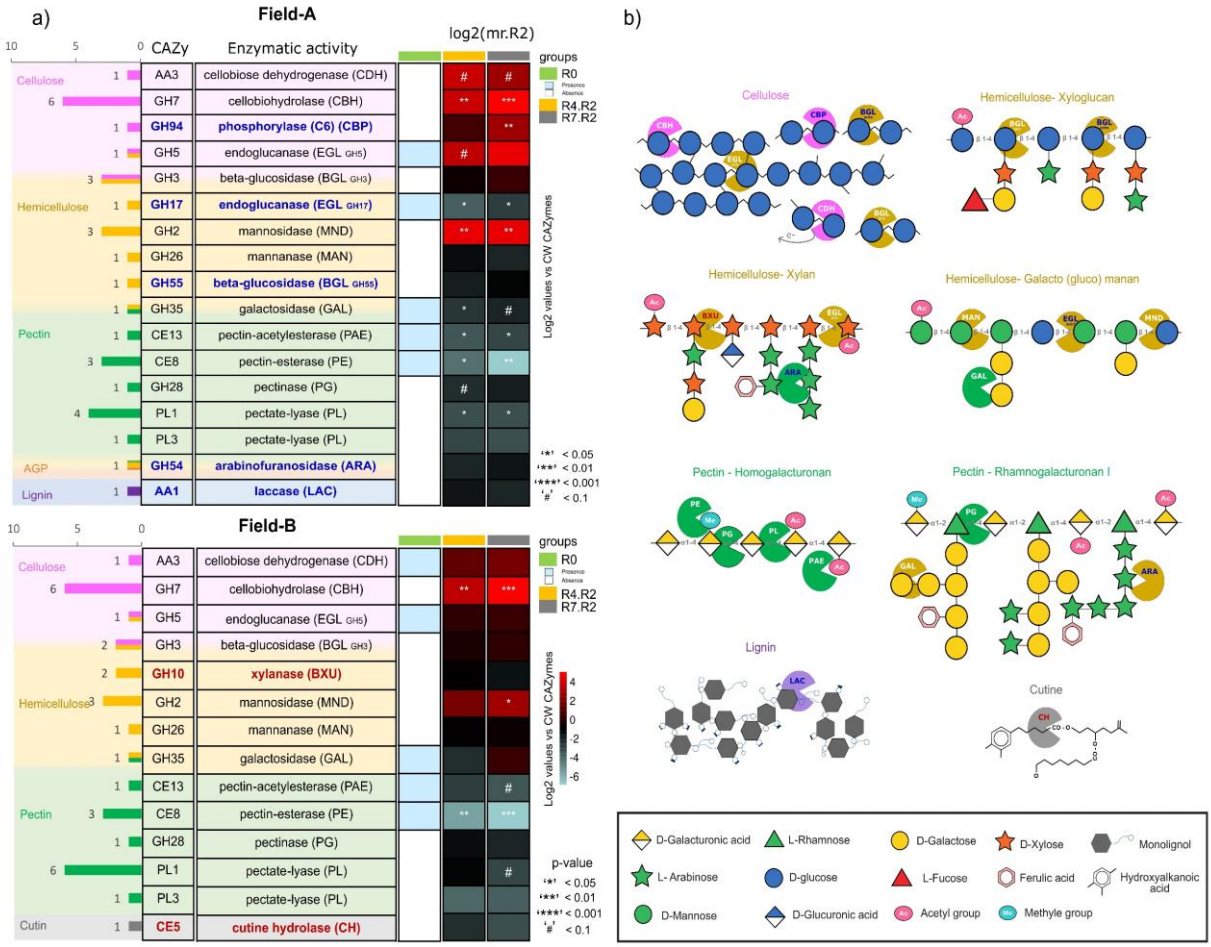

Fig. III.12. Dynamic changes in CAZyme abundances during flax retting in fields A and B.

a) CAZymes were identified within the metaproteome of field A and B and then manually assigned to an enzymatic function and polymer target. CAZymes were then grouped by polymer and enzymatic activities. Numbers in the left barplot diagram indicate the number of unique proteins grouped in each CAZy family. Enzymatic activities specific to field A are shown in blue and enzymatic activities specific to field B are shown in red. The first heatmap column shows presence (light blue) or absence (white) of CAZymes on day 1 (R0); the second and third columns show, respectively, the log2 mean ratio of cumulative abundance values of CAZymes (area under peak) of day 13 (R4) and day 25 (R7) compared to day 6 (R2); n =3, Welsch T-test with FDR. b) schematic representations of plant cell wall polymers and associated degrading enzymes identified in metaproteomes, enzyme abbreviations correspond to those indicated within brackets in (a).

III.2.3.11. CAZymes involved in the degradation of plant wall polymers come mainly from Fungi

As stated above, analysis of the total metaproteome for both fields showed that the majority of proteins (85%) were of bacterial origin. In contrast, analysis of the CAZy proteins acting on cell wall polymers suggested that a little more than half of proteins were of fungal origin. Nineteen (61 %) out of 31 proteins in field A and 17 (57 %) out of 30 proteins in field B come from fungi (**Table III.4**).

All of the fungal CAZymes identified are produced by fungi belonging to the sub-kingdom *Dikarya*. Of these, the majority are *Ascomycota* (classes *Sordariomycetes*, *Saccharomycetes*, *Leotiomycetes*, *Eurotiomycetes*, and *Dothideomycetes*). The *Basidiomycota* are only weakly represented with a single GH7 CAZyme from *Agaricus bisporus* (class *Agaricomycetes*) (**Fig. III.13** and **Table III.4**). Among the fungi identified, some are classified as plant pathogens (*Fusarium oxysporum, Cochliobolus carbonum, Botryotinia fuckeliana*), while others are saprophytic (*Neurospora crassa, Myceliophthora thermophila, Agaricus bisporus*) or endo/epiphytes (*Aureobasidium pullulans)*. It is a little more surprising to find species that are pathogenic for humans, even if they are known to be telluric (*Neosartorya fischeri, Aspergillus clavatus, Aspergillus Niger*).

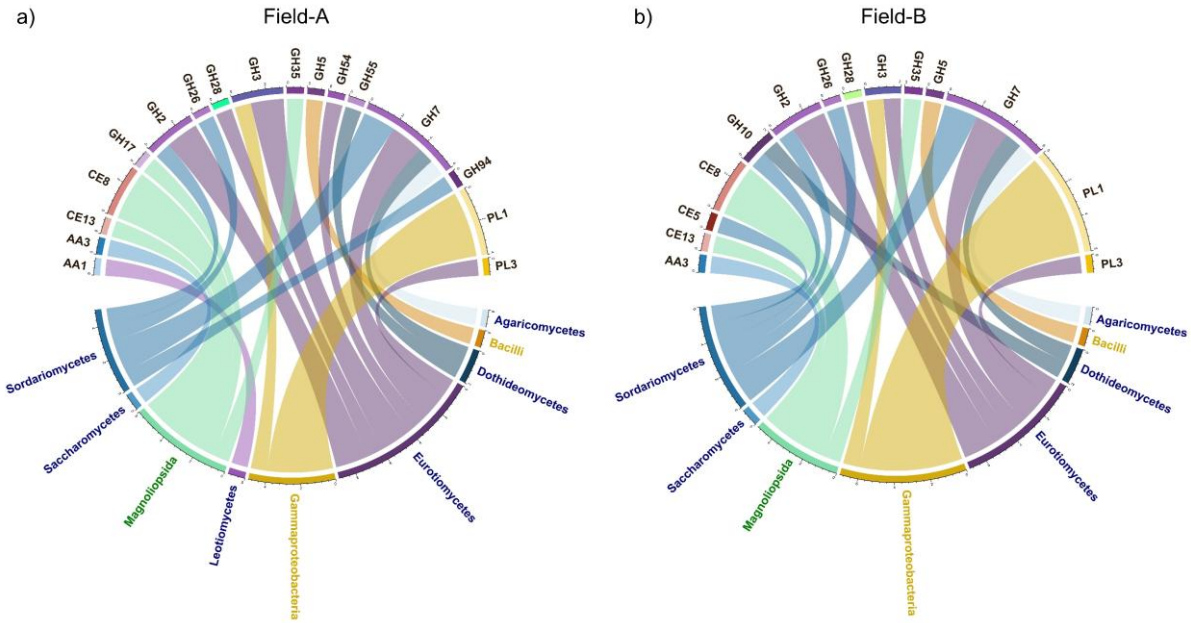

Fig. III.13. Taxonomic origins of CAZymes associated with plant cell wall degradation identified in the metaproteomes of fields A and B.

Chord diagrams show the microbial origin (at the class level) of CAZy families associated with flax cell wall polymer modification during retting in field A (a) and field B (b). CAZy families (in black) are connected to their microbial origin by color chords: Fungal classes are indicated in blue and are connected to their related CAZymes by blue or purple chords; bacterial classes are indicated in yellow and are connected to their related CAZymes by yellow or orange chords; plant (Magnoliopsida) CAZymes are connected with green chords.

Bacterial CAZymes acting on cell wall polymers are less represented with only 6 and 8 proteins identified for fields A and B, respectively. These proteins are mainly produced by two genera (*Pseudomonas* and *Pectobacterium*), that contain plant pathogens and/or saprophytes that are known to produce pectinolytic enzymes. The genus *Paenobacillus* is also present and is represented by the species *lautus* that is a ubiquitous bacillus living on both plants and animals, and well known for producing

polysaccharide degrading enzymes. A little more surprising is the presence of the species *E. Coli* as a GH3 beta-glucosidase cell wall degrading enzyme producer, since this species is commonly associated with the lower intestine habitat. Nonetheless, *E. coli* has been reported to be able to survive in different types of habitats including soil, manure and water (van Elsas et al., 2011).

The chord diagrams were chosen to visually link enzyme classes to their putative origins (Bacteria, Fungi, and Viridiplantae), allowing a clear comparison between fields A and B. While both diagrams appear similar in terms of enzyme origins, subtle differences in the microbial consortia are observed between the fields. Interestingly, despite these similarities, the scutched fibers from each field exhibit distinct physical properties (color, fineness, etc.). This suggests that the final fiber quality is not solely determined by microbial enzyme activity but likely involves other factors, such as microbial interactions or environmental conditions influencing the retting process.

III.2.4. Discussion

Northern France is known to be a favourable region for the growth and retting of fiber flax. Nevertheless, field-to-field variability in fiber quality can still occur even when the same biological variety is cultivated and processed in the same geographical location. In such a situation, plants from different fields are exposed to the same meteorological conditions and it is therefore unlikely that the observed variability is due to differences in plant physiology and fiber formation during growth. In an attempt to see whether such variability might be related to differences in the retting process, we used a biochemical approach combined with a novel metaproteomics strategy to characterize and compare the cell-wall-degrading arsenal in two adjacent fields (A and B) showing variability in both fiber yield and quality.

III.2.4.1. Biochemical analyses identify small differences in retting between fields A and B

A detailed biochemical comparison of cell wall degrading enzyme activities between the two fields during retting revealed that the dynamics were basically similar, although differences in overall activity levels were observed. In both cases, different dynamic profiles could be discerned, broadly according to the cell wall polymer targeted. Endo-polygalacturonase (targeting pectins) and phenol-oxidase/laccase (targeting lignin/polyphenols) activities showed peak activity at the beginning of retting while xylosidase (hemicelluloses) and galactosidase (hemicelluloses and pectins) activities peaked later (R2) before decreasing. Glucosidase (cellulose and hemicellulose) and cellobiohydrolase (cellulose) activities peaked afterward (R3-R4). Overall, these results are similar to the findings of other studies on both flax and hemp retting (Bleuze et al., 2018; Chabbert et al., 2020). The observed activity profiles correspond well with the timing of changes in flax stem anatomy that are known to occur during retting where degradation of the pectin-rich middle lamella is followed by the destruction of the primary cell

walls in the cortex leading to the liberation of fiber bundles from surrounding tissues together with the progressive separation of elementary fibers from each other. The observed lignin/phenol-oxidase activity might be related to the degradation of phenolics in the cuticle of the epidermis and/or low amounts of lignin that can be present in the common compound middle lamella between neighboring bast fibers (Day et al., 2005; Lion et al., 2017). Swathe turning has previously been shown to significantly affect the microbiological consortium during retting (Djemiel et al., 2017), however global enzymatic profiling performed during this study did not reveal any significative effect of this practice.

Comparative compositional analyses of monosaccharides released from hydrolyzed cell wall polymer samples during retting showed very similar patterns for both fields as previously observed during flax or even hemp retting (Bleuze et al., 2018; Chabbert et al., 2020).

Taken together, these results would suggest that the process of retting is basically very similar between the two fields. Such a conclusion is logical given that the fiber quality and yield from both fields is comparable, but not identical. In the light of these observations, it is possible that the biochemical analyses classically utilized in this paper and by other workers to study retting are not sufficiently discriminatory and/or appropriate to detect the underlying parameters responsible for the observed differences. Indeed, the different enzymatic activities measured during retting in this work and previous studies correspond to the sum of the activities of the individual enzymes of a given type extracted from the samples. As an example, the "beta-glucosidase activity" shown in figure 3 and 4, is the sum of the activities of all of the different beta-glucosidase enzymes present in the sample extract. Such an approach therefore does not provide precise enough information about either the identity of the individual enzymes or the (micro) organisms producing such proteins during retting. In an attempt to improve our understanding of these points we previously reported the use of a meta-barcoding approach coupled with the use of the bioinformatic tool PICRUSt (Djemiel et al., 2017). This work identified a high number of new bacterial and fungal species associated with retting as well as predicting what bacterial cell wall degrading CAZymes *might* be present based upon the presence of certain species in the retting microbiome. However, as previously discussed (Djemiel et al., 2020), PICRUSt and similar approaches cannot confirm whether a protein is really present or not in the field.

Several recent studies have demonstrated the value of a metaproteomic approach in providing precise information on the different proteins responsible for enzymatic functions observed in a given habitat (Herbst et al., 2016), including those associated with the degradation of lignocellulosic materials (Hori et al., 2018; Chirania et al., 2022). We, therefore, decided to implement a metaproteomics approach to - i) identify specific cell wall degrading enzymes and associated microorganisms and, ii) evaluate whether such an approach could be powerful enough to detect any differences in the cell wall degrading arsenal of the two fields.

III.2.4.2. Metaproteomics identifies specific proteins present during retting

This approach identified 6032 non-redundant proteins (5702 proteins in field A and 5610 proteins in field B). Compared to other studies involving metaproteomics performed with the same technology, the number of proteins identified in this study is relatively high [(Callister et al., 2018): 4000, (Kipping et al., 2020): 1600, (Hori et al., 2018): 1964]. Nevertheless, other studies based on the analyses of a large number of samples, geographical locations and habitat types (soil, litter, rhizosphere...) have led to the identification of a much higher number of proteins [(Starke et al., 2021), 139127]. Depending upon the samples analysed in this latter study, it was reported that the percentage of CAZymes present varied between 0.2 and 1.4 %. These values are comparable to the 1.23 % (75 proteins) observed in our analyses. A much higher value (14%) was recently reported in a metaproteomic study linked to the decomposition of plant matter, but in this case, the degradation was performed in fermenters where all fractions (liquid, planktonic and solid) were analysed (Chirania et al., 2022). In our study we focused on the identification of proteins in the liquid extracts used for enzyme activity measurements. Although such an approach probably leads to the identification of a lower number of overall proteins, it offers the advantage of targeting those enzymes that are secreted and therefore most likely to be active in the stem tissues during retting.

Given that both bacteria and fungi are generally considered to be involved in retting, our results showing that - i) the great majority (85 %) of proteins identified in the metaproteome come from the bacterial kingdom and, ii) bacteria represent 80 % identified organisms are somewhat surprising. Nevertheless, this latter figure is similar to the results of Starke and colleagues (Starke et al., 2021), who used a metaproteomic approach to study plant litter degradation and showed that bacteria made up between 65 and 75 % of identified organisms. It is possible that such high values might be related to the overrepresentation of bacteria in the databases, which are based on the most studied organisms (Starke et al., 2019).

Despite such an apparent over-representation of bacterial proteins in the metaproteome, the strategy used in this paper is viable for a “functional” investigation of retting (i.e., identification of specific enzymes potentially involved in retting). This is clearly demonstrated by the fact that protein distribution between the different kingdoms becomes much more balanced when only CAZymes are considered with fungal, bacterial and *Streptophyta* proteins representing 41 %, 36 % and 21 % of the total protein content, respectively. When only cell-wall degrading CAZymes are considered (i.e., excluding starch-/glycogen-degrading enzymes) the percentage of fungal CAZymes increases to 61% versus 19.5% for bacteria. A similar preponderance of fungal CAZymes was also observed in a metaproteomic study of plant litter decomposition (Starke et al., 2021). In this case, fungal CAZymes

represented more than 75% of identified CAZymes. Although both situations involve the degradation of lignocellulosic biomass, the higher percentage value observed for fungal CAZymes in the latter case might be related to their different time-frames: a few months for plant litter and only a few weeks for retting. The shorter time involved for retting is unlikely to allow a complete colonization of the stalks by fungi, whose growth is slower than that of bacteria. (Hicks et al., 2019).

Examination of the polymers targeted by the different identified CAZymes indicated that most of the enzymes involved in the degradation of cellulose and hemicelluloses come from fungi. Only 2 proteins (a GH5 endoglucanase and a GH3 beta-glucosidase) are of bacterial origin and 2 enzymes (a GH17 endoglucanase and a GH35 galactosidase) are flax proteins. In contrast, the majority (10 out of 13) of enzymes involved in the degradation of pectins belong to bacteria or flax. These results are similar to those obtained by Starke and colleagues (Starke et al., 2021), who also observed that fungal CAZymes are more associated with the degradation of recalcitrant polymers such as hemicellulose and cellulose, whereas bacterial CAZymes are more associated with the degradation of more accessible polymers such as pectins.

Overall, the bacterial CAZymes identified in this work correspond to those previously predicted to be present based on the use of the bioinformatic tool PICRUSt (Djemiel et al., 2017). Nevertheless, our metaproteomics approach offers two main advantages over PICRUSt. Firstly, and most importantly, PICRUSt is based on the use of rRNA16s sequences and it therefore does not consider fungal CAZymes (Langille et al., 2013). As shown in our study and others (Starke et al., 2021), plant cell wall degrading enzymes are mainly derived from fungi, and therefore predictions based on 16s rRNA using PICRUSt-type tools can only provide a fragmented view of the CAZyme and its dynamics. Secondly, the predictive approach is based on the relative abundance of organisms as determined by OTU (Operational Taxonomic Units) counts. As such, it can only indicate whether organisms containing CAZyme genes in their genomes are present in the retting population. It does not provide any information about the level of expression of these genes, or indeed whether they are expressed. In contrast, the metaproteomics approach provides “real” information about both the presence of a given protein and its relative amount. It therefore becomes possible to establish much more realistic dynamic profiles of the different CAZymes during retting complementary to the analysis of enzymatic activity profiles.

III.2.4.3. Metaproteomics identifies plant enzymes potentially impacting cell wall structure

Of major interest is the fact that plant proteins, mostly from flax, represent 21 % total identified CAZymes. Such an observation raises the possibility that such (plant) enzymes might impact the structure of cell walls thereby contributing to the retting process and/or modifying fiber quality as previously suggested (Chabbert et al., 2020). Among the plant CAZymes identified, certain are related

to pectin metabolism, in particular pectin methylesterases (CE8) and pectin acetylesterases (CE13). These proteins are present at time point R0, still abundant at R2, and then decrease significantly at R4. Pectin-methylesterases (PMEs) catalyse the demethylesterification of homogalacturonan pectins (HGs) in the cell wall. Under block wise action of PMEs, the blocks of demethylesterified HGs can interact with Ca^{2+}, promoting the formation of the so-called "eggs-box" structure and thus stiffening the cell wall (Shin et al., 2021). However, uncoordinated PME action can result in partially demethylesterified HGs that can become a target for pectin-degrading enzymes, such as polygalacturonases, affecting the texture and stiffness of the cell wall and increasing pathogen/saprotroph susceptibility (Levesque-Tremblay et al., 2015). Another flax enzyme involved in pectin metabolism and present in the metaproteome is the Beta-galactosidase BGal1 (GH35). This enzyme is present at the beginning of retting (R0 and R2) and decreases in abundance during the middle and end of retting. A previous study showed that BGal1 β-galactosidase activity is necessary for the dynamic remodelling of polysaccharides that occurs during normal secondary wall development in flax fibers (Roach et al., 2011). The fact that this protein is present throughout retting raises the possibility that it may also play a role in modifying fiber structure post-harvest.

Our results also identified two other cell-wall related (non-CAZy) proteins that showed increasing abundance in field B during retting: cinnamyl alcohol dehydrogenase 7 (CAD7) and CAD8. These enzymes catalyse the last step in the formation of monolignols which are the monomers for lignin and lignans (Wang et al., 2013). Overexpression of *CAD* genes in flax has been associated with an increase in the presence of lignin precursor oligolignols, and lignans (Huis et al., 2012; Chantreau et al., 2014) known for their antimicrobial activities (Huis et al., 2012; Chantreau et al., 2014). Their expression is affected by both injury and stress and it is therefore not surprising to find these proteins in flax stems that have been uprooted, and subjected to the onslaught of pathogenic or saprophytic microorganisms. What is surprising, however, is the presence of these plant proteins at the end of the retting process. While care should be taken since protein presence does not necessarily mean enzyme activity (Campbell et al., 2016), the presence of these plant proteins during retting raises the question of whether retting can be considered as a “simple” degradation process, or whether it also involves plant cell wall remodelling that occurs after uprooting. Similarly, the presence of enzymes associated with the production of anti-microbial compounds (e.g., lignans) would suggest that plants have the ability to modify, post-harvest, the bacterial and fungal communities. In this context, metaproteomics is a powerful tool to gain a better understanding of these interactions, and it would be interesting to combine this approach with meta-metabolomic analyses (Wallenstein et al., 2010; Zhao et al., 2016).

III.2.4.4. Metaproteomics identifies new retting micro-organisms

Specific identification of individual proteins also allowed us to determine what microorganisms were present during flax dew-retting. Many of the CAZyme-producing bacteria identified in this study have already been identified in other studies, either based on a culture approach (Rosemberg, 1965; Sharma, 1986; Tamburini et al., 2003), or by metabarcoding (Liu et al., 2015; Djemiel et al., 2017; Chabbert et al., 2020). Nevertheless, our results also identified, for the first time, CAZyme-producing bacterial species that have been previously associated with field composting such as *Pectobacterium carotovorum* (Ryckeboer et al., 2003) and *Paenibacillus lautus* (Vaz-Moreira et al., 2010). For fungi, only five species out of the 15 identified were previously identified in other retting studies, including *Aspergillus niger* and *Aspergillus flavus* (Fila et al., 2001; Nykter et al., 2008; Ribeiro et al., 2015), *Fusarium oxysporum* (Henriksson et al., 1997; Koivula et al., 2004), *Bipolaris zeicola*, and *Botrytis cinerea* (Nykter et al., 2008; Djemiel et al., 2017; Chabbert et al., 2020).

The taxonomic study of retting has greatly benefited these last years from metagenomic approaches such as 16s/18s rRNA sequencing (Ribeiro et al., 2015), and even more from high throughput sequencing metabarcoding (Djemiel et al., 2017; Chabbert et al., 2020; Xu et al., 2022), although this latter is sometimes limited by the relative poorness of databases, especially for fungi (Starke et al., 2019). The identification of several new bacterial and fungal species in this study demonstrates that the metaproteomic approach, in addition to providing functional information, is also extremely powerful for generating novel taxonomic data.

III.2.4.5. Metaproteomics potentially identifies the reasons for inter-field variability

One of the aims of this work was to assess the ability of metaproteomics to provide biological explanations for the differences in fiber quality observed at the end of retting in two contiguous fields A and B. Our results had indicated that the two characteristics that mainly differentiate fibers are fineness (field A > field B) and strength (field A > field B). Fineness is a parameter that depends directly on the ability of the elementary fibers to be separated, both from each other and from the surrounding tissue (Bourmaud et al., 2010; Chabbert et al., 2020). Proper decohesion of fiber cells requires degradation of the pectins and hemicelluloses, followed by the cellulose present in the primary walls of cortical parenchyma. Comparison of enzyme activity dynamics showed that polygalacturonase, beta-glucosidase and xylosidase activities peaked earlier in field A compared to field B. This pattern could be correlated with the abundances of certain CAZYmes abundances identified in the metaproteome: GH26, GH35, GH55 and GH3 showing maximum abundance before R4. An identified GH2 mannosidase also showed a more significant increase in abundance in field A compared to field B. Taken together, these results could suggest that hemicellulose degradation occurs more slowly in field B compared to field A.

Although further investigation would be required it is plausible that the observed difference in fiber bundle fineness between the two fields might be related to differences in hemicellulose breakdown. Similarly, the general increase in the abundance of CAZymes involved in cellulose degradation (GH7, GH5, GH3) that occurs at the end of the decomposition process is more pronounced in field A than in field B. Such a difference would be expected to favour the degradation of primary cell walls in the stem cortex surrounding the fiber bundles, thereby accelerating fiber (bundle) release and dissociation and leading to increased fineness.

The observed differences in fiber bundle strength between the two fields may also be related to differences in fiber separation resulting from differential degradation of cell wall polymers. Better separated fibers would require less force to extract them from the remaining stem tissues during the subsequent mechanical extraction (scutching) thereby reducing physical damage that could negatively impact their strength (Andersons et al., 2011; Baley et al., 2020). Metaproteomics also revealed the presence of field-specific CAZymes targeting different cell wall polymers. Proteins targeting cellulose (GH94), hemicellulose (GH17, GH55), arabinogalactan proteins (GH54) and lignin (AAI) were found in field A but not field B. In contrast, other proteins targeting hemicellulose (GH10) and cutin (CE5) were only found in field B. It is plausible that such field-specific differences may also contribute to the observed inter-field variability in fiber quality (Jeannin et al., 2024).

Interestingly, further examination of the CAZyme-producing organisms in the two fields highlighted a number of "functional redundancies" (i.e., synthesis of the same CAZyme family protein by different organisms). For example, the polygalacturonase GH28 in field A was produced by *Aspergillus flavus* whereas in field B the GH28 CAZyme came from *Neosartorya fischeri*. These results would suggest that certain functions are universal during the retting process, but do not necessarily come from the same microbial consortium, even in very close fields under the same meteorology.

III.2.5. Conclusion and perspectives

In conclusion, this study has demonstrated that metaproteomics is a powerful tool for the identification of specific cell-wall degrading CAZymes underlying measured enzymatic activities during retting. This technique also allows the identification of organisms whose enzymatic functions are really involved in retting as compared to other approaches such as meta-barcoding that will identify any organisms present in the microbial population. The implementation of the metaproteomic approach as part of a multi-omic strategy including metatranscriptomics, meta-metabolomics and metabarcoding would lead to a much more complete understanding of the biology of retting as previously suggested (Djemiel et al., 2020). Such a strategy would also be useful for the study of retting in other fiber plant species (Aktar et al.,

2024; Bou Orm et al., 2023; Datta et al., 2020; Ribeiro et al., 2015; Xu et al., 2022), as demonstrated in a recent study of the degradation of plant matter in forest litter (Starke et al., 2021).

As well as identifying fungal and bacterial CAZymes, this work also highlighted the possible contribution of plant enzymes to the overall process of cell wall modifications and polymer degradation that occur during retting. The comparative investigation of retting CAZymes in two adjacent fields also allowed us to address the question of inter-field variability in fiber quality. Our results pinpointed a number of key differences that may be responsible for such variability. Although further investigation is obviously necessary this work provides a credible path towards understanding the underlying reasons of the observed differences in fiber quality that are currently limiting the wide-scale utilization of plant fibers in diverse applications.

Finally, the use of metaproteomics in this study made it possible to identify certain CAZymes that are more specific to certain stages of retting regardless of their organism of origin. Such CAZymes could be used as reliable markers for the development of enzymatic and/or antigenic tests embedded on "lab on a chip" type sensors thereby allowing flax farmers to apply agriculture 4.0. practices to flax growth and retting (Griesche and Baeumner, 2020; Fuller et al., 2022).

III.2.6. Supplementary material information

All supplementary material can be found with the Mukherjee et al., 2024, *Industrial Crops & Products* (https://doi.org/10.1016/j.indcrop.2024.119907).

Supplementary material 1 : Supp_data_1
metadata (climate, soil analyses), industrial fiber qualification, fiber yields, enzymatic activities and glycan composition analysis, data relative to **Fig III.2**, **III.3**, **III.4**, **III.5**, **III.6**, **III.7**.

Supplementary material 2 : Supp_data_2
raw metaproteomic data, metaproteomic primary analyses, differential abundance analysis, data relative to **Fig III.8**.

Supplementary material 3 : Supp_data_3
Gene Ontology (GO) annotations of metaproteomes, data relative to **Fig III.9**.

Supplementary material 4 : Supp_data_4
Taxonomic analyses of metaproteomes, data relative to **Fig III.10** and **Fig III.13**.

Supplementary material 5 : Supp_data_5
CAZy annotation of metaproteomes, data relative to **Fig III.11**, **Fig III.12**.

III.3. Enzyme dynamics study in hemp retting

III.3.1. Introduction

Hemp is emerging as a vital natural fiber crop, alongside flax, recognized for its potential in sustainable textile and biocomposite applications (van der Werf and Turunen, 2008; Fike, 2016; Barbhuiya and Bhusan Das, 2022). Both are subjected to dew retting, a crucial pre-process necessary for the bast fiber extraction (explained in Chapter I). While, traditionally, flax has been cultivated in Northern Europe, hemp offers flexibility across diverse climates, including Southern France. This adaptability raises questions about how different environments affect the retting process and the resulting fiber quality.

In this study, we focus on the enzymatic activities involved in hemp retting within Southern France's Mediterranean climate. By conducting both irrigated and non-irrigated field-retting experiments, we aim to simulate the conditions of Northern Europe and compare them with Southern France's warmer, drier environment. As collaborators on a larger project led by PhD student Eliane Bou Orm [from IMT Mines Alès, Polymers and Hybrid Composites Research Unit (PCH) and the Risk Sciences Laboratory (LSR)], our role centers on studying the enzymatic processes during retting, utilizing the same spectrophotometric and fluorometric techniques used to assess global enzyme dynamics in flax. The overarching goals of the main project are to gain a deeper understanding of the microbial processes involved in hemp retting, evaluate its feasibility across varying climates, identify factors that affect hemp fiber quality, and develop tools to optimize the retting process.

By studying enzymatic activities, we aim to understand the effects of climate on hemp dew retting and assess its adaptability (and fiber quality) under changing conditions in Southern France.

III.3.2. Materials and methods

Refer to Section **(§) II.2.4**, **II.6** of Chapter 2

III.3.3. Results

III.3.2.1. Enzyme dynamics of hemp dew retting are similar (watered and non-watered conditions) with flax dew retting.

The measured activities of selected seven groups of enzymes from four retting time points with irrigated (A) and non-irrigated (N-A) experimental sets do not show any statistically significant difference in overall dynamics. Interestingly, similar to what we have seen in flax dew retting, in hemp also, endo-polygalacturonase activity shows a high level in the first week of retting, at R1 before decreasing about 4 times at R4 (**Fig. III.14g**). A similar pattern is observed for phenol-oxidase and peroxidase activities

(**Fig. III.14a, III.14b**), although the decrease in peroxidase activity is more abrupt. The activities of xylosidase, glucosidase, cellobiohydrolase, and galactosidase are initially low but increase until R4 before decreasing at R6 (**Fig. III.14**).

III.3.4. Discussion

The measured activities of seven enzyme groups in both irrigated and non-irrigated experimental sets in Southern France showed no statistically significant differences. This result is rather surprising, as increased humidity and water typically enhance microbial metabolism and enzyme activity (Stanaszek-Tomal, 2020). In Northern France, climatic variations are known to influence the duration of dew retting each year, as shown by our lab's three-year flax dew-retting dataset {comparing retting time of 2014 (described in Djemiel et al., 2017), 2021 campaign (**Chapter III**), 2022 campaign (**Chapter V**)}. A plausible explanation for the lack of differences could be explained by the experimental procedure and particularly the method of water supplementation —insufficient irrigation may have been offset by rapid evaporation due to the high temperature at that period under a dry southern climate. Increasing the irrigation volume to better mimic Northern climate conditions might yield more distinct results. Alternatively, soil composition could be a factor. Soils with high clay or loam content and low sand, such as silty-clay soils, retain more water, leading to higher soil humidity (Réquilé et al., 2021) and promoting greater microbial growth. The soil on which the trial was carried out was rather porous (clayey gravelly soil, with low water holding capacity), which undoubtedly accelerated the drying out of the swaths following the retting (Bou Orm et al., 2024, 2023).

However, when comparing the global enzyme dynamics between hemp and flax, the patterns are quite similar, differing primarily in timing. For example, endopolygalacturonase in flax reached peak activity within one week, while in hemp, this peak occurred after two weeks. This temporal shift in enzyme dynamics could be attributed to the climatic differences between the cold, humid conditions of Northern France (retting 2021) and the dry climate of the south (retting 2021), which affect microbial growth and activity (Robador et al., 2016; Stanaszek-Tomal, 2020). Another possible explanation is the difference in the biochemical composition of flax and hemp stems, particularly the lignin content, which is known to influence the endospheric microbiome (Beckers et al., 2016).

The overall similarity in enzyme dynamics can likely be attributed to the comparable anatomical structures of flax and hemp. Notably, phenol oxidase exhibited a distinct profile in hemp, remaining active until the second week before declining by the fourth week. This activity correlates with the presence of lignin in hemp's outer tissues, unlike flax. These findings suggest that while hemp and flax

undergo dew retting in a similar manner, variations in fiber composition, particularly in lignin content, may account for subtle differences.

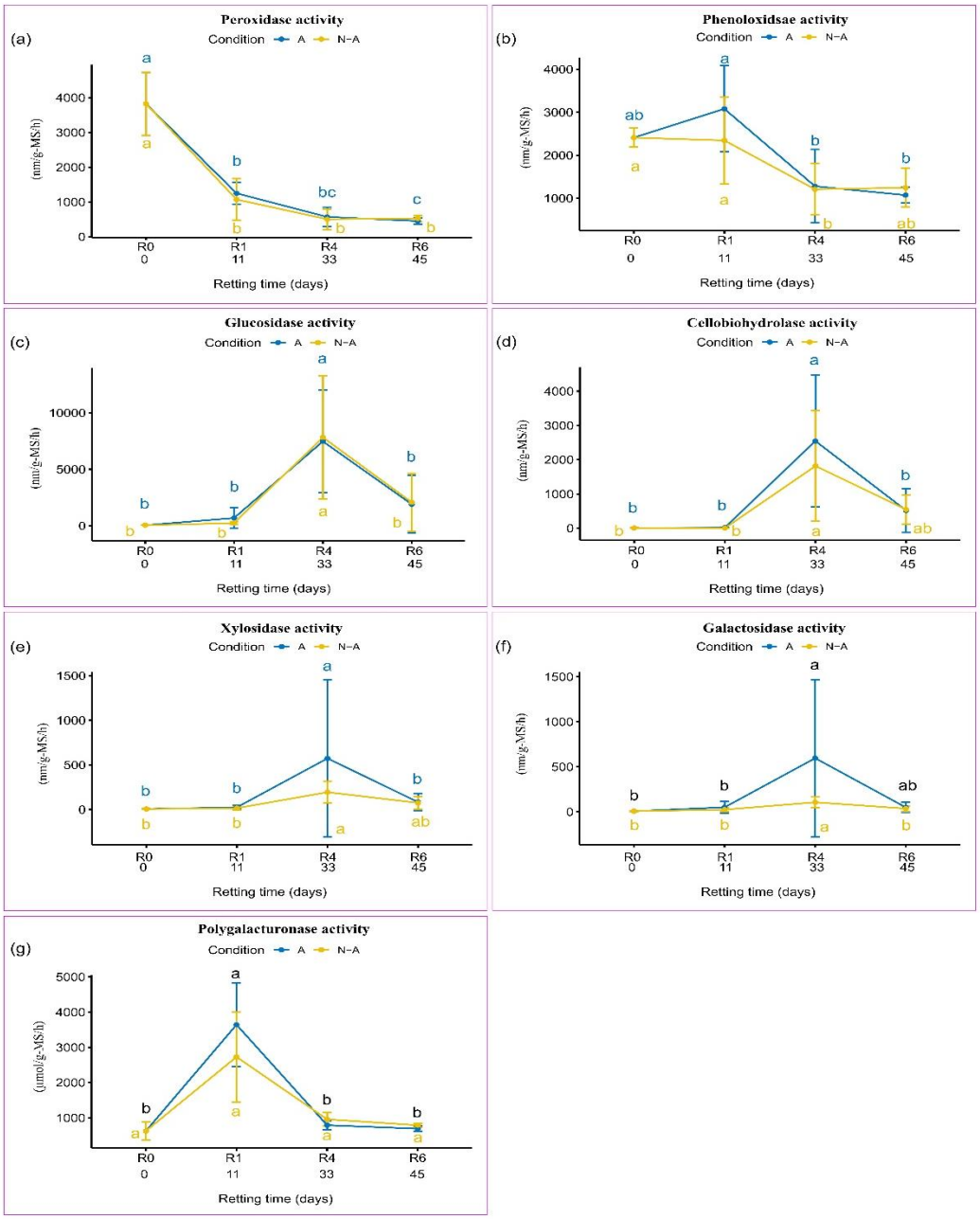

Fig. III.14. Enzyme activity dynamics in outer tissues of hemp stems during dew retting in watered (A) and non-watered (N-A) conditions.

(a) and (b) shows comparative (between A and N-A) Peroxidase Phenol-oxidase activities respectively; (c), (d), (e) and (f) respectively show Glucosidase, Cellobiohydrolase, Xylosidase and Galactosidase activities. (g) shows endo-polygalacturonase activity. All enzyme activities are expressed in $nmol.h^{-1}g^{-1}$ dry matter except polygalacturonase ($\mu mol.h^{-1}g^{-1}$ dry matter); n = 3, with n being the mean of 3 technical replicates, Anova (Tukey's HSD) test between retting points are shown with different letter marking p-Value < 0.05; point to point comparison between two conditions (A and N-A), tested with Pairwise T-Test (p.adjust: Fdr), p-Value < 0.05 are indicated with * if significant (data and tests results are shown in supp-data 1).

III.3.5. Conclusion

In conclusion, hemp dew retting, similar to flax, follows a two-phase enzyme dynamic: an initial increase in polygalacturonase activity leading to pectin degradation, followed by a subsequent rise in glucosidase, cellobiohydrolase, xylosidase, and galactosidase activities that address cellulose and xyloglucan. Although these findings provide a broad understanding of global enzyme trends, the specific dynamics of cell wall-degrading enzymes in hemp dew retting are not defined compared to flax (as we did under FlaxTronic project). Metagenomic studies on hemp dew retting conducted by Eliane Bou Orm (within the main project framework), have shed light on microbial aspects, but the link between microbial activities and enzyme functions remains unclear. This collaborative research highlights both the similarities and differences (information gap) in global enzyme behavior between hemp and flax, emphasizing the need for advanced meta-omics approaches (metaproteomics, meta-transcriptomics, and meta-metabolomics) to explore the relationships between biochemical (enzyme) and structural features (degradation of polysaccharide building block) of bast fiber plants during retting. Such advancements could significantly improve the optimization of retting processes across these species.

III.4. Conclusion of the chapter

This study focused on the dew retting of flax stocks from three fields (A, B, and C) of the Evasion, Terre de Lin cultivar, grown and retted under similar environmental conditions. Field C showed intermediate fiber quality, while Fields A and B exhibited the most contrasting results in both industrial evaluations (USTRL standards) and in-lab assessments (SFTT). Field A consistently produced superior fibers, distinguished by their homogeneity, fineness, and strength, whereas Field B's fibers lagged behind. Consequently, we chose to continue further comparative analysis of the retting process in Fields A and B to understand better the factors behind these differences in fiber yield and quality.

Through extensive biochemical analysis studies (including chemical changes monitoring, and global enzymatic activities) and metaproteomics, we explored the enzymatic activities and microbial communities involved in the degradation of plant cell walls during retting. Our findings identified 6032 non-redundant proteins across four key retting stages (R0, R2, R4, R7), of which 75 were associated with CAZymes—enzymes critical for breaking down cell wall polymers such as pectin, hemicellulose, cellulose, and lignin. The majority of these CAZymes (about 60%) originated from fungal species, although bacteria also played a significant role. While 88% of the proteins were common between the two fields, subtle differences in enzyme abundance and activity, particularly in key CAZyme families, may explain the superior quality of fibers from Field A.

This analysis highlighted the intricate relationship between microbial dynamics and retting efficiency. Small variations in enzyme activity, particularly those involved in cellulose and pectin degradation, had a notable impact on the final fiber quality, despite the proximity of the two fields.

In parallel to the flax study, we conducted an investigation into hemp dew retting as part of a broader research on bast fiber crops. The enzyme dynamics in hemp followed a similar two-phase process to that of flax: an initial increase in polygalacturonase activity led to pectin degradation, followed by the rise of enzymes targeting cellulose and hemicellulose. However, the detailed enzyme dynamics in hemp retting are less defined compared to flax, revealing significant gaps in our understanding. Collaborative metagenomic research on hemp has highlighted the need for advanced meta-omics techniques to better link microbial activities to enzyme functions, especially under varying climate conditions.

In conclusion, the use of metaproteomics and biochemical analyses in this study has deepened our understanding of the factors influencing fiber quality during flax dew retting. The identification of key enzymes and microorganisms responsible for retting not only informs future retting optimization but also highlights the potential of advanced meta-omics technologies in improving fiber processing across bast fiber species like flax and hemp.

Key Findings:

- Metaproteomics enhances our understanding of how retting impacts fiber quality and reveals distinct microbial activities.
- It generates valuable functional taxonomic data, identifying specific organisms and enzymes involved in the retting process.
- Specific CAZymes are linked to distinct stages of retting, regardless of their microbial origin.
- Plant enzymes also play a role in cell wall modification or degradation during retting.
- Hemp and flax follow similar enzyme patterns, but the timing of enzyme activity differs (may be due to climate, composition of polysaccharide building blocks of stem tissues, etc.).

III.5. Reference

Akin, D.E., Gamble, G.R., Morrison III, W.H., Rigsby, L.L., Dodd, R.B., 1996. Chemical and Structural Analysis of Fibre and Core Tissues from Flax. Journal of the Science of Food and Agriculture 72, 155–165. https://doi.org/10.1002/(SICI)1097-0010(199610)72:2<155::AID-JSFA636>3.0.CO;2-X

Akin, D.E., Rigsby, L.L., Henriksson, G., Eriksson, K.-E.L., 1998. Structural Effects on Flax Stems of Three Potential Retting Fungi. Textile Research Journal 68, 515–519. https://doi.org/10.1177/004051759806800708

Aktar, N., Mannan, E., Kabir, S.Md.T., Hasan, R., Hossain, M.S., Ahmed, R., Ahmed, B., Islam, Md.S., 2024. Comparative metagenomics and microbial dynamics of jute retting environment. Int Microbiol 27, 113–126. https://doi.org/10.1007/s10123-023-00377-7

Andersons, J., Poriķe, E., Spārniņš, E., 2011. Modeling strength scatter of elementary flax fibers: The effect of mechanical damage and geometrical characteristics. Composites Part A: Applied Science and Manufacturing 42, 543–549. https://doi.org/10.1016/j.compositesa.2011.01.013

Baley, C., Gomina, M., Breard, J., Bourmaud, A., Davies, P., 2020. Variability of mechanical properties of flax fibres for composite reinforcement. A review. Industrial Crops and Products 145, 111984. https://doi.org/10.1016/j.indcrop.2019.111984

Barbhuiya, S., Bhusan Das, B., 2022. A comprehensive review on the use of hemp in concrete. Construction and Building Materials 341, 127857. https://doi.org/10.1016/j.conbuildmat.2022.127857

Beysens, D., Mongruel, A., Acker, K., 2017. Urban dew and rain in Paris, France: Occurrence and physico-chemical characteristics. Atmospheric Research 189, 152–161. https://doi.org/10.1016/j.atmosres.2017.01.013

Bleuze, L., Lashermes, G., Alavoine, G., Recous, S., Chabbert, B., 2018. Tracking the dynamics of hemp dew retting under controlled environmental conditions. Industrial Crops and Products 123, 55–63. https://doi.org/10.1016/j.indcrop.2018.06.054

Bou Orm, E., Sauvagère, S., Rocher, J., Benezet, J.-C., Bayle, S., Siatka, C., Bergeret, A., Malhautier, L., 2023. Estimating the bias related to DNA recovery from hemp stems for retting microbial community investigation. Appl Microbiol Biotechnol 107, 4665–4681. https://doi.org/10.1007/s00253-023-12582-5

Bou Orm, E., Sutton-Charani, N., Bayle, S., Benezet, J.-C., Bergeret, A., Malhautier, L., 2024. Influence of field retting on physicochemical and biological properties of “Futura 75” hemp stems. Industrial Crops and Products 214, 118487. https://doi.org/10.1016/j.indcrop.2024.118487

Bourmaud, A., Beaugrand, J., Shah, D.U., Placet, V., Baley, C., 2018. Towards the design of high-performance plant fibre composites. Progress in Materials Science 97, 347–408. https://doi.org/10.1016/j.pmatsci.2018.05.005

Bourmaud, A., Morvan, C., Baley, C., 2010. Importance of fiber preparation to optimize the surface and mechanical properties of unitary flax fiber. Industrial Crops and Products 32, 662–667. https://doi.org/10.1016/j.indcrop.2010.08.002

Brown, A.E., 1984. *Epicoccum nigrum*, a primary saprophyte involved in the retting of flax. Transactions of the British Mycological Society 83, 29–35. https://doi.org/10.1016/S0007-1536(84)80242-9

Brown, A.E., Sharma, H. s. s., 1984. Production of polysaccharide-degrading enzymes by saprophytic fungi from glyphosate-treated flax and their involvement in retting. Annals of Applied Biology 105, 65–74. https://doi.org/10.1111/j.1744-7348.1984.tb02803.x

Callister, S.J., Fillmore, T.L., Nicora, C.D., Shaw, J.B., Purvine, S.O., Orton, D.J., White, R.A., Moore, R.J., Burnet, M.C., Nakayasu, E.S., Payne, S.H., Jansson, J.K., Paša-Tolić, L., 2018. Addressing the challenge of soil metaproteome complexity by improving metaproteome depth of coverage through two-dimensional liquid chromatography. Soil Biology and Biochemistry 125, 290–299. https://doi.org/10.1016/j.soilbio.2018.07.018

Campbell, E., Kaltenbach, M., Correy, G.J., Carr, P.D., Porebski, B.T., Livingstone, E.K., Afriat-Jurnou, L., Buckle, A.M., Weik, M., Hollfelder, F., Tokuriki, N., Jackson, C.J., 2016. The role of protein

dynamics in the evolution of new enzyme function. Nat Chem Biol 12, 944–950. https://doi.org/10.1038/nchembio.2175

Chabbert, B., Padovani, J., Djemiel, C., Ossemond, J., Lemaître, A., Yoshinaga, A., Hawkins, S., Grec, S., Beaugrand, J., Kurek, B., 2020. Multimodal assessment of flax dew retting and its functional impact on fibers and natural fiber composites. Industrial Crops and Products 148, 112255. https://doi.org/10.1016/j.indcrop.2020.112255

Chabi, M., Goulas, E., Galinousky, D., Blervacq, A.-S., Lucau, A., Neutelings, G., Grec, S., Day, A., Chabbert, B., Haag, K., Müssig, J., Arribat, S., Planchon, S., Renaut, J., Hawkins, S., 2023. Identification of new potential molecular actors related to fiber quality in flax through Omics. https://doi.org/10.3389/fpls.2023.1204016

Chand, N., Fahim, M., 2020. Tribology of Natural Fiber Polymer Composites. Woodhead Publishing.

Chantreau, M., Portelette, A., Dauwe, R., Kiyoto, S., Crônier, D., Morreel, K., Arribat, S., Neutelings, G., Chabi, M., Boerjan, W., Yoshinaga, A., Mesnard, F., Grec, S., Chabbert, B., Hawkins, S., 2014. Ectopic Lignification in the Flax lignified bast fiber1 Mutant Stem Is Associated with Tissue-Specific Modifications in Gene Expression and Cell Wall Composition. The Plant Cell 26, 4462–4482. https://doi.org/10.1105/tpc.114.130443

Chirania, P., Holwerda, E.K., Giannone, R.J., Liang, X., Poudel, S., Ellis, J.C., Bomble, Y.J., Hettich, R.L., Lynd, L.R., 2022. Metaproteomics reveals enzymatic strategies deployed by anaerobic microbiomes to maintain lignocellulose deconstruction at high solids. Nat Commun 13, 3870. https://doi.org/10.1038/s41467-022-31433-x

Datta, S., Saha, D., Chattopadhyay, L., Majumdar, B., 2020. Genome Comparison Identifies Different Bacillus Species in a Bast Fibre-Retting Bacterial Consortium and Provides Insights into Pectin Degrading Genes. Sci Rep 10, 8169. https://doi.org/10.1038/s41598-020-65228-1

Day, A., Ruel, K., Neutelings, G., Crônier, D., David, H., Hawkins, S., Chabbert, B., 2005. Lignification in the flax stem: evidence for an unusual lignin in bast fibers. Planta 222, 234–245. https://doi.org/10.1007/s00425-005-1537-1

Djemiel, C., Goulas, E., Badalato, N., Chabbert, B., Hawkins, S., Grec, S., 2020. Targeted Metagenomics of Retting in Flax: The Beginning of the Quest to Harness the Secret Powers of the Microbiota. Frontiers in Genetics 11.

Djemiel, C., Grec, S., Hawkins, S., 2017. Characterization of Bacterial and Fungal Community Dynamics by High-Throughput Sequencing (HTS) Metabarcoding during Flax Dew-Retting. Frontiers in Microbiology 8. https://doi.org/doi.org/10.3389/fmicb.2017.02052

Fike, J., 2016. Industrial Hemp: Renewed Opportunities for an Ancient Crop. Critical Reviews in Plant Sciences 35, 406–424. https://doi.org/10.1080/07352689.2016.1257842

Fila, G., Manici, L.M., Caputo, F., 2001. In vitro evaluation of dew-retting of flax by fungi from southern Europe. Annals of Applied Biology 138, 343–351. https://doi.org/10.1111/j.1744-7348.2001.tb00119.x

Fuller, C.W., Padayatti, P.S., Abderrahim, H., Adamiak, L., Alagar, N., Ananthapadmanabhan, N., Baek, J., Chinni, S., Choi, C., Delaney, K.J., Dubielzig, R., Frkanec, J., Garcia, C., Gardner, C., Gebhardt, D., Geiser, T., Gutierrez, Z., Hall, D.A., Hodges, A.P., Hou, G., Jain, S., Jones, T., Lobaton, R., Majzik, Z., Marte, A., Mohan, P., Mola, P., Mudondo, P., Mullinix, J., Nguyen, T., Ollinger, F., Orr, S., Ouyang, Y., Pan, P., Park, N., Porras, D., Prabhu, K., Reese, C., Ruel, T., Sauerbrey, T., Sawyer, J.R., Sinha, P., Tu, J., Venkatesh, A.G., VijayKumar, S., Zheng, L., Jin, S., Tour, J.M., Church, G.M., Mola, P.W., Merriman, B., 2022. Molecular electronics sensors on a scalable semiconductor chip: A platform for single-molecule measurement of binding kinetics and enzyme activity. Proceedings of the National Academy of Sciences 119, e2112812119. https://doi.org/10.1073/pnas.2112812119

Goodman, A.M., Ennos, A.R., Booth, I., 2002. A mechanical study of retting in glyphosate treated flax stems (*Linum usitatissimum*). Industrial Crops and Products 15, 169–177. https://doi.org/10.1016/S0926-6690(01)00108-X

Gorshkova, T., Chernova, T., Mokshina, N., Ageeva, M., Mikshina, P., 2018. Plant 'muscles': fibers with a tertiary cell wall. New Phytologist 218, 66–72. https://doi.org/10.1111/nph.14997

Griesche, C., Baeumner, A.J., 2020. Biosensors to support sustainable agriculture and food safety. TrAC Trends in Analytical Chemistry 128, 115906. https://doi.org/10.1016/j.trac.2020.115906

Henriksson, G., Akin, D.E., Rigsby, L.L., Patel, N., Eriksson, K.-E.L., 1997. Influence of Chelating Agents and Mechanical Pretreatment on Enzymatic Retting of Flax. Textile Research Journal 67, 829–836. https://doi.org/10.1177/004051759706701107

Henriksson, G., Akin, D.E., Slomczynski, D., Eriksson, K.-E.L., 1999. Production of highly efficient enzymes for flax retting by *Rhizomucor pusillus*. Journal of Biotechnology 68, 115–123. https://doi.org/10.1016/S0168-1656(98)00192-8

Herbst, F.-A., Lünsmann, V., Kjeldal, H., Jehmlich, N., Tholey, A., von Bergen, M., Nielsen, J.L., Hettich, R.L., Seifert, J., Nielsen, P.H., 2016. Enhancing metaproteomics—The value of models and defined environmental microbial systems. PROTEOMICS 16, 783–798. https://doi.org/10.1002/pmic.201500305

Hicks, L.C., Ang, R., Leizeaga, A., Rousk, J., 2019. Bacteria constrain the fungal growth response to drying-rewetting. Soil Biology and Biochemistry 134, 108–112. https://doi.org/10.1016/j.soilbio.2019.03.006

Hori, C., Gaskell, J., Cullen, D., Sabat, G., Stewart, P.E., Lail, K., Peng, Y., Barry, K., Grigoriev, I.V., Kohler, A., Fauchery, L., Martin, F., Zeiner, C.A., Bhatnagar, J.M., 2018. Multi-omic Analyses of Extensively Decayed Pinus contorta Reveal Expression of a Diverse Array of Lignocellulose-Degrading Enzymes. Applied and Environmental Microbiology 84, e01133-18. https://doi.org/10.1128/AEM.01133-18

Huis, R., Morreel, K., Fliniaux, O., Lucau-Danila, A., Fénart, S., Grec, S., Neutelings, G., Chabbert, B., Mesnard, F., Boerjan, W., Hawkins, S., 2012. Natural Hypolignification Is Associated with Extensive Oligolignol Accumulation in Flax Stems. Plant Physiology 158, 1893–1915. https://doi.org/10.1104/pp.111.192328

Kipping, L., Holzscheck, N., Maurer, F., Muszynski, S., Noll, M., Jehmlich, N., 2020. Microbial metaproteome data from decayed beech dead wood. Data in Brief 29, 105285. https://doi.org/10.1016/j.dib.2020.105285

Koivula, M., Kymäläinen, H.-R., Vanne, L., Levo, S., Pehkonen, A., Sjöberg, A.-M., 2004. Microbial quality of linseed and fibre hemp plants during growing and harvest seasons.

Langille, M.G.I., Zaneveld, J., Caporaso, J.G., McDonald, D., Knights, D., Reyes, J.A., Clemente, J.C., Burkepile, D.E., Vega Thurber, R.L., Knight, R., Beiko, R.G., Huttenhower, C., 2013. Predictive functional profiling of microbial communities using 16S rRNA marker gene sequences. Nat Biotechnol 31, 814–821. https://doi.org/10.1038/nbt.2676

Lion, C., Simon, C., Huss, B., Blervacq, A.-S., Tirot, L., Toybou, D., Spriet, C., Slomianny, C., Guerardel, Y., Hawkins, S., Biot, C., 2017. BLISS: A Bioorthogonal Dual-Labeling Strategy to Unravel Lignification Dynamics in Plants. Cell Chemical Biology 24, 326–338. https://doi.org/10.1016/j.chembiol.2017.02.009

Liu, D., Li, M., Xi, B., Zhao, Y., Wei, Z., Song, C., Zhu, C., 2015. Metaproteomics reveals major microbial players and their biodegradation functions in a large-scale aerobic composting plant. Microbial Biotechnology 8, 950–960. https://doi.org/10.1111/1751-7915.12290

Liu, M., Thygesen, A., Summerscales, J., Meyer, A.S., 2017. Targeted pre-treatment of hemp bast fibres for optimal performance in biocomposite materials: A review. Industrial Crops and Products 108, 660–683. https://doi.org/10.1016/j.indcrop.2017.07.027

Martin, N., Mouret, N., Davies, P., Baley, C., 2013. Influence of the degree of retting of flax fibers on the tensile properties of single fibers and short fiber/polypropylene composites. Industrial Crops and Products 49, 755–767. https://doi.org/10.1016/j.indcrop.2013.06.012

Meijer, W.J.M., Vertregt, N., Rutgers, B., van de Waart, M., 1995. The pectin content as a measure of the retting and rettability of flax. Industrial Crops and Products 4, 273–284. https://doi.org/10.1016/0926-6690(95)00041-0

Mohanty, A.K., Misra, M., Hinrichsen, G., 2000. Biofibres, biodegradable polymers and biocomposites: An overview. Macromolecular Materials and Engineering 276–277, 1–24. https://doi.org/10.1002/(SICI)1439-2054(20000301)276:1<1::AID-MAME1>3.0.CO;2-W

Morgillo, L., Brionne, L., Melelli, A., Ouagne, P., Scheel, M., Weitkamp, T., Shah, D.U., Abida, M., Beaugrand, J., Bourmaud, A., 2023. Elucidating links between the mechanical performance of flax fibres and their structural defects. Industrial Crops and Products 206, 117722. https://doi.org/10.1016/j.indcrop.2023.117722

Müssig, J., 2010. Industrial Applications of Natural Fibres: Structure, Properties and Technical Applications. John Wiley & Sons.

Mukherjee, S., Goulas, E., Creach, A., Krzewinski, F., Galinousky, D., Blervacq, A.S., D'Arras, P., Ratahiry, S., Menuge, A., Soulat, D., Saliou, J.M., Lacoste, A.S., Hawkins, S., and Grec, S., 2024. Metaproteomics identifies key cell wall degrading enzymes and proteins potentially related to inter-field variability in fiber quality during flax dew retting. Industrial Crops and Products. https://doi.org/10.1016/j.indcrop.2024.119907.

Nykter, M., Kymäläinen, H.-R., Thomsen, A.B., Lilholt, H., Koponen, H., Sjöberg, A.-M., Thygesen, A., 2008. Effects of thermal and enzymatic treatments and harvesting time on the microbial quality and chemical composition of fibre hemp (*Cannabis sativa* L.). Biomass and Bioenergy 32, 392–399. https://doi.org/10.1016/j.biombioe.2007.10.015

Paridah, M.T., Basher, A.B., SaifulAzry, S., Ahmed, Z., 2011. RETTING PROCESS OF SOME BAST PLANT FIBRES AND ITS EFFECT ON FIBRE QUALITY: A REVIEW. BioResources 6, 5260–5281.

Réquilé, S., Mazian, B., Grégoire, M., Musio, S., Gautreau, M., Nuez, L., Day, A., Thiébeau, P., Philippe, F., Chabbert, B., Chamussy, A., Shah, D.U., Beaugrand, J., Placet, V., Benezet, J.-C., le Duigou, A., Bar, M., Malhautier, L., De Luycker, E., Amaducci, S., Baley, C., Bergeret, A., Bourmaud, A., Ouagne, P., 2021. Exploring the dew retting feasibility of hemp in very contrasting European environments: Influence on the tensile mechanical properties of fibres and composites. Industrial Crops and Products 164, 113337. https://doi.org/10.1016/j.indcrop.2021.113337

Ribeiro, A., Pochart, P., Day, A., Mennuni, S., Bono, P., Baret, J.-L., Spadoni, J.-L., Mangin, I., 2015. Microbial diversity observed during hemp retting. Appl Microbiol Biotechnol 99, 4471–4484. https://doi.org/10.1007/s00253-014-6356-5

Roach, M.J., Mokshina, N.Y., Badhan, A., Snegireva, A.V., Hobson, N., Deyholos, M.K., Gorshkova, T.A., 2011. Development of Cellulosic Secondary Walls in Flax Fibers Requires β-Galactosidase. Plant Physiology 156, 1351–1363. https://doi.org/10.1104/pp.111.172676

Robador, A., Müller, A.L., Sawicka, J.E., Berry, D., Hubert, C.R.J., Loy, A., Jørgensen, B.B., Brüchert, V., 2016. Activity and community structures of sulfate-reducing microorganisms in polar, temperate and tropical marine sediments. ISME J 10, 796–809. https://doi.org/10.1038/ismej.2015.157

Rosemberg, J.A., 1965. Bacteria Responsible for the Retting of Brazilian Flax. Applied Microbiology 13, 991–992. https://doi.org/10.1128/am.13.6.991-992.1965

Ryckeboer, J., Mergaert, J., Vaes, K., Klammer, S., Clercq, D.D., Coosemans, J., Insam, H., Swings, J., 2003. A survey of bacteria and fungi occurring during composting and self-heating processes. Ann. Microbiol.

Salmon-minotte, J., Franck, R.R., 2005. 3 - Flax, in: Franck, R.E. (Ed.), Bast and Other Plant Fibres, Woodhead Publishing Series in Textiles. Woodhead Publishing, pp. 94–175. https://doi.org/10.1533/9781845690618.94

Sharma, H.S.S., 1986. The role of bacteria in retting of desiccated flax during damp weather. Appl Microbiol Biotechnol 24, 463–467. https://doi.org/10.1007/BF00250324

Sharma, S., 1992. SHARMA, H.S.S. and VAN SUMERE, C.F. (1992). The Biology and Processing of Flax. M. Publications, Belfast, 576 pp.

Shin, Y., Chane, A., Jung, M., Lee, Y., 2021. Recent Advances in Understanding the Roles of Pectin as an Active Participant in Plant Signaling Networks. Plants (Basel) 10, 1712. https://doi.org/10.3390/plants10081712

Stanaszek-Tomal, E., 2020. Environmental Factors Causing the Development of Microorganisms on the Surfaces of National Cultural Monuments Made of Mineral Building Materials—Review. Coatings 10, 1203. https://doi.org/10.3390/coatings10121203

Starke, R., Jehmlich, N., Bastida, F., 2019. Using proteins to study how microbes contribute to soil ecosystem services: The current state and future perspectives of soil metaproteomics. Journal of Proteomics, 10 Year Anniversary of Proteomics 198, 50–58. https://doi.org/10.1016/j.jprot.2018.11.011

Starke, R., Mondéjar, R.L., Human, Z.R., Navrátilová, D., Štursová, M., Větrovský, T., Olson, H.M., Orton, D.J., Callister, S.J., Lipton, M.S., Howe, A., McCue, L.A., Pennacchio, C., Grigoriev, I., Baldrian, P., 2021. Niche differentiation of bacteria and fungi in carbon and nitrogen cycling of different habitats in a temperate coniferous forest: A metaproteomic approach. Soil Biology and Biochemistry 155, 108170. https://doi.org/10.1016/j.soilbio.2021.108170

Summerscales, J., Dissanayake, N.P.J., Virk, A.S., Hall, W., 2010. A review of bast fibres and their composites. Part 1 – Fibres as reinforcements. Composites Part A: Applied Science and Manufacturing 41, 1329–1335. https://doi.org/10.1016/j.compositesa.2010.06.001

Tamburini, E., León, A.G., Perito, B., Mastromei, G., 2003. Characterization of bacterial pectinolytic strains involved in the water retting process. Environmental Microbiology 5, 730–736. https://doi.org/10.1046/j.1462-2920.2003.00462.x

Tláskal, V., Brabcová, V., Větrovský, T., Jomura, M., López-Mondéjar, R., Oliveira Monteiro, L.M., Saraiva, J.P., Human, Z.R., Cajthaml, T., Nunes da Rocha, U., Baldrian, P., 2021. Complementary Roles of Wood-Inhabiting Fungi and Bacteria Facilitate Deadwood Decomposition. mSystems 6, 10.1128/msystems.01078-20. https://doi.org/10.1128/msystems.01078-20

van der Werf, H.M.G., Turunen, L., 2008. The environmental impacts of the production of hemp and flax textile yarn. Industrial Crops and Products 27, 1–10. https://doi.org/10.1016/j.indcrop.2007.05.003

van Elsas, J.D., Semenov, A.V., Costa, R., Trevors, J.T., 2011. Survival of Escherichia coli in the environment: fundamental and public health aspects. The ISME Journal 5, 173–183. https://doi.org/10.1038/ismej.2010.80

Vaz-Moreira, I., Figueira, V., Lopes, A.R., Pukall, R., Spröer, C., Schumann, P., Nunes, O.C., Manaia, C.M., 2010. Paenibacillus residui sp. nov., isolated from urban waste compost. International Journal of Systematic and Evolutionary Microbiology 60, 2415–2419. https://doi.org/10.1099/ijs.0.014290-0

Voříšková, J., Baldrian, P., 2013. Fungal community on decomposing leaf litter undergoes rapid successional changes. The ISME Journal 7, 477–486. https://doi.org/10.1038/ismej.2012.116

Wallenstein, M.D., Hess, A.M., Lewis, M.R., Steltzer, H., Ayres, E., 2010. Decomposition of aspen leaf litter results in unique metabolomes when decomposed under different tree species. Soil Biology and Biochemistry 42, 484–490. https://doi.org/10.1016/j.soilbio.2009.12.001

Wang, Y., Chantreau, M., Sibout, R., Hawkins, S., 2013. Plant cell wall lignification and monolignol metabolism. Front. Plant Sci. 4. https://doi.org/10.3389/fpls.2013.00220

Xu, H., Zhang, L., Feng, X., Yang, Q., Zheng, K., Duan, S., Cheng, L., 2022. Metagenomic and proteomic analysis of bacterial retting community and proteome profile in the degumming process of kenaf bast. BMC Plant Biology 22, 516. https://doi.org/10.1186/s12870-022-03890-5

Zhao, D., Liu, P., Pan, C., Du, R., Ping, W., Ge, J., 2016. Bacterial succession and metabolite changes during flax (Linum usitatissimum L.) retting with Bacillus cereus HDYM-02. Sci Rep 6, 31812. https://doi.org/10.1038/srep31812

CHAPTER IV

Evaluation of flax dew retting progression and field dynamics (with FT-IR)

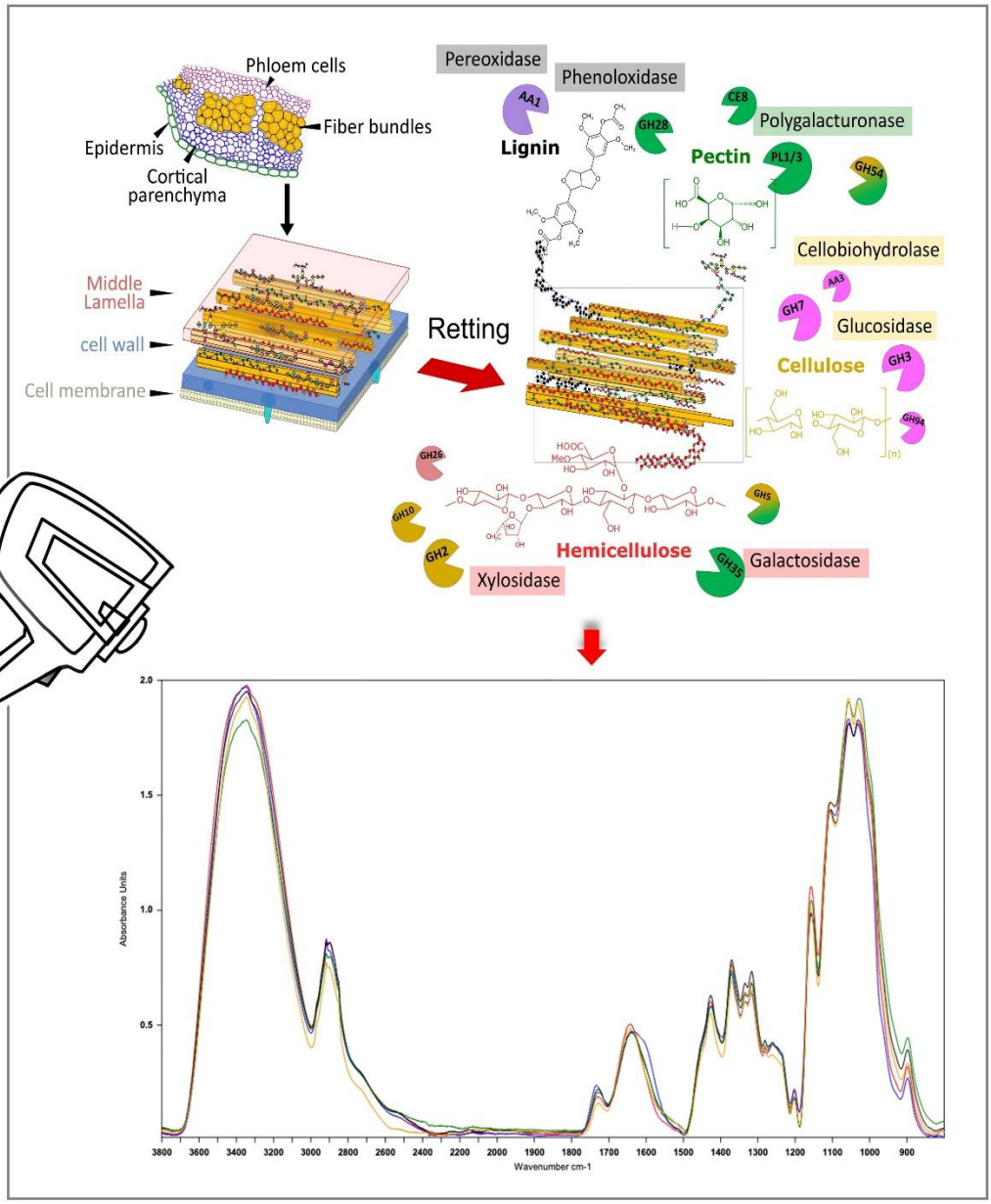

Chapter IV: Evaluation of flax dew retting progression and field dynamics

Contents

Chapter IV: Evaluation of flax dew retting progression and field dynamics 169
IV.1. Context and structure of the chapter 170
IV.2. Flax dew retting tracking: biomarkers of retting and fields dynamics 172
IV.2.1. Introduction 173
IV.2.2. Material and methods 175
IV.2.2.1. Plant Material 175
IV.2.2.2. Preparation of sample for FT-IR spectroscopy 175
IV.2.2.3. FT-IR spectroscopy 175
IV.2.2.4. Spectra treatments for average spectra illustrations 175
IV.2.2.5. Statistical analyses 175
IV.2.3. Retting dynamics in field A 176
IV.2.3.1. Scutched fibers notes 176
IV.2.3.2. Evolution of the global spectral signature during dew retting in field A 176
IV.2.3.3. Analysis of retting spectral profiles by zones: an ‘a priori’ approach in field A 179
IV.2.3.4. Characterization of a suitable workflow for multivariate analysis of field A: a ‘without a priori’ approach 182
IV.2.3.5. Multivariate analysis of field A dataset 183
IV.2.5.1.1. The question of pooling biological and technical repetitions 184
IV.2.5.1.2. Biological and Technical repetitions 185
IV.2.4. Retting dynamics in field B 192
IV.2.4.1. Evolution of the global spectral signature during dew retting in field B 192
IV.2.4.2. Analysis of retting spectral profiles by zones: an ‘a priori’ approach in field B 192
IV.2.4.3. Perspectives for field B 194
IV.2.5. Discussion 195
IV.2.5.1. Flax dew retting spectral profiling 195
IV.2.5.1.1. Methodology 195
IV.2.5.1.2. Specific chemical bonds and pic intensities identifications 196
IV.2.5.2. Enzymes involvement during dew retting 198
IV.2.5.3. Comparison between ‘a priori’ versus ‘without a priori’ approaches in field A 200
IV.3. Conclusions of the chapter 203
IV.4. Reference 204
ANNEXE A: Table FT-IR assignment band 208
ANNEXE B: Table FT-IR assignment band 210

IV.1. Context and structure of the chapter

Retting is a postharvest processing step aiming to release stem fibers from plants dedicated to produce natural fibers such as flax, hemp, kenaf or sisal. One critical element is to finally produce uniform and standardized material for industrial purposes, whereas retting is difficult to appreciate scientifically. As plants reach its optimum of growth, and after up-rooting, two methods are available: chemical one that is considered as the most uniform method but induced heavy cost of enzymes, and the natural one depending on environmental context (meteorology and rhizosphere microorganisms) (Akin et al., 2001; Himmelsbach et al., 2002).

During retting, cohort of enzymes spatially and temporally regulated are produced notably by microorganisms (Tian et al., 2016; Djemiel et al., 2017, 2020). This aims to progressively disorganize outer tissues, and to help releasing elementary fiber from bundles. To achieve this, enzymes will digest cohesive substances that binds fiber to the shive via cortex parenchyma cells.

Usually, farmers use empirical observations to state the end-point of retting: consideration of meteorological factors (rains, temperature variations), visual items via the color of dry stems, and manual mechanical properties (tension strength, elasticity). Beside those factors, scientific parameters could help to define retting process evolution, and to characterize the optimal end-point of retting. Among these parameters, color, enzyme origins (bacteria, fungi, plants) and enzyme activities but also, cell wall dis- and re-organization of outer tissues have been considered in this study that aims to identify reliable markers of retting progression.

The contents of this chapter can be found in the article, entitled "**Tracking flax dew retting by infrared vibrational spectroscopy combined with a powerful multivariate statistical analysis**", co-authored by Mukherjee Suvajit[1], Goulas Estelle[1], De Waele Isabelle[2], Hawkins Simon[1], Grec Sébastien[1], Blervacq Anne-Sophie*[1] ([1]. Univ. Lille, CNRS, UMR 8576 - UGSF - Unité de Glycobiologie Structurale et Fonctionnelle, F-59000 Lille, France, [2]. Univ. Lille, CNRS, UMR 8516 - LASIRE - Laboratoire de Spectroscopie pour les Interactions, la Réactivité et l'Environnement, F-5900 Lille, France, https://doi.org/10.1016/j.indcrop.2025.120798), where we focus on cell wall re- and dis-organization of outer tissues resulting from the putative enzyme activities highlighted previously by meta proteomic (see **Chapter-III**). In this **Chapter IV**, cell wall modifications occurring during the dew retting will be characterized by acquiring spectral profiles based on vibrational spectroscopy (FT-IR) for each retting point.

In a first part, spectra were obtained from stems reduced in coarse powder, at different retting time (R), in the two contrasted fields designed A and B (these fields were chosen as they produced contrasted scutched stems according to their mechanical properties as described in **Chapter III**).

In the second step, flax retting progression is investigated only in the field A. Early and later stages of dew retting are compared upon their vibrational profiles, in order to identify the significant chemical bonds that supported these retting steps. To achieve that, two approaches are developed. Firstly, an '*a priori*' approach identified some peaks in the average spectra. They were therefore considered one by one, evaluated during retting with one-way ANOVA. Their relative interactions or weights, compared to the others, are not considered in this approach. Secondly, an approach 'without *a priori*' was developed on the same datasets. In this more global context, the whole peaks are considered. And their significance level as well as their relative weights to explain variability are considered (PCA, (s)PLS-DA). The relevance of these 2 methods (with or without '*a priori*'), with their advantages and disadvantages, will be debated in the aim to help farmers to define the optimal end-point of retting.

In perspectives, these 2 methods and the first list of significant peaks identified for field A, will be confronted to those from field B, in order to detect potential differences in retting dynamics.

IV.2. Flax dew retting tracking: biomarkers of retting and fields dynamics

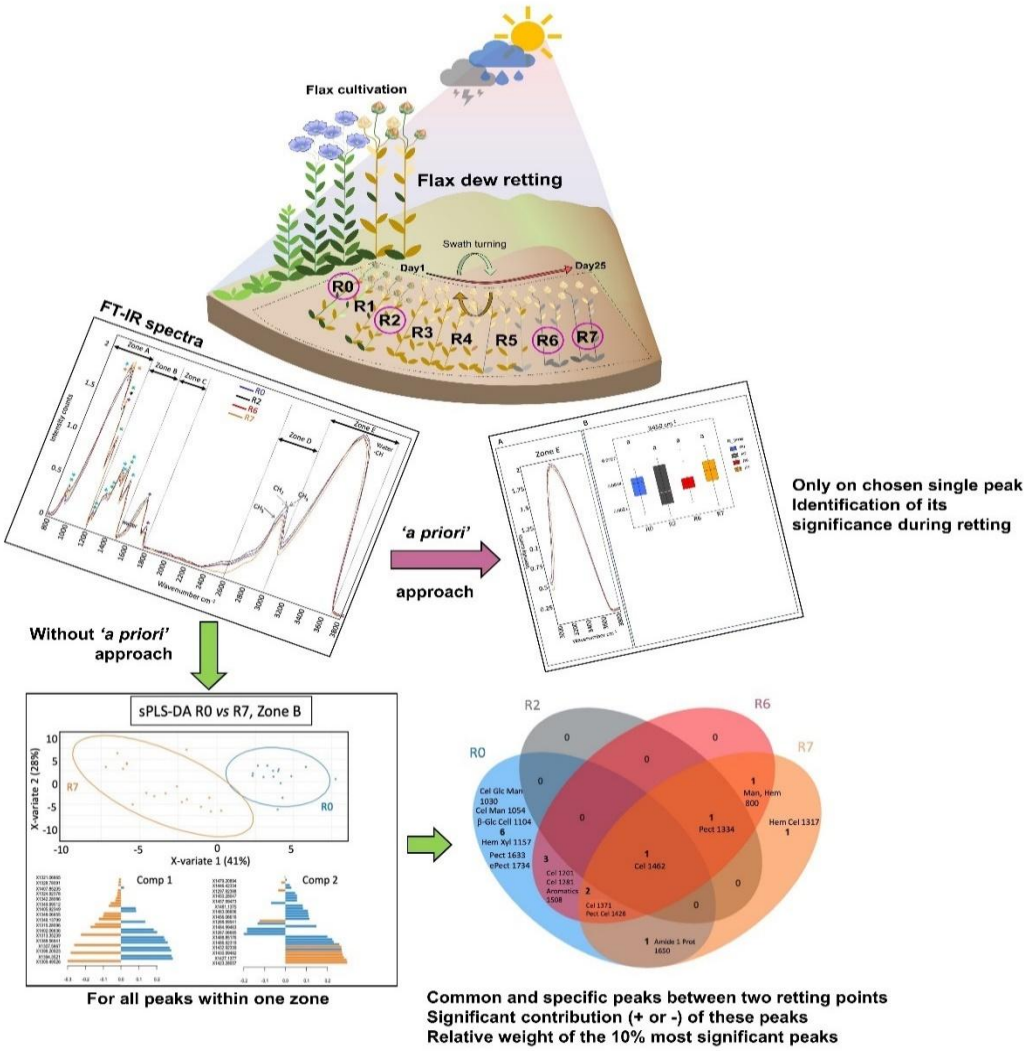

- Is vibrational spectroscopy a suitable tool to monitor flax retting?
- What is the evolution of FT-IR spectral signature during retting?
- What is the convenient statistical approach ('*a priori*' with chosen peak, or 'without *a priori*' considering the whole spectrum) to identify markers of the different stages during the retting?
- Is it possible to estimate the optimal endpoint of retting?

For this chapter, these persons collaborate (in alphabetical order):

Blervacq Anne-Sophie[1], De Waele Isabelle[2], Goulas Estelle[1], Grec Sébastien[1], Hawkins Simon[1]
[1]. Univ. Lille, CNRS, UMR 8576 - UGSF - Unité de Glycobiologie Structurale et Fonctionnelle, F-59000 Lille, France [2]. Univ. Lille, CNRS, UMR 8516 - LASIRE - Laboratoire de Spectroscopie pour les Interactions, la Réactivité et l'Environnement, F-5900 Lille, France

IV.2.1. Introduction

Retting is a crucial postharvest process that significantly facilitates the mechanical release of stem fibers in plants such as in flax (*Linum usitatissimum* L.). During retting, mature flax plants are uprooted (pulled) and spread out in the field for several weeks, where they become colonized by microorganisms (mainly bacteria and fungi). This microbiome is responsible for producing a battery of cell wall degrading enzymes that progressively digest the parenchyma cells surrounding the fibers, thereby facilitating their extraction during the subsequent mechanical step (Archibald et al., 1998; Djemiel et al., 2017, 2020).

The main challenge in the retting process is to ensure the production of uniform fiber batches. This is from an economical interest as biological factors involved may significantly influence the quality of the final linen, making the quality and physical properties of the end products unpredictable. This unpredictability arises partly because retting is a biological process and partly because the rhizosphere community of microorganisms could be different between fields. Furthermore, weather conditions, which are also unpredictable each year, can impact the retting process.

The retting process of fiber's plant such as flax or hemp, is a complex phenomenon, and its endpoint is difficult to appreciate with conventional methods such as stem color (Bleuze et al., 2018), Fried's test (visual scoring of the fiber-release degree after mechanical agitation in hot water treatment), texture, mechanical properties (Archibald et al., 1998). Flax retting monitoring is still based on a highly empirical approach that requires the expertise of the flax grower, and no tools are currently available to assess the status of stalks during retting, to enable this operation to be standardized. As the textile and materials industry requires more batches of fibers of standardized quality, it is crucial to avoid both under-retting and over-retting, as they can result in low-quality fibers. One way to overcome this challenge is to provide dedicated tools to perform precise monitoring of retting progression within the field.

For many decades, FT-IR (Fourier Transform Infra-Red) spectroscopy has been often used in industry, principally on flax scutched fibers. So, alkaline (hydroxide solution), enzymes, and steam-heat treatments (160-220°C, during 0.5-2h) could be used to treat such raw materials. This was a prerequisite treatment in order to increase wettability or to enhance the bonding strength between flax fiber and resins for composite material (Cao et al., 2012). In this context, FT-IR analyses led them to conclude a great cell wall modification of fibers notably with alkaline treatment that also increased the crystallinity index. Moreover, they also noticed an increase of wettability.

Before obtaining scutched fibers, a retting process should happen. Non-natural retting could be the result of many combined factors such as mechanical degradation, thermal and enzymatic treatments

etc. Such a spectroscopic approach has been applied for Indian flax and sisal (*Agave sisalana* L.) in order to validate different mechanical extraction methods in order to obtain more uniform fibers (Nayak et al., 2021). FT-IR profiling and mapping have been already performed in flax, where researchers monitored spectral changes through KBr or BaF2 pellets obtained from stem cross sections (Archibald et al., 1998; Himmelsbach et al., 2002). Such cross sections were exposed to different buffers (with or without chelator, with or without oxalic acid, with enzyme mixture), usually at high temperature (50°C) and for a short period (6h-37h). Another recent technical study describes an ATR-FTIR approach on flax and hemp (*Cannabis sativa* L.), through comparisons of various retting methods (degumming, water- or dew-retting) (Różańska et al., 2023). Higher level of straw extraction was obtained with osmotic degumming, whereas either water- or dew- retting did not show significant differences according to spectral profiles.

Compared to chemical retting, the natural retting process seems eco-friendly and less cost-effective. It is controlled both by abiotic factors (*e.g*., climate, soil properties) and by biotic ones (microorganisms' cohort from the soil and from the phyllosphere) (Djemiel et al., 2017, 2020; Chabbert et al., 2020). As previously mentioned, stem sections or KBr pellets were often used for analysis. Natural biodegradation of Indian flax whole stems was previously followed by FT-IR (Mohapatra and Malik, 2015). But they did not perform any statistics to prove that the difference in the maximum intensity of some peaks, as retting progressed, was significant between their sampling times. Moreover, no information is given according to the 'samples' used to acquire spectra (whole degrading and disorganizing stems, stem sections, whole stem reduced in coarse or fine powder, KBr pellets).

This study proposes to monitor the chemical transformation of the flax outer tissues. This study proposes to monitor the chemical transformation of the flax outer tissues for selected steps during the natural dew retting. The characterization of each retting step was performed by FT-IR onto peeled stem fragments reduced into coarse powder (inner tissues were discarded). The main originality of this study lies in the monitoring of the natural retting conducted in two adjacent fields (247.5 m far from each other) namely A and B that produce, after stem scutching, contrasted fiber. In a first attempt, we decided to validate the process of analysis on field A as the preliminary industrial grade of scutched fiber was higher than in field B. As field A scutched fibers exhibit the best note for the industry, we decided to start analysis with its datasets. In perspective, the validated workflow defined in field A will be tested in field B. The objective is to define a predictive model of retting.

By combining FT-IR spectroscopy, classic and multivariate statistical analysis, with or without *a priori* approaches, this study aims to identify some biomarkers (i.e. spectroscopic peaks) that are specific to different retting stages and that could be referred to determine the optimal end-point retting time.

Defining, and then using objective biological markers for retting, will enable us to rationalize and to better control the variability induced by retting without any doubts.

IV.2.2. Material and Methods

IV.2.2.1. Plant Material

Refer to Section **(§) II.2.1** of Chapter 2

IV.2.2.2. Preparation of sample for FT-IR spectroscopy

Refer to Section **(§) II.10.1** of Chapter 2

IV.2.2.3. FT-IR spectroscopy

Refer to Section **(§) II.10.2** of Chapter 2

IV.2.2.4. Spectra treatments for average spectra illustrations

Refer to Section **(§) II.10.3** of Chapter 2

IV.2.2.5. Statistical analyses

Refer to Section **(§) II.10.4** of Chapter 2

IV.2.2.5.2. Multiple pairwise comparisons by one-way-ANOVA analysis (‘*a priori*’ approach)

Refer to Section **(§) II.10.4.1** of Chapter 2

IV.2.2.5.3. Global statistical analyses (‘without *a priori’* approach)

Refer to Section **(§) II.10.4.2** of Chapter 2

IV.2.2.5.3.1. Unsupervised exploratory analysis by PCA

Refer to Section **(§) II.10.4.2.1** of Chapter 2

IV.2.2.5.3.2. Supervised exploratory analysis by PLS-DA and sPLS-DA

Refer to Section **(§) II.10.4.2.2** of Chapter 2

IV.2.3 Retting dynamics in field A

IV.2.3.1 Scutched fibers notes

One goal to achieve in this study, is to identify markers that reflect field retting dynamics. Indeed, fields could produce different qualities of scutched fibers. Our industrial partner *Van Robaeys Frères* ® measured some technical parameters and affected the global note 65332 for field A, and the global note 65322 for field B (according to USRTL- Union Syndicale des Rouisseurs – Teilleurs de lin Français- notation of scutched fibers, https://www.usrtl-ifl.fr/).

This note is constituted of 5 successive numbers corresponding to these items:

- Nature (flexibility, density, shine) from 1: declassified, to 7: superior (6: good)
- Color (due to retting) from 1: black, to 7: silver (5: half-blue)
- Strength (stretching) from 1: weak, to 4: very solid (3: quite solid)
- Fineness (diameter) from 1: rough to 4: very thin
- Resistance (homogeneity, cleanliness) from 1: marked defect, to 4: very homogenous (2: slight defects).

The note could therefore give an indication of the final quality of the fiber after scutching and multiple combing.

IV.2.3.2. Evolution of the global spectral signature during dew retting in field A

Many questions were addressed in order to build a workflow that could explain what happened in the cell walls from outer stem tissue from flax, during dew retting.

As previously evoked, the main objectives of this study were to determine the chemical composition of the plant cell wall of flax tissues during the retting, what is the dynamic of these changes, and finally is FT-IR able to provide markers that could be used to identify the end of the retting. To meet these objectives, **three main steps in the retting process** are considered:

- Which peaks explain variability observed between R0 *vs* R7, *i.e.*, from the initial retting point R0 to the final one R7
- Which peaks explain variability observed between R0 *vs* R2, *i.e.*, the early period just after up-rooting flax stems
- Which peaks explain variability observed between R6 *vs* R7, *i.e.*, the peaks that could characterize the optimum endpoint. If no significant modifications are observed between these two retting points, over-retting could be soon reached. If significant modifications are noticed, retting is still under processing.

To answer these questions, we have to evaluate the experimental variability significance:

- Is the **biological effect** due to repetitions (the places T1, T2, T3 in the field in which samples were collected) significant?
- Does **technical variability significant**, due to repetitions (rep_1 to rep_n, that corresponds to each powder grain on which a single spectrum was acquired)
- Is there a **kinetic effect** (from R0 to R7)?

In the first attempt, whole average spectra were compared for the 4 selected retting points (R0, R2, R6, R7) for **field A** (**Fig. IV.1**).

Five main zones are observed in the spectral signature of each field:

- Zone A: 1190-800 cm^{-1}
- Zone B: 1500-1191 cm^{-1}
- Zone C: 1785-1501 cm^{-1}
- Zone D: 3000-2600 cm^{-1}
- Zone E: 3800-3000 cm^{-1}

Zone A localized close to the detection limit (below 900 cm^{-1}), a zone corresponding to 750-970 cm^{-1} could be assigned to (1,4) (1,6)-α-D-glucans, (1,3)-α- D-glucans and β-1,4 glycosidic bonds (Szymanska-Chargot and Zdunek, 2013; Różańska et al., 2023). (1,6) and (1,4)-β-D-glucans are more specific fungi cell walls (chitin) and storage (glycogen). In this zone, only the band at 898,6 cm^{-1} was considered since it was associated with amorphous cellulose that is present in all plant primary cell walls (epidermis, cortical parenchyma) as well as in flax bast fibers (Blervacq et al., 2022, 2023).

In Zone A above 900 cm^{-1}, several peaks were assigned to probable plant cell wall polymers: Cellulose (1104,7; 1031,8; 898,6 cm^{-1}), Hemicellulose (xylan, xyloglucan) (1157,1 cm^{-1}), and Pectin (1104,7 cm^{-1}). Other peaks such as Mannan (1054,9; 1031,8 cm^{-1}) and β-1,3 D Glucan (1104,7 cm^{-1}) are also detected.

Zone B covers many peaks corresponding to those from the plant cell wall. They are assigned to Cellulose (1426,7; 1371,2; 1317; 1260; 1201,5 cm^{-1}), Pectin (1426,7; 1334 cm^{-1}) and Hemicelluloses (1317; 1281; 1201,5 cm^{-1}).

Shift towards increasing wave numbers is observed in **Zone C**, and is detected as water is removed during retting. The maximum intensity of this peak is expected to be aligned at 1650 cm^{-1} which could be assigned to pectin, but also to the chemical bond [Amide C-N] in protein. Shoulder could also be slightly present around 1633,2 cm^{-1} (assigned to COO- carboxylate ion stretching in pectin).

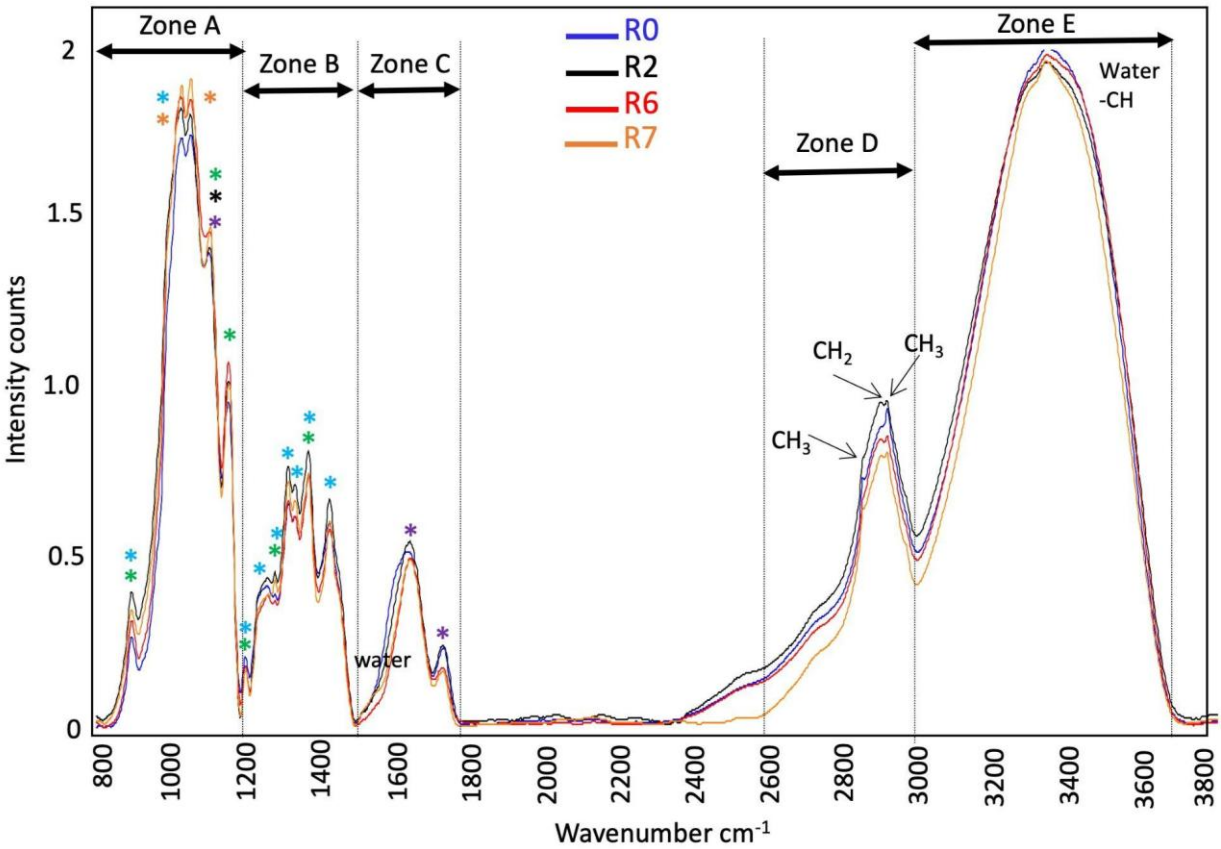

Figure IV.1 Average spectra of the different dew retting time according to the field A. Assignments were done according to the (***ANNEXE A Table Assignment***). Each peak corresponds to a chemical bond between two/three atoms present in polymers *Cellulose; *Hemicellulose-Xylan-Xyloglucan; * β-D Glucan; *Mannan; *Pectin. A minimum of 15 individual spectra (covering all T) was used to calculate the average spectra for each time of dew retting. Normalization was done according to the Min-Max process (OPUS NT software).

Zone C is assigned to pectin major peaks (1733,8; 1650-1633,2 cm^{-1}). The first well-determined peak (1733,8 cm^{-1}) reflects esterified uronic acid and modification of the carbonyl group in esters.

Great modifications were detected in **Zone D,** that corresponds to [CH_2-CH_3-CH_2-OH] chemical bonds (2917,9; 2899,1; 2851,5 cm^{-1}). It probably reflects the whole polysaccharides (*i.e*. carbohydrates) reorganization during retting.

Zone E (3326,7 cm^{-1}) mainly corresponds to water and C-H chemical bonds. Shifts observed between retting points were mainly due to dehydration.

In this field A (**Fig. IV.1**), intensities of major peaks deplete quickly. It means that the chemical context of these chemical bonds changed rapidly probably due to microorganisms' rapid enzymatic action.

IV.2.3.3. Analysis of retting spectral profiles by zones: an '*a priori*' approach in field A

In a first attempt, an '*a priori*' approach was applied in order to explore the major peaks assigned to plant cell wall polymers. With this approach, only one peak is investigated (without considering that other ones could also be significant, and without considering its relative loading weight or 'importance' compared to the other ones). This approach was already applied for animal cells infected by parasites (Vongsvivut et al., 2019), for plant cell wall investigations (Bhagia et al., 2022), and for pollen taxonomy (Kenđel and Zimmermann, 2020).

For that purpose, some peaks are chosen according to their height in our average spectra, according to the literature on cell wall degradation, or according to our own results on enzyme activities (**Chapter III**). The average maximum intensity (avg i_{max} values in $cm^{-1,}$ n = 10 to 15 individual spectra for each retting point) was considered. It corresponds to the maximum height of this chosen peak for the R retting point considered. Its values were statistically tested with a one-way ANOVA (Tuckey's HSD). To assess the dynamic of each peak as significance changes during the retting, point-to-point comparisons were conducted and presented in the following Figures (**Fig. IV.2** to **Fig. IV.6**).

In the zone D (**Fig. IV.5**), corresponding to [CH_2 - CH_3 - CH_2OH] showed no significant difference whatever the peak or the kinetic. The zone C (**Fig. IV.4**), corresponds to esterified pectins (Results can be gathered in **Table IV.1**).

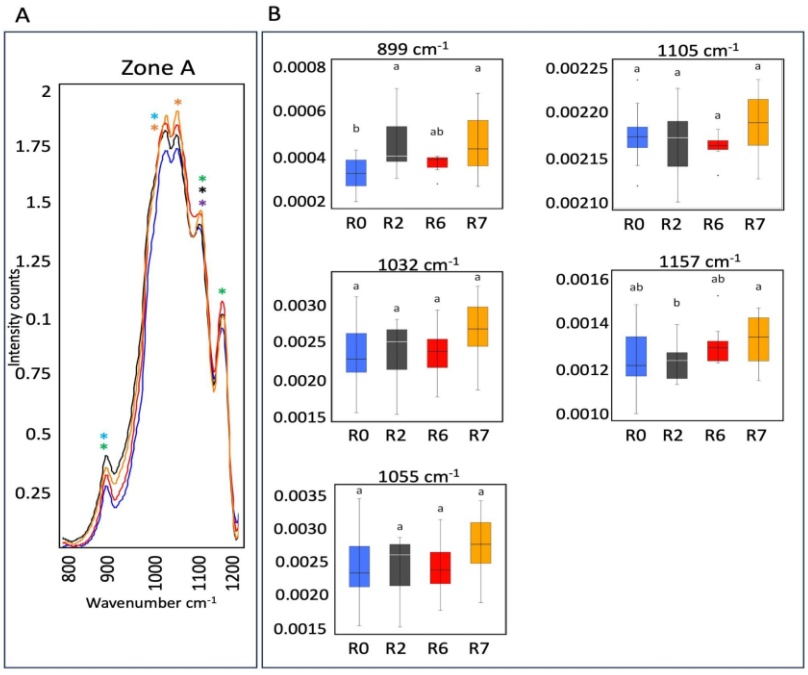

Figure IV.2 Comparative analysis of Zone A in field A. **A**: spectral profile extract (for assignment, see Text). **B**: Box-plots correspond to kinetic retting points (R0, R2, R6, R7). The box-and-whiskers plots represent values of n_{RO}= 15, n_{R2}= 15, n_{R6}= 10, n_{R7}= 17 individual spectra respectively covering all T. Within one time point R, all i_{max} of the technical repetitions were chosen for each of these peaks. Statistical significance with Anova (Tukey's HSD) test between retting points are shown with letter marking where p-Value < 0.05. *Cellulose; *Hemicellulose-Xylan-Xyloglucan; * β-D Glucan; *Mannan; *Pectin.

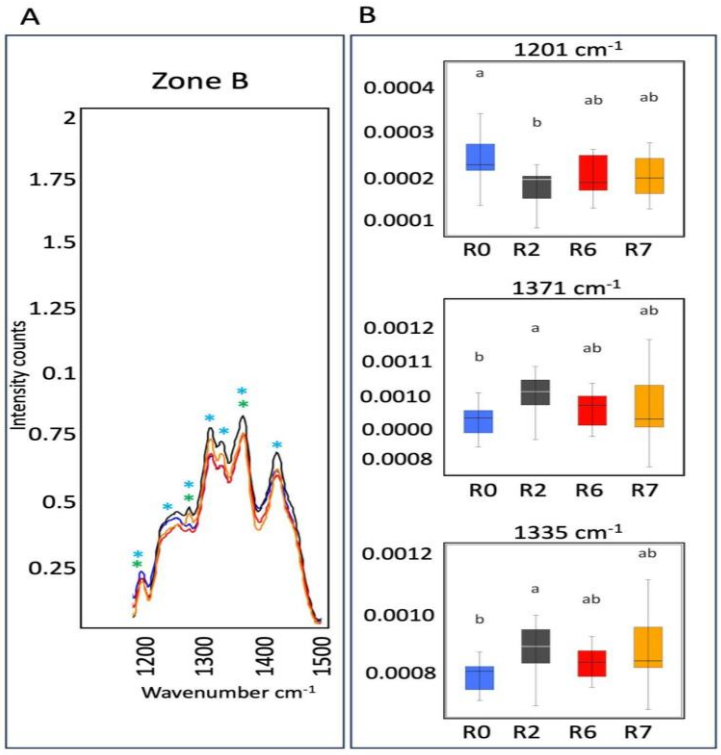

Figure IV.3 Comparative analysis of Zone B in field A. **A**: spectral profile extract (for assignment, see Text). **B**: Box-plots correspond to kinetic retting points (R0, R2, R6, R7). The box-and-whiskers plots represent values of n_{RO}= 15, n_{R2}= 15, n_{R6}= 10, n_{R7}= 17 individual spectra respectively covering all T. Within one time point R, all i_{max} of the technical repetitions were chosen for each of these peaks. Statistical significance with Anova (Tukey's HSD) test between retting points are shown with letter marking where p-Value < 0.05. *Cellulose; *Hemicellulose-Xylan-Xyloglucan

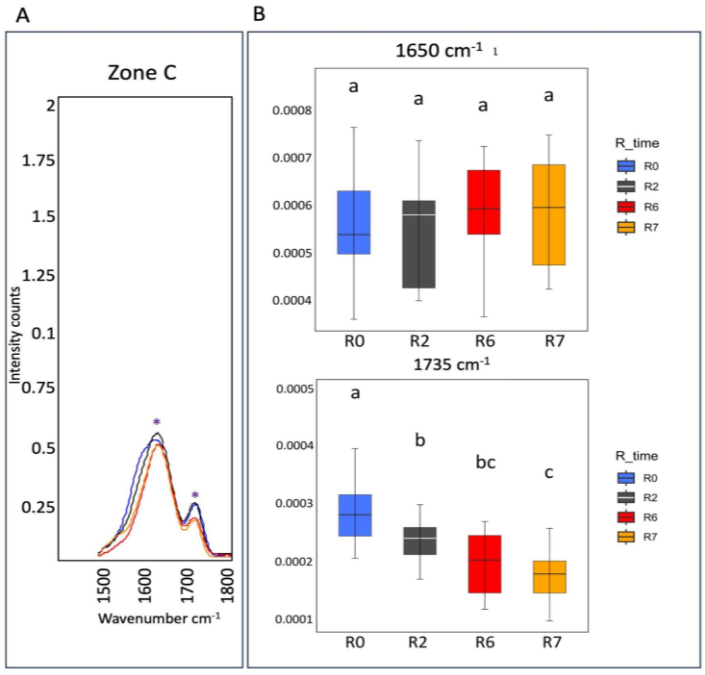

Figure IV.4 Comparative analysis of Zone C in field A. **A**: spectral profile extract (for assignment, see Text). **B**: Box-plots correspond to kinetic retting points (R0, R2, R6, R7). The box-and-whiskers plots represent values of n_{RO}= 15, n_{R2}= 15, n_{R6}= 10, n_{R7}= 17 individual spectra respectively covering all T. Within one time point R, all i_{max} of the technical repetitions were chosen for each of these peaks. Statistical significance with Anova (Tukey's HSD) test between retting points are shown with letter marking where p-Value < 0.05. *Pectin

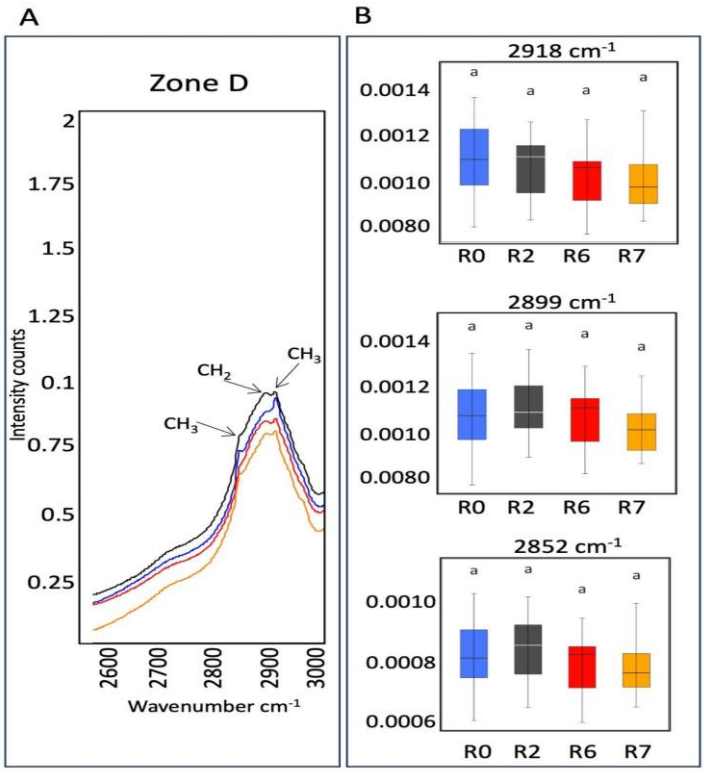

Figure IV.5 Comparative analysis of Zone D in field A. **A**: spectral profile extract (for assignment, see Text). **B**: Box-plots correspond to kinetic retting points (R0, R2, R6, R7). The box-and-whiskers plots represent values of n_{RO}= 15, n_{R2}= 15, n_{R6}= 10, n_{R7}= 17 individual spectra respectively covering all T. Within one time point R, all i_{max} of the technical repetitions were chosen for each of these peaks. Statistical significance with Anova (Tukey's HSD) test between retting points are shown with letter marking where p-Value < 0.05.

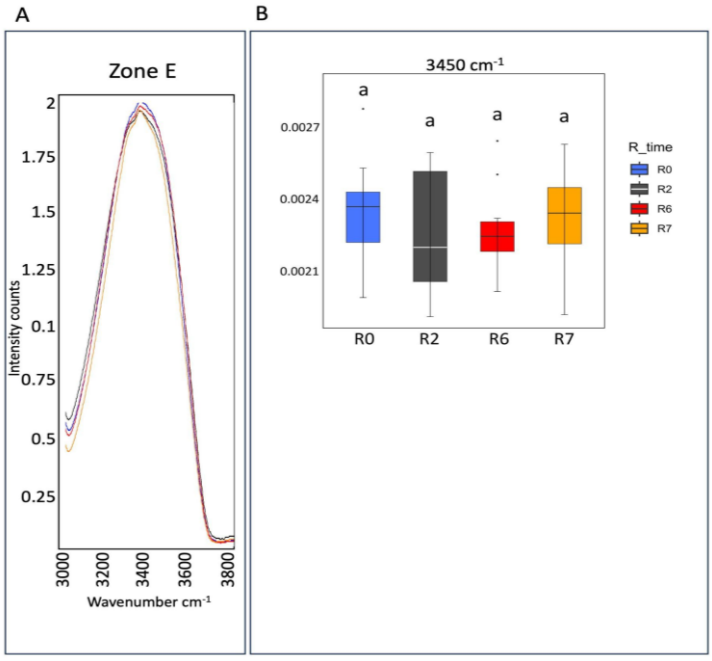

Figure IV.6 Comparative analysis of Zone E in Field A. **A**: spectral profile extract (for assignment, see Text). **B**: Box-plots correspond to kinetic retting points (R0, R2, R6, R7). The box-and-whiskers plots represent values of n_{RO}= 15, n_{R2}= 15, n_{R6}= 10, n_{R7}= 17 individual spectra respectively covering all T. Within one time point R, all i_{max} of the technical repetitions were chosen for each of these peaks. Statistical significance with Anova (Tukey's HSD) test between retting points are shown with letter marking where p-Value < 0.05.

With this '*a priori*' approach (*i.e.* chosen peaks, in each zone) some significant peaks are observed for Field **A**. The early step [R0 vs R2] is characterized by amorphous Cellulose (898,6 cm^{-1}), Xyloglucan and O-H or C-O-C cellulose bonds (1201,5 cm^{-1}), crystalline cellulose (1371,2 cm^{-1}) and pectin (notably esterified or alkyl-esterified, 1733,8 cm^{-1}). No specific peak is identified for the late step

Zone	Peak in cm^{-1}	Related Cell Wall polymer	Comment according to the retting process		
			R0 vs R2	R6 vs R7	R0 vs R7
Zone A	898,6	Cellulose	b,a	ab, a	b, a
	1031,8	Cellulose and AcGM	a,a	a,a	a,a
	1054,9	Cellulose Mannans	a,a	a,a	a,a
	1104,7	Cellulose, Pectin β-D-glucans	a,a	a,a	a,a
	1157,1	Hemicellulose XG	ab,b	ab,ab	ab,a
Zone B	1201,5	Cellulose, XG	a,b	ab,ab	a,ab
	1334,6	Pectin	b,a	ab,ab	b,ab
	1371,2	Crystalline cellulose	b,a	ab,ab	b,ab
Zone C	1650	Pectin, Proteins	a	a	a
	1733,8	Pectin (ester)	a,b	bc,c	a,c
Zone D	2852,3	CH_3	a	a	a
	2899,1	CH_2	a	a	a
	2917,9	CH_3	a	a	a
Zone E	3326,7 3452,5	OH from cellulose, water	a	a	a

Table IV.1 One-way ANOVA of i_{max} value from spectra during the three main steps of the retting process for field A.

The couple of letters (a, b, c) correspond to the significant groups with the one-way ANOVA (Tukey's HSD) based on the whole datasets [R0, R2, R6, R7] (see Fig.IV.2 to Fig.IV.6, and (***ANNEXE A Table Assignment***) for peak assignment). Significant differences between the groups are noticed in the grey boxes. Annotation: AcGM: actyl glucomannan; XG: xyloglucan.
[R6 vs R7], but ANOVA classes of significance often overlap between these two retting points. Overall process [R0 vs R7] led us to identify two major peaks Cellulose (898,6 cm^{-1}) and pectin (1733,8 cm^{-1}).

IV.2.3.4. Characterization of a suitable workflow for multivariate analysis of field A: a 'without *a priori*' approach

Within each field (field A), all individual spectra (rep_1 to rep_{15}) for each retting point, were again considered to proceed for further analyses but in this second approach, no previous expert curation is

performed. Spectra treatment was achieved in order to focus exactly on the same wavenumber window [3400-800 cm^{-1}] for each individual spectrum. Baseline treatment was firstly applied to each individual spectrum (OPUS-NT Software from Brucker). Datasets were normalized (using R software, with Totint method). Previous analysis of average spectra for each retting point, led us to identify five zones (A to E) that could be further separately analyzed (**§ IV.2.3.3.**):

- Zone A: 1190-800 cm^{-1}
- Zone B: 1500-1191 cm^{-1}
- Zone C: 1785-1501 cm^{-1}
- Zone D: 3000-2600 cm^{-1}
- Zone E: 3800-3000 cm^{-1}

Our purpose combining zone and the 'without *a priori* approach', was to try to limit the loading weight (importance) of peak contribution exhibiting very high intensity in the whole spectra, since global analysis of the whole spectra could generate a bias as peaks exhibiting high i_{max} could crush those that showed lower i_{max} (i.e reduce the signal to noise ratio). Previously defined splitted spectra were therefore considered for further 'without *a priori'* analysis. Such a choice to analyze by spectral desired region was previously proposed in flax enzymatic retting (Archibald et al., 1998), for fungal infestation of potato (Erukhimovitch et al., 2010) or for developing cotton fibers (Abidi et al., 2014). For each normalized, baseline corrected spectral sub-datasets from each zone, PCA analyses, PLS-DA (and sPLS-DA) were achieved by using R-package mixOmics.

As a consequence, the workflow for non '*a priori'* statistical analyses were defined as follows (**Fig. IV.7**). PCA were firstly calculated for each step of the retting process (extreme points R0 *vs* R7, early step R0 *vs* R2, and final step R6 *vs* R7). PCA scree plots were produced for each zone (Zone A: 1190-800 cm^{-1}; Zone B: 1500-1191 cm^{-1}; Zone C: 1785-1501 cm^{-1}; Zone D: 3000-2600 cm^{-1}; Zone E: 3800-3000 cm^{-1}). Then the number of PC components to be considered for further analysis was determined in order to reach at least 70 % of the total explained variability.

IV.2.3.5. Multivariate analysis of field A dataset

Partial least square-discriminant analysis (PLS-DA) was chosen to determine whether these FT-IR spectra of the combined [F, T, R] categories could be identified. Such a method could be chosen when a large number of variables constitute the dataset. It helps to describe variability and to obtain the significant peaks (later assigned to plant cell wall polymers), as their relative importance (ponderation), that explained this variability between the biological repetitions (T1-T2-T3), in the field A or retting times (R).

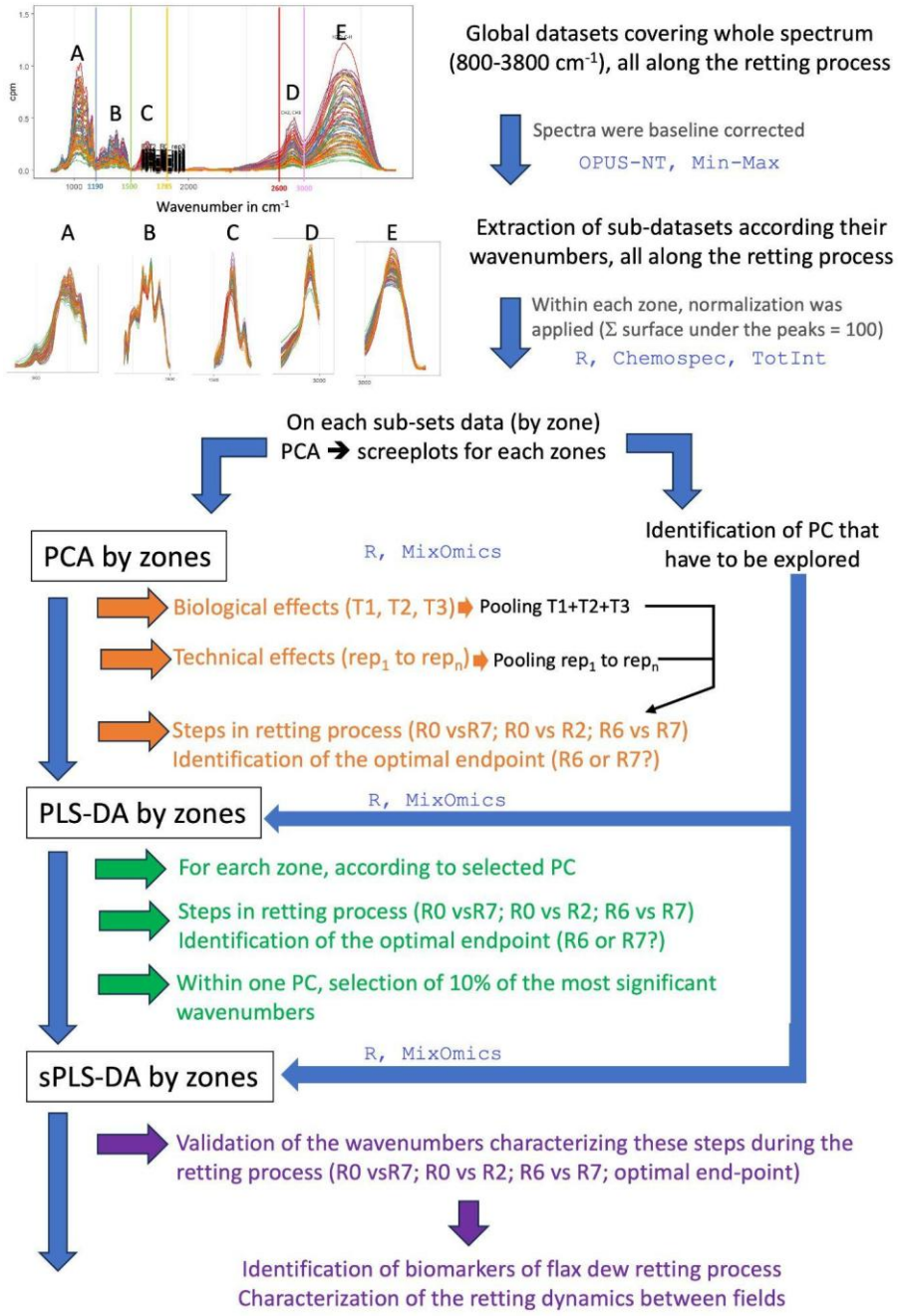

Figure IV.7 Definition of the workflow followed for the multivariate analysis of FT-IR datasets.

IV.2.3.5.1 The question of pooling biological and technical repetitions

The first question to address was to state about pooling either biological repetitions (T1, T2, T3) or technical repetitions (rep_1 to rep_n). PCA led us to notice no differences between technical repetitions whatever the biological repetitions considered. It is the reason why all technical repetitions and biological repetitions were pooled for one given retting point (R) to calculate average spectra. The

number of samples has therefore greatly decreased (from 371 to 57 considering the whole spectral dataset).

IV.2.3.5.2 Biological and Technical repetitions

***At first, the [R0 vs R7] comparison,* which corresponds to the comparison between the start versus end points of the dew retting process**, was illustrated by their respective average spectra (**Fig. IV.8A**). Only 32 conditions were used. A "condition" refers to a dataset combining spectra pooled across locations (T1+T2+T3) and repetitions (rep 1+ .... rep n). The fifth zones (A to E) were splitted then normalized as described previously. PCA was applied on these sub-datasets and three zones appeared clearly interesting: zone A, zone B and zone C since clear separation between groups were observed. Their scree plots gave a component PC1 (69 %, 48 %, and 53 % of explained variability respectively) and a component PC2 (26 % of explained variability for both zones B and C, and 14% for zone A). Both components PC1 and PC2 were considered for further regression analysis, as they explain respectively a total of 83 % (zone A), 74 % (zone B), and 79 % (zone C) of the variability. Then the PLS-DA method was applied on all wavenumbers present in each component confirmed that Principal Component 1 and 2 from these three zones A, B and C, are enough and convenient to discriminate the starting point (R0) from the endpoint (R7) of the dew retting, notably along the X1-component axis (negatively in zone B: 44 % X1-comp; positively in zones A and C: 68 % and 53 % for X1-comp). For zone A, it was X2-variate (15 %) that positively explained variability (**Fig. IV.8B**). A cut-off level was applied to the most 10 % significant wavenumbers from each X-component in the further sparse PLS-DA, in order to select the most predictive or discriminative features in our dataset to classify our retting samples. Most relevant original variables (those with the greatest absolute loading value) and therefore with a higher 'importance' can be seen at the bottom of the sPLS loading plots of each zone (**Fig. IV.8C**).

For zones A and C, peaks selected on the first component are mostly highly abundant in R0 peaks, whereas it is R7 peaks for zone B. In zone A and C, a positive contribution to the first component indicates association with R0 while a negative value is indicative of the R7 retting time. Again, it is the opposite for zone B. On the second component, peaks selected in zone A are all abundant in R0. For zones B and C, the situation is a mixture between R0 and R7, whatever the direction of the contribution. This led us to identify a limited number of the most significant wavenumbers that can be assigned to cell wall polymers (**Fig. IV.11**).

***Then the [R0 vs R2] comparison*, which corresponds to the early events during dew retting process**, was illustrated by their respective average spectra (**Fig. IV.9A**). Only 30 conditions were used. As before, the fifth zones (A to E) were splitted then normalized. PCA showed 2 clearly interesting

zones: zone B and zone C. Their scree plots gave a component PC1 (49 % and 45 % of explained variability respectively) and a component PC2 (22 % and 23 % of explained variability respectively).

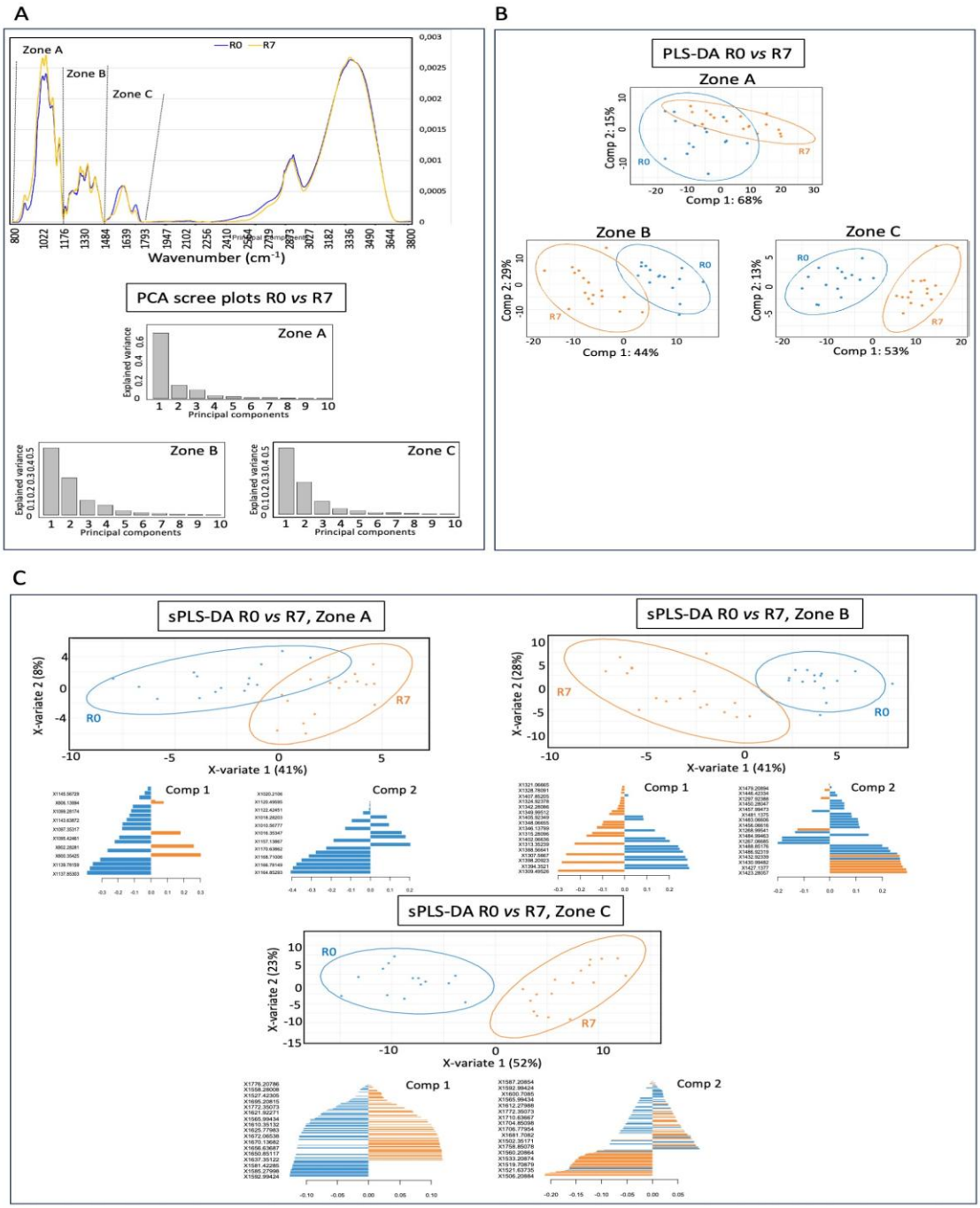

Figure IV.8 [Start vs End] points retting process (R0 vs R7) in field A.

A: comparison between R0 (in marine blue) and R7 (in orange) spectra, only three PCA scree plots were interesting (zone A, zone B, zone C). **B:** PLS-DA biplots for each of the three zones according to the components X1-X2 from these significant zones. **C:** sPLS-DA loadings focussed on the most 10% significant contributions (peaks) and their loading weight in the variability. Loading plots from the sPLS-DA applied to the retting dataset to discriminate retting time. Colors indicate the retting time in

which the median is maximum for each peak. The three biological repetitions (T1+T2+T3) were pooled, up to 7 technical repetitions (rep_1 to rep_7) were used, for two retting points (R0, R7)**.**

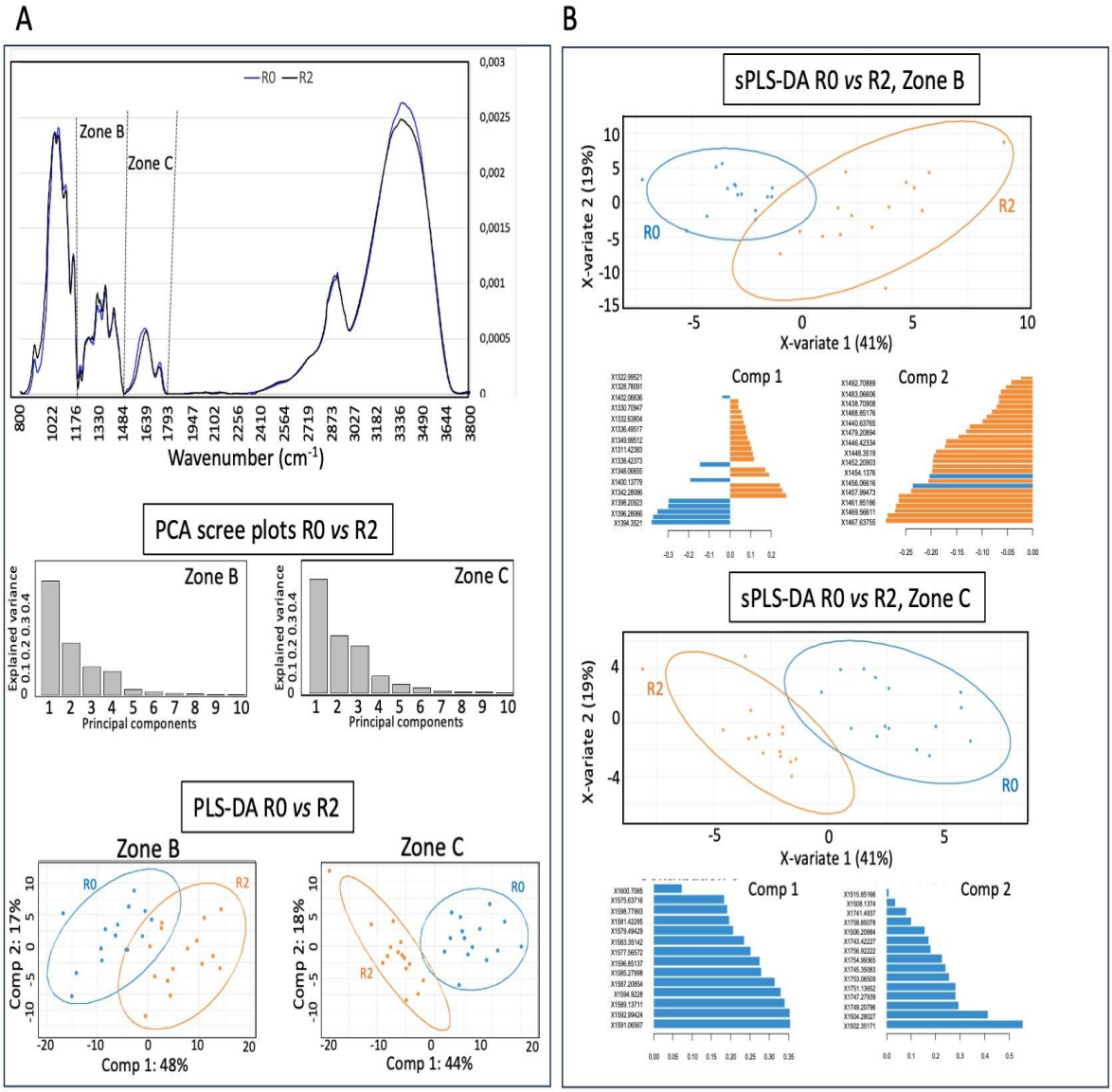

Figure IV.9 Early retting process (R0 vs R2) in field A.

A: comparison between R0 (in marine blue) and R2 (in black) spectra, only two PCA scree plots were interesting (zone B, zone C), and PLS-DA plots based on the components X1-X2 from these significant zones. **B:** sPLS-DA loadings focussed on the most 10% significant contributions (peaks) and their loading weight in the variability. Loading plots from the sPLS-DA, applied to the retting dataset to discriminate retting time. Colors indicate the retting time in which the median is maximum for each peak. The three biological repetitions (T1+T2+T3) were pooled, up to 7 technical repetitions (rep_1 to rep_7) were used, and two retting points (R0, R2).

Both components PC1 and PC2 were further chosen as they explain respectively a total of 71 % and 68 % of the variability. The further PLS-DA confirmed that the PC1 and PC2 from these two zones B and C, are convenient to discriminate what happened during the precocious steps of dew retting,

notably along the X1-component axis (positively in zone B: 48 % X1-comp; negatively in zone C: 44 % for X1-comp) (**Fig. IV.9B**). As before, a cut-off level was applied to the most 10 % significant wavenumbers from each X-component and sPLS-DA led us to identify significant wavenumbers that could be assigned to cell wall polymers (**Fig. IV.11**) as can be seen at the bottom of the sPLS loading plots of each zone (**Fig. IV.9B**). For zone B and C, wavenumbers selected on the first component are mostly highly abundant in or only composed of R0 peaks, respectively. In zone B, a positive contribution to the first component indicates association with R2 while a negative value is indicative of the R0 retting time. Only positive contributions could be observed for zone B. On the second component, wavenumbers selected in zone B are mostly abundant in R2 and with negative contributions, whereas only positive contributions with R0 could be observed. This led us to identify a limited number of the most significant wavenumbers that can be assigned to cell wall polymer.

At last, the late events during the dew retting process **were addressed.** ***[R6 vs R7]*** comparison was illustrated by their respective average spectra (**Fig. IV.10A**) in order to estimate the optimal endpoint of retting. Is the optimal retting already reached at R6 or R7? Indeed, if no significant modifications occurred between R6 and R7, it may indicate an optimal endpoint retting around R6. If there are still significant modifications, it may be explained that retting is still under processing until R7. Only 27 conditions were used. PCA on A to E zones previously splitted and normalized was applied on corresponding sub-datasets and two zones appeared clearly interesting: zone B and zone E. Their scree plots gave a component PC1 (41 % and 64 % of explained variability, respectively) and a component PC2 (31 % and 19 % of explained variability for both zones). Both components PC1 and PC2 were further chosen as they explain respectively a total of 72 % and 83 % of the variability. Further PLS-DA was applied and confirmed that these PC1 and PC2 components from these two zones B and E, are enough and accurate to discriminate what happened during the final steps of dew retting, along the X1-component axis (negatively in zone B: 30 % X1-comp; negatively in zone E: for both X1-comp-57 %, and X2-comp-19 %). sPLS-DA (**Fig. IV.10B**) applied with a 10% cut-off on significant wavenumbers from each X-component allowed to identify significant wavenumbers that were assigned to cell wall polymers (**Fig. IV.11**).

For zone E (**Fig. IV.10B**), peaks selected on both first and second components are mostly highly abundant in R7 peaks, with negative and positive values respectively. Regarding zone B, peaks selected on the first component are similarly abundant in both R6 and R7 peaks. A positive contribution to the first component indicates association with R6 while a negative value is indicative of the R7 retting time. Regarding the second component of zone B, the situation is a mixture between R6 and R7, whatever the direction of the contribution. Overall, these results highlighted a certain number of significant wavenumbers. However, it had to be considered that some of them could correspond to the same peak and as a consequence, to the same vibrated chemical bond related to cell wall polymer. Assignment of

peaks is therefore presented in Venn diagrams based on the conditions tested [R0 vs R7], [R0 vs R2], [R6 vs R7], and all retting points Fig. IV.11.

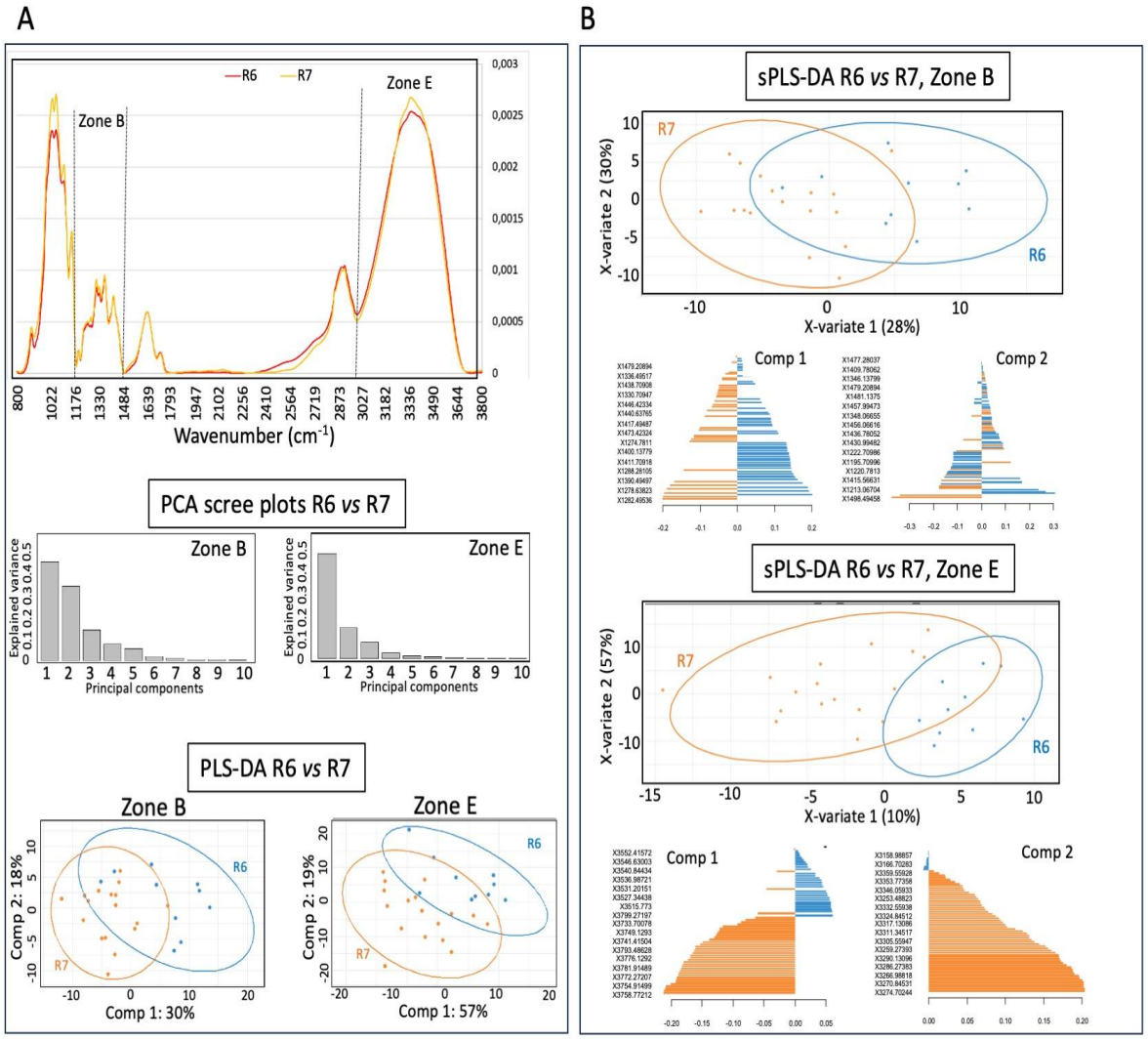

Figure IV.10 Late retting process (R6 vs R7) in Field A.

A: comparison between R6 (in red) and R7 (in orange) spectra, only two PCA scree plots were interesting (zone B, zone E), and PLS-DA plots based on the components X1-X2 from these significant zones. **B:** sPLS-DA loadings focussed on the most 10% significant contributions (peaks) and their loading weight in the variability. Loading plots from the sPLS-DA applied to the retting dataset to discriminate retting time. Colors indicate the retting time in which the median is maximum for each peak. The three biological repetitions (T1+T2+T3) were pooled, up to 7 technical repetitions (rep_1 to rep_7) were used, and two retting points (R6, R7).

These schematic representations easily discriminate specific peaks that characterize one retting time compared to the other one, and putative common peaks between both retting points, that could also be of interest. Indeed, they could have either opposite contributions (positive or negative), or inversely, similar ones. Based on the Venn diagrams, we can conclude that some peaks are common between the two successive retting points (Fig. IV.12A). In contrast, some others appear specific for one of the two successive retting points (Fig. IV.12B). Finally, R0 and R7 exhibited specific peaks that did not appear

during the process; except 1317 cm^{-1} (related to hemicellulose, and cellulose) that is present at R6 and still present at R7. This peak could announce the end of retting.

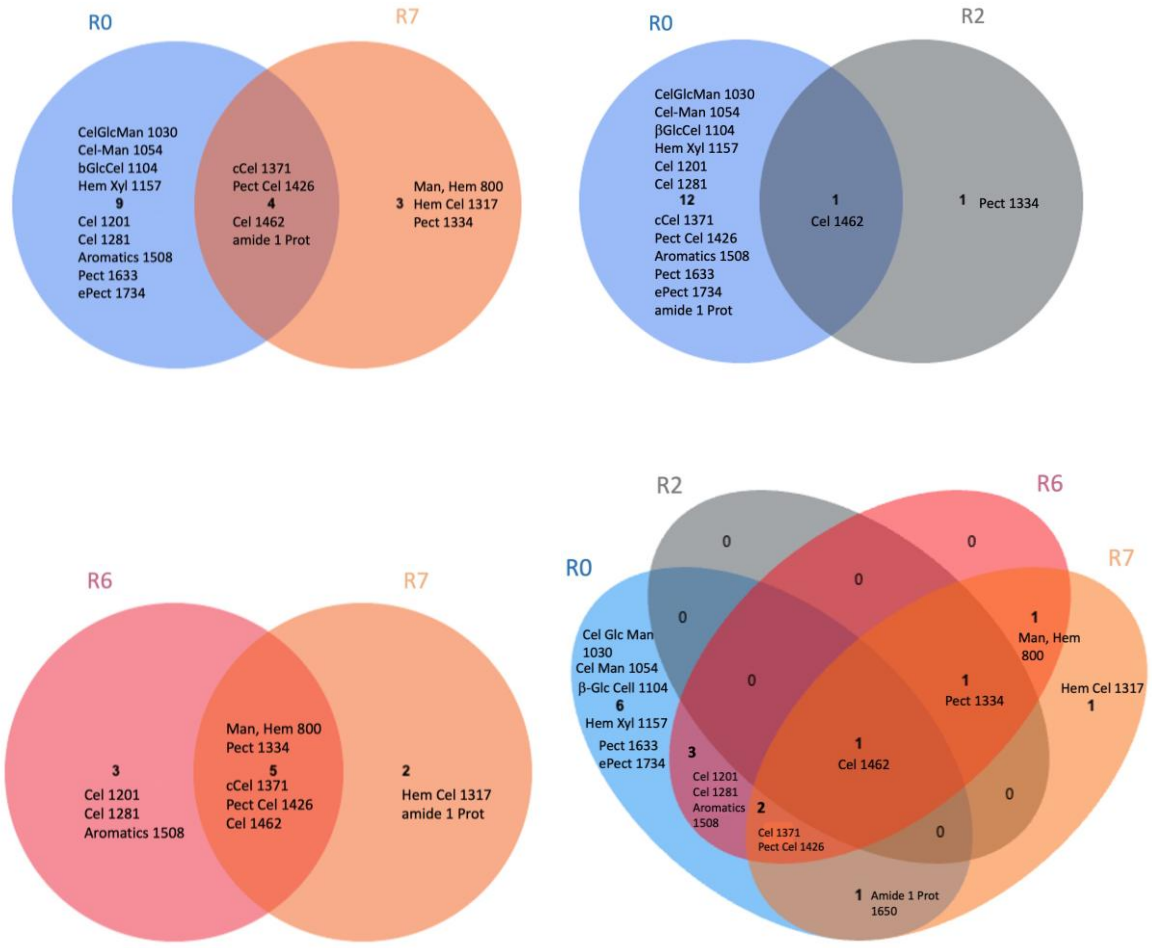

Figure IV.11 Venn Diagrams highlighting significant peaks in Field A.

[Start R0 vs End R7], early [R0 vs R2] and late [R6 vs R7] steps are illustrated. The last Venn diagram covers the whole process [R0, R2, R6, R7]. Lists of significant peaks are built from sPLS-DA PC1 and PC2 loadings (see **Fig. IV.10** to **IV.12**]. The type of contribution (positive or negative) is not considered here. Annotation: Amide 1 Prot: amide I Protein; Cel: Cellulose; cCel: crystalline Cellulose (β)Glc: (β) Glucan; Hem: Hemicellulose; Man: Mannans; NA: not assigned; Pect: Pectin; ePect: esterified Pectin; Xyl: Xylans

Flax dew retting can therefore be characterized depending on the comparisons considered:

- The [Start vs End] points process [R0 vs R7] which is globally characterized by specific R0 negative contribution of chemical bonds related to Acetyl-Glucomannan/Mannan (1031,8 cm^{-1}), Cellulose/Mannan (1054,9 cm^{-1}), β-Glucan (1104,7 cm^{-1}), Hemicellulose/Xylans (1157,1 cm^{-1}) and esterified Pectin (1733,8 cm^{-1}). In this comparison, the final step R7 is specifically characterized by Hemicellulose (1317 cm^{-1}) and Pectin (1334,6 cm^{-1}) with negative contributions and Mannose- Hemicellulose (800 cm^{-1}) with a positive one.

- Early step [R0 vs R2] that shows very few significant peaks. R2 is only specifically characterized by Pectin (1334,6 cm^{-1}) with a positive contribution. In contrast, the start step R0 exhibits numerous significant peaks.
- Late step [R6 vs R7] explains the retting progression toward the final step. Under retting (R6) is characterized by amorphous cellulose (1201,5 and 1281 cm^{-1}) respectively with negative and positive contributions. Aromatics peaks (1508 cm^{-1} shoulder) have also a negative contribution. Progression to the final step R7 is specifically characterized by Hemicellulose (1317 cm^{-1}) and Amide 1 Proteins (1650 cm^{-1}).

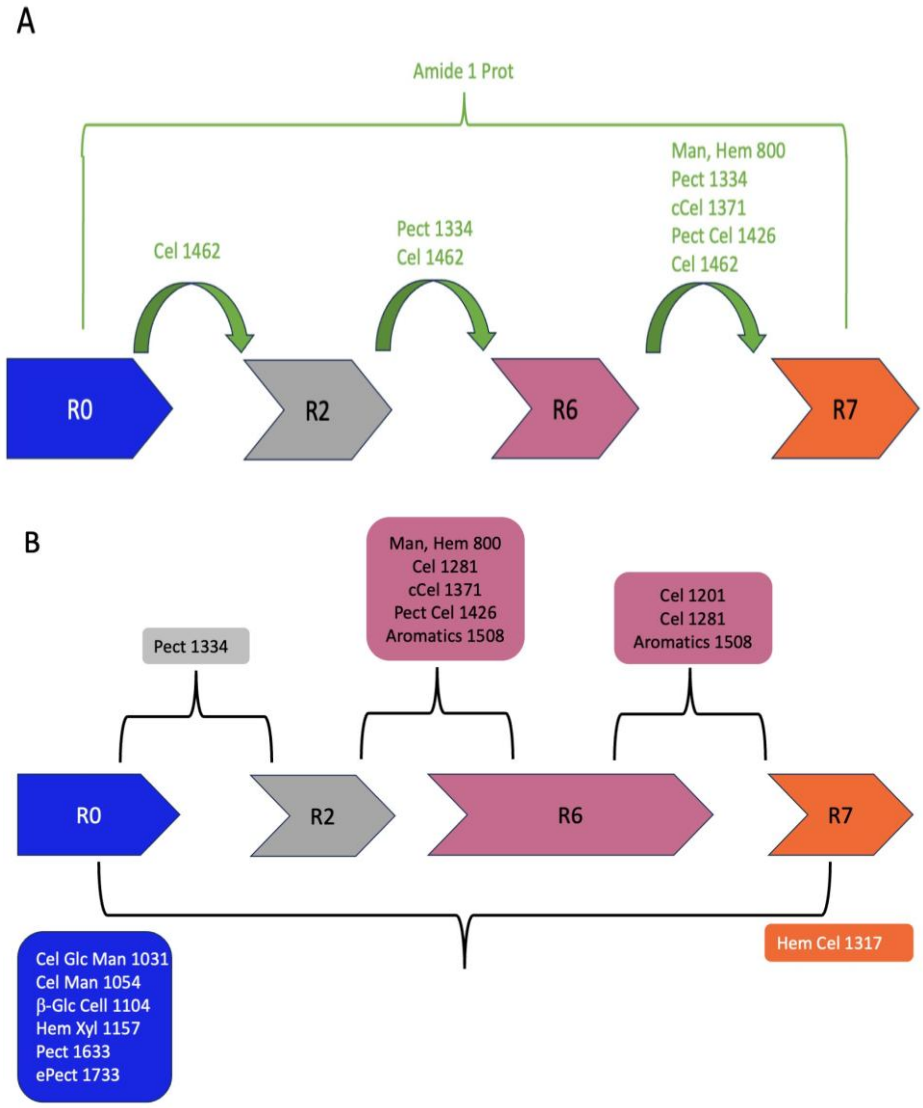

Figure IV.12: Timeline of retting with common and specific peaks characterizing steps.

A: common peaks (indicated in green) between pairwise retting times. **B**: specific peaks from one to the two successive retting points. The color of the box is related to the related retting point (R0: marine blue; R2: pale grey; R6: dark pink; R7: orange). Annotation: Amide 1 Prot: amide I Protein; Cel: Cellulose; cCel: crystalline Cellulose (β)Glc: (β) Glucan; Hem: Hemicellulose; Man: Mannans; Pect: Pectin; ePect: esterified Pectin; Xyl: Xylans.

IV. 2.4 Retting dynamics in field B

IV.2.4.1 Evolution of the global spectral signature during dew retting in field B

As the workflow described in Fig. IV.8 was validated on field A, we started to apply it on field **B** but only on sub-datasets as previously determined. Average spectra for each retting point (R0-R2-R6-R7) are presented in Fig. IV.13.

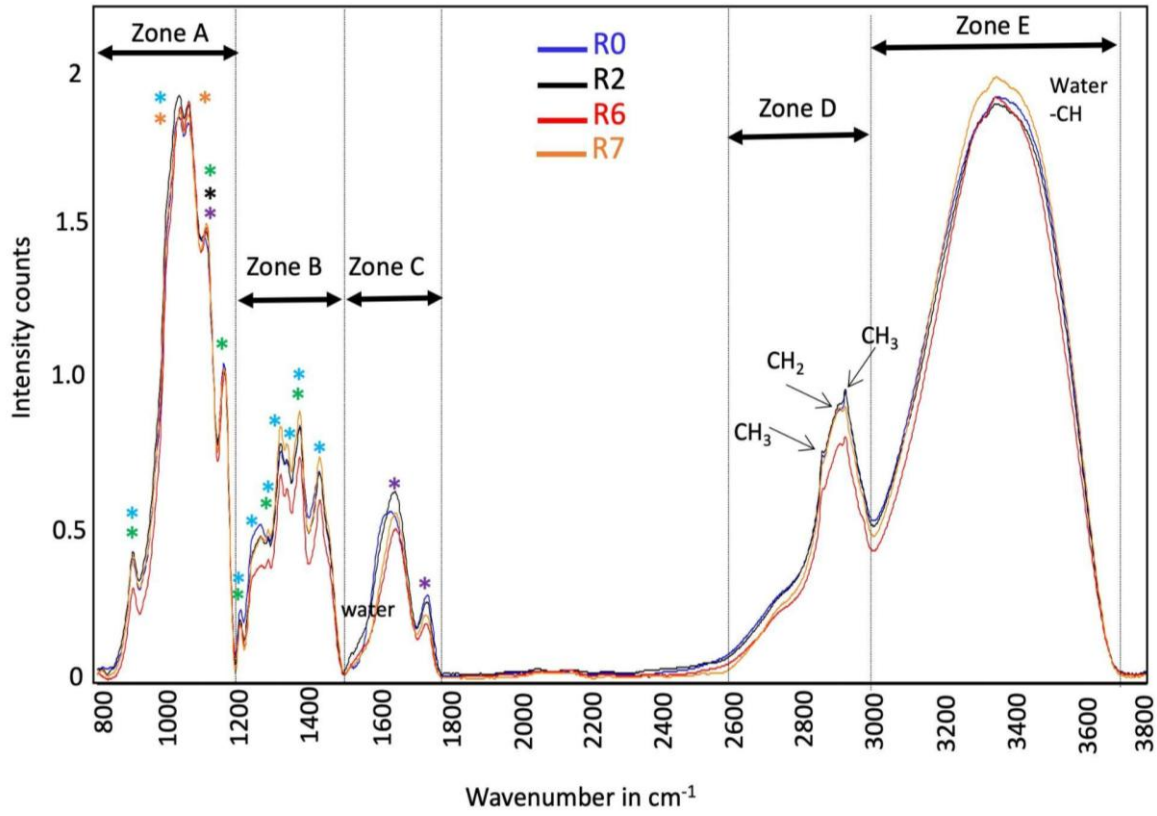

Figure IV.13 Average spectra of the different dew retting times according to the field B.

Assignments were done according to the (***ANNEXE A Table Assignment***) Average spectra were calculated with n_{RO}= 15, n_{R2}= 17, n_{R6}= 17, n_{R7}= 17 individual spectra covering all biological repetitions (T1+T2+T3). Each peak corresponds to a chemical bond between two/three atoms present in polymers *Cellulose; *Hemicellulose-Xylan-Xyloglucan; * β-D Glucan; *Mannan; *Pectin. Normalization was done according to the Min-Max process (OPUS NT software).

Spectral profiling allowed us to identify subtle differences between field A/field B that appeared since the R0.

IV.2.4.2. Analysis of retting spectral profiles by zones: an '*a priori*' approach in field B

The '*a priori*' approach was then applied for each spectral zone (A to E) and i_{max} intensities for each major peak were tested with one-way ANOVA/ Tukey's test Fig. IV.14.

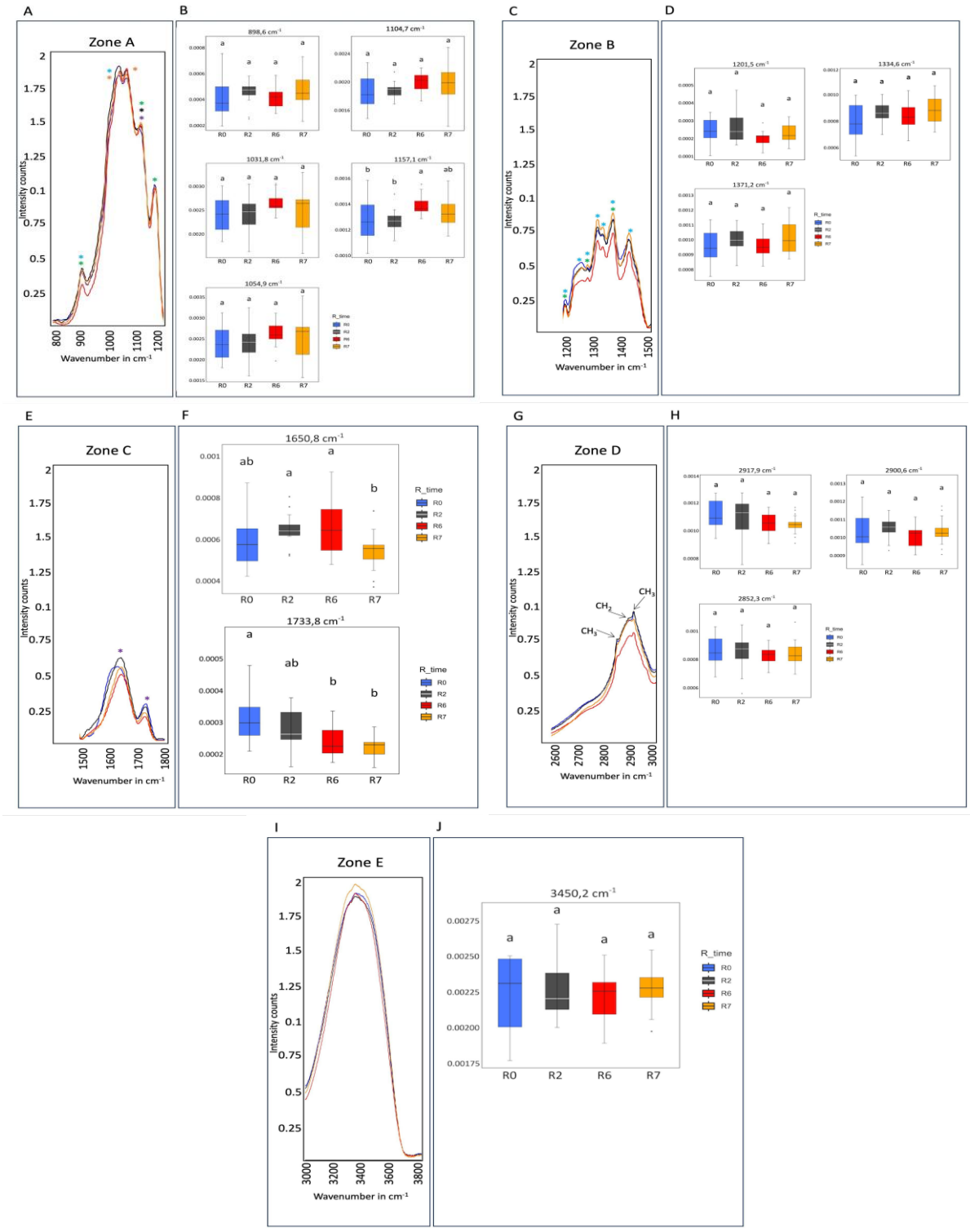

Figure IV.14 Comparative analysis of the five zones, in field B.

Spectral profile extract of each zone, and the related box-and-whiskers plots. *Cellulose; *Hemicellulose-Xylan-Xyloglucan; * β-D Glucan; *Mannan; *Pectin. The box-and-whiskers plots represent values of n_{RO}= 15, n_{R2}= 17, n_{R6}= 17, n_{R7}= 17 individual spectra respectively covering all biological repetitions (T1+T2+T3). Within one time point R, all i_{max} of the technical repetitions were chosen for each of these peaks. Tukey's test was firstly applied to check normality, then a one-way ANOVA was achieved. The *same letters* above each box mean no significant difference at $p = 0.05$. The effect is significant with $p<0.05$.

Results are gathered in Table IV.2.

In this **field B**, for the 4 retting points selected, only two conditions led to significant events. The pectin peak (1650 cm^{-1}) for the late step [R6 vs R7], but another pectin peak related to the esterified form (1733,8 cm^{-1}) for the overall process [R0 vs R7]. This is consistent with the main fact that retting aims to release elementary fibers from their bundles.

By comparison with **field A**, no significant peak appears during the early step [R0 vs R2] in field B. The late stage [R6 vs R7] and the overall process [R0 vs R7], is commonly driven by pectin involvement.

Zone	Peak in cm^{-1}	Related Cell Wall polymer	Comment according to the retting process		
			R0 vs R2	R6 vs R7	R0 vs R7
Zone A	898,6	Cellulose	a,a	a,a	a,a
	1031,8	Cellulose and Acetyl GlcMan	a,a	a,a	a,a
	1054,9	Cellulose, Man	a,a	a,a	a,a
	1104,7	Cellulose β-D-glucans	a,a	a,a	a,a
	1157,1	Hemicellulose XG	b,b	a,ab	b,ab
Zone B	1334,6	Pectin	a, a	a,a	a,a
	1371,2	Crystalline cellulose	a,a	a,a	a,a
	1201,5	Cellulose, XG	a,a	a,a	a,a
Zone C	1650	Pectin	ab,a	a,b	ab,b
	1733,8	Pectin (ester)	a,ab	b,b	a,b
Zone D	2917,9	CH_3	a,a	a,a	a,a
	2899,1	CH_2	a,a	a,a	a,a
	2852,3	CH_3	a,a	a,a	a,a
Zone E	3326,7-3450,2	OH from cellulose, water	a,a	a,a	a,a

Table IV.2 One-way ANOVA of i_{max} value from spectra during the three main steps of the retting process for the field B.

The couple of letters (a, b, c) correspond to the significant groups with the one-way ANOVA (Tukey's HSD) based on the whole datasets [R0, R2, R6, R7] (see ***ANNEXE A Table Assignment***). Significant differences between the groups are noticed in the grey boxes. Annotation: AcGM: actyl glucomannan; XG: xyloglucan.

IV.2.4.3 Perspectives for field B

As this first '*a priori*' approach is completed, the 'without *a priori*' multivariate analysis for field B will have to be soon undertaken. In a middle term perspective, in order to see whether *notes* values of scutched fibers that were measured in field A and B (see § IV.2.3.1, page 176) could be related to *spectrometric* data, we will also calculate correlation coefficients with candidates revealed by both statistical analyses in both fields A and B. Regression lines will reflect positive or negative correlations

between spectrometric and morphometric datasets. In a final perspective, we will aim at a predictive model which will be defined with R-packages such as mixOmics, and further tested with confusion matrices. Such a confusion matrix is indeed a useful tool to estimate the performance of a supervised classification model (Liu et al., 2020). Some field B spectra will be aleatory input in this predictive model (i.e. n= 100 iterations covering R0-R2-R6-R7, and pooling T1+T2+T3), in order to estimate the level of retting (by comparison with the field A). Prediction of retting will be calculated by categorizing aleatory field B-spectra, with known spectra from field A. A binary classification matrix (2 x 2) will indicate False Positives, False Negatives, True Positives and True Negatives that have resulted from the validation test (Liu et al., 2020).

The performance of the model will be estimated according to these two equations (1) and (2):

$$\text{Sensitivity} = \frac{\text{True Positive}}{\text{True Positive + False Negative}} \quad (1)$$

$$[1 - \text{Specificity}] = \frac{\text{False Positive}}{\text{False Positive + True Negative}} \quad (2)$$

A sensitivity value close to 1, and a [1 - specificity] value close to 0 will indicate a highly accurate classifier. Since both sensitivity and [1 - specificity] vary depending on the selected threshold of the classifier in the model, we will ensure the receiver operator characteristic (ROC) curve is a graphical plot of [1 - specificity] *versus* sensitivity where the threshold value is varied. The closer the curve will be to the diagonal, the less accurate the model (Liu et al., 2020). Based on a theoretical retting progression and spectral profiles (early, late, optimal end-point), any spectra potentially obtained in the field with hand-held devices (Cebi et al., 2023) could be tested with this model. The decision of harvesting, or letting the remaining retting process still be processed, will be easier to take.

IV.2.5. Discussion

IV.2.5.1 Flax dew retting spectral profiling

IV. 2.5.1.1. Methodology

If previous study aimed to give information on flax retting, their experimental designs were based on stem cross sections, grounded into powder in order to produce KBr or BaF_2 pellets, and treated with enzyme cocktails (Archibald et al., 1998; Himmelsbach et al., 2002). These experimental designs were supposed to mimic natural retting. In this study, we analyzed flax stems submitted to natural dew retting (so, for a total duration of 25 days). We also decided to use flax stem powder. First attempts with KBr pellets produced greatly heterogeneous grains showing many sizes and colors. So, contrary to literature that did not mention a secondary grounding to build KBr pellets, and in order to homogenate

grains, samples were secondary placed into diamond cells to obtain homogenous grains. This was necessary to limit the significance weight of technical repetitions.

Previous study on flax submitted to artificial retting, established that Raman spectroscopy was better to analyze flax stem powder (Archibald et al., 1998). In our case, it was natural dew retting and stems were submitted to many micro-organisms. Our preliminary tests (not shown) revealed that RAMAN spectra were covered by a high fluorescence making it impossible to use this technique in our study. Such fluorescence could be due to color pigments (as the stems change color during the retting process) (Bleuze et al., 2018), residual chlorophyll from the stem cortical parenchyma (Gamble et al., 2000), and the presence of microorganisms' cell wall residues. But the presence of phenolic constituents could also be involved, and they are known to inhibit cellulase and pectinase actions (Gamble et al., 2000). Aromatic constituents including flavonoids and hydroxy-methoxy cinnamic acids are linked to oligosaccharides, and hydroxy acids through glycosidic linkages (Martin and Akin, 1988). So, to release access for degrading enzymes to outer tissues, such aromatics compounds should be firstly extracted (Akin et al., 1988; Tian et al., 2016). For that reason, FT-IR was preferred and used successfully to achieve our objectives. Moreover, previous studies revealed lignin contributions from flax inner tissues (wood). We were not in this case as our stem fragments were peeled to keep only outer tissues, whereas inner tissues (wood, lignified tissue) were discarded. Therefore, for all these reasons, FT-IR was preferred and used successfully to achieve our objectives.

IV.2.5.1.2. Specific chemical bonds and pic intensities identifications

Our spectral profiling led us to detect visual modifications notably for [CH_2-CH_3-CH_2-OH] chemical bonds (zone D). The relative absorbance of CH_2 chemical bond (2899,1 cm^{-1}) could be associated with proteins, cellulose and pectin (Sene et al., 1994). Two similar bands (2850; 2918 cm^{-1}) were also identified as related to C-H in methyl and methylene groups by (Mohapatra & Malik, 2015) during flax stem degradation onto the fields. However statistical analysis ("a priori") could not find any significance in difference (**Fig. IV.5** for field A; **Fig.IV.14.G, H** for field B). A previous study on artificial retting considered that C-H stretch absorption, which could reflect carbohydrate reorganization or degradation, was poorly related to flax retting (Archibald et al. 2010). Reorganization took place as micro-organisms invaded the flax outer tissues from the stem. To degrade them, such organisms should digest different tissues (epidermis, cortical parenchyma), in order to reach fiber bundles. In these bundles, elementary fibers (*i.e.* one very long single cell) were stuck together with pectin.

As retting involved spatio-temporally cohorts of microorganisms, we also explored literature available on FT-IR from specific fungi cell walls. Most of the studies investigated the impact of fungi/bacteria in plants according to modifications that appeared in the plant wood spectral profiling (Pandey and Pitman, 2003; Chow and Ting, 2019). In such contaminated plants, (Chow and Ting, 2019)

identified a 1377 cm^{-1} peak specific from *Ganoderma goninense* (fungi) that allowed discrimination with bacteria as this peak did not exist in this kingdom (Erukhimovitch et al., 2010). Such a 1377 cm^{-1} peak was not detected in our retting flax stems. (Chow and Ting, 2019) also mentioned that (1,4) (1,6)-α-D-glucans and (1,3)-α-D-glucans are usually detected in fungi as peaks in the window 750-970 cm^{-1} (in which, the specific 898 cm^{-1} corresponds to plant amorphous cellulose, Zone A).

If we focus on the global spectra (*i.e*. whole dataset, 3400-800 cm^{-1}), three major peaks could be suggested to belong to such fungi cell wall: 1104; 1056 and 1030 cm^{-1}, respectively related to β-1,3-D Glucan/chitin and to the mannan residues on proteins (N- and O- glycosylated proteins) (Galichet et al., 2001). Their contributions may be added or subtracted to those originated from the plant (and which could be assigned to another cell wall polymer). As hyphae could be present as dew retting was progressing, the chemical environment could progressively be changed, and chemical bonds could vibrate differently.

Beside cell walls from epidermis, parenchyma that exhibited primary cell walls, the technical properties of the elementary flax fiber are due to the high content of crystalline cellulose (secondary cell walls) (Müller et al., 1998). To obtain high quality fiber, the fiber-cell wall integrity should not be compromised whereas outer surrounding tissues should be degraded. XRD (X-ray Diffraction) led to observing such an increase during hemp retting (Marrot et al., 2013). During flax retting, (Bourmaud et al., 2019) established with XRD and NMR (Nuclear Magnetic Resonance) that an increase of 8% cellulose crystallinity was also established. The authors suggested that it was due to the disappearance of amorphous material that was also mentioned by (Bleuze et al., 2018; Chabbert et al., 2020). In our FT-IR datasets, the 898,6 and 1201,5 cm^{-1} peaks were assigned to amorphous cellulose, and we also showed they were greatly modified during the retting process. Considering the 1371,2 cm^{-1} peak, related to cellulose crystallinity, its contribution is highly positive in R6 compared to R7. This is consistent with NMR results from (Bourmaud et al., 2019) that established a modest increase of crystallinity.

During retting, dehydration also progressively occurred in up-rooted stems (***ANNEXE B, Rains***). However, according to the previous dehydration step of our peeled flax stem in an oven at 45°C/48h (**Chapter II, § II.10.1**, page 113), we would expect that no water was still present in our samples. But (Archibald et al., 1998), working on air-dried flax stems submitted to enzymatic retting, considered that hydration of raw material greatly varied between their samples as it could be for ours. Our observations led us to notice a clear horizontal shift in Zone C (1733,8; 1650; 1633,2 cm^{-1}, containing pectin contributions) that could be due to dehydration, and high (in intensity) and large (in width) peaks at 3326,7 cm^{-1} in Zone E, that seemed major and appear more rapidly in **field A** than in **field B**. Such a phenomenon should also be considered for estimating the retting optimal end-point for each field. Indeed, environmental hygrometry (due to rains for example) can deeply modify

macromolecular structure at the plant cell level (Chen et al., 2018). (Mohapatra and Malik, 2015) washed their flax samples in 70% ethanol then let them air-dried. They also identified a 1637 cm^{-1} peak that they assumed to be related to water adsorption during flax dew retting. In this study, we identify a peak at 1633,2 cm^{-1} that is either related to pectin (Chatjigakis et al., 1998; Szymanska-Chargot and Zdunek, 2013) or to water (Mohapatra and Malik, 2015) contributions. Plant fiber swelling in a wet environment could be a consequence of internal structural changes that induced sorption/desorption/swelling. The OH-groups are involved in such a phenomenon (hysteresis) and, in our context, it particularly concerns amorphous cellulose. Indeed, such hydroxyl sites allow internal cohesion. The other amorphous polysaccharides also provide numerous hydroxyl sites that allow relaxation and deformation of plant cell walls. The fact that no cellulose or hemicellulose peaks are revealed to be significant in this **field B** is questioning. Indeed, outer tissues (epidermis, cortical parenchyma, primary phloem) should be preliminary degraded by enzymes. This is not established statistically.

IV.2.5.2 Enzymes involvement during dew retting

The complexity of the plant cell wall, being a lignocellulosic material, led to the belief that a mixture of enzymes, including cellulases, hemicellulases, and notably pectinases, was necessary for the retting of flax, similar to the natural microbial process associated with wood/litter degradation (Akin, 2013; Sharma, 1992). Research reveals that numerous enzymes, including exopolygalacturonase, α-L-arabinosidase, peroxidase, phenol-oxidase, β-D-xylosidase, β-D-galactosidase, β-D-glucosidase, and cellobiohydrolase, play a key role in the retting process, whether in hemp or flax (Bleuze et al., 2018; Chabbert et al., 2020). In **Chapter III**, we have already explored the enzymology of flax dew retting using spectrophotometry, fluorometry, and a metaproteomic-based approach. We observed a sequential activity of (studied seven) enzymes, where Polygalacturonase (PG) plays a critical role early in retting (R0-R2), (expected to catalyze the breakdown of pectins in the middle lamella), followed by a rise in hemicellulose-degrading enzymes like xylosidase and galactosidase (from R1, till R4) and later by cellulases such as glucosidase and cellobiohydrolase (after R2 till R5), which is known to degrade the cellulose matrix. These enzyme dynamics are also comparably consistent with the changes observed in monosaccharide composition, where arabinose shows significant decreases along with a gradual decrease in galacturonic acid and galactose during early retting (R0-R2), (possibly correlating with seen PG activity).

The FT-IR study of the early retting stages (R0-R2), has shown a significant difference in peaks at wave numbers 1733.8 cm-1 (esterified pectin), 1334.6 cm-1 (pectin), along with 1201.5cm-1 (xyloglucan, amorphous cellulose), 898.6 cm-1 (amorphous cellulose) in the “a priory” approach, might correlates to this enzyme oriented chemical environment change in the bast surrounding tissue of flax straw.

These early-acting PGs are identified as (cell wall-related CAZymes) GH35 (β-galactosidase) and CE8 (pectin methylesterase) from flax, as well as microbial enzymes like GH28 (polygalacturonase) and pectate lyases (PL1 and PL3), were active during R0-R2, compared to later stages (R2-R4 or R2-R7). These enzymes target parenchyma cells surrounding fiber bundles and the pectin-rich middle lamella (Chabbert et al., 2020). Pectin methylesterases (CE8) are particularly involved in esterified pectin de-esterification, which may be associated with the observed 1734 cm^{-1} peak (Zone C). The action of pectinases facilitates access to other cell wall components by other degrading enzymes (Kikot et al., 2009).

In the literature, the hemicellulose degradation by fungi xylanases was necessary to attack the plant primary cell wall (Hatsch et al. 2006; Kikot, Hours, and Alconada 2009). Putative fungi related peaks (1104 cm^{-1} for β-glucan-chitin, and 1056; 1030 cm^{-1} related to N- and O- glycosylated proteins) (Galichet et al. 2001), could also be associated to the progressive invasion of fungi hyphae within these outer tissues. β-mannanases have been identified from *Bacillus licheniformis* after flax water-retting (Ge et al. 2016). In kenaf (*Hibiscus cannabinus*), such enzymes were also identified during dew retting (Xu et al. 2022). We have previously explored the dynamics of hemicellulose-degrading CAZymes (GH17, GH55, GH35, GH10) including mannosidases (GH2, GH26) (detailed in **Chapter III**). In our FT-IR results, hemicelluloses (xylan, xyloglucan) chemical bonds are particularly present in the zones A and B of spectral profiling. Moreover, zone B was often stated as significant through (s)PLS-DA. It means that the chemical context related to hemicellulose polymers was therefore greatly modified during the retting process as previously mentioned by Tian et al. (2016). Such a decrease was also described during hemp retting and was suggested to also affect tensile rigidity (Placet et al., 2017).

As retting progresses (R2-R7), the degradation of xyloglucan and amorphous cellulose intensifies, with increased activity of cellulases (GH7, GH5, GH94) and hemicellulases (GH2) observed at later stages (R6-R7). Monosaccharide analysis reveals a marked decrease in xylose, galactose, and fucose (detailed in **Chapter III**).

The FT-IR analysis supports these findings by showing a reduction in the intensities of peaks corresponding to amorphous cellulose (899, 1201.5, 1281, 1426.7 cm^{-1}) and hemicellulose (1317 cm^{-1}) during the retting process. These structural changes in pectin and hemicellulose supposedly indicate degradation of the middle lamella, a key step that facilitates fiber separation in retting. Degradation of the epidermis and cortical parenchyma by cellulases is essential for accessing fiber bundles (Placet et al., 2017). Such enzymes degrade β-1,4-D glucosidic bonds in the cellulose polymer, and attack amorphous cellulose before the crystalline one (Lee et al., 2020). However, over-retting should be avoided as it could alter mechanical properties of fiber, and therefore their quality (Fila et al., 2001; Placet et al., 2017).

In our 25 days of dew retting study, crystalline cellulose peak (1371 cm^{-1}) showed significant difference with the '*a priori*' approach for [R0 vs R2], and a common significant presence identified with the sPLS-DA between the two retting points tested for each condition. Its common contribution was positive [R0 vs R7] and [R6 vsR7], or negative [R0 vs R2]. Mohapantra & Malik (2015) also noticed with FT-IR such cellulose changes (1372; 1336; 1313; 1280; 1160; 1105 cm^{-1}) during flax biodegradation. Unfortunately, they did not perform any statistics. Such a decrease in the ratio of crystalline cellulose / amorphous components was considered as the first indication of cell wall degradation during hemp retting (Placet et al., 2017). This induced a decrease in the tensile rigidity. In contrast, Bourmaud et al. (2019) established an increase of 8% in crystallinity of the cellulose during flax retting with NMR (Nuclear Magnetic Resonance). During retting crystalline glucose content, along with rhamnose and mannose, does not significantly change in monosaccharide analysis (Mukherjee et al., 2024), consistent with previous reports (Akin, 2013). But in our context, there are also epidermis and cortical parenchyma that contributes to the initial decrease in cellulose (R0 vs R2), coming from their primary cell walls.

Hydrolytic and oxidase activities are also noticed since the flax up-rooting R0 (Chabbert et al. 2020). These combined actions will release cell wall constituents used as nutrients for microorganisms. We suggest that it is reflected by the progressive CH_2-CH_3 depletion of intensity assigned to the main plant cell wall polymers (Zone A, B and C, cellulose, hemicellulose, pectin). Nevertheless, the spatio-temporally presence of these enzymes within outer-tissue cell types, notably oxidases, could be either produced by an endogenous way from the plant itself (before its die) and as retting progressed, by an exogenous origin from the microorganisms from the soil and the phyllosphere (Chabbert et al. 2020; Hodges et al. 2004; Valenzuela et al. 2017)

IV.2.5.3. Comparison between 'a priori' *versus* 'without *a priori*' approaches in field A

In this *Chapter IV,* two approaches for statistical analyses on the same dataset were developed. The '*a priori*' approach considered all over the whole time-course retting process the i_{max} evolution of a limited number of peaks (i.e. wavenumbers) previously chosen by expert curation regarding the literature. This can be considered as a classical approach since such approach is commonly undertaken since years in several studies such as animal cells infected by parasites (Vongsvivut et al., 2019), plant cell wall investigations (Bhagia et al., 2022), or pollen taxonomy (Kendel & Zimmermann, 2020). With such an approach, we were able to identify 2 specific chemical bounds in start vs end retting points comparison, 5 in the early events comparison, and none in the late events comparison (**Table IV.3**). The early event [R0 vs R2] is characterized by modifications of amorphous cellulose and pectins. The initiation of retting is undergoing. The end of retting could be based on two measurements of the

esterified pectin (1733,8 cm^{-1}, but it is more related to R0) and amorphous cellulose (898,6 cm^{-1}, and it is more related to R7).

The 'without *a priori*' approach considered the whole spectrum evolution while series of comparisons of two retting points of the retting process. In this 'without *a priori*' approach, our purpose was to limit the loading weight (importance) of peak contributions exhibiting very high intensity in the whole spectrum, since global analysis of the whole spectra could generate a bias as peaks exhibiting high i_{max} could crush those that showed lower i_{max}. Therefore, we chose to proceed with PCA at first since it is a dimensionality reduction technique that helps to represent a multivariate dataset as a smaller set of variables. Indeed, the power of PCA relies on its ability to represent correlated information from hundreds of spectral channels into a few orthogonal PCs, which provides a convenient way for image visualization and feature extraction (Zhang et al., 2005). However, trends, Clusters and outliers can be visualized, or not be. This is why we further proceed with PLS method searches in order to highlight the highest covariance between our retting variates, which are a linear combination of initial variables, considering all variables in the input matrices. sPLS combine this approach with a Lasso penalization to enable the selection of variables that are the most explanatory of retting discrepancy. Thus, by means of PCA followed by sPLS-DA, we were able to identify much more specific chemical bounds in start *vs* endpoints, early events and late events comparisons than with the '*a priori*' approach (**Table IV.2**). Since two common peaks R0_pectin (1334.6 cm^{-1}) and R2_esterified pectin (1733.8 cm^{-1}), whose putative involvement in accessibility to other cell wall components is discussed above, were observed in both methods, their presence in the larger set of candidates highlighted by means of the 'without *a priori*' approach supports the hypothesis that the other candidates in such approach are reliable.

At last, the other huge advantage of the '*a priori*' method is to be able to pinpoint which of the highlighted variables has a greater "importance" (loading weight) within a very large set of putative candidates, as was for example recently used in a study of the effect of hot air drying on the degradation of polyphenols in red radish (Li et al., 2020). In the **Table IV.2**, by means of Venn diagram (**Fig. IV.11**), we could even decipher what are the peaks whose contribution is significatively specific to this or that retting point of our 25d time-course, as well as if it is *via* a positive or a negative contribution (9, 1, 3 and 4 in R0, R2, R6 and R7, respectively). Such original analysis could be undertaken thanks to advances in bioinformatics tools, as was recently deployed in flax and allowed to highlight relevant candidates that will be used as effective predictors of flax fiber quality parameters (Chabi et al., 2023). At last, one can consider that the choice of the method depends on the objectives. The '*a priori*' approach is technically easy to apply for a hand-portable device that could be calibrated to measure very few peaks. The early event [R0 vs R2] is characterized by modifications of amorphous cellulose and pectins. The initiation of retting is undergoing. The end of retting could be based on two measurements of the esterified pectin (1733,8 cm^{-1}, but it is more related to R0) and amorphous cellulose (898,6 cm^{-1}, and it

is more related to R7). The choice of the 'without *a priori*' method is at first glance more time consuming since it needs to develop a relevant statistical pipeline. But it gives detailed and deeper results as the whole spectrum is used in the analysis. Results from sPLS-DA loadings led us to associated significant peaks to their type of contributions (positive or negative), and their relative loading weight, when two retting points are compared. In consequence, retting evolution is well described and could also be

	[R0 vs R7]	**[R0 vs R2]**	**[R6 vs R7]**
' *a priori*',	898,6 cm^{-1}, aCel 1733,8 cm^{-1}, ePect	898,6 cm^{-1}, aCel 1201,5 cm^{-1}; XG, aCel 1371,2 cm^{-1}, cCel 1334,6 cm^{-1}, Pect 1733,8 cm^{-1}, ePect	none
'without *a priori*' **positive contribution** *negative contribution*	specific for R0: **1031,8 cm^{-1} Cel, GlcMan** *1054,9 cm^{-1}, Man* *1104,7 cm^{-1} βGlc, Cel* *1157,1 cm^{-1},Hem, Xyl* *1201,5 cm^{-1}; XG, aCel* *1281 cm^{-1}, Cel* **1508 cm^{-1}, Aromatics** *1633,2 cm^{-1}, Pect* *1733,8 cm^{-1}, ePect*	specific for R0: none	specific for R6: *1201,5 cm^{-1}; XG, aCel* *1281 cm^{-1}, Cel* *1508 cm^{-1}, Aromatics*
	specific for R7: **800 cm^{-1}, Man, Hem** *1317 cm^{-1}, Hem, Cel* *1334,6 cm^{-1}, Pect*	specific for R2: **1334,6 cm^{-1}, Pect**	specific for R7: **1317 cm^{-1}, Hem, Cel**

Table IV.3 Comparison of the two methods' '*a priori*' and 'without *a priori*'.

The first one considers only a single chosen peak (one-way ANOVA, Tukey's HSD). The second one is based on the whole spectrum (PCA, sPLS-DA, and Venn Diagrams). Annotations: aCel: cellulose; cCel: crystalline cellulose; ePect: esterified pectin; GlcMan: glucomannan; Hem: hemicellulose; Man: mannan; Pect: pectin; Xyl: xylan; XG: xyloglucan. Positive (bold), negative (light) and common (underlined) contributions.

considered with other results such as enzyme activities, technical properties of fiber. We succeeded to highlight a limited number of putative relevant wavenumbers for retting stage monitoring. We do hope the comparison of the two methods can be helpful for further comparable analyses.

IV.3 Conclusions of the chapter

In this Chapter, we promote FT-IR vibrational spectroscopy as a valuable method to characterize the retting process. It allows to discriminate subtle differences in chemical bonds, and in their related cell wall polymers that seem progressively altered. Specifically, early step of cell wall disorganization and later step that finally permit elementary fiber releasing can be deciphered. Retting commitment is characterized by peaks corresponding to cell wall polymers. Cellulose (1260 cm^{-1}, from outer tissues) and pectin (1334,6 cm^{-1}), notably the esterified ones (1733,8 cm^{-1}), are markers of the early step. They are involved in cell cohesion of cells. The amorphous cellulose peaks (1201,5; 1281; 1426,7 cm^{-1}) are greatly decreased during retting. They are related to epidermis and cortex cell disorganization due to enzyme and fungi activities. Such peaks could be considered as markers of a well-retting process. The optimal end-point could be identified with the intensity of peaks related to hemicellulose (1157,1 cm^{-1}). It is theoretically localized around the R7 retting point. Field that exhibits lower speed of retting is expected to not show such a significant peak. We also argue for the development of new approaches based on the use of large spectroscopic datasets and appropriate bioinformatic tools for powerful statistical analyses. The choice of our 'without *a priori*' method is at first glance more time consuming since it needs to develop a relevant statistical pipeline. But it gives more detailed and deeper results as the whole spectrum is used in the analysis. By doing so, we succeeded to highlight a reasonable number of putative relevant wavenumbers for retting stage monitoring, which will be technically easy to use in hand-portable devices as recently developed for food quality control purposes (Cebi et al., 2023).

Key findings:

- Vibrational spectroscopy, notably FT-IR is a suitable tool to monitor retting evolution
- Specific FTIR spectral signatures are identified for each stage (overall, early, and late)
- An '*a priori*' approach based on chosen peak among the spectrum seems convenient but produces very few significant peaks to further operate for technical applications with hand-held device
- The 'without *a priori*' approach needs to firstly define a multivariate analysis workflow based on the whole spectrum. It produces more specific and significant markers of retting stages.
- The optimal endpoint of retting is determined by the 1317 cm^{-1} peak (related to hemicellulose) only significantly and positively present at R7.
- Degradation of flax outer tissues, and therefore cell wall polymers gradual alteration can be documented during the retting process.

IV.4. References

Abidi, N., Cabrales, L., Haigler, C.H., 2014. Changes in the cell wall and cellulose content of developing cotton fibers investigated by FTIR spectroscopy. Carbohydrate Polymers, Biopolymers for Life 100, 9–16. https://doi.org/10.1016/j.carbpol.2013.01.074

Akin, D.E., 2013. Linen Most Useful: Perspectives on Structure, Chemistry, and Enzymes for Retting Flax. ISRN Biotechnology 2013, 1–23. https://doi.org/10.5402/2013/186534

Akin, D.E., Foulk, J.A., Dodd, R.B., McAlister, D.D., 2001. Enzyme-retting of flax and characterization of processed fibers. Journal of Biotechnology, Biotechnology in the Textile Industry - Perspectives for the New Millennium 89, 193–203. https://doi.org/10.1016/S0168-1656(01)00298-X

Akin, D.E., Rigsby, L.L., Theodorou, M.K., Hartley, R.D., 1988. Population changes of fibrolytic rumen bacteria in the presence of phenolic acids and plant extracts. Animal Feed Science and Technology 19, 261–275. https://doi.org/10.1016/0377-8401(88)90089-2

Archibald, D.D., Henrikssen, G., Akin, D.E., Barton, F.E., 1998. Spectroscopic characterization of enzymatic flax retting: Factor analysis of FT-IR and FT-Raman data. AIP Conference Proceedings 430, 653–656. https://doi.org/10.1063/1.55746

Bhagia, S., Ďurkovič, J., Lagaňa, R., Kardošová, M., Kačík, F., Cernescu, A., Schäfer, P., Yoo, C.G., Ragauskas, A.J., 2022. Nanoscale FTIR and Mechanical Mapping of Plant Cell Walls for Understanding Biomass Deconstruction. ACS Sustainable Chem. Eng. 10, 3016–3026. https://doi.org/10.1021/acssuschemeng.1c08163

Blervacq, A.-S., Moreau, M., Duputié, A., De Waele, I., Duponchel, L., Hawkins, S., 2022. Raman spectroscopy mapping of changes in the organization and relative quantities of cell wall polymers in bast fiber cell walls of flax plants exposed to gravitropic stress. Frontiers in Plant Science 13.

Blervacq, A.-S., Moreau, M., Duputié, A., Hawkins, S., 2023. Comparative Analysis of G-Layers in Bast Fiber and Xylem Cell Walls in Flax Using Raman Spectroscopy. Biomolecules 13, 435. https://doi.org/10.3390/biom13030435

Bleuze, L., Lashermes, G., Alavoine, G., Recous, S., Chabbert, B., 2018. Tracking the dynamics of hemp dew retting under controlled environmental conditions. Industrial Crops and Products 123, 55–63. https://doi.org/10.1016/j.indcrop.2018.06.054

Bourmaud, A., Siniscalco, D., Foucat, L., Goudenhooft, C., Falourd, X., Pontoire, B., Arnould, O., Beaugrand, J., Baley, C., 2019. Evolution of flax cell wall ultrastructure and mechanical properties during the retting step. Carbohydrate Polymers 206, 48–56. https://doi.org/10.1016/j.carbpol.2018.10.065

Cao, Y., Chan, F., Chui, Y.-H., Xiao, H., 2012. Characterization of flax fibres modified by alkaline, enzyme, and steam-heat treatments. BioResources 7, 4109–4121. https://doi.org/10.15376/biores.7.3.4109-4121

Cebi, N., Bekiroglu, H., Erarslan, A., Rodriguez-Saona, L., 2023. Rapid Sensing: Hand-Held and Portable FTIR Applications for On-Site Food Quality Control from Farm to Fork. Molecules 28, 3727. https://doi.org/10.3390/molecules28093727

Chabbert, B., Padovani, J., Djemiel, C., Ossemond, J., Lemaître, A., Yoshinaga, A., Hawkins, S., Grec, S., Beaugrand, J., Kurek, B., 2020. Multimodal assessment of flax dew retting and its functional impact on fibers and natural fiber composites. Industrial Crops and Products 148, 112255. https://doi.org/10.1016/j.indcrop.2020.112255

Chabi, M., Goulas, E., Galinousky, D., Blervacq, A.-S., Lucau, A., Neutelings, G., Grec, S., Day, A., Chabbert, B., Haag, K., Müssig, J., Arribat, S., Planchon, S., Renaut, J., Hawkins, S., 2023. Identification of new potential molecular actors related to fiber quality in flax through Omics. https://doi.org/10.3389/fpls.2023.1204016

Chang, S.-S., Salmén, L., Olsson, A.-M., Clair, B., 2014. Deposition and organisation of cell wall polymers during maturation of poplar tension wood by FTIR microspectroscopy. Planta 239, 243–254. https://doi.org/10.1007/s00425-013-1980-3

Chatjigakis, A.K., Pappas, C., N.Proxenia, O.Kalantzi, P.Rodis, Polissiou, M., 1998. FT-IR spectroscopic determination of the degree of esterification of cell wall pectins from stored peaches and correlation to textural changes. Carbohydrate Polymers 37, 395–408. https://doi.org/10.1016/S0144-8617(98)00057-5

Chen, M., Coasne, B., Guyer, R., Derome, D., Carmeliet, J., 2018. Role of hydrogen bonding in hysteresis observed in sorption-induced swelling of soft nanoporous polymers. Nat Commun 9, 3507. https://doi.org/10.1038/s41467-018-05897-9

Chow, Y.Y., Ting, A.S.Y., 2019. Influence of fungal infection on plant tissues: FTIR detects compositional changes to plant cell walls. Fungal Ecology 37, 38–47. https://doi.org/10.1016/j.funeco.2018.10.004

de Sousa Marques, A., de Melo, M.C.N., Cidral, T.A., de Lima, K.M.G., 2014. Feature selection strategies for identification of *Staphylococcus aureus* recovered in blood cultures using FT-IR spectroscopy successive projections algorithm for variable selection: A case study. Journal of Microbiological Methods 98, 26–30. https://doi.org/10.1016/j.mimet.2013.12.015

Djemiel, C., Goulas, E., Badalato, N., Chabbert, B., Hawkins, S., Grec, S., 2020. Targeted Metagenomics of Retting in Flax: The Beginning of the Quest to Harness the Secret Powers of the Microbiota. Frontiers in Genetics 11.

Djemiel, C., Grec, S., Hawkins, S., 2017. Characterization of Bacterial and Fungal Community Dynamics by High-Throughput Sequencing (HTS) Metabarcoding during Flax Dew-Retting. Frontiers in Microbiology 8. https://doi.org/doi.org/10.3389/fmicb.2017.02052

Erukhimovitch, V., Hazanovsky, M., Huleihel, M., 2010. Direct identification of potato's fungal phyto-pathogens by Fourier-transform infrared (FTIR) microscopy. Spectroscopy 24, 609–619. https://doi.org/10.3233/SPE-2010-0483

Galichet, A., Sockalingum, G.D., Belarbi, A., Manfait, M., 2001. FTIR spectroscopic analysis of Saccharomyces cerevisiae cell walls: study of an anomalous strain exhibiting a pink-colored cell phenotype. FEMS microbiology letters 197, 179–186. https://doi.org/10.1111/j.1574-6968.2001.tb10601.x

Gamble, G.R., Snook, M.E., Henriksson, G., Akin, D.E., 2000. Phenolic constituents in flax bast tissue and inhibition of cellulase and pectinase. Biotechnology Letters 22, 741–746. https://doi.org/10.1023/A:1005608304142

Gorzsás, A., Stenlund, H., Persson, P., Trygg, J., Sundberg, B., 2011. Cell-specific chemotyping and multivariate imaging by combined FT-IR microspectroscopy and orthogonal projections to latent structures (OPLS) analysis reveals the chemical landscape of secondary xylem. The Plant Journal 66, 903–914. https://doi.org/10.1111/j.1365-313X.2011.04542.x

Himmelsbach, D.S., Khalili, S., Akin, D.E., 2002. The use of FT-IR microspectroscopic mapping to study the effects of enzymatic retting of flax (Linum usitatissimum L) stems. Journal of the Science of Food and Agriculture 82, 685–696. https://doi.org/10.1002/jsfa.1090

Hori, R., Sugiyama, J., 2003. A combined FT-IR microscopy and principal component analysis on softwood cell walls. Carbohydrate Polymers 52, 449–453. https://doi.org/10.1016/S0144-8617(03)00013-4

Kačuráková, M., Capek, P., Sasinková, V., Wellner, N., Ebringerová, A., 2000. FT-IR study of plant cell wall model compounds: pectic polysaccharides and hemicelluloses. Carbohydrate Polymers 43, 195–203. https://doi.org/10.1016/S0144-8617(00)00151-X

Kenđel, A., Zimmermann, B., 2020. Chemical Analysis of Pollen by FT-Raman and FTIR Spectroscopies. Front. Plant Sci. 11. https://doi.org/10.3389/fpls.2020.00352

Leng, W., He, S., Lu, B., Thirumalai, R.V.K.G., Nayanathara, R.M.O., Shi, J., Zhang, R., Zhang, X., 2022. Raman imaging: An indispensable technique to comprehend the functionalization of lignocellulosic material. International Journal of Biological Macromolecules 220, 159–174. https://doi.org/10.1016/j.ijbiomac.2022.08.084

Li, W., Bi, J., Li, Y., Chen, C., Zhao, X., Zheng, Q., Tan, S., Gao, X., 2020. Chemometric analysis reveals influences of hot air drying on the degradation of polyphenols in red radish. International Journal of Food Engineering 16. https://doi.org/10.1515/ijfe-2019-0387
Liu, X., Renard, C.M.G.C., Bureau, S., Le Bourvellec, C., 2021. Revisiting the contribution of ATR-FTIR spectroscopy to characterize plant cell wall polysaccharides. Carbohydrate Polymers 262, 117935. https://doi.org/10.1016/j.carbpol.2021.117935
Liu, Y.-J., Kyne, M., Wang, C., Yu, X.-Y., 2020. Data mining in Raman imaging in a cellular biological system. Computational and Structural Biotechnology Journal 18, 2920–2930. https://doi.org/10.1016/j.csbj.2020.10.006
Marchessault, R.H., Liang, C.Y., 1962. The infrared spectra of crystalline polysaccharides. VIII. Xylans. Journal of Polymer Science 59, 357–378. https://doi.org/10.1002/pol.1962.1205916813
Marrot, L., Lefeuvre, A., Pontoire, B., Bourmaud, A., Baley, C., 2013. Analysis of the hemp fiber mechanical properties and their scattering (Fedora 17). Industrial Crops and Products 51, 317–327. https://doi.org/10.1016/j.indcrop.2013.09.026
Martin, S.A., Akin, D.E., 1988. Effect of phenolic monomers on the growth and beta-glucosidase activity of Bacteroides ruminicola and on the carboxymethylcellulase, beta-glucosidase, and xylanase activities of Bacteroides succinogenes. Appl Environ Microbiol 54, 3019–3022. https://doi.org/10.1128/aem.54.12.3019-3022.1988
Mazurek, S., Mucciolo, A., Humbel, B.M., Nawrath, C., 2013. Transmission Fourier transform infrared microspectroscopy allows simultaneous assessment of cutin and cell-wall polysaccharides of Arabidopsis petals. The Plant Journal 74, 880–891. https://doi.org/10.1111/tpj.12164
McCann, M.C., Defernez, M., Urbanowicz, B.R., Tewari, J.C., Langewisch, T., Olek, A., Wells, B., Wilson, R.H., Carpita, N.C., 2007. Neural network analyses of infrared spectra for classifying cell wall architectures. Plant Physiology 143, 1314–1326. https://doi.org/10.1104/pp.106.093054
McCann, M.C., Hammouri, M., Wilson, R., Belton, P., Roberts, K., 1992. Fourier transform infrared microspectroscopy is a new way to look at plant cell walls. Plant Physiology 100, 1940–1947. https://doi.org/10.1104/pp.100.4.1940
Mohapatra, H.S., Malik, R.K., 2015. Effect of microorganism on flax and linen. J. Text. Sci. Eng 6, 1000229. https://doi.org/10.4172/2165-8064.1000229
Müller, M., Czihak, C., Vogl, G., Fratzl, P., Schober, H., Riekel, C., 1998. Direct Observation of Microfibril Arrangement in a Single Native Cellulose Fiber by Microbeam Small-Angle X-ray Scattering. Macromolecules 31, 3953–3957. https://doi.org/10.1021/ma980004c
Nayak, L.K., Debnath, S., Shambhu, V.B., Swain, K.C., Baite, H., Kundu, T.K., 2021. Extraction of Flax and Sisal Fibre through Improved Extractor and Their Chemical Characterization. Journal of the Indian Society of Coastal Agricultural Research 39.
Olsson, A.-M., Bjurhager, I., Gerber, L., Sundberg, B., Salmén, L., 2011. Ultra-structural organisation of cell wall polymers in normal and tension wood of aspen revealed by polarisation FTIR microspectroscopy. Planta 233, 1277–1286. https://doi.org/10.1007/s00425-011-1384-1
Pandey, K.K., Pitman, A.J., 2003. FTIR studies of the changes in wood chemistry following decay by brown-rot and white-rot fungi. International Biodeterioration & Biodegradation 52, 151–160. https://doi.org/10.1016/S0964-8305(03)00052-0
Różańska, W., Romanowska, B., Rojewski, S., 2023. The Quantity and Quality of Flax and Hemp Fibers Obtained Using the Osmotic, Water-, and Dew-Retting Processes. Materials 16, 7436. https://doi.org/10.3390/ma16237436
Salih, S., 2012. Fourier Transform: Materials Analysis. BoD – Books on Demand.
Sene, C.F., McCann, M.C., Wilson, R.H., Grinter, R., 1994. Fourier-transform Raman and Fourier-transform infrared spectroscopy (an investigation of five higher plant cell walls and their components). Plant physiology 106, 1623–1631. https://doi.org/10.1104/pp.106.4.1623
Sharma, S., 1992. SHARMA, H.S.S. and VAN SUMERE, C.F. (1992). The Biology and Processing of Flax. M. Publications, Belfast, 576 pp.

Stuart, B.H., 2004. Infrared Spectroscopy: Fundamentals and Applications. John Wiley & Sons.
Szymanska-Chargot, M., Chylinska, M., Kruk, B., Zdunek, A., 2015. Combining FT-IR spectroscopy and multivariate analysis for qualitative and quantitative analysis of the cell wall composition changes during apples development. Carbohydrate Polymers 115, 93–103. https://doi.org/10.1016/j.carbpol.2014.08.039
Szymanska-Chargot, M., Zdunek, A., 2013. Use of FT-IR Spectra and PCA to the Bulk Characterization of Cell Wall Residues of Fruits and Vegetables Along a Fraction Process. Food Biophysics 8, 29–42. https://doi.org/10.1007/s11483-012-9279-7
Tian, Y., Liu, X., Zheng, X., Wang, L., 2016. Antimicrobial properties of flax fibers in the enzyme retting process. Fibres & Textiles in Eastern Europe 15–17. https://doi.org/10.5604/12303666.1172082
Vongsvivut, J., Pérez-Guaita, D., Wood, B.R., Heraud, P., Khambatta, K., Hartnell, D., Hackett, M.J., Tobin, M.J., 2019. Synchrotron macro ATR-FTIR microspectroscopy for high-resolution chemical mapping of single cells. Analyst 144, 3226–3238. https://doi.org/10.1039/C8AN01543K
Zhang, L., Henson, M.J., Sekulic, S.S., 2005. Multivariate data analysis for Raman imaging of a model pharmaceutical tablet. Analytica Chimica Acta 545, 262–278. https://doi.org/10.1016/j.aca.2005.04.080

ANNEXE A: Table FT-IR assignment band

Assignment of our experimental peak according to those from literature and considering the plant cell wall model (dew retting in flax stem, outer tissues). Wavenumber (in cm^{-1}) below 800 cm^{-1} are considered close to the limit of detection of our equipment (in grey boxes).

Experimental cm^{-1}	Literature cm^{-1}	Putative assignment	References
3326,7-3450,2	3429 3344 3336	OH- cellulose, water Intramolecular hydrogen binding, C_5-OH or C_6-0-OH	(Abidi et al., 2014; Nayak et al., 2021; Różańska et al., 2023)
2917,9	2840-3000	asymmetric and symmetric stretching ν(C-H) vibrations of the methylene group of aliphatic compounds shoulder of the 2919 cm^{-1} bands CH_2 - CH_3 - CH_2-OH	(Mazurek et al., 2013; Abidi et al., 2014; Mohapatra and Malik, 2015)
2899,1	2840-3000		
2852,3	2840-3000		
1733,8	1740 1734 1730-1745 1731-1738	Esterified uronic acid ν(C=O) stretching carbonyl group in esters C=O stretching vibration of alkyl ester, pectin ν(C=O) stretching carbonyl group	(Marchessault and Liang, 1962; Sene et al., 1994; Szymanska-Chargot and Zdunek, 2013; Nayak et al., 2021)
1650	1650	Pectin Amide I C-N Protein	(McCann et al., 2007; Szymanska-Chargot and Zdunek, 2013; de Sousa Marques et al., 2014)
1633,2	1630	COO- carboxylate ion stretching, Pectin Water	(Chatjigakis et al., 1998; Szymanska-Chargot and Zdunek, 2013; Mohapatra and Malik, 2015)
1508	1508	C=C, aromatic bonds aryl ring stretching, asymmetric	(Leng et al., 2022; Różańska et al., 2023)
Sh1462	1462	OH- cellulose	(Nayak et al., 2021)
1426,7	1426 1426-1430 1428	HCH and O-CH in plane bending vibration Cellulose COO ester group pectin	(Marchessault and Liang, 1962; Salih, 2012; Szymanska-Chargot and Zdunek, 2013; Chang et al., 2014; Nayak et al., 2021)
1371,2	1365- 1372	in the plane C-H bending Crystalline cellulose	

1334,6	1320-1330 1330-1331	Bending of O-H groups in pyranose ring, pectin	(Gorzsás et al., 2011; Szymanska-Chargot and Zdunek, 2013)
1317	1315-1319 1317 1315	C-H vibration, CH2-rocking vibration at C6, Cellulose, XG and Xylans CH_2-scissors, cellulose, hemicellulose	(Kačuráková et al., 2000; Salih, 2012; Szymanska-Chargot and Zdunek, 2013; Różańska et al., 2023)
1281	1280-1277	CH deformation in cellulose I and cellulose II	(Marchessault and Liang, 1962; Olsson et al., 2011)
1260	1261	C–O stretching, pectin Cellulose	(Olsson et al., 2011)
1201,5	1202-1200 1204 1204	OH in-plane bending in cellulose I and cellulose II Xyloglucan C-O-C symmetric stretching, OH plane deformation	(Salih, 2012; Szymanska-Chargot and Zdunek, 2013; Szymanska-Chargot et al., 2015)
1157,1	1153-1157	Ring vibration (C-OH) overlapped with stretching vibration of side groups and glycosidic bond vibration Hemicellulose, Xyloglucan	
1104,7	1124-1087 1103 1105 1102-1105 1103-1105	C-O, stretching, secondary alcohol C–O stretching, C–C stretching, cellulose (C2-O2) C-H deformation in glucans Pectin β-1,3-D-glucan	(McCann et al., 1992; Galichet et al., 2001; Szymanska-Chargot and Zdunek, 2013)
1054,9	1052-1056 1050-1053	C-O stretching in mannans C-O-C asymmetrical stretching in Cellulose	(Kačuráková et al., 2000; Galichet et al., 2001) (Stuart, 2004; Szymanska-Chargot and Zdunek, 2013)
1031,8	1030 1030-1035 1029	Acetyl glucomannan Cellulose C-O-C bending	(Kačuráková et al., 2000; Hori and Sugiyama, 2003; Szymanska-Chargot et al., 2015; Różańska et al., 2023)
898,6	895-885 s 896 899 896	C=C, bending, alkene disubstituted trans C-H deformation in glucans C1-H bending, cellulose β-linkage of cellulose	(Szymanska-Chargot and Zdunek, 2013) (Abidi et al., 2014)
800	807	Mannose, Hemicellulose	(Liu et al., 2021)
711,9	730-665 713 m	C=C, bending, alkene disubstituted cis C=O	

666,3	730-665	C=C, bending, alkene disubstituted cis	
616,5	Not assigned	Not assigned	

ANNEXE B: Stem water-content evolution during retting

Environmental abiotic factors (wind, rain, sun) affect plant growth, and also, retting process (Lee et al., 2020). Rains were measured in the two fields A and B (separated from 247.5 m) as water content in flax stems is modified if it rains just before collecting samples. Then water-content was estimated.

Protocol:

Individual stems (n= 10) were collected for each of the three biological repetitions (T1, T2, T3). The same samples were also used for this study (FTIR). For each R, stems were firstly peeled to only keep outer tissues. Then fragments of 1 cm-long were cut and crushed to obtain coarse powder. Two grams of fresh weight (initial weight W_i in g) were dehydrated (72h, 50°C, in a hot air oven) in order to determine the related dry weight (final weight W_f in g). First calculations were achieved within each biological repetition (T1, or T2, or T3), independently. The water-content of the retting stems, at each R, was expressed in % with this following equation $[(W_i - W_f) / W_i] \times 100$. A control of dry weight was also performed after 5 days in this hot air oven. In a second step, for illustration, all data (T1+T2+T3) were pooled for each R.

Data of rain quantities were obtained from 'Infoclimat' weather station (https://www.infoclimat.fr/observations-meteo/temps-reel/mazinghem/000RL.html)

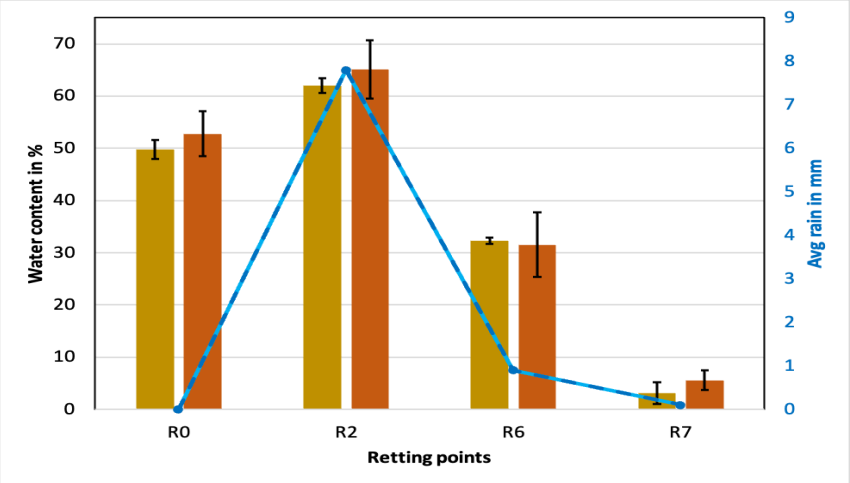

ANNEXE B Stem water-content evolution during retting. Field A in yellow bars, field B in orange bars. The blue curve concerns rains expressed in mm. Within one given field, data for each T were pooled (T1+T2+T3) to calculate water-content averages. Average water content (in %) is represented with standard error.

Result: During summer, few rains are expected, but usually, sunny days are often observed. From the R0 (the day where flax was up-rooted) to the R7 point (25 days after up-rooting), the water content globally decreases. The R2 point is explained by the rain that punctually increases the water content of stems.

N.B.: RWC (relative water content) was not used as the flax stems were not firstly submitted to a water treatment allowing to fill vacuole to its maximum turgid status. The W_i we used here is therefore not representative of the total water capacity of outer tissue cells. As whole plants are progressively dying after up-rooting, the RWC was not relevant.

CHAPTER V

Color change of flax stem surface during dew retting

Chapter V: Studying color change of flax stem surface during dew retting

Contents

Chapter V: Studying color change of flax stem surface during dew retting 211
V.1. Context and structure of the chapter 212
V.2. Quantifying flax stem surface color change for the development of a smart tool to monitor the degree of retting 214
V.2.1. Introduction 215
V.2.2. Materials and Methods 216
V.2.2.1. Plant sample collection and meteorological information 216
V.2.2.2. Collection of Spectral Readings 216
V.2.2.3. Statistical analysis 217
V.2.3. Results 217
V.2.3.1. Weather details during retting 217
V2.3.2. Flax stem surface color change 217
V.2.3.3. *CIELab* color space results. 219
V.2.3.4. (Multivariate analysis) Evolution of the spectral color measurements. 221
V.2.3.5. Prediction of retting stages with confusion matrix made of selected variables (web-lengths) from pooled datasets 228
V.2.3.6. Trend of color evolution in over-retting. 229
V.2.4. Discussions 233
V.2.5. Conclusion. 234
V.3. Reference: 236

V.1. Context and structure of the chapter

The phloem residing fibers or bast cells of the fiber Flax plant (*Linum usitatissimum* L.) are long and rich in crystalline cellulose (i.e. strong and flexible) and used to make high-quality textiles and various composite products (Chand and Fahim, 2020; Mohanty et al., 2000). These fibers are extracted in a step-by-step process starting from retting, followed by mechanical scutching, combing, spinning, and weaving (Gomez-Campos et al., 2021). Retting is a process where the plant's cellular tissues surrounding the extra-phloemien bast-fiber bundles are disaggregated or rot away by the enzymatic action of micro-organisms and moisture that facilitate the separation of the bast fiber bundles from the stem and from each other (Meijer et al., 1995; Djemiel et al., 2017). In Europe, dew retting is practiced widely where uprooted flax plants are left on fields for several weeks under heavy dew falls during night-time and warm summer days accompanied by frequent rainfall. This promotes micro-organisms growth on the flax stems and they partially degrade the cell wall pectin and hemicellulose (Wang et al., 2017) letting loose the single fibers from fiber bundles and other plant tissues (Chabbert et al., 2020). Degradation of these cementing materials let loose the cellulosic fibers which became easier to separate with mechanical steps and retain their high tensile strength (Baley, 2002; Akin, 2013). A prolonged dew-retting can cause the degradation of cellulosic fibers thus impacting the mechanical quality of fibers, a phenomenon known as over-retting (Bratt et al., 1988; Brown and Sharma, 1984; Meijer et al., 1995). On the other hand, under-retted fibers are not easily separated from the stem tissue, often causing cuticle contamination and reducing the fiber quality in fineness and homogeneity (Akin, 2013). Despite all this knowledge, there is no real-time standardization of flax dew retting and farmers still decide when to stop retting depending on their experience. Constant fiber quality management of dew-retted flax is still very much empirical. Farmers often depend upon the straw color change or manual in-hand evaluation of ease of fiber separation (Fried test) and decide to stop retting (Akin et al., 1996). Several studies, attempting to produce a tool to test the degree of retting using both physical (Brown et al., 1986; Donaghy et al., 1992; Meijer et al., 1995; Seaby and Mercer, 1984; Sharma and Faughey, 1999) and biochemical properties (Meijer et al., 1995; Sharma and Faughey, 1999), suggested that a more sensitive and multimodal method is needed to determine flax's initial rettability and monitor the degree of retting in the field. To date, no reliable ideal tool has been demonstrated as the proposed models are either destructive, too cumbersome, or unreliable (Meijer et al., 1995). The change in stem surface color during dew-retting, although well-known and still used by experts to define retting, is rarely explored scientifically.

In this chapter, we use optical spectroscopy to measure the optical spectrum of flax stems in various degrees of retting. Following this, the optical data is subjected to a statistical analysis to identify spectral peaks that can be used as tracers which indicate the degree of retting. The first part of the chapter contextualizes the color changes in flax stems within a broader framework of color variations in plants

and their applications. Following this, we will present and analyze the collected data using detailed statistical methods. The findings will demonstrate that specific tracer peaks in the optical spectrum can be correlated with the degree of retting in flax. Finally, we will discuss the potential applications of these observations in the context of smart agriculture.

The contents of this chapter are being structured as an article, entitled "**Quantifying flax stem surface color change for the development of a smart tool to monitor the degree of retting**", co-authored by Mukherjee Suvajit[1,2], Grec Sébastien[1*], Blervacq Anne- Sophie[1], Arscott Steve[2*] ([1]. Univ. Lille, CNRS, UMR 8576 - UGSF - Unité de Glycobiologie Structurale et Fonctionnelle, F-59000 Lille, France ; [2]Univ. Lille, CNRS, Centrale Lille, Junia, Univ. Polytechnique Hauts-de-France, UMR 8520 - IEMN - Institut d'Electronique de Microélectronique et de Nanotechnologie, F-59000 Lille, France).

V.2. Quantifying flax stem surface color change for the development of a smart tool to monitor the degree of retting

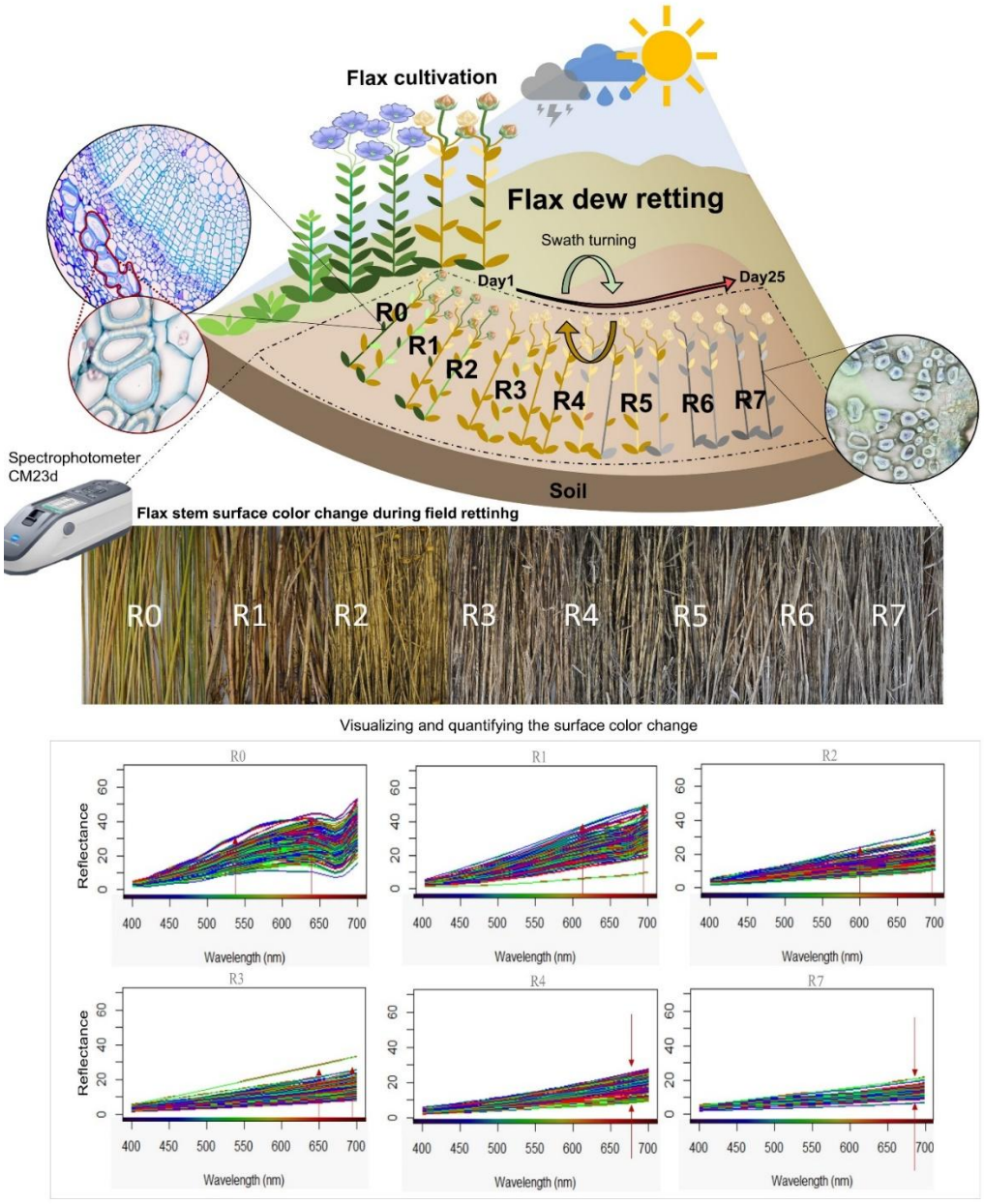

❖ What insights can the surface color change of flax stems provide about the dew retting process?

❖ Can we quantify these changes, develop a structured data analysis pipeline, and propose a potential color-based, non-invasive tool to monitor flax dew retting?

For this chapter, these persons collaborate (in alphabetical order):

Blervacq Anne-Sophie[1], Grec Sébastien[1], Stephen Arscott[2]
[1]. Univ. Lille, CNRS, UMR 8576 - UGSF - Unité de Glycobiologie Structurale et Fonctionnelle, F-59000 Lille, France., [2]Univ. Lille, CNRS, Centrale Lille, Junia, Univ. Polytechnique Hauts-de-France, UMR 8520 - IEMN - Institut d'Electronique de Microélectronique et de Nanotechnologie, F-59000 Lille, France

V.2.1. Introduction

Color is regarded as a perception that arises from light's interaction with things and the observer's sensory systems in both philosophy and science. Within his idea of direct realism, Scottish philosopher Thomas Reid (1764) suggested that color is not an intrinsic feature of objects but rather a sense resulting from light interacting with the human eye and brain (Reid, 1810). According to science, color is created when particular light wavelengths are absorbed and reflected; variations in hue signify chemical or physical changes. Such changes occur naturally, as demonstrated by the vivid reds, oranges, and yellows of fall foliage caused by the breakdown of chlorophyll during senescence (Rossotti, 1985), which reveals carotenoid and anthocyanin pigments (Gan, 2008). For millennia, humans have utilized color changes to assess plant and crop health, as well as fruit ripeness. In crops, changes in leaf color from green to yellow or brown indicate nutrient shortages or environmental stress (Abadía, 1992; Ougham et al., 2008). Similar to this, as fruit ripens, it frequently exhibits a decline in chlorophyll and an increase in pigments such as carotenoids and anthocyanins, which indicate when to pick the fruit at its best (Espley and Jaakola, 2023).

Recent advancements in color sensing technology have opened new avenues for smart agriculture applications, ranging from plant health monitoring (Kuricheti and Supriya, 2019) to harvest scheduling optimization (Darwin et al., 2021). These advanced sensors can detect minute variations in leaf color, enabling assessments of water stress, nutrient deficiencies, and disease onset (Mahlein, 2016). Moreover, real-time determinations of fruit ripeness and sugar content through colorimetric sensing enhance precision agriculture and reduce waste (Li et al., 2018; Yang et al., 2021). These technological advancements facilitate accurate and timely identification of crop conditions, promoting sustainable agricultural practices and efficient decision-making and resource management (Pathan et al., 2020; Qazi et al., 2022).

Nevertheless, many agricultural sectors still lack such sensors, presenting opportunities for development. For instance, the dew retting of bast fiber plants like flax and hemp, where noticeable color changes in straw occur (Bleuze et al., 2018); and is still assessed empirically using the Fred test (Akin et al., 1996). During this decay process, surface color changes of flax/hemp straw result from the cumulative effects of chlorophyll degradation (making carotenoids more visible), enzymatic oxidation of released phenolics, microbial colonization, and the sequential degradation of plant polysaccharides. Such changes have previously been observed for hemp dew retting (Bleuze et al., 2018), where the stems experience significant color transformations during the retting process, transitioning from a vibrant green to a bright yellow within just one week. By the second week, black spots begin to appear; by the fourth week, the color shifts to pale gray with more black spots; and by the sixth week, they become dark gray with numerous black spots (Bleuze et al., 2018; Mazian et al., 2019; Bou Orm et al., 2024). A

similar pattern is found in the case of flax dew retting. However, surprisingly, to date few studies have reported this change; one such study is by (Bleuze et al., 2018), who employed colorimetry and infrared spectroscopy to analyze the CIELAB components. Stem surface color change is a promising simple measure, non-destructive parameter candidate for the basis of a reliable tool. In this study, we carry out a detailed investigation into the retting-induced color changes in flax stems for several retting cycles. The results indicate that optical spectroscopy could be a reliable parameter to determine the beginning of the optimal retting phase. The results enable one to envisage a reliable, non-invasive tool that integrates color spectroscopy, drone technology, statistical techniques, and machine learning (AI).

V.2.2. Materials and Methods

V.2.2.1. Plant sample collection and meteorological information

Refer to Section **(§) II.2.** of Chapter 2.

Flax dew retting sampling	Retting 2022 Field A	Retting 2022 Field B	Retting 2021 Field A	Retting 2021 Field B	Retting 2014
Duration (days)	55	52	25	25	44
Sampling point numbers (R)	R0 to R18	R0 to R15	R0 to R7	R0 to R7	R0 to R6
Sampling point used in color study	R0, R3, R6, R9, R13, R15 (R17, R18)	R0, R4, R7, R10, R13, R15	R0, R1, R2, R4, R6, R7	R0, R1, R2, R4, R6, R7	R0, R1, R2, R3, R4, R5, R6
In days	1, 13, 23, 34, 44, 55 (69, 90)	1, 13, 24, 34, 45, 52	1, 4, 6, 13, 18, 20, 25	1, 4, 6, 13, 18, 20, 25	1, 6, 12, 19 26, 33, 44
Total readings (SCI+SCE)	800+ 150	800	640	640	1470

Table V.1. Details of sampling from five flax dew retting experimental sets.

The number of sampling points (R) used in spectral color analysis and resulting total readings are mentioned. The over retting sampling points and respective days and readings are colored in red. Taken from **Table II.1** in material and methods, for details please check **§ II.2**, **II.11**, page 98, Chapter 2.

V.2.2.2. Collection of Spectral Readings

Refer to Section **(§) II.11.1** of Chapter 2.

V.2.2.3. Statistical analysis

Refer to Section (§) II.11.2 of Chapter 2.

V.2.3. Results

V.2.3.1. Weather details during retting

In 2021, rainfall and temperature were unevenly distributed during the retting period (23 July–16 August). The highest precipitation occurred in the first week (24–27 July), peaking at 41.8 mm on 26 July. The average temperature was 17.7°C, with a maximum of 25.5°C (23 July, 12 August, 15 August) and a minimum of 9.5°C (4 August, 11 August). The average daily rainfall was 5.67 mm (Fig. V.1.a).

In contrast, 2022 experienced significantly lower rainfall, likely extending the retting process. The maximum precipitation during retting was 5.2 mm (16 August), with only two other notable rainfall days. The average temperature during retting was 20.5°C, and the average daily rainfall was just 0.31 mm. The highest temperature during 2022 reached 38°C (19 July), while the minimum was 10.7°C (8 July). Over-retting saw the highest precipitation, with 17 mm recorded on day 60 (8 September), accompanied by an average temperature of 19.5°C and daily rainfall of 1.89 mm (Fig. V.1.b).

In 2014, rainfall was more evenly distributed, with the highest precipitation of 41.3 mm on 25 August. The maximum temperature, 29°C, was recorded on the first day of retting, while the lowest, 8.7°C, occurred on 24 August. The average temperature was 17°C, and the average daily rainfall was 3.9 mm (Fig. V.1.c).

V2.3.2. Flax stem surface color change

Our visual observation of the flax stem samples (bundle of 50-60 stems), collected at various retting stages from 2022 showed a similar color evolution as described for hemp by (Bleuze et al., 2018). Visually, the color transitions were distinct, with the stems changing from green-yellow at early stages (R0, R1) to grey (R7), and eventually to a blue-grey hue (R12, R13). Over-retted flax exhibited dark brown coloration or became black (R16, R17) (Fig. V.2).

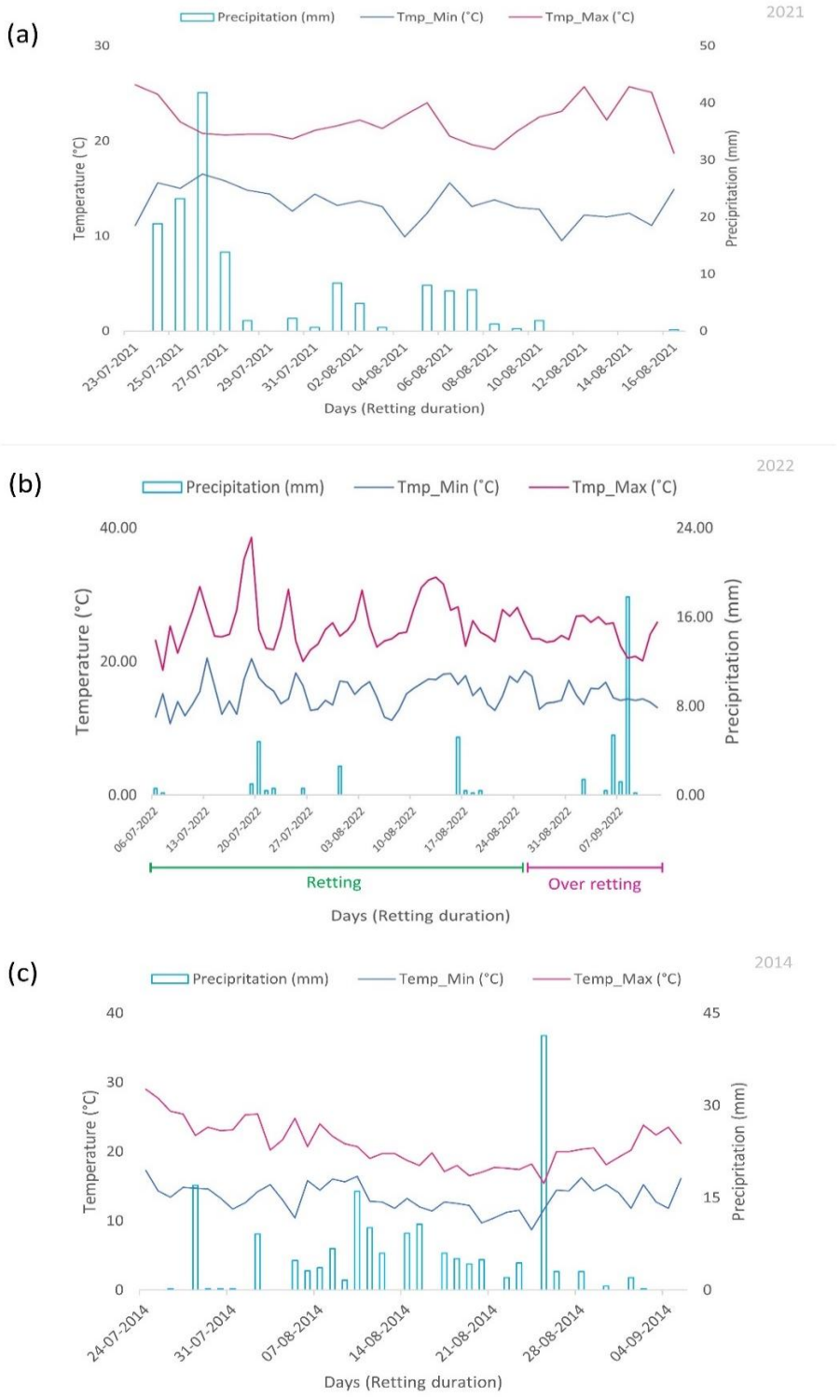

Figure V.1. Climate data (temperature and rainfall) during flax dew retting in three sampling years.

(a) Climate during the retting period in 2021 (23rd July – 16th August), data sourced from Mazinghem weather station. (b) Climate during the retting period in 2022 (6th July – 29th August, with over-retting extending until 12th September), data sourced from Bergues weather station. (c) Climate during the retting period in 2014 (24th July – 5th September), data sourced from Abbeville80 weather station. Climate website https://www.infoclimat.fr/.

Figure V.2. Photographs of flax stem bundles in various stages of retting.

These photographs are from the 2022 sampling. The flax stems were gathered periodically from 05/07/22 to 17/09/22. Photographs of straw color change are taken with NIKON D5000 (24mega-pixel, aperture f/4.8), in auto settings (ISO 400, exposure time 1/90 second) with indoor light conditions and from 90° angle to present the changes visually, for each experiment set.

V.2.3.3. *CIELab* color space results

The spectrophotometer (cm23d Konica) quantitatively measured these color changes by capturing surface reflectance data across the visual spectrum and expressing them in the CIELab color space. This system uses three values to represent color: the b* value for the blue-yellow axis (negative values indicate blue, positive indicate yellow), the a* value for the green-red axis (negative values indicate green, positive indicate red), and the L* value for lightness (ranging from 0 to 100). Its perceptually uniform design ensures consistent color representation across different devices.

In all five retting sample sets across the three years, the b* value decreased by more than half during the first and last weeks of retting (**Fig. V.3**), indicating a shift in color from yellow toward blue. Similarly, the decreasing a* values suggest a transition from a greener hue toward red. The lightness (L*) values showed more pronounced changes in longer retting experiments, such as those conducted in 2014 and 2022, compared to the shorter retting period of 2021. These findings imply that analyzing spectral data could provide insights into the degree of retting and whether a specific color (wavelength) can be associated with the optimal stop time for retting. While the *CIELab* color space with RGB data may be limiting for detecting subtle changes, it necessitates a multivariate analysis of the color data across the visual spectrum.

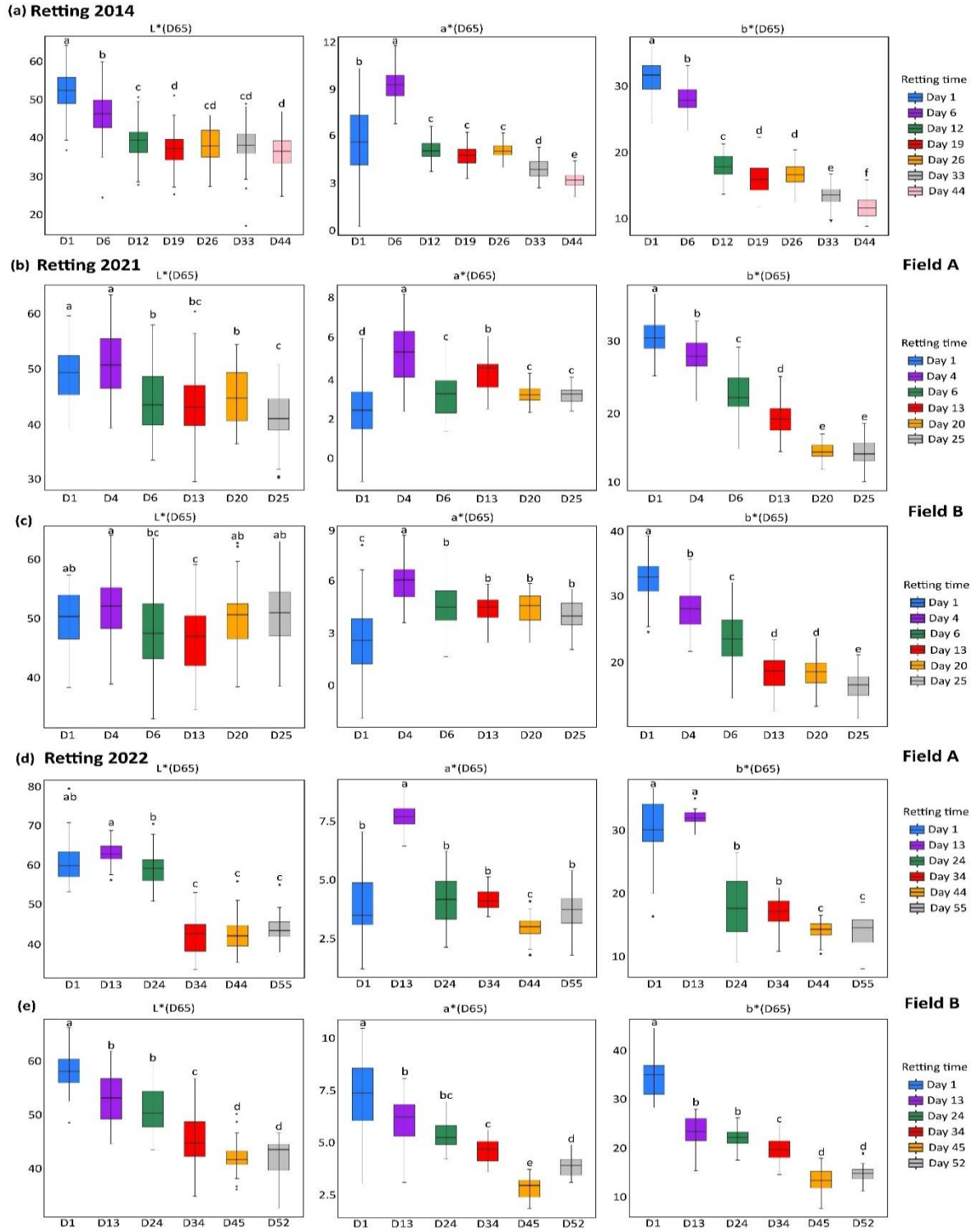

Figure V.3. Box plot of L*a*b* values of color retting samples (where L* = lightness, a* = green-redness, b* = blue-yellowness).

(a) *CIELab* color space of retting 2014; (b & c) retting 2021, field A & B; (d & e) retting 2022, field A & B. The letters represent statistical significance between days (ANOVA, Tukey's HSD test, $p \leq 0.05$).

V.2.3.4. (Multivariate analysis) Evolution of the spectral color measurements

Empirical observations combined with CIE L*a*b* color space evaluation reveal significant alterations in stem surface color during the retting process. These changes require detailed analysis across the visible spectrum to identify potential retting patterns and determine specific wavelengths responsible for these variations.

To begin, an unsupervised Principal Component Analysis (PCA) was conducted, for example, on color data set retting 2014 (44 days of retting). Scree plots indicated that selecting PC1 and PC2 would capture approximately 90% of the explained variance (Ferreira et al., 2017) (**Fig. V.4a**). Subsequently, Partial Least Squares Discriminant Analysis (PLS-DA) was applied to all wavelengths within each component. This analysis confirmed that PC1 and PC2 are effective in discriminating the various stages of color change during retting. As hypothesized, the initial stage (D1-D6) is primarily explained by the positive X2-variate from PLS-DA (30%), while the middle stage (up to D26, influenced by overlapping clouds in pls-da) and the final stage (beginning at D33) are accounted for by the positive X1-variate from PLS-DA (69%) (**Fig. V.4b**). The loadings for Comp 1 and Comp 2 (**Fig. V.4c**) allowed us to identify significant contributions and their corresponding weights, with positive (in orange) and negative (in blue) values indicating the correlation of specific wavelengths with the principal components.

Subsequently, hierarchical clustering (HC) was performed using Comp 1 and Comp 2 (**Fig. V.4d**), revealing the following patterns:

- **Early Stage:** The D1 and D6 sub-datasets differ in a reduction of wavelength contributions, initially positive (600-700 nm), particularly between 640-660 and 690-700 nm. A significant increase in contribution was observed at 520-600 nm at the end of the early stage.
- **Middle Stage:** Until D26, the contributions from the entire spectrum (400-700 nm) were regular and low.
- **Advanced Stage:** The two endpoints, D33 and D45, exhibit similar contribution patterns, which can be divided into three distinct blocks: very low (570-700 nm; 0 to -1.74 from the color key), low (530-560 nm, 0 to +1.74 from the color key), and high (400-520 nm, > +1.74 from the color key).

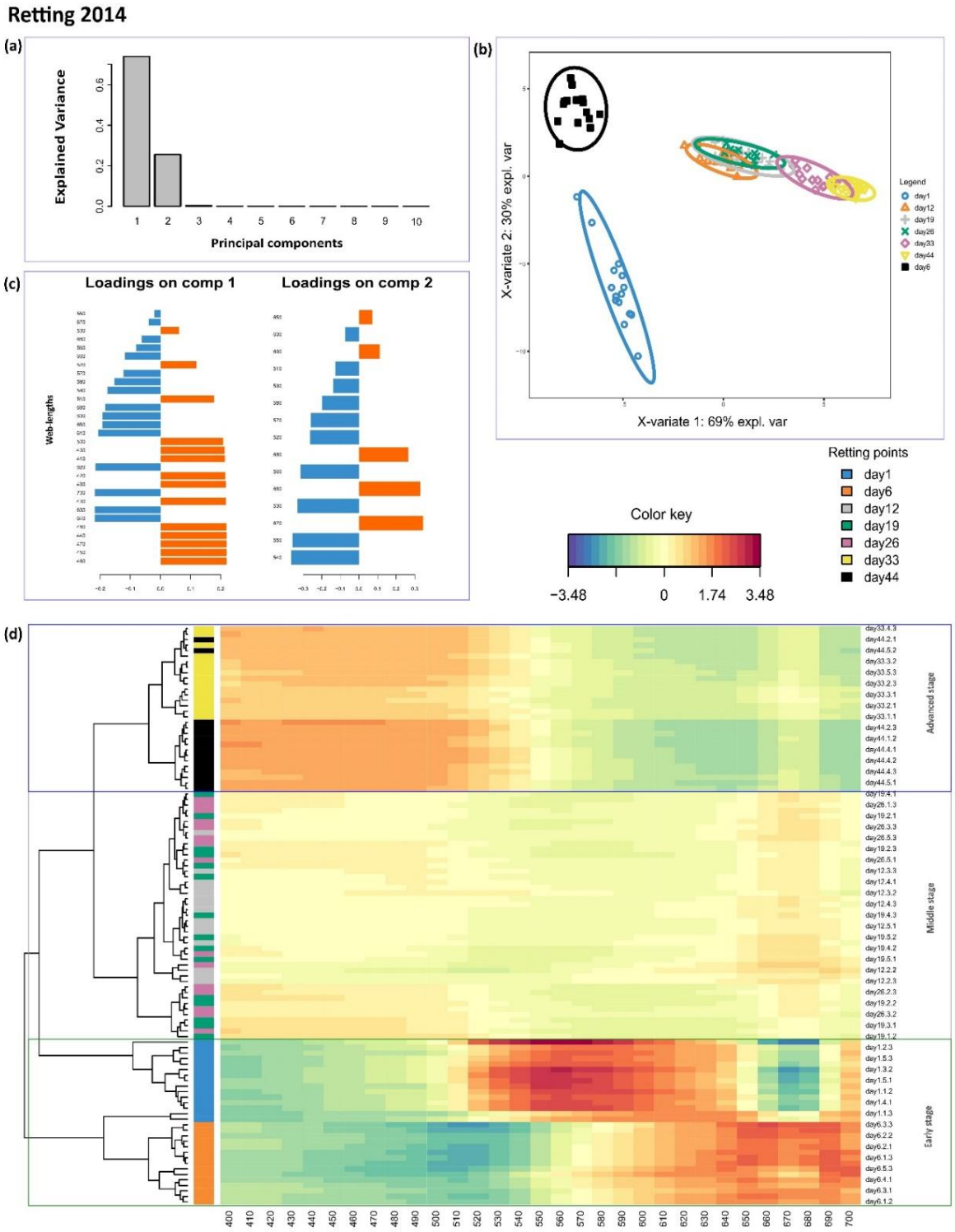

Figure V.4. Spectral analysis of retting 2014.

(a) Scree plot of PC components (1-10) of the data set; (b) PLS-DA analysis of spectral data, comp1 explains 69%, and comp2 30% of the variance in the data variables; (c) Loadings & respective wavelengths in comp1 & comp2; (d) is the clustered image mapping of color datasets according to the day (left side of the panel); the green, gray and blue rectangles represent manually distinguished Early, Middle and Advanced stages of retting based on color values.

The same analysis is conducted across all five data sets. For the color data from the 2021 retting fields A and B (25-day retting period) (**Fig. V.5** and **V.6**), similar trends are observed as in 2014. In field A, the early retting stages (D1-D4) were explained by a positive X2-variate from PLS-DA, accounting for 23% of the variation, while the later stages (D6-D25) were predominantly explained by the positive X1-variate, accounting for 74% (**Fig. V.5b**). For field B, the early stages contributed 28% to the positive X2-variate, and the later stages accounted for 70% of the positive X1- variate (**Fig. V.6b**). The clustered image analysis also shows a similar pattern where the early stage, between D1-D4, is defined with initially positive color values at 520-630, 700 nm; and also, a significantly increasing contribution at 650-680 (0 to +2 from the color key) from D1 to D4, in Field A (**Fig. V.5c**). The middle stage (D6 – D13) with regular and low contributions throughout the spectrum. And finally, the advanced stage (D20 – D25), is again divided into three distinct blocks: very low (520-640, 690-700 nm; 0 to -2 from the color key), low (650-680 nm, 0 to +1.36 from the color key), and high (400-510 nm, > +1.36 from the color key), in Filed A (**Fig. V.5c**). A similar result is found in Filed B (**Fig. V.6c**).

In the 2022 retting color data set for both Fields A and B (with 55 days of retting), a consistent pattern is observed in PLS-DA and Clustered Image Analysis (**Fig. V.7** and **V.8**). During the early stage (D1–D13), there are initially positive color values at 520-630 nm and 700 nm, with D1 showing this trend most clearly. By the end of the early stage (D13), there's a noticeable increase in color values at 640-690 nm. In the middle stage (D24-D34), the color values remain uniformly low. In the advanced stage (D45-D52/D55), there is a typical increase in color values between 400-510 nm (**Fig. V.7d** and **V.8d**).

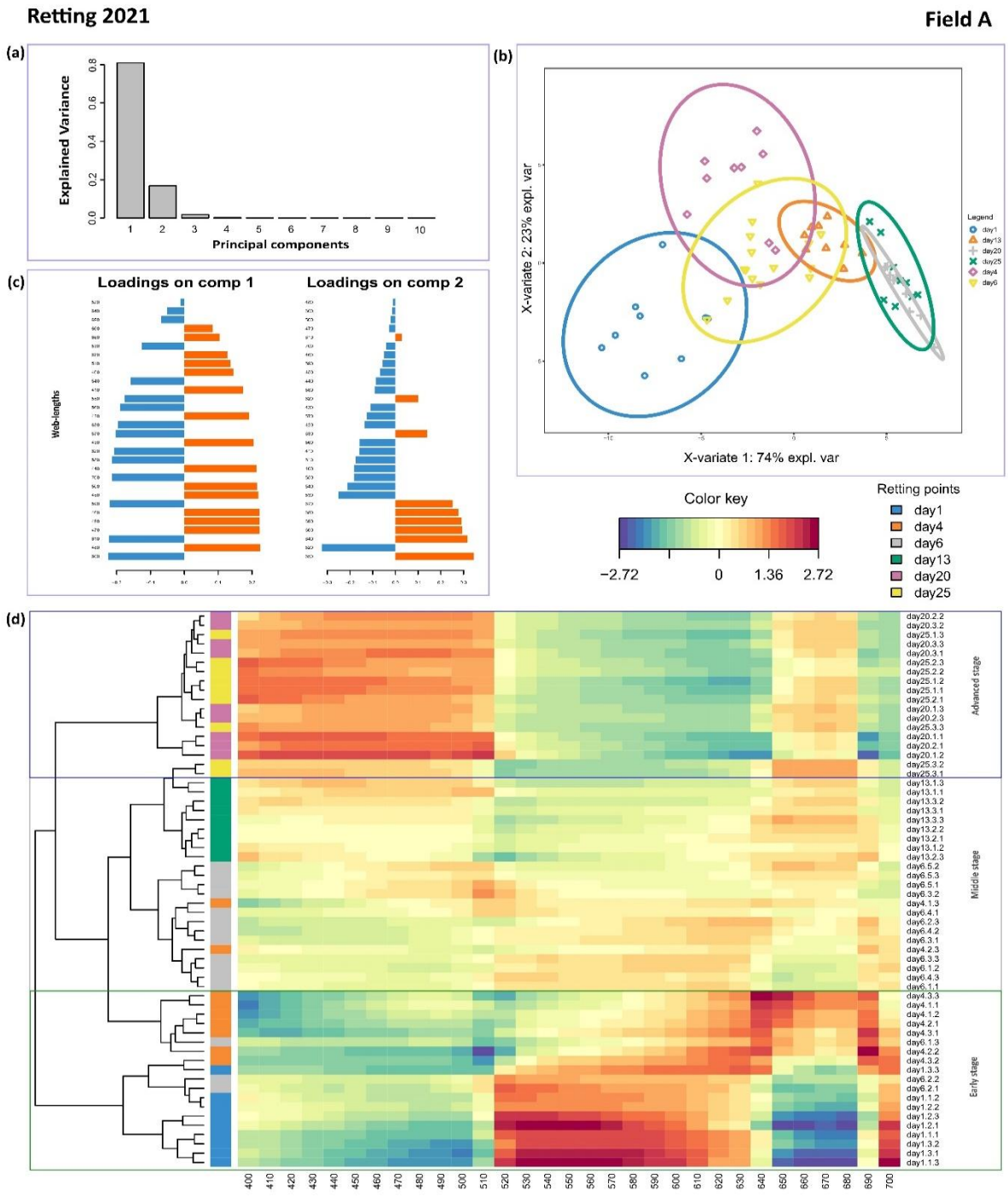

Figure V.5. Spectral analysis of retting 2021 filed A.

(a) Scree plot of PC components (1-10) of the data set; (b) PLS-DA analysis of spectral data, comp1 explains 74%, and comp2 23% of the variance in the data variables; (c) Loadings & respective wavelengths in comp1 & comp2; (d) is the clustered image mapping of color datasets according to the day (left side of the panel); the green, gray and blue rectangles represent manually distinguished Early, Middle and Advanced stages of retting based on color values.

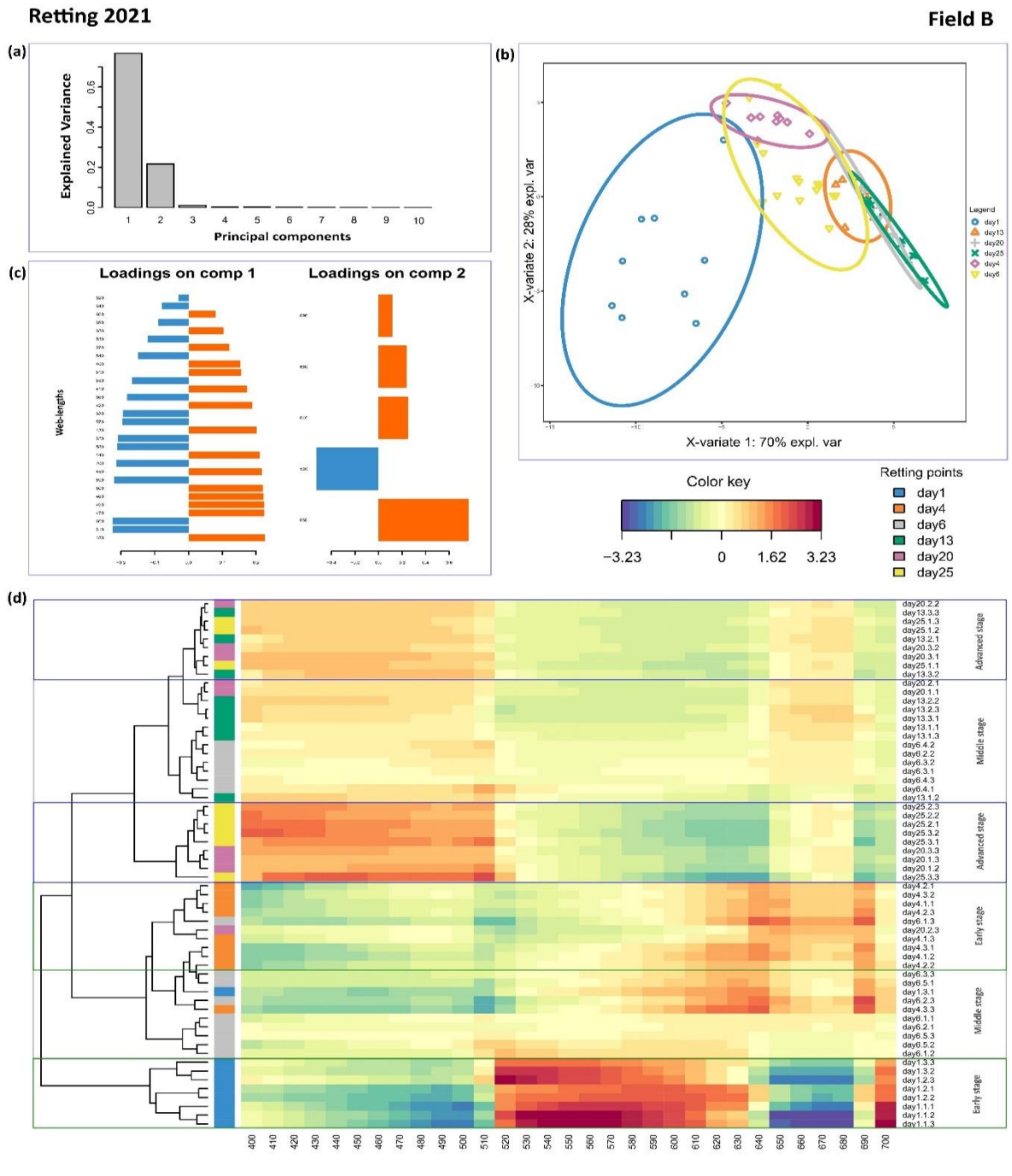

Figure V.6. Spectral analysis of retting 2021 filed B.

(a) Scree plot of PC components (1-10) of the data set; (b) PLS-DA analysis of spectral data, comp1 explains 70%, and comp2 28% of the variance in the data variables; (c) Loadings & respective wavelengths in comp1 & comp2; (d) is the clustered image mapping of color datasets according to the day (left side of the panel); the green, gray and blue rectangles represent manually distinguished Early, Middle and Advanced stages of retting based on color values.

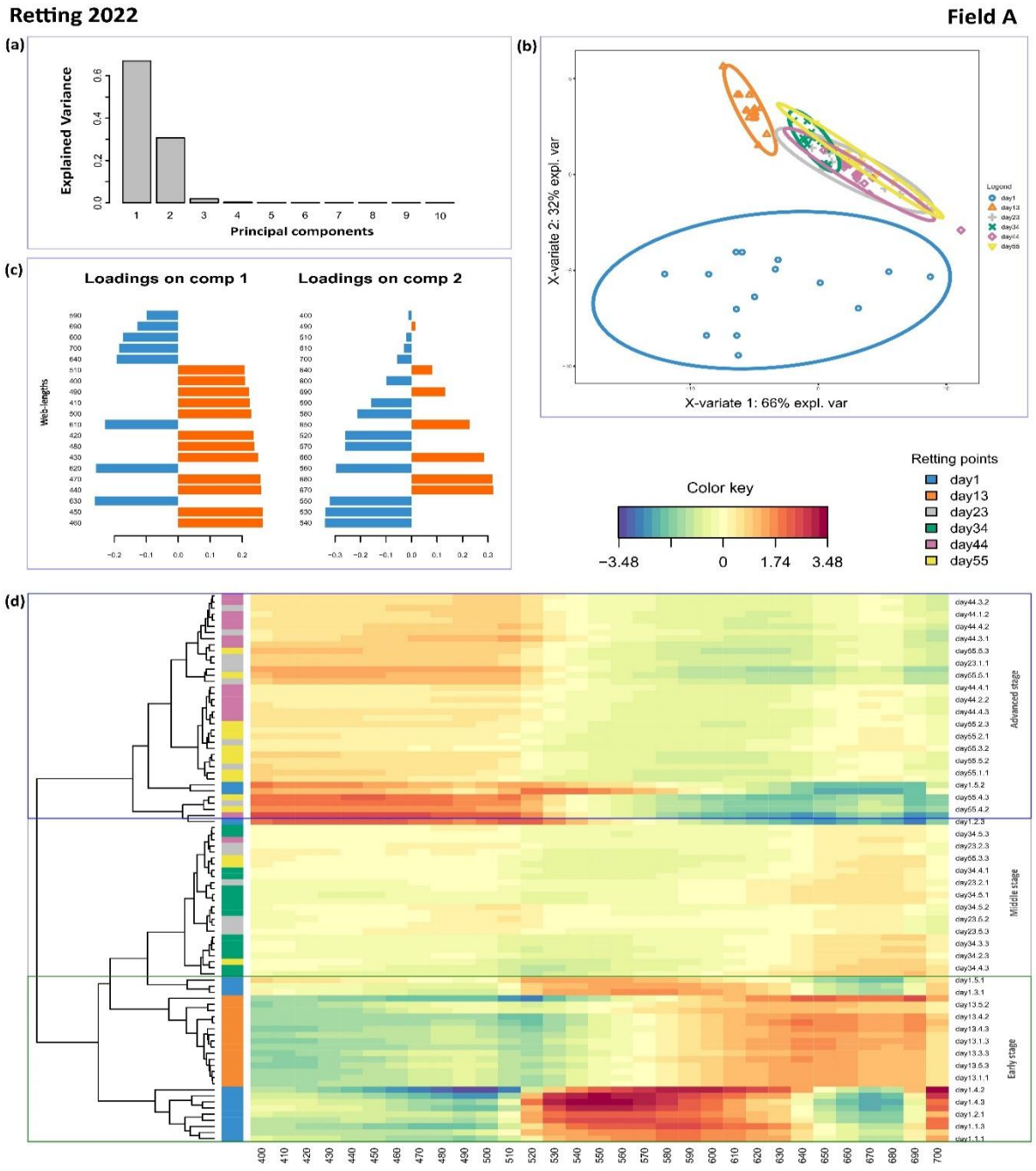

Figure V.7. Spectral analysis of retting 2022 filed A.

(a) Scree plot of PC components (1-10) of the data set; (b) PLS-DA analysis of spectral data, comp1 explains 66%, and comp2 32% of the variance in the data variables; (c) Loadings & respective wavelengths in comp1 & comp2; (d) is the clustered image mapping of color datasets according to the day (left side of the panel); the green, gray and blue rectangles represent manually distinguished Early, Middle and Advanced stages of retting based on color values.

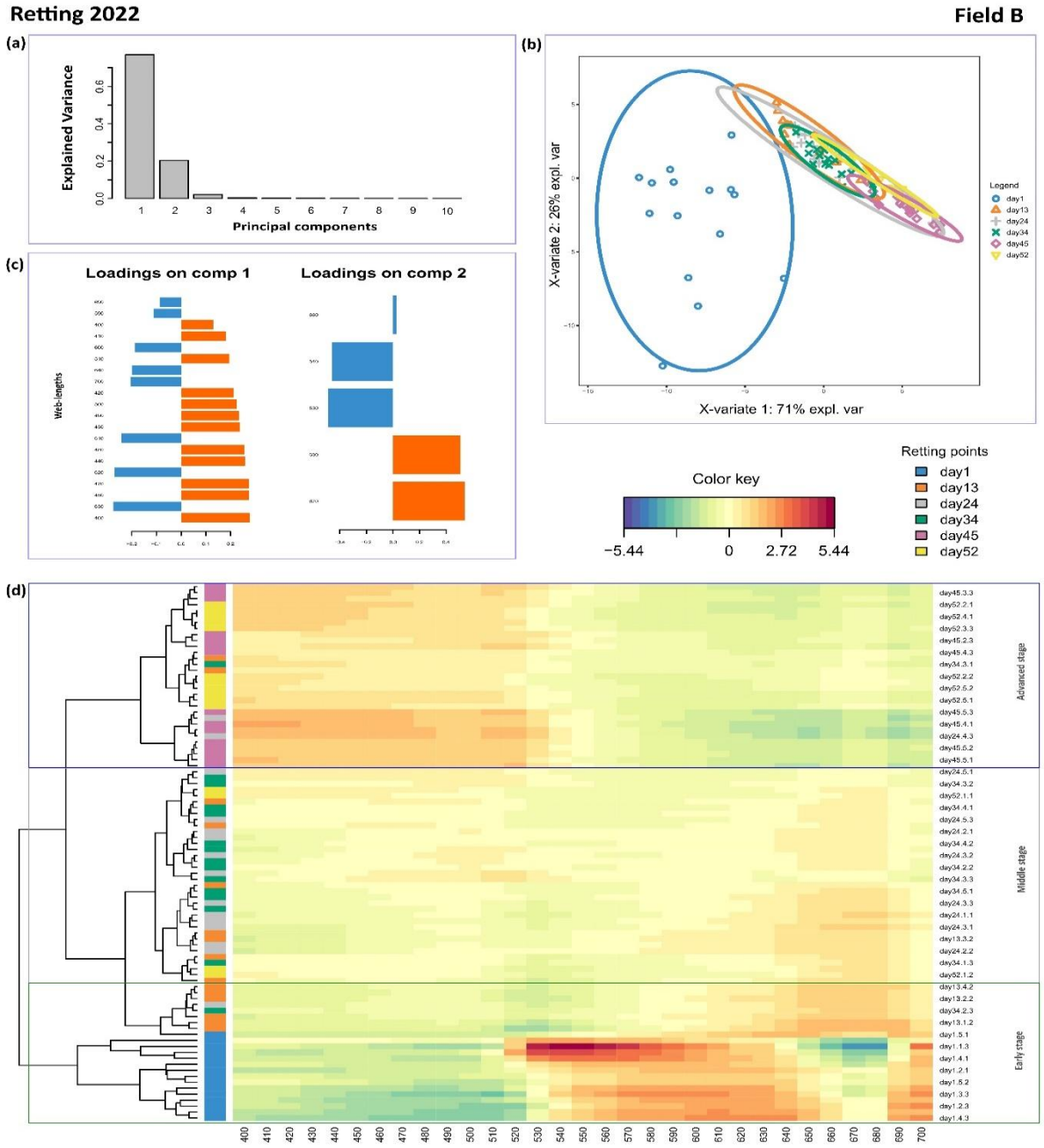

Figure V.8. Spectral analysis of retting 2022 filed B.

(a) Scree plot of PC components (1-10) of the data set; (b) PLS-DA analysis of spectral data, comp1 explains 71%, and comp2 26% of the variance in the data variables; (c) Loadings & respective wavelengths in comp1 & comp2; (d) is the clustered image mapping of color datasets according to the day (left side of the panel); the green, gray and blue rectangles represent manually distinguished Early, Middle and Advanced stages of retting based on color values.

V.2.3.5. Prediction of retting stages with confusion matrix made of selected variables (web-lengths) from pooled datasets

The loadings on component 1 from the sPLS-DA analysis of all five color datasets were compared (Table V.2), and four wavelengths (two positives, two negatives) from the top common loadings were selected (highlighted in red) to interpret the observed differences.

Wave lengths	Loadings Field -2014	Loadings Field-2021A	Loadings Field-2021B	Loadings Field-2022A	Loadings Field-2022B	Average Loading
400	0.21059421	0.16343468	0.15464563	0.20478207	0.17714951	0.182121
410	0.211449	0.17803695	0.16825297	0.20926752	0.18501682	0.190405
420	0.21293998	0.18723882	0.17874982	0.21004848	0.18975848	0.195747
430	0.215457705	0.19379504	0.1885152	0.20945191	0.19348307	0.200141
440	0.2155654	0.19836794	0.19625035	0.20917796	0.19751903	0.203376
450	0.21590655	0.2002755	0.20042067	0.20738394	0.20150891	0.205099
460	0.2157319	0.20113356	0.20344382	0.20581672	0.20504803	0.206235
480	0.21437054	0.20223418	0.20671583	0.20421261	0.21116133	0.207739
490	0.21240031	0.20186956	0.20571763	0.20341184	0.21237081	0.207154
500	0.20443597	0.19608217	0.19919075	0.2032166	0.20917521	0.20242
510	0.17723462	0.14618078	0.13907585	0.18675914	0.19399908	0.16865
560	-0.09944652	-0.1938976	-0.1962652	-0.14968233	-0.18434564	-0.16473
570	-0.13479928	-0.20009385	-0.20293757	-0.17697301	-0.20202573	-0.18337
580	-0.16135255	-0.2055176	-0.20890343	-0.20161439	-0.21351425	-0.19818
590	-0.18026739	-0.20882777	-0.0937723	-0.21986347	-0.21909868	-0.18437
600	-0.19487663	-0.21018075	-0.21222617	-0.23106285	-0.2207448	-0.21382
610	-0.20672008	-0.20675243	-0.20768433	-0.23578052	-0.21964553	-0.21532
620	-0.21276972	-0.19588843	-0.19096871	-0.23221158	-0.21505249	-0.20938
630	-0.2148749	-0.18813063	-0.17856194	-0.22456224	-0.20945389	-0.20312
640	-0.21407539	-0.10690403	-0.08894939	-0.18895062	-0.18389613	-0.15656
690	-0.18170463	-0.10707899	-0.0937723	-0.14260532	-0.15826757	-0.13669
700	-0.21329171	-0.19948015	-0.20375145	-0.19574366	-0.20663539	-0.20378

Table V.2: Loadings of principle component 1 with positive and negative contributions, from respective retting color data sets.

In the clustered image analysis of the five datasets, the samples were manually categorized into Early, Middle, and Advanced retting stages. The data for the selected wavelengths were then pooled across all datasets and renamed into six categories, S1-S6 (Table V.3), for further interpretation.

Experimental sets (pooled data renaming)	Early stage		Middle stage		Advanced stage	
	S0	S1	S2	S3	S4	S5
Retting 2014	Day1	Day6	Day12	Day26	Day33	Day44
Retting 2021 Field-A	Day1	Day4	Day6	Day13	Day20	Day25
Retting 2021 Field-B	Day1	Day4	Day6	Day13	Day20	Day25
Retting 2022 Field-A	Day1	Day13	Day23	Day34	Day44	Day55
Retting 2022 Field-B	Day1	Day13	Day24	Day34	Day45	Day52

Table V.3: Pooling of five retting color data sets (from three years with different durations) into Early, Middle, and Advanced stages based on clustered image analysis.

The pooled data was processed using the same method as before and subsequently employed to generate the clustered image analysis. This extensive pooled dataset was then utilized to create a confusion matrix in R's mixOmics package. The model was trained on the complete dataset, with one year of data excluded as the test set, and then evaluated on each year's data to produce the ROC-AUC curve. This approach allowed for assessing the model's performance across different retting stages by comparing true positive and false positive rates, with the AUC providing a comprehensive measure of classification accuracy.

The 4 variables in the pooled data set discriminate the 6 retting times points (S0-S5) with a positive 100% X1-variate from PLS-DA (**Fig. V.9a**), and the resulting clustered image analysis shows a simpler version, where **Early** sage (S0, S1) is marked with an initial positive value of 600 and 610 nm (≥1 in color scale) and negative values at 480 and 490nm (≤0 in the color scale) (**Fig. V.9c**). The **Middle** stage (S2, S3) represents the transition phase with overall low uniform values. Finally, the **Advanced** stage (S4, S5) is marked with positive values at 480 and 490nm (≥1 in the color scale) and a low to negative value of 600 and 610 nm (≤0 in the color scale) (**Fig. V.9c**).

The ROC-AUC curve, trained on the pooled data excluding the test set (e.g., Retting 2014), demonstrates the model's ability to distinguish the early stages (S1, S2) and advanced stages (S4, S5) from other stages, with a prediction score exceeding 0.9 (where a score of 1 indicates perfect distinguishability) (**Fig. V.9b**). Comparable prediction scores are achieved when the four other retting color data sets are used as test models (**Fig. V.10**).

V.2.3.6. Trend of color evolution in over-retting

The 2022 Field A samples were examined for over-retting (as detailed in the Methods section). The Cl*ab** values revealed a significant decrease in L* (lightness) and b* (yellow-blue) during the over-retting stages (D69, D90), compared to D55 (the standard industrial termination of retting), indicating that the samples become duller and bluer over time (**Fig. V.11a**). This change is distinguishable from the initial early-stage color data. Therefore, for spectral analysis, we focused on examining the changes between D34 and D90 using the same statistical pipeline as before (**Fig. V.11b**). The over-retted stage, especially D90, is primarily explained by the positive X2-variate from PLS-DA (29%). While D69 is more overlapped with D44 and D55, accounted for by the positive X1-variate from PLS-DA (70%).

The difference in D90 compared to the other days is more pronounced in the cluster image analysis (**Fig. V.11c**), showing positive values at 660-700 nm and around 400-440 nm (≥ 0 on the color scale). Interestingly, the over-retting at D69 exhibits mostly positive values (≥ 0 on the color scale) between 400-580 nm and negative values (≤ 0 on the color scale) between 590-700 nm.

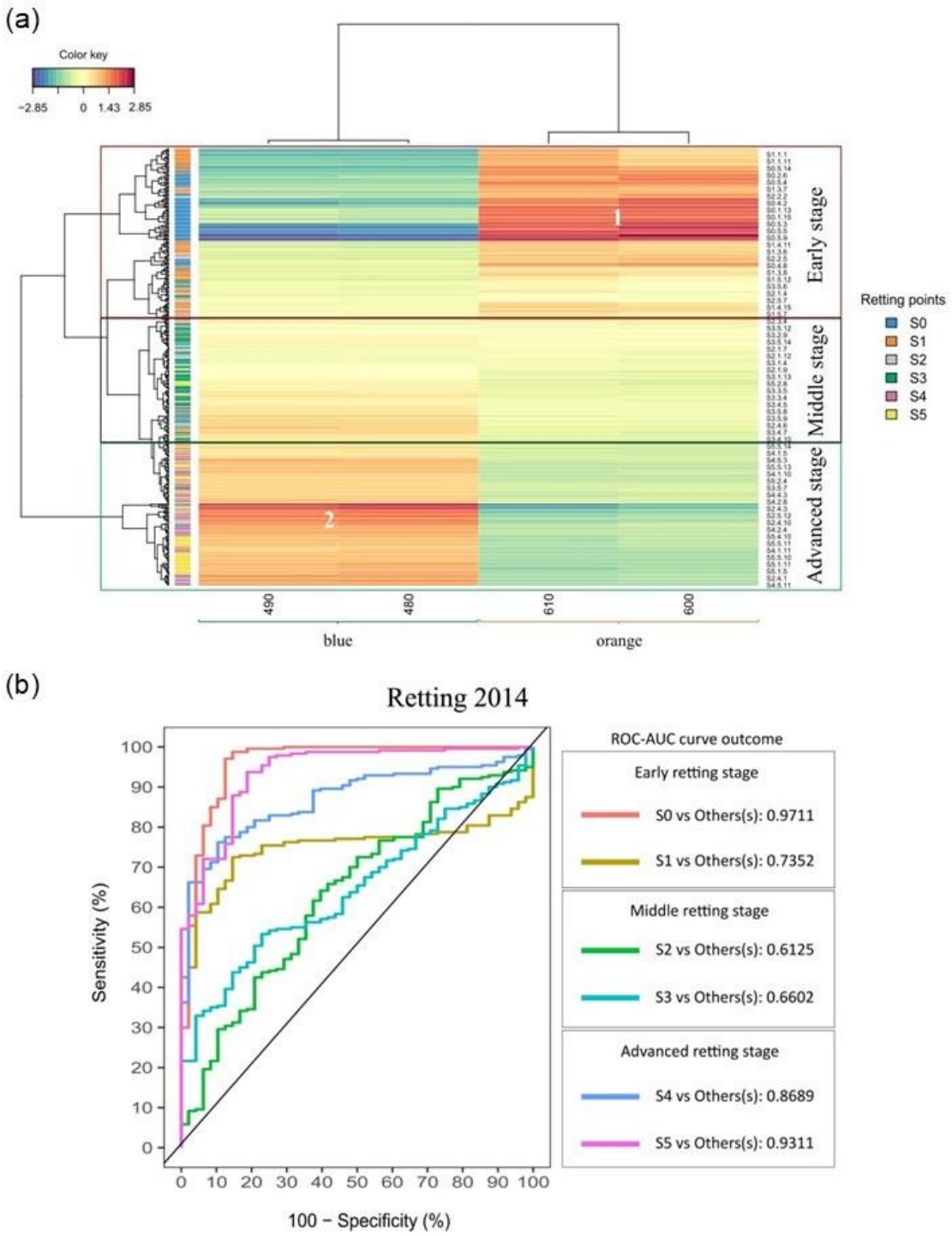

Figure V.9. Spectral analysis of pooled color data with selected four variables from comp-1, from all five retting color data sets.

(a) clustered image mapping of pooled color datasets according to the groups S0-S5 (left side of the panel); the green, gray and blue rectangles represent manually distinguished Early, Middle and Advanced stages of retting based on color values on selected wavelengths; (b) ROC curve with AUC score of retting 2014 with prediction model trained from pooled data (where 1 indicates perfect performance and 0.5 indicates random guessing).

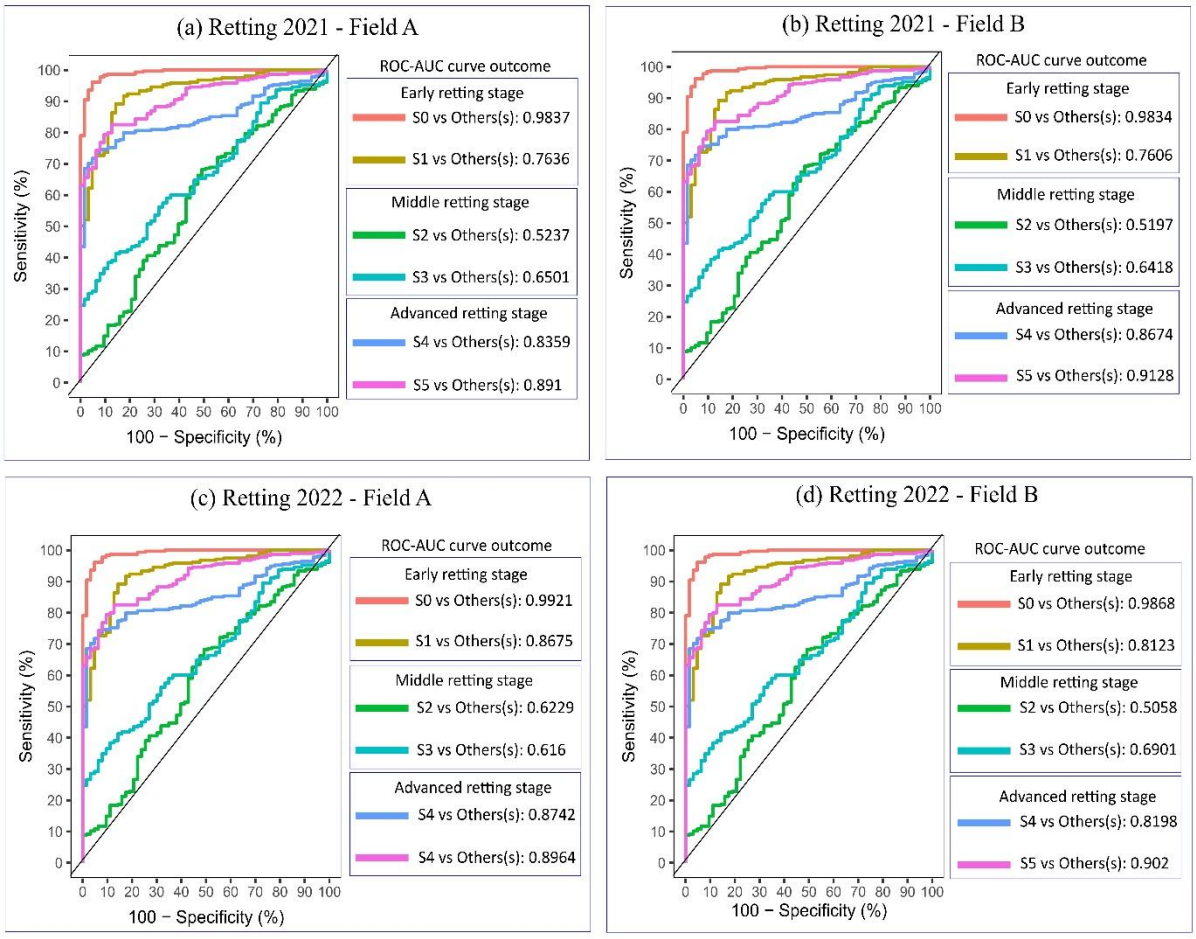

Figure V.10. ROC curve with AUC score of different retting color data sets.

(a) ROC AUC curve of retting 2021 filed A color data set; (b) retting 2021 filed B color data set; (c) retting 2022 filed A color data set. (d) retting 2022 filed B color data set, is tested with prediction model trained from pooled data (where 1 indicates perfect performance and 0.5 indicates random guessing).

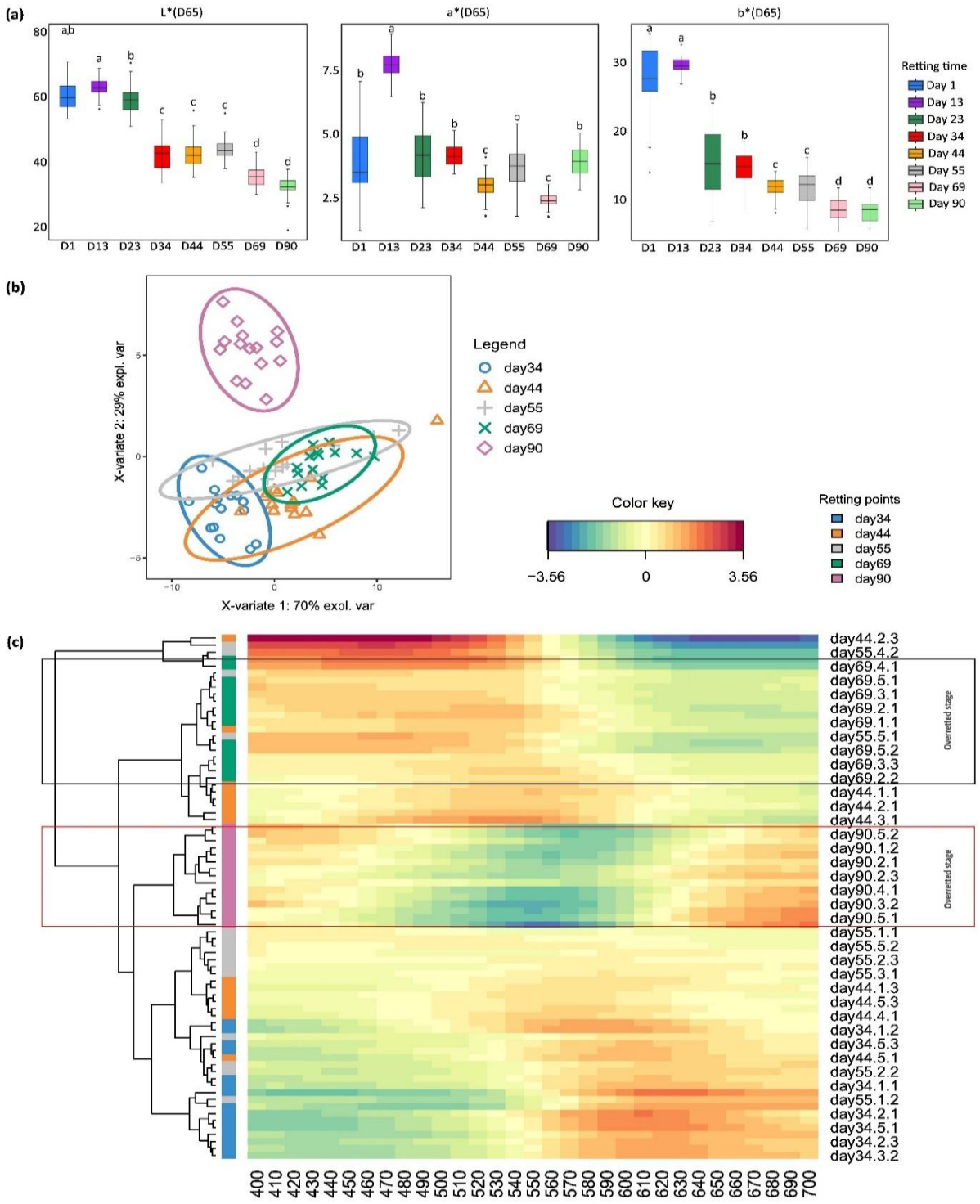

Figure V.11: Spectral analysis of color data from retting 2022 Field A with over-retted samples.

(a) Box plot of Cl*a*b* values (ANOVA, Tukey's HSD test, $p \leq 0.05$). b) PLS-DA analysis of spectral data, comp1 explains 70% and comp2 29% of the variance in the data variables; (c) is the clustered image mapping color retting 20222 Filed A datasets, including over retting, according to the days (left side of the panel); the black and red rectangles represent over retting samples from D69 and D90 respectively.

V.2.4. Discussions

The observed color changes during retting are primarily due to variations in light reflectance within the visible spectrum by the sample surface (Wyszecki and Stiles, 2000). When the surface absorbs all wavelengths except those between 380-459 nm, the sample appears violet. Similarly, wavelengths in the range of 450-495 nm result in a blue appearance, around 500 nm in cyan, 495-570 nm in green, 570-590 nm in yellow, 590-620 nm in orange, and 620-700 nm in red. The CIELAB color space simplifies these color changes during flax dew retting into three components: red-green (a*), yellow-blue (b*), and lightness (L*) values.

Although previous research has addressed subjective color changes on flax and hemp stem surfaces during retting (Mazian et al., 2019; Bou Orm et al., 2024), objective studies have focused on color changes in extracted retted fibers. (Akin et al., 2000; Chabbert et al., 2020). However, a few studies have quantified the color changes on stem surfaces using colorimetry during retting (Bleuze et al., 2018). According to visual observations, stem samples initially present a Vivid green color, which turns Bright yellow within the first week. By the second week, black spots begin to appear, and by the fourth week, the appearance shifts to pale gray with additional black spots. By the sixth week, the stems become dark gray with numerous black spots (Bleuze et al., 2018; Bou Orm et al., 2024; Mazian et al., 2019). Our

study shows a similar evolution of the stem surface color during retting (**Fig. V.2**), consistent with these earlier findings. The literature claims that a mix of biological and chemical processes causes the dying plants' color to change during the dew retting process. Chlorophyll, the pigment that gives plants their green hue, breaks down (releasing the pyrrole rings) as a plant senses or dies, causing a noticeable change to yellow, orange, or brown. Enzymatic processes and environmental stressors like sun exposure and oxidation cause this degradation, which turns chlorophyll into non-colored molecules and makes other pigments like carotenoids more noticeable (Hu et al., 2021; Sousa, 2022). Microbial action during retting further speeds up these modifications. Phenolic chemicals are released when bacteria and fungi break down structural elements such pectin, xyloglucans and lignin, further oxidizing and darkening the surface of the stem (Chowdhary et al., 2021). Reactive oxygen species produced during this breakdown add to oxidative browning, which intensifies the darkening over time (Hu et al., 2021). Additional environmental influences on these alterations include moisture, UV radiation, and atmospheric oxygen. These interplaying biological and chemical processes can explain the gradual color change in the stems of retted plants but certainly need to be studied in the context of flax retting.

The analysis of CIELAB color components for hemp stem surfaces during retting shows that the L* value decreases by 18.5%, reflecting the transition from bright to pale and eventually to darker colors. The a* and b* values decline by 32.2% and 32.4%, respectively, approaching zero, which

corresponds to the color shift from green to gray (achromatic) (Bleuze et al., 2018). In our study, encompassing five retting sets over three years, we observed that the a* and b* values decreased by more than 50% from the start to the end of retting. Although the L* value showed a general decreasing trend, this was not consistent across the three years of retting samples. These changes align with the visual observations noted earlier and are likely due to the degradation of plant pigments through photodegradation, biodegradation, and microbial colonization. The appearance of black spots is attributed to microbial colonization, as noted in previous hemp dew-retting studies (Akin et al., 1998; Bleuze et al., 2018; Jankauskienė and Gruzdevienė, 2013).

Revisiting the original spectral data from the CIELAB color space analysis and examining the entire visual spectrum in detail reveals a consistent pattern of wavelength changes during retting. This pattern is very similar across all five experimental sets from three years of retting samples, highlighting key wavelengths that account for most of the observed changes. Specifically, we found that during retting, the values at 480 nm and 490 nm increase from the early to advanced stages, while the values at 600 nm and 610 nm decrease. This change is readily identifiable using a confusion matrix trained with pooled data sets, suggesting the potential for an automated color sensor capable of predicting transitions from early to middle to advanced stages of dew retting.

Further examination of over-retted samples from one year shows that color changes in the stem surface continue in a distinctive manner beyond the advanced stage. By day 69, the values at 480 nm and 490 nm continue to remain positive. Concurrently, the values at 600 nm and 610 nm decrease, reflecting a reduction in the orange-red component. However, with prolonged retting, both ends of the visible spectrum show positive values, indicating a indicating an ongoing shift towards a bluish or bluish-purple hue on the stem surfaces. The CIELAB values for these samples display the lowest L* value, indicating a duller and darker appearance, along with the lowest a* and b* values, which further represent this bluish shift.

V.2.5. Conclusions

The dynamics of stem surface color change during retting is not scientifically well explored but has an industrial interest as it is an essential means for following retting by experts. Reading the stem color change with Cl*a*b* color space values with a portable spectrophotometer reveals the visually recognized patterns of changes in a quantitative digital form which is again limited to RGB colors and not a perfect means to detect small color changes, throughout the visual spectrum. The critical analysis of large 3-year data sets and 5 retting sets of color data helps us to conclude, that color change can help to follow retting in events, not with precision. Following specific web lengths, for example, increasing values at 480 and 490 nm (between 1 to 2.85 in the color scale) can indicate an advanced stage of retting

(with a predictive score > 0.9) and indicate the retting might finish in the following week. With more years of data, a better predictive model could work with better precision (predictive score = 1).

While the current analysis highlights the potential of an automated color sensor to monitor retting progress by tracking spectral changes, it is important to consider other environmental factors that may influence these observations. Factors such as humidity and temperature could play a significant role in altering the spectral characteristics of the stem surfaces during retting. For instance, variations in humidity might affect the rate of microbial colonization, which in turn could impact the observed color changes. Similarly, temperature fluctuations could accelerate or slow down the biochemical processes responsible for pigment degradation, leading to variations in the timing and intensity of the color shifts.

Exploring these environmental variables in conjunction with spectral data could provide a more comprehensive understanding of the retting process. It may also enhance the accuracy of the automated sensor by accounting for conditions that could otherwise introduce variability into the measurements. Future research in this direction could refine the sensor's predictive capabilities, making it more robust and reliable across different retting environments. This would be particularly valuable for industrial applications where consistent fiber quality is critical, regardless of the specific environmental conditions present during retting.

Key Findings:

- Flax straw color changes during retting are quantifiable and follow a distinct, stage-specific pattern.
- Specific wavelengths (e.g., 490 nm and 610 nm) enable easy, non-destructive monitoring of retting, revealing early, middle, and advanced stages.

V.3. Reference:

Abadía, J., 1992. Leaf responses to Fe deficiency: A review. Journal of Plant Nutrition 15, 1699–1713. https://doi.org/10.1080/01904169209364432

Akin, D.E., 2013. Linen Most Useful: Perspectives on Structure, Chemistry, and Enzymes for Retting Flax. ISRN Biotechnology 2013, 1–23. https://doi.org/10.5402/2013/186534

Akin, D.E., Epps, H.H., Archibald, D.D., Sharma, H.S.S., 2000. Color Measurement of Flax Retted by Various Means. Textile Research Journal 70, 852–858. https://doi.org/10.1177/004051750007001002

Akin, D.E., Gamble, G.R., Morrison III, W.H., Rigsby, L.L., Dodd, R.B., 1996. Chemical and Structural Analysis of Fibre and Core Tissues from Flax. Journal of the Science of Food and Agriculture 72, 155–165. https://doi.org/10.1002/(SICI)1097-0010(199610)72:2<155::AID-JSFA636>3.0.CO;2-X

Akin, D.E., Rigsby, L.L., Henriksson, G., Eriksson, K.-E.L., 1998. Structural Effects on Flax Stems of Three Potential Retting Fungi. Textile Research Journal 68, 515–519. https://doi.org/10.1177/004051759806800708

Baley, C., 2002. Analysis of the flax fibres tensile behaviour and analysis of the tensile stiffness increase. Composites Part A: Applied Science and Manufacturing 33, 939–948. https://doi.org/10.1016/S1359-835X(02)00040-4

Bleuze, L., Lashermes, G., Alavoine, G., Recous, S., Chabbert, B., 2018. Tracking the dynamics of hemp dew retting under controlled environmental conditions. Industrial Crops and Products 123, 55–63. https://doi.org/10.1016/j.indcrop.2018.06.054

Bou Orm, E., Sutton-Charani, N., Bayle, S., Benezet, J.-C., Bergeret, A., Malhautier, L., 2024. Influence of field retting on physicochemical and biological properties of “Futura 75” hemp stems. Industrial Crops and Products 214, 118487. https://doi.org/10.1016/j.indcrop.2024.118487

Bratt, R.P., Mercer, P.C., Brown, A.E., 1988. Degradation of flax stems by Botrytis cinerea. Transactions of the British Mycological Society 90, 537–544. https://doi.org/10.1016/S0007-1536(88)80004-4

Brown, A.E., Sharma, H. s. s., 1984. Production of polysaccharide-degrading enzymes by saprophytic fungi from glyphosate-treated flax and their involvement in retting. Annals of Applied Biology 105, 65–74. https://doi.org/10.1111/j.1744-7348.1984.tb02803.x

Brown, A.E., Sharma, H.S.S., Black, D.L.R., 1986. Relationship between pectin content of stems of flax cultivars, fungal cell wall-degrading enzymes and pre-harvest retting. Annals of Applied Biology 109, 345–351. https://doi.org/10.1111/j.1744-7348.1986.tb05326.x

Chabbert, B., Padovani, J., Djemiel, C., Ossemond, J., Lemaître, A., Yoshinaga, A., Hawkins, S., Grec, S., Beaugrand, J., Kurek, B., 2020. Multimodal assessment of flax dew retting and its functional impact on fibers and natural fiber composites. Industrial Crops and Products 148, 112255. https://doi.org/10.1016/j.indcrop.2020.112255

Chand, N., Fahim, M., 2020. Tribology of Natural Fiber Polymer Composites. Woodhead Publishing.

Chowdhary, V., Alooparampil, S., Pandya, R.V., Tank, J.G., 2021. Physiological function of phenolic compounds in plant defense system. Phenolic compounds-chemistry, synthesis, diversity, non-conventional industrial, pharmaceutical and therapeutic applications.

Darwin, B., Dharmaraj, P., Prince, S., Popescu, D.E., Hemanth, D.J., 2021. Recognition of Bloom/Yield in Crop Images Using Deep Learning Models for Smart Agriculture: A Review. Agronomy 11, 646. https://doi.org/10.3390/agronomy11040646

Djemiel, C., Grec, S., Hawkins, S., 2017. Characterization of Bacterial and Fungal Community Dynamics by High-Throughput Sequencing (HTS) Metabarcoding during Flax Dew-Retting. Frontiers in Microbiology 8. https://doi.org/doi.org/10.3389/fmicb.2017.02052

Donaghy, J.A., Boomer, J.H., Haylock, R.W., 1992. An assessment of the quality and yield of flax fiber produced by the use of pure bacterial cultures in flax rets. Enzyme and Microbial Technology 14, 131–134. https://doi.org/10.1016/0141-0229(92)90170-S

Espley, R.V., Jaakola, L., 2023. The role of environmental stress in fruit pigmentation. Plant, Cell & Environment 46, 3663–3679. https://doi.org/10.1111/pce.14684

Ferreira, K.B., Oliveira, A.G.G., Gonçalves, A.S., Gomes, J.A., 2017. Evaluation of Hyperspectral Imaging Visible/Near Infrared Spectroscopy as a forensic tool for automotive paint distinction. Forensic Chemistry 5, 46–52. https://doi.org/10.1016/j.forc.2017.06.001

Gan, S., 2008. Annual Plant Reviews, Senescence Processes in Plants. John Wiley & Sons.

Gomez-Campos, A., Vialle, C., Rouilly, A., Sablayrolles, C., Hamelin, L., 2021. Flax fiber for technical textile: A life cycle inventory. Journal of Cleaner Production 281, 125177. https://doi.org/10.1016/j.jclepro.2020.125177

Hu, X., Gu, T., Khan, I., Zada, A., Jia, T., 2021. Research Progress in the Interconversion, Turnover and Degradation of Chlorophyll. Cells 10, 3134. https://doi.org/10.3390/cells10113134

Jankauskienė, Z., Gruzdevienė, E., 2013. Physical parameters of dew refitted and water refitted hemp (Cannabis sativa L.) fibres. Zemdirbyste-Agriculture 100, 71–80.

Kuricheti, G., Supriya, P., 2019. Computer Vision Based Turmeric Leaf Disease Detection and Classification: A Step to Smart Agriculture, in: 2019 3rd International Conference on Trends in Electronics and Informatics (ICOEI). Presented at the 2019 3rd International Conference on Trends in Electronics and Informatics (ICOEI), pp. 545–549. https://doi.org/10.1109/ICOEI.2019.8862706

Li, B., Lecourt, J., Bishop, G., 2018. Advances in Non-Destructive Early Assessment of Fruit Ripeness towards Defining Optimal Time of Harvest and Yield Prediction—A Review. Plants 7, 3. https://doi.org/10.3390/plants7010003

Mahlein, A.-K., 2016. Plant Disease Detection by Imaging Sensors – Parallels and Specific Demands for Precision Agriculture and Plant Phenotyping. Plant Disease 100, 241–251. https://doi.org/10.1094/PDIS-03-15-0340-FE

Mazian, B., Cariou, S., Chaignaud, M., Fanlo, J.-L., Fauconnier, M.-L., Bergeret, A., Malhautier, L., 2019. Evolution of temporal dynamic of volatile organic compounds (VOCs) and odors of hemp stem during field retting. Planta 250, 1983–1996. https://doi.org/10.1007/s00425-019-03280-6

Meijer, W.J.M., Vertregt, N., Rutgers, B., van de Waart, M., 1995. The pectin content as a measure of the retting and rettability of flax. Industrial Crops and Products 4, 273–284. https://doi.org/10.1016/0926-6690(95)00041-0

Mohanty, A.K., Misra, M., Hinrichsen, G., 2000. Biofibres, biodegradable polymers and biocomposites: An overview. Macromolecular Materials and Engineering 276–277, 1–24. https://doi.org/10.1002/(SICI)1439-2054(20000301)276:1<1::AID-MAME1>3.0.CO;2-W

Ougham, H., Thomas, H., Archetti, M., 2008. The Adaptive Value of Leaf Colour. The New Phytologist 179, 9–13.

Pathan, M., Patel, N., Yagnik, H., Shah, M., 2020. Artificial cognition for applications in smart agriculture: A comprehensive review. Artificial Intelligence in Agriculture 4, 81–95. https://doi.org/10.1016/j.aiia.2020.06.001

Qazi, S., Khawaja, B.A., Farooq, Q.U., 2022. IoT-Equipped and AI-Enabled Next Generation Smart Agriculture: A Critical Review, Current Challenges and Future Trends. IEEE Access 10, 21219–21235. https://doi.org/10.1109/ACCESS.2022.3152544

Reid, T., 1810. An Inquiry Into the Human Mind .. 6th Ed. Bell&Bradfute.

Rossotti, H., 1985. Colour: Why the World Isn't Grey. Princeton University Press.

Seaby, D.A., Mercer, P.C., 1984. Development of a hand tool to test the degree of retting of flax straw. Annals of Applied Biology 104, 567–573. https://doi.org/10.1111/j.1744-7348.1984.tb03040.x

Sharma, H.S.S., Faughey, G.J., 1999. Comparison of subjective and objective methods to assess flax straw cultivars and fibre quality after dew-retting. Annals of Applied Biology 135, 495–501. https://doi.org/10.1111/j.1744-7348.1999.tb00879.x

Sousa, C., 2022. Anthocyanins, Carotenoids and Chlorophylls in Edible Plant Leaves Unveiled by Tandem Mass Spectrometry. Foods 11, 1924. https://doi.org/10.3390/foods11131924

Wang, Q., Chen, H., Fang, G., Chen, A., Yuan, P., Liu, J., 2017. Isolation of Bacillus cereus P05 and Pseudomonas sp. X12 and their application in the ramie retting. Industrial Crops and Products 97, 518–524. https://doi.org/10.1016/j.indcrop.2016.12.047

Wyszecki, G., Stiles, W.S., 2000. Color Science: Concepts and Methods, Quantitative Data and Formulae. John Wiley & Sons.

Yang, X., Liu, G., He, J., Kang, N., Yuan, R., Fan, N., 2021. Determination of sugar content in Lingwu jujube by NIR–hyperspectral imaging. Journal of Food Science 86, 1201–1214. https://doi.org/10.1111/1750-3841.15674

CHAPTER VI

Discussion, Conclusion, and Perspective

Chapter VI: Overall Discussion, Conclusion, and Perspective of the Thesis

Contents

Chapter VI: Overall Discussion, Conclusion, and Perspective of the Thesis 239
VI.1. Discussion 240
VI.1.1. Context: 240
VI.1.2. Breakthrough in understanding the biology of retting thanks to a combination of enzymatic, wet chemistry and metaproteomic approaches 240
VI.1.3. Question the relevance of using vibrational spectral approaches (with RAMAN/FT-IR) to provide a tool (at the level of chemical bonds) for monitoring retting in the field. 244
VI.1.4. Objective-III: Assess the feasibility of using physical color changes in flax stems, analyzed through a simple spectroscopic approach (spectral color analysis), to monitor retting in the field. 246
VI.1.5. Building a toolbox by combining literature, biological, spectral, and physical results... 246
VI.2. General Conclusion of the Thesis 249
VI.3. Perspective of the Thesis 250
VI.4. References 252

VI.1. Discussion

VI.1.1. Context:

The "FlaxTronic" project aims to establish a more scientific approach to evaluating retting progress, moving beyond empirical methods by identifying reliable biological, spectral, and physical markers. The primary objective is to deepen the understanding of the biological/chemical/physical aspects of dew retting and address the variability introduced during the process. To achieve this, four key objectives were defined: (1) exploring the biological basis of retting variability, (2) assessing the relevance of vibrational spectroscopy (e.g., Raman/FTIR) for monitoring retting in the field, (3) evaluating the feasibility of using spectral changes, such as stem color, to track retting progress, and (4) proposing a toolbox that integrates biological, spectral, and physical approaches (**Chapter I**). These objectives were pursued through three experimental approaches: combination of enzymology, wet chemistry and metaproteomics (**Chapter III**), vibrational spectroscopy (**Chapter IV**), and visual color spectrometry (**Chapter V**) (**Fig. VI.I**). Each approach plays a critical role in addressing the objectives, offering valuable insights into the mechanisms of retting and presenting potential tools for its monitoring. The results of these experiments are discussed below, individually, within the broader context of the FlaxTronic project's overarching goals, the potential development of the "FlaxTronic" toolbox.

The following sections (VI.2 and VI.3) will detail the outcomes of these experiments, culminating in concluding remarks that explore technological perspectives.

VI.1.2. Breakthrough in understanding the biology of retting thanks to a combination of enzymatic, wet chemistry and metaproteomic approaches

The biology of retting involves microbial degradation of plant stem tissues through the secretion of enzymes, a process explored in various studies (Bleuze et al., 2018; Chabbert et al., 2020; Djemiel, 2017; Mazian, 2018). Recent metabarcoding analyses (Chabbert et al., 2020; Djemiel et al., 2017) have highlighted the microbial composition of retting, showing a predominance of fungal species (215 fungal and 95 bacterial species). Despite advances in understanding global enzyme dynamics during flax retting, such as the activity of pectinases and glucosidases (Chabbert et al., 2020), no specific enzymes responsible for these global activities were identified. Our study addresses for the first time the missing link between global activities, cell-wall composition, enzymes (CAZymes), and the microorganisms that produced them. Moreover, our study underlines the power of metaproteomics to reveal new enzymes and their dynamic enzyme strategies involved in lignocellulose deconstruction during flax dew retting (**Chapter III**; Mukherjee et al., 2024, https://doi.org/10.1016/j.indcrop.2024.119907).

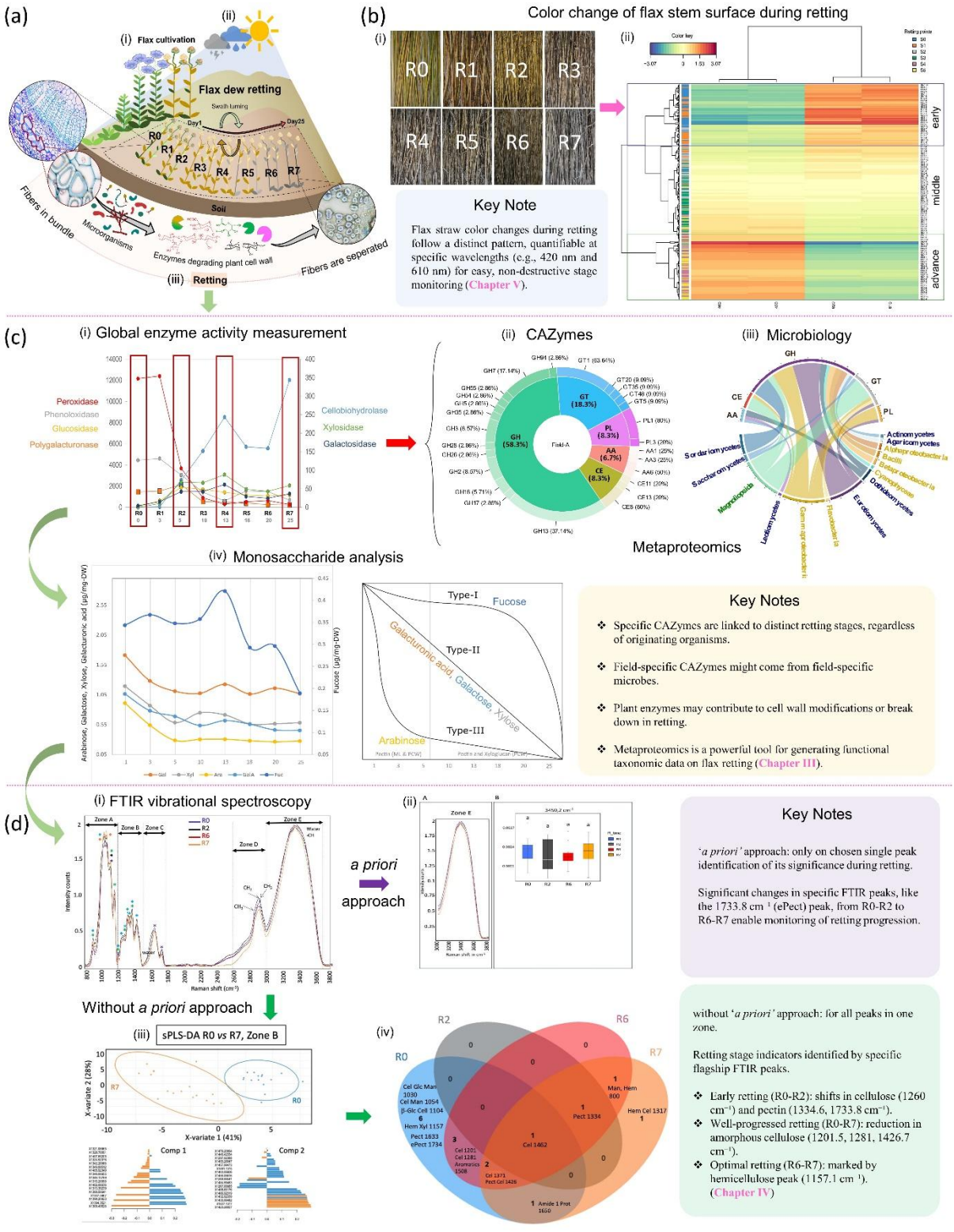

Figure. VI.1. Biology of Retting and the Search for Retting Markers.

(a) dew retting and sampling; (b) quantifying flax stem surface color change during dew retting (detailed in chapter V); (c) enzyme dynamics with metaproteomics and biochemical changes during retting (detailed in Chapter III); (d) FTIR vibrational spectroscopy to follow retting progress (detailed in Chapter IV).

By integrating functional taxonomic data, we successfully bridge the gap between the microbial community and the global enzyme activities observed in previous studies. To establish a framework for metaproteomic analysis, we first tracked the activity of seven key enzyme groups using spectrophotometric and fluorometric assays [as described in (Chabbert et al., 2020)]. This provided insights into global enzyme dynamics and enabled us to select four key retting time points for in-depth proteomic analysis (**Fig.VI.I C(i)**), which correspond to the start point (R0), the beginning (R2), the intermediate corresponding to the turning of the swaths (R4) and the end (R7). Including the intermediate retting points could have refined the kinetics, but we do not believe that this would have allowed other proteins to be identified. Metaproteomics data not shown for point R6 on field B show, for example, that no differentially abundant proteins between R6 and R7 could be identified, and that the points chosen for the metaproteomics are the main stages in the retting process. In addition, this would undoubtedly have added complexity to the analysis and significant additional analysis costs.

This study focused exclusively on the outer tissue (manually extracted) of flax stems, containing the bast fibers while discarding the woody core. Adapted from the same strategy chosen by Chabbert et al, 2020, based on the experience of the hemp retting study (Bleuze et al, 2017), which showed that including the whole stem for global enzymatic activities reduced the significance of what can be observed in external tissues. The limitation of this strategy is that the degradation of the woody part is not considered. Focusing on the external issues is a way to focus on what happens to the fiber surrounding environment and the enzymes that can directly affect fiber quality. In another study, it will also be interesting to focus on the internal tissues because their organization is different, mainly consisting of lignified secondary xylem, the enzymatic cocktail capable of degrading them might certainly be very different, including more lignolytic enzymes.

For both enzyme assays and metaproteomics analyses, we utilized manually extracted outer tissue from flax stems, primarily focusing on the soluble fraction while initially discarding the insoluble pellet. However, recent literature shows that some activities are still present in the pellet fraction (Chirania et al., 2022) and we checked this afterward. Our preliminary experiments indicated that residual enzymatic activity persisted within these discarded insoluble fractions from the early stages (R0) to the later stages (R7) of retting (data not shown), suggesting that critical insights into the retting process may have been overlooked. This suggests a role for membrane-bound proteins (such as pectinases, cellulases, and lignin-degrading enzymes) as well as enzymes attached to cell wall polysaccharides with carbohydrate-binding motifs, which likely contribute to cell wall modification during retting (Gilbert, 2010; Linder and Teeri, 1997). To overcome this limitation, future studies should adopt a sequential extraction approach to analyze both soluble and insoluble fractions. This comprehensive strategy would enhance our understanding of enzyme compartmentalization and the

dynamics of enzymatic activity throughout the retting process. Nonetheless, the focus of our current study was justified by the objective of establishing a quantifiable link between the overall activity measured in the supernatant and the identification of specific enzymes involved. The identification of proteins with carbohydrate-binding domains underscores the efficacy of our methodology in detecting proteins potentially associated with the cell wall, which may also reside in the pellet. Thus, we can reasonably conclude that our approach remains effective in identifying these proteins, even if some are retained in the insoluble fractions.

We conducted our study in two adjacent fields (250 meters apart) that produced contrasting fiber qualities based on industrial assessments (U.S.R.T.L. standards) and in-lab quantitative assessments using single fiber tensile strength (SFTT) tests (detailed in **Chapters II** and **III**). The aim was then to identify differences at the biological level that could explain the qualitative variability of batch fibers often observed at the end of the retting process Despite the differences in fiber quality, enzyme dynamics followed similar overall (average) patterns in both fields. This pattern allowed us to divide retting into two distinct phases. In the first phase, peroxidase and phenol-oxidase activities (which target lignin and polyphenols) decreased while polygalacturonase, targeting pectins, peaked. In the second phase, xylosidase (targeting hemicelluloses) and galactosidase (targeting hemicelluloses and pectins) reached peak activity at R2 (day6), followed by peaks in glucosidase (cellulose and hemicellulose) and cellobiohydrolase (cellulose) activities at R3 (day11) - R4 (day13). This enzyme pattern is more or less similar to other studies carried out on flax and hemp (Bleuze et al., 2018; Chabbert et al., 2020), as well as with anatomical changes in flax stems, where pectin-rich middle lamellae degrade first, followed by the breakdown of primary cell walls in the cortex, liberating fiber bundles (Akin et al., 2001). The observed peroxidase and phenol-oxidase activities might be linked to phenolic degradation in the epidermis cuticle or low levels of lignin in the middle lamella between neighboring bast fibers (Day et al., 2005; Lion et al., 2017). It is widely accepted that pectinase alone is sufficient to conduct retting (Akin et al., 2001), and the increase in cellulase activities could signal over-retting, a key focus for future studies.

Metaproteomic analysis identified 6,032 non-redundant proteins (5,702 in Field A and 5,610 in Field B) across four key retting stages (R0/day 1, R2/day 6, R4/day 13, and R7/day 25), including 75 proteins with CAZy (Carbohydrate Active Enzyme) motifs from 31 different CAZy families across all five CAZy classes. Of these, 31 CAZymes in Field A and 30 in Field B were related to plant cell wall degradation. Taxonomically, 85% of the proteins were bacterial, 13% fungal, and 2% plant-derived, though ~60% of CAZymes involved in plant cell wall degradation originated from fungi (detailed in **Chapter III**) (**Fig.VI.I C(ii), C(iii)**). We observed both shared and field-specific CAZymes across the two adjacent fields A and B that provided contrasted fiber quality at the endpoint of dew retting. This

observation suggests that even if the retting is carried out by a protein main core (enzyme pool), niche-specific enzymes (such as GH94, GH55, GH54, AA1 in field A, and GH10, CE5 in field B) and therefore microorganisms might influence retting activity. Some CAZymes, such as GH3, were constant across both fields and could originate from either bacteria or fungi.

Plant CAZymes, primarily β-galactosidase and pectin methyl esterases, were active throughout retting, suggesting that retting is not just a degradation process but also involves cell wall modification. β-galactosidase is crucial for polysaccharide remodeling during secondary wall development in flax fibers (Roach et al., 2011), and pectin methylesterases modulate cell wall loosening or strengthening (Levesque-Tremblay et al., 2015).

The enzyme dynamics between retting time points showed a consistent reduction in pectinase activity early on and increased cellulase activity later in the retting process in both fields. However, field-specific differences in enzyme activity dynamics likely contribute to the observed variability in fiber quality (detailed in **Chapter III**). The idea of studying adjacent fields was to be able to look at biological differences while having few varying environmental factors. However, it will now be necessary to carry out the same study on more contrasting fields, or even on different campaigns. This will enable more robust identification of the enzymes and microorganisms involved in the main core of the retting process.

VI.1.3. Question the relevance of using vibrational spectral approaches (with RAMAN/FT-IR) to provide a tool (at the level of chemical bonds) for monitoring retting in the field

Considering possible retting markers, previous studies, such as (Meijer et al., 1995), have established that the biochemical changes during retting, particularly the reduction in pectin content (notably galacturonic acid), serve as potential indicators of retting progress.

Vibrational spectroscopies (such as Raman or FTIR) led us to observe the vibration of chemical bonds. These bonds could be related to many cell wall polymers (from flax, or microorganisms) depending on their wavenumbers n. It is related to their close chemical environment that could change during retting and let the chemical bond between 2-3 atoms vibrate more, or less. At a macroscopical level, we must take into account the gradual flax stem degradation and tissue disorganization. To detect overall chemical changes during retting, we prepared a coarse powder from the outer tissue of retted stem samples for vibrational spectroscopy analysis. As it was heterogeneous, we must use a diamond cell in order to obtain fine powder and therefore, repeatable spectra acquisition (technical repetitions). Using two statistical approaches ("*a priori*" and "without *a priori*"), we successfully differentiated retting time points based on significant spectral/ chemical changes. The "*a priori*" approach, which

compared selected peaks from literature (explained in **Chapter IV**; Mukherjee et al., 2025a, https://doi.org/10.1016/j.indcrop.2025.120798), showed that FT-IR peaks associated with polysaccharides changed notably across retting time points. For instance, the 1733.8 cm^{-1} peak (assigned to n(C=O) stretching carbonyl group in esters and uronic acid that could be assigned to esterified pectin) showed a marked shift from (R0-R2) to (R6-R7). In contrast, the "without *a priori*" approach, examined the entire spectral range (800-3400 cm^{-1}) marking changes throughout the retting stages. Early retting (R0 vs R2) was marked by changes in chemical bonds related to amorphous cellulose (1260 cm^{-1}) and to pectin (1334.6 and 1733.8 cm^{-1}), progressing retting by a reduction in the intensity of peaks related to amorphous cellulose (1201.5, 1281, and 1426.7 cm^{-1}), and optimal retting endpoint (close to R7) by a specific significant peak related to glycosidic bonds (C-OH) present in hemicellulose and xylan (1157.1 cm^{-1}).

While a reduction in pectin content is a proposed marker for retting, it is not easily applicable in field settings (Meijer et al., 1995). To address this, we drew inspiration from handheld FT-IR devices used in industries (to assess fruit quality) (Cebi et al., 2023), hypothesizing that a similar method could be adapted for flax. FT-IR has been tested for evaluating retted scutched fibers (Feleke et al., 2023; Kwiatkowska et al., 2024) and enzyme-retted flax stems (Archibald et al., 1998); but we tested it, for the first time, on naturally dew-retted flax stems, focusing on the outer tissue (after removing the woody core).

Besides a direct technical application in the field (with one or very few peaks to measure), and in a more fundamental aspect, the "without *a priori*" approach considers the whole contributions of any of the material present at one retting time, whatever its origin (plant, microorganisms). It makes a link between them according to the relative loading weight and proportion of one given peak face to the others. Effectively, outer tissue is similar to a "complex system". Not only one peak could explain the whole retting event. Indeed, all peaks could contribute simultaneously. This global approach as well as the multivariate analysis undergone in this thesis, give robust and detailed elements to further decipher dew retting.

These findings demonstrate that FT-IR is a reliable tool for tracking flax dew retting by monitoring specific wavenumber changes associated with chemical environment transformations. This approach could provide a foundation for developing portable FT-IR devices to monitor flax retting in the field (if flax powder can be produced directly on the field). However, interpreting FT-IR spectra from biological samples requires caution, as the peaks result from contributions related to complex plant systems, or to microbial molecules. Thus, attributing a peak to a single molecule or polymer, or determining its exact origin can be challenging in a complex biological system. Additionally, the lack of over-retting data and reliance on a single year's samples make these initial findings preliminary,

accounting for further validation. Testing this approach directly on stems could help assess the feasibility of applying FT-IR through portable handheld devices for real-time retting monitoring.

VI.1.4. Objective-III: Assess the feasibility of using physical color changes in flax stems, analyzed through a simple spectroscopic approach (spectral color analysis), to monitor retting in the field

To develop a noninvasive approach for monitoring retting, we decided to focus on quantifying surface color changes, as experts still rely on visual assessments to track retting progress. Using a simple usage industrial hand-held portable spectrophotometer (CM23d), we measured surface color changes in flax stems during retting, sampling across three years and five different retting fields (detailed in **Chapter II**). Statistical analysis revealed that the color of flax straw undergoes quantifiable changes during retting, following a distinct, stage-specific pattern. Specific wavelengths, such as 420 nm and 610 nm, were identified as key indicators, enabling the non-destructive monitoring of early, middle, and advanced stages of retting (detailed in **Chapter V**).

To our knowledge, this is the first time that flax straw color changes during retting have been quantified using spectral color analysis across a large dataset. Our findings lay the groundwork for the future development of color-based, non-invasive tools to monitor flax dew retting. However, it is important to note that while color changes can track retting progress in broad stages (early, middle, advanced), they cannot pinpoint precise timing, which remains a limitation. Moreover, environmental factors such as humidity and temperature must be considered when using color sensors to monitor retting, as they can significantly affect spectral characteristics and the resulting color changes (Cloutis et al., 2019). Incorporating these environmental variables alongside robust spectral data could provide a more comprehensive understanding of the retting process. Over time, gathering more data from multiple years and diverse locations will enable the refinement of predictive models for retting detection based on color analysis, improving their accuracy and usability. Furthermore, exploring non-visible spectra, such as UV, could reveal additional insights into the color changes associated with retting, enriching the dataset and refining monitoring tools. By addressing these limitations, we can strengthen the reliability of our predictive models for color-based assessments of the retting process.

VI.1.5. Building a toolbox by combining literature, biological, spectral, and physical results

The multimodal approach we employed in monitoring retting provides a deep understanding of the biochemical and structural changes occurring during the process. A key finding from our spectrophotometric and fluorometric enzyme assays is the sequential activity of cell wall-degrading enzymes. Polygalacturonase (PG) plays a critical role early in retting (R0-R2), catalyzing the breakdown of pectins in the middle lamella. This is followed by a rise in hemicellulose-degrading enzymes like

xylosidase and galactosidase (from R1, till R4), and later by cellulases such as glucosidase and cellobiohydrolase (after R2 till R5), which is known to degrade the cellulose matrix (detailed in **Chapter III**). These enzyme dynamics are consistent with the changes observed in monosaccharide composition, where arabinose shows significant decreases (Type III, in **Fig.VI.1. C(iv)**) along with a gradual decrease (Type II, in **Fig.VI.1. C(iv)**) in galacturonic acid and galactose during early retting (R0-R2), possibly correlating with seen PG activity. At the same time (R0-R2), FTIR has seen a significant difference in peaks at wave numbers 1733.8 cm-1 (esterified pectin), 1334.6 cm-1 (pectin), along with 1201.5cm-1 (xyloglucan, amorphous cellulose), 898.6 cm-1 (amorphous cellulose) in the "a priory" approach, supports the finding. These early-acting PGs are found to be cell wall-related CAZymes (active between R0-R2 compared to R2-R4 or R2-R7), such as GH35 (β-galactosidase), CE8 (pectin methylesterase) from flax, and GH28 (polygalacturonase), and the pectate lyases PL1 and PL3 from microbes.

As retting progresses (R2-R7), the degradation of xyloglucan and amorphous cellulose by hemicellulases and cellulases becomes more prominent, which was reflected in our monosaccharide and FT-IR analysis respectively (**Fig.VI.1. C**). At the advanced (R6-R7) stage of retting where cellulases, including GH7 (cellobiohydrolase), GH5 (endoglucanase), and GH94 (cellobiose phosphorylase), alongside hemicellulases like GH2 (mannanase), are increasing compared to R2; we see xylose and galactose continued to decrease (type II in **Fig.VI.1. C(iv)**) along with fucose (type I in **Fig.VI.1. C(iv)**) in monosaccharide analysis. This effect is seen with a reduction in amorphous cellulose (1201.5, 1281, 1426.7 cm^{-1}) and hemicellulose (1317 cm-1) in the FT-IR study, throughout the retting. These structural changes in pectin and hemicellulose are indicative of middle lamella degradation, leading to fiber separation, a critical step in the retting process.

Crystalline glucose content along with Rhamnose and mannose don't change significantly in monosaccharide analysis, which is supported by previous reports (Akin, 2013). The FT-IR study noted an increase in cellulose crystallinity during retting, as evidenced by specific peaks, such as at 1371.2 cm^{-1}, which again aligned with previous studies (Bourmaud et al., 2019).

The exposure of phenolic components, such as pyrroles of chlorophyll, occurs as the plant begins to die, and their oxidation, coupled with microbial colonization of the stem surface, contributes to the visible color changes observed in flax straws during retting. The FT-IR peaks associated with fungal cell wall components (1104, 1056, and 1030 cm^{-1}), including β-1,3-D-glucan, chitin, and mannan, suggest that fungi play an active role during the retting process (already confirmed by fungal proteins). These microbial activities likely modify the biochemical environment on the surface of the stems, potentially accelerating cell wall degradation.

Our color analysis has shown the ability to distinguish between different stages of retting, particularly the transitions from early (R0-R2) to middle (R3-R5) and advanced stages (R6-R7). These

observations align with the enzymatic and FT-IR data, indicating that changes at the levels of enzymatic activity, microbial action, and polysaccharide degradation may be monitored through FT-IR analysis. Furthermore, the resulting color changes can be assessed using color spectral analysis. Thus, the integration of colorimetric methods with biochemical assays and spectral analysis could offer a valuable approach to standardizing the retting process, although further investigation is needed to establish definitive correlations.

In the future, the integration of biological and physical data, analyzed using Pearson and Spearman rank correlations, will offer a valuable statistical framework for interpreting the retting process (**Fig.VI.2**). This combined approach could not only enhance our understanding of the sequential degradation of plant cell wall components but also pave the way for the development of advanced monitoring tools for retting. For instance, a drone equipped with a camera and color sensor could perform color spectroscopy to assess the retting progress, effectively indicating when the process is nearing its endpoint. Farmers could then utilize a portable hand-held FTIR device or biochemical sensors to intervene during the retting process. The application of antibodies would enable targeted assays to quantify key proteins, including cellulase and pectinase, along with specific polysaccharides like pectin. Integrating this biochemical data with FTIR measurements would create a robust framework for real-time monitoring and standardization of retting. This approach has the potential to enhance retting efficiency, minimize variability, and ultimately optimize the quality of the harvested fibers.

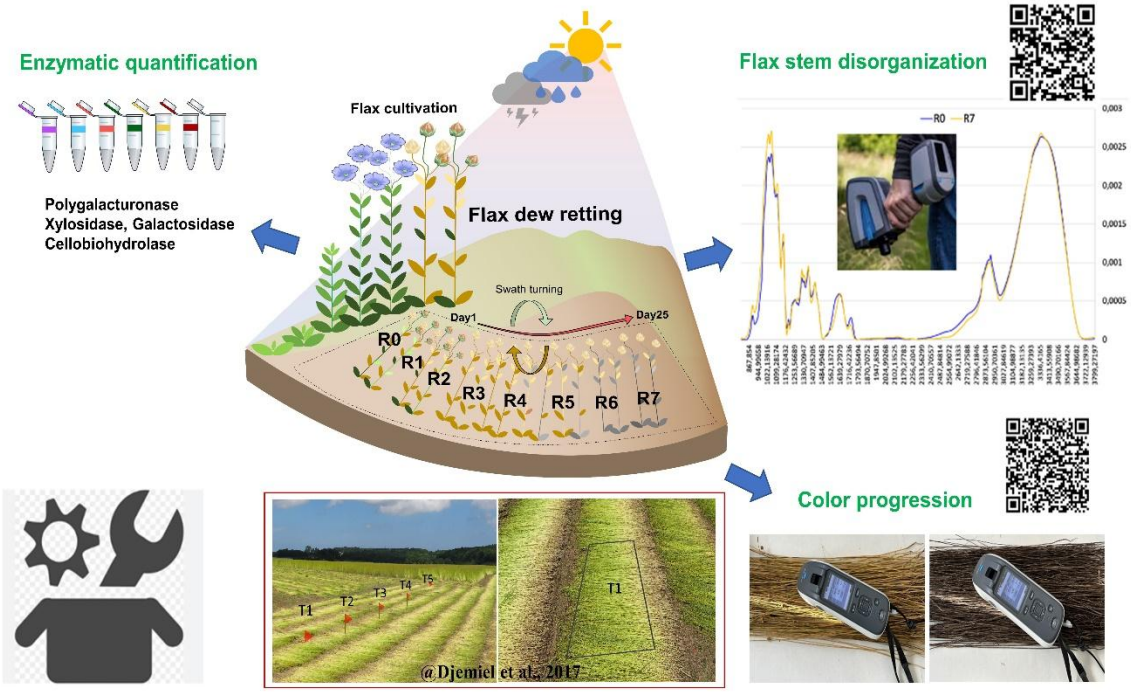

Figure. VI.2. A concept of a toolbox combining proposed methods.

QR codes are related to one example of portable FTIR (not used in this thesis), and the color spectrophotometer cm23d (from Konica) used in this thesis.

VI.2. General Conclusion of the Thesis

In this thesis, under the FlaxTronic project, we addressed the gaps between known microbiological processes and the dynamics of enzyme activities in the flax dew retting process, while also exploring potential retting markers to scientifically monitor and standardize the process (proposing technical solutions).

Utilizing a metaproteomics-based approach, we bridged the knowledge gap between known microbial communities and the global enzyme activities involved in fiber degradation. Our findings identified critical bacterial and fungal CAZymes, but also highlighted the significant role of plant-derived enzymes in cell wall modification and polymer degradation during retting. This work offers a deeper insight into how these enzymatic activities drive fiber separation, particularly through the disorganization of cellulose and pectin components, as characterized by monosaccharide analysis and FT-IR spectroscopy.

Through comparative field studies, we identified notable inter-field variability in retting enzyme profiles, which may explain the differences in fiber quality. This discovery paves the way for further investigations into the environmental and microbial factors influencing retting efficiency. Vibrational spectroscopy, specifically FT-IR, proved invaluable in detecting subtle chemical changes during retting, offering clear markers for early-stage cell wall breakdown and optimal fiber release points, such as the progressive decline in amorphous cellulose peaks and the emergence of hemicellulose signals.

In parallel, our exploration of stem surface color changes using spectrophotometry revealed the potential for a predictive model to monitor retting progress (in stages). By tracking specific wavelengths in the color spectrum, we observed that shifts in color intensity correlated with advanced retting stages, particularly around the optimal retting point. However, the precision of color monitoring remains limited, necessitating further refinement, particularly in the context of variable environmental conditions like humidity and temperature, which can significantly impact retting dynamics.

In conclusion, the integration of metaproteomics, vibrational spectroscopy, and colorimetric analysis offers a comprehensive toolkit for better understanding and monitoring retting. These methods not only enhance our ability to predict retting outcomes with greater accuracy but also contribute to the European Green Deal's goal of advancing sustainable textile technologies. Future work on correlation-based data integration along with valorization and refining of proposed predictive models will be crucial in optimizing retting for consistent fiber quality, regardless of field-specific conditions.

VI.3. Perspective of the Thesis

For enzyme assays and metaproteomics, we focused on the soluble fraction of manually extracted flax stem outer tissue, discarding the insoluble part. However, preliminary tests on the discarded tissue revealed residual enzyme activity. In future analyses, including both the soluble fraction and sequential extracts from the insoluble tissue could offer deeper insights into enzyme compartmentalization during retting. This comprehensive approach would enhance our understanding of secretory and cell wall-bound enzymes, providing a more complete enzymatic profile during the retting process.

The application of meta-omics approaches, including metagenomics, metaproteomics, metatranscriptomics, and metabolomics, offers a powerful framework for unraveling the complexities of microbe-microbe and plant-microbial interactions during retting. Metagenomics, particularly through shotgun sequencing, not only reveals "who is there" but also the enzymatic potential within the microbial community. However, it does not indicate which genes are actively expressed or translated into functional proteins. This gap is addressed by metatranscriptomics, which identifies "what they do" by highlighting gene expression, regulation, and post-transcriptional modifications. Metaproteomics further connects the microbial community to actual enzymatic activities, and metabolomics provides direct evidence of microbial metabolic functions, such as plant polysaccharide degradation. Together, these tools offer a more comprehensive biological understanding of retting. Applying these methods to other bast fiber plants with different anatomical features could also be an exciting direction for future research.

Additionally, the inclusion of over-retting samples in future studies could reveal important differences in microbial enzyme strategies and chemical changes in the fibers. For FT-IR-based analysis, studying over-retted samples (beyond R7) may yield new spectral peaks that distinguish between retting and over-retting stages. Comparing the predictive model developed for Field A with that of Field B will help validate our findings, potentially allowing us to explain the differences in fiber quality (under-retted or over-retted) and finalize the predictive retting model.

The application of Raman vibrational spectroscopy to study the gradual deconstruction of plant polymers during flax dew retting offers the potential to obtain tissue-specific insights (with 1µm leaser) into the changing chemical environment. This method provides greater precision in identifying localized chemical changes compared to non-tissue-specific techniques. However, during preliminary trials, the analysis encountered technical challenges, particularly due to autofluorescence, which proved difficult to overcome within a short timeframe. As a result, FTIR vibrational spectroscopy was employed. In future studies, Raman spectroscopy could complement FTIR findings by providing more detailed

localization of chemical modifications at the tissue level, thereby enhancing our understanding of the retting process.

Our current FT-IR studies were conducted on homogenous powder samples from retted flax stem external tissue. Moving forward, it will be of interest to apply FT-IR directly to the stems in a non-destructive manner. If similar results are achieved, this approach could be adapted for a portable, hand-held device, enabling real-time retting monitoring in the field. This would address the industry's need to reduce the reliance on expert evaluations for monitoring dew retting.

Our color change quantification demonstrated that tracking retting through color variations can be effective for monitoring the retting process in stages (early, middle, and advanced), which aligns with industrial needs. However, these tests were conducted in indoor conditions on dried samples. It is essential to incorporate environmental factors such as humidity and temperature when using color sensors in the field, as these conditions can significantly influence spectral characteristics and color changes. Expanding the data set with more in-field measurements and studying these environmental variables will improve the predictive model’s accuracy.

Lastly, integrating the multivariate data sets obtained in our studies with statistical analyses to identify the most significant correlated variables that define the retting status could be incorporated into a complete toolbox for the standardization of the dew retting process in the future. This approach holds promise not only for flax but also for other bast fiber plants, such as hemp and ramie, where limited data are currently available. Expanding this technique to these plants could improve retting processes and support the development of monitoring tools, further enhancing fiber quality and process control.

VI.4. References

Akin, D.E., 2013. Linen Most Useful: Perspectives on Structure, Chemistry, and Enzymes for Retting Flax. ISRN Biotechnology 2013, 1–23. https://doi.org/10.5402/2013/186534

Akin, D.E., Foulk, J.A., Dodd, R.B., McAlister, D.D., 2001. Enzyme-retting of flax and characterization of processed fibers. Journal of Biotechnology, Biotechnology in the Textile Industry - Perspectives for the New Millennium 89, 193–203. https://doi.org/10.1016/S0168-1656(01)00298-X

Archibald, D.D., Henrikssen, G., Akin, D.E., Barton, F.E., 1998. Spectroscopic characterization of enzymatic flax retting: Factor analysis of FT-IR and FT-Raman data. AIP Conference Proceedings 430, 653–656. https://doi.org/10.1063/1.55746

Bleuze, L., Lashermes, G., Alavoine, G., Recous, S., Chabbert, B., 2018. Tracking the dynamics of hemp dew retting under controlled environmental conditions. Industrial Crops and Products 123, 55–63. https://doi.org/10.1016/j.indcrop.2018.06.054

Bourmaud, A., Siniscalco, D., Foucat, L., Goudenhooft, C., Falourd, X., Pontoire, B., Arnould, O., Beaugrand, J., Baley, C., 2019. Evolution of flax cell wall ultrastructure and mechanical properties during the retting step. Carbohydrate Polymers 206, 48–56. https://doi.org/10.1016/j.carbpol.2018.10.065

Cebi, N., Bekiroglu, H., Erarslan, A., Rodriguez-Saona, L., 2023. Rapid Sensing: Hand-Held and Portable FTIR Applications for On-Site Food Quality Control from Farm to Fork. Molecules 28, 3727. https://doi.org/10.3390/molecules28093727

Chabbert, B., Padovani, J., Djemiel, C., Ossemond, J., Lemaître, A., Yoshinaga, A., Hawkins, S., Grec, S., Beaugrand, J., Kurek, B., 2020. Multimodal assessment of flax dew retting and its functional impact on fibers and natural fiber composites. Industrial Crops and Products 148, 112255. https://doi.org/10.1016/j.indcrop.2020.112255

Chirania, P., Holwerda, E.K., Giannone, R.J., Liang, X., Poudel, S., Ellis, J.C., Bomble, Y.J., Hettich, R.L., Lynd, L.R., 2022. Metaproteomics reveals enzymatic strategies deployed by anaerobic microbiomes to maintain lignocellulose deconstruction at high solids. Nat Commun 13, 3870. https://doi.org/10.1038/s41467-022-31433-x

Cloutis, E., Beck, P., Gillis-Davis, J.J., Helbert, J., Loeffler, M.J., 2019. Effects of Environmental Conditions on Spectral Measurements, in: Bell III, J.F., Bishop, J.L., Moersch, J.E. (Eds.), Remote Compositional Analysis: Techniques for Understanding Spectroscopy, Mineralogy, and Geochemistry of Planetary Surfaces, Cambridge Planetary Science. Cambridge University Press, Cambridge, pp. 289–306. https://doi.org/10.1017/9781316888872.015

Day, A., Ruel, K., Neutelings, G., Crônier, D., David, H., Hawkins, S., Chabbert, B., 2005. Lignification in the flax stem: evidence for an unusual lignin in bast fibers. Planta 222, 234–245. https://doi.org/10.1007/s00425-005-1537-1

Djemiel, C., 2017. Étude de la diversité du domaine Bacteria et du règne Fungi au cours du rouissage du lin sur champ par une approche de metabarcoding (These de doctorat). Lille 1.

Djemiel, C., Grec, S., Hawkins, S., 2017. Characterization of Bacterial and Fungal Community Dynamics by High-Throughput Sequencing (HTS) Metabarcoding during Flax Dew-Retting. Frontiers in Microbiology 8. https://doi.org/doi.org/10.3389/fmicb.2017.02052

Feleke, K., Thothadri, G., Beri Tufa, H., Rajhi, A.A., Ahmed, G.M.S., 2023. Extraction and Characterization of Fiber and Cellulose from Ethiopian Linseed Straw: Determination of Retting Period and Optimization of Multi-Step Alkaline Peroxide Process. Polymers 15, 469. https://doi.org/10.3390/polym15020469

Gilbert, H.J., 2010. The Biochemistry and Structural Biology of Plant Cell Wall Deconstruction. Plant Physiology 153, 444–455. https://doi.org/10.1104/pp.110.156646

Kwiatkowska, E., Zimniewska, M., Gryszczyńska, A., Przybylska, P., Różańska, W., 2024. The Effect of Drought on the Content of Active Substances of Flax Fibers. Journal of Natural Fibers 21, 2310679. https://doi.org/10.1080/15440478.2024.2310679

Levesque-Tremblay, G., Pelloux, J., Braybrook, S.A., Müller, K., 2015. Tuning of pectin methylesterification: consequences for cell wall biomechanics and development. Planta 242, 791–811. https://doi.org/10.1007/s00425-015-2358-5

Linder, M., Teeri, T.T., 1997. The roles and function of cellulose-binding domains. Journal of Biotechnology, Biochemistry and genetics of cellulases and hemicellulases and their application 57, 15–28. https://doi.org/10.1016/S0168-1656(97)00087-4

Lion, C., Simon, C., Huss, B., Blervacq, A.-S., Tirot, L., Toybou, D., Spriet, C., Slomianny, C., Guerardel, Y., Hawkins, S., Biot, C., 2017. BLISS: A Bioorthogonal Dual-Labeling Strategy to Unravel Lignification Dynamics in Plants. Cell Chemical Biology 24, 326–338. https://doi.org/10.1016/j.chembiol.2017.02.009

Mazian, B., 2018. Approche intégrée du procédé de rouissage des fibres de chanvre : Vers une amélioration de la qualité des intrants pour la fabrication des matériaux biocomposites (phdthesis). IMT - MINES ALES - IMT - Mines Alès Ecole Mines - Télécom.

Meijer, W.J.M., Vertregt, N., Rutgers, B., van de Waart, M., 1995. The pectin content as a measure of the retting and rettability of flax. Industrial Crops and Products 4, 273–284. https://doi.org/10.1016/0926-6690(95)00041-0

Mukherjee, S., Goulas, E., Creach, A., Krzewinski, F., Galinousky, D., Blervacq, A.S., D'Arras, P., Ratahiry, S., Menuge, A., Soulat, D., Saliou, J.M., Lacoste, A.S., Hawkins, S., and Grec, S., 2024. Metaproteomics identifies key cell wall degrading enzymes and proteins potentially related to inter-field variability in fiber quality during flax dew retting. Industrial Crops and Products. https://doi.org/10.1016/j.indcrop.2024.119907.

Roach, M.J., Mokshina, N.Y., Badhan, A., Snegireva, A.V., Hobson, N., Deyholos, M.K., Gorshkova, T.A., 2011. Development of Cellulosic Secondary Walls in Flax Fibers Requires β-Galactosidase. Plant Physiology 156, 1351–1363. https://doi.org/10.1104/pp.111.172676

Analyse multimodale du processus de rouissage sur champs du lin : étude fonctionnelle et spectrales en vue d'améliorer la qualité des fibres

Résumé

Le lin (Linum usitatissimum L.) est considéré comme une alternative durable aux fibres synthétiques pour les applications textiles et matériaux. Les fibres de lin se trouvant dans la tige, leur extraction commence par le rouissage sur champ. Les tiges sont couchées sur le sol et les microorganismes décomposent les polymères qui lient les fibres aux autres tissus de la tige. Ce processus naturel introduit de la variabilité dans la qualité des fibres. L'objectif de cette thèse (Flaxtronix, PEARLI-Site) et d'améliorer les connaissances du rouissage et d'identifier des marqueurs permettant un suivi en champs par des capteurs (Agriculture 4.0). Une approche combinant enzymologie, chimie, et métaprotéomique ont permis d'identifier des enzymes et de microorganismes associés au rouissage. Il a également été démontré que la spectroscopie infrarouge (FT-IR) et l'analyse spectrale des couleurs peuvent fournir des marqueurs pertinents permettant de prédire la fin du rouissage.

Deciphering Flax dew retting by a multimodal approach

Abstract

Flax (Linum usitatissimum L.) represents a sustainable alternative to synthetic fibers in textiles and composites. The fiber extraction process begins with retting, during which microorganisms decompose the pectic substances that bind the fibers to the stem. This biological process depends on many factors and introduces variability in fiber batches. This thesis (FlaxTronic, PEARL I-site), aims to help for standardizing flax dew-retting by proposing a possible sensor-based system for real-time decision-making (Agriculture 4.0). Key objectives include understanding the biology of retting by using enzymology, chemistry, and metaproteomic; vibrational spectroscopy (FT-IR); and assessing stem color changes as non-invasive markers. As the main results, metaproteomics identified carbohydrate-active enzymes (CAZymes) and microorganisms involved in cell wall degradation, while FT-IR spectroscopy and color spectrophotometry might provide valuable monitoring tools to predict retting achievement.